



Universiteit  
Leiden  
The Netherlands

**Potentialiation of Gram-positive specific antibiotics against Gram-negative bacteria through outer membrane disruption**  
Wesseling, C.M.J.

**Citation**

Wesseling, C. M. J. (2022, July 5). *Potentialiation of Gram-positive specific antibiotics against Gram-negative bacteria through outer membrane disruption*. Retrieved from <https://hdl.handle.net/1887/3421483>

Version: Publisher's Version

License: [Licence agreement concerning inclusion of doctoral thesis in the Institutional Repository of the University of Leiden](#)

Downloaded from: <https://hdl.handle.net/1887/3421483>

**Note:** To cite this publication please use the final published version (if applicable).

# Potential of Gram-positive specific antibiotics against Gram-negative bacteria through outer membrane disruption

Proefschrift

ter verkrijging van  
de graad van doctor aan de Universiteit Leiden,  
op gezag van rector magnificus prof.dr.ir. H. Bijl,  
volgens besluit van het college voor promoties  
te verdedigen op dinsdag 5 juli 2022  
klokke 11:15 uur

door

Charlotte Marie José Wesseling  
geboren te Woerden  
in 1990

Promotores: Prof. dr. Nathaniel I. Martin  
Prof. dr. Suzan H.M. Rooijakkers (UMC Utrecht)

Doctorate committee: Prof. dr. Gilles P. van Wezel  
Prof. dr. Dennis Claessen  
Prof. dr. Sander I. van Kasteren  
Prof. dr. Nina M. van Sorge (Amsterdam UMC - UvA)  
Prof. dr. Oscar P. Kuipers (Rijksuniversiteit Groningen)

Cover image depicts a photograph of the checkerboard kitchen floor of C.M.J. Wesseling covered with fallen tulip petals.

This Ph.D. program was financially supported by:

ZonMW

The printing of this thesis was financially supported by:

Universiteit Leiden

Shimadzu Benelux BV

Printed by: proefschriften.net

Cover lay-out: A.J.B. Wesseling

Lay-out: C.M.J. Wesseling

ISBN: 978-94-6421-770-4

“Cruciaal is dat je jezelf overhaalt om van de wereld te houden. Als je de schoonheid ziet van de breekbare menselijke soort, van bouwkunst, sport, staatsrecht, gastronomie en al die andere manieren die we verzonnen hebben om ons biologische repertoire te verfijnen, dan pas kun je je eigen bijdrage, hoe klein ook, naar waarde schatten. Dat is een grote troost als je weet dat alles doorgaat als jij er niet meer bent.”

- René Gude





# Table of contents

<b>List of abbreviations</b>	<b>6</b>
<b>Chapter 1</b>	<b>9</b>
Introduction. Synergy by perturbing the Gram-negative outer membrane: opening the door for Gram-positive specific antibiotics	
<b>Chapter 2</b>	<b>63</b>
Structure-activity studies with bis-amidines that potentiate Gram-positive specific antibiotics against Gram-negative pathogens	
<b>Chapter 3</b>	<b>153</b>
Thrombin-derived peptides potentiate the activity of Gram-positive specific antibiotics against Gram-negative bacteria	
<b>Chapter 4</b>	<b>203</b>
Exploring Gram-positive specific antibiotics potentiation by human serum against Gram-negative bacteria	
<b>Chapter 5</b>	<b>245</b>
Intrinsic antimicrobial activity of bis-amidines against Gram-positive bacteria	
<b>Chapter 6</b>	<b>271</b>
Summary and Future Outlook	
<b>Appendices</b>	<b>280</b>
Samenvatting	
Sources of bacterial strains	

## List of abbreviations

$\Delta F$	$\alpha,\beta$ -didehydrophenylalanine
AA	amino acid
Ac <sub>2</sub> O	acetic anhydride
AcOH	acetic acid
ACS	American Chemical Society
alle	D- <i>allo</i> -isoleucine
AMP	antimicrobial peptides
AMR	antimicrobial resistance
ATCC	American Type Culture Collection
Bip	biphenylalanine
BPEI	branched polyethylenimine
BPI	bactericidal/permeability-increasing protein
Boc	tert-butyloxycarbonyl
tBu	tert-butyl
tBuOH	tert-butanol
Boc	tert-butyloxycarbonyl
BOP	(benzotriazol-1-yloxy)tris(dimethylamino)phosphonium hexafluorophosphate
C6	hexanoyl
C8	octanoyl
C10	decanoyl
CBr <sub>4</sub>	carbon tetrabromide
Cbz	benzyloxycarbonyl
CDCl <sub>3</sub>	deuterated chloroform
Cha	cyclohexylalanyl
CLSI	Clinical & Laboratory Standards Institute
Dab	2,4-diaminobutyric acid
DAPB	deacylpolymyxin B
DIC	N,N-Diisopropylcarbodiimide
DIPEA	N,N-diisopropylethylamine
DMF	N,N-dimethylformamide
dUSCL	dilipid ultrashort cationic lipopeptide
dUSTBP	dilipid ultrashort tetrabasic peptidomimetic
EDTA	ethylenediaminetetraacetate
ESBL	extended spectrum $\beta$ -lactamase
EtOAc	ethyl acetate
EtOH	ethanol
FICI	fractional inhibitory concentration index
Fmoc	fluorenylmethyloxycarbonyl
H <sub>2</sub> SO <sub>4</sub>	sulfuric acid
HCl	hydrogen chloride
HFIP	1,1,1,3,3,3-hexafluoro-2-propanol
HMP	hexametaphosphate
HPLC	high-performance liquid chromatography
HTS	high throughput screening
LB	Lysogeny Broth
LPS	lipopolysaccharide
MAC	membrane attack complex
MDR	multidrug-resistant
MeOH	methanol
MIC	minimum inhibitory concentration
MOX	moxifloxacin
MSC	minimum synergistic concentration
MTBE	methyl tert-butyl ether

Na <sub>2</sub> SO <sub>4</sub>	sodium sulfate
Nal	β-naphthylalanine
NDM-1	New Delhi β-lactamase 1
NEB	nebramine
NMP	1-(1-naphthylmethyl)-piperazine
NPN	N-phenyl-napthalen-1-amine
NR	no data reported
OAK	oligo-acyl-lysyl
OM	outer membrane
Oxyma	ethyl cyanohydroxyiminoacetate
PAR	paroxetine
Pbf	2,2,4,6,7-pentamethyldihydrobenzofuran-5-sulfonyl
PEDES	PEptide DEscriptors from Sequence
PG	phosphatidylglycerol
PMB	polymyxin B
PMBH	polymyxin B heptapeptide
PMBN	polymyxin B nonapeptide
PMBO	polymyxin B octapeptide
PPh <sub>3</sub>	triphenylphosphine
SAR	structure-activity relationship
SM	squalamine mimics
THF	tetrahydrofuran
TIS	triisopropylsilane
TOB	tobramycin
TPP	tetraphenylphosphonium
TriA <sub>1</sub>	Tridecaptin A <sub>1</sub>
Trt	trityl
UTBLP	ultrashort tetrabasic lipopeptide
WHO	World Health Organization

### Amino acids

Ala	A	Alanine
Arg	R	Arginine
Asn	N	Asparagine
Asp	D	Aspartic acid
Cys	C	Cysteine
Glu	E	Glutamic acid
Gln	Q	Glutamine
Gly	G	Glycine
His	H	Histidine
Ile	I	Isoleucine
Leu	L	Leucine
Lys	K	Lysine
Met	M	Methionine
Phe	F	Phenylalanine
Pro	P	Proline
Ser	S	Serine
Thr	T	Threonine
Trp	W	Tryptophan
Tyr	Y	Tyrosine
Val	V	Valine



# Chapter 1

## Introduction. Synergy by perturbing the Gram-negative outer membrane: opening the door for Gram-positive specific antibiotics

Charlotte M.J. Wesseling and Nathaniel I. Martin

Parts of this chapter have been submitted for publication

### Abstract

New approaches to target antibacterial agents towards Gram-negative bacteria are key given the rise of antibiotic resistance. Since the discovery of polymyxin B nonapeptide as a potent Gram-negative outer membrane (OM) permeabilizing synergist in the early 1980s, a vast amount of literature on such synergists has been published. This review addresses a range of peptide-based and small organic compounds that disrupt the OM to elicit a synergistic effect with antibiotics that are otherwise inactive towards Gram-negative bacteria, with synergy defined as a fractional inhibitory concentration index of  $<0.5$ . Another requirement for the inclusion of the synergists here covered is their potentiation of a specific set of clinically used antibiotics: erythromycin, rifampicin, novobiocin, or vancomycin. In addition, we have focused on those synergists with reported activity against Gram-negative members of the ESKAPE family of pathogens namely, *Escherichia coli*, *Pseudomonas aeruginosa*, *Klebsiella pneumoniae*, and/or *Acinetobacter baumannii*. In cases where the FICI values were not directly reported in the primary literature but could be calculated from the published data we have done so, allowing for more direct comparison of potency with other synergists. We also address the hemolytic activity of the various OM disrupting synergists reported in the literature, an effect that is often downplayed but of key importance in assessing the selectivity of such compounds for Gram-negative bacteria.

## 1. Introduction

The increasing occurrence of antibiotic resistance among Gram-negative pathogens highlights the need for novel antibacterial agents and therapeutic strategies. It is well established that Gram-negative bacteria are inherently harder to kill with antibiotics than Gram-positives given the presence of the Gram-negative outer membrane (OM) as well as efflux pumps.<sup>1-4</sup> Among the limited number of clinically effective anti-Gram-negative agents, several are labeled as last resort further underscoring the urgent need for new treatments against Gram-negative pathogens.<sup>5-7</sup> This troubling reality is further exacerbated by increasing accounts of emerging resistance mechanisms against Gram-negative antibiotics including: extended spectrum beta-lactamases (ESBLs) that can render even fifth generation cephalosporins and carbapenems inactive,<sup>8-11</sup> enzymes that structurally modify and deactivate aminoglycosides,<sup>12-15</sup> and *mcr*-mediated polymyxin resistance.<sup>16-27</sup> In this context, the World Health Organization (WHO) recently listed *Acinetobacter baumannii* (carbapenem-resistant), *Pseudomonas aeruginosa* (carbapenem-resistant), and the *Enterobacteriaceae* (carbapenem-resistant and ESBL-producing strains) as the bacterial pathogens of highest priority for the development of new antibiotics.<sup>28</sup>

The Gram-negative OM functions as a barrier that prevents many antibiotics, that are otherwise active against Gram-positive species, from reaching their targets.<sup>3,29</sup> The OM itself consists of an asymmetrical lipid bilayer (See Figure 1A).<sup>30</sup> The inner leaflet consist mostly of phospholipids and is similar to the cytoplasmic membrane.<sup>31</sup> The outer leaflet is made up of an organized and fortified structure of densely packed lipopolysaccharides (LPS) and  $Mg^{2+}/Ca^{2+}$  cations that bridge the negatively charged phosphate groups of the lipid A component of LPS (See Figure 1B).<sup>3,32</sup> Furthermore, the tightly packed saturated acyl chains result in a low level of membrane fluidity that limits the diffusion of hydrophobic compounds across the OM.<sup>2,3</sup> The OM also contains porins which function as size exclusion channels across the OM that mediate the diffusion of small hydrophilic molecules between the periplasm and the extracellular environment while keeping large, hydrophobic molecules, including many antibiotics, out.<sup>1,2,29</sup> Additionally, when lipophilic or amphiphilic antibiotics do manage to cross the OM, multidrug efflux pumps can transport these molecules back out.<sup>1-3,29</sup> In many cases, the over-expression of efflux pumps provides an effective means for a Gram-negative pathogen to decrease its susceptibility to antibiotics.<sup>3,33</sup> Taken together, their diverse resistance mechanisms and unique cellular features provide Gram-negative bacteria with a formidable range of defenses against antibacterial agents.

To address the specific challenges posed by Gram-negative bacteria a number of new and innovative approaches are currently under investigation. Such strategies include interfering with LPS biosynthesis,<sup>34-37</sup> targeting OM proteins such as the BAM complex,<sup>34,38,39</sup> developing siderophore-antibiotic conjugates as Trojan horse agents,<sup>40-42</sup> co-administering different antibiotics to restrict or reverse antibiotic resistance,<sup>43,44</sup> and blocking efflux pumps.<sup>45-48</sup> In addition to these promising strategies, the development of agents that can selectively disrupt the OM offers the possibility of sensitizing Gram-negative bacteria to antibiotics that otherwise function only against Gram-positive bacteria.<sup>3,7,32</sup> The pursuit of such synergists continues to be a very active field of research and is the basis for this review.

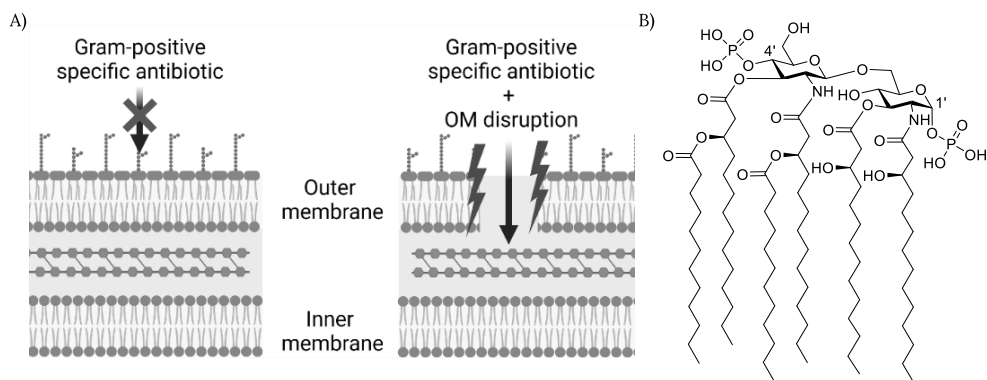


**Figure 1.** A) Schematic depiction of the OM disruption required for potentiation of Gram-positive specific antibiotics (created with BioRender.com); B) Lipid A (from *Escherichia coli* K-12), the hydrophobic anchor of LPS.

The best studied example of an OM disrupting synergist is polymyxin B nonapeptide (PMBN) which is obtained by enzymatic degradation of the clinically used lipopeptide polymyxin B (PMB).<sup>7,32</sup> The potentiating effects of PMBN were first reported in the 1980s, and in the decades since a growing number of OM disrupting synergists have been discovered.<sup>7,32,49</sup> To date, a number of reviews have been published on the general topic of antibiotic synergy,<sup>50–57</sup> including compounds that potentiate Gram-positive antibiotics through interactions with the OM<sup>58</sup> and OM disrupting synergists.<sup>32,59–63</sup> However, a comprehensive overview of OM disrupting synergists that also provides the reader with a direct comparison of both the potency and selectivity of these compounds has, to date, been lacking. In this regard, the most widely accepted benchmark for synergistic activity is the so called fractional inhibitory concentration index (FICI, Box 1). In this review we discuss only those synergists for which FICI values are reported or could be calculated from published data. The other criterion we have also chosen to emphasize is the selectivity of OM disruption associated with these synergists. In this regard, we pay special attention to the hemolytic activity reported for the various OM disruptors as a means of assessing their membrane specificity.

Among the Gram-negative bacteria for which OM disrupting synergists have been reported, we have selected those pathogens noted on the WHO's priority list: *A. baumannii*, *Escherichia coli*, *Klebsiella pneumoniae*, or *P. aeruginosa*.<sup>28</sup> As for Gram-positive specific antibiotics whose activity is potentiated by OM disrupting synergists, we have chosen to focus on clinically used agents that are most commonly evaluated for synergy with OM disruptors: erythromycin, rifampicin, vancomycin, and novobiocin.<sup>7,58</sup> This criterion has, for example, led to the exclusion of OM disrupting agents for which synergy was reported with macrolide antibiotics other than erythromycin.<sup>64–67</sup> Also, to further streamline the review, synergists for which an OM disrupting mechanism was not clearly demonstrated are not here discussed in detail.<sup>68–76</sup> In addition, synergists that



specifically engage with Gram-negative targets and subsequently cause OM disruption as a secondary effect are not discussed in this review.<sup>77–85</sup>

**Box 1.** An important formalism in the field of synergy is the fractional inhibitory concentration index (FICI). The FICI is calculated from experimental minimum inhibitory concentration (MIC) data as shown in Equation 1. A synergistic combination is generally defined as an FICI  $\leq 0.5$ . Additionally, it allows for a straightforward comparison of the potency of the synergistic combinations: the lower the FICI, the more potent the combination. Apart from the FICI, the minimum synergistic concentration (MSC) values are also relevant parameters. The MSCs represent the concentrations of each component required for synergy and are therefore also of clinical relevance.

$$\text{FICI} = \frac{\text{MSC}_{\text{ant}}}{\text{MIC}_{\text{ant}}} + \frac{\text{MSC}_{\text{syn}}}{\text{MIC}_{\text{syn}}} \quad (1)$$

**Equation 1.** Calculation of FICI.  $\text{MSC}_{\text{ant}}$  = MIC of antibiotic in combination with synergist;  $\text{MIC}_{\text{ant}}$  = MIC of antibiotic alone;  $\text{MSC}_{\text{syn}}$  = MIC of synergist in combination with antibiotic;  $\text{MIC}_{\text{syn}}$  = MIC of synergist alone.

The scope of the synergists included in this review ranges from peptides to synthetic small-molecules and small polymers of <1500 Da. In this regard, protein-based OM disruptors such as the membrane attack complex (MAC)<sup>86</sup>, lactoferrin,<sup>87</sup> and the bactericidal/permeability-increasing protein (BPI)<sup>88</sup> or larger polymers or polymer-like agents<sup>89–92,92–96</sup> will not be discussed. This review is further organized based on the chemical families of the synergists covered. We begin with cyclic peptides based on PMBN, followed by linear peptides, cationic steroids, peptide-steroids hybrids, and small molecules. For each subgroup of synergists a summary table has been assembled to provide a convenient comparative overview of FICI values. These tables also include the identity of the Gram-negative species and companion antibiotics employed in generating the FICIs. In addition, where possible, we have included the reported hemolytic activity of each synergist to provide an indication of their selectivity for Gram-negative cells.

## 2. Peptide-based potentiators

### 2.1. Polymyxin derived synergists

Polymyxin derived synergists have been extensively reviewed in the past and therefore only a concise summary of these analogues is here included.<sup>7,32,63</sup> PMBN is a derivative of the parent lipopeptide PMB (see Figure 2A). Unlike its parent compound, PMBN has no inherent antimicrobial activity nor is it nephrotoxic.<sup>7,97</sup> In their landmark 1983 paper, Martti and Timo Vaara demonstrated that the combination of PMBN with hydrophobic, generally Gram-positive specific, antibiotics results in a potent synergistic effect (See Table 1).<sup>32,49</sup> In this regard, PMBN is often used as a benchmark for synergistic activity.<sup>7</sup> Apart from PMBN, other truncated derivatives of PMB, like deacylpolymyxin B (DAPB), polymyxin B octapeptide (PMBO) and polymyxin B heptapeptide (PMBH) also display synergistic activity (Figure 1A and Table 1).<sup>32</sup> The peptide macrocycle is of key importance for these synergists as linear PMBN variants lose their synergistic activity.<sup>98</sup>

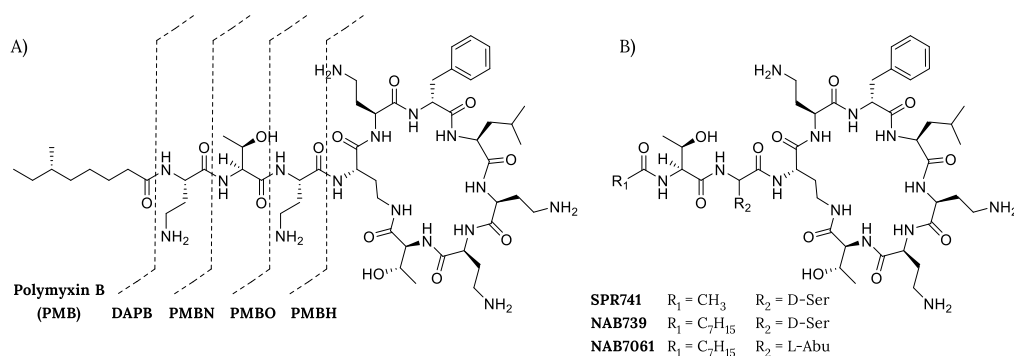


**Figure 2.** Molecular structures of A) polymyxin B (PMB), deacylpolymyxin B (DAPB), polymyxin B nonapeptide (PMBN), polymyxin B octapeptide (PMBO), and polymyxin B heptapeptide (PMBH); B) PMBN analogues SPR741, NAB739, and NAB7061.

A new generation of PMBN analogues containing only three positive charges was developed more recently.<sup>99,100</sup> SPR741, previously named NAB741, has passed the Phase I clinical trials (See Figure 2B).<sup>7</sup> Like PMBN, SPR741 has no lipophilic tail resulting in improved renal clearance compared to PMB and other analogues including a lipophilic tail such as NAB739 and NAB7061.<sup>100</sup> NAB7061 has little inherent antimicrobial activity, but is a very potent synergist, while NAB739 has very potent antimicrobial activity (Table 1).<sup>101</sup> Remarkably, this difference in activity between NAB739 and NAB7061 is attributed to the absence of one hydroxyl group in NAB7061 (See Figure 2B).<sup>99</sup> NAB739 has been reported to exhibit generally moderate synergistic activity against wild-type strains with the exception of the *A. baumannii* strain indicated in Table 1.<sup>99,102</sup> Interestingly, against *mcr*-positive strains, the loss of antimicrobial activity for NAB739 is accompanied by a significant increase in its synergistic activity, an effect also noted for colistin.<sup>102,103</sup>

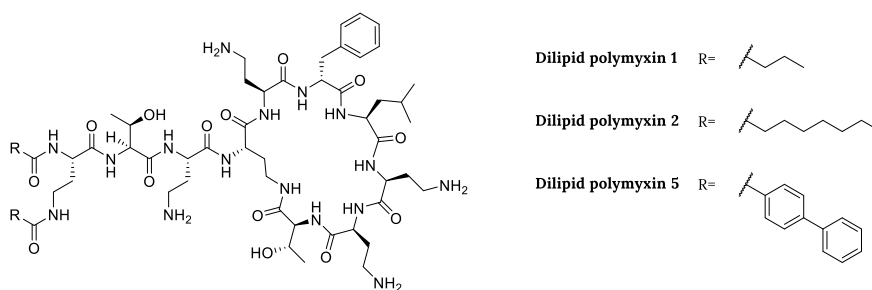
**Table 1.** Synergistic activity of polymyxin analogues.

Name	Ref.	FICI	Pathogen	Antibiotic
PMBN	104	0.013*	<i>E. coli</i>	rifampicin
PMBO	104	0.013*	<i>E. coli</i>	rifampicin
PMBH	104	0.020*	<i>E. coli</i>	rifampicin
DAPB	104	0.043*	<i>E. coli</i>	rifampicin
SPR741	105	0.06	<i>E. coli</i>	rifampicin
NAB739	99	0.126	<i>A. baumannii</i>	rifampicin
NAB7061	99	0.055	<i>E. coli</i>	rifampicin

\*FICI calculated from MSC and MIC values reported in the cited reference.

## 2.2. Dilipidated polymyxins

Polymyxin analogues bearing an additional lipid tail have also been explored to test the hypothesis that additional hydrophobicity might enhance membrane interactions.<sup>106</sup> To generate these variants a variety of acyl tails were added to both amino groups of the N-terminal 2,4-diaminobutyric acid (Dab) residue of PMB (Figure 3).<sup>106,107</sup> The introduction of simple propyl lipids as in analogue **1** led to a complete loss of inherent activity ( $\leq 128$   $\mu\text{g/mL}$ ), while the analogues **2** and **5**, bearing larger, more hydrophobic groups, maintained moderate activity with MICs of 4–64  $\mu\text{g/mL}$  against most Gram-negative bacteria.<sup>106</sup> Notably, the reduced inherent activity was accompanied by a higher synergistic potential (Table 2), indicating that these dilipidated analogues have an increased capacity to disrupt the OM.<sup>106</sup> Also, of note is the reported activity of analogues **2** and **5** against Gram-positive bacteria (MICs of 8–32  $\mu\text{g/mL}$ ) compared to colistin, which has no such activity (MICs of  $\leq 128$   $\mu\text{g/mL}$ ).<sup>106</sup>

**Figure 3.** Molecular structures of the dilipidated polymyxin analogues.**Table 2.** Synergistic activities of dilipidated polymyxin analogues.

Name	Ref.	FICI	Pathogen	Antibiotic	Hemolytic activity <sup>a</sup>
Dilipid polymyxin 1	106	0.02	<i>P. aeruginosa</i>	rifampicin	<10% (1h)
Dilipid polymyxin 2	106	0.26	<i>P. aeruginosa</i>	novobiocin	<10% (1h)
Dilipid polymyxin 5	106	0.31	<i>P. aeruginosa</i>	rifampicin	<10% (1h)

<sup>a</sup>Non-hemolytic is defined as <10% hemolysis compared to positive control with incubation times denoted in parentheses

### 2.3. Linear peptide-based synergists

In most reviews published on the topic of OM-targeting synergists, relatively little attention has been paid to linear peptides. Peptides have several drawbacks including poor metabolic stability, low bioavailability, potential immunogenicity, and high production costs.<sup>108-110</sup> To improve their metabolic stability, the structures of peptides can be adapted by a number of approaches including: peptidomimetics, lipidation, head-to-tail cyclization, N- and C-terminus modifications, backbone stereochemistry changes, and incorporation of unnatural amino acids.<sup>108,109,111-115</sup> Improvements to the bioavailability of peptides have also been explored by applying formulation techniques, adjusting the properties of peptides, or linking them to a moiety to improve passage over the blood-brain barrier.<sup>108-110</sup> These advances, combined with the development of more economical methods for peptide synthesis support a future role for peptide-based therapeutics with a number of antimicrobial peptides already in (pre)clinical development.<sup>116-120</sup>

In the literature an increasing number of peptides synergists that function through OM disruption have been reported (see Table 3). In some studies, panels of structurally similar peptides are screened, resulting in the identification of multiple hits with FICIs lower than 0.5. In such cases we have opted to select up to four of the most potent synergists to limit the number of peptides. Given that most peptide-based synergists are derived from specific lead proteins or antimicrobial peptides (AMPs), we have divided the linear peptide synergists accordingly, both in the discussion below and in the overview Table 3.

#### 2.3.1. Cathelicidin antimicrobial peptides

The cathelicidins are AMPs that play an important role in the innate immune defense system of mammals and function by binding to bacterial membranes resulting in their destabilization and lysis.<sup>121-124</sup> In addition to their direct antibacterial activity, cathelicidins have also been found to play a role in recruiting immune cells to the site of infection as well as in LPS neutralization.<sup>56,121,125</sup> The sole human cathelicidin-AMP gene encodes for hCAP-18 which cleaved by proteases into the active LL-37.<sup>122-124</sup> The mature LL-37 peptide forms an amphipathic  $\alpha$ -helix that upon interaction with bacterial cell surfaces is associated with a detergent-like antimicrobial activity.<sup>126-128</sup> Recently, a truncated version of LL-37, termed FK16, was reported to potentiate the activity of vancomycin against *P. aeruginosa* (Table 3).<sup>129</sup> Similarly, the Kuipers group showed that another LL-37 derived sequence termed KR-12-2, is able to synergize with azithromycin (and erythromycin, Table 3).<sup>130</sup> Further optimization of the peptide sequence resulted in peptide L11 which was also synthesized as the D-amino acid variant (D11) as a means of improving serum stability (Table 3).<sup>130,131</sup> These peptides were screened in combination with multiple antibiotics against different Gram-negative strains and OM disruption assays verified their mode of action.<sup>130-132</sup>

In addition to the human cathelicidins, derivatives of cathelicidins from other mammals have also been screened for synergistic activity including novicidin (sheep), bactenectin (bovine), and indolicidin (bovine).<sup>121,133,134</sup> Among these, only novicidin was reported to display potent synergy (Table 3).<sup>133</sup> In the case of bactenectin, which normally contains a disulfide bridge, a number of linear analogues have been prepared, including peptides G2, R2, and DP7 which were found to exhibit OM disruption and exhibit moderate synergy (Table 3).<sup>134-136,137</sup> In the case of indolicidin, structure-activity relationship (SAR) studies have led to the discovery of the synergists Indopt 10 and

CLS001 (Table 3). CLS001 is particularly effective and displays synergy with both vancomycin and azithromycin against multiple Gram-negative pathogens.<sup>134,137</sup> Marketed under the name Omiganan, CLS001 is also much less hemolytic than indolicidin and is currently in clinical trials for the treatment of skin-related infections.<sup>101,138,139</sup>

### 2.3.2. Lactoferrin-derived peptides

Lactoferrin is a multifunctional protein found in mammals and plays key roles in the human immune system. Lactoferrin has inherent activity against a range of bacterial, fungal, and viral pathogens and in the case of Gram-negative bacteria, it can disrupt the OM.<sup>87</sup> Based on the LPS binding region of lactoferrin known as LF11, the Martínez-de-Tejada group synthesized a series of LF11 homologues (Table 3) which were screened in combination with novobiocin for synergistic activity.<sup>140</sup> Based on these findings a new generation of peptide synergists was designed using PEptide DEscriptors from Sequence (PEDES) software to predict OM permeabilizing sequences.<sup>141</sup> The peptides thus obtained (i.e. peptide P2-16, Table 3) generally showed synergistic activity on par with the original series.<sup>141</sup> Given the abundance of lactoferrins in other mammals, Svendsen and coworkers also investigated a series of peptides derived from bovine lactoferrin, both for antimicrobial activity and synergistic activity.<sup>142-145</sup> This led to the identification of a 12-mer peptide termed P12, along with P15, a 15-mer containing biphenylalanine (Bip), and a longer 18-mer termed P18 all of which were found to exhibit moderate synergy with erythromycin when tested against *E. coli* (Table 3).

### 2.3.3. Thrombin-derived peptides

Thrombin is an enzyme that plays a critical role in coagulation and recent studies have also shown that certain thrombin-derived C-terminal peptides are capable of binding to LPS and neutralizing its toxic and inflammatory effects.<sup>146</sup> Given the capacity of PMB to also bind and neutralize LPS, our group was interested in assessing whether these thrombin-derived peptides might also exhibit the synergistic behavior of PMB. To this end we prepared a series of 12-mer thrombin-derived peptides and showed that a number of them are indeed potent synergists.<sup>147</sup> The most active synergist thus identified (Peptide **6**, Table 3) was further investigated by means of an alanine scan, leading to the discovery of more potent variants (Peptides **14** and **19**, Table 3). Notably, these peptides were found to be non-hemolytic and their synergistic activity was shown to extend to rifampicin, erythromycin, and novobiocin against multiple Gram-negative strains including those with *mcr*-mediated resistance.<sup>147</sup>

### 2.3.4. Histatins

The histatins are a unique group of histidine-rich peptides found in human saliva that play roles in both defending against infection as well as in aiding wound-healing.<sup>148</sup> Among the most common histatins, the 24 amino acid Histatin **5** has been shown to bind Lipid A and has endotoxin neutralizing properties.<sup>149</sup> SAR studies with Histatin **5** led to the identification of a 12-mer sub region termed P-113 that exhibits antimicrobial activity against Gram-positive and Gram-negative bacteria.<sup>148,150-152</sup> Further structural optimization to enhance the stability of P-113 led to analogues incorporating  $\beta$ -naphthylalanine (Nal) and Bip residues to yield Nal-P-113 and Bip-P-113 and wherein the 4th, 5th, and 12th histidine residues were replaced by Nal or Bip respectively (Table 3).<sup>152</sup> Bip-P-113 and Nal-P-113 exhibit antimicrobial activity, improved serum proteolytic

stability, and were also found to permeabilize LPS containing large unilamellar vesicles used to model the Gram-negative OM.<sup>152,153</sup> These findings prompted investigation of vancomycin potentiation by Bip-P-113 and Nal-P-113 revealing both to exhibit moderate synergy.<sup>154</sup> However, a notable drawback of Bip-P-113 and Nal-P-113 is their significantly increased hemolytic activity relative to P-113.<sup>152</sup>

### 2.3.5. Other Natural AMPs, their hybrids, and derivatives

A number of other naturally occurring AMPs have been reported to potentiate antibiotics that are otherwise excluded by the OM. These AMPs are all polycationic and include: buforrin II, esculentin 1b, sphistatin, HE2 $\alpha$ , HE2 $\beta$ 2, anoplin, magainin II, and cecropin A (Table 3).<sup>155–159</sup> The sources of these AMPs are diverse and include toads, wasp venom, or even the human male reproductive tract.<sup>157,158,160</sup> The AMPs here discussed have all been reported to disrupt the OM,<sup>156,158,161–163</sup> bind to LPS, and/or show endotoxin neutralizing activity.<sup>155,159,164</sup> In general, these AMPs exhibit modest FICIs (0.2–0.36) which has also led to interest in hybrids and derivatives with enhanced synergistic activity. For example, Park and coworkers developed a series of hybrid peptide synergists, termed CAME, CAMA, and HPMA containing sequences derived from cecropin A, magainin II, and melittin (Table 3).<sup>164,165</sup> Other approaches include truncation as in the case of the lipopeptide AMP Tridecaptin A<sub>1</sub> (TriA<sub>1</sub>), which exhibits potent inherent anti-Gram-negative activity, were found to be effective synergists. Notably, removal of the TriA<sub>1</sub> N-terminal lipid yielded H-TriA<sub>1</sub> which was found to be much less active as an antibiotic but exhibited very potent synergism when combined with rifampicin resulting in an FICI of 0.002 against *E. coli* (Table 3).<sup>166,167</sup> Like the tridecaptins, the recently discovered paenipeptins contain a number of Dab residues and have been subject to SAR studies.<sup>168</sup> These efforts led to the discovery of a potent paenipeptin inspired synergist termed SLAP-S25 which effectively potentiates the activity of rifampicin and vancomycin against *E. coli* (Table 3).<sup>169</sup> In addition to OM disruption, the binding of SLAP-S25 to LPS and phosphatidylglycerol (PG) was established, suggesting that SLAP-S25 is also an inner membrane disruptor.<sup>169</sup> This was confirmed by dose-dependent uptake of propidium iodide and release of cellular contents in cells treated with SLAP-S25.<sup>169</sup> Notably, SLAP-S25 was also demonstrated to effectively enhance the *in vivo* activity of colistin against a colistin-resistant strain of *E. coli* in both *G. mellonella* and mouse infection models.<sup>169</sup>

Originally isolated from wasp venom, anoplin is one of the smallest known amphipathic,  $\alpha$ -helical AMPs.<sup>158,160</sup> Multiple SAR investigations have been performed to improve its antimicrobial activity and stability.<sup>170–174</sup> A recent study with anoplin reported the systematic introduction of tryptophan and lysine residues to determine the optimal hydrophobicity, amphipathicity, and number of positive charges required for antibacterial activity and minimal cytotoxicity.<sup>158</sup> A number of these analogues were also found to be synergistic when combined with rifampicin (see peptides A13, A17, and A21 in Table 3) via a mechanism involving OM disruption.<sup>158</sup> A similar study with Mastoparan-C, a peptide found in the venom of the European hornet, led to the identification of an analogue termed L7A (Table 3) which also displays synergy via OM perturbation.<sup>138</sup> Another example of a synergist derived from a toxic peptide is myotoxin II which is isolated from certain snake venoms. Studies with peptide sequences based on the C-terminus of myotoxin II resulted in the generation of peptide S1 (Table 3) which showed a good balance of synergy with vancomycin and low hemolytic activity.<sup>175,176</sup> Attempts at further improving the S1 peptide involved the introduction of Nal residues at the C-terminus to generate S1-Nal which exhibited enhanced synergistic activity and S1-Nal-

Nal which also exhibited enhanced synergistic activity but at the expense of increased hemolytic activity (Table 3).<sup>177–180</sup>

### 2.3.6. Peptide synergists discovered via library screening

Guardabassi and coworkers recently reported the development and validation of an assay meant to enable high throughput screens for identifying OM disruption agents.<sup>181</sup> To this end they applied a whole-cell screening platform that allows for detection of OM permeabilization in *E. coli* based on the signal generated by a chromogenic substrate reporter for a cytoplasmic  $\beta$ -galactosidase. To validate the assay, a library of peptides and peptidomimetics was screened which generated a notable hit termed peptide 79 that showed potentiation of various antibiotics at therapeutically relevant levels (Table 3).<sup>181</sup> In a follow-up study the same group went on to develop two improved synergists termed Peptides **1** and **2** along with the all D-amino acid variants which were also found to effectively potentiate rifampicin against *K. pneumoniae* (Table 3).<sup>70,181</sup>

### 2.3.7. Peptide synergists from phage display

Phage display techniques have also been applied to identify novel peptides capable of interaction with the OM. In one such investigation, a phage library displaying random 12-mer peptides was screened for the ability to bind to the cell surface of Gram-negative bacteria.<sup>182</sup> Specificity for the Gram-negative OM was ensured by removal of peptides binding to Gram-positive bacteria by pre-incubation of the library with *Staphylococcus aureus*.<sup>182</sup> This approach led to the identification of a peptide termed EC5, that exhibits moderate antibacterial activity against *E. coli* and *P. aeruginosa*, with MICs in the range of 8–16  $\mu\text{g/mL}$  against both.<sup>182</sup> The EC5 peptide was shown to cause OM disruption and cytoplasmic membrane depolarization while exhibiting very little hemolytic activity.<sup>182</sup> Subsequent synergy studies showed that the peptide was also capable of potentiating the activity of erythromycin, clarithromycin, and telithromycin against *P. aeruginosa*.<sup>130</sup>

### 2.3.8. Rationally designed peptide synergists

Inspired by the structure of DAPB (see Figure 2), Vaara and coworkers designed a series of linear and cyclic peptides for evaluation as synergists.<sup>183</sup> The sequences of these peptides were based on an ABB<sub>n</sub> motif in which A is a basic amino acid and B a hydrophobic residue (see Peptides 4 and 5 in Table 3).<sup>183</sup> Cyclic peptides were also prepared bearing a similar AB<sub>n</sub> motif (see Peptide 7, Table 3).<sup>183</sup> All peptides were screened for synergistic activity with erythromycin, rifampicin, novobiocin, and fusidic acid with the rifampicin combinations being the most potent (Table 3).<sup>183</sup> While the synergistic activity of these peptides could be correlated to their OM disrupting activity, the effect was not specific given their high hemolytic activity.<sup>183</sup>

*De novo*-designed peptides have also been explored as a means of generating novel synergists. To this end the Sahal group developed a number of peptides incorporating key elements found in AMPs and synergists including amphipathicity, positive charge, and helical conformation.<sup>184,185</sup> Of note was the introduction of  $\alpha,\beta$ -didehydrophenylalanine ( $\Delta\text{F}$ ) into the peptides as a means of constraining the helical conformation of the peptides.<sup>186–188</sup> Using this approach two peptides termed  $\Delta\text{Fm}$  and  $\Delta\text{Fmscr}$  were identified as effective synergists with low toxicity towards mammalian cells (Table 3).<sup>187</sup>

In another recent approach to identifying novel peptide synergists, Yu and colleagues reported the construction of a small library wherein amphipathic peptides were subjected to a proline-scanning strategy to generate novel hinged peptides.<sup>194</sup> Such proline hinged peptides are reported to have lower toxicity towards mammalian cells given that their membrane binding is reduced compared to conventional AMPs with a high  $\alpha$ -helical conformation.<sup>189</sup> Proline scanning of two model peptides, LK (LKKLLKLLKKLLKL) and KL (KLLKLLKKLLKLLK), provided a set of peptides that were screened for synergistic activity with the four most potent peptides displayed in Table 3. The peptides were also screened for hemolysis which led to identification of peptide KL-L9P as the most promising hit. This peptide was subsequently shown to permeabilize the OM, as evidenced by uptake of N-phenylnaphthalen-1-amine (NPN), and was also found to bind LPS without disturbing the inner membrane.<sup>190</sup> Mouse sepsis studies were also performed to evaluate the *in vivo* synergistic effect of KL-L9P, which displayed a significant potentiation of a number of clinically used antibiotics and resulted in improved overall survival.<sup>190</sup>

In another recently reported study, Zeng et al. described the application of rational design approaches to generate novel helix-forming AMPs based on cytolytic peptide toxins produced by highly virulent strains of *S. aureus*.<sup>191,192</sup> The peptides thus obtained were shown to have improved physicochemical properties and antibacterial activity, while maintaining low hemolytic activity and cytotoxicity. Among the 16-mers thus generated, two peptides, termed zp12 and zp16, were also found to exhibit potent synergy (Table 3). Notable in this regard is the finding that peptide zp16 specifically potentiates the effect of the glycopeptide antibiotics vancomycin and teicoplanin against highly pathogenic *K. pneumonia*.<sup>192</sup> The vancomycin-zp16 combination exhibits negligible toxicity *in vitro* and *in vivo* and mechanistic studies indicate that zp16 enhances vancomycin's cell permeability, leading to markedly reduced biofilm formation and rapid bactericidal effect.<sup>192</sup>

In 2022 the group of Ni reported the potentiation of multiple antibiotics, including rifampicin, by two rationally designed peptides named K4 and K5 (Table 3).<sup>193</sup> These peptides were selected from a library of variants all containing a repeating motif (WRX)<sub>n</sub> wherein X represents I, K, L, F, and W.<sup>194</sup> Hemolysis and cytotoxicity assays led to the selection of peptides K4 and K5 as leads.<sup>194</sup> The finding that these peptides permeabilize the OM resulted in follow-up studies on the potentiation of antibiotics against Gram-negative bacteria.<sup>193</sup> Apart from synergy, a 15-day resistance assay was also performed for the K4 and K5 peptides, with or without antibiotics, showing no significant resistance development.<sup>193,194</sup> Also of note, while the inherent activity of K4 was found to be comparable to PMB, K4 was reported to display significantly less toxicity.<sup>194</sup>

## 2.4. Lipopeptide synergists

In addition to the exclusively peptide-based synergists described above, lipopeptides have also been explored as synergists. We here cover examples of lipopeptides that do not possess potent inherent antibacterial activity but rather have the capacity to effectively potentiate the activity of other antibiotics. A recent example are the synthetic paenipeptins developed by Huang and coworkers.<sup>195</sup> The design of these lipopeptides is based on peptides produced by *Paenibacillus* sp. strain OSY-N that contain a number of unnatural and D-amino acids. Using low hemolytic activity as a selection criterion, a subset of these lipopeptides were selected and screened for synergistic activity. This led



to the identification of paenipeptins 1, 9, 15, and 16 which exhibit potent synergy (Table 3).<sup>195,196</sup> These lipopeptides were further shown to have OM disrupting activity as indicated by the NPN assay. Furthermore, in an murine thigh infection model, paenipeptin **1** was shown to effectively potentiate the *in vivo* activity of both clarithromycin and rifampin against polymyxin-resistant *E. coli*.<sup>196</sup>

Small cationic lipopeptides have also been explored as synergists with the aim of identifying smaller, less hemolytic agents. To this end Schweizer and coworkers recently reported a series of “dilipid ultrashort cationic lipopeptides” (dUSCLs) capable of enhancing the activity of clinically used antibiotics against Gram-negative bacteria. The design of these dUSCLs consists of lysine rich tetrapeptides bearing various lipids at the N-terminal residue as illustrated in Figure 4A. It was found that dUSCLs bearing lipids of  $\geq 11$  carbon atoms caused significant hemolysis. However, analogues with slightly shorter lipid were found to achieve an acceptable balance of low hemolytic activity and synergistic activity. This led to the identification of dUSCLs **2** and **6** as the most promising synergists (Table 3) capable of sensitizing a range of Gram-negative strains to various antibiotics. The authors also noted that in addition to permeabilizing the OM, the dUSCLs may also function by indirectly disrupting antibiotic efflux.<sup>197</sup>

The Schweizer group also recently reported a series of ultrashort tetrabasic lipopeptides (UTBLPs) synergists.<sup>198</sup> These compounds were specifically prepared to assess the effect of lysine N- $\zeta$ -methylation on the potentiation of antibiotics and was inspired by reports suggesting N-methylation can lead to reduced hemolysis, increased proteolytic stability, and improved antibacterial activity.<sup>199–201</sup> Compared to the dUSCLs, UTBLP **5** and **6** contain an extra lysine while an octanoyl group was employed as the lipophilic moiety (Figure 4B).<sup>197,198</sup> Methylation of the lysine side-chain resulted in a reduction of potentiation for rifampicin and novobiocin in both wild-type and resistant Gram-negative strains.<sup>198</sup> A correlation between the number of methyl groups and loss of activity was seen, while the increase in NPN fluorescence of the tri-methylated UTBLP were on par their un- or mono-methylated analogues.<sup>198</sup>

## 2.5. Lipopeptidomimetic synergists

The Schweizer group also expanded the scope of their dUSCLs by exploring a series of dilipid ultrashort tetrabasic peptidomimetics (dUSTBPs) as a proteolytically stable alternative.<sup>202</sup> In a focused SAR study they prepared dUSTBPs consisting of three basic amino acids separated by a molecular scaffold, bis(3-aminopropyl)glycine, along with ligation to simple fatty acids (see Figure 4C).<sup>202</sup> This led to identification of a number of dUSTBPs capable of potentiating the activity of several antibiotics against pathogenic Gram-negative bacteria while exhibiting low hemolytic activity (Table 3). In particular, dUSTBP **8**, consisting of three L-arginine units and a dilipid of 8 carbons long, was found to potentiate novobiocin and rifampicin against multidrug-resistant (MDR) clinical isolates of *P. aeruginosa*, *A. baumannii*, and *Enterobacteriaceae* species.<sup>202</sup>

In 2007 Mor and coworkers introduced the oligo-acyl-lysyls (OAKs) as peptidomimetics of the antimalarial peptide dermaseptin S3 (Figure 4D) that were initially evaluated primarily for antimicrobial activity.<sup>203–205</sup> Among the first series of analogues prepared, OAK C<sub>12(ω7)</sub> was found to adhere to the OM with minimal insertion and its antibacterial activity against Gram-negative bacteria improved in combination with ethylenediaminetetraacetate (EDTA).<sup>205–207</sup> The introduction of a double bond in OAK C<sub>12(ω7)</sub> resulted in significant reduction of hemolytic activity compared to OAK C<sub>12</sub> while

the slightly less hydrophobic OAK C<sub>10</sub> and OAK C<sub>8</sub> analogues also showed no hemolytic activity.<sup>205,208</sup> In 2013 these four OAKs, as well as the more recently described OAK C<sub>14(ω5)</sub>OOc<sub>10</sub>O containing ornithine instead of lysine (Figure 4D), were reported to potentiate rifampicin against Gram-negative bacteria (Table 3).<sup>208,209</sup> Interestingly, the synergistic activity of the OAKs was maintained in human plasma but was suppressed by addition of anti-complement antibodies, suggesting that these compounds sensitize Gram-negative bacteria to the action of antibacterial innate immune mechanisms.<sup>252</sup>

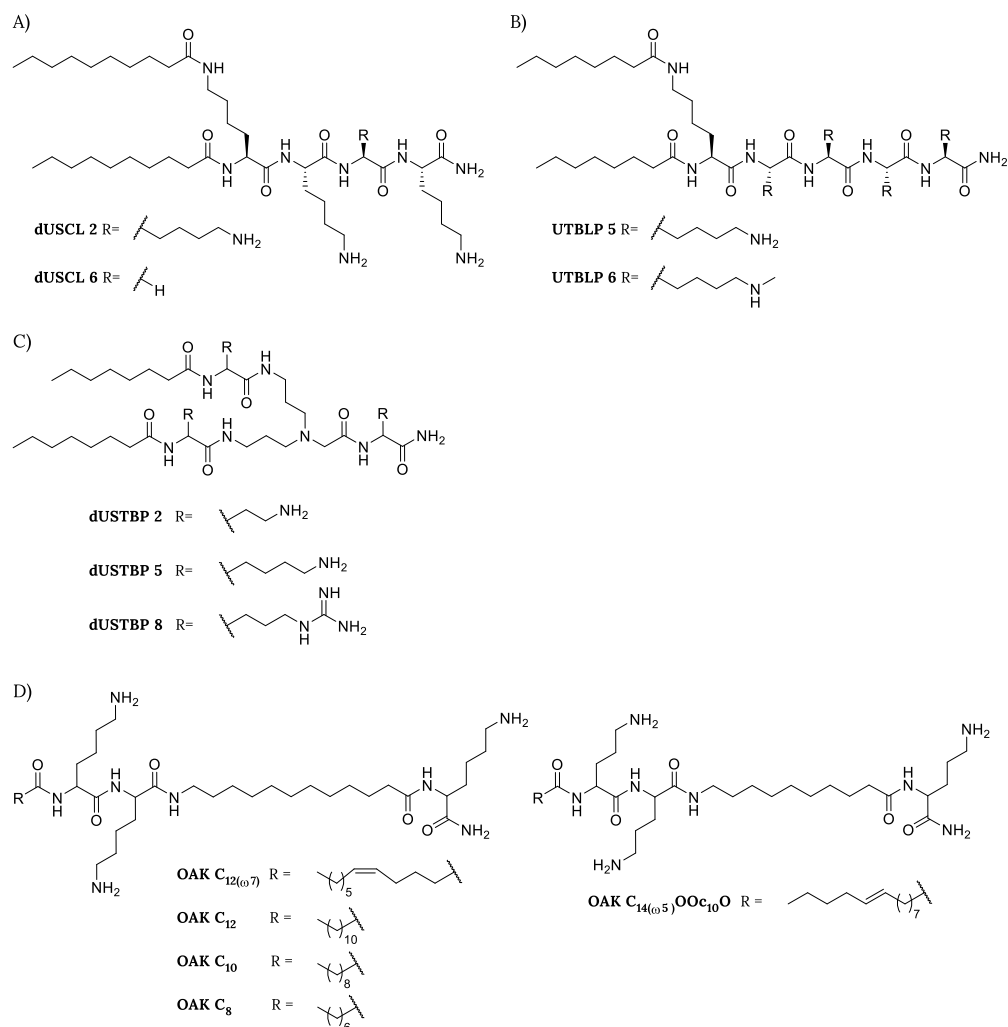


**Figure 4.** Lipopeptide and lipopeptidomimetic synergists. Representative structures of A) dilipid ultrashort cationic lipopeptides (dUSCLs); B) Ultrashort tetrabasic lipopeptides (UTBLPs); C) dilipid ultrashort tetrabasic peptidomimetics (dUSTBPs); and D) oligo-acyl-lysyls (OAKs).

**Table 3.** Overview of linear peptide-based synergists (compound names provided as given in the cited literature references).

Name	Ref	Peptide sequence <sup>a</sup>	FICI	Pathogen	Antibiotic	Hemolytic activity <sup>b</sup>
<b>Cathelicidin derived peptides</b>						
<b>FK16</b>	129	FKRIVQRIKDFLRNLV	0.25	<i>P. aeruginosa</i>	vancomycin	<10% (1h)
<b>KR-12-a2</b>	130,210	KRIVQRIKKWLR-NH <sub>2</sub>	0.156	<i>P. aeruginosa</i>	erythromycin	<10% (1h)
<b>L-11</b>	131	RIVQRIKKWLR-NH <sub>2</sub>	0.070	<i>A. baumannii</i>	vancomycin	NR
<b>D-11</b>	131,132	rivqrikkwlr-NH <sub>2</sub>	0.032	<i>A. baumannii</i>	rifampicin	<10% (1h)
<b>Novicidin</b>	133	KNLRRRIIRKGIHIKKYF	0.018	<i>E. coli</i>	rifampicin	<10% (1h)
<b>G2</b>	134	RGARIVVIRVAR-NH <sub>2</sub>	0.38	<i>P. aeruginosa</i>	erythromycin	NR
<b>R2</b>	134	RRARIVVIRVAR-NH <sub>2</sub>	0.27	<i>P. aeruginosa</i>	erythromycin	NR
<b>DP7</b>	137,211	VQWRIRVAVIRK	0.25	<i>P. aeruginosa</i>	vancomycin	<10% (1h)
<b>Indopt 10</b>	134	ILKWKIFKWKWFR-NH <sub>2</sub>	0.38	<i>P. aeruginosa</i>	erythromycin	NR
<b>CLS001</b>	137,139	ILRWPWWPWRRK-NH <sub>2</sub>	0.28	<i>P. aeruginosa</i>	vancomycin	10% (30 min)
<b>Lactoferrin derived peptides</b>						
<b>P10</b>	140	FWQRNIRKVKKK-NH <sub>2</sub>	0.113	<i>P. aeruginosa</i>	novobiocin	<10% (1h)
<b>P14</b>	140	FWQRNIRKVKKKI-NH <sub>2</sub>	0.113	<i>P. aeruginosa</i>	novobiocin	<10% (1h)
<b>P22</b>	140	RFWQRNIRKYRR-NH <sub>2</sub>	0.431	<i>P. aeruginosa</i>	novobiocin	<10% (1h)
<b>P2-16</b>	141	FWRNIRIWRN-NH <sub>2</sub>	0.116	<i>P. aeruginosa</i>	novobiocin	NR
<b>P12</b>	144,212	RRWQWRMKKLGA	0.43	<i>E. coli</i>	erythromycin	<10% (2h)
<b>P15</b>	144	FK-Bip-RRWQWRMKKLGA <sup>c</sup>	0.38	<i>E. coli</i>	erythromycin	NR
<b>P18</b>	144	PAWFKARRWAWRMLKKA <sup>a</sup>	0.38	<i>E. coli</i>	erythromycin	NR
<b>Thrombin derived peptides</b>						
<b>Peptide 6</b>	147	VFRLKKWIQKVI-NH <sub>2</sub>	0.094	<i>E. coli</i>	rifampicin	<10% (20h)
<b>Peptide 14</b>	147	VFRLKKAIQKVI-NH <sub>2</sub>	0.078	<i>E. coli</i>	erythromycin	<10% (20h)
<b>Peptide 19</b>	147	VFRLKKWIQKVA-NH <sub>2</sub>	0.078	<i>E. coli</i>	rifampicin	<10% (20h)
<b>Histatin derived peptides</b>						
<b>Nal-P-113</b>	152,154	Ac-AKR-Nal-Nal-GYKRKF-Nal-NH <sub>2</sub> <sup>d</sup>	0.38	<i>E. coli</i>	vancomycin	>10% (1h)
<b>Bip-P-113</b>	152,154	Ac-AKR-Bip-Bip-GYKRKF-Bip-NH <sub>2</sub> <sup>c</sup>	0.38	<i>E. coli</i>	vancomycin	>10% (1h)
<b>Other Natural AMPs, their hybrids, and derivatives</b>						
<b>Buforin II</b>	155,213	TRSSRAGLQFPVGRVHRLLRK	0.312	<i>A. baumannii</i>	rifampicin	<10% (1h)
<b>Esculentin 1b</b>	156,214	GIFSKLAGKKLKNLLISG-NH <sub>2</sub>	0.36	<i>E. coli</i>	erythromycin	>10% (1h)
<b>HE2α</b>	157,161	VHISHREARGPSFRICVGFLGPRWARGCSTGNGDVPPIGIRNTICRMQQG	0.3	<i>E. coli</i>	rifampicin	<10% (1h)
<b>HE2β2</b>	157,161	ICRLFFCHSGTGQQHRQRCG	0.2	<i>E. coli</i>	rifampicin	<10% (1h)
<b>Anoplin</b>	158	GLLKRIKTLL	0.3125	<i>P. aeruginosa</i>	rifampicin	<10% (1h)

<b>Magainin II</b>	159,213	GIGKFLHAAKKFAKAFV AEIMNS-NH2	0.312	<i>P. aeruginosa</i>	rifampicin	>10% (1h)
<b>Cecropin A</b>	159,164	KWKLFKKIEKVGQNIRD GIKAGPAVAVVGQATQ IAK-NH2	0.312	<i>P. aeruginosa</i>	rifampicin	<10% (1h)
<b>CAME</b>	215,216	KWKLFKKIGIGAVLKVL TTG-NH2	0.375	<i>A. baumannii</i>	erythromycin	<10% (1h)
<b>CAMA</b>	215,216	KWKLFKKIGIGKFLHSA KKF-NH2	0.25	<i>A. baumannii</i>	erythromycin	<10% (1h)
<b>HPMA</b>	215,217	AKKVFKRLGIGKFLHSA KKF-NH2	0.313	<i>A. baumannii</i>	erythromycin	<10% (1h) <sup>#</sup>
<b>H-TriA<sub>1</sub></b>	166,167	v-dab-Gsw-Dab- dab-FEI-allele-A <sup>e, f</sup> Ac-Dab-I-Dab-I- Dab-fL-Dab-vLA- NH2	0.002	<i>E. coli</i>	rifampicin	<10% (30 min) <sup>#</sup>
<b>SLAP-S25</b>	169	Dab-fL-Dab-vLA- NH2	0.031	<i>E. coli</i>	rifampicin	<10% (1h)
<b>A13</b>	158	GWKKRIKTWW	0.375	<i>K. pneumoniae</i>	rifampicin	<10% (1h)
<b>A17</b>	158	KWWKRWKKWW	0.3125	<i>P. aeruginosa</i>	rifampicin	>10% (1h)
<b>A21</b>	158	KWWKRWKKWW	0.3125	<i>K. pneumoniae</i>	rifampicin	<10% (1h)
<b>L7A</b>	138	LNLKALAAVAKKIL- NH2	0.31	<i>E. coli</i>	rifampicin	<10% (1h)
<b>S1</b>	177,180	Ac-KKWRKWLAKK-NH2	0.38	<i>A. baumannii</i>	vancomycin	<10% (1h) <sup>#</sup>
<b>S1-Nal</b>	177,180	Ac-KKWRKWLAKK- Nal-NH2	0.27	<i>A. baumannii</i>	vancomycin	<10% (1h) <sup>#</sup>
<b>S1-Nal-Nal</b>	177,180	Ac-KKWRKWLAKK- Nal-Nal-NH2	0.27	<i>A. baumannii</i>	vancomycin	>10% (1h)

#### Peptide synergists via library screening

<b>Peptide 79</b>	176,181	KKWRKWLKWLAKK-NH2	0.14	<i>E. coli</i>	rifampicin	<10% (1h)
<b>Peptide 1</b>	70,218	KLWKWKWKWLK-NH2	0.02	<i>K. pneumoniae</i>	rifampicin	<10% (1h)
<b>Peptide 2</b>	70,184	GKWKILGKLIR-NH2	0.04	<i>K. pneumoniae</i>	rifampicin	<10% (1h)
<b>Peptide D1</b>	70	klwkkwkwlk-NH2	≤0.03	<i>K. pneumoniae</i>	rifampicin	NR
<b>Peptide D2</b>	70	gkwkklgklir-NH2	≤0.04	<i>K. pneumoniae</i>	rifampicin	NR

#### Peptide synergists from phage display

<b>EC5</b>	130,182	RLFRKIRRLKR	0.266	<i>P. aeruginosa</i>	erythromycin	<10% (24h)
------------	---------	-------------	-------	----------------------	--------------	------------

#### Designed peptides

<b>Peptide 4</b>	183	KFFKFFKFF	0.03	<i>E. coli</i>	rifampicin	>10% (30 min)
<b>Peptide 5</b>	183	IKFLKFLKFL	0.06	<i>E. coli</i>	rifampicin	NR
<b>Peptide 7</b>	183	CKFKFKFKFC	0.20	<i>E. coli</i>	rifampicin	NR
<b>ΔFm</b>	187	Ac-GΔFRKΔFHKΔFWA- NH2 <sup>g</sup>	0.3	<i>E. coli</i>	rifampicin	<10% (1h)
<b>ΔFmscr</b>	187	Ac-GΔFRKΔFKAΔFWH- NH2 <sup>g</sup>	0.14	<i>E. coli</i>	rifampicin	<10% (1h)
<b>LK-L8P</b>	219	Ac- LKKLLKLPKKLLKL- NH2	0.18	<i>E. coli</i>	erythromycin	<10% (4h)
<b>LK-L11P</b>	219	Ac- LKKLLKLLKKPLKL- NH2	0.47	<i>E. coli</i>	erythromycin	<10% (4h)
<b>KL-L6P</b>	219	Ac- LKKLLPLKKLLKL- NH2	0.33	<i>E. coli</i>	erythromycin	>10% (4h)

<b>KL-L9P</b>	219	Ac- LKKLLKLLPKLLKL- NH <sub>2</sub>	0.12	<i>E. coli</i>	erythromycin	<10% (4h)
<b>zp12</b>	192	GIKRGI IKI IKRIKRI- NH <sub>2</sub>	0.25	<i>K. pneumoniae</i>	vancomycin	NR
<b>zp16</b>	192	GIKRGI IKI IRRIKRI- NH <sub>2</sub>	0.06	<i>K. pneumoniae</i>	vancomycin	<10% (1h)
<b>K4</b>	193,194	WRKWRKWRKWRK-NH <sub>2</sub>	0.2	<i>K. pneumoniae</i>	rifampicin	<10% (1h)
<b>K5</b>	193,194	WRKWRKWRKWRKWRK- NH <sub>2</sub>	0.2	<i>E. coli</i>	rifampicin	<10% (1h)

#### Lipopeptide Synergists

<b>Paenipeptin 1</b>	195,196	C <sub>6</sub> -Dab-I-Dab-fL- Dab-vLS-NH <sub>2</sub> <sup>h</sup>	0.125*	<i>E. coli</i>	rifampicin	<10% (30 min)
<b>Paenipeptin 9</b>	195	C <sub>8</sub> -Dab-I-Dab-fL- Dab-vL-Dab-NH <sub>2</sub> <sup>i</sup>	≤0.03*	<i>K. pneumoniae</i>	rifampicin	<10% (30 min)
<b>Paenipeptin 15</b>	195	Cbz-Dab-I-Dab-fL- Dab-vLS-NH <sub>2</sub> <sup>j</sup>	≤0.03*	<i>K. pneumoniae</i>	rifampicin	<10% (30 min)
<b>Paenipeptin 16</b>	195	Cha-Dab-I-Dab-fL- Dab-vLS-NH <sub>2</sub> <sup>k</sup>	0.06*	<i>K. pneumoniae</i>	rifampicin	<10% (30 min)
<b>dUSCL 2</b>	197	C <sub>10</sub> -K (C <sub>10</sub> ) KKK-NH <sub>2</sub> <sup>l</sup> (Figure 4A)	0.07	<i>P. aeruginosa</i>	rifampicin	<10% (1h)
<b>dUSCL 6</b>	197	C <sub>10</sub> -K (C <sub>10</sub> ) KGK-NH <sub>2</sub> <sup>l</sup> (Figure 4A)	0.25	<i>P. aeruginosa</i>	rifampicin	<10% (1h)
<b>UTBLP 5</b>	198	C <sub>8</sub> -K (C <sub>8</sub> ) KKKK-NH <sub>2</sub> <sup>i</sup> (Figure 4B)	≥0.016	<i>P. aeruginosa</i>	novobiocin	NR
<b>UTBLP 6</b>	198	C <sub>8</sub> - K (C <sub>8</sub> ) K (Me) K (Me) K (M e) K (Me) -NH <sub>2</sub> <sup>i</sup> (Figure 4B)	0.047	<i>A. baumannii</i>	rifampicin	NR

#### Lipopeptidomimetic Synergists

<b>dUSTBP 2</b>	202	Figure 4C	≥0.250	<i>P. aeruginosa</i>	rifampicin	<10% (1h)
<b>dUSTBP 5</b>	202	Figure 4C	≥0.125	<i>P. aeruginosa</i>	rifampicin	<10% (1h)
<b>dUSTBP 8</b>	202	Figure 4C	≥0.002	<i>A. baumannii</i>	novobiocin	<10% (1h)
<b>OAK C<sub>12</sub>(ω<sub>7</sub>)</b>	208	Figure 4D	≤0.073*	<i>E. coli</i>	rifampicin	>10% (3h)
<b>OAK C<sub>12</sub></b>	208	Figure 4D	≤0.211*	<i>E. coli</i>	rifampicin	>10% (3h)
<b>OAK C<sub>10</sub></b>	208	Figure 4D	≤0.036*	<i>E. coli</i>	rifampicin	<10% (3h)#
<b>OAK C<sub>8</sub></b>	208	Figure 4D	≤0.078*	<i>E. coli</i>	rifampicin	<10% (3h)#
<b>OAK C<sub>14</sub>(ω<sub>5</sub>)OOC<sub>10</sub>O</b>	209	Figure 4D	0.20*	<i>K. pneumoniae</i>	rifampicin	<10% (3h)#

<sup>a</sup>Lower case letters indicate D-amino acids; <sup>b</sup>Non-hemolytic is defined as <10% hemolysis compared to positive control with incubation times denoted in parentheses, NR denotes no data reported; <sup>c</sup>Bip, biphenylalanine; <sup>d</sup>Nal, β-naphthylalanine; <sup>e</sup>Dab, 2,4-diaminobutyric acid; <sup>f</sup>alle, D-allo-isoleucine; <sup>g</sup>ΔF, α,β-didehydrophenylalanine; <sup>h</sup>C<sub>6</sub>, hexanoyl; <sup>i</sup>C<sub>8</sub>, octanoyl; <sup>j</sup>Cbz, benzyloxycarbonyl; <sup>k</sup>Cha, cyclohexylalanyl; <sup>l</sup>C<sub>10</sub>, decanoyl; #denotes that the concentration tested was lower than 100 µg/mL; \*FICI calculated from MSC and MIC values reported in the cited literature reference.

### 3. Cationic steroids

In 1993 the isolation of squalamine from tissues of the dogfish shark *Squalus acanthias* was reported.<sup>220</sup> Squalamine consists of a steroid core linked to a spermidine moiety (Figure 5A) and was found to exhibit broad antimicrobial activity.<sup>220</sup> Later, it was established that squalamine disrupts membranes and is also hemolytic. Notably, investigations into its synergistic activity showed that it was unable to potentiate erythromycin against wild-type strains, showing an effect only against a *P. aeruginosa* strain overproducing MexAB-OprM efflux pumps (See Table 4).<sup>221,222</sup> A few years after its discovery, novel squalamine mimics (SMs) were synthesized in an attempt to enhance antibacterial activities (Figure 5B).<sup>223</sup> These synthetic analogues consist of cholic and deoxycholic acid as the steroid backbone to which a spermidine chain is appended. This approach resulted in the identification of analogue SM-7, which was found to potentiate rifampicin against multiple Gram-negative bacteria (Table 4).<sup>223</sup> However, like squalamine, SM-7 also possesses significant hemolytic activity limiting its potential for systemic use.<sup>223</sup>

In another approach, the Savage group also employed the cholic acid backbone but with the aim of mimicking polymyxins through the amphiphilic positioning of positive charges (Figure 5C and 5D).<sup>224,225</sup> In doing so, a variety of cationic steroids were developed and screened both for inherent antimicrobial activity as well as the capacity to potentiate antibiotics against Gram-negative bacteria.<sup>225–233</sup> The orientation of the hydroxyl groups of cholic acid backbone provide convenient functionalities for the incorporation of positively charged moieties via formation of ether (Figure 5C) or ester (Figure 5D) linkages. Among the ether-linked series, an analogue bearing three carbon atom spacers between the steroid and the primary amine groups, along with an N-benzylated tertiary amino group at the C24 position (analogue **I**, Figure 5C), was found to exhibit both inherent antimicrobial and synergistic activity.<sup>225</sup> Interestingly, replacement of the lipophilic N-benzyl moiety with a hydroxyl group led to analogue **II** which showed a significant reduction of inherent activity while maintaining a strong ability to potentiate the activity of erythromycin against *E. coli*.<sup>224,225</sup> The decreased lipophilicity of analogue **II** also reduced the hemolytic activity seen with analogue **I** (Table 4). Follow-up studies revealed that conversion of the free hydroxyl group at the C24 position to the propyl ether as in analogue **III** significantly increased hemolytic activity.<sup>226,227</sup> Notably, addition of a terminal amino group to the propyl ether moiety provided analogue **IV** which exhibited significantly reduced hemolysis relative to analogue **III** while maintaining effective synergistic activity (Table 4).<sup>228</sup> A series of ester linked analogues were also prepared by the Savage group (Figure 5D), wherein compounds **V**, **VI**, and **VII** exhibited synergistic activity comparable to the corresponding ether variants (Table 4).<sup>229,230</sup> Amide analogues were also explored, however, they exhibited a significant lower potentiation of erythromycin, presumably due to conformational constraints relative to the more active esters.<sup>229</sup>

In addition to the polycationic steroids described above, steroid-peptide hybrids have also been explored as synergists.<sup>233–235</sup> In a one case, Bavikar *et. al* reported a series of hybrids wherein simple tetrapeptides were coupled to cholic acid in an attempt to mimic the squalamine tail (Figure 5E).<sup>235</sup> As indicated in Table 4, these steroid-peptide hybrids exhibit potent synergy with erythromycin against *E. coli*. While the hemolytic activity of these compounds was not reported, they were described as having low cytotoxicity towards HEK293 and MCF-7 cells.<sup>235</sup>

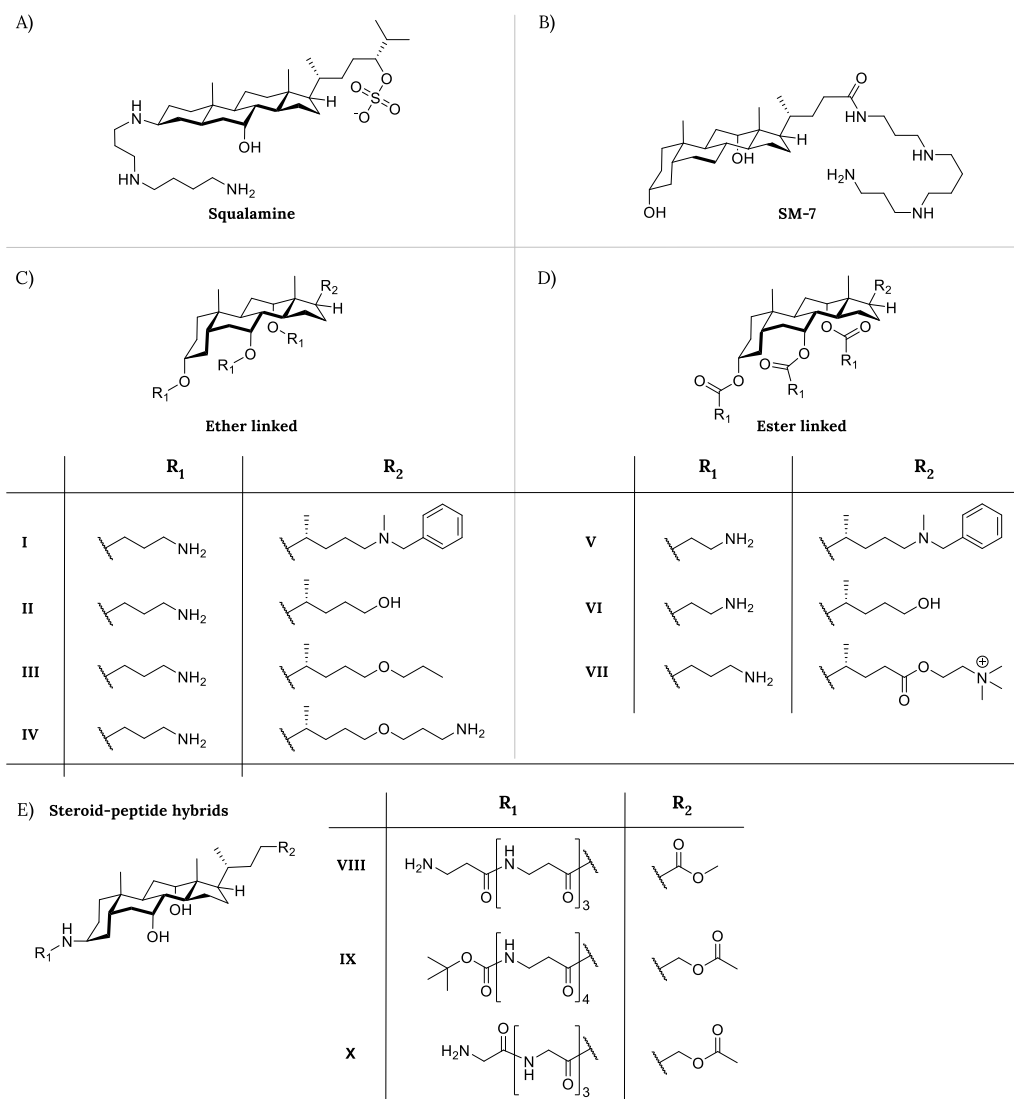


**Figure 5.** Overview of the synergistic steroids A) Squalamine; B) squalamine mimic SM-7; C) polycationic cholic acid ether linked steroid synergists; D) polycationic cholic acid ester linked steroid synergists; and E) steroid-peptide hybrids.

**Table 4.** Overview of synergists based on cationic steroids.

Name	Ref.	FICI	Pathogen	Antibiotic	Hemolytic activity <sup>a</sup>
<b>Squalamine</b>	220,222	0.35*	<i>P. aeruginosa</i>	erythromycin	>10% (10 min)
<b>SM-7</b>	223	0.063	<i>K. pneumoniae</i>	rifampicin	<10% (24h)
<b>Polycationic cholic acid analogues</b>					
<b>Ether linked</b>					
<b>I</b>	225,226	0.035	<i>K. pneumoniae</i>	rifampicin	>10% (24h)
<b>II</b>	226	0.029	<i>K. pneumoniae</i>	novobiocin	<10% (24h)
<b>III</b>	226	0.022	<i>K. pneumoniae</i>	novobiocin	>10% (24h)
<b>IV</b>	228	0.13	<i>K. pneumoniae</i>	rifampicin	<10% (24h)
<b>Ester linked</b>					
<b>V</b>	229	0.057*	<i>E. coli</i>	erythromycin	NR
<b>VI</b>	229	0.064*	<i>E. coli</i>	erythromycin	NR
<b>VII</b>	230	0.176*	<i>E. coli</i>	erythromycin	<10% (24h)
<b>Steroid-peptide hybrids</b>					
<b>VIII</b>	235	0.099	<i>E. coli</i>	erythromycin	NR
<b>IX</b>	235	0.093	<i>E. coli</i>	erythromycin	NR
<b>X</b>	235	0.078	<i>E. coli</i>	erythromycin	NR

<sup>a</sup>Non-hemolytic is defined as <10% hemolysis compared to positive control with incubation times denoted in parentheses, NR denotes no data reported; \*FICI calculated from MSC and MIC values reported in the cited literature reference.



## 4. Non-steroid small molecule synergists

### 4.1. Synergists based on approved drugs

Recently, Brown and coworkers reported an innovative screening platform for the identification of non-lethal, OM-active compounds with potential as adjuvants for conventional antibiotics.<sup>236</sup> They applied their screen to a library of 1,440 previously approved drugs which resulted in the identification of three hits. Among the three hits identified, the antiprotozoal agent pentamidine (Figure 6A), was subsequently found to display the highest synergistic potency (Table 5).<sup>236</sup> Notably, while pentamidine's OM targeting mechanism was found to be driven by interaction with LPS, *mcr*-resistance did not affect its synergistic potential.<sup>236</sup> The potentiation of novobiocin by pentamidine was also established *in vivo* against wild-type and resistant *A. baumannii*.<sup>236</sup> Subsequently, a focused SAR study using commercially available bis-amidines similar in structure to pentamidine led to the identification of compound **9** as an even more potent synergist (Figure 6A and Table 5).<sup>236</sup>

Inspired by these findings, our group recently undertook a broad SAR investigation wherein a number of structurally unique bis-amidines were synthesized and evaluated as synergists.<sup>237</sup> Specifically we focused our attention on the length and rigidity of the linker motif as well as the geometry of the amidine groups on the aromatic rings. In addition to assessing the synergistic activity of the new bis-amidines prepared, we also performed hemolysis assays with each compound to ascertain OM selectivity. Given the potent synergy previously reported for bis-amidine **9**<sup>236</sup> we also synthesized it to use as a benchmark. Among the compounds prepared in our study, bis-amidine **21**, containing an *ortho*-substituted benzene linker, was found to be significantly more synergistic than pentamidine and displayed no hemolytic activity (Figure 6A and Table 5).<sup>237</sup> We also found that the introduction of additional aromatic groups to the linker, such as in compound **38**, led to further enhancement of synergy, however, this came at the costs of increased hemolytic activity (Table 5). Interesting, our studies also revealed benchmark bis-amidine **9** to be hemolytic. These findings further highlight the importance of assessing OM selectivity when pursuing synergists.<sup>237</sup>

The Brown group also recently reported a follow-up SAR study aimed at further enhancing the therapeutic potential of bis-amidines synergists.<sup>238</sup> Similar to our own SAR study, the rigidity, conformation flexibility, and lipophilicity were further explored. In addition, the role of chirality and charge were also investigated.<sup>238</sup> A key focus of this study was to identify bis-amidine synergists with improved off-target effects relative to pentamidine, especially the QT prolongation resulting from its effect on the hERG ion channel.<sup>238–240</sup> This led to compound **P35** which was shown to have the same synergistic mode of action as pentamidine, displayed a strong potentiation of novobiocin, and no hemolytic activity (Table 5). Furthermore, compound **P35** outperformed pentamidine on multiple levels: an improvement in cytotoxicity, a higher efficacy in a mouse infection model, and reduced hERG inhibition.<sup>238</sup>

Wang and coworkers also recently reported a study wherein the Prestwick Chemical Library, comprising 158 FDA-approved drugs, was assessed for compounds exhibiting synergy with doxycycline.<sup>240</sup> This led to the finding that metformin, a commonly prescribed anti-diabetic agent (Figure 6B), effectively potentiates vancomycin as well as tetracycline antibiotics, particularly doxycycline and minocycline, against MDR *S. aureus*, *Enterococcus faecalis*, *E. coli*, and *Salmonella enteritidis*.<sup>240</sup> The capacity for

28

metformin to disturb the OM was assessed using the NPN assay, revealing an increase in *E. coli* OM permeability in a dose-dependent manner. Of particular note was the finding that metformin was also able to fully restore the activity of doxycycline in animal infection models.<sup>241</sup>

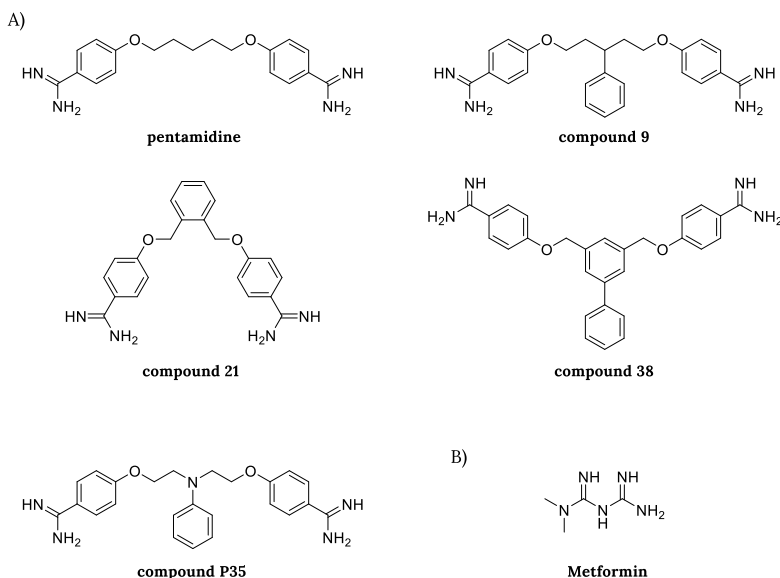


**Figure 6.** Representative structures of reported A) bis-amidine synergists; and B) metformin.

## 4.2. Small molecule synergists via high throughput screening

Following the success in applying their OM perturbation reporter assay to identify pentamidine as a potent synergist, the Brown group applied the same approach in a much larger high throughput screening (HTS) campaign with a library of ca. 140 000 synthetic compounds.<sup>236,242</sup> This in turn led to the identification of 39 hits that were subsequently screened for synergistic activity with rifampicin.<sup>242</sup> Among these hits MAC-0568743 and liproxstatin-1 and (Figure 7A) were found to be particularly active synergists (Table 5).<sup>242</sup> Both compounds were found to potentiate the activity of the Gram-positive-targeting antibiotics rifampicin, novobiocin, erythromycin, and linezolid. This potentiation was further shown to be due to selective disruption of the OM, driven by interactions with LPS, and neither compound impacted the inner membrane.<sup>242</sup>

In another recently reported campaign, Datta and coworkers screened a focused library of 3000 drug-like compounds for antibiotic synergy using a whole-cell-based phenotypic assay.<sup>243</sup> This led to the identification of a series of azaindoles that potentiate the MICs of macrolides, novobiocin, and rifampicin, by 100–1000-fold vs. Gram-negative bacteria. Optimization studies led to compounds BWC-Aza1 and BWC-Aza2 (See Figure 7B) both of which were screened for synergistic activity with an extensive panel of antibiotics against *E. coli* (Table 5). The OM permeabilizing activity of the azaindoles was also probed using the NPN assay revealing dose-dependent disruption.<sup>243</sup>

### 4.3. Small molecule polyamine synergists

In recent years the polyamines norspermine and norspermidine have been explored as starting points for the development of antibacterial and antibiofilm agents.<sup>244,245</sup> Building on this work, the Halder group recently reported the development of D-LANA-14 comprised of a norspermidine core linked to two D-lysine along with conjugation to a tetradecanoyl chain at the central secondary amine (Figure 7C).<sup>246</sup> D-LANA-14 showed potent synergy with tetracycline or rifampicin against meropenem-resistant *A. baumannii* and *P. aeruginosa* clinical isolates (Table 5) and importantly was also found to disrupt established biofilms formed by these pathogens.<sup>246</sup> D-LANA-14 was shown to perturb the OM by means of the NPN assay and importantly also found to exhibit potent *in vivo* activity when combined with rifampicin resulting in a significant reduction of bacterial burden in a mouse model of burn-wound infection.<sup>246</sup>

In another study involving small molecule polyamines, Katsu and coworkers investigated synthetic analogues of the joro spider toxin as OM disrupting agents leading to the identification of naphthylacetylspermine (Figure 7D) which was found to potentiate the activity of novobiocin against *E. coli* (Table 5).<sup>247</sup> Mechanistic studies revealed that administration of naphthylacetylspermine causes OM disruption, which was attributed to displacement of LPS-associated  $\text{Ca}^{2+}$ . In addition, naphthylacetylspermine was found to promote cellular uptake of the tetraphenylphosphonium ( $\text{TPP}^+$ ), indicating membrane permeabilization, a finding similar to that obtained with PMBN.<sup>247,248</sup> Interestingly, spermidine and spermine were also found to induce loss of  $\text{Ca}^{2+}$  but did not cause uptake of  $\text{TPP}^+$ , pointing to the importance of the naphthyl moiety for membrane permeabilization.<sup>248</sup> Given that no hemolysis data was reported for naphthylacetylspermine, it is not possible to assess the selectivity of its OM activity.

The David group also reported the development of acylated polyamines as LPS neutralizing agents capable of functioning as OM disrupting synergists.<sup>249–251</sup> A series of monoacyl- and bisacyl-homospermines were prepared and evaluated as potentiators of rifampicin resulting in the identification of two potent synergists, compounds **8a** and **8b** (see Figure 7E and Table 5).<sup>249</sup> A clear correlation between length of the lipophilic tails and hemolytic activity was seen with compound **8a** appearing to strike an optimal balance.<sup>249</sup> Using a similar approach, Copp and coworkers introduced the indole-3-acrylamido-spermine conjugates inspired by a class of indole spermidine alkaloid natural products.<sup>252,253</sup> A SAR study led to the development of spermidine analogues like **14** and **17** which exhibited effective synergy with various antibiotics (Figure 7F and Table 5).<sup>252,254</sup> These compounds affect bacterial membrane integrity, show low cytotoxicity and hemolytic activity. Interestingly, compound **14** was also found to inhibit bacterial efflux pumps suggesting that the potentiation of antibiotics by these compounds may be attributed to a dual mechanism of action.<sup>252,254</sup>

Given the inclusion criteria noted in the introduction, only small molecules synergists (MW under 1500 kDa) are included in this review and as such we do not discuss larger polycationic polymers even though some have been shown to exhibit synergistic activity.<sup>89–95,255,256</sup> It is noteworthy, however, that branched polyethylenimine (BPEI) with a MW of 600 Da shows synergistic activity (Figure 7G, Table 5) and can also eradicate biofilms when co-administered with a variety of antibiotics.<sup>257</sup> Mechanistic studies using isothermal titration calorimetry and fluorescence spectroscopy indicate that at the concentration required for antibiotic potentiation, 600 Da BPEI reduces diffusion barriers from LPS without disrupting the OM itself.<sup>257</sup>

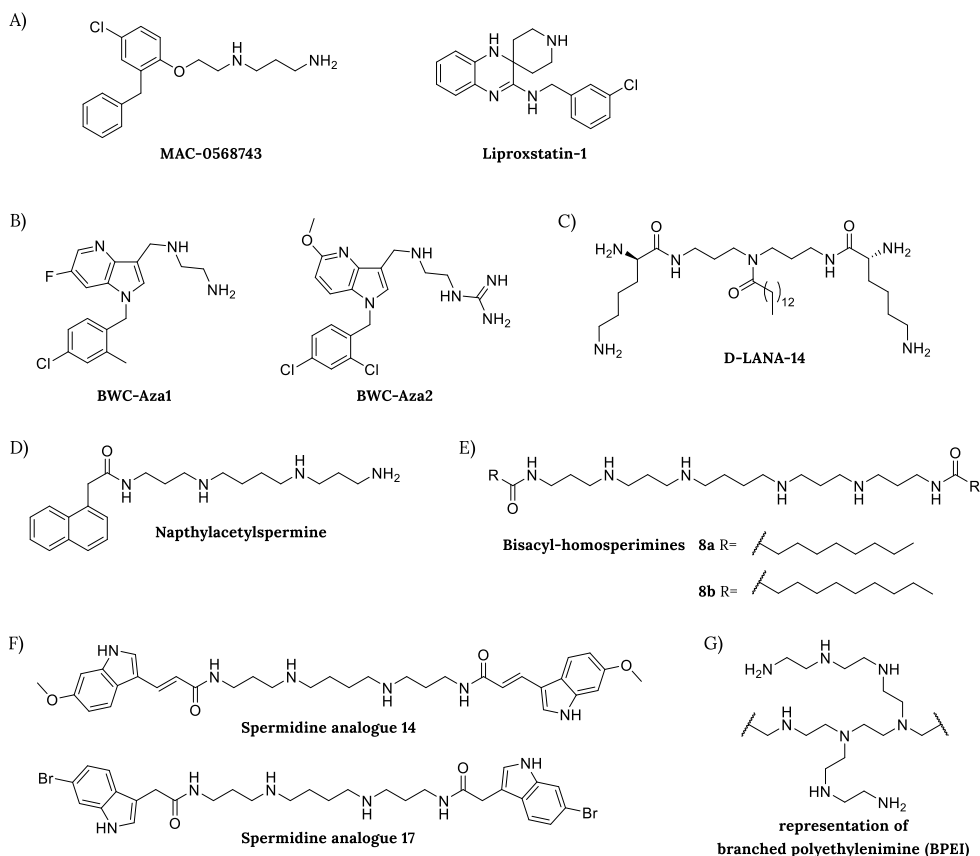


**Figure 7.** Non-steroid small molecule synergists A) synergists identified via HTS; B) azaindole synergists; C) D-LANA-14 based on a norspermidine core linked to two D-lysine residues and a central tetradecanoyl moiety; D) joro spider toxin inspired naphylacetylspermine; E) bisacyl-homospermines; F) indole-3-acrylamido-spermine conjugates; and G) representation of 600 Da branched polyethylenimine (BPEI).

#### 4.4. Plant derived synergists

A number of plant-derived compounds have also been reported to potentiate the activity of antibiotics against Gram-negative bacteria (Table 5). These include natural products like eugenol, a major component of cloves oil, linalool which can be isolated from coriander, thymol which is extracted from thyme, and cinnamaldehyde and cinnamic acid which are found in the bark and leaves of the cinnamon tree (Figure 8).<sup>258-264</sup> Important to note is that only pure compounds derived from plants are included in our assessment. We refer the reader to other reviews on the synergistic activity of essential oils or crude extracts.<sup>265,266</sup> Notably, most plant-derived compounds reported to potentiate antibiotics against Gram-negative bacteria are not cationic, setting them apart from most other synergists. Despite their lack of positive charge, a number of investigations have shown that the synergy associated with these compounds is a function of their ability induce OM permeabilization (Table 6).<sup>258,259,267-269</sup> The broad range of biological activities associated with cinnamic acid and its derivatives, including ferulic acid, 3,4-dimethoxycinnamic acid, and 2,4,5-trimethoxy cinnamic acid (Figure 9), have been recently reviewed including synergistic effects associated with OM disruption.<sup>270</sup> Interestingly, despite its clear structural similarities with cinnamic acid, studies with cinnamaldehyde suggest it may operate via a different synergist mechanism. Unlike cinnamic acid, cinnamaldehyde does not increase OM permeabilization based on the NPN assay, but does exhibit synergistic effects with erythromycin and novobiocin (Table 5).<sup>267,269</sup>

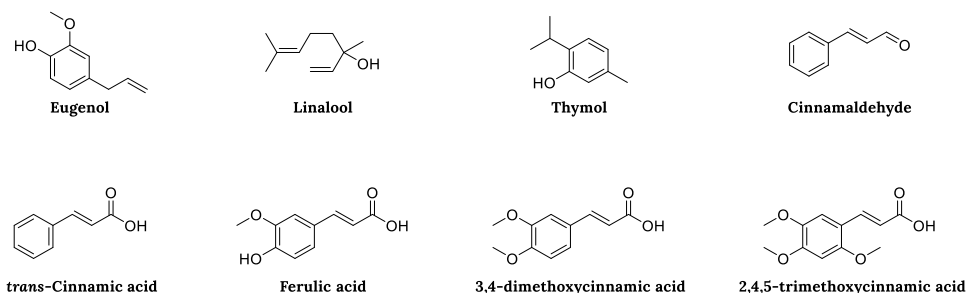


**Figure 8.** Plant-derived natural products reported to potential the activity of antibiotics against Gram-negative bacteria.

**Table 5.** Overview of non-steroid small molecule synergists (compound names provided as given in the cited literature references).

Name	Ref	FICI	Pathogen	Antibiotic	Hemolytic activity <sup>a</sup>
<b>Synergists based on approved drugs</b>					
<b>Pentamidine</b>	236,237	0.25	<i>E. coli</i>	rifampicin	<10% (20h)
<b>Compound 9</b>	236,237	<0.047	<i>E. coli</i>	rifampicin	>10% (20h)
<b>Compound 21</b>	237	≤0.094	<i>E. coli</i>	rifampicin	<10% (20h)
<b>Compound 38</b>	237	≤0.039	<i>E. coli</i>	rifampicin	>10% (20h)
<b>Compound P35</b>	238	0.094	<i>A. baumannii</i>	novobiocin	<10% (45 min)#
<b>Metformin</b>	241	0.375	<i>E coli</i>	vancomycin	<10% (1h)

High throughput screening (HTS)-hits					
MAC-0568743	242	≤0.16	<i>E. coli</i>	rifampicin	NR
Liproxstatin-1	242	0.25*	<i>E. coli</i>	rifampicin	NR
BWC-Aza1	243	0.258	<i>E. coli</i>	rifampicin	<10% (45 min)
BWC-Aza2	243	0.06	<i>A. baumannii</i>	rifampicin	<10% (45 min)
Peptidomimetics					
OAK C <sub>12</sub> ( <sub>w7</sub> )	208	≤0.073*	<i>E. coli</i>	rifampicin	>10% (3h)
OAK C <sub>12</sub>	208	≤0.211*	<i>E. coli</i>	rifampicin	>10% (3h)
OAK C <sub>10</sub>	208	≤0.036*	<i>E. coli</i>	rifampicin	<10% (3h)#
OAK C <sub>8</sub>	208	≤0.078*	<i>E. coli</i>	rifampicin	<10% (3h)#
C <sub>14</sub> ( <sub>w5</sub> )OOC <sub>10</sub> O	209	0.20*	<i>K. pneumoniae</i>	rifampicin	<10% (3h)#
dUSTBP 2	202	≥0.250	<i>P. aeruginosa</i>	rifampicin	<10% (1h)
dUSTBP 5	202	≥0.125	<i>P. aeruginosa</i>	rifampicin	<10% (1h)
dUSTBP 8	202	≥0.002	<i>A. baumannii</i>	novobiocin	<10% (1h)
Synergists with a polyamine motif					
D-LANA-14	245,246	0.09	<i>P. aeruginosa</i>	rifampicin	<10% (1h)
Naphthylacetylspermine	247	0.125*	<i>E. coli</i>	novobiocin	NR
Bisacyl-homospermine 8a	249	0.304*	<i>E. coli</i>	rifampicin	<10% (30min)
Bisacyl-homospermine 8b	249	0.297*	<i>E. coli</i>	rifampicin	>10% (30min)
Spermidine analogue 14	254	0.255*	<i>E. coli</i>	erythromycin	<10% (1h)#
Spermidine analogue 17	254	0.255*	<i>P. aeruginosa</i>	erythromycin	<10% (1h)#
600-Da BPEI	257,271	0.26	<i>P. aeruginosa</i>	erythromycin	<10% (1h)
Plant derived synergists					
Eugenol	258,272	≤0.2*	<i>P. aeruginosa</i>	rifampicin	<10% (24h)
Linalool	259,273	0.37	<i>E. coli</i>	erythromycin	<10% (4h)
Thymol	267,274	0.25	<i>E. coli</i>	erythromycin	<10% (1h)
Cinnamaldehyde	267,275	0.24	<i>E. coli</i>	erythromycin	<10% (48h)
trans-Cinnamic acid	268,276	0.36	<i>E. coli</i>	erythromycin	<50% (1h)
Ferulic acid	268,276	0.48	<i>E. coli</i>	erythromycin	<50% (1h)
3,4-dimethoxycinnamic acid	268,276	0.42	<i>E. coli</i>	erythromycin	<50% (1h)
2,4,5-trimethoxycinnamic acid	268,276	0.22	<i>E. coli</i>	erythromycin	<50% (1h)

<sup>a</sup>Non-hemolytic is defined as <10% hemolysis compared to positive control with incubation times denoted in parentheses; NR denotes no data reported; #denotes that the concentration tested was lower than 100 µg/mL; \*FICI calculated from MSC and MIC values reported in the cited literature reference.

## 5. Antibiotic-derived synergists

In general, the antibiotic potentiators discussed above show little-to-no inherent antibacterial activity. There are, however, a number of reports describing antibacterial compounds that also exhibit OM disrupting effects and in doing so synergize with antibiotics that are otherwise inactive towards Gram-negative bacteria. The synergists described in this section are specifically included based upon their OM disrupting activity rather than a contribution of their inherent activity to synergy. We therefore do not include the combination of rifampicin with imipenem or trimethoprim which is solely based on functional synergy.<sup>277,278</sup> In addition, we also do not cover reports describing systems where an OM perturbing motif like PMBN is covalently linked to another antibiotic as a means of enhancing anti-Gram-negative activity.<sup>39,279–281</sup>

### 5.1. Tobramycin-derived synergists

Tobramycin (Figure 9A) belongs to the aminoglycoside class of antibiotics that function by inhibiting ribosomal protein synthesis in bacteria. Recent studies have also revealed that aminoglycosides like tobramycin also interact with bacterial membranes by specifically binding to LPS and in doing so cause membrane depolarization.<sup>282–286</sup> Building on these insights Schweizer and coworkers have prepared and assessed a number of conjugates wherein one tobramycin molecule is linked to a second antibiotic providing hybrid systems that possess both inherent antibacterial activity as well as potent synergy with other antibiotics (Figure 9A).<sup>287–290,279,291–297</sup> Among the first hybrids prepared was a series tobramycin-fluoroquinolone conjugates.<sup>287,288</sup> Both the optimal sites of conjugation and linker lengths between the two antibiotics were investigated revealing TOB-MOX, a tobramycin-moxifloxacin hybrid, and tobramycin-ciprofloxacin conjugate **1e** to be potent synergists (Table 6).<sup>288</sup> Notably, the conjugates generally showed lower inherent antibacterial activity than the parent antibiotics indicating that their synergistic activity comes at the price of inherent activity.<sup>287,288</sup> OM disruption was confirmed for both hybrids using the NPN assay and both were found to potentiate multiple antibiotics including rifampicin, erythromycin, novobiocin, and vancomycin.<sup>287,288</sup> Also of note was the finding that these hybrids exhibited a significantly reduced capacity to inhibit of protein translation compared to that of tobramycin.<sup>287,288</sup> Conversely, the hybrids were found to maintain, and some cases exceed, the gyrase inhibiting activity of the parent fluoroquinolones.<sup>287,288</sup> Another series of hybrids were prepared by coupling tobramycin with rifampicin, which targets the bacterial RNA polymerase.<sup>289</sup> As for the fluoroquinolone conjugates, the inherent activity of the tobramycin-rifampicin conjugates was significantly reduced compared to the parent antibiotics. Again, however, some hybrids were found to exhibit synergy via an OM-disrupting mechanism (see tobramycin-rifampicin **1**, **2**, **3**, Figure 9A).<sup>288–290,298</sup>

A number of other hybrids have also been reported by the Schweizer group wherein tobramycin was coupled to various other small molecules known to engage with different bacterial targets. In one case, tobramycin was coupled to a lysine-based amphiphile known to function as membrane permeabilizer (see tobramycin-lysine **3**, Figure 9A).<sup>290,299</sup> This conjugate was found to effectively potentiate the activity of novobiocin, erythromycin, and vancomycin (Table 6).<sup>290,300</sup> The same group also explored hybrids wherein tobramycin was coupled to small molecule efflux pumps inhibitors such as 1-(1-naphthylmethyl)-piperazine (NMP) and paroxetine (PAR) (Figure 9A).<sup>45,291,301–303</sup> Along with potent synergy against *P. aeruginosa* (Table 6), these hybrids were also found

to cause OM disruption and inner membrane depolarization.<sup>315,316</sup> Two additional generations of tobramycin conjugates were also reported: tobramycin homodimers and tobramycin coupled to chelating cyclams (Figure 9A).<sup>293,294</sup> The dimerization of tobramycin was conveniently achieved by means of copper catalyzed azide-alkyne click chemistry, resulting in potent synergists that also exhibit enhanced OM disruption relative to tobramycin itself (Table 6).<sup>293</sup> A combination of novobiocin and tobramycin homodimer **1** (both administered at 50 µg/mL) was further shown to have *in vivo* efficacy against *A. baumannii* in a wax worm larvae model.<sup>293</sup> Studies with the corresponding monomeric tobramycin azide and alkyne precursors revealed neither to be synergistic, underscoring the need for dimerization to achieve synergy.<sup>293</sup> In the case of the tobramycin-cyclam conjugates, the introduction of the cyclam chelating group was hypothesized to aid in the OM permeabilization by sequestration of divalent cations bridging the Lipid A phosphate groups.<sup>294,304–306</sup> While tobramycin-cyclam hybrids **1**, **2**, and **3** effectively potentiated novobiocin, rifampicin, vancomycin and erythromycin (Table 6), it is also particularly noteworthy that they also enhanced the activity of meropenem against both carbapenem-resistant and -sensitive strains.<sup>294</sup> This effect was abrogated by the addition of excess MgCl<sub>2</sub> further supporting a mode of action driven by OM disruption.<sup>294</sup>

## 5.2. Nebramine-derived synergists

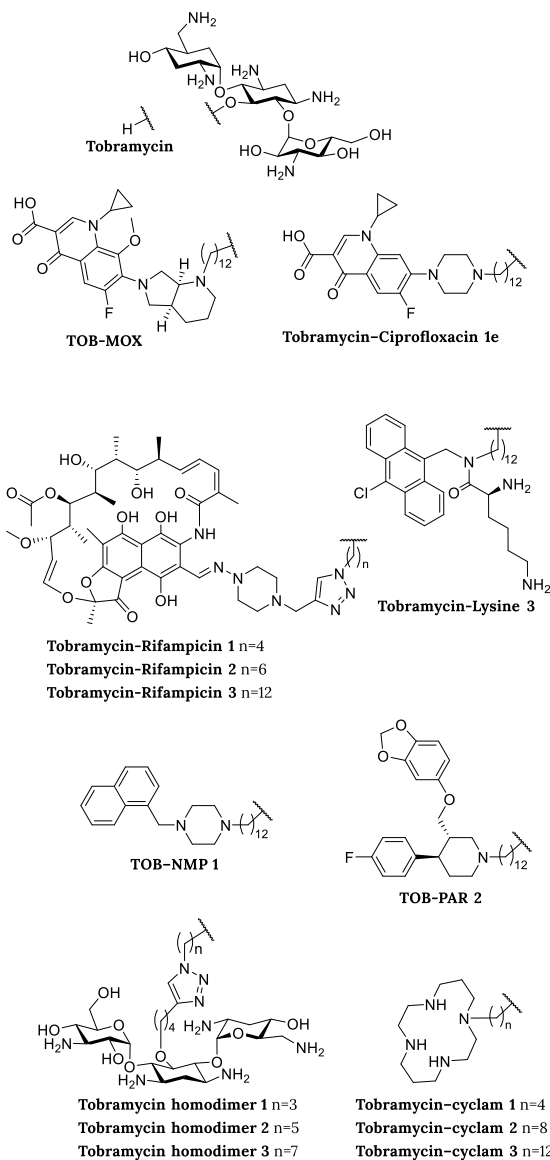
Following on their work with tobramycin hybrids, the Schweizer group also prepared a number of analogous nebramine conjugates (Figure 9B). Nebramine (NEB) is a disaccharide subunit of tobramycin that interestingly displays activity against tobramycin resistant strains and also interacts with the OM.<sup>283,307–313</sup> The NEB hybrids synthesized included conjugates with moxifloxacin (MOX), ciprofloxacin (CIP), NMP, and cyclam (Figure 9B).<sup>295,296</sup> These hybrids were all found to effectively potentiate the activity of multiple classes of antibiotics against a range of Gram-negative bacteria (Table 6). Furthermore, NEB-MOX **1a**, NEB-CIP **1b**, and NEB-NMP **2** were also reported to dissipate proton motive force and proposed to cause OM disruption as for the corresponding tobramycin conjugates.<sup>287,290,291,295,296</sup>

## 5.3. Levofloxacin derived synergists

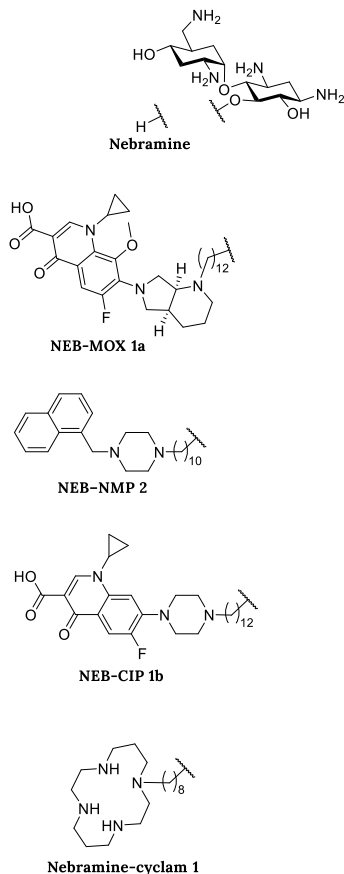
Schweizer and coworkers also recently reported another class of antibiotic based synergists based on polybasic peptide-levofloxacin conjugates (Figure 9C).<sup>297</sup> While these levofloxacin-peptide hybrids were found to be non-hemolytic, they were also shown to be essentially devoid of inherent antimicrobial activity (MICs typically > 128 µg/mL). They did however, exhibit strong potentiation of numerous antibiotics against MDR clinical isolates of *P. aeruginosa*, *E. coli*, *K. pneumoniae* and to a lesser extent, *A. baumannii* (Table 6).<sup>297</sup> Preliminary mechanistic studies indicate that these conjugates potentiate other antibiotics by both blocking active efflux and by permeabilization of the OM.<sup>297</sup>



A) Tobramycin conjugates



B) Nebramine conjugates



C)

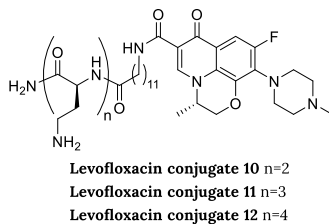


**Figure 9.** Synergists based on clinically used antibiotics. A) Tobramycin (TOB) conjugates; B) Nebramine (NEB) analogues; and C) polybasic conjugated levofloxacin hybrids.

**Table 6.** Overview of synergists based on clinically used antibiotics (compound names provided as given in the cited literature references).

Name	Ref	FICI	Pathogen	Antibiotic	Hemolytic activity <sup>a</sup>
<b>Tobramycin derivatives</b>					
TOB-MOX 1	287	0.125	<i>P. aeruginosa</i>	novobiocin	<10% (30 min)
Tobramycin-Ciprofloxacin 1e	288	<0.04	<i>P. aeruginosa</i>	rifampicin	<10% (30 min)
Tobramycin-Rifampicin 1	289	0.28	<i>P. aeruginosa</i>	rifampicin	<10% (1h)
Tobramycin-Rifampicin 2	289	0.15	<i>P. aeruginosa</i>	erythromycin	<10% (1h)
Tobramycin-Rifampicin 3	289	0.06	<i>P. aeruginosa</i>	erythromycin	<10% (1h)
Tobramycin-Lysine 3	290	0.008	<i>P. aeruginosa</i>	novobiocin	<10% (1 h)
TOB-NMP 1	292	≥0.008	<i>P. aeruginosa</i>	rifampicin	<10% (30 min)
TOB-PAR 2	292	≥0.008	<i>P. aeruginosa</i>	rifampicin	<10% (30 min)
Tobramycin homodimer 1	293	0.07	<i>P. aeruginosa</i>	novobiocin	<10% (1h)
Tobramycin homodimer 2	293	0.08	<i>P. aeruginosa</i>	novobiocin	<10% (1h)
Tobramycin homodimer 3	293	0.05	<i>P. aeruginosa</i>	novobiocin	<10% (1h)
Tobramycin-Cyclam 1	294	0.13	<i>P. aeruginosa</i>	novobiocin	<10% (30 min)
Tobramycin-Cyclam 2	294	0.13	<i>P. aeruginosa</i>	novobiocin	<10% (30 min)
Tobramycin-Cyclam 3	294	0.08	<i>P. aeruginosa</i>	novobiocin	<10% (30 min)
<b>Nebramine derivatives</b>					
NEB-MOX 1a	295	≥0.002	<i>K. pneumoniae</i>	rifampicin	NR
NEB-CIP 1b	295	≥0.008	<i>P. aeruginosa</i>	rifampicin	<10% (1h)
NEB-NMP 2	295	≥0.004	<i>P. aeruginosa</i>	rifampicin	NR
Nebramine-cyclam	296	0.25	<i>P. aeruginosa</i>	rifampicin	<10% (1h)
<b>Levofloxacin derivatives</b>					
Levofloxacin conjugate 10	297	0.10	<i>P. aeruginosa</i>	rifampicin	<10% (1h)
Levofloxacin conjugate 11	297	0.10	<i>P. aeruginosa</i>	novobiocin	<10% (1h)
Levofloxacin conjugate 12	297	0.08	<i>P. aeruginosa</i>	novobiocin	<10% (1h)

<sup>a</sup>Non-hemolytic is defined as <10% hemolysis compared to positive control with incubation times denoted in parentheses, NR denotes no data reported.

## 6. Chelating agents as OM disrupting synergists

The activity of antibiotics can also be potentiated by chelating agents that disturb the integrity of the OM by sequestering the divalent cations  $Mg^{2+}$  or  $Ca^{2+}$  coordinated by the phosphate groups of the lipid A core of LPS (Figure 1B).<sup>32</sup> The preeminent chelating agent, EDTA (Figure 10) is a well described synergist and its reported ability to potentiate antibiotics actually predates the reported synergistic activity of PMBN.<sup>49,314–317</sup> Exposure of Gram-negative bacteria to EDTA is accompanied by the significant release of LPS and, as for treatment with PMBN, also results in the increased uptake of NPN.<sup>318–320</sup> While the potentiating effects of EDTA on antibiotics such as novobiocin and rifampicin are well documented, FICI values have not been reported in literature and cannot be readily calculated from published data.<sup>316,317,319,321</sup> Similarly, for the other chelating here discussed, no FICI values could be found in the literature and as such we do not provide a summary table as done for the other synergists discussed in this review.

In addition to his seminal work with PMBN, Vaara also reported the potentiation of hydrophobic antibiotics by sodium hexametaphosphate (HMP, Figure 10) against Gram-negative bacteria as well as the increase in NPN uptake in cells treated with this potent  $Ca^{2+}$  binding agent.<sup>322</sup> In a similar study, Ayres and Russell also described sodium polyphosphates as potent synergist with several antibiotics (structures not shown).<sup>323</sup> In the same study, citric acid (Figure 10) was also demonstrated to exhibit synergistic activity with erythromycin, novobiocin, rifampicin, methicillin, and gentamicin.<sup>323</sup> In addition, 2,3-dimercaptosuccinic acid (Figure 10), clinically used in the treatment of lead intoxication, was also found to potentiate the activity of hydrophobic antibiotics.<sup>319</sup> The synergistic activity of 2,3-dimercaptosuccinic acid was attributed to an OM permeabilizing mechanism as evidenced by increased NPN uptake in bacterial cells treated with the compound.<sup>319</sup>

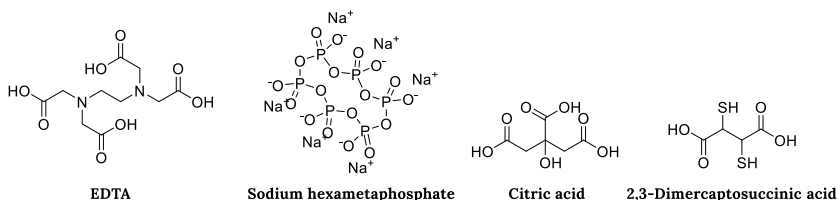


**Figure 10.** Chelating agents with demonstrated synergistic activity.

## 7. Concluding remarks

New strategies are required to address the growing threat posed by MDR Gram-negative pathogens. To this end, a large and growing number of synergists capable of potentiating Gram-positive specific antibiotics against Gram-negative bacteria have been described in literature to date. Within this review we provide the reader with a comprehensive and up-to-date overview of those synergists reported to have a demonstrated OM targeting mechanism. We also draw attention to the importance of selective OM disruption, a factor that has often been overlooked by researchers when characterizing their synergists. In this regard, and based on our assessment of the literature, the majority of hemolysis studies reported for such synergists use relatively short incubation times compared to the incubation times actually used in assessing synergy (i.e. in checkerboard assays). Based on our own experience, not only is the concentration at which hemolysis is assessed relevant, but incubation time can also make a significant difference in describing a compound as hemolytic or not. For example, in cases where 5% hemolysis is reported after one hour, it is our experience that such compounds are often much more hemolytic after overnight incubation. For this reason we have included both the concentrations and incubation times of the synergists described in this review. Doing so provides for a more honest and accurate assessment of the OM specificity of these synergists.

To provide a means of comparing the relative activity of the synergists here summarized, we have emphasized their FICI values, a descriptor broadly applied as a scale to quantify synergistic potency. However, another important consideration that is not directly revealed by the FICI is of course the concentration at which a synergist actually potentiates the companion antibiotic. Related to this is the importance of the pharmacokinetic/pharmacodynamic profile of the synergist and how well it matches that of the antibiotic it potentiates. Given that the vast majority of synergists covered in this review have only been characterized using cell-based *in vitro* and biochemical assays, we have not touched on this. It is clear, however, that establishing and optimizing such parameters will be essential to the (pre)clinical development of any such synergist.

## 8. Thesis outline

This thesis describes the development of novel synergists designed to selectively disrupt the outer membrane of Gram-negative bacteria.

**Chapter 2** reports the optimization of bis-amidines as outer membrane disrupting agents that can potentiate Gram-positive specific antibiotics. The synthesis of a number of unique bis-amidines was followed by an initial screening with checkerboard assays revealing the most potent synergists. The compounds were also evaluated for hemolytic activity to provide a rough measure of their selectivity. The most potent, non-hemolytic compounds were then evaluated in combination with rifampicin against multiple strains of Gram-negative bacteria. Lastly, their outer membrane disrupting activity was compared to the well-known synergist PMBN.

**Chapter 3** describes the development of peptide-based synergists with the capacity to enhance the activity of antibiotics against Gram-negative bacteria. The approach taken was inspired by recent reports of LPS-binding activity by thrombin-derived peptides. This prompted us to further evaluate these peptides as outer membrane disrupting synergists. The structures of the peptides were optimized by adjusting the C- and N-termini as well as by applying an alanine scan. In addition, hemolysis and outer membrane disrupting assays were performed to establish the selectivity of the peptides for the outer membrane of Gram-negative bacteria. The synergistic potential of the lead peptides was evaluated with several Gram-positive antibiotics and for multiple Gram-negative bacterial strains.

In **Chapter 4** the focus was shifted from outer membrane disrupting synergists based on synthetic small molecules and peptides, to the synergistic activity of the complement system found in with human serum. A broad range of Gram-positive specific antibiotics was evaluated with serum in two assays: an inner membrane permeability assay serving as a screen, followed by a bacterial viability assay allowing for a validation of the hits. In addition, four antibiotics of the glycopeptide class were also evaluated to allow for an in-class comparison of synergy with the complement system.

**Chapter 5** diverges from the synergy theme of this thesis: in this chapter the inherent anti-Gram-positive activity of the bis-amidines described in Chapter 2 is described. In addition to the previously synthesized bis-amidines, four new bis-amidines were prepared and evaluated for hemolytic and antimicrobial activity. In addition to the screening of several Gram-positive bacteria, the effects of different media were also evaluated.

## References

- (1) Delcour, A. H. Outer Membrane Permeability and Antibiotic Resistance. *Biochim. Biophys. Acta BBA - Proteins Proteomics* **2009**, 1794 (5), 808–816. <https://doi.org/10.1016/j.bbapap.2008.11.005>.
- (2) Nikaido, H. Molecular Basis of Bacterial Outer Membrane Permeability Revisited. *Microbiol. Mol. Biol. Rev.* **2003**, 67 (4), 593–656. <https://doi.org/10.1128/MMBR.67.4.593-656.2003>.
- (3) Nikaido, H. The Role of Outer Membrane and Efflux Pumps in the Resistance of Gram-Negative Bacteria. Can We Improve Drug Access? *Drug Resist. Updat.* **1998**, 1 (2), 93–98. [https://doi.org/10.1016/S1368-7646\(98\)80023-X](https://doi.org/10.1016/S1368-7646(98)80023-X).
- (4) Silhavy, T. J.; Kahne, D.; Walker, S. The Bacterial Cell Envelope. *Cold Spring Harb. Perspect. Biol.* **2010**, 2 (5), a000414. <https://doi.org/10.1101/cshperspect.a000414>.
- (5) Freire-Moran, L.; Aronsson, B.; Manz, C.; Gyssens, I. C.; So, A. D.; Monnet, D. L.; Cars, O. Critical Shortage of New Antibiotics in Development against Multidrug-Resistant Bacteria—Time to React Is Now. *Drug Resist. Updat.* **2011**, 14 (2), 118–124. <https://doi.org/10.1016/j.drup.2011.02.003>.
- (6) Nicolau, D. P. Carbapenems: A Potent Class of Antibiotics. *Expert Opin. Pharmacother.* **2008**, 9 (1), 23–37. <https://doi.org/10.1517/14656566.9.1.23>.
- (7) Vaara, M. Polymyxin Derivatives That Sensitize Gram-Negative Bacteria to Other Antibiotics. *Molecules* **2019**, 24 (2), 249. <https://doi.org/10.3390/molecules24020249>.
- (8) Bustos, C.; Pozo, J. L. D. Emerging Agents to Combat Complicated and Resistant Infections: Focus on Ceftobiprole. *Infect. Drug Resist.* **2010**, 3, 5–14. <https://doi.org/10.2147/IDR.S3681>.
- (9) Riccobene, T. A.; Su, S. F.; Rank, D. Single- and Multiple-Dose Study To Determine the Safety, Tolerability, and Pharmacokinetics of Ceftaroline Fosamil in Combination with Avibactam in Healthy Subjects. *Antimicrob. Agents Chemother.* **2013**, 57 (3), 1496–1504. <https://doi.org/10.1128/AAC.02134-12>.
- (10) Kisgen, J.; Whitney, D. Ceftobiprole, a Broad-Spectrum Cephalosporin With Activity against Methicillin-Resistant *Staphylococcus Aureus* (MRSA). *Pharm. Ther.* **2008**, 33 (11), 631–641.
- (11) Chaudhary, U.; Aggarwal, R. Extended Spectrum  $\beta$ -Lactamases (ESBL) – an Emerging Threat to Clinical Therapeutics. *Indian J. Med. Microbiol.* **2004**, 22 (2), 75–80. [https://doi.org/10.1016/S0255-0857\(21\)02884-X](https://doi.org/10.1016/S0255-0857(21)02884-X).
- (12) Mingeot-Leclercq, M.-P.; Glupczynski, Y.; Tulkens, P. M. Aminoglycosides: Activity and Resistance. *Antimicrob. Agents Chemother.* **1999**, 43 (4), 727–737. <https://doi.org/10.1128/AAC.43.4.727>.
- (13) Shaw, K. J.; Rather, P. N.; Hare, R. S.; Miller, G. H. Molecular Genetics of Aminoglycoside Resistance Genes and Familial Relationships of the Aminoglycoside-Modifying Enzymes. *Microbiol. Rev.* **1993**, 57 (1), 138–163. <https://doi.org/10.1128/mr.57.1.138-163.1993>.
- (14) Ramirez, M. S.; Tolmasky, M. E. Aminoglycoside Modifying Enzymes. *Drug Resist. Updat.* **2010**, 13 (6), 151–171. <https://doi.org/10.1016/j.drup.2010.08.003>.
- (15) Poole, K. Aminoglycoside Resistance in *Pseudomonas Aeruginosa*. *Antimicrob. Agents Chemother.* **2005**, 49 (2), 479–487. <https://doi.org/10.1128/AAC.49.2.479-487.2005>.
- (16) Liu, Y. Y.; Wang, Y.; Walsh, T. R.; Yi, L. X.; Zhang, R.; Spencer, J.; Doi, Y.; Tian, G.; Dong, B.; Huang, X.; Yu, L. F.; Gu, D.; Ren, H.; Chen, X.; Lv, L.; He, D.; Zhou, H.; Liang, Z.; Liu, J. H.; Shen, J. Emergence of Plasmid-Mediated Colistin Resistance Mechanism MCR-1 in Animals and Human Beings in China: A Microbiological and Molecular Biological Study. *Lancet Infect. Dis.* **2016**, 16 (2), 161–168. [https://doi.org/10.1016/S1473-3099\(15\)00424-7](https://doi.org/10.1016/S1473-3099(15)00424-7).
- (17) Partridge, S. R.; Di Pilato, V.; Doi, Y.; Feldgarden, M.; Haft, D. H.; Klimke, W.; Kumar-Singh, S.; Liu, J.-H.; Malhotra-Kumar, S.; Prasad, A.; Rossolini, G. M.; Schwarz, S.; Shen, J.; Walsh, T.; Wang, Y.; Xavier, B. B. Proposal for Assignment of Allele Numbers for Mobile Colistin Resistance (Mcr) Genes. *J. Antimicrob. Chemother.* **2018**, 73 (10), 2625–2630. <https://doi.org/10.1093/jac/dky262>.
- (18) Xavier, B. B.; Lammens, C.; Ruhal, R.; Kumar-Singh, S.; Butaye, P.; Goossens, H.; Malhotra-Kumar, S. Identification of a Novel Plasmid-Mediated Colistin-Resistance Gene, Mcr-2, in

- Escherichia Coli, Belgium, June 2016. *Eurosurveillance* **2016**, 21 (27), 30280. <https://doi.org/10.2807/1560-7917.ES.2016.21.27.30280>.
- (19) Yin, W.; Li, H.; Shen, Y.; Liu, Z.; Wang, S.; Shen, Z.; Zhang, R.; Walsh, T. R.; Shen, J.; Wang, Y. Novel Plasmid-Mediated Colistin Resistance Gene Mcr-3 in Escherichia Coli. *mBio* **2017**, 8 (3), e00543-17. <https://doi.org/10.1128/mBio.00543-17>.
  - (20) Carattoli, A.; Villa, L.; Feudi, C.; Curcio, L.; Orsini, S.; Luppi, A.; Pezzotti, G.; Magistrali, C. F. Novel Plasmid-Mediated Colistin Resistance Mcr-4 Gene in Salmonella and Escherichia Coli, Italy 2013, Spain and Belgium, 2015 to 2016. *Eurosurveillance* **2017**, 22 (31), 30589. <https://doi.org/10.2807/1560-7917.ES.2017.22.31.30589>.
  - (21) Borowiak, M.; Fischer, J.; Hammerl, J. A.; Hendriksen, R. S.; Szabo, I.; Malorny, B. Identification of a Novel Transposon-Associated Phosphoethanolamine Transferase Gene, Mcr-5, Conferring Colistin Resistance in d-Tartrate Fermenting Salmonella Enterica Subsp. Enterica Serovar Paratyphi B. *J. Antimicrob. Chemother.* **2017**, 72 (12), 3317-3324. <https://doi.org/10.1093/jac/dkx327>.
  - (22) AbuOun, M.; Stubberfield, E. J.; Duggett, N. A.; Kirchner, M.; Dormer, L.; Nunez-Garcia, J.; Randall, L. P.; Lemma, F.; Crook, D. W.; Teale, C.; Smith, R. P.; Anjum, M. F. Mcr-1 and Mcr-2 (Mcr-6.1) Variant Genes Identified in Moraxella Species Isolated from Pigs in Great Britain from 2014 to 2015. *J. Antimicrob. Chemother.* **2017**, 72 (10), 2745-2749. <https://doi.org/10.1093/jac/dkx286>.
  - (23) Yang, Y.-Q.; Li, Y.-X.; Lei, C.-W.; Zhang, A.-Y.; Wang, H.-N. Novel Plasmid-Mediated Colistin Resistance Gene Mcr-7.1 in Klebsiella Pneumoniae. *J. Antimicrob. Chemother.* **2018**, 73 (7), 1791-1795. <https://doi.org/10.1093/jac/dky111>.
  - (24) Wang, X.; Wang, Y.; Zhou, Y.; Li, J.; Yin, W.; Wang, S.; Zhang, S.; Shen, J.; Shen, Z.; Wang, Y. Emergence of a Novel Mobile Colistin Resistance Gene, Mcr-8, in NDM-Producing Klebsiella Pneumoniae. *Emerg. Microbes Infect.* **2018**, 7 (1), 1-9. <https://doi.org/10.1038/s41426-018-0124-z>.
  - (25) Carroll, L. M.; Gaballa, A.; Guldemann, C.; Sullivan, G.; Henderson, L. O.; Wiedmann, M. Identification of Novel Mobilized Colistin Resistance Gene Mcr-9 in a Multidrug-Resistant, Colistin-Susceptible Salmonella Enterica Serotype Typhimurium Isolate. *mBio* **2019** 10 (3), e00853-19. <https://doi.org/10.1128/mBio.00853-19>.
  - (26) Wang, C.; Feng, Y.; Liu, L.; Wei, L.; Kang, M.; Zong, Z. Identification of Novel Mobile Colistin Resistance Gene Mcr-10. *Emerg. Microbes Infect.* **2020**, 9 (1), 508-516. <https://doi.org/10.1080/22221751.2020.1732231>.
  - (27) Hussein, N. H.; AL-Kadmy, I. M. S.; Taha, B. M.; Hussein, J. D. Mobilized Colistin Resistance (Mcr) Genes from 1 to 10: A Comprehensive Review. *Mol. Biol. Rep.* **2021**, 48 (3), 2897-2907. <https://doi.org/10.1007/s11033-021-06307-y>.
  - (28) World Health Organization. Prioritization of Pathogens to Guide Discovery, Research and Development of New Antibiotics for Drug-Resistant Bacterial Infections, Including Tuberculosis; WHO/EMP/IAU/2017.12; World Health Organization, 2017.
  - (29) Ghai, I.; Ghai, S. Understanding Antibiotic Resistance via Outer Membrane Permeability. *Infect. Drug Resist.* **2018**, 11, 523-530. <https://doi.org/10.2147/IDR.S156995>.
  - (30) Kamio, Y.; Nikaido, H. Outer Membrane of Salmonella Typhimurium: Accessibility of Phospholipid Head Groups to Phospholipase C and Cyanogen Bromide Activated Dextran in the External Medium. *Biochemistry* **1976**, 15 (12), 2561-2570. <https://doi.org/10.1021/bi00657a012>.
  - (31) Kadner, R. J. Cytoplasmic: Membrane. In F. C. Neidhardt, R. Curtiss III, J. L. Ingraham, E. C. C. Lin, K. B. Low, B. Magasanik, W. S. Reznikoff, M. Riley, M. Schaechter, and H. E. Umbarger (ed.) Cytoplasmic membrane. In *Escherichia coli and Salmonella: Cellular and Molecular Biology*; American Society for Microbiology Press: Washington, D.C., 1996; Vol. I, pp 58-87.
  - (32) Vaara, M. Agents That Increase the Permeability of the Outer Membrane. *Microbiol. Rev.* **1992**, 56 (3), 395-411.
  - (33) Poole, K. Efflux-Mediated Antimicrobial Resistance. *J. Antimicrob. Chemother.* **2005**, 56 (1), 20-51.

- (34) Robinson, J. A. Folded Synthetic Peptides and Other Molecules Targeting Outer Membrane Protein Complexes in Gram-Negative Bacteria. *Front. Chem.* **2019**, 7, 45. <https://doi.org/10.3389/fchem.2019.00045>.
- (35) Högenauer, G.; Woisetschlager, M. A Diazaborine Derivative Inhibits Lipopolysaccharide Biosynthesis. *Nature* **1981**, 293 (5834), 662–664. <https://doi.org/10.1038/293662a0>.
- (36) Onishi, H. R.; Pelak, B. A.; Gerckens, L. S.; Silver, L. L.; Kahan, F. M.; Chen, M.-H.; Patchett, A. A.; Galloway, S. M.; Hyland, S. A.; Anderson, M. S.; Raetz, C. R. H. Antibacterial Agents That Inhibit Lipid a Biosynthesis. *Science* **1996**, 274 (5289), 980–982.
- (37) Hammond, S. M.; Claesson, A.; Jansson, A. M.; Larsson, L.-G.; Pring, B. G.; Town, C. M.; Ekström, B. A New Class of Synthetic Antibacterials Acting on Lipopolysaccharide Biosynthesis. *Nature* **1987**, 327 (6124), 730–732. <https://doi.org/10.1038/327730a0>.
- (38) Imai, Y.; Meyer, K. J.; Iinishi, A.; Favre-Godal, Q.; Green, R.; Manuse, S.; Caboni, M.; Mori, M.; Niles, S.; Ghiglieri, M.; Honrao, C.; Ma, X.; Guo, J. J.; Makriyannis, A.; Linares-Otoya, L.; Böhringer, N.; Wuisan, Z. G.; Kaur, H.; Wu, R.; Mateus, A.; Typas, A.; Savitski, M. M.; Espinoza, J. L.; O'Rourke, A.; Nelson, K. E.; Hiller, S.; Noinaj, N.; Schäberle, T. F.; D'Onofrio, A.; Lewis, K. A New Antibiotic Selectively Kills Gram-Negative Pathogens. *Nature* **2019**, 576 (7787), 459–464. <https://doi.org/10.1038/s41586-019-1791-1>.
- (39) Luther, A.; Urfer, M.; Zahn, M.; Müller, M.; Wang, S.-Y.; Mondal, M.; Vitale, A.; Hartmann, J.-B.; Sharpe, T.; Monte, F. L.; Kocherla, H.; Cline, E.; Pessi, G.; Rath, P.; Modaresi, S. M.; Chiquet, P.; Stiegeler, S.; Verbree, C.; Remus, T.; Schmitt, M.; Kolopp, C.; Westwood, M.-A.; Desjonquères, N.; Brabet, E.; Hell, S.; LePoupon, K.; Vermeulen, A.; Jaisson, R.; Rithié, V.; Upert, G.; Lederer, A.; Zbinden, P.; Wach, A.; Moehle, K.; Zerbe, K.; Locher, H. H.; Bernardini, F.; Dale, G. E.; Eberl, L.; Wollscheid, B.; Hiller, S.; Robinson, J. A.; Obrecht, D. Chimeric Peptidomimetic Antibiotics against Gram-Negative Bacteria. *Nature* **2019**, 576 (7787), 452–458. <https://doi.org/10.1038/s41586-019-1665-6>.
- (40) Zähler, H.; Diddens, H.; Keller-Schierlein, W.; Nägeli, H. U. Some Experiments with Semisynthetic Sideromycins. *Jpn. J. Antibiot.* **1977**, 30 Suppl, 201–206.
- (41) Arisawa, M.; Sekine, Y.; Shimizu, S.; Takano, H.; Angehrn, P.; Then, R. L. In Vitro and in Vivo Evaluation of Ro 09-1428, a New Parenteral Cephalosporin with High Antipseudomonal Activity. *Antimicrob. Agents Chemother.* **1991**, 35 (4), 653–659. <https://doi.org/10.1128/AAC.35.4.653>.
- (42) Möllmann, U.; Heinisch, L.; Bauernfeind, A.; Köhler, T.; Ankel-Fuchs, D. Siderophores as Drug Delivery Agents: Application of the “Trojan Horse” Strategy. *BioMetals* **2009**, 22 (4), 615–624. <https://doi.org/10.1007/s10534-009-9219-2>.
- (43) Baym, M.; Stone, L. K.; Kishony, R. Multidrug Evolutionary Strategies to Reverse Antibiotic Resistance. *Science* **2016**, 351 (6268), aad3292. <https://doi.org/10.1126/science.aad3292>.
- (44) Brown, E. D.; Wright, G. D. Antibacterial Drug Discovery in the Resistance Era. *Nature* **2016**, 529 (7586), 336–343. <https://doi.org/10.1038/nature17042>.
- (45) Van Bambeke, F.; Pagès, J.-M.; Lee, V. J. Inhibitors of Bacterial Efflux Pumps as Adjuvants in Antibiotic Treatments and Diagnostic Tools for Detection of Resistance by Efflux. *Recent Patents Anti-Infect. Drug Disc.* **2006**, 1 (2), 157–175. <https://doi.org/10.2174/15748910677452692>.
- (46) Pagès, J.-M.; Amaral, L. Mechanisms of Drug Efflux and Strategies to Combat Them: Challenging the Efflux Pump of Gram-Negative Bacteria. *Biochim. Biophys. Acta BBA - Proteins Proteomics* **2009**, 1794 (5), 826–833. <https://doi.org/10.1016/j.bbapap.2008.12.011>.
- (47) Blanco, P.; Sanz-García, F.; Hernando-Amado, S.; Martínez, J. L.; Alcalde-Rico, M. The Development of Efflux Pump Inhibitors to Treat Gram-Negative Infections. *Expert Opin. Drug Discov.* **2018**, 13 (10), 919–931. <https://doi.org/10.1080/17460441.2018.1514386>.
- (48) Cox, G.; Wright, G. D. Intrinsic Antibiotic Resistance: Mechanisms, Origins, Challenges and Solutions. *Int. J. Med. Microbiol.* **2013**, 303 (6), 287–292. <https://doi.org/10.1016/j.ijmm.2013.02.009>.
- (49) Vaara, M.; Vaara, T. Sensitization of Gram-Negative Bacteria to Antibiotics and Complement by a Nontoxic Oligopeptide. *Nature* **1983**, 303 (5917), 526–528. <https://doi.org/10.1038/303526a0>.



- (50) Gadelli, A.; Hassan, K.-O.; Hakansson, A. P. Sensitizing Agents to Restore Antibiotic Resistance. In *Antibiotic Drug Resistance*; John Wiley & Sons, Ltd, 2019; pp 429–452. <https://doi.org/10.1002/9781119282549.ch17>.
- (51) Schweizer, F. Repurposing Antibiotics to Treat Resistant Gram-Negative Pathogens. In *Antibiotic Drug Resistance*; John Wiley & Sons, Ltd, 2019; pp 453–476. <https://doi.org/10.1002/9781119282549.ch18>.
- (52) Bernal, P.; Molina-Santiago, C.; Daddaoua, A.; Llamas, M. A. Antibiotic Adjuvants: Identification and Clinical Use. *Microb. Biotechnol.* **2013**, 6 (5), 445–449. <https://doi.org/10.1111/1751-7915.12044>.
- (53) Worthington, R. J.; Melander, C. Combination Approaches to Combat Multidrug-Resistant Bacteria. *Trends Biotechnol.* **2013**, 31 (3), 177–184. <https://doi.org/10.1016/j.tibtech.2012.12.006>.
- (54) Melander, R. J.; Melander, C. Antibiotic Adjuvants. In *Antibacterials: Volume I*; Fisher, J. F., Mobashery, S., Miller, M. J., Eds.; Topics in Medicinal Chemistry; Springer International Publishing: Cham, 2018; pp 89–118. [https://doi.org/10.1007/7355\\_2017\\_10](https://doi.org/10.1007/7355_2017_10).
- (55) Tyers, M.; Wright, G. D. Drug Combinations: A Strategy to Extend the Life of Antibiotics in the 21st century. *Nat. Rev. Microbiol.* **2019**, 17 (3), 141–155. <https://doi.org/10.1038/s41579-018-0141-x>.
- (56) Wright, G. D. Antibiotic Adjuvants: Rescuing Antibiotics from Resistance. *Trends Microbiol.* **2016**, 24 (11), 862–871. <https://doi.org/10.1016/j.tim.2016.06.009>.
- (57) Liu, Y.; Li, R.; Xiao, X.; Wang, Z. Antibiotic Adjuvants: An Alternative Approach to Overcome Multi-Drug Resistant Gram-Negative Bacteria. *Crit. Rev. Microbiol.* **2019**, 45 (3), 301–314. <https://doi.org/10.1080/1040841X.2019.1599813>.
- (58) Klobucar, K.; Brown, E. D. New Potentiators of Ineffective Antibiotics: Targeting the Gram-Negative Outer Membrane to Overcome Intrinsic Resistance. *Curr. Opin. Chem. Biol.* **2022**, 66, 102099. <https://doi.org/10.1016/j.cbpa.2021.102099>.
- (59) Savage, P. B. Multidrug-Resistant Bacteria: Overcoming Antibiotic Permeability Barriers of Gram-Negative Bacteria. *Ann. Med.* **2001**, 33 (3), 167–171. <https://doi.org/10.3109/07853890109002073>.
- (60) Nikaido, H.; Vaara, M. Molecular Basis of Bacterial Outer Membrane Permeability. *Microbiol. Rev.* **1985**, 49 (1), 1–32. <https://doi.org/10.1128/mr.49.1.1-32.1985>.
- (61) Hancock, R. E. Alterations in Outer Membrane Permeability. *Annu. Rev. Microbiol.* **1984**, 38, 237–264. <https://doi.org/10.1146/annurev.mi.38.100184.001321>.
- (62) Douafer, H.; Andrieu, V.; Phanstiel, O.; Brunel, J. M. Antibiotic Adjuvants: Make Antibiotics Great Again! *J. Med. Chem.* **2019**, 62 (19), 8665–8681. <https://doi.org/10.1021/acs.jmedchem.8b01781>.
- (63) Zabawa, T. P.; Pucci, M. J.; Parr, T. R.; Lister, T. Treatment of Gram-Negative Bacterial Infections by Potentiation of Antibiotics. *Curr. Opin. Microbiol.* **2016**, 33, 7–12. <https://doi.org/10.1016/j.mib.2016.05.005>.
- (64) Blankson, G.; Parhi, A. K.; Kaul, M.; Pilch, D. S.; LaVoie, E. J. Structure-Activity Relationships of Potentiators of the Antibiotic Activity of Clarithromycin against *Escherichia Coli*. *Eur. J. Med. Chem.* **2019**, 178, 30–38. <https://doi.org/10.1016/j.ejmech.2019.05.075>.
- (65) Giacometti, A.; Cirioni, O.; Del Prete, M. S.; Paggi, A. M.; D'Errico, M. M.; Scalise, G. Combination Studies between Polycationic Peptides and Clinically Used Antibiotics against Gram-Positive and Gram-Negative Bacteria. *Peptides* **2000**, 21 (8), 1155–1160. [https://doi.org/10.1016/S0196-9781\(00\)00254-0](https://doi.org/10.1016/S0196-9781(00)00254-0).
- (66) Belanger, C. R.; Lee, A. H.-Y.; Pletzer, D.; Dhillon, B. K.; Falsafi, R.; Hancock, R. E. W. Identification of Novel Targets of Azithromycin Activity against *Pseudomonas Aeruginosa* Grown in Physiologically Relevant Media. *Proc. Natl. Acad. Sci.* **2020**, 117 (52), 33519–33529. <https://doi.org/10.1073/pnas.2007626117>.
- (67) Maisuria, V. B.; Okshevsky, M.; Déziel, E.; Tufenkji, N. Proanthocyanidin Interferes with Intrinsic Antibiotic Resistance Mechanisms of Gram-Negative Bacteria. *Adv. Sci. Wein. Baden-Wurt. Ger.* **2019**, 6 (15), 1802333. <https://doi.org/10.1002/adv.201802333>.
- (68) Rahman, Md. S.; Choi, Y. H.; Choi, Y. S.; Yoo, J. C. Glycin-Rich Antimicrobial Peptide YD1 from *B. Amyloliquefaciens*, Induced Morphological Alteration in and Showed Affinity for

- Plasmid DNA of *E. Coli*. *AMB Express* **2017**, 7 (1), 8. <https://doi.org/10.1186/s13568-016-0315-8>.
- (69) Subratti, A.; Ramkisson, A.; Lalgee, L. J.; Jalsa, N. K. Synthesis and Evaluation of the Antibiotic-Adjuvant Activity of Carbohydrate-Based Phosphoramidate Derivatives. *Carbohydr. Res.* **2021**, 500, 108216. <https://doi.org/10.1016/j.carres.2020.108216>.
  - (70) Baker, K. R.; Jana, B.; Hansen, A. M.; Vissing, K. J.; Nielsen, H. M.; Franzky, H.; Guardabassi, L. Repurposing Azithromycin and Rifampicin against Gram-Negative Pathogens by Combination with Peptide Potentiators. *Int. J. Antimicrob. Agents* **2019**, 53 (6), 868–872. <https://doi.org/10.1016/j.ijantimicag.2018.10.025>.
  - (71) Faure, M.-E. Engineering Therapies against *Pseudomonas Aeruginosa* Based on Iron Chelation. Ph.D., King's College London, 2021.
  - (72) Lee, H.; Hwang, J. S.; Lee, and D. G. Periplanetasin-2 Enhances the Antibacterial Properties of Vancomycin or Chloramphenicol in *Escherichia Coli*. *J. Microbiol. Biotechnol.* **2021**, 31 (2), 189–196. <https://doi.org/10.4014/jmb.2010.10058>.
  - (73) Domalaon, R.; Sanchak, Y.; Koskei, L. C.; Lyu, Y.; Zhanel, G. G.; Arthur, G.; Schweizer, F. Short Proline-Rich Lipopeptide Potentiates Minocycline and Rifampin against Multidrug- and Extensively Drug-Resistant *Pseudomonas Aeruginosa*. *Antimicrob. Agents Chemother.* **2018**, 62 (4), e02374–17. <https://doi.org/10.1128/AAC.02374-17>.
  - (74) Mangoni, M.; Rinaldi, A.; Di Giulio, A.; Giuseppina, M.; Bozzi, A.; D.Barra; Simmaco, M. Structure-Function Relationships of Temporins, Small Antimicrobial Peptides from Amphibian Skin. *Eur J Biochem* **2000**, 267 (5), 1447–1454. <https://doi.org/10.1046/j.1432-1327.2000.01143.x>.
  - (75) Liu, J.; Chen, F.; Wang, X.; Peng, H.; Zhang, H.; Wang, K.-J. The Synergistic Effect of Mud Crab Antimicrobial Peptides Sphistin and Sph12–38 With Antibiotics Azithromycin and Rifampicin Enhances Bactericidal Activity Against *Pseudomonas Aeruginosa*. *Front. Cell. Infect. Microbiol.* **2020**, 10, 572849. <https://doi.org/10.3389/fcimb.2020.572849>.
  - (76) Almaaytah, A.; Qaoud, M. T.; Abualhaijaa, A.; Al-Balas, Q.; Alzoubi, K. H. Hybridization and Antibiotic Synergism as a Tool for Reducing the Cytotoxicity of Antimicrobial Peptides. *Infect. Drug Resist.* **2018**, 11, 835–847. <https://doi.org/10.2147/IDR.S166236>.
  - (77) Taylor, P. L.; Rossi, L.; De Pascale, G.; Wright, G. D. A Forward Chemical Screen Identifies Antibiotic Adjuvants in *Escherichia Coli*. *ACS Chem. Biol.* **2012**, 7 (9), 1547–1555. <https://doi.org/10.1021/cb300269g>.
  - (78) Wang, G.; Brunel, J.-M.; Bolla, J.-M.; Van Bambeke, F. The Polyaminoisoprenyl Potentiator NV716 Revives Old Disused Antibiotics against Intracellular Forms of Infection by *Pseudomonas Aeruginosa*. *Antimicrob. Agents Chemother.* **2021**, 65 (3), e02028–20. <https://doi.org/10.1128/AAC.02028-20>.
  - (79) Borselli, D.; Blanchet, M.; Bolla, J.; Muth, A.; Skrubber, K.; Phanstiel, O.; Brunel, J. M. Motuporamine Derivatives as Antimicrobial Agents and Antibiotic Enhancers against Resistant Gram-Negative Bacteria. *Chembiochem* **2017**, 18 (3), 276–283. <https://doi.org/10.1002/cbic.201600532>.
  - (80) Lamers, R. P.; Cavallari, J. F.; Burrows, L. L. The Efflux Inhibitor Phenylalanine-Arginine Beta-Naphthylamide (PAβN) Permeabilizes the Outer Membrane of Gram-Negative Bacteria. *PLOS ONE* **2013**, 8 (3), e060666. <https://doi.org/10.1371/journal.pone.0060666>.
  - (81) Kaur, U. J.; Chopra, A.; Preet, S.; Raj, K.; Kondepudi, K. K.; Gupta, V.; Rishi, P. Potential of 1-(1-Naphthylmethyl)-Piperazine, an Efflux Pump Inhibitor against Cadmium-Induced Multidrug Resistance in *Salmonella Enterica* Serovar Typhi as an Adjunct to Antibiotics. *Braz. J. Microbiol.* **2021**, 52 (3), 1303–1313. <https://doi.org/10.1007/s42770-021-00492-5>.
  - (82) Blankson, G. A.; Parhi, A. K.; Kaul, M.; Pilch, D. S.; LaVoie, E. J. Advances in the Structural Studies of Antibiotic Potentiators against *Escherichia Coli*. *Bioorg. Med. Chem.* **2019**, 27 (15), 3254–3278. <https://doi.org/10.1016/j.bmc.2019.06.003>.
  - (83) Hart, E. M.; Mitchell, A. M.; Konovalova, A.; Grabowicz, M.; Sheng, J.; Han, X.; Rodriguez-Rivera, F. P.; Schwaid, A. G.; Malinverni, J. C.; Balibar, C. J.; Bodea, S.; Si, Q.; Wang, H.; Homsher, M. F.; Painter, R. E.; Ogawa, A. K.; Sutterlin, H.; Roemer, T.; Black, T. A.; Rothman, D. M.; Walker, S. S.; Silhavy, T. J. A Small-Molecule Inhibitor of BamA Impervious to Efflux

- and the Outer Membrane Permeability Barrier. *Proc. Natl. Acad. Sci.* **2019**, 116 (43), 21748–21757. <https://doi.org/10.1073/pnas.1912345116>.
- (84) Muheim, C.; Götzke, H.; Eriksson, A. U.; Lindberg, S.; Lauritsen, I.; Nørholm, M. H. H.; Daley, D. O. Increasing the Permeability of Escherichia Coli Using MAC13243. *Sci. Rep.* **2017**, 7 (1), 17629. <https://doi.org/10.1038/s41598-017-17772-6>.
  - (85) Kotzialampou, A.; Protonotariou, E.; Skoura, L.; Sivropoulou, A. Synergistic Antibacterial and Antibiofilm Activity of the MreB Inhibitor A22 Hydrochloride in Combination with Conventional Antibiotics against Pseudomonas Aeruginosa and Escherichia Coli Clinical Isolates. *Int. J. Microbiol.* **2021**, 2021, e3057754. <https://doi.org/10.1155/2021/3057754>.
  - (86) Heesterbeek, D. a. C.; Martin, N. I.; Velthuisen, A.; Duijst, M.; Ruyken, M.; Wubbolts, R.; Rooijakkers, S. H. M.; Bardool, B. W. Complement-Dependent Outer Membrane Perturbation Sensitizes Gram-Negative Bacteria to Gram-Positive Specific Antibiotics. *Sci. Rep.* **2019**, 9 (1), 3074. <https://doi.org/10.1038/s41598-019-38577-9>.
  - (87) Ellison, R. T.; Giehl, T. J.; LaForce, F. M. Damage of the Outer Membrane of Enteric Gram-Negative Bacteria by Lactoferrin and Transferrin. *Infect. Immun.* **1988**, 56 (11), 2774–2781. <https://doi.org/10.1128/iai.56.11.2774-2781.1988>.
  - (88) Weiss, J.; Victor, M.; Elsbach, P. Role of Charge and Hydrophobic Interactions in the Action of Bactericidal/Permeability-Increasing Protein of Neutrophils on Gram-Negative Bacteria. *J. Clin. Invest.* **1983**, 71 (3), 540–549. <https://doi.org/10.1172/JCI110798>.
  - (89) Barman, S.; Mukherjee, S.; Ghosh, S.; Haldar, J. Amino-Acid-Conjugated Polymer-Rifampicin Combination: Effective at Tackling Drug-Resistant Gram-Negative Clinical Isolates. *ACS Appl. Bio Mater.* **2019**, 2 (12), 5404–5414. <https://doi.org/10.1021/acsabm.9b00732>.
  - (90) Kim, J.-H.; Yu, D.; Eom, S.-H.; Kim, S.-H.; Oh, J.; Jung, W.-K.; Kim, Y.-M. Synergistic Antibacterial Effects of Chitosan-Caffeic Acid Conjugate against Antibiotic-Resistant Acne-Related Bacteria. *Mar. Drugs* **2017**, 15 (6), 167. <https://doi.org/10.3390/md15060167>.
  - (91) Je, J.-Y.; Kim, S.-K. Chitosan Derivatives Killed Bacteria by Disrupting the Outer and Inner Membrane. *J. Agric. Food Chem.* **2006**, 54 (18), 6629–6633. <https://doi.org/10.1021/jf061310p>.
  - (92) Qiao, J.; Purro, M.; Liu, Z.; Xiong, M. P. Effects of Polyethylen Glycol-Desferrioxamine:Gallium Conjugates on Pseudomonas Aeruginosa Outer Membrane Permeability and Vancomycin Potentiation. *Mol. Pharm.* **2021**, 18 (2), 735–742. <https://doi.org/10.1021/acs.molpharmaceut.0c00820>.
  - (93) Qiao, J.; Liu, Z.; Purro, M.; Xiong, M. P. Antibacterial and Potentiation Properties of Charge-Optimized Polyrotaxanes for Combating Opportunistic Bacteria. *J. Mater. Chem. B* **2018**, 6 (33), 5353–5361. <https://doi.org/10.1039/C8TB01610K>.
  - (94) Tantisuwanno, C.; Dang, F.; Bender, K.; Spencer, J. D.; Jennings, M. E.; Barton, H. A.; Joy, A. Synergism between Rifampicin and Cationic Polyurethanes Overcomes Intrinsic Resistance of Escherichia Coli. *Biomacromolecules* **2021**, 22 (7), 2910–2920. <https://doi.org/10.1021/acs.biomac.1c00306>.
  - (95) Livne, L.; Epand, R. F.; Papahadjopoulos-Sternberg, B.; Epand, R. M.; Mor, A. OAK-Based Cochleates as a Novel Approach to Overcome Multidrug Resistance in Bacteria. *FASEB J.* **2010**, 24 (12), 5092–5101. <https://doi.org/10.1096/fj.10.167809>.
  - (96) Si, Z.; Hou, Z.; Vikhe, Y. S.; Thappeta, K. R. V.; Marimuthu, K.; De, P. P.; Ng, O. T.; Li, P.; Zhu, Y.; Pethe, K.; Chan-Park, M. B. Antimicrobial Effect of a Novel Chitosan Derivative and Its Synergistic Effect with Antibiotics. *ACS Appl. Mater. Interfaces* **2021**, 13 (2), 3237–3245. <https://doi.org/10.1021/acsami.0c20881>.
  - (97) Danner, R. L.; Joiner, K. A.; Rubin, M.; Patterson, W. H.; Johnson, N.; Ayers, K. M.; Parrillo, J. E. Purification, Toxicity, and Antiendotoxin Activity of Polymyxin B Nonapeptide. *Antimicrob. Agents Chemother.* **1989**, 33 (9), 1428–1434. <https://doi.org/10.1128/AAC.33.9.1428>.
  - (98) Vaara, M. The Outer Membrane Permeability-Increasing Action of Linear Analogues of Polymyxin B Nonapeptide. *Drugs Exp. Clin. Res.* **1991**, 17 (9), 437–443.
  - (99) Vaara, M.; Fox, J.; Loidl, G.; Siikanen, O.; Apajalahti, J.; Hansen, F.; Frimodt-Møller, N.; Nagai, J.; Takano, M.; Vaara, T. Novel Polymyxin Derivatives Carrying Only Three Positive Charges

- Are Effective Antibacterial Agents. *Antimicrob. Agents Chemother.* **2008**, 52 (9), 3229–3236. <https://doi.org/10.1128/AAC.00405-08>.
- (100) Vaara, M.; Siikanen, O.; Apajalahti, J.; Fox, J.; Frimodt-Møller, N.; He, H.; Poudyal, A.; Li, J.; Nation, R. L.; Vaara, T. A Novel Polymyxin Derivative That Lacks the Fatty Acid Tail and Carries Only Three Positive Charges Has Strong Synergism with Agents Excluded by the Intact Outer Membrane. *Antimicrob. Agents Chemother.* **2010**, 54 (8), 3341–3346. <https://doi.org/10.1128/AAC.01439-09>.
- (101) Vaara, M. New Approaches in Peptide Antibiotics. *Curr. Opin. Pharmacol.* **2009**, 9 (5), 571–576. <https://doi.org/10.1016/j.coph.2009.08.002>.
- (102) MacNair, C. R.; Stokes, J. M.; Carfrae, L. A.; Fiebig-Comyn, A. A.; Coombes, B. K.; Mulvey, M. R.; Brown, E. D. Overcoming Mcr-1 Mediated Colistin Resistance with Colistin in Combination with Other Antibiotics. *Nat. Commun.* **2018**, 9 (1), 458. <https://doi.org/10.1038/s41467-018-02875-z>.
- (103) Tyrrell, J. M.; Aboklaish, A. F.; Walsh, T. R.; Vaara, M. The Polymyxin Derivative NAB739 Is Synergistic with Several Antibiotics against Polymyxin-Resistant Strains of *Escherichia Coli*, *Klebsiella Pneumoniae* and *Acinetobacter Baumannii*. *Peptides* **2019**, 112, 149–153. <https://doi.org/10.1016/j.peptides.2018.12.006>.
- (104) Kimura, Y.; Matsunaga, H.; Vaara, M. Polymyxin B Octapeptide and Polymyxin B Heptapeptide Are Potent Outer Membrane Permeability-Increasing Agents. *J. Antibiot. (Tokyo)* **1992**, 45 (5), 742–749. <https://doi.org/10.7164/antibiotics.45.742>.
- (105) Corbett, D.; Wise, A.; Langley, T.; Skinner, K.; Trimby, E.; Birchall, S.; Dorali, A.; Sandiford, S.; Williams, J.; Warn, P.; Vaara, M.; Lister, T. Potentiation of Antibiotic Activity by a Novel Cationic Peptide: Potency and Spectrum of Activity of SPR741. *Antimicrob. Agents Chemother.* **2017**, 61 (8), e00200–17. <https://doi.org/10.1128/AAC.00200-17>.
- (106) Domalaon, R.; Berry, L.; Tays, Q.; Zhanel, G. G.; Schweizer, F. Development of Dilipid Polymyxins: Investigation on the Effect of Hydrophobicity through Its Fatty Acyl Component. *Bioorganic Chem.* **2018**, 80, 639–648. <https://doi.org/10.1016/j.bioorg.2018.07.018>.
- (107) Kanazawa, K.; Sato, Y.; Ohki, K.; Okimura, K.; Uchida, Y.; Shindo, M.; Sakura, N. Contribution of Each Amino Acid Residue in Polymyxin B3 to Antimicrobial and Lipopolysaccharide Binding Activity. *Chem. Pharm. Bull. (Tokyo)* **2009**, 57 (3), 240–244. <https://doi.org/10.1248/cpb.57.240>.
- (108) Seo, M.-D.; Won, H.-S.; Kim, J.-H.; Mishig-Ochir, T.; Lee, B.-J. Antimicrobial Peptides for Therapeutic Applications: A Review. *Molecules* **2012**, 17 (10), 12276–12286. <https://doi.org/10.3390/molecules171012276>.
- (109) Adessi, C.; Soto, C. Converting a Peptide into a Drug: Strategies to Improve Stability and Bioavailability. *Curr. Med. Chem.* **2002**, 9 (9), 963–978. <https://doi.org/10.2174/0929867024606731>.
- (110) Bruckdorfer, T.; Marder, O.; Albericio, F. From Production of Peptides in Milligram Amounts for Research to Multi-Tons Quantities for Drugs of the Future. *Curr. Pharm. Biotechnol.* **2004**, 5 (1), 29–43. <https://doi.org/10.2174/1389201043489620>.
- (111) Ovidia, O.; Greenberg, S.; Laufer, B.; Gilon, C.; Hoffman, A.; Kessler, H. Improvement of Drug-like Properties of Peptides: The Somatostatin Paradigm. *Expert Opin. Drug Discov.* **2010**, 5 (7), 655–671. <https://doi.org/10.1517/17460441.2010.493935>.
- (112) Godballe, T.; Nilsson, L. L.; Petersen, P. D.; Jenssen, H. Antimicrobial  $\beta$ -Peptides and  $\alpha$ -Peptoids. *Chem. Biol. Drug Des.* **2011**, 77 (2), 107–116. <https://doi.org/10.1111/j.1747-0285.2010.01067.x>.
- (113) Zhang, L.; Bulaj, G. Converting Peptides into Drug Leads by Lipidation. *Curr. Med. Chem.* **2012**, 19 (11), 1602–1618. <https://doi.org/10.2174/092986712799945003>.
- (114) Gentilucci, L.; De Marco, R.; Cerisoli, L. Chemical Modifications Designed to Improve Peptide Stability: Incorporation of Non-Natural Amino Acids, Pseudo-Peptide Bonds, and Cyclization. *Curr. Pharm. Des.* **2010**, 16 (28), 3185–3203. <https://doi.org/10.2174/138161210793292555>.

- (115) deGruyter, J. N.; Malins, L. R.; Baran, P. S. Residue-Specific Peptide Modification: A Chemist's Guide. *Biochemistry* **2017**, 56 (30), 3863–3873. <https://doi.org/10.1021/acs.biochem.7b00536>.
- (116) Fox, J. L. Antimicrobial Peptides Stage a Comeback. *Nat. Biotechnol.* **2013**, 31 (5), 379–382. <https://doi.org/10.1038/nbt.2572>.
- (117) Zhu, Y.; Hao, W.; Wang, X.; Ouyang, J.; Deng, X.; Yu, H.; Wang, Y. Antimicrobial Peptides, Conventional Antibiotics, and Their Synergistic Utility for the Treatment of Drug-Resistant Infections. *Med. Res. Rev.* n/a (n/a). <https://doi.org/10.1002/med.21879>.
- (118) Hancock, R. E. W.; Sahl, H.-G. Antimicrobial and Host-Defense Peptides as New Anti-Infective Therapeutic Strategies. *Nat. Biotechnol.* **2006**, 24 (12), 1551–1557. <https://doi.org/10.1038/nbt1267>.
- (119) Zompra, A. A.; Galanis, A. S.; Werbitzky, O.; Albericio, F. Manufacturing Peptides as Active Pharmaceutical Ingredients. *Future Med. Chem.* **2009**, 1 (2), 361–377. <https://doi.org/10.4155/fmc.09.23>.
- (120) Albericio, F.; Kruger, H. G. Therapeutic Peptides. *Future Med. Chem.* **2012**, 4 (12), 1527–1531. <https://doi.org/10.4155/fmc.12.94>.
- (121) Bals, R.; Wilson, J. M. Cathelicidins - a Family of Multifunctional Antimicrobial Peptides. *Cell. Mol. Life Sci. CMLS* **2003**, 60 (4), 711–720. <https://doi.org/10.1007/s00018-003-2186-9>.
- (122) Nijnik, A.; Hancock, R. E. The Roles of Cathelicidin LL-37 in Immune Defences and Novel Clinical Applications. *Curr. Opin. Hematol.* **2009**, 16 (1), 41–47. <https://doi.org/10.1097/MOH.0b013e32831ac517>.
- (123) Hancock, R. E. W.; Haney, E. F.; Gill, E. E. The Immunology of Host Defence Peptides: Beyond Antimicrobial Activity. *Nat. Rev. Immunol.* **2016**, 16 (5), 321–334. <https://doi.org/10.1038/nri.2016.29>.
- (124) Bowdish, D. M. E.; Davidson, D. J.; Hancock, R. E. W. Immunomodulatory Properties of Defensins and Cathelicidins. In *Antimicrobial Peptides and Human Disease*; Shafer, W. M., Ed.; Current Topics in Microbiology and Immunology; Springer: Berlin, Heidelberg, 2006; pp 27–66. [https://doi.org/10.1007/3-540-29916-5\\_2](https://doi.org/10.1007/3-540-29916-5_2).
- (125) Scott, M. G.; Davidson, D. J.; Gold, M. R.; Bowdish, D.; Hancock, R. E. W. The Human Antimicrobial Peptide LL-37 Is a Multifunctional Modulator of Innate Immune Responses. *J. Immunol.* **2002**, 169 (7), 3883–3891. <https://doi.org/10.4049/jimmunol.169.7.3883>.
- (126) Gudmundsson, G. H.; Agerberth, B.; Odeberg, J.; Bergman, T.; Olsson, B.; Salcedo, R. The Human Gene FALL39 and Processing of the Cathelin Precursor to the Antibacterial Peptide LL-37 in Granulocytes. *Eur. J. Biochem.* **1996**, 238 (2), 325–332. <https://doi.org/10.1111/j.1432-1033.1996.0325z.x>.
- (127) Oren, Z.; Lerman, J. C.; Gudmundsson, G. H.; Agerberth, B.; Shai, Y. Structure and Organization of the Human Antimicrobial Peptide LL-37 in Phospholipid Membranes: Relevance to the Molecular Basis for Its Non-Cell-Selective Activity. *Biochem. J.* **1999**, 341 (Pt 3), 501–513.
- (128) Agerberth, B.; Gunne, H.; Odeberg, J.; Kogner, P.; Boman, H. G.; Gudmundsson, G. H. FALL-39, a Putative Human Peptide Antibiotic, Is Cysteine-Free and Expressed in Bone Marrow and Testis. *Proc. Natl. Acad. Sci.* **1995**, 92 (1), 195–199. <https://doi.org/10.1073/pnas.92.1.195>.
- (129) Mohammed, I.; Said, D. G.; Nubile, M.; Mastropasqua, L.; Dua, H. S. Cathelicidin-Derived Synthetic Peptide Improves Therapeutic Potential of Vancomycin Against *Pseudomonas Aeruginosa*. *Front. Microbiol.* **2019**, 10, 2190. <https://doi.org/10.3389/fmicb.2019.02190>.
- (130) Xia, Y.; Cebrián, R.; Xu, C.; Jong, A. de; Wu, W.; Kuipers, O. P. Elucidating the Mechanism by Which Synthetic Helper Peptides Sensitize *Pseudomonas Aeruginosa* to Multiple Antibiotics. *PLOS Pathog.* **2021**, 17 (9), e1009909. <https://doi.org/10.1371/journal.ppat.1009909>.
- (131) Li, Q.; Cebrián, R.; Montalbán-López, M.; Ren, H.; Wu, W.; Kuipers, O. P. Outer-Membrane-Acting Peptides and Lipid II-Targeting Antibiotics Cooperatively Kill Gram-Negative Pathogens. *Commun. Biol.* **2021**, 4 (1), 1–11. <https://doi.org/10.1038/s42003-020-01511-1>.

- (132) Cebrián, R.; Xu, C.; Xia, Y.; Wu, W.; Kuipers, O. P. The Cathelicidin-Derived Close-to-Nature Peptide D-11 Sensitises *Klebsiella Pneumoniae* to a Range of Antibiotics in Vitro, Ex Vivo and in Vivo. *Int. J. Antimicrob. Agents* **2021**, 58 (5), 106434. <https://doi.org/10.1016/j.ijantimicag.2021.106434>.
- (133) Soren, O.; Brinch, K. S.; Patel, D.; Liu, Y.; Liu, A.; Coates, A.; Hu, Y. Antimicrobial Peptide Novicidin Synergizes with Rifampin, Ceftriaxone, and Ceftazidime against Antibiotic-Resistant Enterobacteriaceae In Vitro. *Antimicrob. Agents Chemother.* **2015**, 59 (10), 6233–6240. <https://doi.org/10.1128/AAC.01245-15>.
- (134) Ruden, S.; Rieder, A.; Chis Ster, I.; Schwartz, T.; Mikut, R.; Hilpert, K. Synergy Pattern of Short Cationic Antimicrobial Peptides Against Multidrug-Resistant *Pseudomonas Aeruginosa*. *Front. Microbiol.* 2019, 10, 2740. <https://doi.org/10.3389/fmicb.2019.02740>.
- (135) Liu, F.; Wang, H.; Cao, S.; Jiang, C.; Hou, J. Characterization of Antibacterial Activity and Mechanisms of Two Linear Derivatives of Bactenecin. *LWT* **2019**, 107, 89–97. <https://doi.org/10.1016/j.lwt.2019.02.073>.
- (136) Hilpert, K.; Volkmer-Engert, R.; Walter, T.; Hancock, R. E. W. High-Throughput Generation of Small Antibacterial Peptides with Improved Activity. *Nat. Biotechnol.* **2005**, 23 (8), 1008–1012. <https://doi.org/10.1038/nbt1113>.
- (137) Wu, X.; Li, Z.; Li, X.; Tian, Y.; Fan, Y.; Yu, C.; Zhou, B.; Liu, Y.; Xiang, R.; Yang, L. Synergistic Effects of Antimicrobial Peptide DP7 Combined with Antibiotics against Multidrug-Resistant Bacteria. *Drug Des. Devel. Ther.* **2017**, 11, 939–946. <https://doi.org/10.2147/DDDT.S107195>.
- (138) Zhu, N.; Zhong, C.; Liu, T.; Zhu, Y.; Gou, S.; Bao, H.; Yao, J.; Ni, J. Newly Designed Antimicrobial Peptides with Potent Bioactivity and Enhanced Cell Selectivity Prevent and Reverse Rifampin Resistance in Gram-Negative Bacteria. *Eur. J. Pharm. Sci.* **2021**, 158, 105665. <https://doi.org/10.1016/j.ejps.2020.105665>.
- (139) Faccone, D.; Veliz, O.; Corso, A.; Noguera, M.; Martínez, M.; Payes, C.; Semorile, L.; Maffia, P. C. Antimicrobial Activity of de Novo Designed Cationic Peptides against Multi-Resistant Clinical Isolates. *Eur. J. Med. Chem.* **2014**, 71, 31–35. <https://doi.org/10.1016/j.ejmech.2013.10.065>.
- (140) Sánchez-Gómez, S.; Lamata, M.; Leiva, J.; Blondelle, S. E.; Jerala, R.; Andrä, J.; Brandenburg, K.; Lohner, K.; Moriyón, I.; Martínez-de-Tejada, G. Comparative Analysis of Selected Methods for the Assessment of Antimicrobial and Membrane-Permeabilizing Activity: A Case Study for Lactoferricin Derived Peptides. *BMC Microbiol.* **2008**, 8 (1), 196. <https://doi.org/10.1186/1471-2180-8-196>.
- (141) Sánchez-Gómez, S.; Japelj, B.; Jerala, R.; Moriyón, I.; Fernández Alonso, M.; Leiva, J.; Blondelle, S. E.; Andrä, J.; Brandenburg, K.; Lohner, K.; Martínez de Tejada, G. Structural Features Governing the Activity of Lactoferricin-Derived Peptides That Act in Synergy with Antibiotics against *Pseudomonas Aeruginosa* In Vitro and In Vivo. *Antimicrob. Agents Chemother.* **2011**, 55 (1), 218–228. <https://doi.org/10.1128/AAC.00904-10>.
- (142) Strøm, M. B.; Haug, B. E.; Rekdal, Ø.; Skar, M. L.; Stensen, W.; Svendsen, J. S. Important Structural Features of 15-Residue Lactoferricin Derivatives and Methods for Improvement of Antimicrobial Activity. *Biochem. Cell Biol.* **2002**, 80 (1), 65–74. <https://doi.org/10.1139/o01-236>.
- (143) Strøm, M. B.; Svendsen, J. S.; Rekdal, Ø. Antibacterial Activity of 15-Residue Lactoferricin Derivatives. *J. Pept. Res.* **2000**, 56 (5), 265–274. <https://doi.org/10.1034/j.1399-3011.2000.00770.x>.
- (144) Ulvatne, H.; Karoliussen, S.; Stiberg, T.; Rekdal, Ø.; Svendsen, J. S. Short Antibacterial Peptides and Erythromycin Act Synergically against *Escherichia Coli*. *J. Antimicrob. Chemother.* **2001**, 48 (2), 203–208. <https://doi.org/10.1093/jac/48.2.203>.
- (145) Rekdal, Ø.; Andersen, J.; Vorland, L. H.; Svendsen, J. S. Construction and Synthesis of Lactoferricin Derivatives with Enhanced Antibacterial Activity. *J. Pept. Sci.* **1999**, 5 (1), 32–45.
- (146) Saravanan, R.; Holdbrook, D. A.; Petrlova, J.; Singh, S.; Berglund, N. A.; Choong, Y. K.; Kjellström, S.; Bond, P. J.; Malmsten, M.; Schmidtchen, A. Structural Basis for Endotoxin

- Neutralisation and Anti-Inflammatory Activity of Thrombin-Derived C-Terminal Peptides. *Nat. Commun.* **2018**, 9 (1), 2762. <https://doi.org/10.1038/s41467-018-05242-0>.
- (147) Wesseling, C. M. J.; Wood, T. M.; Bertheussen, K.; Lok, S.; Martin, N. I. Thrombin-Derived Peptides Potentiate the Activity of Gram-Positive-Specific Antibiotics against Gram-Negative Bacteria. *Molecules* **2021**, 26 (7), 1954. <https://doi.org/10.3390/molecules26071954>.
- (148) Giacometti, A.; Cirioni, O.; Kamysz, W.; D'Amato, G.; Silvestri, C.; Prete, M. S. D.; Licci, A.; Riva, A.; Lukasiak, J.; Scalise, G. In Vitro Activity of the Histatin Derivative P-113 against Multidrug-Resistant Pathogens Responsible for Pneumonia in Immunocompromised Patients. *Antimicrob. Agents Chemother.* **2005**, 49 (3), 1249–1252. <https://doi.org/10.1128/AAC.49.3.1249-1252.2005>.
- (149) Sugiyama, K. Anti-Lipopolysaccharide Activity of Histatins, Peptides from Human Saliva. *Experientia* **1993**, 49 (12), 1095–1097. <https://doi.org/10.1007/BF01929920>.
- (150) Sajjan, U. S.; Tran, L. T.; Sole, N.; Rovaldi, C.; Akiyama, A.; Friden, P. M.; Forstner, J. F.; Rothstein, D. M. P-113D, an Antimicrobial Peptide Active against *Pseudomonas Aeruginosa*, Retains Activity in the Presence of Sputum from Cystic Fibrosis Patients. *Antimicrob. Agents Chemother.* **2001**, 45 (12), 3437–3444. <https://doi.org/10.1128/AAC.45.12.3437-3444.2001>.
- (151) Cirioni, O.; Giacometti, A.; Ghiselli, R.; Orlando, F.; Kamysz, W.; D'Amato, G.; Mocchegiani, F.; Lukasiak, J.; Silvestri, C.; Saba, V.; Scalise, G. Potential Therapeutic Role of Histatin Derivative P-113d in Experimental Rat Models of *Pseudomonas Aeruginosa* Sepsis. *J. Infect. Dis.* **2004**, 190 (2), 356–364. <https://doi.org/10.1086/421913>.
- (152) Yu, H.-Y.; Tu, C.-H.; Yip, B.-S.; Chen, H.-L.; Cheng, H.-T.; Huang, K.-C.; Lo, H.-J.; Cheng, J.-W. Easy Strategy To Increase Salt Resistance of Antimicrobial Peptides. *Antimicrob. Agents Chemother.* **2011**.
- (153) Chih, Y.-H.; Wang, S.-Y.; Yip, B.-S.; Cheng, K.-T.; Hsu, S.-Y.; Wu, C.-L.; Yu, H.-Y.; Cheng, J.-W. Dependence on Size and Shape of Non-Nature Amino Acids in the Enhancement of Lipopolysaccharide (LPS) Neutralizing Activities of Antimicrobial Peptides. *J. Colloid Interface Sci.* **2019**, 533, 492–502. <https://doi.org/10.1016/j.jcis.2018.08.042>.
- (154) Wu, C.-L.; Hsueh, J.-Y.; Yip, B.-S.; Chih, Y.-H.; Peng, K.-L.; Cheng, J.-W. Antimicrobial Peptides Display Strong Synergy with Vancomycin Against Vancomycin-Resistant *E. Faecium*, *S. Aureus*, and Wild-Type *E. Coli*. *Int. J. Mol. Sci.* **2020**, 21 (13), 4578. <https://doi.org/10.3390/ijms21134578>.
- (155) Cirioni, O.; Silvestri, C.; Ghiselli, R.; Orlando, F.; Riva, A.; Gabrielli, E.; Mocchegiani, F.; Cianforlini, N.; Trombetta, M. M. C.; Saba, V.; Scalise, G.; Giacometti, A. Therapeutic Efficacy of Buforin II and Rifampin in a Rat Model of *Acinetobacter Baumannii* Sepsis. *Crit. Care Med.* **2009**, 37 (4), 1403–1407. <https://doi.org/10.1097/CCM.0b013e31819c3e22>.
- (156) Marcellini, L.; Borro, M.; Gentile, G.; Rinaldi, A.; Stella, L.; Aimola, P.; Barra, D.; Mangoni, M. Esculentin-1b(1-18) - A Membrane-Active Antimicrobial Peptide That Synergizes with Antibiotics and Modifies the Expression Level of a Limited Number of Proteins in *Escherichia Coli*. *FEBS J.* **2009**, 276, 5647–5664. <https://doi.org/10.1111/j.1742-4658.2009.07257.x>.
- (157) Yenugu, S.; Narmadha, G. The Human Male Reproductive Tract Antimicrobial Peptides of the HE2 Family Exhibit Potent Synergy with Standard Antibiotics. *J. Pept. Sci.* **2010**, 16 (7), 337–341. <https://doi.org/10.1002/psc.1246>.
- (158) Gou, S.; Li, B.; Ouyang, X.; Ba, Z.; Zhong, C.; Zhang, T.; Chang, L.; Zhu, Y.; Zhang, J.; Zhu, N.; Zhang, Y.; Liu, H.; Ni, J. Novel Broad-Spectrum Antimicrobial Peptide Derived from Anoplin and Its Activity on Bacterial Pneumonia in Mice. *J. Med. Chem.* **2021**, 64 (15), 11247–11266. <https://doi.org/10.1021/acs.jmedchem.1c00614>.
- (159) Cirioni, O.; Silvestri, C.; Ghiselli, R.; Orlando, F.; Riva, A.; Mocchegiani, F.; Chiodi, L.; Castelletti, S.; Gabrielli, E.; Saba, V.; Scalise, G.; Giacometti, A. Protective Effects of the Combination of  $\alpha$ -Helical Antimicrobial Peptides and Rifampicin in Three Rat Models of *Pseudomonas Aeruginosa* Infection. *J. Antimicrob. Chemother.* **2008**, 62 (6), 1332–1338. <https://doi.org/10.1093/jac/dkn393>.

- (160) Konno, K.; Hisada, M.; Fontana, R.; Lorenzi, C. C. B.; Naoki, H.; Itagaki, Y.; Miwa, A.; Kawai, N.; Nakata, Y.; Yasuhara, T.; Ruggiero Neto, J.; de Azevedo, W. F.; Palma, M. S.; Nakajima, T. Anoplin, a Novel Antimicrobial Peptide from the Venom of the Solitary Wasp *Anoplius Samariensis*. *Biochim. Biophys. Acta BBA - Protein Struct. Mol. Enzymol.* **2001**, 1550 (1), 70–80. [https://doi.org/10.1016/S0167-4838\(01\)00271-0](https://doi.org/10.1016/S0167-4838(01)00271-0).
- (161) Yenugu, S.; Hamil, K. G.; Birse, C. E.; Ruben, S. M.; French, F. S.; Hall, S. H. Antibacterial Properties of the Sperm-Binding Proteins and Peptides of Human Epididymis 2 (HE2) Family; Salt Sensitivity, Structural Dependence and Their Interaction with Outer and Cytoplasmic Membranes of *Escherichia Coli*. *Biochem. J.* **2003**, 372 (2), 473–483. <https://doi.org/10.1042/bj20030225>.
- (162) Ajish, C.; Yang, S.; Kumar, S. D.; Shin, S. Y. Proadrenomedullin N-Terminal 20 Peptide (PAMP) and Its C-Terminal 12-Residue Peptide, PAMP(9–20): Cell Selectivity and Antimicrobial Mechanism. *Biochem. Biophys. Res. Commun.* **2020**, 527 (3), 744–750. <https://doi.org/10.1016/j.bbrc.2020.04.063>.
- (163) Kim, M. K.; Kang, N. H.; Ko, S. J.; Park, J.; Park, E.; Shin, D. W.; Kim, S. H.; Lee, S. A.; Lee, J. I.; Lee, S. H.; Ha, E. G.; Jeon, S. H.; Park, Y. Antibacterial and Antibiofilm Activity and Mode of Action of Magainin 2 against Drug-Resistant *Acinetobacter Baumannii*. *Int. J. Mol. Sci.* **2018**, 19 (10), 3041. <https://doi.org/10.3390/ijms19103041>.
- (164) Lee, E.; Shin, A.; Kim, Y. Anti-Inflammatory Activities of Cecropin a and Its Mechanism of Action. *Arch. Insect Biochem. Physiol.* **2015**, 88 (1), 31–44. <https://doi.org/10.1002/arch.21193>.
- (165) Scott, M. G.; Yan, H.; Hancock, R. E. W. Biological Properties of Structurally Related  $\alpha$ -Helical Cationic Antimicrobial Peptides. *Infect. Immun.* **1999**. <https://doi.org/10.1128/IAI.67.4.2005-2009.1999>.
- (166) Cochrane, S. A.; Vederas, J. C. Unacylated Tridecaptin A<sub>1</sub> Acts as an Effective Sensitiser of Gram-Negative Bacteria to Other Antibiotics. *Int. J. Antimicrob. Agents* **2014**, 44 (6), 493–499. <https://doi.org/10.1016/j.ijantimicag.2014.08.008>.
- (167) Cochrane, S. A.; Lohans, C. T.; Brandelli, J. R.; Mulvey, G.; Armstrong, G. D.; Vederas, J. C. Synthesis and Structure-Activity Relationship Studies of N-Terminal Analogues of the Antimicrobial Peptide Tridecaptin A<sub>1</sub>. *J. Med. Chem.* **2014**, 57 (3), 1127–1131. <https://doi.org/10.1021/jm401779d>.
- (168) Liu, Y.; Ding, S.; Shen, J.; Zhu, K. Nonribosomal Antibacterial Peptides That Target Multidrug-Resistant Bacteria. *Nat. Prod. Rep.* **2019**, 36 (4), 573–592. <https://doi.org/10.1039/C8NP00031J>.
- (169) Song, M.; Liu, Y.; Huang, X.; Ding, S.; Wang, Y.; Shen, J.; Zhu, K. A Broad-Spectrum Antibiotic Adjuvant Reverses Multidrug-Resistant Gram-Negative Pathogens. *Nat. Microbiol.* **2020**, 5 (8), 1040–1050. <https://doi.org/10.1038/s41564-020-0723-z>.
- (170) Slootweg, J. C.; van Schaik, T. B.; Quarles van Ufford, H. (Linda) C.; Breukink, E.; Liskamp, R. M. J.; Rijkers, D. T. S. Improving the Biological Activity of the Antimicrobial Peptide Anoplin by Membrane Anchoring through a Lipophilic Amino Acid Derivative. *Bioorg. Med. Chem. Lett.* **2013**, 23 (13), 3749–3752. <https://doi.org/10.1016/j.bmcl.2013.05.002>.
- (171) Wang, Y.; Chen, J.; Zheng, X.; Yang, X.; Ma, P.; Cai, Y.; Zhang, B.; Chen, Y. Design of Novel Analogues of Short Antimicrobial Peptide Anoplin with Improved Antimicrobial Activity. *J. Pept. Sci.* **2014**, 20 (12), 945–951. <https://doi.org/10.1002/psc.2705>.
- (172) Munk, J. K.; Ritz, C.; Flidner, F. P.; Frimodt-Møller, N.; Hansen, P. R. Novel Method To Identify the Optimal Antimicrobial Peptide in a Combination Matrix, Using Anoplin as an Example. *Antimicrob. Agents Chemother.* **2014**, 58 (2), 1063–1070. <https://doi.org/10.1128/AAC.02369-13>.
- (173) Libardo, M. D. J.; Nagella, S.; Lugo, A.; Pierce, S.; Angeles-Boza, A. M. Copper-Binding Tripeptide Motif Increases Potency of the Antimicrobial Peptide Anoplin via Reactive Oxygen Species Generation. *Biochem. Biophys. Res. Commun.* **2015**, 456 (1), 446–451. <https://doi.org/10.1016/j.bbrc.2014.11.104>.
- (174) Zhong, C.; Liu, T.; Gou, S.; He, Y.; Zhu, N.; Zhu, Y.; Wang, L.; Liu, H.; Zhang, Y.; Yao, J.; Ni, J. Design and Synthesis of New N-Terminal Fatty Acid Modified-Antimicrobial Peptide



- Analogues with Potent in Vitro Biological Activity. *Eur. J. Med. Chem.* **2019**, 182, 111636. <https://doi.org/10.1016/j.ejmech.2019.111636>.
- (175) Santamaría, C.; Larios, S.; Angulo, Y.; Pizarro-Cerda, J.; Gorvel, J.-P.; Moreno, E.; Lomonte, B. Antimicrobial Activity of Myotoxic Phospholipases A2 from Crotalid Snake Venoms and Synthetic Peptide Variants Derived from Their C-Terminal Region. *Toxicon* **2005**, 45 (7), 807–815. <https://doi.org/10.1016/j.toxicon.2004.09.012>.
- (176) Yu, H.-Y.; Huang, K.-C.; Yip, B.-S.; Tu, C.-H.; Chen, H.-L.; Cheng, H.-T.; Cheng, J.-W. Rational Design of Tryptophan-Rich Antimicrobial Peptides with Enhanced Antimicrobial Activities and Specificities. *ChemBioChem* **2010**, 11 (16), 2273–2282. <https://doi.org/10.1002/cbic.201000372>.
- (177) Chu, H.-L.; Yu, H.-Y.; Yip, B.-S.; Chih, Y.-H.; Liang, C.-W.; Cheng, H.-T.; Cheng, J.-W. Boosting Salt Resistance of Short Antimicrobial Peptides. *Antimicrob. Agents Chemother.* **2013**, 57 (8), 4050–4052. <https://doi.org/10.1128/AAC.00252-13>
- (178) Chih, Y.-H.; Lin, Y.-S.; Yip, B.-S.; Wei, H.-J.; Chu, H.-L.; Yu, H.-Y.; Cheng, H.-T.; Chou, Y.-T.; Cheng, J.-W. Ultrashort Antimicrobial Peptides with Antidotoxin Properties. *Antimicrob. Agents Chemother.* **2015**, 59 (8) 5052–5056. <https://doi.org/10.1128/AAC.00519-15>
- (179) Yu, H.-Y.; Chen, Y.-A.; Yip, B.-S.; Wang, S.-Y.; Wei, H.-J.; Chih, Y.-H.; Chen, K.-H.; Cheng, J.-W. Role of  $\beta$ -Naphthylalanine End-Tags in the Enhancement of Antidotoxin Activities: Solution Structure of the Antimicrobial Peptide S1-Nal-Nal in Complex with Lipopolysaccharide. *Biochim. Biophys. Acta BBA - Biomembr.* **2017**, 1859 (6), 1114–1123. <https://doi.org/10.1016/j.bbamem.2017.03.007>.
- (180) Wu, C.-L.; Peng, K.-L.; Yip, B.-S.; Chih, Y.-H.; Cheng, J.-W. Boosting Synergistic Effects of Short Antimicrobial Peptides With Conventional Antibiotics Against Resistant Bacteria. *Front. Microbiol.* **2021**, 12, 3145. <https://doi.org/10.3389/fmicb.2021.747760>.
- (181) Baker, K. R.; Jana, B.; Franzyk, H.; Guardabassi, L. A High-Throughput Approach To Identify Compounds That Impair Envelope Integrity in Escherichia Coli. *Antimicrob. Agents Chemother.* **2016**, 60 (10), 5995–6002. <https://doi.org/10.1128/AAC.00537-16>.
- (182) Rao, S. S.; Mohan, K. V. K.; Atreya, C. D. A Peptide Derived from Phage Display Library Exhibits Antibacterial Activity against E. Coli and Pseudomonas Aeruginosa. *PLOS ONE* **2013**, 8 (2), e56081. <https://doi.org/10.1371/journal.pone.0056081>.
- (183) Vaara, M.; Porro, M. Group of Peptides That Act Synergistically with Hydrophobic Antibiotics against Gram-Negative Enteric Bacteria. *Antimicrob. Agents Chemother.* **1996**, 40 (8), 1801–1805. <https://doi.org/10.1128/AAC.40.8.1801>.
- (184) Monincová, L.; Buděšínský, M.; Slaninová, J.; Hovorka, O.; Cvačka, J.; Voburka, Z.; Fučík, V.; Borovičková, L.; Bednářová, L.; Straka, J.; Čefovský, V. Novel Antimicrobial Peptides from the Venom of the Eusocial Bee Halictus Sexcinctus (Hymenoptera: Halictidae) and Their Analogs. *Amino Acids* **2010**, 39 (3), 763–775. <https://doi.org/10.1007/s00726-010-0519-1>.
- (185) Dewan, P. C.; Anantharaman, A.; Chauhan, V. S.; Sahal, D. Antimicrobial Action of Prototypic Amphipathic Cationic Decapeptides and Their Branched Dimers. *Biochemistry* **2009**, 48 (24), 5642–5657. <https://doi.org/10.1021/bi900272r>.
- (186) Ramagopal, U. A.; Ramakumar, S.; Sahal, D.; Chauhan, V. S. De Novo Design and Characterization of an Apolar Helical Hairpin Peptide at Atomic Resolution: Compaction Mediated by Weak Interactions. *Proc. Natl. Acad. Sci. U. S. A.* **2001**, 98 (3), 870–874.
- (187) Anantharaman, A.; Rizvi, M. S.; Sahal, D. Synergy with Rifampin and Kanamycin Enhances Potency, Kill Kinetics, and Selectivity of DeNovo-Designed Antimicrobial Peptides. *Antimicrob. Agents Chemother.* **2010**, 54 (5), 1693–1699. <https://doi.org/10.1128/AAC.01231-09>.
- (188) Yeaman, M. R.; Yount, N. Y. Mechanisms of Antimicrobial Peptide Action and Resistance. *Pharmacol. Rev.* **2003**, 55 (1), 27–55. <https://doi.org/10.1124/pr.55.1.2>.
- (189) Fernandez, D. I.; Lee, T.-H.; Sani, M.-A.; Aguilar, M.-I.; Separovic, F. Proline Facilitates Membrane Insertion of the Antimicrobial Peptide Maculatin 1.1 via Surface Indentation and Subsequent Lipid Disordering. *Biophys. J.* **2013**, 104 (7), 1495–1507. <https://doi.org/10.1016/j.bpj.2013.01.059>.
- (190) Hyun, S.; Choi, Y.; Jo, D.; Choo, S.; Park, T. W.; Park, S.-J.; Kim, S.; Lee, S.; Park, S.; Jin, S. M.; Cheon, D. H.; Yoo, W.; Arya, R.; Chong, Y. P.; Kim, K. K.; Kim, Y. S.; Lee, Y.; Yu, J. Proline

- Hinged Amphipathic  $\alpha$ -Helical Peptide Sensitizes Gram-Negative Bacteria to Various Gram-Positive Antibiotics. *J. Med. Chem.* **2020**, 63 (23), 14937–14950. <https://doi.org/10.1021/acs.jmedchem.0c01506>.
- (191) Zeng, P.; Xu, C.; Cheng, Q.; Liu, J.; Gao, W.; Yang, X.; Wong, K.-Y.; Chen, S.; Chan, K.-F. Phenol-Soluble-Modulin-Inspired Amphipathic Peptides Have Bactericidal Activity against Multidrug-Resistant Bacteria. *ChemMedChem* **2019**, 14 (16), 1547–1559. <https://doi.org/10.1002/cmdc.201900364>.
- (192) Zeng, P.; Xu, C.; Liu, C.; Liu, J.; Cheng, Q.; Gao, W.; Yang, X.; Chen, S.; Chan, K.-F.; Wong, K.-Y. De Novo Designed Hexadecapeptides Synergize Glycopeptide Antibiotics Vancomycin and Teicoplanin against Pathogenic *Klebsiella Pneumoniae* via Disruption of Cell Permeability and Potential. *ACS Appl. Bio Mater.* **2020**, 3 (3), 1738–1752. <https://doi.org/10.1021/acsabm.0c00044>.
- (193) Zhang, F.; Zhong, C.; Yao, J.; Zhang, J.; Zhang, T.; Li, B.; Gou, S.; Ni, J. Antimicrobial Peptides–Antibiotics Combination: An Effective Strategy Targeting Drug-Resistant Gram-Negative Bacteria. *Pept. Sci.* **2022**, e24261. <https://doi.org/10.1002/pep2.24261>.
- (194) Zhong, C.; Zhang, F.; Yao, J.; Zhu, Y.; Zhu, N.; Zhang, J.; Ouyang, X.; Zhang, T.; Li, B.; Xie, J.; Ni, J. New Antimicrobial Peptides with Repeating Unit against Multidrug-Resistant Bacteria. *ACS Infect. Dis.* **2021**, 7 (6), 1619–1637. <https://doi.org/10.1021/acsinfecdis.0c00797>.
- (195) Moon, S. H.; Zhang, X.; Zheng, G.; Meeker, D. G.; Smeltzer, M. S.; Huang, E. Novel Linear Lipopeptide Paenipeptins with Potential for Eradicating Biofilms and Sensitizing Gram-Negative Bacteria to Rifampicin and Clarithromycin. *J. Med. Chem.* **2017**, 60 (23), 9630–9640. <https://doi.org/10.1021/acs.jmedchem.7b01064>.
- (196) Moon, S. H.; Kaufmann, Y.; Huang, E. Paenipeptin Analogues Potentiate Clarithromycin and Rifampin against Mcr-1-Mediated Polymyxin-Resistant *Escherichia Coli* In Vivo. *Antimicrob. Agents Chemother.* **2020**, 64 (4), e02045-19. <https://doi.org/10.1128/AAC.02045-19>.
- (197) Domalaon, R.; Brizuela, M.; Eisner, B.; Findlay, B.; Zhanel, G. G.; Schweizer, F. Dilipid Ultrashort Cationic Lipopeptides as Adjuvants for Chloramphenicol and Other Conventional Antibiotics against Gram-Negative Bacteria. *Amino Acids* **2019**, 51 (3), 383–393. <https://doi.org/10.1007/s00726-018-2673-9>.
- (198) Schweizer, L.; Ramirez, D.; Schweizer, F. Effects of Lysine N- $\zeta$ -Methylation in Ultrashort Tetrabasic Lipopeptides (UTBLPs) on the Potentiation of Rifampicin, Novobiocin, and Niclosamide in Gram-Negative Bacteria. *Antibiotics* **2022**, 11 (3), 335. <https://doi.org/10.3390/antibiotics11030335>.
- (199) Qian, Y.; Deng, S.; Cong, Z.; Zhang, H.; Lu, Z.; Shao, N.; Bhatti, S. A.; Zhou, C.; Cheng, J.; Gellman, S. H.; Liu, R. Secondary Amine Pendant  $\beta$ -Peptide Polymers Displaying Potent Antibacterial Activity and Promising Therapeutic Potential in Treating MRSA-Induced Wound Infections and Keratitis. *J. Am. Chem. Soc.* **2022**, 144 (4), 1690–1699. <https://doi.org/10.1021/jacs.1c10659>.
- (200) Li, H.; Hu, Y.; Pu, Q.; He, T.; Zhang, Q.; Wu, W.; Xia, X.; Zhang, J. Novel Stapling by Lysine Tethering Provides Stable and Low Hemolytic Cationic Antimicrobial Peptides. *J. Med. Chem.* **2020**, 63 (8), 4081–4089. <https://doi.org/10.1021/acs.jmedchem.9b02025>.
- (201) Fernández-Reyes, M.; Díaz, D.; de la Torre, B. G.; Cabrales-Rico, A.; Vallès-Miret, M.; Jiménez-Barbero, J.; Andreu, D.; Rivas, L. Lysine N(Epsilon)-Trimethylation, a Tool for Improving the Selectivity of Antimicrobial Peptides. *J. Med. Chem.* **2010**, 53 (15), 5587–5596. <https://doi.org/10.1021/jm100261r>.
- (202) Ramirez, D.; Berry, L.; Domalaon, R.; Brizuela, M.; Schweizer, F. Dilipid Ultrashort Tetrabasic Peptidomimetics Potentiate Novobiocin and Rifampicin Against Multidrug-Resistant Gram-Negative Bacteria. *ACS Infect. Dis.* **2020**, 6 (6), 1413–1426. <https://doi.org/10.1021/acsinfecdis.0c00017>.
- (203) Radzishewsky, I. S.; Rotem, S.; Bourdetsky, D.; Navon-Venezia, S.; Carmeli, Y.; Mor, A. Improved Antimicrobial Peptides Based on Acyl-Lysine Oligomers. *Nat. Biotechnol.* **2007**, 25 (6), 657–659. <https://doi.org/10.1038/nbt1309>.

- (204) Radzishevsky, I.; Krugliak, M.; Ginsburg, H.; Mor, A. Antiplasmodial Activity of Lauryl-Lysine Oligomers. *Antimicrob. Agents Chemother.* **2007**, 51 (5), 1753–1759. <https://doi.org/10.1128/AAC.01288-06>.
- (205) Sarig, H.; Livne, L.; Held-Kuznetsov, V.; Zaknoon, F.; Ivankin, A.; Gidalevitz, D.; Mor, A. A Miniature Mimic of Host Defense Peptides with Systemic Antibacterial Efficacy. *FASEB J.* **2010**, 24 (6), 1904–1913. <https://doi.org/10.1096/fj.09-149427>.
- (206) Rotem, S.; Radzishevsky, I. S.; Bourdetsky, D.; Navon-Venezia, S.; Carmeli, Y.; Mor, A. Analogous Oligo-Acyl-Lysines with Distinct Antibacterial Mechanisms. *FASEB J.* **2008**, 22 (8), 2652–2661. <https://doi.org/10.1096/fj.07-105015>.
- (207) Epand, R. F.; Sarig, H.; Mor, A.; Epand, R. M. Cell-Wall Interactions and the Selective Bacteriostatic Activity of a Miniature Oligo-Acyl-Lysyl. *Biophys. J.* **2009**, 97 (8), 2250–2257. <https://doi.org/10.1016/j.bpj.2009.08.006>.
- (208) Jammal, J.; Zaknoon, F.; Kaneti, G.; Goldberg, K.; Mor, A. Sensitization of Gram-Negative Bacteria to Rifampin and OAK Combinations. *Sci. Rep.* **2015**, 5 (1), 9216. <https://doi.org/10.1038/srep09216>.
- (209) Zaknoon, F.; Meir, O.; Mor, A. Mechanistic Studies of Antibiotic Adjuvants Reducing Kidney's Bacterial Loads upon Systemic Monotherapy. *Pharmaceutics* **2021**, 13 (11), 1947. <https://doi.org/10.3390/pharmaceutics13111947>.
- (210) Jacob, B.; Park, I.-S.; Bang, J.-K.; Shin, S. Y. Short KR-12 Analogs Designed from Human Cathelicidin LL-37 Possessing Both Antimicrobial and Antiendotoxic Activities without Mammalian Cell Toxicity. *J. Pept. Sci.* **2013**, 19 (11), 700–707. <https://doi.org/10.1002/psc.2552>.
- (211) Wu, X.; Wang, Z.; Li, X.; Fan, Y.; He, G.; Wan, Y.; Yu, C.; Tang, J.; Li, M.; Zhang, X.; Zhang, H.; Xiang, R.; Pan, Y.; Liu, Y.; Lu, L.; Yang, L. In Vitro and In Vivo Activities of Antimicrobial Peptides Developed Using an Amino Acid-Based Activity Prediction Method. *Antimicrob. Agents Chemother.* **2014** 58 (9), 5342–5349. <https://doi.org/10.1128/AAC.02823-14>.
- (212) Huertas, N. de J.; Rivera Monroy, Z. J.; Fierro Medina, R.; García Castañeda, J. E. Antimicrobial Activity of Truncated and Polyvalent Peptides Derived from the FKRRWQWRMKKGLA Sequence against *Escherichia Coli* ATCC 25922 and *Staphylococcus Aureus* ATCC 25923. *Mol. J. Synth. Chem. Nat. Prod. Chem.* **2017**, 22 (6), 987. <https://doi.org/10.3390/molecules22060987>.
- (213) Meng, H.; Kumar, K. Antimicrobial Activity and Protease Stability of Peptides Containing Fluorinated Amino Acids. *J. Am. Chem. Soc.* **2007**, 129 (50), 15615–15622. <https://doi.org/10.1021/ja075373f>.
- (214) Mangoni, M. L.; Fiocco, D.; Mignogna, G.; Barra, D.; Simmaco, M. Functional Characterisation of the 1–18 Fragment of Esculentin-1b, an Antimicrobial Peptide from *Rana Esculenta*. *Peptides* **2003**, 24 (11), 1771–1777. <https://doi.org/10.1016/j.peptides.2003.07.029>.
- (215) Gopal, R.; Kim, Y. G.; Lee, J. H.; Lee, S. K.; Chae, J. D.; Son, B. K.; Seo, C. H.; Park, Y. Synergistic Effects and Antibiofilm Properties of Chimeric Peptides against Multidrug-Resistant *Acinetobacter Baumannii* Strains. *Antimicrob. Agents Chemother.* **2014**, 58 (3), 1622–1629. <https://doi.org/10.1128/AAC.02473-13>.
- (216) Shin, S. Y.; Kang, J. H.; Lee, M. K.; Kim, S. Y.; Kim, Y.; Hahm, K.-S. Cecropin a – Magainin 2 Hybrid Peptides Having Potent Antimicrobial Activity with Low Hemolytic Effect. *IUBMB Life* **1998**, 44 (6), 1119–1126. <https://doi.org/10.1080/15216549800202192>.
- (217) Keun Kim, H.; Gun Lee, D.; Park, Y.; Nam Kim, H.; Hwa Choi, B.; Choi, C.-H.; Hahm, K.-S. Antibacterial Activities of Peptides Designed as Hybrids of Antimicrobial Peptides. *Biotechnol. Lett.* **2002**, 24 (5), 347–353. <https://doi.org/10.1023/A:1014573005866>.
- (218) Park, K. H.; Nan, Y. H.; Park, Y.; Kim, J. I.; Park, I.-S.; Hahm, K.-S.; Shin, S. Y. Cell Specificity, Anti-Inflammatory Activity, and Plausible Bactericidal Mechanism of Designed Trp-Rich Model Antimicrobial Peptides. *Biochim. Biophys. Acta BBA – Biomembr.* **2009**, 1788 (5), 1193–1203. <https://doi.org/10.1016/j.bbamem.2009.02.020>.
- (219) Yunhwa, C. Proline Hinged Amphipathic  $\alpha$ -Helical Peptide Enhances Synergistic Antimicrobial Activity with Various Antibiotics by Perturbing Outer Membrane of Gram-Negative Bacteria. Thesis, 서울대학교 대학원, 2017.

- (220) Moore, K. S.; Wehrli, S.; Roder, H.; Rogers, M.; Forrest, J. N.; McCrimmon, D.; Zasloff, M. Squalamine: An Aminosterol Antibiotic from the Shark. *Proc. Natl. Acad. Sci.* **1993**, 90 (4), 1354–1358. <https://doi.org/10.1073/pnas.90.4.1354>.
- (221) Salmi, C.; Loncle, C.; Vidal, N.; Letourneux, Y.; Fantini, J.; Maresca, M.; Taïeb, N.; Pagès, J.-M.; Brunel, J. M. Squalamine: An Appropriate Strategy against the Emergence of Multidrug Resistant Gram-Negative Bacteria? *PLOS ONE* **2008**, 3 (7), e2765. <https://doi.org/10.1371/journal.pone.0002765>.
- (222) Lavigne, J.-P.; Brunel, J.-M.; Chevalier, J.; Pagès, J.-M. Squalamine, an Original Chemosensitizer to Combat Antibiotic-Resistant Gram-Negative Bacteria. *J. Antimicrob. Chemother.* **2010**, 65 (4), 799–801. <https://doi.org/10.1093/jac/dkq031>.
- (223) Kikuchi, K.; Bernard, E. M.; Sadownik, A.; Regen, S. L.; Armstrong, D. Antimicrobial Activities of Squalamine Mimics. *Antimicrob. Agents Chemother.* **1997**, 41 (7), 1433–1438. <https://doi.org/10.1128/AAC.41.7.1433>.
- (224) Savage, P. B.; Li, C. Cholic Acid Derivatives: Novel Antimicrobials. *Expert Opin. Investig. Drugs* **2000**, 9 (2), 263–272. <https://doi.org/10.1517/13543784.9.2.263>.
- (225) Li, C.; Peters, A. S.; Meredith, E. L.; Allman, G. W.; Savage, P. B. Design and Synthesis of Potent Sensitizers of Gram-Negative Bacteria Based on a Cholic Acid Scaffolding. *J. Am. Chem. Soc.* **1998**, 120 (12), 2961–2962. <https://doi.org/10.1021/ja973881r>.
- (226) Li, C.; Lewis, M. R.; Gilbert, A. B.; Noel, M. D.; Scoville, D. H.; Allman, G. W.; Savage, P. B. Antimicrobial Activities of Amine- and Guanidine-Functionalized Cholic Acid Derivatives. *Antimicrob. Agents Chemother.* **1999**, 43 (6), 1347–1349. <https://doi.org/10.1128/AAC.43.6.1347>.
- (227) Li, C.; Budge, L. P.; Driscoll, C. D.; Willardson, B. M.; Allman, G. W.; Savage, P. B. Incremental Conversion of Outer-Membrane Permeabilizers into Potent Antibiotics for Gram-Negative Bacteria. *J. Am. Chem. Soc.* **1999**, 121 (5), 931–940. <https://doi.org/10.1021/ja982938m>.
- (228) Schmidt, E. J.; Boswell, J. S.; Walsh, J. P.; Schellenberg, M. M.; Winter, T. W.; Li, C.; Allman, G. W.; Savage, P. B. Activities of Cholic Acid-Derived Antimicrobial Agents against Multidrug-Resistant Bacteria. *J. Antimicrob. Chemother.* **2001**, 47 (5), 671–674. <https://doi.org/10.1093/jac/47.5.671>.
- (229) Atiq-ur-Rehman; Li, C.; Budge, L. P.; Street, S. E.; Savage, P. B. Preparation of Amino Acid-Appended Cholic Acid Derivatives as Sensitizers of Gram-Negative Bacteria. *Tetrahedron Lett.* **1999**, 40 (10), 1865–1868. [https://doi.org/10.1016/S0040-4039\(99\)00075-1](https://doi.org/10.1016/S0040-4039(99)00075-1).
- (230) Guan, Q.; Li, C.; Schmidt, E. J.; Boswell, J. S.; Walsh, J. P.; Allman, G. W.; Savage, P. B. Preparation and Characterization of Cholic Acid-Derived Antimicrobial Agents with Controlled Stabilities. *Org. Lett.* **2000**, 2 (18), 2837–2840. <https://doi.org/10.1021/ol0062704>.
- (231) Savage, P. B.; Li, C.; Taotafa, U.; Ding, B.; Guan, Q. Antibacterial Properties of Cationic Steroid Antibiotics. *FEMS Microbiol. Lett.* **2002**, 217 (1), 1–7. <https://doi.org/10.1111/j.1574-6968.2002.tb11448.x>.
- (232) Ding, B.; Taotofa, U.; Orsak, T.; Chadwell, M.; Savage, P. B. Synthesis and Characterization of Peptide-Cationic Steroid Antibiotic Conjugates. *Org. Lett.* **2004**, 6 (20), 3433–3436. <https://doi.org/10.1021/ol048845t>.
- (233) Lai, X.-Z.; Feng, Y.; Pollard, J.; Chin, J. N.; Rybak, M. J.; Bucki, R.; Epand, R. F.; Epand, R. M.; Savage, P. B. Ceragenins: Cholic Acid-Based Mimics of Antimicrobial Peptides. *Acc. Chem. Res.* **2008**, 41 (10), 1233–1240. <https://doi.org/10.1021/ar700270t>.
- (234) Saha, S.; Savage, P. b.; Bal, M. Enhancement of the Efficacy of Erythromycin in Multiple Antibiotic-Resistant Gram-Negative Bacterial Pathogens. *J. Appl. Microbiol.* **2008**, 105 (3), 822–828. <https://doi.org/10.1111/j.1365-2672.2008.03820.x>.
- (235) Bavikar, S. N.; Salunke, D. B.; Hazra, B. G.; Pore, V. S.; Dodd, R. H.; Thierry, J.; Shirazi, F.; Deshpande, M. V.; Kadreppa, S.; Chattopadhyay, S. Synthesis of Chimeric Tetrapeptide-Linked Cholic Acid Derivatives: Impending Synergistic Agents. *Bioorg. Med. Chem. Lett.* **2008**, 18 (20), 5512–5517. <https://doi.org/10.1016/j.bmcl.2008.09.013>.
- (236) Stokes, J. M.; MacNair, C. R.; Ilyas, B.; French, S.; Côté, J.-P.; Bouwman, C.; Farha, M. A.; Sieron, A. O.; Whitfield, C.; Coombes, B. K.; Brown, E. D. Pentamidine Sensitizes Gram-

- Negative Pathogens to Antibiotics and Overcomes Acquired Colistin Resistance. *Nat. Microbiol.* **2017**, 2 (5), 1–8. <https://doi.org/10.1038/nmicrobiol.2017.28>.
- (237) Wesseling, C. M. J.; Slingerland, C. J.; Veraar, S.; Lok, S.; Martin, N. I. Structure–Activity Studies with Bis-Amidines That Potentiate Gram-Positive Specific Antibiotics against Gram-Negative Pathogens. *ACS Infect. Dis.* **2021**. <https://doi.org/10.1021/acsinfecdis.1c00466>.
- (238) MacNair, C. R.; Farha, M. A.; Serrano-Wu, M. H.; Lee, K. K.; Hubbard, B.; Côté, J.-P.; Carfrae, L. A.; Tu, M. M.; Gaulin, J. L.; Hunt, D. K.; Hung, D. T.; Brown, E. D. Preclinical Development of Pentamidine Analogs Identifies a Potent and Nontoxic Antibiotic Adjuvant. *ACS Infect. Dis.* **2022**. <https://doi.org/10.1021/acsinfecdis.1c00482>.
- (239) Sands, M.; Kron, M. A.; Brown, R. B. Pentamidine: A Review. *Rev. Infect. Dis.* **1985**, 7 (5), 625–634. <https://doi.org/10.1093/clinids/7.5.625>.
- (240) Kuryshv, Y. A.; Ficker, E.; Wang, L.; Hawryluk, P.; Dennis, A. T.; Wible, B. A.; Brown, A. M.; Kang, J.; Chen, X.-L.; Sawamura, K.; Reynolds, W.; Rampe, D. Pentamidine-Induced Long QT Syndrome and Block of HERG Trafficking. *J. Pharmacol. Exp. Ther.* **2005**, 312 (1), 316–323. <https://doi.org/10.1124/jpet.104.073692>.
- (241) Liu, Y.; Jia, Y.; Yang, K.; Li, R.; Xiao, X.; Zhu, K.; Wang, Z. Metformin Restores Tetracyclines Susceptibility against Multidrug Resistant Bacteria. *Adv. Sci.* **2020**, 7 (12), 1902227. <https://doi.org/10.1002/advs.201902227>.
- (242) Klobucar, K.; Côté, J.-P.; French, S.; Borrillo, L.; Guo, A. B. Y.; Serrano-Wu, M. H.; Lee, K. K.; Hubbard, B.; Johnson, J. W.; Gaulin, J. L.; Magolan, J.; Hung, D. T.; Brown, E. D. Chemical Screen for Vancomycin Antagonism Uncovers Probes of the Gram-Negative Outer Membrane. *ACS Chem. Biol.* **2021**, 16 (5), 929–942. <https://doi.org/10.1021/acscchembio.1c00179>.
- (243) Sharma, S.; Rao, R.; Reeve, S. M.; Phelps, G. A.; Bharatham, N.; Katagihallimath, N.; Ramachandran, V.; Raveendran, S.; Sarma, M.; Nath, A.; Thomas, T.; Manickam, D.; Nagaraj, S.; Balasubramanian, V.; Lee, R. E.; Hameed P, S.; Datta, S. Azaindole Based Potentiator of Antibiotics against Gram-Negative Bacteria. *ACS Infect. Dis.* **2021**, 7 (11), 3009–3024. <https://doi.org/10.1021/acsinfecdis.1c00171>.
- (244) Böttcher, T.; Kolodkin-Gal, I.; Kolter, R.; Losick, R.; Clardy, J. Synthesis and Activity of Biomimetic Biofilm Disruptors. *J. Am. Chem. Soc.* **2013**, 135 (8), 2927–2930. <https://doi.org/10.1021/ja3120955>.
- (245) Konai, M. M.; Haldar, J. Lysine-Based Small Molecules That Disrupt Biofilms and Kill Both Actively Growing Planktonic and Nondividing Stationary Phase Bacteria. *ACS Infect. Dis.* **2015**, 1 (10), 469–478. <https://doi.org/10.1021/acsinfecdis.5b00056>.
- (246) Konai, M. M.; Haldar, J. Lysine-Based Small Molecule Sensitizes Rifampicin and Tetracycline against Multidrug-Resistant *Acinetobacter Baumannii* and *Pseudomonas Aeruginosa*. *ACS Infect. Dis.* **2020**, 6 (1), 91–99. <https://doi.org/10.1021/acsinfecdis.9b00221>.
- (247) Yasuda, K.; Ohmizo, C.; Katsu, T. Mode of Action of Novel Polyamines Increasing the Permeability of Bacterial Outer Membrane. *Int. J. Antimicrob. Agents* **2004**, 24 (1), 67–71. <https://doi.org/10.1016/j.ijantimicag.2004.01.006>.
- (248) Katsu, T.; Nakagawa, H.; Yasuda, K. Interaction between Polyamines and Bacterial Outer Membranes as Investigated with Ion-Selective Electrodes. *Antimicrob. Agents Chemother.* **2002**, 46 (4), 1073–1079. <https://doi.org/10.1128/AAC.46.4.1073-1079.2002>.
- (249) Balakrishna, R.; Wood, S. J.; Nguyen, T. B.; Miller, K. A.; Suresh Kumar, E. V. K.; Datta, A.; David, S. A. Structural Correlates of Antibacterial and Membrane-Permeabilizing Activities in Acylpolyamines. *Antimicrob. Agents Chemother.* **2006**, 50 (3), 852–861. <https://doi.org/10.1128/AAC.50.3.852-861.2006>.
- (250) David, S. A. Towards a Rational Development of Anti-Endotoxin Agents: Novel Approaches to Sequestration of Bacterial Endotoxins with Small Molecules. *J. Mol. Recognit.* **2001**, 14 (6), 370–387. <https://doi.org/10.1002/jmr.549>.
- (251) David, S. A.; Silverstein, R.; Amura, C. R.; Kielian, T.; Morrison, D. C. Lipopolyamines: Novel Antiendotoxin Compounds That Reduce Mortality in Experimental Sepsis Caused by

- Gram-Negative Bacteria. *Antimicrob. Agents Chemother.* **1999**, 43 (4), 912–919. <https://doi.org/10.1128/AAC.43.4.912>.
- (252) Li, S. A.; Cadelis, M. M.; Sue, K.; Blanchet, M.; Vidal, N.; Brunel, J. M.; Bourguet-Kondracki, M.-L.; Copp, B. R. 6-Bromindolglyoxylamido Derivatives as Antimicrobial Agents and Antibiotic Enhancers. *Bioorg. Med. Chem.* **2019**, 27 (10), 2090–2099. <https://doi.org/10.1016/j.bmc.2019.04.004>.
- (253) Finlayson, R.; Pearce, A. N.; Page, M. J.; Kaiser, M.; Bourguet-Kondracki, M.-L.; Harper, J. L.; Webb, V. L.; Copp, B. R. Didemnidines A and B, Indole Spermidine Alkaloids from the New Zealand Ascidian *Didemnum* Sp. *J. Nat. Prod.* **2011**, 74 (4), 888–892. <https://doi.org/10.1021/np1008619>.
- (254) Cadelis, M. M.; Li, S. A.; Bourguet-Kondracki, M.-L.; Blanchet, M.; Douafer, H.; Brunel, J. M.; Copp, B. R. Spermine Derivatives of Indole-3-Carboxylic Acid, Indole-3-Acetic Acid and Indole-3-Acrylic Acid as Gram-Negative Antibiotic Adjuvants. *ChemMedChem* **2021**, 16 (3), 513–523. <https://doi.org/10.1002/cmdc.202000359>.
- (255) Helander, I. M.; Nurmiaho-Lassila, E.-L.; Ahvenainen, R.; Rhoades, J.; Roller, S. Chitosan Disrupts the Barrier Properties of the Outer Membrane of Gram-Negative Bacteria. *Int. J. Food Microbiol.* **2001**, 71 (2), 235–244. [https://doi.org/10.1016/S0168-1605\(01\)00609-2](https://doi.org/10.1016/S0168-1605(01)00609-2).
- (256) Helander, I. M.; Latva-Kala, K.; Lounatmaa, K. 1998. Permeabilizing Action of Polyethyleneimine on *Salmonella Typhimurium* Involves Disruption of the Outer Membrane and Interactions with Lipopolysaccharide. *Microbiology* **1998** 144 (2), 385–390. <https://doi.org/10.1099/00221287-144-2-385>.
- (257) Lam, A. K.; Panlilio, H.; Pusavat, J.; Wouters, C. L.; Moen, E. L.; Rice, C. V. Overcoming Multidrug Resistance and Biofilms of *Pseudomonas Aeruginosa* with a Single Dual-Function Potentiator of  $\beta$ -Lactams. *ACS Infect. Dis.* **2020**, 6 (5), 1085–1097. <https://doi.org/10.1021/acsinfecdis.9b00486>.
- (258) Hemaiswarya, S.; Doble, M. Synergistic Interaction of Eugenol with Antibiotics against Gram Negative Bacteria. *Phytomedicine* **2009**, 16 (11), 997–1005. <https://doi.org/10.1016/j.phymed.2009.04.006>.
- (259) Aelenei, P.; Rimbu, C. M.; Guguianu, E.; Dimitriu, G.; Aprotosoia, A. C.; Brebu, M.; Horhoge, C. E.; Miron, A. Coriander Essential Oil and Linalool - Interactions with Antibiotics against Gram-Positive and Gram-Negative Bacteria. *Lett. Appl. Microbiol.* **2019**, 68 (2), 156–164. <https://doi.org/10.1111/lam.13100>.
- (260) Farag, R. S.; Daw, Z. Y.; Hewedi, F. M.; El-Baroty, G. S. A. Antimicrobial Activity of Some Egyptian Spice Essential Oils. *J. Food Prot.* **1989**, 52 (9), 665–667. <https://doi.org/10.4315/0362-028X-52.9.665>.
- (261) Bauer, K.; Garbe, D.; Surburg, H. *Common Fragrance and Flavor Materials: Preparation, Properties and Uses*; John Wiley & Sons, 2008.
- (262) Burt, S. Essential Oils: Their Antibacterial Properties and Potential Applications in Foods—a Review. *Int. J. Food Microbiol.* **2004**, 94 (3), 223–253. <https://doi.org/10.1016/j.ijfoodmicro.2004.03.022>.
- (263) Wijesekera, R. O. B.; Chichester, C. O. The Chemistry and Technology of Cinnamon. *C R C Crit. Rev. Food Sci. Nutr.* **1978**, 10 (1), 1–30. <https://doi.org/10.1080/10408397809527243>.
- (264) ter Heide, R. Qualitative Analysis of the Essential Oil of Cassia (*Cinnamomum Cassia* Blume). *J Agric Food Chem* **1972**, 20 (4), 747–751.
- (265) Langeveld, W. T.; Veldhuizen, E. J. A.; Burt, S. A. Synergy between Essential Oil Components and Antibiotics: A Review. *Crit. Rev. Microbiol.* **2014**, 40 (1), 76–94. <https://doi.org/10.3109/1040841X.2013.763219>.
- (266) Aelenei, P.; Miron, A.; Trifan, A.; Bujor, A.; Gille, E.; Aprotosoia, A. C. Essential Oils and Their Components as Modulators of Antibiotic Activity against Gram-Negative Bacteria. *Medicines* **2016**, 3 (3), 19. <https://doi.org/10.3390/medicines3030019>.
- (267) Palaniappan, K.; Holley, R. A. Use of Natural Antimicrobials to Increase Antibiotic Susceptibility of Drug Resistant Bacteria. *Int. J. Food Microbiol.* **2010**, 140 (2), 164–168. <https://doi.org/10.1016/j.ijfoodmicro.2010.04.001>.

- (268) Hemaiswarya, S.; Doble, M. Synergistic Interaction of Phenylpropanoids with Antibiotics against Bacteria. *J. Med. Microbiol.* **2010**, *59*, 1469–1476. <https://doi.org/10.1099/jmm.0.022426-0>.
- (269) Helander, I. M.; Alakomi, H.-L.; Latva-Kala, K.; Mattila-Sandholm, T.; Pol, I.; Smid, E. J.; Gorris, L. G. M.; von Wright, A. Characterization of the Action of Selected Essential Oil Components on Gram-Negative Bacteria. *J. Agric. Food Chem.* **1998**, *46* (9), 3590–3595. <https://doi.org/10.1021/jf980154m>.
- (270) Ruwizhi, N.; Aderibigbe, B. A. Cinnamic Acid Derivatives and Their Biological Efficacy. *Int. J. Mol. Sci.* **2020**, *21* (16), 5712. <https://doi.org/10.3390/ijms21165712>.
- (271) Gibney, K.; Sovadinova, I.; Lopez, A. I.; Urban, M.; Ridgway, Z.; Caputo, G. A.; Kuroda, K. Poly(Ethylene Imine)s as Antimicrobial Agents with Selective Activity. *Macromol. Biosci.* **2012**, *12* (9), 1279–1289. <https://doi.org/10.1002/mabi.201200052>.
- (272) Pontes, K. A. O.; Silva, L. S.; Santos, E. C.; Pinheiro, A. S.; Teixeira, D. E.; Peruchetti, D. B.; Silva-Aguiar, R. P.; Wendt, C. H. C.; Miranda, K. R.; Coelho-de-Souza, A. N.; Leal-Cardoso, J. H.; Caruso-Neves, C.; Pinheiro, A. A. S. Eugenol Disrupts Plasmodium Falciparum Intracellular Development during the Erythrocytic Cycle and Protects against Cerebral Malaria. *Biochim. Biophys. Acta BBA - Gen. Subj.* **2021**, *1865* (3), 129813. <https://doi.org/10.1016/j.bbagen.2020.129813>.
- (273) Togashi, N.; Hamashima, H.; Shiraishi, A.; Inoue, Y.; Takano, A. Antibacterial Activities Against Staphylococcus Aureus of Terpene Alcohols With Aliphatic Carbon Chains. *J. Essent. Oil Res.* **2010**, *22* (3), 263–269. <https://doi.org/10.1080/10412905.2010.9700321>.
- (274) Ahmad, A.; Khan, A.; Akhtar, F.; Yousuf, S.; Xess, I.; Khan, L. A.; Manzoor, N. Fungicidal Activity of Thymol and Carvacrol by Disrupting Ergosterol Biosynthesis and Membrane Integrity against Candida. *Eur. J. Clin. Microbiol. Infect. Dis.* **2011**, *30* (1), 41–50. <https://doi.org/10.1007/s10096-010-1050-8>.
- (275) Theurer, M.; Shaik, N.; Lang, F. Stimulation of Suicidal Erythrocyte Death by Trans-Cinnamaldehyde. *Phytomedicine* **2013**, *20* (12), 1119–1123. <https://doi.org/10.1016/j.phymed.2013.05.006>.
- (276) Hemaiswarya, S.; Doble, M. Combination of Phenylpropanoids with 5-Fluorouracil as Anti-Cancer Agents against Human Cervical Cancer (HeLa) Cell Line. *Phytomedicine* **2013**, *20* (2), 151–158. <https://doi.org/10.1016/j.phymed.2012.10.009>.
- (277) Farrell, W.; Wilks, M.; Drasar, F. A. The Action of Trimethoprim and Rifampicin in Combination against Gram-Negative Rods Resistant to Gentamicin. *J. Antimicrob. Chemother.* **1977**, *3* (5), 459–462. <https://doi.org/10.1093/jac/3.5.459>.
- (278) Wang, Y.; Bao, W.; Guo, N.; Chen, H.; Cheng, W.; Jin, K.; Shen, F.; Xu, J.; Zhang, Q.; Wang, C.; An, Y.; Zhang, K.; Zhang, F.; Yu, L. Antimicrobial Activity of the Imipenem/Rifampicin Combination against Clinical Isolates of Acinetobacter Baumannii Grown in Planktonic and Biofilm Cultures. *World J. Microbiol. Biotechnol.* **2014**, *30* (12), 3015–3025. <https://doi.org/10.1007/s11274-014-1728-7>.
- (279) Domalaon, R.; Yang, X.; Lyu, Y.; Zhanel, G. G.; Schweizer, F. Polymyxin B3-Tobramycin Hybrids with Pseudomonas Aeruginosa-Selective Antibacterial Activity and Strong Potentiation of Rifampicin, Minocycline, and Vancomycin. *ACS Infect. Dis.* **2017**, *3* (12), 941–954. <https://doi.org/10.1021/acsinfecdis.7b00145>.
- (280) Wood, T. M.; Slingerland, C. J.; Martin, N. I. A Convenient Chemoenzymatic Preparation of Chimeric Macrocytic Peptide Antibiotics with Potent Activity against Gram-Negative Pathogens. *J. Med. Chem.* **2021**, *64* (15), 10890–10899. <https://doi.org/10.1021/acs.jmedchem.1c00176>.
- (281) van Groesen, E.; Slingerland, C. J.; Innocenti, P.; Mihajlovic, M.; Masereeuw, R.; Martin, N. I. Vancomyxins: Vancomycin-Polymyxin Nonapeptide Conjugates That Retain Anti-Gram-Positive Activity with Enhanced Potency against Gram-Negative Strains. *ACS Infect. Dis.* **2021**, *7* (9), 2746–2754. <https://doi.org/10.1021/acsinfecdis.1c00318>.
- (282) Herzog, I. M.; Green, K. D.; Berkov-Zrihen, Y.; Feldman, M.; Vidavski, R. R.; Eldar-Boock, A.; Satchi-Fainaro, R.; Eldar, A.; Garneau-Tsodikova, S.; Fridman, M. 6''-Thioether Tobramycin Analogues: Towards Selective Targeting of Bacterial Membranes. *Angew. Chem.* **2012**, *124* (23), 5750–5754. <https://doi.org/10.1002/ange.201200761>.

- (283) Ouberai, M.; El Garch, F.; Bussiere, A.; Riou, M.; Alsteens, D.; Lins, L.; Baussanne, I.; Dufrêne, Y. F.; Brasseur, R.; Decout, J.-L.; Mingeot-Leclercq, M.-P. The *Pseudomonas Aeruginosa* Membranes: A Target for a New Amphiphilic Aminoglycoside Derivative? *Biochim. Biophys. Acta BBA – Biomembr.* **2011**, 1808 (6), 1716–1727. <https://doi.org/10.1016/j.bbamem.2011.01.014>.
- (284) Guchhait, G.; Altieri, A.; Gorityala, B.; Yang, X.; Findlay, B.; Zhanel, G. G.; Mookherjee, N.; Schweizer, F. Amphiphilic Tobramycins with Immunomodulatory Properties. *Angew. Chem. Int. Ed.* **2015**, 54 (21), 6278–6282. <https://doi.org/10.1002/anie.201500598>.
- (285) Loh, B.; Grant, C.; Hancock, R. E. Use of the Fluorescent Probe 1-N-Phenyl-naphthylamine to Study the Interactions of Aminoglycoside Antibiotics with the Outer Membrane of *Pseudomonas Aeruginosa*. *Antimicrob. Agents Chemother.* **1984**, 26 (4), 546–551. <https://doi.org/10.1128/AAC.26.4.546>.
- (286) Bulitta, J. B.; Ly, N. S.; Landersdorfer, C. B.; Wanigaratne, N. A.; Velkov, T.; Yadav, R.; Oliver, A.; Martin, L.; Shin, B. S.; Forrest, A.; Tsuji, B. T. Two Mechanisms of Killing of *Pseudomonas Aeruginosa* by Tobramycin Assessed at Multiple Inocula via Mechanism-Based Modeling. *Antimicrob. Agents Chemother.* **2015**, 59 (4), 2315–2327. <https://doi.org/10.1128/AAC.04099-14>.
- (287) Gorityala, B. K.; Guchhait, G.; Goswami, S.; Fernando, D. M.; Kumar, A.; Zhanel, G. G.; Schweizer, F. Hybrid Antibiotic Overcomes Resistance in *P. Aeruginosa* by Enhancing Outer Membrane Penetration and Reducing Efflux. *J. Med. Chem.* **2016**, 59 (18), 8441–8455. <https://doi.org/10.1021/acs.jmedchem.6b00867>.
- (288) Gorityala, B. K.; Guchhait, G.; Fernando, D. M.; Deo, S.; McKenna, S. A.; Zhanel, G. G.; Kumar, A.; Schweizer, F. Adjuvants Based on Hybrid Antibiotics Overcome Resistance in *Pseudomonas Aeruginosa* and Enhance Fluoroquinolone Efficacy. *Angew. Chem. Int. Ed.* **2016**, 55 (2), 555–559. <https://doi.org/10.1002/anie.201508330>.
- (289) Idowu, T.; Arthur, G.; Zhanel, G. G.; Schweizer, F. Heterodimeric Rifampicin–Tobramycin Conjugates Break Intrinsic Resistance of *Pseudomonas Aeruginosa* to Doxycycline and Chloramphenicol in Vitro and in a *Galleria Mellonella* in Vivo Model. *Eur. J. Med. Chem.* **2019**, 174, 16–32. <https://doi.org/10.1016/j.ejmech.2019.04.034>.
- (290) Lyu, Y.; Yang, X.; Goswami, S.; Gorityala, B. K.; Idowu, T.; Domalaon, R.; Zhanel, G. G.; Shan, A.; Schweizer, F. Amphiphilic Tobramycin–Lysine Conjugates Sensitize Multidrug Resistant Gram-Negative Bacteria to Rifampicin and Minocycline. *J. Med. Chem.* **2017**, 60 (9), 3684–3702. <https://doi.org/10.1021/acs.jmedchem.6b01742>.
- (291) Yang, X.; Goswami, S.; Gorityala, B. K.; Domalaon, R.; Lyu, Y.; Kumar, A.; Zhanel, G. G.; Schweizer, F. A Tobramycin Vector Enhances Synergy and Efficacy of Efflux Pump Inhibitors against Multidrug-Resistant Gram-Negative Bacteria. *J. Med. Chem.* **2017**, 60 (9), 3913–3932. <https://doi.org/10.1021/acs.jmedchem.7b00156>.
- (292) Yang, X.; Domalaon, R.; Lyu, Y.; Zhanel, G. G.; Schweizer, F. Tobramycin-Linked Efflux Pump Inhibitor Conjugates Synergize Fluoroquinolones, Rifampicin and Fosfomycin against Multidrug-Resistant *Pseudomonas Aeruginosa*. *J. Clin. Med.* **2018**, 7 (7), 158. <https://doi.org/10.3390/jcm7070158>.
- (293) Idowu, T.; Ammeter, D.; Rossong, H.; Zhanel, G. G.; Schweizer, F. Homodimeric Tobramycin Adjuvant Repurposes Novobiocin as an Effective Antibacterial Agent against Gram-Negative Bacteria. *J. Med. Chem.* **2019**, 62 (20), 9103–9115. <https://doi.org/10.1021/acs.jmedchem.9b00876>.
- (294) Idowu, T.; Ammeter, D.; Arthur, G.; Zhanel, G. G.; Schweizer, F. Potentiation of  $\beta$ -Lactam Antibiotics and  $\beta$ -Lactam/ $\beta$ -Lactamase Inhibitor Combinations against MDR and XDR *Pseudomonas Aeruginosa* Using Non-Ribosomal Tobramycin–Cyclam Conjugates. *J. Antimicrob. Chemother.* **2019**, 74 (9), 2640–2648. <https://doi.org/10.1093/jac/dkz228>.
- (295) Yang, X.; Ammeter, D.; Idowu, T.; Domalaon, R.; Brizuela, M.; Okunnu, O.; Bi, L.; Guerrero, Y. A.; Zhanel, G. G.; Kumar, A.; Schweizer, F. Amphiphilic Nebramine-Based Hybrids Rescue Legacy Antibiotics from Intrinsic Resistance in Multidrug-Resistant Gram-Negative Bacilli. *Eur. J. Med. Chem.* **2019**, 175, 187–200. <https://doi.org/10.1016/j.ejmech.2019.05.003>.
- (296) Ammeter, D.; Idowu, T.; Zhanel, G. G.; Schweizer, F. Development of a Nebramine–Cyclam Conjugate as an Antibacterial Adjuvant to Potentiate  $\beta$ -Lactam Antibiotics against



- Multidrug-Resistant *P. Aeruginosa*. *J. Antibiot. (Tokyo)* **2019**, 72 (11), 816–826. <https://doi.org/10.1038/s41429-019-0221-9>.
- (297) Berry, L.; Domalaon, R.; Brizuela, M.; Zhanel, G. G.; Schweizer, F. Polybasic Peptide–Levofloxacin Conjugates Potentiate Fluoroquinolones and Other Classes of Antibiotics against Multidrug-Resistant Gram-Negative Bacteria. *MedChemComm* **2019**, 10 (4), 517–527. <https://doi.org/10.1039/C9MD00051H>.
- (298) Domalaon, R.; Idowu, T.; Zhanel, G. G.; Schweizer, F. Antibiotic Hybrids: The Next Generation of Agents and Adjuvants against Gram-Negative Pathogens? *Clin. Microbiol. Rev.* **2018**. <https://doi.org/10.1128/CMR.00077-17>.
- (299) Ghosh, C.; Manjunath, G. B.; Akkapeddi, P.; Yarlagadda, V.; Hoque, J.; Uppu, D. S. S. M.; Konai, M. M.; Haldar, J. Small Molecular Antibacterial Peptoid Mimics: The Simpler the Better! *J. Med. Chem.* **2014**, 57 (4), 1428–1436. <https://doi.org/10.1021/jm401680a>.
- (300) Lyu, Y.; Domalaon, R.; Yang, X.; Schweizer, F. Amphiphilic Lysine Conjugated to Tobramycin Synergizes Legacy Antibiotics against Wild-Type and Multidrug-Resistant *Pseudomonas Aeruginosa*. *Pept. Sci.* **2019**, 111 (1), e23091. <https://doi.org/10.1002/bip.23091>.
- (301) Bohnert, J. A.; Kern, W. V. Selected Arylpiperazines Are Capable of Reversing Multidrug Resistance in *Escherichia Coli* Overexpressing RND Efflux Pumps. *Antimicrob. Agents Chemother.* **2005**, 49 (2), 849–852. <https://doi.org/10.1128/AAC.49.2.849-852.2005>.
- (302) Kaatz, G. W.; Moudgal, V. V.; Seo, S. M.; Hansen, J. B.; Kristiansen, J. E. Phenylpiperidine Selective Serotonin Reuptake Inhibitors Interfere with Multidrug Efflux Pump Activity in *Staphylococcus Aureus*. *Int. J. Antimicrob. Agents* **2003**, 22 (3), 254–261. [https://doi.org/10.1016/s0924-8579\(03\)00220-6](https://doi.org/10.1016/s0924-8579(03)00220-6).
- (303) Kriengkauykat, J.; Porter, E.; Lomovskaya, O.; Wong-Beringer, A. Use of an Efflux Pump Inhibitor To Determine the Prevalence of Efflux Pump-Mediated Fluoroquinolone Resistance and Multidrug Resistance in *Pseudomonas Aeruginosa*. *Antimicrob. Agents Chemother.* **2005**, 49 (2), 565–570. <https://doi.org/10.1128/AAC.49.2.565-570.2005>.
- (304) Conejo, M. C.; García, I.; Martínez-Martínez, L.; Picabea, L.; Pascual, Á. Zinc Eluted from Silicized Latex Urinary Catheters Decreases OprD Expression, Causing Carbapenem Resistance in *Pseudomonas Aeruginosa*. *Antimicrob. Agents Chemother.* **2003**, 47 (7), 2313–2315. <https://doi.org/10.1128/AAC.47.7.2313-2315.2003>.
- (305) Perron, K.; Caille, O.; Rossier, C.; Van Delden, C.; Dumas, J.-L.; Köhler, T. CzcR–CzcS, a Two-Component System Involved in Heavy Metal and Carbapenem Resistance in *Pseudomonas Aeruginosa*. *J. Biol. Chem.* **2004**, 279 (10), 8761–8768. <https://doi.org/10.1074/jbc.M312080200>.
- (306) Caille, O.; Rossier, C.; Perron, K. A Copper-Activated Two-Component System Interacts with Zinc and Imipenem Resistance in *Pseudomonas Aeruginosa*. *J. Bacteriol.* **2007**, 189 (13), 4561–4568. <https://doi.org/10.1128/JB.00095-07>.
- (307) Zimmermann, L.; Kempf, J.; Briée, F.; Swain, J.; Mingeot-Leclercq, M.-P.; Décout, J.-L. Broad-Spectrum Antibacterial Amphiphilic Aminoglycosides: A New Focus on the Structure of the Lipophilic Groups Extends the Series of Active Dialkyl Neamines. *Eur. J. Med. Chem.* **2018**, 157, 1512–1525. <https://doi.org/10.1016/j.ejmech.2018.08.022>.
- (308) Zimmermann, L.; Das, I.; Désiré, J.; Sautrey, G.; Barros R. S., V.; El Khoury, M.; Mingeot-Leclercq, M.-P.; Décout, J.-L. New Broad-Spectrum Antibacterial Amphiphilic Aminoglycosides Active against Resistant Bacteria: From Neamine Derivatives to Smaller Neosamine Analogues. *J. Med. Chem.* **2016**, 59 (20), 9350–9369. <https://doi.org/10.1021/acs.jmedchem.6b00818>.
- (309) Fourmy, D.; Recht, M. I.; Puglisi, J. D. Binding of Neomycin-Class Aminoglycoside Antibiotics to the A-Site of 16 s rRNA Edited by I. Tinoco. *J. Mol. Biol.* **1998**, 277 (2), 347–362. <https://doi.org/10.1006/jmbi.1997.1552>.
- (310) Fourmy, D.; Recht, M. I.; Blanchard, S. C.; Puglisi, J. D. Structure of the A Site of *Escherichia Coli* 16S Ribosomal RNA Complexed with an Aminoglycoside Antibiotic. *Science* **1996**, 274 (5291), 1367–1371. <https://doi.org/10.1126/science.274.5291.1367>.
- (311) Agnelli, F.; Sucheck, S. J.; Marby, K. A.; Rabuka, D.; Yao, S.-L.; Sears, P. S.; Liang, F.-S.; Wong, C.-H. Dimeric Aminoglycosides as Antibiotics. *Angew. Chem. Int. Ed.* **2004**, 43 (12), 1562–1566. <https://doi.org/10.1002/anie.200353225>.

- (312) Vicens, Q.; Westhof, E. Crystal Structure of a Complex between the Aminoglycoside Tobramycin and an Oligonucleotide Containing the Ribosomal Decoding A Site. *Chem. Biol.* **2002**, 9 (6), 747–755. [https://doi.org/10.1016/S1074-5521\(02\)00153-9](https://doi.org/10.1016/S1074-5521(02)00153-9).
- (313) Lynch, S. R.; Gonzalez, R. L.; Puglisi, J. D. Comparison of X-Ray Crystal Structure of the 30S Subunit-Antibiotic Complex with NMR Structure of Decoding Site Oligonucleotide-Paromomycin Complex. *Structure* **2003**, 11 (1), 43–53. [https://doi.org/10.1016/S0969-2126\(02\)00934-6](https://doi.org/10.1016/S0969-2126(02)00934-6).
- (314) Russell, A. D. Effect of Magnesium Ions and Ethylenediamine Tetra-Acetic Acid on the Activity of Vancomycin against Escherichia Coli and Staphylococcus Aureus. *J. Appl. Bacteriol.* **1967**, 30 (2), 395–401. <https://doi.org/10.1111/j.1365-2672.1967.tb00314.x>.
- (315) Russell, A. D. Chapter 3G - Ethylenediaminetetra-Acetic Acid. In *Inhibition and Destruction of the Microbial Cell*; Hugo, W. B., Ed.; Academic Press, **1971**; pp 209–224. <https://doi.org/10.1016/B978-0-12-361150-5.50013-4>.
- (316) Leive, L. The Barrier Function of the Gram-Negative Envelope. *Ann. N. Y. Acad. Sci.* **1974**, 235 (1), 109–129. <https://doi.org/10.1111/j.1749-6632.1974.tb43261.x>.
- (317) Mosteller, R. D.; Yanofsky, C. Transcription of the Tryptophan Operon in Escherichia Coli: Rifampicin as an Inhibitor of Initiation. *J. Mol. Biol.* **1970**, 48 (3), 525–531. [https://doi.org/10.1016/0022-2836\(70\)90064-1](https://doi.org/10.1016/0022-2836(70)90064-1).
- (318) Hancock, R. E.; Wong, P. G. Compounds Which Increase the Permeability of the Pseudomonas Aeruginosa Outer Membrane. *Antimicrob. Agents Chemother.* **1984**, 26 (1), 48–52.
- (319) Alakomi, H.-L.; Paananen, A.; Suihko, M.-L.; Helander, I. M.; Saarela, M. Weakening Effect of Cell Permeabilizers on Gram-Negative Bacteria Causing Biodeterioration. *Appl. Environ. Microbiol.* **2006**, 72 (7), 4695–4703. <https://doi.org/10.1128/AEM.00142-06>.
- (320) Leive, L. Release of Lipopolysaccharide by EDTA Treatment of E. Coli. *Biochem. Biophys. Res. Commun.* **1965**, 21 (4), 290–296. [https://doi.org/10.1016/0006-291X\(65\)90191-9](https://doi.org/10.1016/0006-291X(65)90191-9).
- (321) Scudamore, R. A.; Beveridge, T. J.; Goldner, M. Outer-Membrane Penetration Barriers as Components of Intrinsic Resistance to Beta-Lactam and Other Antibiotics in Escherichia Coli K-12. *Antimicrob. Agents Chemother.* **1979**. <https://doi.org/10.1128/AAC.15.2.182>.
- (322) Vaara, M.; Jaakkola, J. Sodium Hexametaphosphate Sensitizes Pseudomonas Aeruginosa, Several Other Species of Pseudomonas, and Escherichia Coli to Hydrophobic Drugs. *Antimicrob. Agents Chemother.* **1989**, 33 (10), 1741–1747. <https://doi.org/10.1128/AAC.33.10.1741>.
- (323) Ayres, H. M.; Furr, J. R.; Russell, A. D. Effect of Permeabilizers on Antibiotic Sensitivity of Pseudomonas Aeruginosa. *Lett. Appl. Microbiol.* **1999**, 28 (1), 13–16. <https://doi.org/10.1046/j.1365-2672.1999.00486.x>.



## Chapter 2

# Structure-activity studies with bis-amidines that potentiate Gram-positive specific antibiotics against Gram-negative pathogens

Charlotte M.J. Wesseling, Cornelis J. Slingerland, Shanice Veraar, Samantha Lok, and Nathaniel I. Martin

Parts of this chapter have been published: *ACS Infect. Dis.* **2021**.

### Abstract

Pentamidine, an FDA approved antiparasitic drug, was recently identified as an outer membrane disrupting synergist that potentiates erythromycin, rifampicin, and novobiocin against Gram-negative bacteria. The same study also described a preliminary structure-activity relationship study using commercially available pentamidine analogues. We here report the design, synthesis, and evaluation of a broader panel of bis-amidines inspired by pentamidine. The present study both validates the previously observed synergistic activity reported for pentamidine, while further assessing the capacity for structurally similar bis-amidines to also potentiate Gram-positive specific antibiotics against Gram-negative pathogens. Among the bis-amidines prepared, a number were found to exhibit synergistic activity greater than pentamidine. These synergists were shown to effectively potentiate the activity of Gram-positive specific antibiotics against multiple Gram-negative pathogens such as *A. baumannii*, *K. pneumoniae*, *P. aeruginosa* and *E. coli*, including polymyxin- and carbapenem-resistant strains.

## 1. Introduction

The growing threat of antimicrobial resistance (AMR) has led to projections that by 2050 the world may be confronted with as many as 10 million annual AMR-associated deaths.<sup>1</sup> Society is already dealing with the rising tide posed by this global health challenge: each year, 700,000 people die due to infections with drug-resistant pathogens.<sup>2</sup> At present, the most critical threats are presented by Gram-negative pathogens, including *Acinetobacter baumannii* (carbapenem-resistant), *Pseudomonas aeruginosa* (carbapenem-resistant), and the *Enterobacteriaceae* (carbapenem-resistant and ESBL-producing strains), such as *Escherichia coli* and *Klebsiella pneumoniae*, according to the World Health Organization (WHO).<sup>3</sup>

In treating infections due to Gram-negative bacteria there is an increased interest in strategies aimed at disrupting the outer membrane (OM) so as to potentiate a number of clinically used antibiotics that on their own are only effective against Gram-positive bacteria.<sup>4-6</sup> In an elegant approach recently reported by Brown and coworkers, a panel of 1440 previously approved drugs was screened to identify compounds capable of disrupting the OM of Gram-negative bacteria.<sup>7</sup> The assay used in the screen was based on findings that at low temperatures, OM synthesis is altered in *E. coli* making it more susceptible to vancomycin.<sup>8,9</sup> This led to the hypothesis that compounds that antagonize vancomycin in *E. coli* grown at 15°C would likely also impact the OM integrity.<sup>7,10</sup> Among the hits identified using this innovative screen, the small molecule bis-amidine pentamidine (**1**) (Figure 1) exhibited the most effective capacity to antagonize the activity of vancomycin.<sup>7</sup>

Pentamidine is used clinically to treat *Pneumocystis jiroveci* pneumonia, trypanosomiasis, and leishmaniasis.<sup>11-13</sup> Apart from its antiprotozoal activity, pentamidine is also known to have moderate antibacterial activity against Gram-positive species.<sup>14,15</sup> Furthermore, pentamidine has also been shown to have anti-cancer activity by restoring the tumor-suppressing activity of p53, is capable to bind A/T-rich regions of double-stranded DNA, and can non-specifically bind and disrupt tRNA secondary structures.<sup>16-19</sup> Unsurprisingly, this broadly active compound has a high incidence of side effects such as nephrotoxicity, hypotension, hypoglycaemia, or local reactions to the injection.<sup>11-13</sup> The Brown group's discovery that pentamidine potentiates the anti-Gram-negative activity of rifampicin, erythromycin, and novobiocin further highlights the multifaceted nature of the compound.<sup>7</sup>

It is well established that the disruption of the Gram-negative OM, for example, with the well-studied polymyxin B nonapeptide (PMBN), can potentiate the activity of hydrophobic, Gram-positive specific antibiotics.<sup>7,20</sup> In keeping with these findings, it is also known that polymyxin-resistance also reduces the synergistic potential of PMBN.<sup>7,20</sup> In this regard, it is notable that the synergistic activity of pentamidine in combination with novobiocin, when evaluated against wild-type and polymyxin-resistant strains of *A. baumannii*, was observed both *in vitro* and *in vivo*.<sup>7</sup>

In addition to pentamidine, Brown and coworkers also examined the synergistic activity of other commercially available bis-amidines by performing checkerboard assays, from which the fractional inhibitory concentration index (FICI) was derived, serving as a measure of synergistic activity.<sup>7,21</sup> These studies highlighted the necessity of two amidine groups for effective potentiation of Gram-positive antibiotics against an *E. coli* indicator

strain.<sup>7</sup> In addition, the linker used to connect the benzamidine moieties was also found to play a key role in determining the activity of the compounds evaluated.<sup>7</sup> Based on these studies, two analogues were identified as having enhanced synergistic activities relative to pentamidine (compounds **2** and **3**, Figure 1). The conclusions drawn from these studies suggest that increased linker length and hydrophobicity, along with decreased linker flexibility, contributes to an increase in synergistic activity for these bis-amidines.<sup>7</sup>

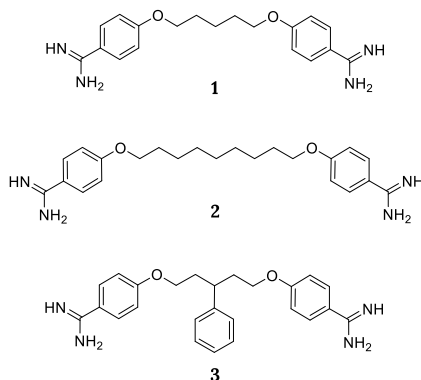


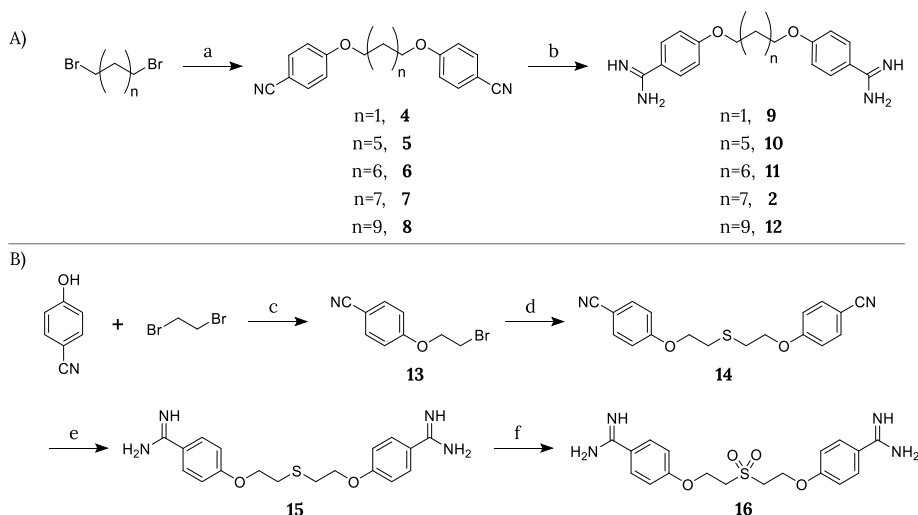
**Figure 1.** Structures of pentamidine (**1**) and analogues **2** and **3** previously found to exhibit synergy with Gram-positive antibiotics against Gram-negative species.<sup>7</sup>

Inspired by these findings, we here describe structure-activity relationship (SAR) studies designed to provide a broad understanding of the structural features required for potent and selective synergy by bis-amidines. While the previous study of Brown and coworkers evaluated the synergistic potential of commercially available bis-amidines, we here report the design, synthesis, and evaluation of a number of novel bis-amidines. In addition to screening for synergistic activity, the new compounds here studied were also assessed for their capacity to selectively target the Gram-negative OM membrane rather than act as non-specific membrane disruptors. Our findings serve to both validate published accounts, while also revealing new, more potent, and selective bis-amidine based synergists.

## 2. Results and Discussion

### 2.1. Synthesis and initial screening

**Linear linkers.** To further explore the correlation between linker length and synergistic activity, a set of linear pentamidine analogues was selected. In addition to the previously reported nonamidine (**2**) and propamidine (**9**), we also synthesized heptamidine (**10**), octamidine (**11**), and undecamidine (**12**) analogues (Scheme 1A). Pentamidine (**1**) was also synthesized by the same route to allow for comparison with the commercial material (Supporting information, Scheme S1), which subsequently revealed no difference in the synergistic activity of the in-house prepared and commercial materials (data not shown).



**Scheme 1.** Synthesis of pentamidine analogues containing different linear spacers between the benzamidine groups. Reagents and conditions: (a) 4-Cyanophenol, NaH, DMF, 80°C, 1h (59%-quant.); (b) i) LHMDs, THF, 48h, rt, ii) HCl (dioxane), 0°C to rt, overnight (49%-quant.); (c) K<sub>2</sub>CO<sub>3</sub>, DMF, 100°C, 5h (43%); (d) Na<sub>2</sub>S·9H<sub>2</sub>O, DMSO, 115°C, 1h (93%); (e) i) LHMDs, THF, rt, 48h; ii) HCl (dioxane), rt, overnight (64%); (f) *m*-CPBA, DCM, 0°C, 2h (32%).

As shown in Scheme 1A, the dibenzonitrile intermediates were prepared from the commercially available  $\alpha,\omega$ -dibromo-alkanes via a Williamson ether synthesis according to literature protocols.<sup>22</sup> Crystallization from ethanol resulted in the pure intermediates **4-8** in good to excellent yields. The transformation of the nitrile groups into the corresponding amidine is classically performed via the Pinner reaction followed by treatment with ammonia.<sup>23-27</sup> However, recent publications have described the same transformation by the more convenient use of a lithium bis(trimethylsilyl)amide (LHMDs) solution followed by an acidic quench.<sup>28-31</sup> In the synthesis of pentamidine we therefore evaluated the treatment of the corresponding bis-nitrile precursor with LHMDs (1 M in tetrahydrofuran (THF)) followed by a quench with saturated ethanolic HCl, 4 M HCl in dioxane, or 1 M HCl (aq) (See Supporting information, Scheme S1 and S2). These trial experiments revealed that quenching with 4 M HCl in dioxane resulted in the highest yield, and these conditions were therefore also applied in the preparation of the bis-amidines **2**, **9-12**, which were subsequently isolated in good yields after high-



performance liquid chromatography (HPLC) purification. In addition to probing linker length, we also explored the impact of heteroatom substitution in the linker. Notably, thioether analogue **15** has been previously prepared and tested for antimicrobial activity.<sup>15,32</sup> Thioether **15** was therefore synthesized as indicated in Scheme 1B, also providing ready access to the more hydrophilic sulfone analogue **16** obtained by *m*-CPBA treatment of **15**.

The inherent antibacterial activities of pentamidine (**1**) and the bis-amidines **2**, **3**, **9-12**, **15**, and **16** were first assessed against an indicator strain *E. coli* BW25113. This revealed a trend wherein compounds containing linkers of eight or more carbons exhibited moderate antibacterial activity with minimum inhibitory concentration (MIC) values of 50 µg/mL (See Table 1). Neither the thioether linked species **15** or sulfone linked **16** showed any inherent activity up to the maximum concentration tested (200 µg/mL). Next, the synergistic activity of the compounds was assessed in combination with both erythromycin and rifampicin using the same indicator *E. coli* strain. Checkerboard assays were performed in which a dilution series of the synergist was evaluated in combination with the antibiotic of interest, also serially diluted. The resulting “checkerboard” or 2-dimensional MIC readout, makes it possible to identify the lowest concentration of both components that results in the most potent synergistic effect. The highest concentrations tested among the synergists correspond to their inherent MIC values (or up to 200 µg/mL in case where no antibacterial activity was observed). For erythromycin the highest concentration tested was 200 µg/mL and for rifampicin it was 12 µg/mL.

In general, a trend was observed wherein bis-amidines with longer linker lengths showed a great capacity to potentiate the activity of erythromycin (Table 1). Compared with pentamidine (FICI 0.500), nonamidine (**2**), and heptamidine (**10**) were found to be the most effective synergists with FICI values of 0.094 and 0.125, respectively, while the shorter propamidine (**9**) exhibited activity on par with pentamidine (Figure 2). The synergistic activities observed when the same panel of bis-amidines was evaluated with rifampicin corroborates the findings with erythromycin (Table 1 and Supporting information Figure S2). These findings highlight the importance of linker length and hydrophobicity for synergistic activity. All analogues containing linkers greater than five carbon atoms demonstrated more potent synergy than the observed for pentamidine. By comparison, propamidine (**9**), containing a three carbon spacer and thioether **15** (isosteric to pentamidine) exhibited synergistic activities comparable to pentamidine. It is also interesting to note that the introduction of the more polar sulfone-linker as in **16** led a complete loss of synergistic activity (Table 1, Supporting information, Figure S1, S2, and Table S1, S2).

Examination of the effect of these bis-amidines on red blood cells revealed another feature that correlates with linker length. Specifically, the enhanced antimicrobial activity and synergistic potential in combination with erythromycin observed for analogues containing longer linkers is accompanied by an increase in hemolytic activity (Table 1 and Supporting information Figures S17 and S18 and Table S17). While propamidine (**9**) and pentamidine (**1**) have little inherent antibacterial activity (MIC of 200 µg/mL or higher) and are moderate synergists with erythromycin (FICI of 0.500), they are also non-hemolytic (erythrocytes treated with compounds at 200 µg/mL for 20 h. at 37°C, non-hemolytic defined as <10%<sup>33</sup>). By comparison, the slightly longer heptamidine (**10**) has an inherent antimicrobial activity (MIC 200 µg/mL) along with enhanced synergistic activity with erythromycin (FICI ≤0.125) but also a slight increase in



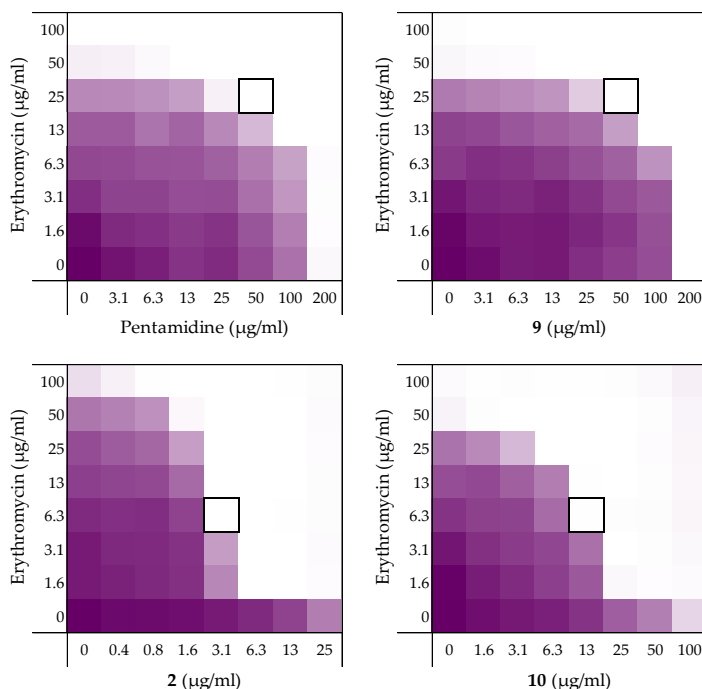


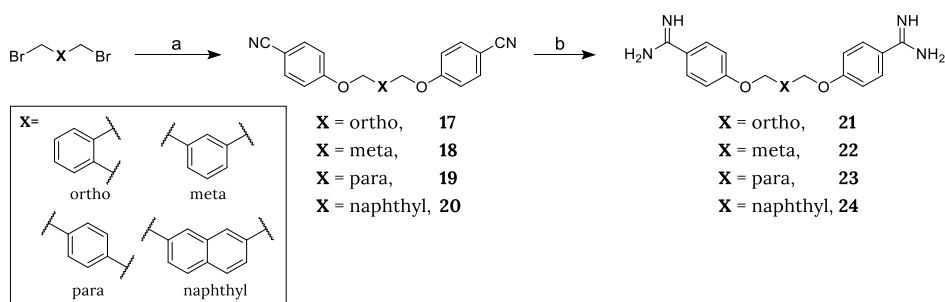
**Figure 2.** Representative checkerboard assays for pentamidine (**1**), propamidine (**9**), nonamidine (**2**) and heptamidine (**10**) in combination with erythromycin versus *E. coli* BW25113. In each case, the bounded box in the checkerboard assays indicates the combination of compound and antibiotic resulting in the lowest FICI (See Table 1). OD<sub>600</sub> values were measured using a plate reader and transformed to a gradient: purple represents growth, white represents no growth. An overview of all checkerboard assays with erythromycin can be found in the Supporting information, Figure S1.

hemolytic activity to 9.2%. However, the longer octamidine (**11**), nonamidine (**2**), and undecamidine (**12**) exhibit very significant levels of hemolysis (16–87%), suggesting that both the inherent antimicrobial activity (MIC 50 µg/mL) and potent synergistic activity in combination with erythromycin (FICI ≤0.094–0.156) of these analogues are driven by a general membrane disruption mechanism and not a selective disruption of the Gram-negative OM. Based on these findings, it appears that the “tipping point” associated with the desirable synergistic effects versus the unwanted hemolytic activity appears to be for C<sub>7</sub> spaced bis-amidine analogue heptamidine (**10**). These findings served to inform the design of the next series of analogues.

## 2.2. Linkers with reduced flexibility

Building on our initial findings with the linear bis-amidines, we next examined the effect of reducing the rotational flexibility of the linker. In the Brown group’s earlier study, it was noted that phenyl substituted bis-amidine **3** (Figure 1) was an extremely effective synergist, an effect that was attributed in part to its decreased molecular flexibility.<sup>7</sup> To this end, we prepared a series of bis-amidines (Scheme 2, compounds **21–24**) that incorporate linkers comprising different planar, aromatic motifs as a means of even further restricting flexibility. For purposes of comparison, we also prepared compound **3**

(Supporting information Scheme S3) and confirmed its synergistic activity (Table 1, Supporting information Figure S1 and S2). Notable, however, was the finding that compound **3** also exhibits significant hemolytic activity (above 10%<sup>33</sup>) (See Table 1 and Supporting information, Figure S18 and Table S17) suggesting that impressive synergistic activity associated with the compound is not selective for the Gram-negative OM and is due instead to general membrane disruption. The synthetic route used to access bis-amidines **21–24** is shown in Scheme 2 and was based largely on the published preparation of these and similar compounds previously evaluated as anti-parasitic agents.<sup>22,34–39</sup> The *meta*-oriented linker in compound **22** most closely mimics the 5-carbon spacer found in pentamidine, while analogues **21** and **23** differ slightly due to the *ortho*- and *para*-orientations of the benzene core. In the case of compound **24**, a 2,7-disubstituted naphthalene motif was envisioned to mimic of the 7-carbon spacer found in heptamidine (**10**). The synthesis of compounds **21–24** started from the corresponding commercially available dibromo-xylenes or 2,7-bis(bromomethyl)naphthalene, which were transformed into the corresponding bis-nitriles **17–20** by treatment with 4-cyanophenol and NaH in dimethylformamide (DMF) at 80°C. In this case, recrystallization of the intermediates **17**, **19**, and **20** from ethanol was not successful. However, based on an acceptable purity (as assessed by NMR), the crude bis-nitriles **19** and **20** could be used directly without a need for further purification, while bis-nitrile **17** was purified using column chromatography. Transformation into the corresponding bis-amidines was in turn performed by treatment with LHMDS<sup>34</sup> followed by acidic quench with 4 M HCl in dioxane to provide compounds **21–24** in acceptable yields after HPLC purification.



**Scheme 2.** Synthesis of bis-amidines containing rigid aromatic spacers. Reagents and conditions: (a) 4-Cyanophenol, NaH, DMF, 80°C, 1h (79%-quant.); (b) i) LHMDS, THF, 48h; ii) HCl (dioxane, 0°C to rt, overnight (19–83%).

Evaluation of the inherent antimicrobial activity of compounds **21–24** as well as their ability to synergize with erythromycin revealed **22** and **24** to be the most effective of these four of compounds (FICI of  $\leq 0.094$  with erythromycin) (Figure 3 and Table 1). *o*-Xylene analogue **21** also exhibited enhanced synergistic activity relative to pentamidine ( $\leq 0.125$  vs. 0.500) while *p*-xylene analogue **23** showed less activity (FICI  $\leq 0.313$ ). Interestingly, while none of compounds **21–24** showed any inherent antibacterial activity up to 200  $\mu\text{g/mL}$ , the 2,7-naphthalene linked analogue **24** was found to exhibit significant hemolytic activity (75%) (See Table 1). These findings are in line with previous studies in which compound **24** was evaluated as an anti-protozoal where it was also found to exhibit

significant toxicity against a rat L6 muscle cell line.<sup>38</sup> By comparison, compounds **21** and **22** were found to be non-hemolytic and demonstrate potent synergy when combined with erythromycin with FICI values of  $\leq 0.125$  and  $\leq 0.094$ , respectively (Table 1). Similarly, **21** and **22** were also found to significantly potentiate the activity of rifampicin against the same *E. coli* indicator strain with FICI values of  $\leq 0.094$  and  $\leq 0.188$ , respectively (Table 1). These findings support the hypothesis that reduced linker flexibility is beneficial for synergistic activity and also reveal the importance of the orientation of the benzamidines on the aromatic nucleus. This is most clearly demonstrated by the potent synergy exhibited by the *ortho*- and *meta*-xylene analogues **21** and **22** (FICI  $\leq 0.094$ – $0.188$ ) in contrast to the much less active *para*-xylene linked **23** (FICI  $\leq 0.313$ – $0.375$ ).

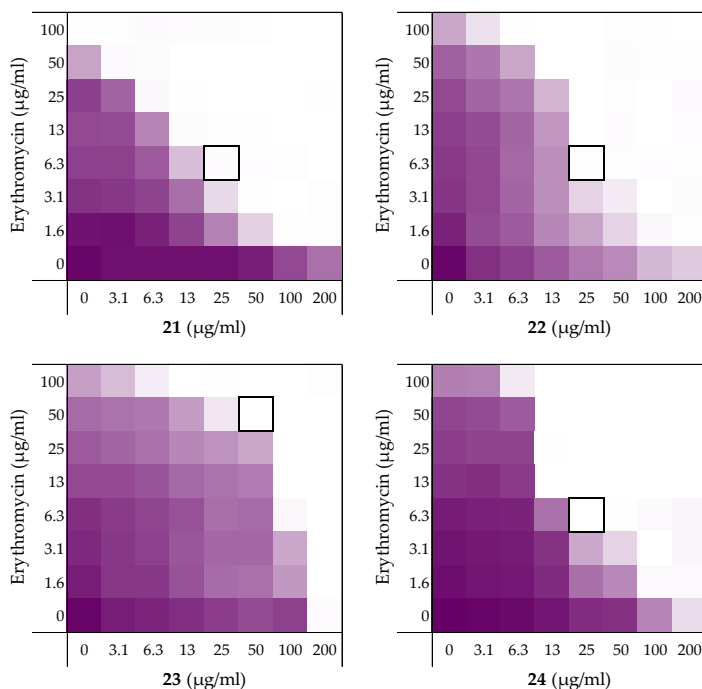
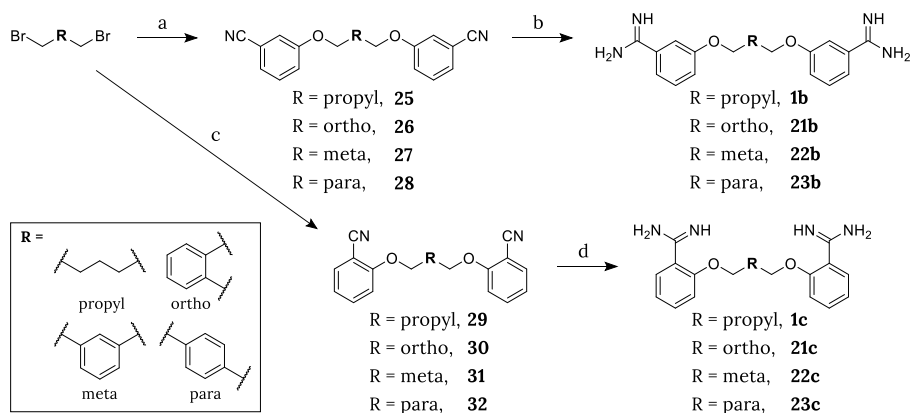


**Figure 3.** Checkerboard assays for compounds **21**–**24** in combination with erythromycin versus *E. coli* BW25113. In each case, the bounded box in the checkerboard assays indicates the combination of compound and antibiotic resulting in the lowest FICI (see Table 1). OD<sub>600</sub> values were measured using a plate reader and transformed to a gradient: purple represents growth, white represents no growth. An overview of all checkerboard assays with erythromycin can be found in the Supporting information, Figure S1.

### 2.3. Altering the position of the amidine moiety

The rigidity of the xylene-based linkers described above not only affects the spacing but also the positioning of the amidine groups. In the case of pentamidine (**1**) and compounds **21**–**23**, the amidine moieties are positioned *para* relative to the linker. We, therefore, next prepared a series of analogues wherein the positioning of the amidine groups was shifted to either the *meta*- or *ortho*-positions (Scheme 3). While the *meta*-amidine analogues **1b**,

**21b-23b** are known in the literature,<sup>24,35,38-41</sup> *ortho*-amidine analogues **1c**, **21c-23c** have not been previously described. The synthesis of the *meta*-amidine analogues was performed following the same protocol employed for the preparation of the corresponding *para*-amidines but using 3-cyanophenol in place of 4-cyanophenol (Scheme 3). For the preparation of the *ortho*-amidine analogues, the intermediate bis-nitriles were prepared in an analogous fashion, however, conversion to the product bis-amidines required a different set of conditions. Unlike the route used in the preparation of the *para*- and *meta*-bis-amidines, treatment of the *ortho*-bis-nitrile intermediates **29-32** with LHMDS failed to yield the expected amidine product. For this reason, an alternative, previously reported three-step procedure for the conversion of nitriles to amidines, was instead employed.<sup>42</sup> In doing so, the nitrile is first converted to the corresponding N-hydroxyamidine by treatment with hydroxylamine hydrochloride. The N-hydroxy group is then acetylated with Ac<sub>2</sub>O followed by reduction to the amidine product using zinc powder (Scheme 3). After HPLC purification, the *ortho*-bis-amidines (**1c**, **21c-23c**) were obtained in yields suitable for subsequent evaluation.



**Scheme 3.** Synthesis of bis-amidine analogues **1b**, **21b-23b** and **1c**, **21c-23c**. Reagents and conditions: (a) 3-Cyanophenol, NaH, DMF, 80°C, 1h (63%-quant); (b) i) LHMDS, THF, 48h, ii) HCl (dioxane), 0°C to rt, overnight (72%-quant); (c) 2-Cyanophenol, NaH, DMF, 80°C, 1h (83-99%); (d) (i) NH<sub>2</sub>OH·HCl, DIPEA, EtOH, 85°C, 6h; (ii) Ac<sub>2</sub>O, AcOH, rt, 4h; (iii) Zn powder, AcOH, 35°C, 6h (12-48%).

As for pentamidine (**1**) and the other *para*-bis-amidines **21-23**, no inherent antimicrobial activity or hemolysis was observed for the *meta*-substituted analogues **1b**, **21b-23b** or the *ortho*-substitute analogues **1c**, **21c-23c** (Table 1). Assessment of synergy with erythromycin showed that the *meta*-bis-amidines maintain a reasonable degree of synergistic activity (Figure 4) while the *ortho*-bis-amidines show no such ability (Table 1). In general, the *meta*-orientated bis-amidines are less effective synergists than the corresponding *para*-oriented compounds, a trend also observed in synergy studies with rifampicin (Table 1). An exception to this was observed for compounds **23** and **23b** both containing the *p*-xylene linker. In this case, the placement of the amidine groups at the *meta*-position relative to the linker results in a slight decrease in FICI from 0.313 for compound **23** to 0.250 for **23b** when tested in combination with erythromycin. An even more pronounced potentiation effect was seen when these compounds were evaluated with rifampicin. In this case, compound **23** was found to have an FICI value of 0.375 while

for **23b**, the FICI value calculated was 0.156, making it one of the most potent, non-hemolytic, rifampicin synergists identified (Table 1). Collectively, these findings indicate that both the geometry of the linker and the positioning of the amidines in the benzamidine moieties are interrelated structural features that play a key role in dictating optimal synergistic activity.

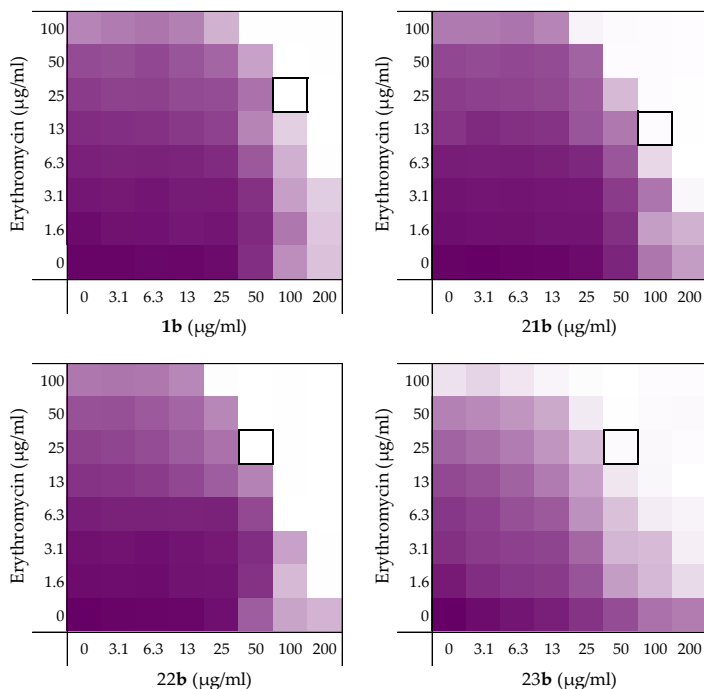


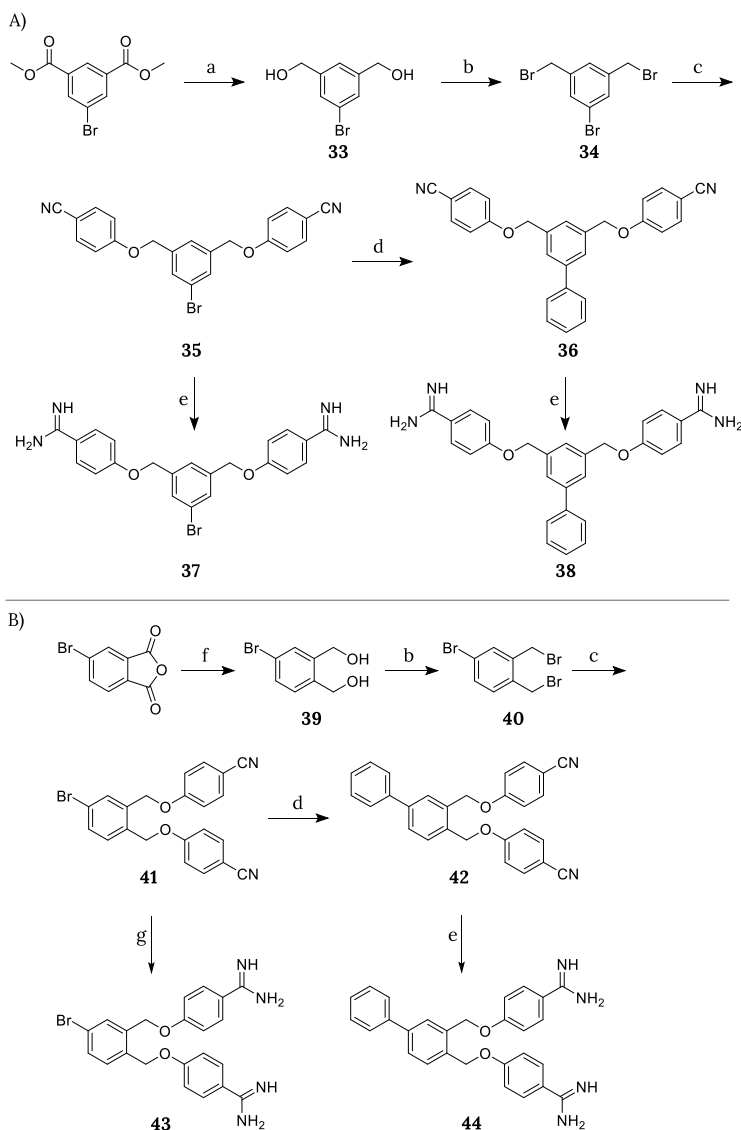
**Figure 4.** Checkerboard assays for compounds **1b**, **21b**–**23b** in combination with erythromycin versus *E. coli* BW25113. In each case, the bounded box in the checkerboard assays indicates the combination of compound and antibiotic resulting in the lowest FICI (see Table 1). OD<sub>600</sub> values were measured using a plate reader and transformed to a gradient: purple represents growth, white represents no growth. An overview of all checkerboard assays with erythromycin can be found in the Supporting information, Figure S1.

## 2.4. Increasing linker hydrophobicity

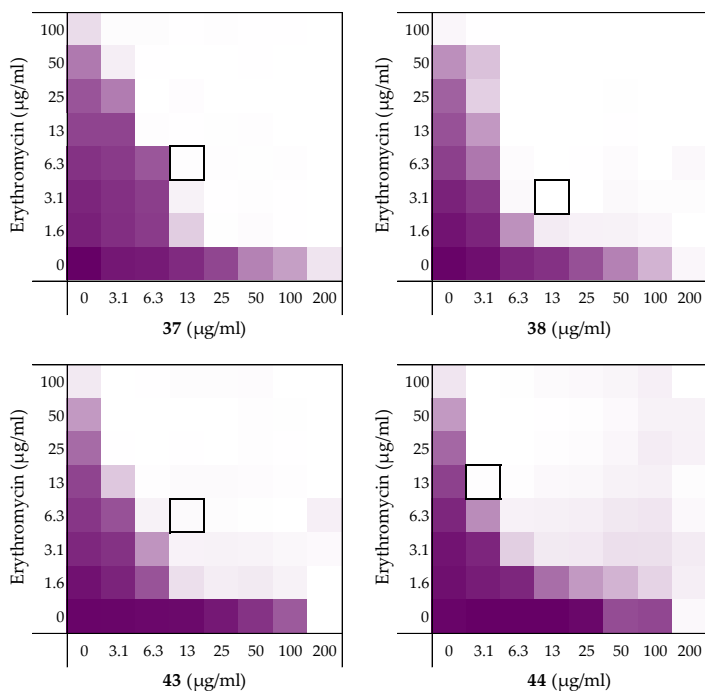
As described above, bis-amidines with more hydrophobic linkers typically show enhanced synergistic activity but often at the cost of increased hemolysis. In this light, compounds **21** and **22** were deemed to be particularly interesting given that they exhibit potent synergistic activity with both erythromycin and rifampicin while displaying no appreciable hemolytic activity. To examine the possibility of further enhancing these compounds we next prepared analogues wherein an additional phenyl group, as for compound **3**, was added as a substituent to the aromatic linkers in both **21** and **22** to give analogues **38** and **44** (Scheme 4). The synthetic route used also provided ready access to brominated intermediates **35** and **41**. Given the hydrophobic character of halogen atoms,<sup>43</sup> we opted to also convert these intermediates to the corresponding bis-amidines **37** and **43**. The synthesis of *meta*-linked analogues **37** and **38** started with the reduction

of dimethyl 5-bromoisophthalate to give diol **33**.<sup>44</sup> An Appel reaction was then applied to transform the diol into tribromide **34**,<sup>45</sup> followed by reaction with 4-cyanophenol to yield bis-nitrile **35**.<sup>22</sup> A portion of **35** was subsequently used in a Suzuki coupling employing phenylboronic acid resulting in intermediate **36**.<sup>46-48</sup> Both **35** and **36** were then converted to the corresponding bis-amidines by treatment with LHMDS followed by HCl quench and HPLC purification to give **37** and **38**. The preparation of **43** and **44** followed a similar synthetic strategy but started with the reduction of 4-bromophthalic anhydride using lithium aluminum hydride and ZnCl<sub>2</sub>.<sup>49</sup> The resulting diol **39** was cleanly converted to tribromide **40**, which was subsequently transformed into the brominated bis-nitrile intermediate **41**. A portion of **41** was then transformed into intermediate **42** using the same Suzuki conditions applied in the previous preparation of **36**.<sup>46-48</sup> Notably, while bis-nitrile **42** was readily transformed into the desired bis-amidine **44** using the LHMDS protocol, when the same conditions were applied to **41** an unexpected dehalogenation occurred. As an alternative, the same three-step process, described above for the preparation of **21b-23b**, was successfully applied to convert the bis-nitrile to the desired bis-amidine **43**.<sup>42</sup>

Compounds **37**, **38**, **43**, and **44** were found to show no significant inherent antimicrobial activity when tested against *E. coli* BW25113 (Table 1). As expected, the introduction of the hydrophobic side-chains improved the synergistic activity with FICI values ranging from 0.047 to 0.094 (Figure 5 and Table 1). Unfortunately, however, and not entirely unexpectedly, the increased hydrophobicity of these analogues was also found to result in a severe increase in hemolytic activity (Table 1) indicating that the enhanced synergistic activity observed is likely due to non-specific membrane disruption.



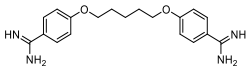
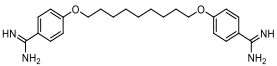
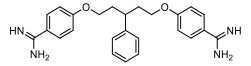
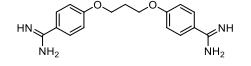
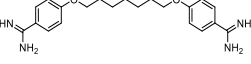
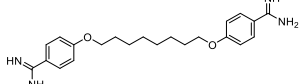
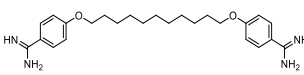
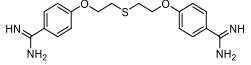
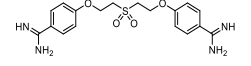
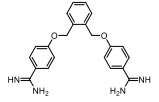
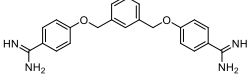
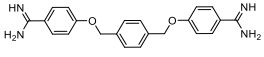
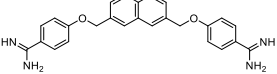
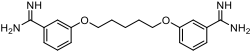
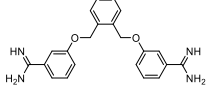
**Scheme 4.** Synthesis of A) *meta*-linked or B) *ortho*-linked bis-amidines containing bromo (**37**, **43**) or phenyl substitution (**38**, **44**) on the central aromatic core. Reagents and conditions: a) i) DIBALH, DCM, 0°C, 1h; ii) Rochelle salt (quench), rt, overnight (96%); (b) PPh<sub>3</sub>, CBr<sub>4</sub>, DCM, rt, 2h (55–74%); (c) 4-Cyanophenol, NaH, DMF, 80°C, 1h (87–99%); (d) Phenylboronic acid, Pd(dppf)Cl<sub>2</sub>·DCM, THF/Na<sub>2</sub>CO<sub>3</sub> (aq) (1:1), 65°C, 8–18h (8–80%); (e) i) LHMDS, THF, rt, 48h; ii) HCl (dioxane), 0°C – rt, overnight (17–75%); f) i) LAH, ZnCl<sub>2</sub>, THF, rt, 6h; ii) Rochelle salt (quench), rt, overnight (95%); (g) i) NH<sub>2</sub>OH·HCl, DIPEA, EtOH, 85°C, 6h; ii) Ac<sub>2</sub>O, AcOH, rt, 4h; iii) Zn powder, AcOH, 35°C, 6h (7%).



**Figure 5.** Checkerboard assays for compounds **37**, **38**, **43**, and **44** in combination with erythromycin versus *E. coli* BW25113. In each case, the bounded box in the checkerboard assays indicates the combination of compound and antibiotic resulting in the lowest FICI (see Table 1). OD<sub>600</sub> values were measured using a plate reader and transformed to a gradient: purple represents growth, white represents no growth. An overview of all checkerboard assays with erythromycin can be found in the Supporting information, Figure S1.



**Table 1.** Overview of synergy with erythromycin against *E. coli* BW25113 and hemolysis data.

Structures	MIC ( $\mu\text{g/mL}$ )	erythromycin		rifampicin		HA (%) <sup>b</sup>
		MIC ( $\mu\text{g/mL}$ )	FICI <sup>a</sup>	MIC ( $\mu\text{g/mL}$ )	FICI	
<b>1</b> 	200	100	0.500	12	0.375	0.4
<b>2</b> 	50	>100	$\leq 0.094$	6	$\leq 0.094$	82
<b>3</b> 	>200	>100	$\leq 0.063$	6	$\leq 0.063$	13
<b>9</b> 	$\geq 200$	100	0.500	12	$\leq 0.500$	0.6
<b>10</b> 	>100	100	$\leq 0.125$	12	0.078	9.2
<b>11</b> 	50	>100	$\leq 0.156$	12	$\leq 0.125$	16
<b>12</b> 	50	>100	$\leq 0.133$	12	$\leq 0.078$	87
<b>15</b> 	>200	100	$\leq 0.375$	6	$\leq 0.500$	0.0
<b>16</b> 	>200	50	>0.5	6	>0.5	0.1
<b>21</b> 	>200	100	$\leq 0.125$	12	$\leq 0.094$	0.5
<b>22</b> 	>200	>100	$\leq 0.094$	12	$\leq 0.188$	1.1
<b>23</b> 	$\geq 200$	>100	$\leq 0.313$	6	0.375	0.4
<b>24</b> 	$\geq 200$	>100	$\leq 0.094$	12	0.031	75
<b>1b</b> 	>200	>100	$\leq 0.375$	12	$\leq 0.375$	0.1
<b>21b</b> 	>200	>100	$\leq 0.313$	6	$\leq 0.313$	0.4

<b>22b</b>		>200	>100	≤0.250	6	≤0.250	1.6
<b>23b</b>		>200	>100	≤0.250	>12	≤0.156	3.7
<b>1c</b>		>200	>100	>0.5	12	>0.5	0.7
<b>21c</b>		>200	>100	>0.5	12	>0.5	0.4
<b>22c</b>		>200	>100	>0.5	12	>0.5	0.0
<b>23c</b>		>200	>100	>0.5	12	>0.5	0.0
<b>37</b>		>100	>100	≤0.063	>12	≤0.125	57
<b>38</b>		≥100	>100	≤0.047	>12	≤0.039	58
<b>43</b>		≥100	>100	≤0.094	12	0.094	57
<b>44</b>		≥200	>100	≤0.078	12	≤0.047	82
<b>PMBN</b>		>200	200	≤0.125	3	≤0.039	-

<sup>a</sup>Synergy defined as FICI ≤0.5.<sup>21</sup> See Supporting Information Tables S1 and S2 for full data used in calculating the FICIs with erythromycin and rifampicin respectively; <sup>b</sup>Hemolytic activity of all compounds after 20 hours of incubation at 200 µg/mL. Values <10% were defined as non-hemolytic.<sup>33</sup>

## 2.5. Exploring the synergistic range

Erythromycin, rifampicin, novobiocin, and vancomycin are typically used to treat Gram-positive infections.<sup>50–55</sup> However, when combined with OM disrupting agents, these antibiotics can also display efficacy against Gram-negative bacteria.<sup>6,20</sup> The Brown group's recent study with pentamidine showed that erythromycin, rifampicin, and novobiocin were most effectively potentiated by this bis-amidine.<sup>7</sup> With this in mind, we next investigated the broader synergy of the most promising compounds identified in our present study, namely, compounds **21**, **22**, and **23b**. As noted above, these three compounds were all found to be more active than pentamidine in potentiating the activity of erythromycin and rifampicin against an indicator *E. coli* stain while showing no hemolytic activity. To this end, compounds **21**, **22**, and **23b** were evaluated against an expanded panel of organisms, including several *E. coli* strains (including carbapenem- and polymyxin-resistant strains) and ATCC strains of *A. baumannii*, *K. pneumoniae*, and *P. aeruginosa*. In addition, the well-studied OM disruptor PMBN and pentamidine itself were taken along as benchmarks in the expanded assessment of compounds **21**, **22**, and **23b**.

### 2.5.1. Synergy with novobiocin and vancomycin

Building from the synergy studies with erythromycin and rifampicin described above, compounds **21**, **22**, and **23b** were next tested for the ability to potentiate novobiocin and vancomycin, along with pentamidine (**1**) and PMBN (Figure 6, Supporting information Figures S3 and S4). In agreement with previous studies, novobiocin and vancomycin showed no antimicrobial activity against the indicator *E. coli* BW25113 strain at the highest concentration tested of 200 µg/mL.<sup>7,56</sup> Checkerboard assays with compounds **21**, **22**, and **23b** in combination with novobiocin revealed the compounds to be superior synergists compared to pentamidine (Table 2, Figure 6), a finding in line with the results obtained when the same bis-amidines were evaluated with erythromycin and rifampicin. In general, PMBN was found to be a more potent synergist than the bis-amidines with the exception of compound **22** in combination with erythromycin which resulted in very effective growth prevention of the *E. coli* indicator strain. When tested in combination with vancomycin, none of the bis-amidines showed any synergistic activity, while PMBN maintained a potent effect (Table 2). These findings are in line with previously reported observations in which pentamidine was found not to synergize with vancomycin.<sup>7</sup>

**Table 2.** FICI values of pentamidine (**1**), **21**, **22**, **23b**, and PMBN against *E. coli* BW25113 in combination with Gram-positive-specific antibiotics rifampicin, novobiocin, and vancomycin.<sup>a</sup>

	Erythromycin	Rifampicin	Novobiocin	Vancomycin
Pentamidine ( <b>1</b> )	0.500	0.375	≤0.281	>0.5 <sup>b</sup>
<b>21</b>	≤0.125	≤0.094	≤0.125	>0.5 <sup>b</sup>
<b>22</b>	≤0.094	≤0.188	≤0.078	>0.5 <sup>b</sup>
<b>23b</b>	≤0.250	≤0.156	≤0.188	>0.5 <sup>b</sup>
PMBN	≤0.125	≤0.039	≤0.047	≤0.156

<sup>a</sup>MIC and minimal synergistic concentrations (MSC) data can be found in the Supporting information, Table S1–S4. <sup>b</sup>Synergy defined as an FICI ≤0.5.<sup>21</sup>

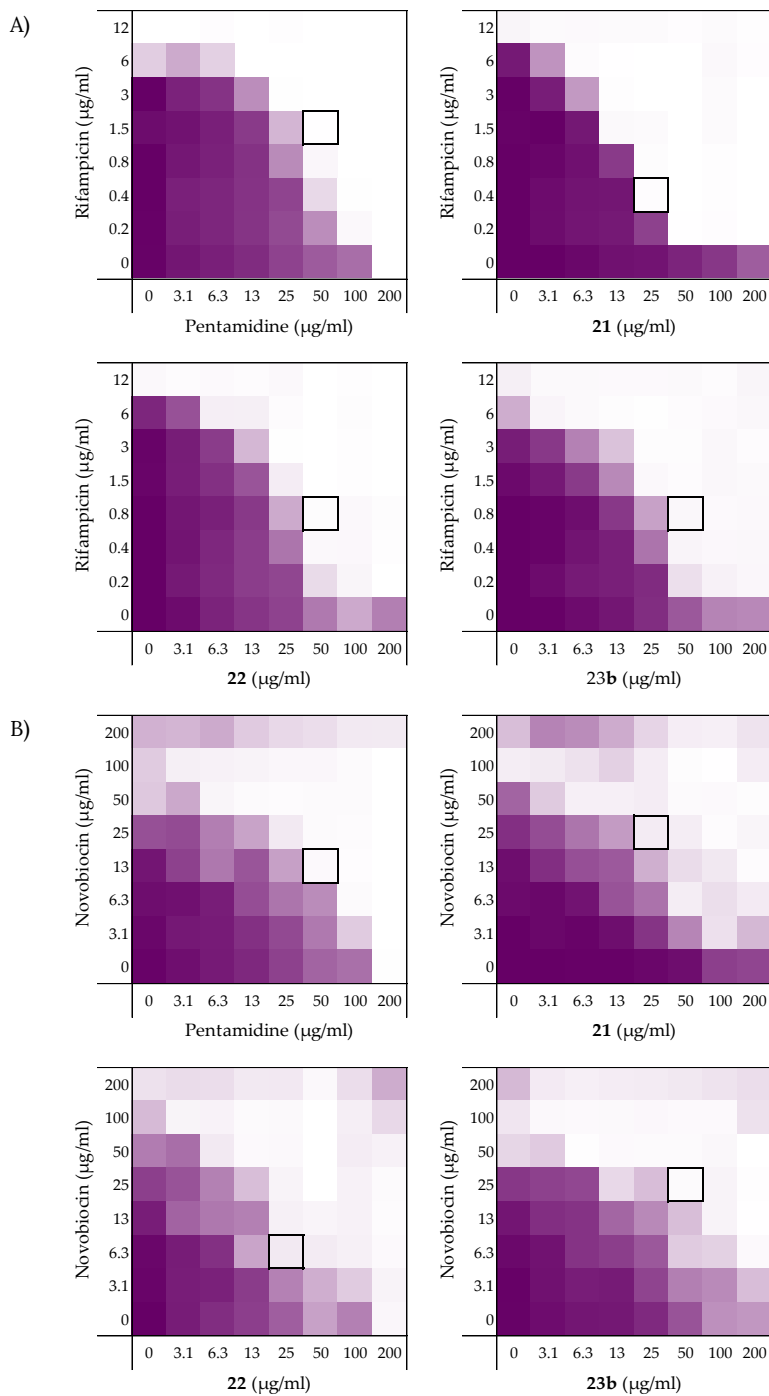


**Figure 6.** Checkerboard assays of compounds pentamidine (**1**), **21**, **22**, and **23b** in combination with A) rifampicin and B) novobiocin against *E. coli* BW25113. In each case, the bounded box in the checkerboard assays indicates the combination of compound and antibiotic resulting in the lowest

FICI (see Table 2). OD<sub>600</sub> values were measured using a plate reader and transformed to a gradient: purple represents growth, white represents no growth. The poor aqueous solubility of novobiocin results in the background signal observed in the OD<sub>600</sub> read-out at when tested at concentrations  $\geq 100$   $\mu\text{g/mL}$ . An overview of all checkerboard assays with rifampicin, novobiocin and vancomycin can be found in the Supporting information, Figure S2-S4.

### 2.5.2. Synergy against other *E. coli* strains.

The next phase of our investigation involved assessing the synergistic activity of the most promising compounds identified against an expanded panel of *E. coli* strains. For these screens, we opted to focus on rifampicin as the companion antibiotic given that it is bactericidal while erythromycin is considered to be bacteriostatic.<sup>11,57</sup> In our initial screens, a more clear-cut distinction of growth versus no growth was indeed observed for rifampicin, possibly due to its bactericidal nature (see Figures 3 and 6A). Furthermore, given that the MIC of rifampicin is significantly lower against the Gram-negative strains used versus the MICs of erythromycin or novobiocin, potential solubility issues at the highest antibiotic concentrations tested were not a problem.

In selecting an expanded panel of *E. coli* strains, we sought to examine a variety of features ranging from the OM composition to resistance profile. In the case of *E. coli*, the structure of the lipopolysaccharide (LPS) layer is known to affect their susceptibility to antibiotics<sup>58</sup> and we therefore reasoned that it could also play a role in the synergistic activity of compounds targeting the OM. This was seen as particularly relevant for the pentamidine analogues investigated here, given that previous studies have suggested that pentamidine interacts with lipid A.<sup>7</sup> With this in mind, *E. coli* ATCC25922 (smooth LPS) and *E. coli* W3110 (rough LPS) were selected, along with the indicator lab strain *E. coli* BW25113 also known to possess a rough LPS layer.<sup>59-61</sup> Additionally, a clinical isolate *E. coli* 552060.1 was included, which, like most clinical isolates, has a smooth LPS layer.<sup>58,62</sup> The inherent antimicrobial activity of rifampicin, pentamidine (**1**), compounds **21**, **22**, **23b**, and PMBN was first established against these *E. coli* strains (Supporting information Figures S5-S7 and Tables S5-S7). In keeping with our initial checkerboard assays with rifampicin and the *E. coli* BW25113 strain (Table 1), compound **21** in nearly all cases showed the lowest FICI values among the bis-amidines evaluated against the expanded *E. coli* panel (Figure 7A and Table 3). In general, the bis-amidines tested all showed effective synergy with little difference observed for the rough or smooth LPS strains.

The expanded screening was continued with *E. coli* bearing *mcr*-1, *mcr*-2, and *mcr*-3 genotypes known to confer polymyxin resistance. For this purpose, a lab strain *E. coli* BW25113 *mcr*-1, transformed with the pGDP2 plasmid, was also included to directly assess the effect of the phosphoethanolamine transferase responsible for lipid A modification.<sup>63-65</sup> The bis-amidines displayed synergy with rifampicin against all *mcr*-positive strains evaluated (Figure 7B, Table 3, Supporting information Figures S8-S12, and Tables S8-S12). Again, in nearly all cases, compound **21** gave the lowest FICI values among the bis-amidines evaluated, with synergy comparable to that of PMBN, which was found to be generally less effective against *mcr*-positive strains than non-*mcr* strains (Table 3).

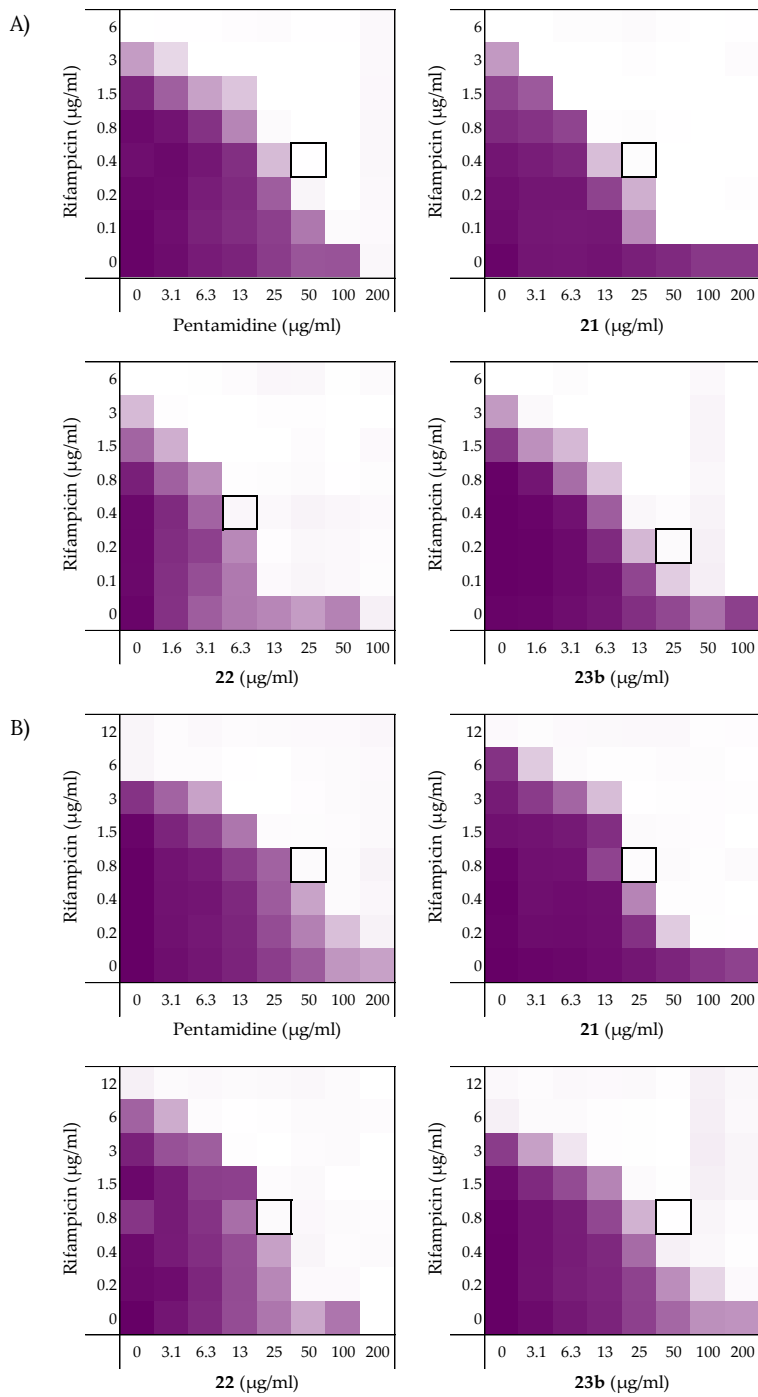
In addition, carbapenem-resistant *E. coli* RC0089, a clinical isolate producing New Delhi  $\beta$ -lactamase 1 (NDM-1), was also evaluated to assess whether this resistance mechanism affected the synergistic activity of the bis-amidines here studied. Notably, the MIC of rifampicin was significantly elevated against this strain (MIC of  $>192$   $\mu\text{g/mL}$ ,

see Supporting information Figure S13 and Table S13). While the bis-amidines were again found to synergize with rifampicin, the FICI values calculated were elevated, with the exception of compound **22** (Figure 7C and Table 3). Interestingly, this strain also resulted in an increased FICI for PMBN.

**Table 3.** FICI values of pentamidine (**1**), **21**, **22**, **23b**, and PMBN in combination with rifampicin against different *E. coli* strains including polymyxin- and carbapenem-resistant strains.<sup>a</sup>

Strain	Pentamidine ( <b>1</b> )	<b>21</b>	<b>22</b>	<b>23b</b>	PMBN
<b>Wild-type</b>					
BW25113	0.375	≤0.094	≤0.188	≤0.156	≤0.039
ATCC25922	0.313	≤0.125	0.094	0.156	≤0.047
W3110	≤0.188	≤0.188	0.313	≤0.188	≤0.031
552060.1	0.375	≤0.094	0.250	≤0.188	≤0.047
<b>Polymyxin-resistant</b>					
BW25113 mcr-1	≤0.250	≤0.094	≤0.156	≤0.188	≤0.156
mcr-1	≤0.188	≤0.188	≤0.188	≤0.188	≤0.094
EQASmcr-1	≤0.250	≤0.125	0.188	≤0.188	≤0.125
EQASmcr-2	0.375	≤0.125	0.313	≤0.125	≤0.156
EQASmcr-3	≤0.188	≤0.125	≤0.188	≤0.188	≤0.094
<b>Carbapenem-resistant</b>					
RC0089	≤0.375	≤0.250	≤0.156	≤0.375	≤0.188

<sup>a</sup>MIC and minimal synergistic concentrations (MSC) data can be found in the Supporting information, Table S2, S5-S13.



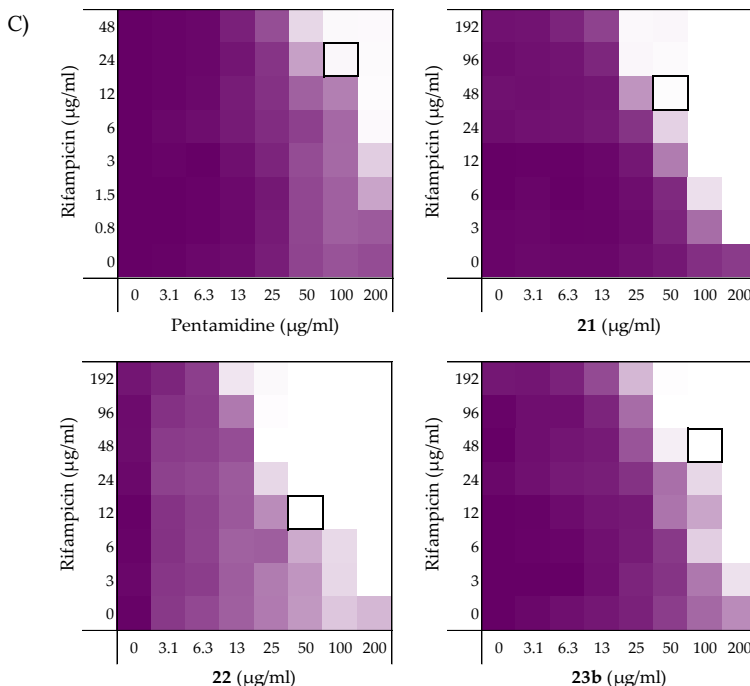


**Figure 7.** Checkerboard assays of compounds pentamidine (**1**), **21**, **22**, and **23b** in combination with rifampicin versus A) *E. coli* ATCC25922; B) *E. coli* EQASmcr-1; C) *E. coli* RC0089. In each case, the bounded box in the checkerboard assays indicates the combination of compound and antibiotic resulting in the lowest FICI (see Table 3). OD<sub>600</sub> values were measured using a plate reader and transformed to a gradient: purple represents growth, white represents no growth. An overview of all checkerboard assays with rifampicin with the *E. coli* strains can be found in the Supporting information, Figure S5–S13.

### 2.5.3. Synergy against *A. baumannii*, *K. pneumoniae*, and *P. aeruginosa*

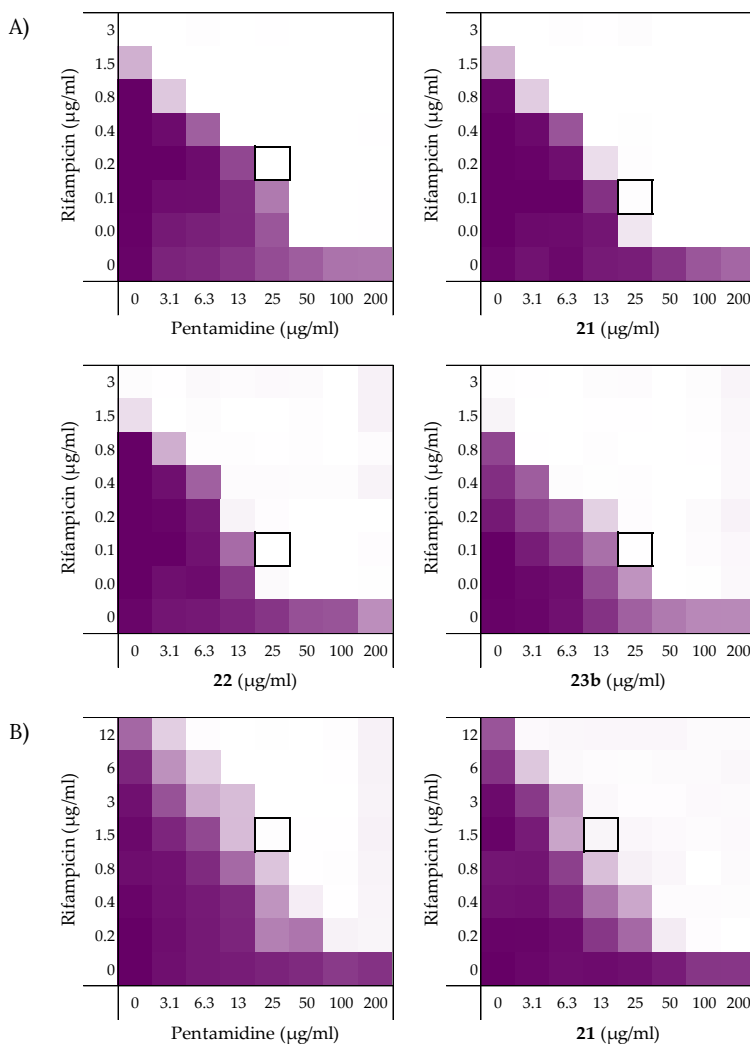
In addition to studying the synergistic activity of the selected bis-amidines against the *E. coli* strains described above, we also investigated their capacity to potentiate the activity of rifampicin against the selected strains of *A. baumannii*, *K. pneumoniae*, and *P. aeruginosa* (Figure 8, Table 4). As for the *E. coli* strains, the inherent antimicrobial activities of rifampicin, pentamidine (**1**), compounds **21**, **22**, **23b**, and PMBN were first established against each strain (Supporting information Table S14–S16). Full checkerboard assays with the *A. baumannii* and *K. pneumoniae* strains tested showed the bis-amidines and PMBN to be effective synergists. In general, compounds **21**, **22**, and **23b** were found to be more potent than pentamidine (**1**), while PMBN was found to be an even more effective synergist. Among the bis-amidines tested, compound **22** displayed the most effective potentiation of rifampicin. Interestingly, when tested against *P. aeruginosa*, the FICIs determined for pentamidine and compounds **21**, **22**, and **23b** were significantly elevated while PMBN maintained potent synergistic activity.



**Table 4.** FICI values of pentamidine (**1**), **21**, **22**, **23b**, and PMBN in combination with rifampicin against different Gram-negative pathogens.<sup>a</sup>

Strain	Pentamidine ( <b>1</b> )	<b>21</b>	<b>22</b>	<b>23b</b>	PMBN
<i>A. baumannii</i> ATCC17978	≤0.125	≤0.094	≤0.094	≤0.094	≤0.023
<i>K. pneumoniae</i> ATCC13883	≤0.125	≤0.094	≤0.078	≤0.125	≤0.070
<i>P. aeruginosa</i> ATCC27853	≤0.500	≤0.313	≤0.250	≤0.375	0.031

<sup>a</sup>MIC and minimal synergistic concentrations (MSC) data can be found in the Supporting information, Tables S14–S16.



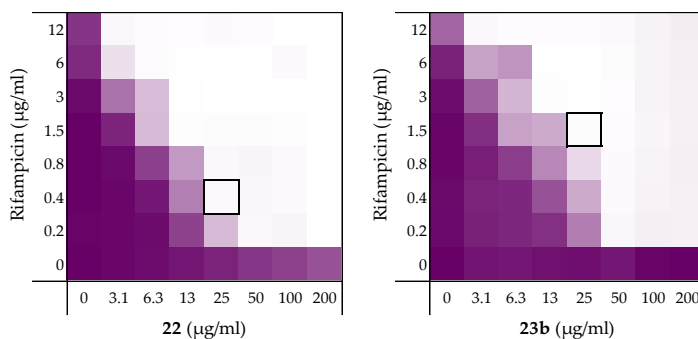


**Figure 8.** Checkerboard assays of pentamidine (**1**), **21**, **22**, and **23b** in combination with rifampicin and versus A) *A. baumannii* ATCC17978 and B) *K. pneumoniae* ATCC13883. In each case, the bounded box in the checkerboard assays indicates the combination of compound and antibiotic resulting in the lowest FICI (see Table 4). OD<sub>600</sub> values were measured using a plate reader and transformed to a gradient: purple represents growth, white represents no growth. An overview of all checkerboard assays with rifampicin with the *E. coli* strains can be found in the Supporting information, Figures S14–S16.

## 2.6. Mechanistic studies

To characterize the mechanism of action of the bis-amidines here studied, we next investigated the capacity of the most active compounds to disrupt the Gram-negative OM. This line of investigation was based in part on the previously noted interaction of pentamidine with lipid A and also on the knowledge that the potentiation of antibiotics like erythromycin, rifampicin, and novobiocin generally relies on OM disruption.<sup>7,20,66</sup> To this end, we employed an established assay relying on the fluorescent properties of N-phenyl-naphthalen-1-amine (NPN) allowing for the real time monitoring and quantification of OM disruption.<sup>67</sup> In the presence of intact bacterial cells, NPN exhibits relatively low levels of fluorescence. However, in the event that the OM is disrupted, NPN can gain entry to the phospholipid layer resulting in a detectable increase in fluorescence that can, in turn, be measured.<sup>67</sup> For this assay, we selected compounds **21** and **22** based on their consistently potent activity in the various synergy assays described above. The bacterial strain used was *E. coli* BW25113 and pentamidine (**1**) and PMBN were taken along as benchmarks. As illustrated in Figure 9, a clear, dose-dependent increase in the fluorescent signal is observed for both **21** and **22**, indicating effective OM disruption. In general, both compounds appear to outperform pentamidine in their ability to disrupt the OM with compound **22** also exhibiting a stronger effect than PMBN (see Supporting information, Figure S19 for NPN fluorescence at higher concentrations of bis-amidines and PMBN).

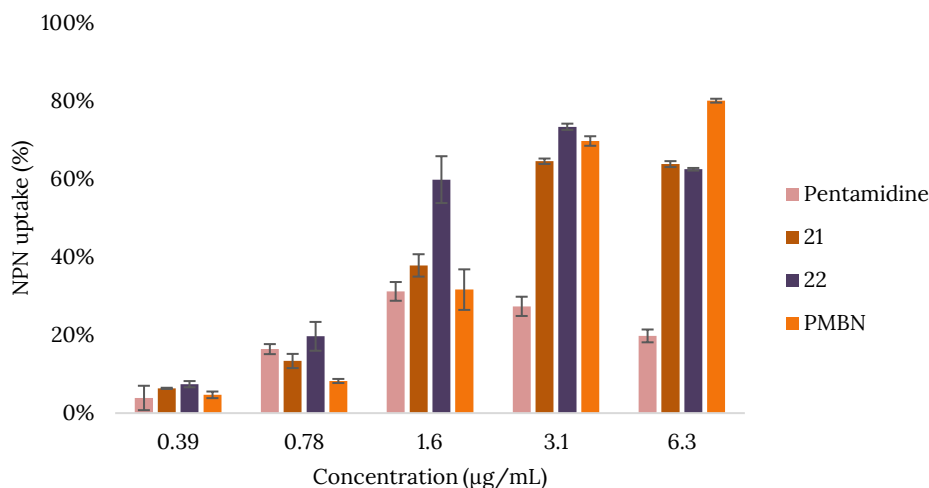


**Figure 9.** Outer membrane permeabilization assay of pentamidine (**1**), compounds **21**, **22**, and PMBN with *E. coli* BW25113 using N-phenyl-1-naphthylamine (NPN) as fluorescent probe. The read-out was performed after 60 minutes of incubation using a plate reader with  $\lambda_{\text{ex}}$  355 nm and  $\lambda_{\text{em}}$  420 nm. The NPN uptake values shown are relative to the uptake signal obtained upon treating the cells with 100 µg/mL colistin as previously reported.<sup>68</sup> All values corrected for background signal of the negative control. Error bars represent the standard deviation based on n=3 technical replicates.

### 3. Conclusion

We here describe structure-activity relationship studies aimed at delivering new insights into the capacity for small-molecule bis-amidines to potentiate the activity of Gram-positive specific antibiotics against Gram-negative bacteria. Inspired by the finding that the anti-parasitic drug pentamidine disrupts the Gram-negative OM to synergize with antibiotics like erythromycin, rifampicin, and novobiocin, we prepared a number of structurally similar bis-amidines and characterized their synergistic potential with the same antibiotics. Our studies confirm that the length, rigidity, and hydrophobicity of the linker unit present in these bis-amidines play an important role in determining their ability to potentiate Gram-positive specific antibiotics.<sup>7</sup> Also of note, however, is the finding that the potent synergy exhibited by bis-amidines containing long, hydrophobic linkers is likely driven by nonspecific membrane disruption as indicated by the strong hemolytic activity associated with these analogues. Further assessment of the linker motif also revealed that, in general, a single aromatic ring provides a desirable balance of enhanced synergistic activity relative to pentamidine, without introducing hemolytic activity. Further examination of the relative positioning of the benzamidine groups on the aromatic linker and as well as the *ortho*-, *meta*-, and *para*-, geometry of the amidine moieties themselves, identified compounds **21**, **22**, and **23b** as most promising. These compounds were found to consistently outperform pentamidine in their ability to potentiate the activity of erythromycin, rifampicin, and novobiocin against a number of *E. coli* strains including polymyxin-resistant and carbapenem-resistant variants. Additional screening showed that among the bis-amidines here studied, compounds **21**, **22**, and **23b** maintain their superior synergistic activity against other Gram-negative pathogens including *A. baumannii*, *K. pneumoniae*, and *P. aeruginosa*. Mechanistic studies also confirm that these bis-amidines effectively induce Gram-negative OM disruption. Taken together, the findings here reported provide a broader understanding of the potential for bis-amidines to be used as synergists in expanding the activity of Gram-positive specific antibiotics against Gram-negative bacteria.

## 4. Materials and methods

**General procedures.** All reagents employed were of American Chemical Society (ACS) grade or finer and were used without further purification unless otherwise stated. For compound characterization, <sup>1</sup>H NMR spectra were recorded at 400 MHz with chemical shifts reported in parts per million (ppm) downfield relative to CHCl<sub>3</sub> (7.26) or DMSO (δ 2.50). <sup>1</sup>H NMR data are reported in the following order: multiplicity (s, singlet; d, doublet; t, triplet; q, quartet and m, multiplet), coupling constant (J) in hertz (Hz) and the number of protons. Where appropriate, the multiplicity is preceded by br, indicating that the signal was broad. <sup>13</sup>C NMR spectra were recorded at 101 MHz with chemical shifts reported relative to CDCl<sub>3</sub> (δ 77.16) or DMSO (δ 39.52). HRMS analysis was performed on a Shimadzu Nexera X2 UHPLC system with a Waters Acquity HSS C18 column (2.1 × 100 mm, 1.8 μm) at 30 °C and equipped with a diode array detector. The following solvent system, at a flow rate of 0.5 mL/min, was used: solvent A, 0.1 % formic acid in water; solvent B, 0.1 % formic acid in acetonitrile. Gradient elution was as follows: 95:5 (A/B) for 1 min, 95:5 to 15:85 (A/B) over 6 min, 15:85 to 0:100 (A/B) over 1 min, 0:100 (A/B) for 3 min, then reversion back to 95:5 (A/B) for 3 min. This system was connected to a Shimadzu 9030 QTOF mass spectrometer (ESI ionisation) calibrated internally with Agilent's API-TOF reference mass solution kit (5.0 mM purine, 100.0 mM ammonium trifluoroacetate and 2.5 mM hexakis(1H,1H,3H-tetrafluoropropoxy)phosphazine) diluted to achieve a mass count of 10000. Compounds **13**, **14**, **33**, and **34** were synthesized as previously described and had NMR spectra and mass spectra consistent with the assigned structures.<sup>32,69</sup> Compounds **1**, **2**, **4-6**, **8-11**, **15**, **18**, **19**, **21-23**, **1b**, **21b-23b**, **39**, **40**, **45**, **47**, and **48** were synthesized using optimized protocols as described below and gave NMR spectra and mass spectra consistent for the same compounds previously described in literature.<sup>22,29,32,34,38,39,70-74</sup> Purity of the final compounds **1-3**, **9-12**, **15**, **16**, **21-24**, **1b**, **21b-23b**, **1c**, **21c-23c**, **37**, **38**, **43**, and **44** was confirmed to be ≥ 95% by analytical RP-HPLC using a Shimadzu Prominence-i LC-2030 system with a Dr. Maisch Reprosil Gold 120 C18 column (4.6 × 250 mm, 5 μm) at 30 °C and equipped with a UV detector monitoring at 214 nm. The following solvent system, at a flow rate of 1 mL/min, was used: solvent A, 0.1 % TFA in water/acetonitrile, 95/5; solvent B, 0.1 % TFA in water/acetonitrile, 5/95. Gradient elution was as follows: 95:5 (A/B) for 2 min, 95:5 to 0:100 (A/B) over 30 min, 0:100 (A/B) for 1 min, then reversion back to 95:5 (A/B) over 1 min, 95:5 (A/B) for 3 min. The compounds were purified via preparative HPLC using a BESTA-Technik system with a Dr. Maisch Reprosil Gold 120 C18 column (25 × 250 mm, 10 μm) and equipped with a ECOM Flash UV detector monitoring at 214 nm. The following solvent system, at a flow rate of 12 mL/min, was used: solvent A, 0.1 % TFA in water/acetonitrile 95/5; solvent B, 0.1 % TFA in water/acetonitrile 5/95. Unless stated otherwise in the protocol, the gradient elution was as follows: 100:0 (A/B) to 0:100 (A/B) over 25 min, 0:100 (A/B) for 3 min, then reversion back to 100:0 (A/B) over 1 min, 100:0 (A/B) for 1 min.

### 4.1. Synthesis

**4,4'-(pentane-1,5-diylbis(oxy))dibenzimidamide/pentamidine (1)** This protocol was based on the synthesis of structurally similar amidine containing compounds previously described in literature.<sup>28-31</sup> 4,4'-(pentane-1,5-diylbis(oxy))dibenzonitrile (94 mg, 0.3 mmol) was dissolved in dry THF (2 mL) under argon atmosphere and LHMDs (1.2 mL, 1 M THF solution, 4.0 eq.) was added. The reaction was stirred at room temperature for 48 hours or longer until complete conversion to the bis-amidine (monitored by LCMS). The solution was cooled to 0 °C and quenched with HCl (4.5 mL, 4 M dioxane solution, 60 eq.). The mixture was stirred at room temperature overnight, then diluted with diethyl ether and filtered. The precipitate was purified by preparative HPLC with the gradient 0-100% in 30 minutes to give pentamidine (**1**) (120 mg, quant.). <sup>1</sup>H NMR (400 MHz, DMSO-d<sub>6</sub>) δ 9.14 (s, 4H), 9.06 (s, 4H), 7.81 (d, J = 8.9 Hz, 4H), 7.15 (d, J = 8.9 Hz, 4H), 4.12 (t, J = 6.4 Hz, 4H), 1.88 – 1.75 (m, 4H), 1.65 – 1.52 (m, 2H). <sup>13</sup>C NMR (101 MHz, DMSO) δ 164.70, 163.06, 130.19, 119.50, 114.79, 68.05, 28.21, 22.09. HRMS (ESI): calculated for C<sub>19</sub>H<sub>24</sub>N<sub>4</sub>O<sub>2</sub> [M+H]<sup>+</sup> 341.1977, found 341.1977.

**4,4'-((nonane-1,9-diylbis(oxy))dibenzimidamide/nonamidine (2)** Following the procedure as described for compound **1**, using compound **7** (100 mg, 0.28 mmol), LHMDS (1.5 mL, 1 M THF solution, 5.4 eq.) and HCl (5 mL, 4 M dioxane solution, 71 eq.), afforded the crude product. Purification by preparative HPLC with the gradient 20–100% in 30 minutes afforded compound **2** (86 mg, 84%). <sup>1</sup>H NMR (400 MHz, DMSO-*d*<sub>6</sub>) δ 9.14 (d, *J* = 6.2 Hz, 8H), 7.81 (d, *J* = 8.9 Hz, 4H), 7.13 (d, *J* = 9.0 Hz, 4H), 4.07 (t, *J* = 6.5 Hz, 4H), 1.78 – 1.67 (m, 4H), 1.48 – 1.27 (m, 10H). <sup>13</sup>C NMR (101 MHz, DMSO) δ 164.82, 163.12, 130.21, 119.50, 114.82, 68.16, 29.01, 28.77, 28.52, 25.47. HRMS (ESI): calculated for C<sub>23</sub>H<sub>32</sub>N<sub>4</sub>O<sub>2</sub> [M+H]<sup>+</sup> 397.2604, found 397.2597.

**4,4'-((3-phenylpentane-1,5-diyl)bis(oxy))dibenzimidamide (3)** 4,4'-((3-phenylpentane-1,5-diyl)bis(oxy))dibenzonitrile (109 mg, 0.28 mmol) was dissolved in the LHMDS solution (1.1 mL, 1 M THF solution, 4.0 eq.) under argon atmosphere. The reaction was stirred at room temperature for 48 hours or longer until complete conversion to the bis-amidine (monitored by LCMS). The solution was cooled to 0 °C and quenched with HCl (4.5 mL, 4 M dioxane solution, 60 eq.). The mixture was stirred at room temperature overnight, then diluted with diethyl ether and filtered. The precipitate was purified by preparative HPLC with the gradient 20–100% in 30 minutes to give compound **3** (27.4 mg, 23%). <sup>1</sup>H NMR (400 MHz, DMSO-*d*<sub>6</sub>) δ 9.11 (d, *J* = 12.6 Hz, 8H), 7.77 (d, *J* = 8.9 Hz, 4H), 7.34 – 7.16 (m, 5H), 7.05 (d, *J* = 9.0 Hz, 4H), 4.00 – 3.90 (m, 2H), 3.83 (dd, *J* = 15.0, 8.9 Hz, 2H), 3.14 – 3.04 (m, 1H), 2.29 – 2.16 (m, 2H), 2.13 – 2.00 (m, 2H). <sup>13</sup>C NMR (101 MHz, DMSO) δ 164.81, 162.92, 143.38, 130.21, 128.62, 127.69, 126.58, 119.64, 66.21, 38.31, 35.10. HRMS (ESI): calculated for C<sub>25</sub>H<sub>28</sub>N<sub>4</sub>O<sub>2</sub> [M+H]<sup>+</sup> 417.2291, found 417.2287.

**4,4'-((propane-1,3-diylbis(oxy))dibenzonitrile (4)** These conditions were based on literature protocols.<sup>22</sup> 4-cyanophenol (0.29 g, 2.4 mmol, 2.4 eq.) was suspended in dry DMF (3 mL) under argon atmosphere. The suspension was cooled to 0 °C using an ice bath and NaH (96 mg, 60% dispersion in mineral oil, 2.4 eq.) was slowly added. The reaction was stirred until a clear solution appeared, the ice bath was removed and 1,3-dibromopropane (202 mg, 1 mmol) was added. The reaction mixture was heated to 80 °C for 1 hour and then cooled to room temperature. Water (10 mL) was added to the mixture to obtain precipitation. The precipitate was filtered, washed with water and recrystallized from EtOH to give compound **4** as white crystals (164 mg, 59%). <sup>1</sup>H NMR (400 MHz, CDCl<sub>3</sub>) δ 7.59 (d, *J* = 8.9 Hz, 4H), 6.95 (d, *J* = 8.9 Hz, 4H), 4.21 (t, *J* = 6.0 Hz, 4H), 2.37 – 2.27 (m, 2H). <sup>13</sup>C NMR (101 MHz, CDCl<sub>3</sub>) δ 162.09, 134.19, 119.26, 115.29, 104.39, 64.56, 28.96.

**4,4'-((heptane-1,7-diylbis(oxy))dibenzonitrile (5)** Following the procedure as described above for compound **4**, using 1,7-dibromoheptane (0.60 mL, 3.5 mmol), afforded compound **5** (1.17 g, quant.). <sup>1</sup>H NMR (400 MHz, CDCl<sub>3</sub>) δ 7.56 (d, *J* = 8.8 Hz, 4H), 6.92 (d, *J* = 8.8 Hz, 4H), 3.99 (t, *J* = 6.4 Hz, 4H), 1.89 – 1.76 (m, 4H), 1.55 – 1.40 (m, 6H). <sup>13</sup>C NMR (101 MHz, CDCl<sub>3</sub>) δ 162.49, 134.09, 119.42, 115.26, 103.82, 68.38, 29.14, 29.03, 26.00.

**4,4'-((octane-1,8-diylbis(oxy))dibenzonitrile (6)** Following the procedure as described above for compound **4**, using 1,8-dibromooctane (0.64 mL, 3.5 mmol), afforded compound **6** (1.10 g, 90%). <sup>1</sup>H NMR (400 MHz, CDCl<sub>3</sub>) δ 7.57 (d, *J* = 8.9 Hz, 4H), 6.93 (d, *J* = 8.9 Hz, 4H), 3.99 (t, *J* = 6.5 Hz, 4H), 1.84 – 1.77 (m, 4H), 1.51 – 1.43 (m, 4H), 1.43 – 1.35 (m, 4H). <sup>13</sup>C NMR (101 MHz, CDCl<sub>3</sub>) δ 162.54, 134.12, 119.45, 115.29, 103.86, 68.46, 29.37, 29.11, 26.04.

**4,4'-((nonane-1,9-diylbis(oxy))dibenzonitrile (7)** Following the procedure as described above for compound **4**, using 1,9-dibromononane (0.71 mL, 3.5 mmol), afforded compound **7** (1.26 g, 99%). <sup>1</sup>H NMR (400 MHz, CDCl<sub>3</sub>) δ 7.57 (d, *J* = 8.9 Hz, 4H), 6.93 (d, *J* = 8.8 Hz, 4H), 3.99 (t, *J* = 6.5

Hz, 4H), 1.86 – 1.75 (m, 4H), 1.51 – 1.41 (m, 4H), 1.40 – 1.30 (m, 6H). <sup>13</sup>C NMR (101 MHz, CDCl<sub>3</sub>) δ 162.55, 134.11, 119.46, 115.29, 103.82, 68.49, 29.56, 29.39, 29.11, 26.07.

**4,4'-(undecane-1,11-diylbis(oxy))dibenzonitrile (8)** Following the procedure as described above for compound **4**, using 1,11-dibromoundecane (0.82 mL, 3.5 mmol), afforded compound **8** (1.24 g, 92%). <sup>1</sup>H NMR (400 MHz, CDCl<sub>3</sub>) δ 7.57 (d, J = 8.9 Hz, 4H), 6.93 (d, J = 8.9 Hz, 4H), 3.99 (t, J = 6.5 Hz, 4H), 1.84 – 1.75 (m, 4H), 1.49 – 1.40 (m, 4H), 1.39 – 1.28 (m, 10H). <sup>13</sup>C NMR (101 MHz, CDCl<sub>3</sub>) δ 162.57, 134.11, 119.47, 115.30, 103.80, 68.53, 29.65, 29.63, 29.46, 29.12, 26.08.

**4,4'-(propane-1,3-diylbis(oxy))dibenzimidamide/propamidine (9)** Following the procedure as described above for pentamidine (**1**), using compound **4** (60 mg, 0.2 mmol). After LCMS analysis of the reaction mixture at 48 hours, LHMDS (0.2 mL, 1 M THF solution, 1 eq) was added. The HCl quench was therefore also increased (4 mL, 4 M dioxane solution, 75 eq). Compound **9** was obtained after HPLC purification (33 mg, 49%). <sup>1</sup>H NMR (400 MHz, DMSO-*d*<sub>6</sub>) δ 9.15 (d, J = 9.4 Hz, 8H), 7.82 (d, J = 8.9 Hz, 4H), 7.18 (d, J = 8.9 Hz, 4H), 4.27 (t, J = 6.2 Hz, 4H), 2.24 (p, J = 6.2 Hz, 2H). <sup>13</sup>C NMR (101 MHz, DMSO) δ 164.73, 162.82, 130.22, 119.76, 114.84, 64.84, 28.26. HRMS (ESI): calculated for C<sub>17</sub>H<sub>20</sub>N<sub>4</sub>O<sub>2</sub> [M+H]<sup>+</sup> 313.1664, found 313.1662.

**4,4'-(heptane-1,7-diylbis(oxy))dibenzimidamide/heptamidine (10)** Following the procedure as described above for compound **3**, using compound **5** (100 mg, 0.3 mmol), LHMDS (1.5 mL, 1 M THF solution, 5 eq.) and HCl (5 mL, 4 M dioxane solution, 67 eq.), afforded compound **10** (95.3 mg, 86%). <sup>1</sup>H NMR (400 MHz, DMSO-*d*<sub>6</sub>) δ 9.13 (d, J = 17.8 Hz, 8H), 7.81 (d, J = 8.9 Hz, 4H), 7.14 (d, J = 9.0 Hz, 4H), 4.08 (t, J = 6.5 Hz, 4H), 1.81 – 1.69 (m, 4H), 1.49 – 1.36 (m, 6H). <sup>13</sup>C NMR (101 MHz, DMSO) δ 164.80, 163.12, 130.21, 119.50, 114.82, 68.14, 28.51, 28.47, 25.43. HRMS (ESI): calculated for C<sub>21</sub>H<sub>28</sub>N<sub>4</sub>O<sub>2</sub> [M+H]<sup>+</sup> 369.2290, found 369.2290.

**4,4'-(octane-1,8-diylbis(oxy))dibenzimidamide/octamidine (11)** Following the procedure as described above for compound **3**, using compound **6** (100 mg, 0.29 mmol). After LCMS analysis of the reaction mixture at 48 hours, LHMDS (0.3 mL, 1 M THF solution, 1 eq) was added, bringing the total of equivalents to 5. After an acidic quench with HCl (5 mL, 4 M dioxane solution, 69 eq.) the reaction was stirred overnight. HPLC purification afforded the product **11** (41 mg, 41%). <sup>1</sup>H NMR (400 MHz, DMSO-*d*<sub>6</sub>) δ 8.95 (br, 8H), 7.78 (d, J = 8.9 Hz, 4H), 7.13 (d, J = 8.9 Hz, 4H), 4.06 (t, J = 6.5 Hz, 4H), 1.79 – 1.67 (m, 4H), 1.46 – 1.31 (m, 8H). <sup>13</sup>C NMR (101 MHz, DMSO) δ 164.75, 163.19, 130.29, 119.49, 114.88, 68.22, 28.81, 28.55, 25.50. HRMS (ESI): calculated for C<sub>22</sub>H<sub>30</sub>N<sub>4</sub>O<sub>2</sub> [M+H]<sup>+</sup> 383.2447, found 383.2446.

**4,4'-(undecane-1,11-diylbis(oxy))dibenzimidamide/undecamidine (12)** Following the procedure as described above for compound **3**, using compound **8** (98 mg, 0.25 mmol), LHMDS (1 mL, 1 M THF solution, 4 eq.) and HCl (2 mL, 4M dioxane solution, 32 eq.), afforded the product **12** (68 mg, 64%). <sup>1</sup>H NMR (400 MHz, DMSO-*d*<sub>6</sub>) δ 8.96 (br, 8H), 7.79 (d, J = 8.8 Hz, 4H), 7.14 (d, J = 8.9 Hz, 4H), 4.07 (t, J = 6.5 Hz, 4H), 1.78 – 1.67 (m, 4H), 1.44 – 1.26 (m, 14H). <sup>13</sup>C NMR (101 MHz, DMSO) δ 164.81, 163.12, 130.20, 119.48, 114.81, 68.15, 29.06, 29.02, 28.82, 28.52, 25.48. HRMS (ESI): calculated for C<sub>25</sub>H<sub>36</sub>N<sub>4</sub>O<sub>2</sub> [M+H]<sup>+</sup> 425.2916, found 425.2919.

**4-(2-bromoethoxy)benzonitrile (13)** Protocol as described in literature.<sup>69</sup> 1,2-dibromoethane (4.3 mL, 50 mmol, 5 eq.), 4-cyanophenol (1.2 g, 10 mmol) and K<sub>2</sub>CO<sub>3</sub> (4.2 g, 30 mmol, 3 eq.) were suspended in dry DMF (20 mL) under argon atmosphere. The mixture was stirred at 100 °C for 5 hours, cooled to room temperature and EtOAc and

water were added. The organic layer was separated, washed with brine, dried over Na<sub>2</sub>SO<sub>4</sub> and concentrated in vacuo. The crude product was purified by column chromatography (petroleum ether/EtOAc = 9:1) to afford compound **13** (0.97 g, 43%). <sup>1</sup>H NMR (400 MHz, CDCl<sub>3</sub>) δ 7.60 (d, J = 9.0 Hz, 2H), 6.96 (d, J = 8.9 Hz, 2H), 4.33 (t, J = 6.1 Hz, 2H), 3.66 (t, J = 6.1 Hz, 2H). <sup>13</sup>C NMR (101 MHz, CDCl<sub>3</sub>) δ 161.44, 134.24, 119.11, 115.44, 104.88, 68.08, 28.47.

**4,4'-((thiobis(ethane-2,1-diyl))bis(oxy))dibenzonitrile (**14**)** Protocol as described in literature.<sup>32</sup> Compound **13** (0.96 g, 4.3 mmol, 2 eq.) and Na<sub>2</sub>S·9H<sub>2</sub>O (0.51 g, 2.1 mmol) were dissolved in DMSO (5 mL) and the mixture was stirred at 115 °C under argon atmosphere. After 1 hour, the mixture was poured into ice water (25 mL) and left for 24 hours in the fridge. The precipitate was filtered, washed with cold water and recrystallized from EtOH to obtain compound **14** (0.65 g, 93%). <sup>1</sup>H NMR (400 MHz, CDCl<sub>3</sub>) δ 7.58 (d, J = 8.9 Hz, 4H), 6.94 (d, J = 8.9 Hz, 4H), 4.23 (t, J = 6.4 Hz, 4H), 3.05 (t, J = 6.4 Hz, 4H). <sup>13</sup>C NMR (101 MHz, CDCl<sub>3</sub>) δ 161.73, 134.20, 119.15, 115.31, 104.61, 68.35, 31.71.

**4,4'-((thiobis(ethane-2,1-diyl))bis(oxy))dibenzimidamide (**15**)** Following the procedure as described above for compound **3**, using compound **14** (100 mg, 0.31 mmol), LHMDS (1.55 mL, 1 M THF solution, 5 eq.) and quenched with and HCl (5.2 mL, 4 M dioxane solution, 67 eq.), afforded the product **15** (71 mg, 64%). <sup>1</sup>H NMR (400 MHz, DMSO-*d*<sub>6</sub>) δ 9.00 (s, 6H), 7.81 (d, J = 8.9 Hz, 4H), 7.18 (d, J = 8.9 Hz, 4H), 4.29 (t, J = 6.4 Hz, 4H), 3.04 (t, J = 6.4 Hz, 4H). <sup>13</sup>C NMR (101 MHz, DMSO) δ 164.61, 162.61, 130.24, 119.80, 114.86, 68.01, 30.54. HRMS (ESI): calculated for C<sub>18</sub>H<sub>22</sub>N<sub>4</sub>O<sub>2</sub>S [M+H]<sup>+</sup> 359.1541, found 359.1541.

**4,4'-((sulfonylbis(ethane-2,1-diyl))bis(oxy))dibenzimidamide (**16**)** Compound **15** (100 mg, 0.22 mmol) was dissolved in dry DCM (10 mL) under argon atmosphere. The solution was cooled to 0 °C using an ice bath and *m*-CPBA (54 mg, 77% aqueous solution, 1.1 eq.) was added. The mixture was stirred at 0 °C for 2 hours and then concentrated in vacuo. After HPLC purification with a 0-100% gradient in 30 minutes to obtain compound **16** (27 mg, 32%). <sup>1</sup>H NMR (400 MHz, DMSO-*d*<sub>6</sub>) δ 9.18 (s, 4H), 8.99 (s, 4H), 7.83 (d, J = 8.9 Hz, 4H), 7.21 (d, J = 9.0 Hz, 4H), 4.52 (t, J = 5.5 Hz, 4H), 3.79 (t, J = 5.5 Hz, 4H). <sup>13</sup>C NMR (101 MHz, DMSO) δ 164.65, 162.00, 130.29, 120.39, 114.94, 62.19, 53.38. HRMS (ESI): calculated for C<sub>18</sub>H<sub>22</sub>N<sub>4</sub>O<sub>4</sub>S [M+H]<sup>+</sup> 391.1441, found 391.1434.

**4,4'-((1,2-phenylenebis(methylene))bis(oxy))dibenzonitrile (**17**)** Following the procedure as described above for compound **4**, using 1,2-bis(bromomethyl)benzene (1.0 g, 3.8 mmol), afforded the title compound as crude product. No precipitation occurred upon addition of water. Therefore the mixture was concentrated under reduced pressure and the crude product was purified by column chromatography (petroleum ether/EtOAc = 19:1) to obtain compound **17** (1.2 g, 96%). <sup>1</sup>H NMR (400 MHz, CDCl<sub>3</sub>) δ 7.59 (d, J = 8.0 Hz, 4H), 7.46 (dd, 4H), 6.99 (d, J = 8.0 Hz, 4H), 5.21 (s, 4H). <sup>13</sup>C NMR (101 MHz, CDCl<sub>3</sub>) δ 161.76, 134.26, 134.12, 129.56, 129.27, 119.12, 115.57, 104.79, 68.46.

**4,4'-((1,3-phenylenebis(methylene))bis(oxy))dibenzonitrile (**18**)** Following the procedure as described above for compound **4**, using 1,3-bis(bromomethyl)benzene (0.92 g, 3.5 mmol), afforded compound **18** (0.94 g, 79%). <sup>1</sup>H NMR (400 MHz, CDCl<sub>3</sub>) δ 7.59 (d, J = 8.8 Hz, 4H), 7.50 – 7.37 (m, 4H), 7.02 (d, J = 8.8 Hz, 4H), 5.13 (s, 4H). <sup>13</sup>C NMR (101 MHz, CDCl<sub>3</sub>) δ 161.92, 136.51, 134.19, 129.37, 127.60, 126.52, 119.21, 115.66, 104.54, 70.09.

**4,4'-((1,4-phenylenebis(methylene))bis(oxy))dibenzonitrile (**19**)** Following the procedure as described above for compound **4**, using 1,4-bis(bromomethyl)benzene (0.92 g, 3.5 mmol), afforded compound **19** as a crude product. The crude product was not



recrystallized due to insolubility issues and was used in the next step without further purification based on a purity assessment (NMR) (1.2 g, 97%). <sup>1</sup>H NMR (400 MHz, DMSO-*d*<sub>6</sub>) δ 7.78 (d, *J* = 8.8 Hz, 4H), 7.48 (s, 4H), 7.18 (d, *J* = 8.9 Hz, 4H), 5.22 (s, 4H). <sup>13</sup>C NMR (101 MHz, DMSO) δ 161.74, 136.11, 134.24, 128.08, 119.13, 115.92, 103.05, 69.36.

**4,4'-((2-benzylpropane-1,3-diyl)bis(oxy))dibenzonitrile (20)** Following the procedure as described above for compound **4**, using 2,7-bis(bromomethyl)naphthalene (0.20 g, 0.64 mmol), afforded compound **20** as a crude product. The crude product was not recrystallized due to insolubility issues and was used in the next step without further purification based on a purity assessment (NMR) (0.25 g, quant.). <sup>1</sup>H NMR (400 MHz, CDCl<sub>3</sub>) δ 7.90 (d, *J* = 8.5 Hz, 2H), 7.87 (s, 2H), 7.60 (d, *J* = 8.9 Hz, 4H), 7.54 (dd, *J* = 8.5, 1.7 Hz, 2H), 7.06 (d, *J* = 8.9 Hz, 4H), 5.29 (s, 4H). <sup>13</sup>C NMR (101 MHz, CDCl<sub>3</sub>) δ 134.23, 134.04, 133.08, 128.74, 126.61, 125.65, 119.26, 115.77, 104.56, 70.42.

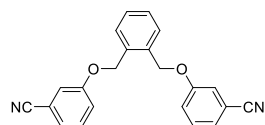
**4,4'-((1,2-phenylenebis(methylene))bis(oxy))dibenzimidamide (21)** Following the procedure as described above for compound **3**, using compound **17** (102 mg, 0.3 mmol), LHMDS (1.5 mL, 1 M THF solution, 5 eq.) and HCl (5.0 mL, 4 M dioxane solution, 67 eq.), afforded the product **21** (63 mg, 56%). <sup>1</sup>H NMR (400 MHz, DMSO-*d*<sub>6</sub>) δ 9.14 (s, 4H), 9.04 (s, 4H), 7.81 (d, *J* = 8.9 Hz, 4H), 7.55 (dd, *J* = 5.6, 3.4 Hz, 2H), 7.40 (dd, *J* = 5.7, 3.3 Hz, 2H), 7.24 (d, *J* = 9.0 Hz, 4H), 5.38 (s, 4H). <sup>13</sup>C NMR (101 MHz, DMSO) δ 164.70, 162.45, 134.57, 130.19, 128.82, 128.44, 120.04, 115.18, 67.51. HRMS (ESI): calculated for C<sub>22</sub>H<sub>22</sub>N<sub>4</sub>O<sub>2</sub> [M+H]<sup>+</sup> 375.1821, found 375.1821.

**4,4'-((1,3-phenylenebis(methylene))bis(oxy))dibenzimidamide (22)** Following the procedure as described above for compound **3**, using compound **18** (100 mg, 0.29 mmol), LHMDS (2.35 mL, 1 M THF solution, 8 eq.) and HCl (4.35 mL, 4 M dioxane solution, 60 eq.), afforded the product **22** (91 mg, 83%). <sup>1</sup>H NMR (400 MHz, DMSO-*d*<sub>6</sub>) δ 9.13 (s, 4H), 8.85 (s, 4H), 7.80 (d, *J* = 8.9 Hz, 4H), 7.56 (s, 1H), 7.44 (d, *J* = 1.3 Hz, 3H), 7.23 (d, *J* = 9.0 Hz, 4H), 5.24 (s, 4H). <sup>13</sup>C NMR (101 MHz, DMSO) δ 164.60, 162.61, 136.67, 130.24, 127.66, 127.19, 119.90, 115.15, 69.54. HRMS (ESI): calculated for C<sub>22</sub>H<sub>22</sub>N<sub>4</sub>O<sub>2</sub> [M+H]<sup>+</sup> 375.1821, found 375.1821.

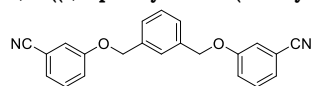
**4,4'-((1,4-phenylenebis(methylene))bis(oxy))dibenzimidamide (23)** Following the procedure as described above for compound **3**, using compound **19** (102 mg, 0.3 mmol), LHMDS (1.5 mL, 1 M THF solution, 5 eq.) and HCl (5 mL, 4 M dioxane solution, 67 eq.), afforded the product **23** (21 mg, 19%). <sup>1</sup>H NMR (400 MHz, DMSO-*d*<sub>6</sub>) δ 9.15 (s, 4H), 9.04 (s, 4H), 7.81 (d, *J* = 8.9 Hz, 4H), 7.50 (s, 4H), 7.23 (d, *J* = 9.0 Hz, 4H), 5.25 (s, 4H). <sup>13</sup>C NMR (101 MHz, DMSO) δ 164.71, 162.55, 136.21, 130.20, 128.05, 119.93, 115.19, 69.34. HRMS (ESI): calculated for C<sub>22</sub>H<sub>22</sub>N<sub>4</sub>O<sub>2</sub> [M+H]<sup>+</sup> 375.1821, found 375.1820.

**4,4'-((naphthalene-2,7-diylbis(methylene))bis(oxy))dibenzimidamide (24)** Following the procedure as described above for compound **3**, using compound **20** (117 mg, 0.3 mmol) and LHMDS (1.5 mL, 1 M THF solution, 5 eq.). After LCMS analysis of the reaction mixture at 48 hours, LHMDS (0.5 mL, 1 M THF solution, 1.7 eq) was added. The reaction was quenched using HCl (6 mL, 4M dioxane solution, 80 eq.). Compound **24** was obtained in a 26% yield (33 mg). <sup>1</sup>H NMR (400 MHz, DMSO-*d*<sub>6</sub>) δ 9.14 (s, 4H), 9.07 (s, 4H), 8.04 – 7.95 (m, 4H), 7.82 (d, *J* = 9.0 Hz, 4H), 7.61 (dd, *J* = 8.4, 1.7 Hz, 2H), 7.29 (d, *J* = 9.0 Hz, 4H), 5.42 (s, 4H). <sup>13</sup>C NMR (101 MHz, DMSO) δ 164.74, 162.58, 134.48, 132.52, 132.25, 130.21, 128.15, 126.59, 126.04, 119.98, 115.27, 69.68. HRMS (ESI): calculated for C<sub>26</sub>H<sub>24</sub>N<sub>4</sub>O<sub>2</sub> [M+H]<sup>+</sup> 425.1977, found 425.1977.

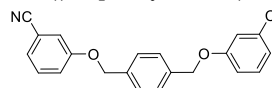
**3,3'-((pentane-1,5-diylbis(oxy))dibenzonitrile (25))** Following the procedure as described above for compound **4**, using 1,5-dibromopentane (0.48 mL, 3.5 mmol) and 3-cyanophenol (1 g, 8.4 mmol), afforded compound **25** (0.68 g, 63%). <sup>1</sup>H NMR (400 MHz, CDCl<sub>3</sub>) δ 7.39 – 7.34 (m, 2H), 7.25 – 7.21 (m, 2H), 7.15 – 7.10 (m, 4H), 4.00 (t, J = 6.3 Hz, 4H), 1.93 – 1.83 (m, 4H), 1.72 – 1.61 (m, 2H). <sup>13</sup>C NMR (101 MHz, CDCl<sub>3</sub>) δ 159.19, 130.48, 124.59, 119.92, 118.91, 117.46, 113.32, 68.20, 28.90, 22.79.



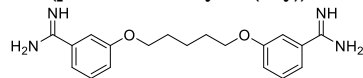
**3,3'-((1,2-phenylenebis(methylene))bis(oxy))dibenzonitrile (26)** Following the procedure as described above for compound **4**, using 1,2-bis(bromomethyl)benzene (1.0 g, 3.8 mmol) and 3-cyanophenol (1.1 g, 9.1 mmol, 2.4 eq.), afforded the title compound as a crude product. The crude product did not precipitate but had very high viscosity. During filtration a minimal amount of acetone was used to prevent clogging. The precipitate was collected and the filtrate was concentrated under reduced pressure to evaporate the acetone. The precipitate in the aqueous solution was filtered again with a minimal amount of acetone. This process was repeated three times to obtain compound **26** (1.1 g, 85%). <sup>1</sup>H NMR (400 MHz, CDCl<sub>3</sub>) δ 7.53 – 7.47 (m, 2H), 7.45 – 7.35 (m, 4H), 7.28 – 7.27 (m, 1H), 7.26 – 7.25 (m, 1H), 7.20 – 7.16 (m, 4H), 5.18 (s, 4H). <sup>13</sup>C NMR (101 MHz, CDCl<sub>3</sub>) δ 158.65, 134.27, 130.67, 129.54, 129.22, 125.21, 120.18, 118.71, 117.74, 113.49, 68.55.



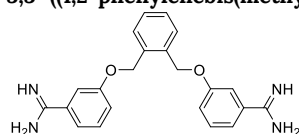
**3,3'-((1,3-phenylenebis(methylene))bis(oxy))dibenzonitrile (27)** Following the procedure as described above for compound **4**, using 1,3-bis(bromomethyl)benzene (0.92 g, 3.5 mmol) and 3-cyanophenol (1.0 g, 8.4 mmol, 2.4 eq.), afforded compound **27** as a crude product. The crude product was not recrystallized due to insolubility issues and was used in the next step without further purification based on a purity assessment (NMR) (1.2 g, quant.). <sup>1</sup>H NMR (400 MHz, CDCl<sub>3</sub>) δ 7.51 – 7.34 (m, 6H), 7.28 – 7.24 (m, 2H), 7.23 – 7.17 (m, 4H), 5.11 (s, 4H). <sup>13</sup>C NMR (101 MHz, CDCl<sub>3</sub>) δ 158.73, 136.65, 130.56, 129.34, 127.48, 126.41, 125.02, 120.22, 118.77, 117.91, 113.38, 70.14.



**3,3'-((1,4-phenylenebis(methylene))bis(oxy))dibenzonitrile (28)** Following the procedure as described above for compound **4**, using 1,4-bis(bromomethyl)benzene (0.9 g, 4 mmol) and 3-cyanophenol (1.1 g, 9.6 mmol, 2.4 eq.), produced compound **28** (1.3 g, 97%). <sup>1</sup>H NMR (400 MHz, CDCl<sub>3</sub>) δ 7.46 (s, 4H), 7.41 – 7.35 (m, 2H), 7.29 – 7.24 (m, 3H), 7.20 (m, 4H), 5.10 (s, 4H). <sup>13</sup>C NMR (101 MHz, CDCl<sub>3</sub>) δ 158.78, 136.21, 130.58, 127.96, 125.03, 120.27, 118.80, 117.93, 113.42, 70.08.



**3,3'-((pentane-1,5-diylbis(oxy))dibenzimidamide (1b))** Following the procedure as described above for compound **3**, using compound **25** (92 mg, 0.3 mmol). LHMDS (1.5 mL, 1 M THF solution, 5 eq.) was added and after LCMS analysis of the reaction mixture at 48 hours, LHMDS (3.0 mL, 1 M THF solution, 10 eq.) was additionally added. A quench with HCl (5.0 mL, 4 M dioxane solution, 67 eq.), afforded the crude product. The crude product was purified using HPLC affording compound **1b** (93 mg, 91%). <sup>1</sup>H NMR (400 MHz, DMSO-*d*<sub>6</sub>) δ 9.46 (s, 4H), 9.32 (s, 4H), 7.52 (t, J = 8.1 Hz, 2H), 7.38 (d, J = 6.6 Hz, 4H), 7.29 (d, J = 8.8 Hz, 2H), 4.09 (t, J = 6.3 Hz, 4H), 1.90 – 1.74 (m, 4H), 1.68 – 1.52 (m, 2H). <sup>13</sup>C NMR (101 MHz, DMSO) δ 165.55, 158.72, 130.35, 129.48, 119.92, 113.80, 67.87, 28.29, 22.22. HRMS (ESI): calculated for C<sub>19</sub>H<sub>24</sub>N<sub>4</sub>O<sub>2</sub> [M+H]<sup>+</sup> 341.1977, found 341.1977.



**3,3'-((1,2-phenylenebis(methylene))bis(oxy))dibenzimidamide (21b)** Following the procedure as described above for compound **3**, using compound **26** (102 mg, 0.3 mmol). LHMDS (1.5 mL, 1 M THF solution, 5 eq.) was added and after LCMS analysis of the reaction mixture at 48 hours, LHMDS (3.0 mL, 1 M THF solution, 10 eq.) was additionally added. A quench with HCl (5.0 mL, 4 M dioxane solution, 67 eq.), afforded the crude product.

The crude product was purified using HPLC affording compound **21b** (80.4 mg, 72%). <sup>1</sup>H NMR (400 MHz, DMSO-*d*<sub>6</sub>) δ 9.45 (s, 4H), 9.33 (s, 4H), 7.59 – 7.54 (m, 2H), 7.53 (s, 1H), 7.52 – 7.46 (m, 3H), 7.45 – 7.35 (m, 6H), 5.34 (s, 4H). <sup>13</sup>C NMR (101 MHz, DMSO) δ 165.43, 158.25, 134.76, 130.37, 129.52, 128.84, 128.44, 120.46, 119.94, 114.63, 67.52. HRMS (ESI): calculated for C<sub>22</sub>H<sub>22</sub>N<sub>4</sub>O<sub>2</sub> [M+H]<sup>+</sup> 375.1821, found 375.1821.

**3,3'-((1,3-phenylenebis(methylene))bis(oxy))dibenzimidamide (22b)** Following the procedure as described above for compound **3**, using compound **27** (102 mg, 0.3 mmol). LHMDS (1.5 mL, 1 M THF solution, 5 eq.) was added and after LCMS analysis of the reaction mixture at 48 hours, LHMDS (2.0 mL, 1 M THF solution, 6.7 eq.) was additionally added. A quench with HCl (5.0 mL, 4 M dioxane solution, 67 eq.), afforded the crude product. The crude product was purified using HPLC affording compound **22b** (88 mg, 78%). <sup>1</sup>H NMR (400 MHz, DMSO-*d*<sub>6</sub>) δ 9.46 (s, 4H), 9.34 (s, 4H), 7.62 – 7.52 (m, 3H), 7.50 (s, 2H), 7.47 (s, 3H), 7.44 – 7.36 (m, 4H), 5.23 (s, 4H). <sup>13</sup>C NMR (101 MHz, DMSO) δ 165.44, 158.38, 136.84, 130.41, 129.52, 128.84, 127.59, 127.13, 120.41, 120.03, 114.43, 69.59. HRMS (ESI): calculated for C<sub>22</sub>H<sub>22</sub>N<sub>4</sub>O<sub>2</sub> [M+H]<sup>+</sup> 375.1821, found 375.1821.

**3,3'-[1,4-Phenylenebis(methyleneoxy)]dibenzenecarboximidamide (23b)** Following the procedure as described above for compound **3**, using compound **28** (102 mg, 0.3 mmol), LHMDS (2.4 mL, 1 M THF solution, 8 eq.) and HCl (4.5 mL, 4 M dioxane solution, 60 eq.) produced compound **23b** (114 mg, quant.). <sup>1</sup>H NMR (400 MHz, DMSO-*d*<sub>6</sub>) δ 9.30 (d, J = 19.8 Hz, 8H), 7.54 – 7.38 (m, 8H), 7.38 – 7.26 (m, 4H), 5.16 (s, 4H). <sup>13</sup>C NMR (101 MHz, DMSO) δ 165.40, 158.35, 136.33, 130.41, 129.51, 128.04, 120.40, 120.03, 114.47, 69.42. HRMS (ESI): calculated for C<sub>22</sub>H<sub>22</sub>N<sub>4</sub>O<sub>2</sub> [M+H]<sup>+</sup> 375.1821, found 375.1818.

**2,2'-(pentane-1,5-diylbis(oxy))dibenzonitrile (29)** Following the procedure as described above for compound **4**, using 1,5-dibromopentane (0.54 mL, 4 mmol) and 2-cyanophenol (1.14 g, 9.6 mmol, 2.4 eq.), afforded compound **29** (1.20 g, 97%). <sup>1</sup>H NMR (400 MHz, CDCl<sub>3</sub>) δ 7.61 – 7.45 (m, 4H), 7.04 – 6.92 (m, 4H), 4.12 (t, J = 6.2 Hz, 4H), 1.95 (m, 4H), 1.85 – 1.69 (m, 2H). <sup>13</sup>C NMR (101 MHz, CDCl<sub>3</sub>) δ 160.85, 134.49, 133.85, 120.77, 116.70, 112.37, 102.08, 68.88, 28.58, 22.70.

**2,2'-((1,2-phenylenebis(methylene))bis(oxy))dibenzonitrile (30)** Following the procedure as described above for compound **4**, using 1,2-bis(bromomethyl)benzene (0.53 g, 2 mmol) and 2-cyanophenol (0.57 g, 4.8 mmol, 2.4 eq.), afforded compound **30** (0.56 g, 83%). <sup>1</sup>H NMR (400 MHz, CDCl<sub>3</sub>) δ 7.62 – 7.46 (m, 6H), 7.45 – 7.36 (m, 2H), 7.15 (d, J = 8.4 Hz, 2H), 6.99 (td, J = 7.6, 0.9 Hz, 2H), 5.39 (s, 4H). <sup>13</sup>C NMR (101 MHz, CDCl<sub>3</sub>) δ 160.13, 134.72, 133.97, 133.87, 129.30, 129.05, 121.32, 116.66, 112.91, 102.09, 69.45.

**2,2'-((1,3-phenylenebis(methylene))bis(oxy))dibenzonitrile (31)** Following the procedure as described above for compound **4**, using 1,3-bis(bromomethyl)benzene (0.53 g, 2 mmol) and 2-cyanophenol (0.57 g, 4.8 mmol, 2.4 eq.), afforded compound **31** (0.60 g, 88%). <sup>1</sup>H NMR (400 MHz, CDCl<sub>3</sub>) δ 7.58 (dd, J = 8.1, 1.7 Hz, 2H), 7.55 – 7.48 (m, 3H), 7.44 (m, 3H), 7.05 – 6.96 (m, 4H), 5.23 (s, 4H). <sup>13</sup>C NMR (101 MHz, CDCl<sub>3</sub>) δ 160.29, 136.37, 134.51, 134.00, 129.40, 127.02, 125.20, 121.31, 116.57, 111.95, 102.53, 77.48, 77.16, 76.84, 70.49.

**2,2'-((1,4-phenylenebis(methylene))bis(oxy))dibenzonitrile (32)** Following the procedure as described above for compound **4**, using 1,4-bis(bromomethyl)benzene (0.92 g, 3.5 mmol), 2-cyanophenol (1.1 g, 9.6 mmol, 2.6 eq.), and NaH (0.38 g, 60% dispersion in mineral oil, 2.6 eq.) afforded compound **32** (1.2 g, 99%). <sup>1</sup>H NMR (400 MHz, CDCl<sub>3</sub>) δ 7.59 (dd, J = 7.6, 1.7 Hz, 2H), 7.55 – 7.44

(m, 6H), 7.08 – 6.95 (m, 4H), 5.22 (s, 4H).  $^{13}\text{C}$  NMR (101 MHz,  $\text{CDCl}_3$ )  $\delta$  160.31, 135.86, 134.46, 134.04, 127.49, 121.30, 116.55, 112.99, 102.58, 70.37.

**2,2'-(pentane-1,5-diylbis(oxy))dibenzimidamide (1c)** These conditions were based on literature protocols.<sup>42</sup> To a suspension of compound **29** (190 mg, 0.62 mmol) and DIPEA (0.56 mL, 3.2 mmol, 5 eq.) in EtOH (10 mL) was added  $\text{NH}_2\text{OH}\cdot\text{HCl}$  (208 mg, 3 mmol, 4.8 eq.). The reaction mixture was stirred at 85 °C overnight. The mixture was concentrated in vacuo and the residue was dissolved in AcOH (4.2 mL) and  $\text{Ac}_2\text{O}$  (0.29 mL, 3 mmol, 4.8 eq.) was added. The reaction was stirred for 4 hours and then concentrated in vacuo. The residue was co-evaporated with toluene three times and then suspended in AcOH (7.5 mL) under argon atmosphere. Zinc powder (60 mg, 0.92 mmol, 1.5 eq.) was added and the mixture was stirred at 35 °C overnight. Upon completion, the reaction mixture was filtered through Celite®, the celite was rinsed with acetone and all collected fractions were concentrated in vacuo. The crude product purified by preparative HPLC (gradient 20–100%, 30 minutes) to afford the final compound **1c** (102 mg, 48%).  $^1\text{H}$  NMR (400 MHz,  $\text{DMSO}-d_6$ )  $\delta$  9.32 (s, 4H), 9.12 (s, 4H), 7.60 (t,  $J$  = 7.9 Hz, 2H), 7.51 (d,  $J$  = 7.5 Hz, 2H), 7.25 (d,  $J$  = 8.4 Hz, 2H), 7.11 (t,  $J$  = 7.5 Hz, 2H), 4.09 (t,  $J$  = 6.4 Hz, 4H), 1.81 (p,  $J$  = 6.9 Hz, 4H), 1.56 (p,  $J$  = 7.6 Hz, 2H).  $^{13}\text{C}$  NMR (101 MHz, DMSO)  $\delta$  164.64, 156.10, 133.82, 129.53, 120.35, 118.55, 113.07, 68.28, 28.01, 21.76. HRMS (ESI): calculated for  $\text{C}_{19}\text{H}_{24}\text{N}_4\text{O}_2$   $[\text{M}+\text{H}]^+$  341.1977, found 341.1972.

**2,2'-((1,2-phenylenebis(methylene))bis(oxy))dibenzimidamide (21c)** Following the procedure as described above for compound **1c**, using compound **30** (211 mg, 0.62 mmol), afforded compound **21c** (43 mg, 18%).  $^1\text{H}$  NMR (400 MHz,  $\text{DMSO}-d_6$ )  $\delta$  9.46 (s, 4H), 9.24 (s, 4H), 7.67 – 7.58 (m, 4H), 7.55 (dd,  $J$  = 7.6, 1.7 Hz, 2H), 7.44 – 7.31 (m, 4H), 7.15 (td,  $J$  = 7.5, 0.8 Hz, 2H), 5.35 (s, 4H).  $^{13}\text{C}$  NMR (101 MHz, DMSO)  $\delta$  164.75, 155.41, 134.33, 133.66, 129.61, 128.31, 128.22, 120.79, 119.07, 113.41, 67.37. HRMS (ESI): calculated for  $\text{C}_{22}\text{H}_{22}\text{N}_4\text{O}_2$   $[\text{M}+\text{H}]^+$  375.1821, found 375.1815.

**2,2'-((1,3-phenylenebis(methylene))bis(oxy))dibenzimidamide (22c)** Following the procedure as described above for compound **1c**, using compound **31** (210 mg, 0.62 mmol), afforded compound **22c** (49 mg, 21%).  $^1\text{H}$  NMR (400 MHz,  $\text{DMSO}-d_6$ )  $\delta$  9.46 (s, 4H), 9.22 (s, 4H), 7.62 (ddd,  $J$  = 8.8, 7.4, 1.7 Hz, 2H), 7.58 – 7.42 (m, 6H), 7.33 (d,  $J$  = 8.4 Hz, 2H), 7.15 (td,  $J$  = 7.6, 0.8 Hz, 2H), 5.23 (s, 4H).  $^{13}\text{C}$  NMR (101 MHz, DMSO)  $\delta$  164.69, 155.69, 136.70, 133.76, 129.65, 128.80, 127.31, 126.80, 120.77, 118.98, 113.46, 69.95. HRMS (ESI): calculated for  $\text{C}_{22}\text{H}_{22}\text{N}_4\text{O}_2$   $[\text{M}+\text{H}]^+$  375.1821, found 375.1816.

**2,2'-((1,4-phenylenebis(methylene))bis(oxy))dibenzimidamide (23c)** Following the procedure as described above for compound **1c**, using compound **32** (211 mg, 0.62 mmol), afforded compound **23c** (27 mg, 12%).  $^1\text{H}$  NMR (400 MHz,  $\text{DMSO}-d_6$ )  $\delta$  9.33 (s, 4H), 9.21 (s, 4H), 7.62 (ddd,  $J$  = 8.8, 7.4, 1.8 Hz, 2H), 7.57 – 7.49 (m, 6H), 7.33 (d,  $J$  = 8.8 Hz, 2H), 7.14 (td,  $J$  = 7.6, 0.9 Hz, 2H), 5.23 (s, 4H).  $^{13}\text{C}$  NMR (101 MHz, DMSO)  $\delta$  164.62, 155.66, 136.23, 133.75, 129.65, 127.79, 120.72, 118.92, 113.39, 69.75. HRMS (ESI): calculated for  $\text{C}_{22}\text{H}_{22}\text{N}_4\text{O}_2$   $[\text{M}+\text{H}]^+$  375.1821, found 375.1816.

**(5-bromo-1,3-phenylene)dimethanol (33)** Protocol as described in literature.<sup>44</sup> Dimethyl 5-bromoisophthalate (2.3 g, 8.3 mmol) was dissolved in dry DCM (25 mL) under argon atmosphere. The solution was then cooled to 0 °C using an ice bath and DIBALH (40 mL, 1 M hexane solution, 4.8 eq.) was added dropwise. The mixture was stirred from 0 °C to room temperature for 1 hour. The reaction was quenched with Rochelle salt (60 mL, sat. aq.) and the biphasic mixture was stirred at room temperature overnight. The layers were separated and the aqueous layer was two times extracted with diethyl ether. The organic layers were combined, washed with water and brine, dried over  $\text{Na}_2\text{SO}_4$  and concentrated in vacuo. The crude product was purified using column chromatography (DCM/EtOAc = 1:1) and afforded

compound **33** (1.8 g, 96%). <sup>1</sup>H NMR (400 MHz, MeOD) δ 7.42 (s, 2H), 7.28 (s, 1H), 4.58 (s, 4H), 3.35 (s, 2H). <sup>13</sup>C NMR (101 MHz, MeOD) δ 145.51, 129.42, 124.82, 123.31, 64.29.

**1-bromo-3,5-bis(bromomethyl)benzene (34)** Protocol as described in literature.<sup>45</sup> To a solution of compound **33** (1.0 g, 4.6 mmol) in dry DCM (50 mL) was added PPh<sub>3</sub> (2.5 g, 9.7 mmol, 2.1 eq.) and CBr<sub>4</sub> (3.2 g, 9.7 mmol, 2.1 eq.) and the mixture was stirred at room temperature for two hours under argon atmosphere. The reaction was quenched with water (30 mL) and the product was extracted from the aqueous layer with DCM three times. The combined organic layers were washed with water and brine, dried over Na<sub>2</sub>SO<sub>4</sub> and concentrated in vacuo. The crude product was purified by column chromatography (petroleum ether 100%) to give compound **34** (0.87 g, 55%). <sup>1</sup>H NMR (400 MHz, CDCl<sub>3</sub>) δ 7.51 – 7.45 (m, 2H), 7.34 (s, 1H), 4.53 (d, J = 4.0 Hz, 1H), 4.41 (d, J = 4.2 Hz, 3H). <sup>13</sup>C NMR (101 MHz, CDCl<sub>3</sub>) δ 140.42, 140.11, 132.11, 132.09, 131.64, 128.40, 127.90, 122.83, 44.89, 31.64, 31.59.

**4,4'-(((5-bromo-1,3-phenylene)bis(methylene))bis(oxy))dibenzonitrile (35)** Following the procedure as described above for compound **4**, using compound **34** (0.82 g, 2.4 mmol), afforded compound **35** as a crude product. The crude product was not recrystallized due to insolubility issues and was used in the next step without further purification based on a purity assessment (NMR) (1.0 g, quant.). <sup>1</sup>H NMR (400 MHz, CDCl<sub>3</sub>) δ 7.66 – 7.57 (m, 4H), 7.57 – 7.53 (m, 1H), 7.04 – 6.96 (m, 4H), 5.15 – 5.05 (m, 4H). <sup>13</sup>C NMR (101 MHz, CDCl<sub>3</sub>) δ 161.57, 138.62, 134.25, 130.33, 124.72, 123.30, 119.09, 115.62, 104.87, 69.18.

**4,4'-(((1,1'-biphenyl)-3,5-diylbis(methylene))bis(oxy))dibenzonitrile (36)** Conditions were based on protocols described in literature.<sup>47,48</sup> Dibenzonitrile intermediate **35** (0.30 g, 0.72 mmol) was dissolved in a 3:1 mixture of THF and 2 M Na<sub>2</sub>CO<sub>3</sub> (aq.) of 8 mL, respectively. Phenylboronic acid (0.13 g, 1.1 mmol, 1.5 eq.) and Pd(dppf)Cl<sub>2</sub>·DCM (58 mg, 0.07 mmol, 0.1 eq.) were added. The reaction mixture was heated to 65 °C for 18 hours and then partitioned between DCM and NaHCO<sub>3</sub> (sat. aq.). The aqueous layer was three times extracted with DCM, the organic layers were combined and dried over Na<sub>2</sub>SO<sub>4</sub>. The solvent was evaporated under reduced pressure and the crude product was purified using column chromatography (petroleum ether/EtOAc = 4:1) to obtain compound **36** (0.28 g, 94%). <sup>1</sup>H NMR (400 MHz, CDCl<sub>3</sub>) δ 7.66 – 7.57 (m, 8H), 7.50 – 7.36 (m, 4H), 7.05 (d, J = 8.8 Hz, 4H), 5.19 (s, 4H). <sup>13</sup>C NMR (101 MHz, CDCl<sub>3</sub>) δ 161.90, 142.59, 140.22, 137.05, 134.21, 129.06, 128.03, 127.31, 126.40, 125.32, 119.19, 115.67, 104.57, 70.12.

**4,4'-(((5-bromo-1,3-phenylene)bis(methylene))bis(oxy))dibenzimidamide (37)** Following the procedure as described above for compound **3**, using compound **35** (126 mg, 0.3 mmol), LHMDS (3.0 mL, 1 M THF solution, 10 eq.) and HCl (10 mL, 4 M dioxane solution, 133 eq.), afforded the product **37** (23 mg, 17%). <sup>1</sup>H NMR (400 MHz, DMSO-*d*<sub>6</sub>) δ 9.17 (s, 3H), 9.09 (s, 3H), 7.83 (d, J = 8.9 Hz, 4H), 7.67 (d, J = 1.1 Hz, 2H), 7.58 (s, 1H), 7.24 (d, J = 9.0 Hz, 4H), 5.27 (s, 4H). <sup>13</sup>C NMR (101 MHz, DMSO) δ 164.78, 162.35, 139.43, 130.28, 130.05, 125.93, 121.85, 120.20, 115.20, 68.57. HRMS (ESI): calculated for C<sub>22</sub>H<sub>21</sub>BrN<sub>4</sub>O<sub>2</sub> [M+H]<sup>+</sup> 453.0926, found 453.0924.

**4,4'-(((1,1'-biphenyl)-3,5-diylbis(methylene))bis(oxy))dibenzimidamide (38)** Following the procedure as described above for compound **3**, using compound **36** (0.28 g, 0.67 mmol), LHMDS (5.4 mL, 1 M THF solution, 8 eq.) and HCl (10 mL, 4 M dioxane solution, 60 eq.). HPLC purification using a 30–100% gradient for 30 minutes afforded compound **38** (0.23 g, 74%). <sup>1</sup>H NMR (400 MHz, DMSO-*d*<sub>6</sub>) δ 9.15 (d, J = 15.3 Hz, 8H), 7.83 (d, J = 9.0 Hz, 4H), 7.76 (s, 2H), 7.69 (d, J = 7.2 Hz, 2H), 7.58 (s, 1H), 7.50 (t, J = 7.6

Hz, 2H), 7.40 (t,  $J = 7.3$  Hz, 1H), 7.27 (d,  $J = 9.0$  Hz, 4H), 5.33 (s, 4H).  $^{13}\text{C}$  NMR (101 MHz, DMSO)  $\delta$  164.83, 162.61, 140.77, 139.54, 137.54, 130.26, 129.14, 127.94, 126.84, 126.19, 126.03, 120.04, 115.25, 69.51. HRMS (ESI): calculated for  $\text{C}_{28}\text{H}_{26}\text{N}_4\text{O}_2$   $[\text{M}+\text{H}]^+$  451.2135, found 451.2130.

**(4-bromo-1,2-phenylene)dimethanol (39)** Conditions were based on protocol reported in literature.<sup>49</sup> LAH (15 mL, 1 M THF solution, 2 eq.) and  $\text{ZnCl}_2$  (0.61 g, 4.5 mmol, 0.6 eq.) were suspended in dry THF (30 mL) and cooled to 0 °C, then 4-bromophthalic anhydride (1.7 g, 7.5 mmol) was slowly added. The mixture was stirred at room temperature for 6 hours under argon atmosphere. The mixture was cooled to 0 °C and quenched with Rochelle salt (30 mL, sat. aq.) and the biphasic mixture was stirred at room temperature overnight. The layers were separated and the aqueous layer was extracted with diethyl ether two times and the combined organic layers were washed with water and brine, dried over  $\text{Na}_2\text{SO}_4$  and concentrated in vacuo. The crude product was purified by column chromatography (DCM/EtOAc = 1:1) to give compound **39** (1.5 g, 95%).  $^1\text{H}$  NMR (400 MHz,  $\text{CDCl}_3$ )  $\delta$  7.48 (d,  $J = 2.1$  Hz, 1H), 7.42 (dd,  $J = 8.0$ , 2.1 Hz, 1H), 7.18 (d,  $J = 8.0$  Hz, 1H), 4.62 (d,  $J = 2.6$  Hz, 4H), 3.20 (s, 2H).  $^{13}\text{C}$  NMR (101 MHz,  $\text{CDCl}_3$ )  $\delta$  141.49, 138.18, 129.88, 128.77, 127.92, 122.30, 64.53, 64.40, 64.31, 63.49, 63.47, 31.08, 23.80.

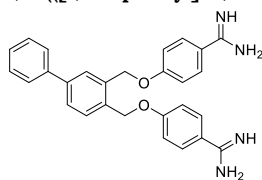
**4-bromo-1,2-bis(bromomethyl)benzene (40)** Following the procedure described for compound **34**, using compound **39** (1.5 g, 7.0 mmol) as starting material, afforded compound **40** (1.8 g, 74%).  $^1\text{H}$  NMR (400 MHz,  $\text{CDCl}_3$ )  $\delta$  7.52 (d,  $J = 2.1$  Hz, 1H), 7.43 (dd,  $J = 8.2$ , 2.1 Hz, 1H), 7.24 (d,  $J = 8.2$  Hz, 1H), 4.59 (s, 2H), 4.58 (s, 2H).  $^{13}\text{C}$  NMR (101 MHz,  $\text{CDCl}_3$ )  $\delta$  138.65, 135.67, 134.02, 132.69, 132.58, 131.24, 129.60, 123.17, 66.00, 42.46, 42.32, 30.14, 29.32, 29.12, 29.00, 28.83, 15.43.

**4,4'-(((4-bromo-1,2-phenylene)bis(methylene))bis(oxy))dibenzonitrile (41)** Following the procedure as described above for compound **4**, using compound **40** (0.80 g, 2.3 mmol), afforded compound **41** as a crude product. The crude product was not recrystallized due to insolubility issues and was used in the next step without further purification (1.1 g, quant.).  $^1\text{H}$  NMR (400 MHz,  $\text{CDCl}_3$ )  $\delta$  7.67 (d,  $J = 2.1$  Hz, 1H), 7.62 – 7.57 (m, 4H), 7.54 (dd,  $J = 8.1$ , 2.1 Hz, 1H), 7.37 (d,  $J = 8.1$  Hz, 1H), 6.99 (dd,  $J = 8.9$ , 4.6 Hz, 4H), 5.15 (d,  $J = 6.0$  Hz, 4H).  $^{13}\text{C}$  NMR (101 MHz,  $\text{CDCl}_3$ )  $\delta$  161.46, 136.30, 134.29, 134.27, 132.83, 132.15, 132.10, 131.05, 129.52, 129.23, 123.21, 118.99, 115.52, 105.06, 104.99, 67.83, 67.51.

**4,4'-(((1,1'-biphenyl)-3,4-diylbis(methylene))bis(oxy))dibenzonitrile (42)** Following the procedure as described above for compound **36**, using compound **41** (0.33 g, 0.79 mmol), a 3:1 mixture of THF and 2M  $\text{Na}_2\text{CO}_3$  (aq.) (8.0 mL), phenylboronic acid (0.13 g, 1.1 mmol, 1.5 eq.) and  $\text{Pd}(\text{dppf})\text{Cl}_2\text{-DCM}$  (58 mg, 0.07 mmol, 0.1 eq) afforded compound **42** (0.28 g, 84%).  $^1\text{H}$  NMR (400 MHz,  $\text{CDCl}_3$ )  $\delta$  7.72 (s, 1H), 7.66 – 7.57 (m, 8H), 7.49 – 7.44 (m, 2H), 7.41 – 7.36 (m, 1H), 7.04 – 7.00 (m, 4H), 5.25 (d,  $J = 7.1$  Hz, 4H).  $^{13}\text{C}$  NMR (101 MHz,  $\text{CDCl}_3$ )  $\delta$  161.76, 142.35, 140.07, 134.61, 134.27, 132.94, 130.17, 129.54, 129.26, 129.09, 128.37, 128.04, 127.82, 127.27, 119.11, 115.58, 104.84, 104.80, 68.55, 68.27.

**4,4'-(((4-bromo-1,2-phenylene)bis(methylene))bis(oxy))dibenzimidamide (43)** Following the procedure as described above for compound **1c**, using compound **41** (172 mg, 0.41 mmol), affording compound **43** (72 mg, 39%).  $^1\text{H}$  NMR (400 MHz,  $\text{DMSO}-d_6$ )  $\delta$  9.14 (d,  $J = 18.5$  Hz, 8H), 7.82 (dd,  $J = 9.0$ , 3.2 Hz, 4H), 7.77 (d,  $J = 2.1$  Hz, 1H), 7.62 (dd,  $J = 8.2$ , 2.1 Hz, 1H), 7.51 (d,  $J = 8.3$  Hz, 1H), 7.33 – 7.20 (m, 4H), 5.37 (d,  $J = 10.1$  Hz, 4H).  $^{13}\text{C}$  NMR (101 MHz,  $\text{DMSO}-d_6$ )  $\delta$  164.76, 164.74, 162.24, 162.17, 137.22, 133.96, 131.16, 131.01, 130.76, 130.25, 130.21, 121.48, 120.32, 120.23, 115.22, 66.83, 66.59, 40.15, 39.94, 39.73, 39.52, 39.31, 39.10, 38.89. HRMS (ESI): calculated for  $\text{C}_{22}\text{H}_{21}\text{BrN}_4\text{O}_2$   $[\text{M}+\text{H}]^+$  453.0926, found 453.0923.

#### 4,4'-((([1,1'-biphenyl]-3,4-diylbis(methylene))bis(oxy))dibenzimidamide (44)



Following the procedure as described above for compound **3**, using compound **42** (0.28 g, 0.66 mmol), LHMDS (5.4 mL, 1 M THF solution, 8 eq.) and HCl (10 mL, 4 M dioxane solution, 60 eq.), afforded the crude product. The crude product was purified using HPLC with a 30–100% gradient for 30 minutes to obtain the pure compound **44** (35 mg, 12%). <sup>1</sup>H NMR (400 MHz, DMSO-*d*<sub>6</sub>) δ 9.14 (d, *J* = 5.2 Hz, 4H), 9.00 (d, *J* = 4.8 Hz, 4H), 7.88 (d, *J* = 2.0 Hz, 1H), 7.81 (dd, *J* = 8.9, 3.2 Hz, 4H), 7.72 – 7.61 (m, 4H), 7.48 (t, *J* = 7.6 Hz, 2H), 7.39 (t, *J* = 7.3 Hz, 1H), 7.28 (t, *J* = 8.6 Hz, 4H), 5.44 (d, *J* = 10.4 Hz, 4H). <sup>13</sup>C NMR (101 MHz, DMSO) δ 164.72, 162.49, 162.45, 140.20, 139.34, 135.20, 133.89, 130.25, 129.56, 129.11, 127.37, 126.75, 120.10, 120.08, 115.26, 115.23, 67.64, 67.31. HRMS (ESI): calculated for C<sub>28</sub>H<sub>26</sub>N<sub>4</sub>O<sub>2</sub> [M+H]<sup>+</sup> 451.2135, found 451.2129.

#### 4.2. Antimicrobial assays

All compounds were screened for antimicrobial activity against *E. coli* BW25113. A select group of the pentamidine analogues was further tested against *E. coli* ATCC25922, *E. coli* W3110, *E. coli* 552060.1, *E. coli* BW25113 transformed with pGDP2-mcr-1 (the plasmid was a gift from Gerard Wright (Addgene plasmid # 118404; <http://n2t.net/addgene:118404>; RRID:Addgene\_118404)<sup>63</sup>), *E. coli* mcr-1, *E. coli* EQASmcr-1 (EQAS 2016 412016126), *E. coli* EQASmcr-2 (EQAS 2016 KP37), *E. coli* EQASmcr-3 (EQAS 2017 2013-SQ352), *E. coli* RC0089, *K. pneumoniae* ATCC13883, *P. aeruginosa* ATCC27853 and *A. baumannii* ATCC17978. The antimicrobial assay was performed according to CLSI guidelines. Bacteria were plated out directly from their glycerol stocks on blood agar plates, incubated overnight at 37 °C, and then kept in the fridge. The blood agar plates were only used for 2 weeks and then replaced.

#### 4.3. MIC assays

A single colony from a blood agar plate was inoculated in Lysogeny Broth (LB) at 37 °C until a 0.5 optical density at 600nm (OD<sub>600</sub>) was reached (compared to the sterility control of LB). The bacterial suspension was diluted in fresh LB to 2.0 × 10<sup>6</sup> CFU/mL. The serial dilutions were prepared in polypropylene microtiter plates: a stock of the test compounds was prepared with a 2x final concentration in LB. 100 µl of the stock was added to the wells of the top row of which 50 µl was used for the serial dilution. The bottom row of each plate was used as the positive (50 µl of LB) and negative controls (100 µl of LB) (6 wells each). 50 µl of the 2.0 × 10<sup>6</sup> CFU/mL bacterial stock was added to each well except for the negative controls, adding up to a total volume of 100 µl per well. The plates were sealed with a breathable seal and incubated for 20 hours at 37 °C and 600 rpm. The MIC was visually determined after centrifuging the plates for 2 minutes at 3000 rpm.

#### 4.4. Checkerboard assays

Dilution series of both the test compound and antibiotic to be evaluated was prepared in LB media. To evaluate synergy, 25 µL of the test compound solutions were added to wells containing 25 µL of the antibiotic solution. This was replicated in three columns for each combination so as to obtain triplicates. To the resulting 50 µL volume of antibiotic + test compound was next added 50 µL of bacterial stock (See MIC assays) and the plates sealed. After incubation for 20 hours at 37 °C while shaking at 600 rpm, the breathable seals were removed and the plates shaken using a bench top shaker to ensure even suspension of the bacterial cells as established by visual inspection. The plates were then transferred to a Tecan Spark plate reader and following another brief shaking (20 seconds) the density of the bacterial suspensions measured at 600 nm (OD<sub>600</sub>). The resulting OD<sub>600</sub> values were transformed to a 2D gradient to visualize the growth/no-growth results. The FICI was calculated using Equation 1, with an FICI ≤ 0.5 indicating synergy.<sup>21</sup>

$$FICI = \frac{MSC_{ant}}{MIC_{ant}} + \frac{MSC_{syn}}{MIC_{syn}} \quad (1)$$

**Equation 1.** Calculation of FICI.  $MSC_{ant}$  = MIC of antibiotic in combination with synergist;  $MIC_{ant}$  = MIC of antibiotic alone;  $MSC_{syn}$  = MIC of synergist in combination with antibiotic;  $MIC_{syn}$  = MIC of synergist alone. In cases where the MIC of the antibiotic or synergist was found to exceed the highest concentration tested, the next highest concentration in the dilution series was used in determining the FICI and the result reported as  $\leq$  the calculated value.

#### 4.5. Hemolysis assays

The hemolytic activity of each analogue was assessed in triplicate. Red blood cells from defibrinated sheep blood obtained from Thermo Fisher were centrifuged (400 g for 15 minutes at 4°C) and washed with Phosphate-Buffered Saline (PBS) containing 0.002% Tween20 (buffer) for five times. Then, the red blood cells were normalized to obtain a positive control read-out between 2.5 and 3.0 at 415 nm to stay within the linear range with the maximum sensitivity. A serial dilution of the compounds (200 – 6.25 µg/mL, 75 µL) was prepared in a 96-well plate. The outer border of the plate was filled with 75 µL buffer. Each plate contained a positive control (0.1% Triton-X final concentration, 75 µL) and a negative control (buffer, 75 µL) in triplicate. The normalized blood cells (75 µL) were added and the plates were incubated at 37 °C for 1 hour or 20 hours while shaking at 500 rpm. A flat-bottom plate of polystyrene with 100 µL buffer in each well was prepared. After incubation, the plates were centrifuged (800 g for 5 minutes at room temperature) and 25 µL of the supernatant was transferred to their respective wells in the flat-bottom plate. The values obtained from a read-out at 415 nm were corrected for background (negative control) and transformed to a percentage relative to the positive control.

#### 4.6. Membrane permeability assay using N-phenylnaphthalen-1-amine (NPN)

The assay was performed based on protocols adapted from those described in literature.<sup>67,68</sup> Bacteria were inoculated overnight at 37 °C in LB, diluted the next day 50x in LB and grown to  $OD_{600}$  of 0.5. The bacterial suspension was then centrifuged for 10 minutes at 1000 g at 25 °C. The pellet of bacteria was suspended in 5 mM HEPES buffer containing 20mM glucose to a final concentration of  $OD_{600}$  of 1.0. The compounds were serially diluted (25 µL) in triplicate in a black ½ area clear-bottom 96-well plate. 100 µg/mL final concentration of colistin in triplicate served as the positive control. Three wells were filled with 25 µL buffer to serve as the negative control. Additional controls of the compounds were made in triplicate using 25 µL of the highest concentration to detect interactions of the compounds with NPN in the absence of bacteria. A stock of 0.5 mM of NPN in acetone was prepared and diluted 12.5x in the buffer. 25 µL of the NPN solution was added to each well. 50 µL of the 1.0  $OD_{600}$  bacterial stock was then added to each well except for the controls of the compounds with NPN. To these wells 50 µL of buffer was added. After 60 minutes the plate was measured using Tecan plate reader with  $\lambda_{ex}$  355 nm  $\pm$  20 nm and  $\lambda_{em}$  420 nm  $\pm$  20 nm. The fluorescence values obtained were then transformed into a NPN uptake percentage using the following equation 2:

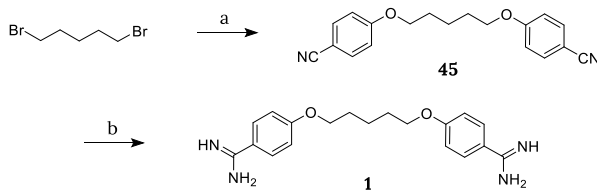
$$NPN \text{ uptake (\%)} = (F_{obs} - F_0) / (F_{100} - F_0) \times 100\%, \quad (2)$$

**Equation 2:** NPN uptake. The observed fluorescence ( $F_{obs}$ ) is corrected for background using the negative control ( $F_0$ ). This value is divided by the positive control corrected for background ( $F_{100} - F_0$ ) and multiplied by 100% to obtain the percentage NPN uptake.<sup>68,75</sup>



## Supporting information

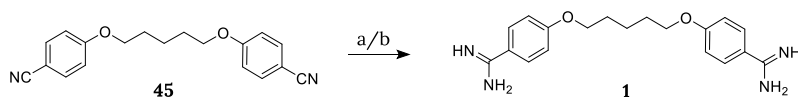
### Synthesis



**Scheme S1.** Synthesis of pentamidine (**1**). Reagents and conditions: (a) 4-Cyanophenol, NaH, DMF, 80°C, 1h (78%); (b) i) LHMDs, THF, 48h, rt, ii) 4M HCl (dioxane), 0°C to rt, overnight (quant.).

**4,4'-(pentane-1,5-diylbis(oxy))dibenzonitrile (**45**)** 4-cyanophenol (1.14 g, 9.6 mmol, 2.4 eq.) was suspended in dry DMF (12 mL) under argon atmosphere. The suspension was cooled to 0 °C using an ice bath and NaH (384 mg, 60% dispersion in mineral oil, 2.4 eq.) was slowly added. The reaction was stirred until a clear solution appeared, the ice bath was removed and 1,5-dibromopentane (0.92 g, 4.0 mmol) was added. The reaction mixture was heated to 80 °C for 1 hour and then cooled to room temperature. Water (35 mL) was added to the mixture to obtain precipitation. The precipitate was filtered, washed with water and recrystallized from EtOH to give compound **45** as white crystals (0.95 g, 78%). <sup>1</sup>H NMR (400 MHz, CDCl<sub>3</sub>) δ 7.57 (d, J = 8.9 Hz, 4H), 6.93 (d, J = 8.9 Hz, 4H), 4.03 (t, J = 6.3 Hz, 4H), 1.93 – 1.84 (m, 4H), 1.72 – 1.61 (m, 2H). <sup>13</sup>C NMR (101 MHz, CDCl<sub>3</sub>) δ 162.37, 134.09, 119.36, 115.24, 103.91, 68.14, 28.81, 22.73.

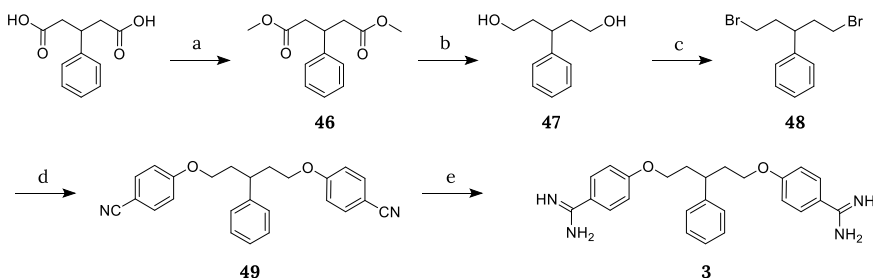
**4,4'-(pentane-1,5-diylbis(oxy))dibenzimidamide (**1**)** Compound **45** (94 mg, 0.3 mmol) was dissolved in dry THF (2 mL) under argon atmosphere and LHMDs (1.2 mL, 1 M THF solution, 4.0 eq.) was added. The reaction was stirred at room temperature for 48 hours or longer until complete conversion to the bis-amidine (monitored by LCMS). The solution was cooled to 0 °C and quenched with HCl (4.5 mL, 4 M dioxane solution, 60 eq.). The mixture was stirred at room temperature overnight, then diluted with diethyl ether and filtered. The precipitate was purified by preparative HPLC with the gradient 0–100% in 30 minutes. The samples were analyzed and the combined pure fractions were dried to give pentamidine (**1**) (120 mg, quant.). <sup>1</sup>H NMR (400 MHz, DMSO-*d*<sub>6</sub>) δ 9.14 (s, 3H), 9.06 (s, 3H), 7.81 (d, J = 8.9 Hz, 4H), 7.15 (d, J = 8.9 Hz, 4H), 4.12 (t, J = 6.4 Hz, 4H), 1.88 – 1.75 (m, 4H), 1.65 – 1.52 (m, 2H). <sup>13</sup>C NMR (101 MHz, DMSO) δ 164.70, 163.06, 130.19, 119.50, 114.79, 68.05, 28.21, 22.09. HRMS (ESI): calculated for C<sub>19</sub>H<sub>24</sub>N<sub>4</sub>O<sub>2</sub> [M+H]<sup>+</sup> 341.1977, found 341.1977.



**Scheme S2.** Exploration of the optimal acidic quench. Reagents and conditions: (a) i) LHMDs, THF, 48h, ii) 2M HCl (aq), 0°C to rt, overnight (68%) or (b) i) LHMDs, THF, 48h, ii) sat. ethanolic HCl, 0°C to rt, overnight (9%).

**4,4'-(pentane-1,5-diylbis(oxy))dibenzimidamide (1) using 2M HCl (aq)** Following the procedure as described for compound **1** except for using 2 M HCl (aq) (20 mL) as acidic quench afforded pentamidine (**1**) (71 mg, 68%). <sup>1</sup>H NMR (400 MHz, DMSO-*d*<sub>6</sub>) δ 9.14 (s, 4H), 9.06 (s, 4H), 7.81 (d, *J* = 8.9 Hz, 4H), 7.15 (d, *J* = 8.9 Hz, 4H), 4.12 (t, *J* = 6.4 Hz, 4H), 1.88 – 1.75 (m, 4H), 1.65 – 1.52 (m, 2H). <sup>13</sup>C NMR (101 MHz, DMSO) δ 164.70, 163.06, 130.19, 119.50, 114.79, 68.05, 28.21, 22.09. HRMS (ESI): calculated for C<sub>19</sub>H<sub>24</sub>N<sub>4</sub>O<sub>2</sub> [M+H]<sup>+</sup> 341.1977, found 341.1977.

**4,4'-(pentane-1,5-diylbis(oxy))dibenzimidamide (1) using sat. ethanolic HCl** Following the procedure as described for compound **1** except for using freshly prepared sat. ethanolic HCl (20 mL) as acidic quench afforded pentamidine (**1**) (9 mg, 9%). <sup>1</sup>H NMR (400 MHz, DMSO-*d*<sub>6</sub>) δ 9.14 (s, 4H), 9.06 (s, 4H), 7.81 (d, *J* = 8.9 Hz, 4H), 7.15 (d, *J* = 8.9 Hz, 4H), 4.12 (t, *J* = 6.4 Hz, 4H), 1.88 – 1.75 (m, 4H), 1.65 – 1.52 (m, 2H). <sup>13</sup>C NMR (101 MHz, DMSO) δ 164.70, 163.06, 130.19, 119.50, 114.79, 68.05, 28.21, 22.09. HRMS (ESI): calculated for C<sub>19</sub>H<sub>24</sub>N<sub>4</sub>O<sub>2</sub> [M+H]<sup>+</sup> 341.1977, found 341.1977.



**Scheme S3.** Synthesis of 4,4'-((3-phenylpentane-1,5-diyl)bis(oxy))dibenzimidamide (**3**). Reagents and conditions: (a) H<sub>2</sub>SO<sub>4</sub>, MeOH, 70°C, overnight (91%); (b) DIBAL-H, DCM, 0°C, 1 hour (quant.); (c) NBS, PPh<sub>3</sub>, DCM, 0°C to rt, 2 hours (62%) (d) 4-Cyanophenol, NaH, DMF, 80°C, 1h (89%); (e) i) LHMDS, THF, 48h, ii) 4M HCl (dioxane), 0°C to rt, overnight (23%).

**Dimethyl 3-phenylpentanedioate (46)** 3-phenylpentanedioic acid (1.04 g, 5 mmol) was dissolved in MeOH (20 mL) and a few drops of H<sub>2</sub>SO<sub>4</sub> were added to the solution. The reaction mixture was refluxed at 70 °C overnight, concentrated in vacuo and redissolved in DCM (50 mL). The organic layer was washed with water (4 mL) five times. The organic layer was then washed with brine, dried over Na<sub>2</sub>SO<sub>4</sub> and concentrated in vacuo. The crude product was purified using column chromatography (petroleum ether/EtOAc = 17:3) to give dimethyl ester **46** (1.08 g, 92%). <sup>1</sup>H NMR (400 MHz, CDCl<sub>3</sub>) δ 7.33 – 7.26 (m, 2H), 7.25 – 7.18 (m, 3H), 3.70 – 3.61 (m, 1H), 3.59 (s, 6H), 2.73 (dd, *J* = 15.6, 7.2 Hz, 2H), 2.65 (dd, *J* = 15.6, 7.9 Hz, 2H). <sup>13</sup>C NMR (101 MHz, CDCl<sub>3</sub>) δ 172.19, 142.67, 128.74, 127.28, 127.10, 51.75, 40.53, 38.36.

**3-phenylpentane-1,5-diol (47)** Dimethyl ester **46** (1.07 mg, 4.5 mmol) was dissolved in dry DCM (12.5 mL) under argon atmosphere. The mixture was cooled to 0 °C using an ice bath. DIBAL-H (21.7 mL, 1M dioxane solution, 4.8 eq.) was added dropwise to the cooled solution and stirred for 1 hour. The reaction was quenched with Rochelle salt (30 mL, sat. aq.) and the biphasic mixture was stirred at room temperature overnight. The layers were separated and the aqueous layer was extracted two times with diethyl ether. The organic layers were combined, washed with water and brine, dried over Na<sub>2</sub>SO<sub>4</sub> and concentrated in vacuo. The diol **47** (863 mg, quant.) was used in the next step without further purification. <sup>1</sup>H NMR (400 MHz, CDCl<sub>3</sub>) δ 7.34 – 7.27 (m, 2H), 7.24 – 7.15 (m, 3H), 3.62 – 3.52 (m, 2H), 3.52 – 3.43 (m, 2H), 2.98

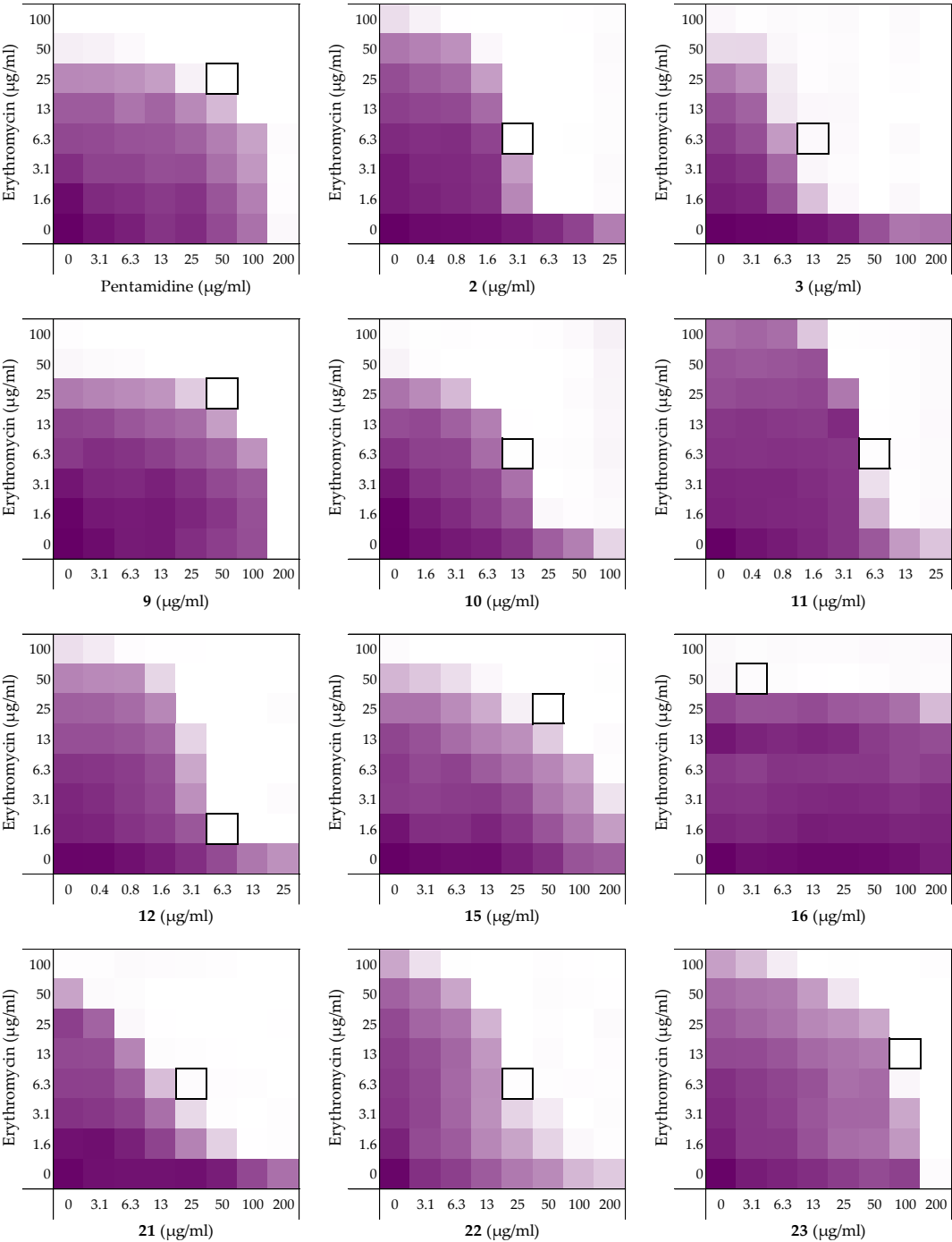
– 2.84 (m, 1H), 2.01 – 1.79 (m, 4H).  $^{13}\text{C}$  NMR (101 MHz,  $\text{CDCl}_3$ )  $\delta$  144.48, 128.80, 127.73, 126.63, 61.04, 39.55, 38.94.

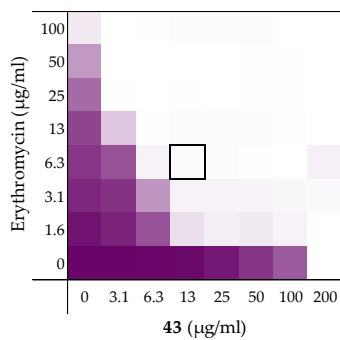
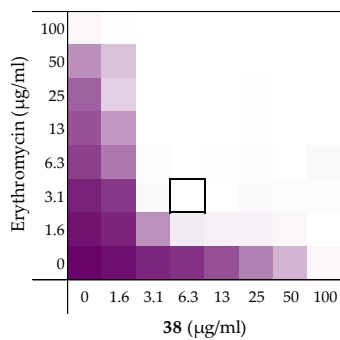
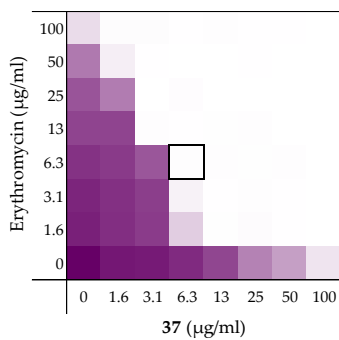
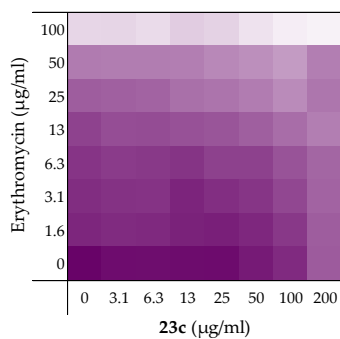
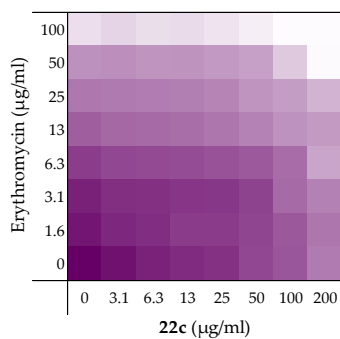
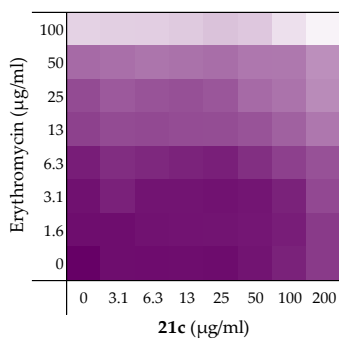
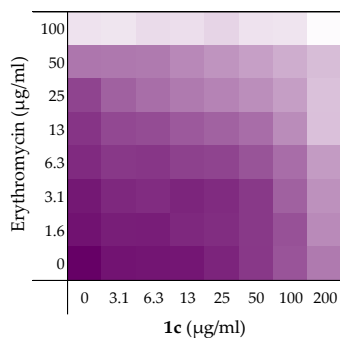
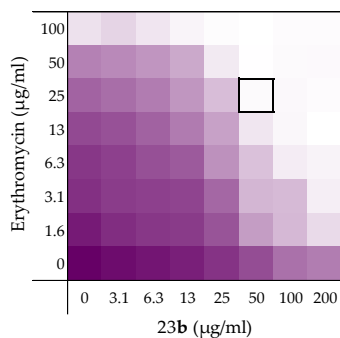
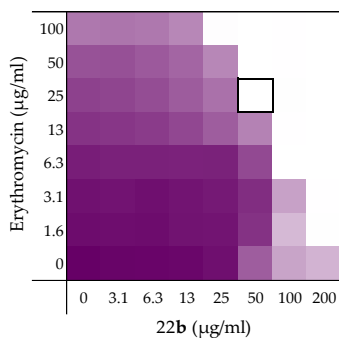
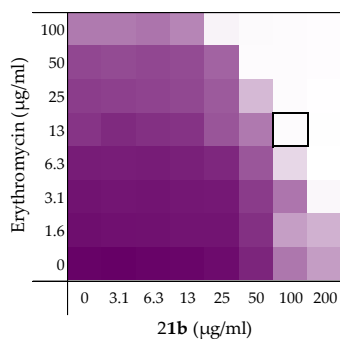
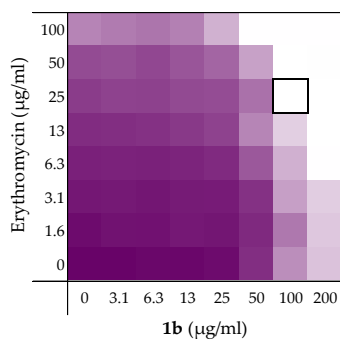
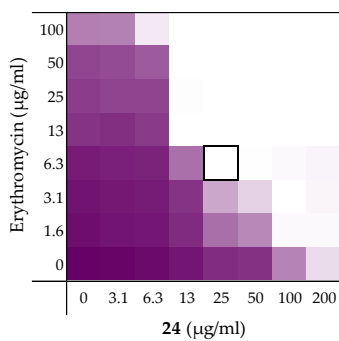
**(1,5-dibromopentane-3-yl)benzene (48)** Compound **47** (400 mg, 2.2 mmol) was dissolved in dry DCM (10 mL),  $\text{PPh}_3$  (1.46 g, 5.5 mmol, 2.5 eq.) was added, and the mixture under argon was cooled to 0 °C using an ice bath. N-bromosuccinimide (0.65 g, 5.5 mmol, 2.5 eq.) was added portion wise. After the addition, the ice bath was removed and the reaction was stirred at room temperature for 2 hours. The reaction mixture was concentrated under reduced pressure and the crude product was purified by column chromatography (petroleum ether/EtOAc = 99:1) to give compound **48** (415 mg, 62%).  $^1\text{H}$  NMR (400 MHz,  $\text{CDCl}_3$ )  $\delta$  7.34 – 7.33 (m, 3H), 7.22 – 7.16 (m, 2H), 3.28 (ddd,  $J$  = 10.0, 6.6, 5.5 Hz, 2H), 3.21 – 2.94 (m, 3H), 2.20 – 2.13 (m, 4H).  $^{13}\text{C}$  NMR (101 MHz,  $\text{CDCl}_3$ ) (including  $\text{PPh}_3=\text{O}$  peaks)  $\delta$  134.00, 133.81, 132.37, 132.27, 129.09, 129.05, 128.78, 128.74, 128.67, 127.88, 127.23, 42.79, 39.34, 31.54.

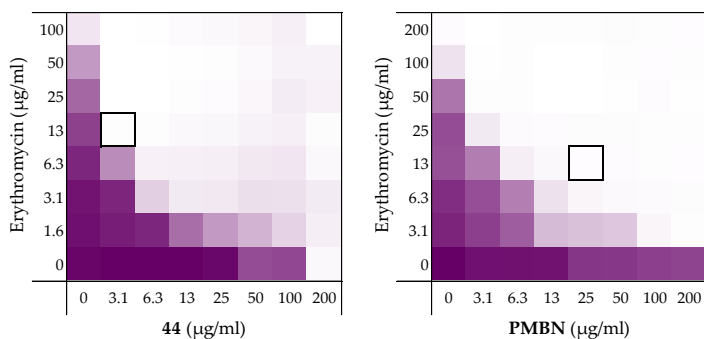
**4,4'-((3-phenylpentane-1,5-diyl)bis(oxy))dibenzonitrile (49)** Following the procedure as described above for compound **45**, using compound **48** (500 mg, 1.6 mmol), afforded crude compound **49** (546 mg, 89%). The crude product was used in the next step without further purification.  $^1\text{H}$  NMR (400 MHz,  $\text{CDCl}_3$ )  $\delta$  7.51 – 7.40 (m, 5H), 7.24 – 7.24 (m, 2H), 7.12 – 7.08 (m, 2H), 6.82 – 6.67 (m, 4H), 3.81 (ddd,  $J$  = 9.4, 6.6, 4.9 Hz, 2H), 3.72 (ddd,  $J$  = 9.4, 8.1, 6.0 Hz, 2H), 3.11 – 2.96 (m, 1H), 2.24 – 2.12 (m, 2H), 2.09 – 1.98 (m, 2H).  $^{13}\text{C}$  NMR (101 MHz,  $\text{CDCl}_3$ )  $\delta$  162.23, 142.69, 137.35, 137.24, 134.08, 133.96, 133.77, 128.84, 128.66, 128.59, 127.69, 127.13, 119.34, 115.25, 104.02, 66.21, 39.00, 36.00, 29.84.

**4,4'-((3-phenylpentane-1,5-diyl)bis(oxy))dibenzimidamide (3)** Compound **49** (109 mg, 0.28 mmol) was dissolved in the LHMDs solution (1.1 mL, 1 M THF solution, 4.0 eq.) under argon atmosphere. The reaction was stirred at room temperature for 48 hours or longer until complete conversion to the bis-amidine (monitored by LCMS). The solution was cooled to 0 °C and quenched with HCl (4.5 mL, 4 M dioxane solution, 60 eq.). The mixture was stirred at room temperature overnight, then diluted with diethyl ether and filtered. The precipitate was purified by preparative HPLC with the gradient 20–100% in 30 minutes. The samples were analyzed and the combined pure fractions were dried to give compound **3** (27.4 mg, 23%).  $^1\text{H}$  NMR (400 MHz,  $\text{DMSO}-d_6$ )  $\delta$  9.11 (d,  $J$  = 12.6 Hz, 8H), 7.77 (d,  $J$  = 8.9 Hz, 4H), 7.34 – 7.16 (m, 5H), 7.05 (d,  $J$  = 9.0 Hz, 4H), 4.00 – 3.90 (m, 2H), 3.83 (dd,  $J$  = 15.0, 8.9 Hz, 2H), 3.14 – 3.04 (m, 1H), 2.29 – 2.16 (m, 2H), 2.13 – 2.00 (m, 2H).  $^{13}\text{C}$  NMR (101 MHz,  $\text{DMSO}$ )  $\delta$  164.81, 162.92, 143.38, 130.21, 128.62, 127.69, 126.58, 119.64, 66.21, 38.31, 35.10. HRMS (ESI): calculated for  $\text{C}_{25}\text{H}_{28}\text{N}_4\text{O}_2$   $[\text{M}+\text{H}]^+$  417.2291, found 417.2287.

Checkerboard assays and FICI data against *E. coli* BW25113 with erythromycin

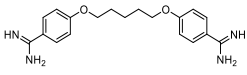
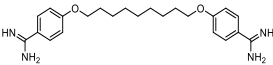
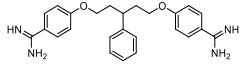
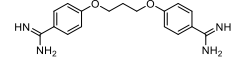
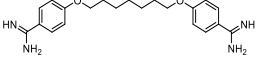
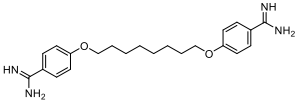
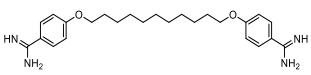
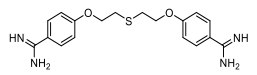
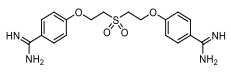
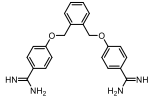
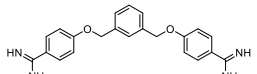
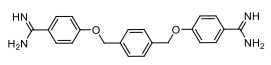
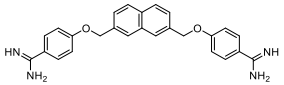
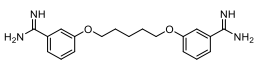


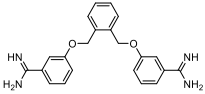
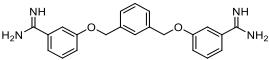
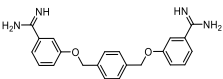
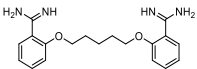
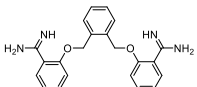
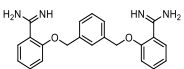
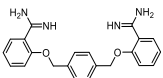
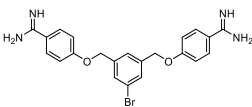
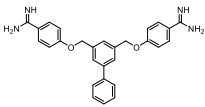
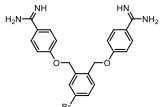
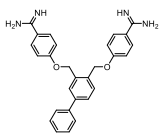




**Figure S1.** Checkerboard assays of the compounds and PMBN in combination with erythromycin versus *E. coli* BW25113. OD600 values were measured using a plate reader and transformed to a gradient: purple represents growth, white represents no growth. In each case, the bounded box in the checkerboard assays indicates the minimal synergistic concentration (MSC) of compound and antibiotic resulting in the lowest FICI.

**Table S1.** Synergistic data of compounds and PMBN of the checkerboard assays with erythromycin as shown in Figure S1. All minimal inhibitory concentrations (MICs) and minimal synergistic concentrations (MSCs) are in  $\mu\text{g/mL}$ .

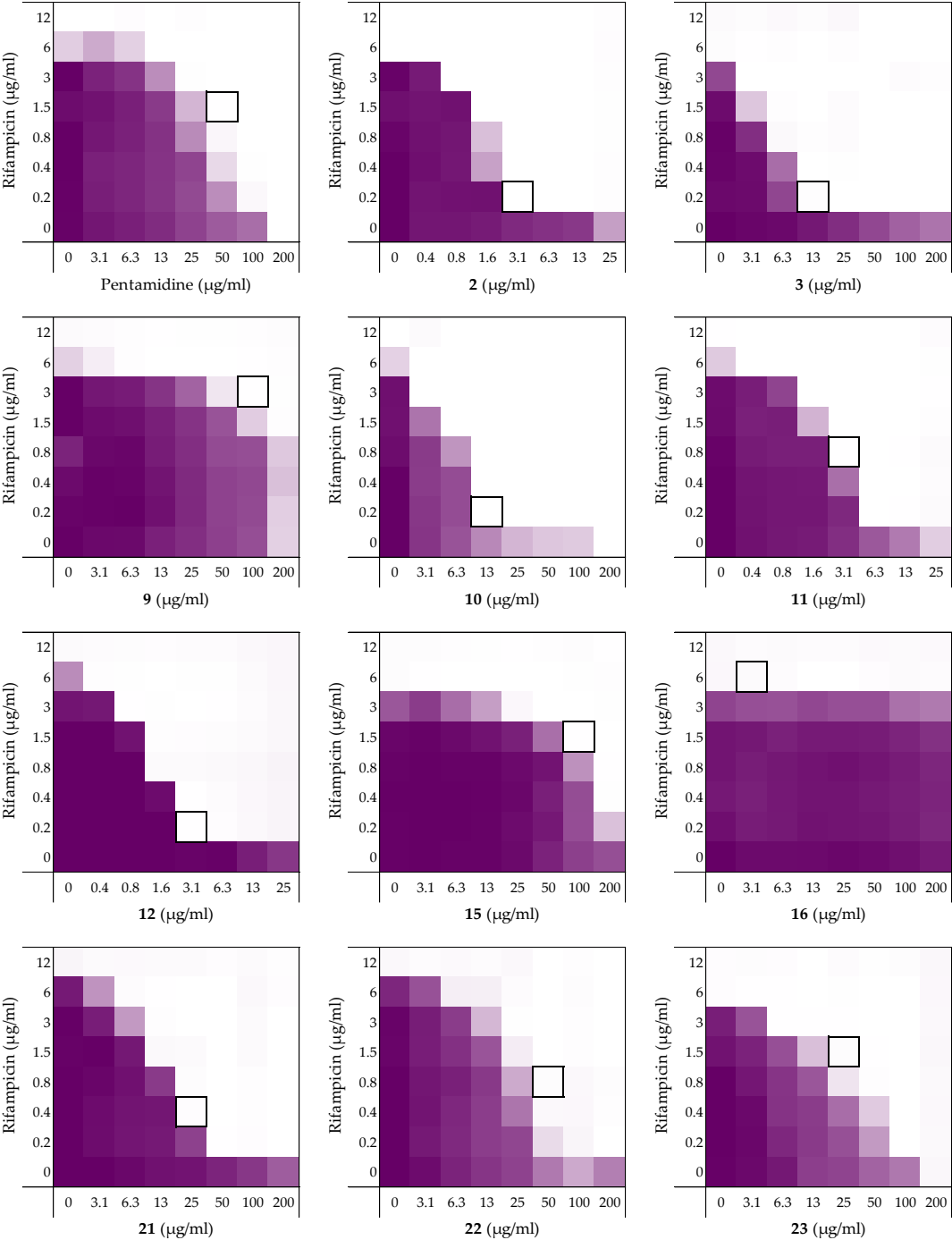
	Structures	MIC	MSC	MIC ery	MSC ery	FICI
<b>1</b>		200	50	100	25	0.500
<b>2</b>		>25	3.13	>100	6.25	$\leq 0.094$
<b>3</b>		>200	12.5	>100	6.25	$\leq 0.063$
<b>9</b>		200	50	100	25	0.500
<b>10</b>		>100	12.5	100	6.25	$\leq 0.125$
<b>11</b>		>25	6.25	>100	6.25	$\leq 0.156$
<b>12</b>		>25	6.25	>100	1.56	$\leq 0.133$
<b>15</b>		>200	50	100	25	$\leq 0.375$
<b>16</b>		>200	3.13	50	50	$>0.5^a$
<b>21</b>		>200	25	100	6.25	$\leq 0.125$
<b>22</b>		>200	25	>100	6.25	$\leq 0.094$
<b>23</b>		>200	100	>100	12.5	$\leq 0.313$
<b>24</b>		>200	25	>100	6.25	$\leq 0.094$
<b>1b</b>		>200	100	>100	25	$\leq 0.375$

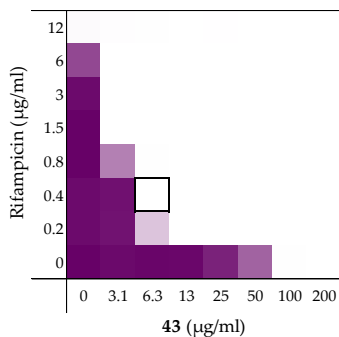
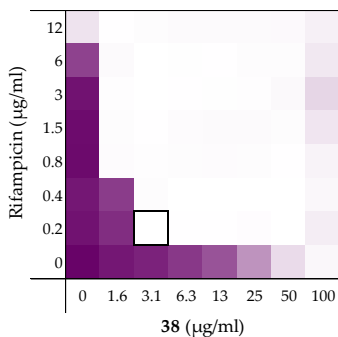
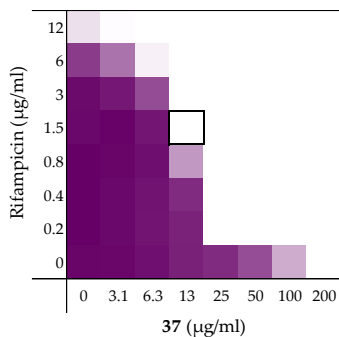
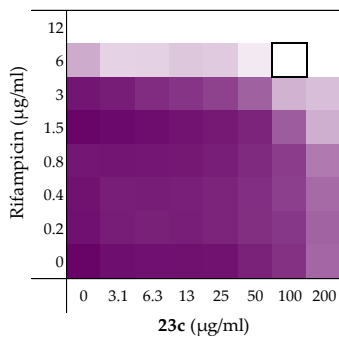
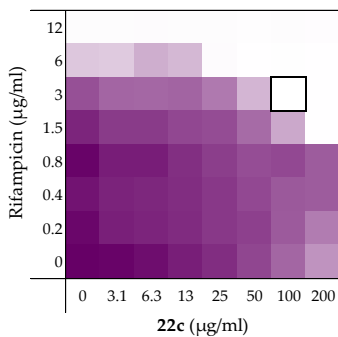
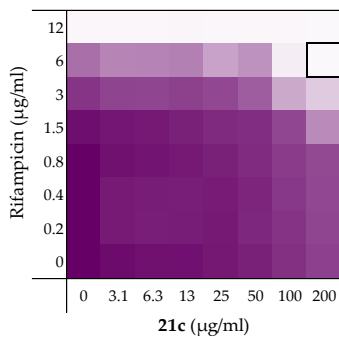
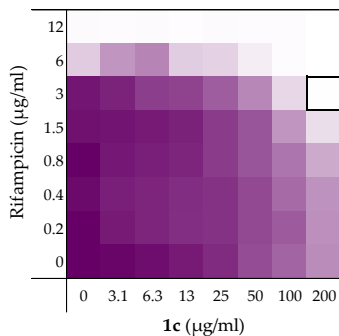
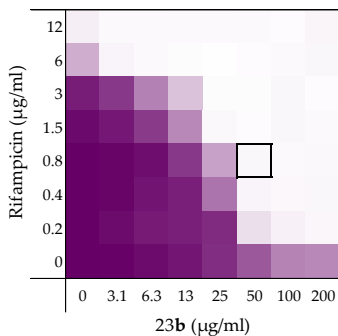
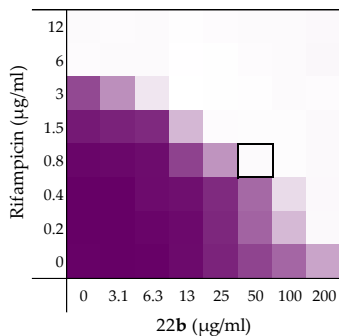
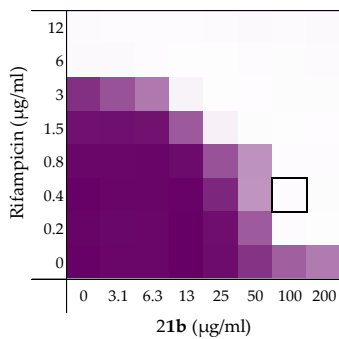
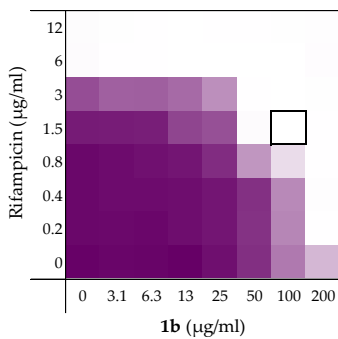
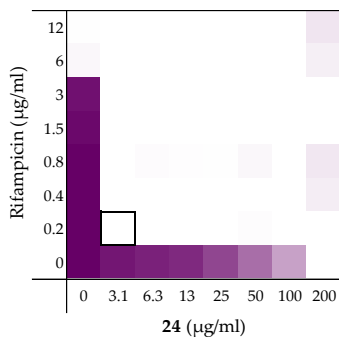
<b>21b</b>		>200	100	>100	12.5	≤0.313
<b>22b</b>		>200	50	>100	25	≤0.250
<b>23b</b>		>200	50	>100	25	≤0.250
<b>1c</b>		>200	nd.	>100	nd.	>0.5 <sup>a</sup>
<b>21c</b>		>200	nd.	>100	nd.	>0.5 <sup>a</sup>
<b>22c</b>		>200	nd.	>100	nd.	>0.5 <sup>a</sup>
<b>23c</b>		>200	nd.	>100	nd.	>0.5 <sup>a</sup>
<b>37</b>		>100	6.25	>100	6.25	≤0.063
<b>38</b>		>100	6.25	>100	3.13	≤0.047
<b>43</b>		200	12.5	>100	6.25	≤0.094
<b>44</b>		200	3.13	>100	12.5	≤0.078
<b>PMBN</b>		>200	25	200	12.5	≤0.125

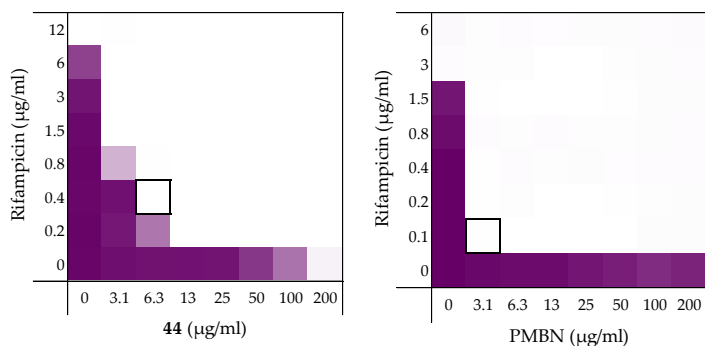
<sup>a</sup> Synergy is defined as FICI ≤0.5.<sup>21</sup>



Checkerboard assays and FICI data against *E. coli* BW25113 with rifampicin

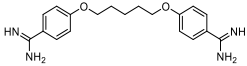
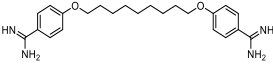
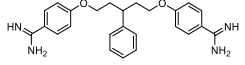
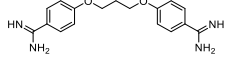
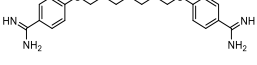
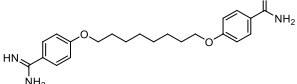
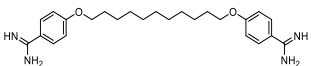
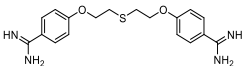
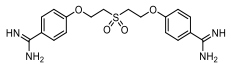
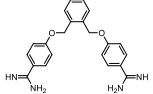
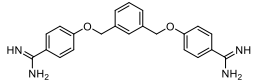
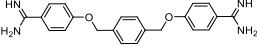
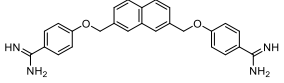
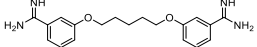
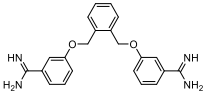


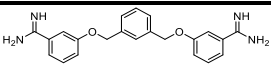
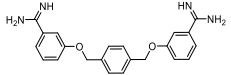
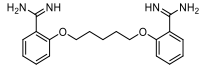
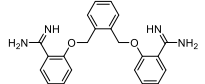
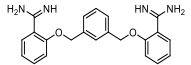
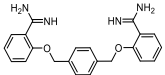
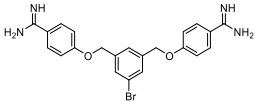
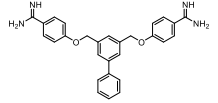
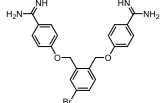
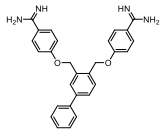




**Figure S2.** Checkerboard assays of the compounds and PMBN in combination with rifampicin versus *E. coli* BW25113. OD600 values were measured using a plate reader and transformed to a gradient: purple represents growth, white represents no growth. In each case, the bounded box in the checkerboard assays indicates the minimal synergistic concentration (MSC) of compound and antibiotic resulting in the lowest FICI.

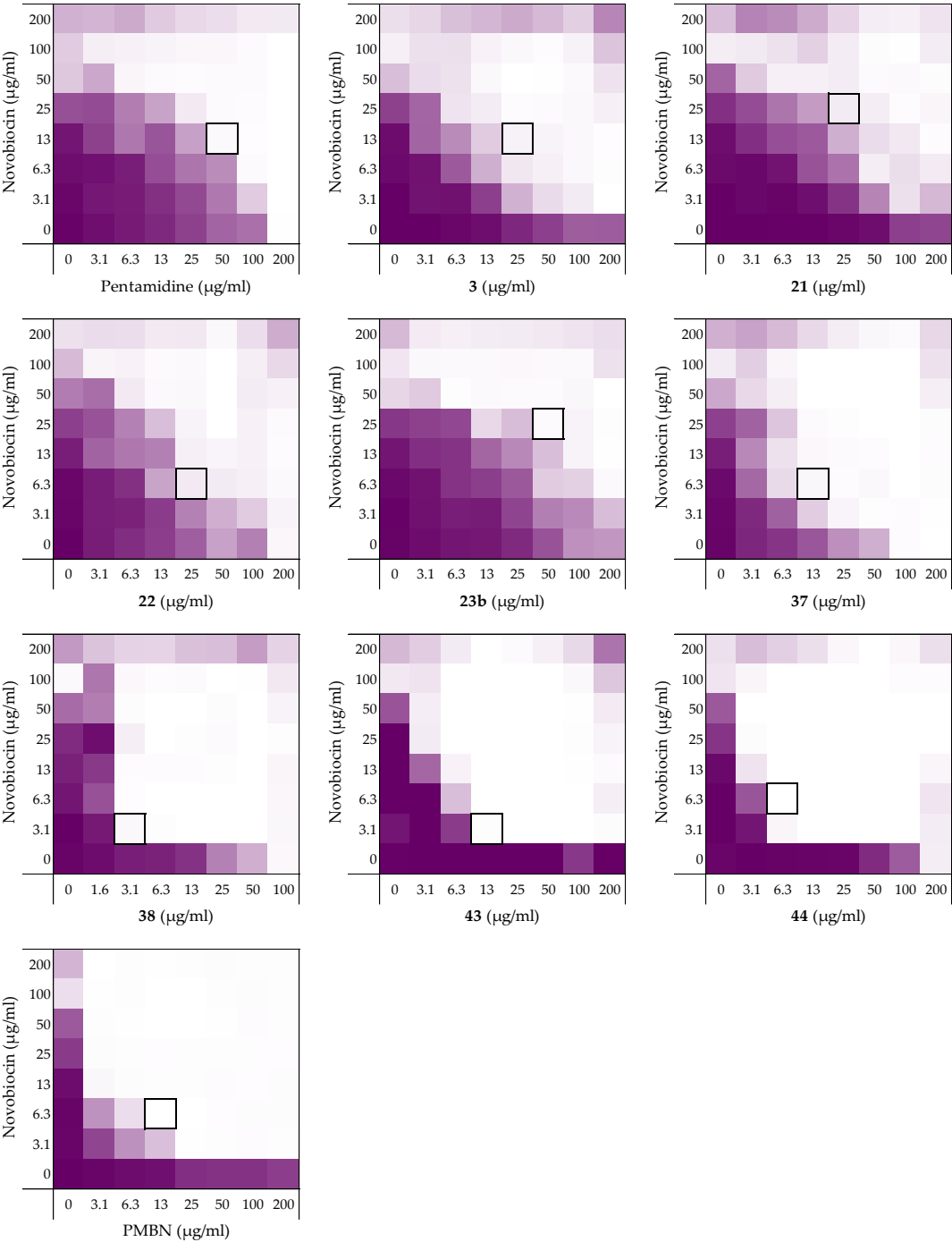
**Table S2.** Synergistic data of compounds and PMBN of the checkerboard assays with rifampicin as shown in Figure S2. All minimal inhibitory concentrations (MICs) and minimal synergistic concentrations (MSCs) are in  $\mu\text{g/mL}$ .

	Structures	MIC	MSC	MIC rif	MSC rif	FICI
1		200	50	12	1.5	0.375
2		>25	3.13	6	0.19	$\leq 0.094$
3		>200	12.5	6	0.19	$\leq 0.063$
9		>200	100	12	3	$\leq 0.500$
10		200	12.5	12	0.19	0.078
11		>25	3.13	12	0.75	$\leq 0.125$
12		>25	3.13	12	0.19	$\leq 0.078$
15		>200	100	6	1.5	$\leq 0.500$
16		>200	3.13	6	6	$>0.5^a$
21		>200	25	12	0.38	$\leq 0.094$
22		>200	50	12	0.75	$\leq 0.188$
23		200	25	6	1.5	0.375
24		200	3.13	12	0.19	0.031
1b		>200	100	12	1.5	$\leq 0.375$
21b		>200	100	6	0.38	$\leq 0.313$

<b>22b</b>		>200	50	6	0.75	≤0.250
<b>23b</b>		>200	50	>12	0.75	≤0.156
<b>1c</b>		>200	nd.	12	nd.	>0.5 <sup>a</sup>
<b>21c</b>		>200	nd.	12	nd.	>0.5 <sup>a</sup>
<b>22c</b>		>200	nd.	12	nd.	>0.5 <sup>a</sup>
<b>23c</b>		>200	nd.	12	nd.	>0.5 <sup>a</sup>
<b>37</b>		200	12.5	>12	1.5	≤0.125
<b>38</b>		100	3.13	>12	0.19	≤0.039
<b>43</b>		100	6.25	12	0.38	0.094
<b>44</b>		>200	6.25	12	0.38	≤0.047
<b>PMBN</b>		>200	3.125	3	0.09	≤0.039

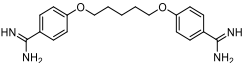
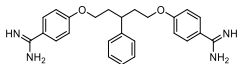
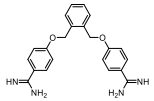
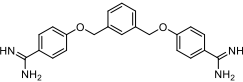
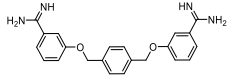
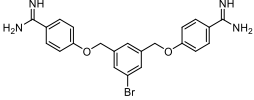
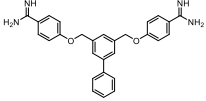
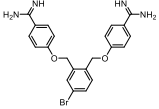
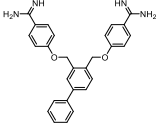
<sup>a</sup> Synergy is defined as FICI ≤0.5.<sup>21</sup>

Checkerboard assays and FICI data against *E. coli* BW25113 with novobiocin

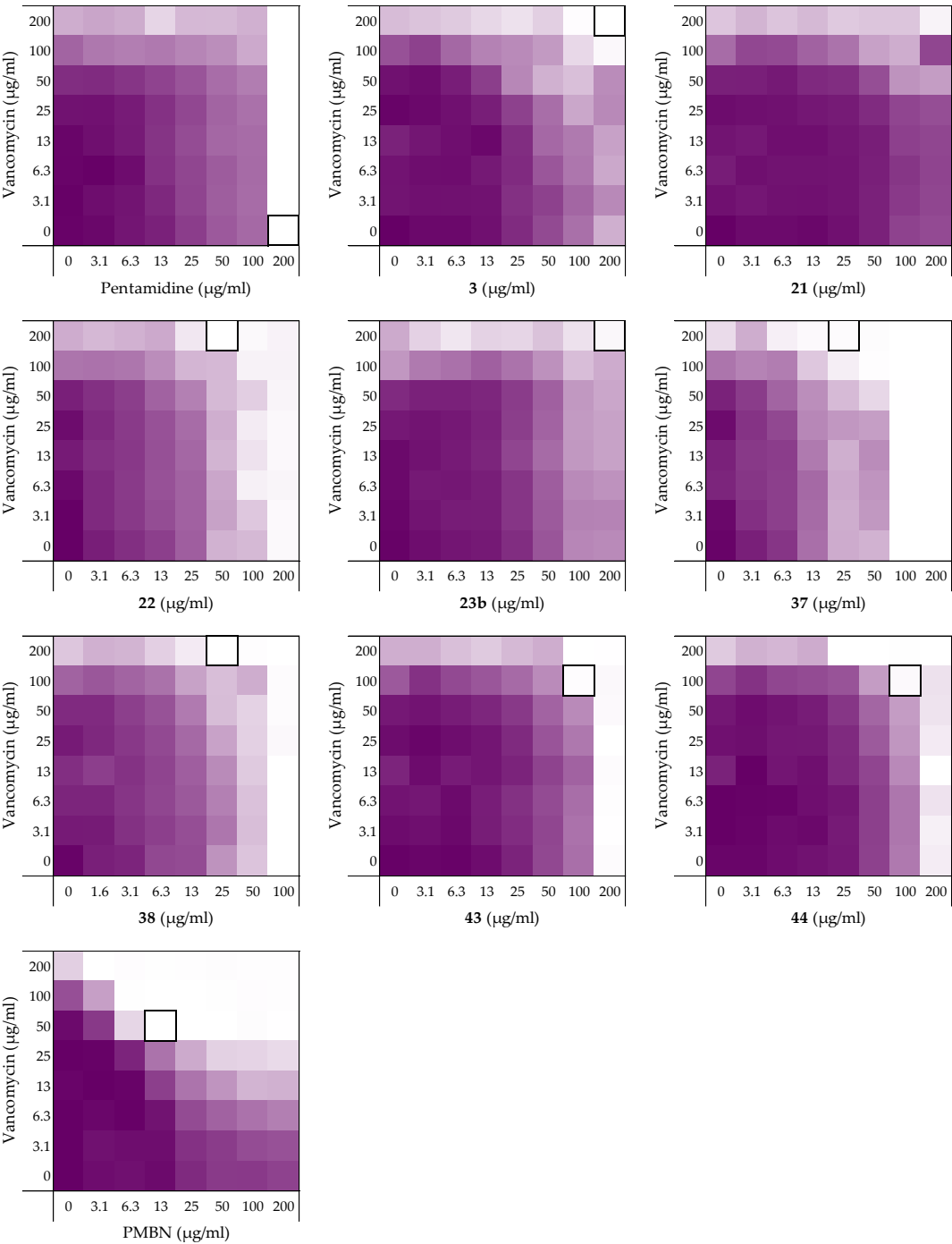


**Figure S3.** Checkerboard assays of compounds **1**, **3**, **21**, **22**, **23b**, **37**, **38**, **43**, **44**, and PMBN in combination with novobiocin versus *E. coli* BW25113. OD<sub>600</sub> values were measured using a plate reader and transformed to a gradient: purple represents growth, white represents no growth. In each case, the bounded box in the checkerboard assays indicates the minimal synergistic concentration (MSC) of compound and antibiotic resulting in the lowest FICI.

**Table S3.** Synergistic data of compounds **1**, **3**, **21**, **22**, **23b**, **37**, **38**, **43**, **44**, and PMBN of the checkerboard results for *E. coli* BW25113 with novobiocin as shown in Figure S3. All minimal inhibitory concentrations (MICs) and minimal synergistic concentrations (MSCs) are in µg/mL.

	Structures	MIC	MSC	MIC nov	MSC nov	FICI
<b>1</b>		200	50	>200	12.5	≤0.281
<b>3</b>		>200	25	>200	12.5	≤0.094
<b>21</b>		>200	25	>200	25	≤0.125
<b>22</b>		>200	25	>200	6.25	≤0.078
<b>23b</b>		>200	50	>200	25	≤0.188
<b>37</b>		200	12.5	>200	6.25	≤0.078
<b>38</b>		100	3.13	>200	3.13	≤0.039
<b>43</b>		>200	12.5	>200	3.13	≤0.039
<b>44</b>		>200	6.25	>200	6.25	≤0.031
<b>PMBN</b>		>200	12.5	>200	6.25	≤0.047

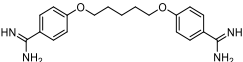
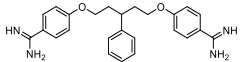
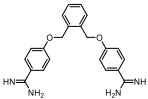
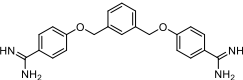
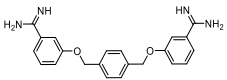
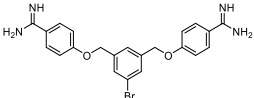
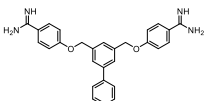
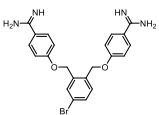
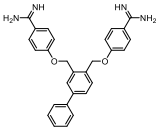
Checkerboard assays and FICI data against *E. coli* BW25113 with vancomycin





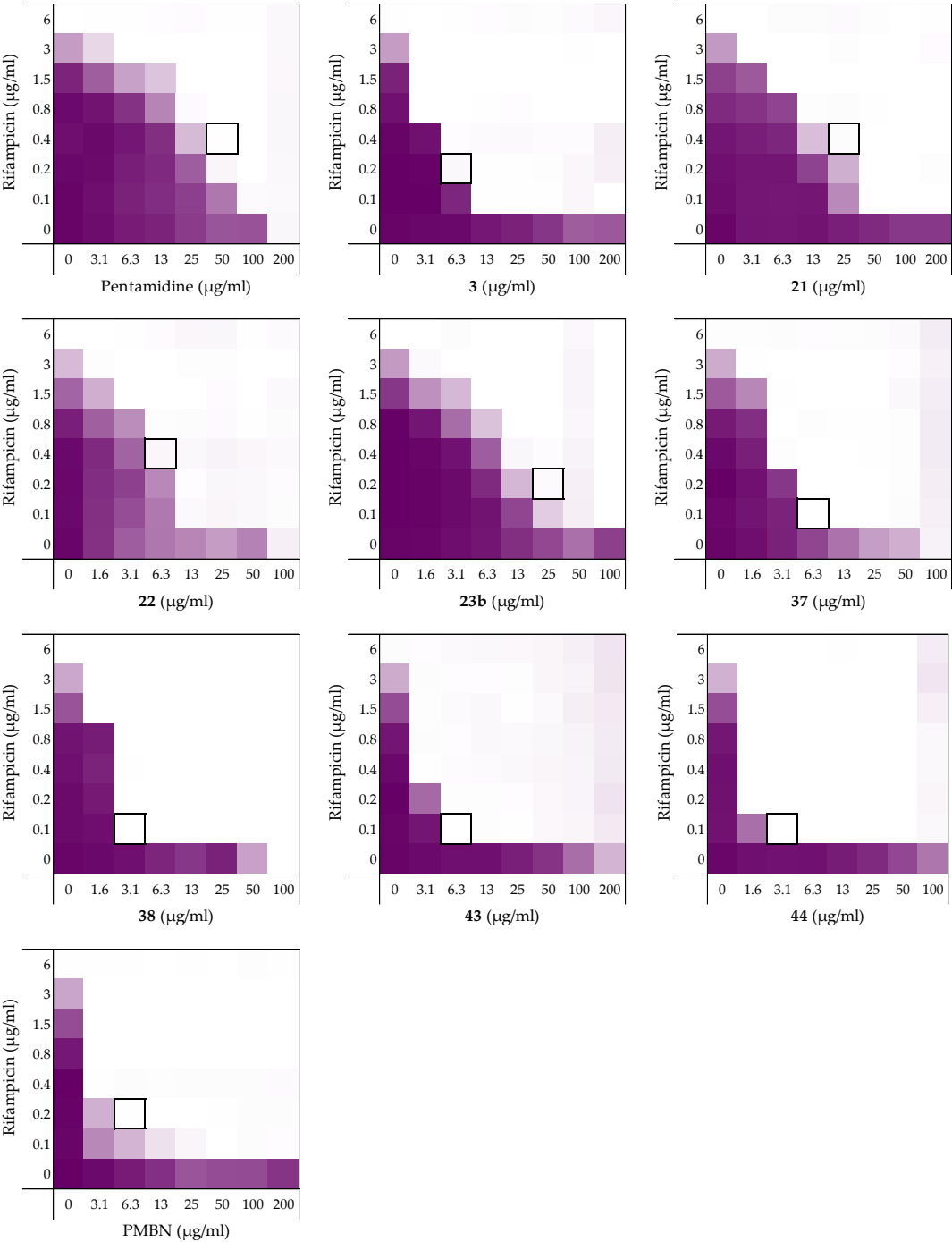
**Figure S4.** Checkerboard assays of compounds **1**, **3**, **21**, **22**, **23b**, **37**, **38**, **43**, **44**, and PMBN in combination with vancomycin versus *E. coli* BW25113. OD<sub>600</sub> values were measured using a plate reader and transformed to a gradient: purple represents growth, white represents no growth. In each case, the bounded box in the checkerboard assays indicates the minimal synergistic concentration (MSC) of compound and antibiotic resulting in the lowest FICI.

**Table S4.** Synergistic data of compounds **1**, **3**, **21**, **22**, **23b**, **37**, **38**, **43**, **44**, and PMBN of the checkerboard results for *E. coli* BW25113 with vancomycin as shown in Figure S4. All minimal inhibitory concentrations (MICs) and minimal synergistic concentrations (MSCs) are in µg/mL.

	Structures	MIC	MSC	MIC van	MSC van	FICI
<b>1</b>		200	200	>200	-	>0.5 <sup>a</sup>
<b>3</b>		>200	200	>200	200	>0.5 <sup>a</sup>
<b>21</b>		>200	>200	>200	>200	>0.5 <sup>a</sup>
<b>22</b>		>200	50	>200	200	>0.5 <sup>a</sup>
<b>23b</b>		>200	200	>200	200	>0.5 <sup>a</sup>
<b>37</b>		100	25	>200	200	>0.5 <sup>a</sup>
<b>38</b>		100	25	>200	200	>0.5 <sup>a</sup>
<b>43</b>		200	100	>200	100	>0.5 <sup>a</sup>
<b>44</b>		>200	100	>200	100	≤0.500
<b>PMBN</b>		>200	12.5	>200	50	≤0.156

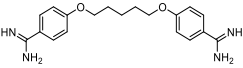
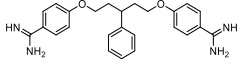
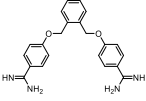
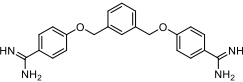
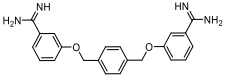
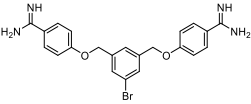
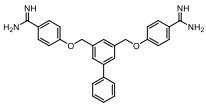
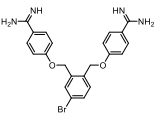
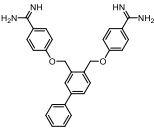
<sup>a</sup> Synergy is defined as FICI ≤ 0.5.<sup>21</sup>

Checkerboard assays and FICI data against *E. coli* ATCC25922 with rifampicin

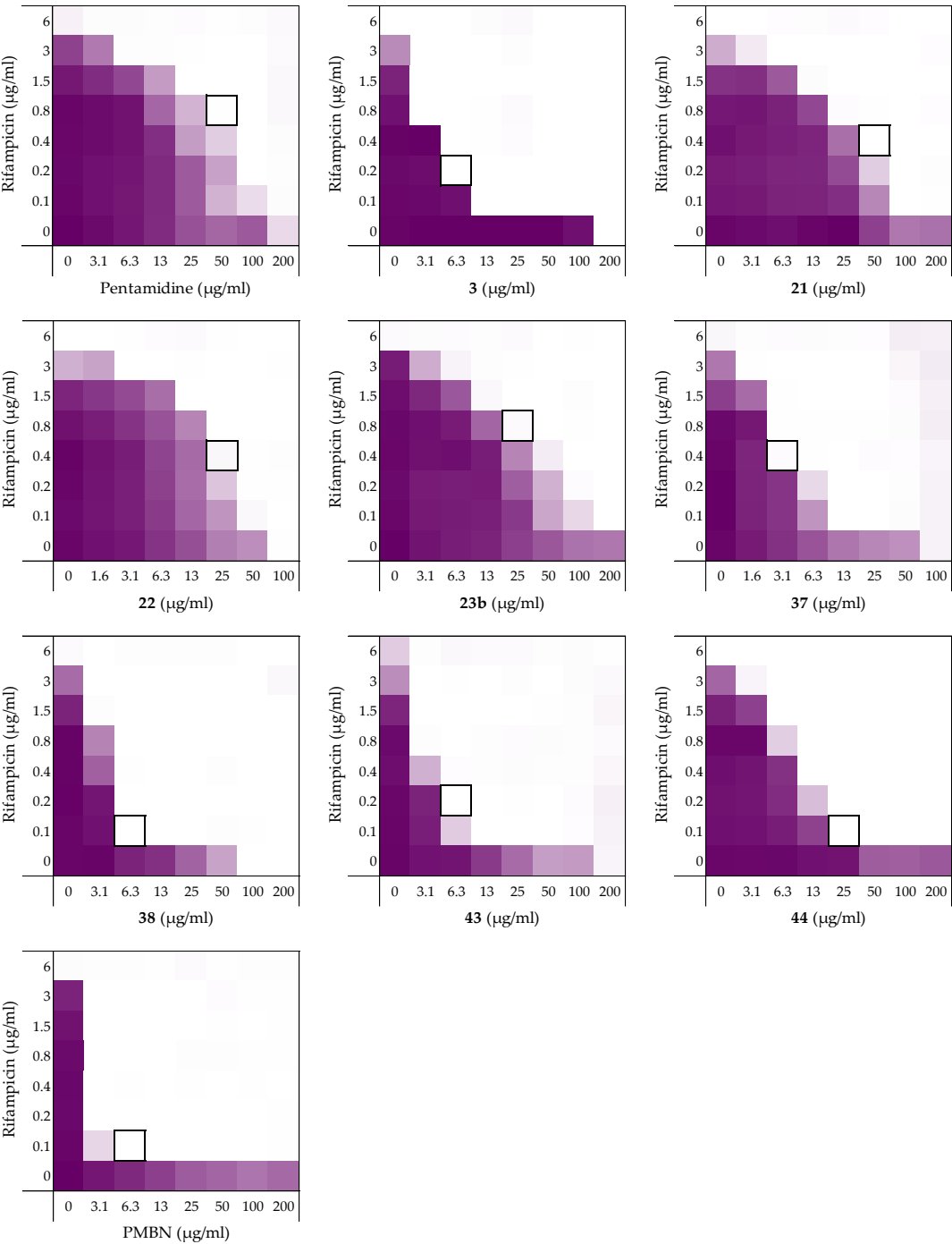


**Figure S5.** Checkerboard assays of compounds **1**, **3**, **21**, **22**, **23b**, **37**, **38**, **43**, **44**, and PMBN in combination with rifampicin versus *E. coli* ATCC25922. OD<sub>600</sub> values were measured using a plate reader and transformed to a gradient: purple represents growth, white represents no growth. In each case, the bounded box in the checkerboard assays indicates the minimal synergistic concentration (MSC) of compound and antibiotic resulting in the lowest FICI.

**Table S5.** Synergistic data of compounds **1**, **3**, **21**, **22**, **23b**, **37**, **38**, **43**, **44**, and PMBN of the checkerboard results for *E. coli* ATCC25922 with rifampicin as shown in Figure S5. All minimal inhibitory concentrations (MICs) and minimal synergistic concentrations (MSCs) are in µg/mL.

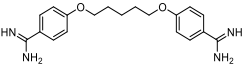
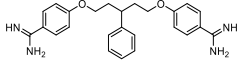
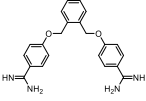
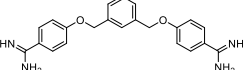
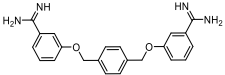
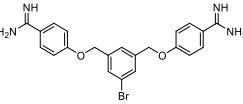
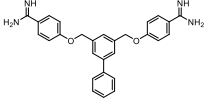
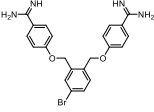
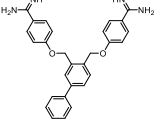
	Structures	MIC	MSC	MIC rif	MSC rif	FICI
<b>1</b>		200	50	6	0.38	0.313
<b>3</b>		>200	6.25	6	0.19	≤0.047
<b>21</b>		>200	25	6	0.38	≤0.125
<b>22</b>		200	6.25	6	0.38	0.094
<b>23b</b>		200	25	6	0.19	0.156
<b>37</b>		100	6.25	6	0.09	0.078
<b>38</b>		100	3.13	6	0.09	0.047
<b>43</b>		>200	6.25	6	0.09	≤0.031
<b>44</b>		200	3.13	6	0.09	0.031
<b>PMBN</b>		>200	6.25	6	0.19	≤0.047

Checkerboard assays and FICI data against *E. coli* W3110 with rifampicin

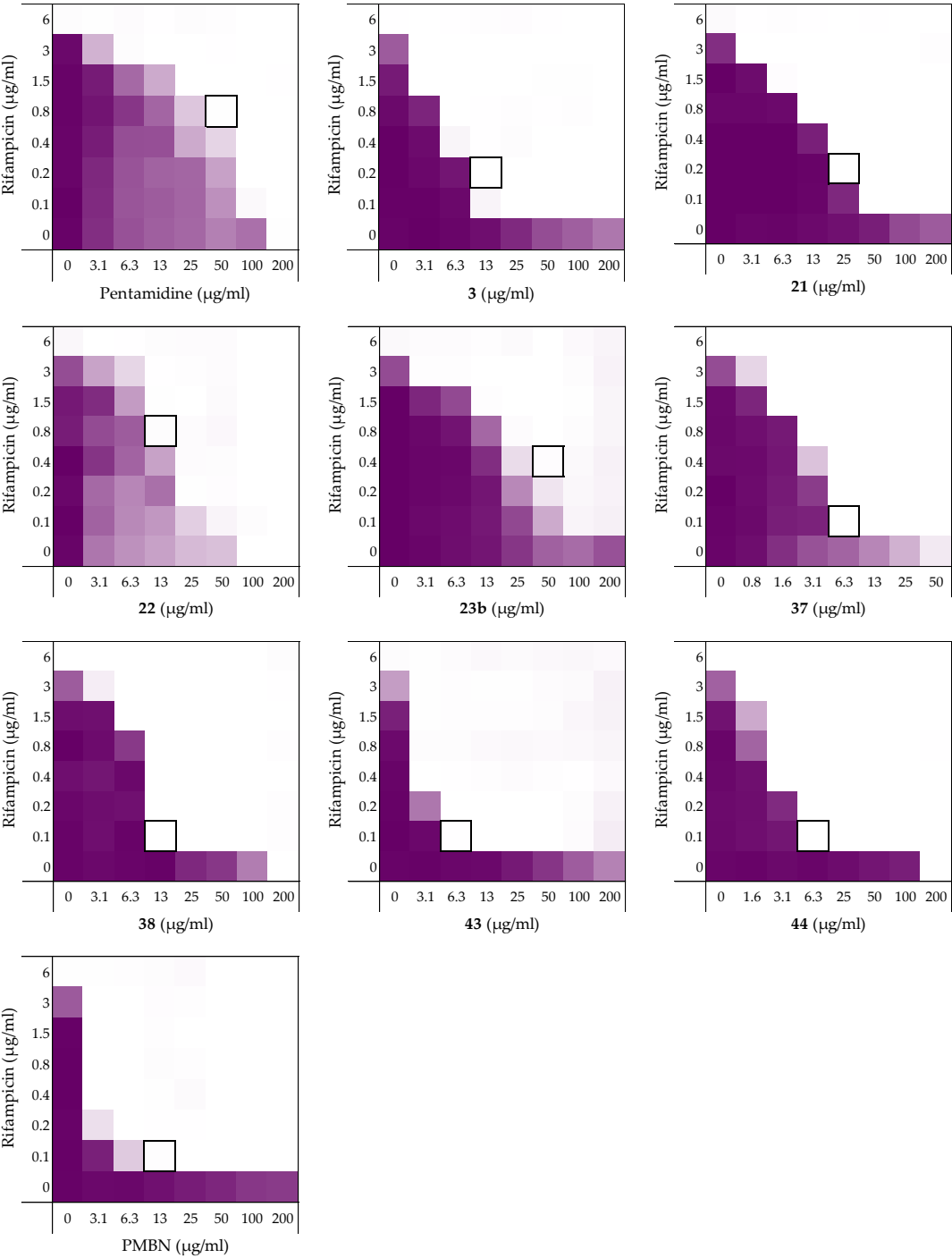


**Figure S6.** Checkerboard assays of compounds **1**, **3**, **21**, **22**, **23b**, **37**, **38**, **43**, **44**, and PMBN in combination with rifampicin versus *E. coli* W3110. OD<sub>600</sub> values were measured using a plate reader and transformed to a gradient: purple represents growth, white represents no growth. In each case, the bounded box in the checkerboard assays indicates the minimal synergistic concentration (MSC) of compound and antibiotic resulting in the lowest FICI.

**Table S6.** Synergistic data of compounds **1**, **3**, **21**, **22**, **23b**, **37**, **38**, **43**, **44**, and PMBN of the checkerboard results for *E. coli* W3110 with rifampicin as shown in Figure S6. All minimal inhibitory concentrations (MICs) and minimal synergistic concentrations (MSCs) are in µg/mL.

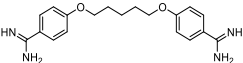
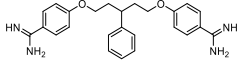
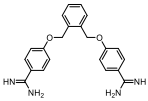
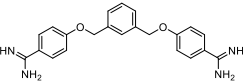
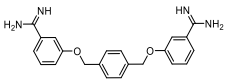
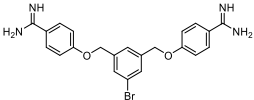
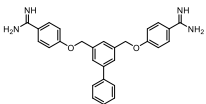
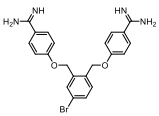
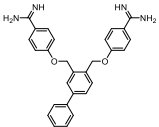
	Structures	MIC	MSC	MIC rif	MSC rif	FICI
<b>1</b>		>200	50	>6	0.75	≤0.188
<b>3</b>		200	6.25	6	0.19	0.063
<b>21</b>		>200	50	6	0.38	≤0.188
<b>22</b>		100	25	6	0.38	0.313
<b>23b</b>		>200	25	6	0.75	≤0.188
<b>37</b>		100	3.13	>6	0.38	≤0.063
<b>38</b>		100	6.25	>6	0.09	≤0.070
<b>43</b>		200	6.25	>6	0.19	≤0.047
<b>44</b>		>200	25	6	0.09	≤0.078
<b>PMBN</b>		>200	6.25	6	0.09	≤0.031

Checkerboard assays and FICI data against *E. coli* 552060.1 with rifampicin

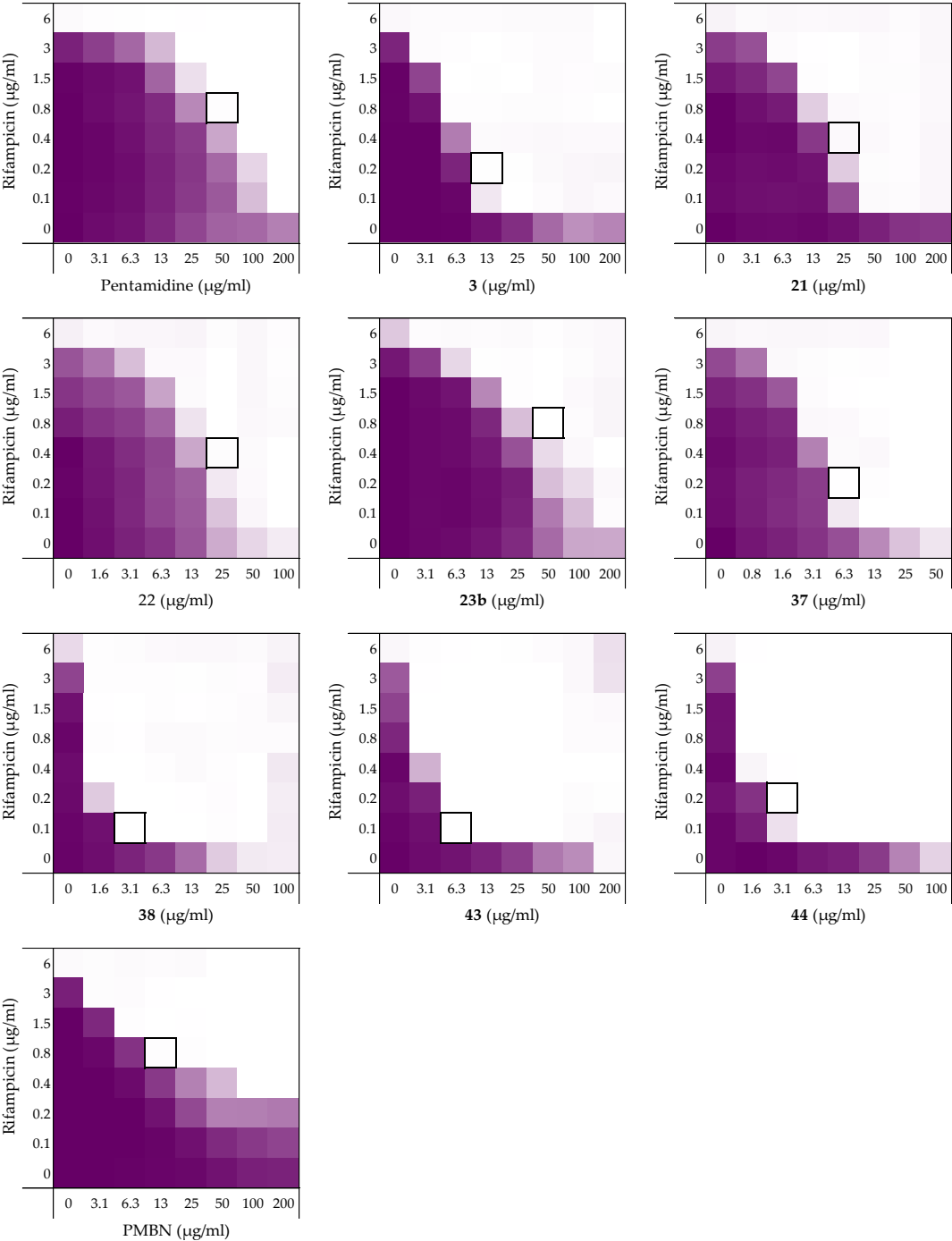


**Figure S7.** Checkerboard assays of compounds **1**, **3**, **21**, **22**, **23b**, **37**, **38**, **43**, **44**, and PMBN in combination with rifampicin versus *E. coli* 552060.1. OD<sub>600</sub> values were measured using a plate reader and transformed to a gradient: purple represents growth, white represents no growth. In each case, the bounded box in the checkerboard assays indicates the minimal synergistic concentration (MSC) of compound and antibiotic resulting in the lowest FICI.

**Table S7.** Synergistic data of compounds **1**, **3**, **21**, **22**, **23b**, **37**, **38**, **43**, **44**, and PMBN of the checkerboard results for *E. coli* 552060.1 with rifampicin as shown in Figure S7. All minimal inhibitory concentrations (MICs) and minimal synergistic concentrations (MSCs) are in µg/mL.

	Structures	MIC	MSC	MIC rif	MSC rif	FICI
<b>1</b>		200	50	6	0.75	0.375
<b>3</b>		>200	12.5	6	0.19	≤0.063
<b>21</b>		>200	25	6	0.19	≤0.094
<b>22</b>		100	12.5	6	0.75	0.250
<b>23b</b>		>200	50	6	0.38	≤0.188
<b>37</b>		100	6.25	6	0.09	0.078
<b>38</b>		200	12.5	6	0.09	0.078
<b>43</b>		>200	6.25	6	0.09	≤0.031
<b>44</b>		200	6.25	6	0.09	0.047
<b>PMBN</b>		>200	12.5	6	0.09	≤0.047

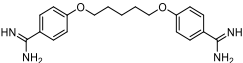
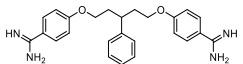
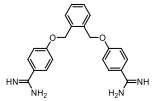
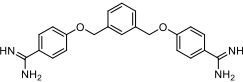
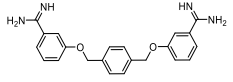
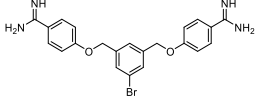
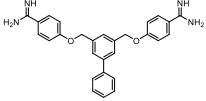
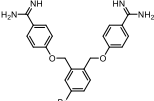
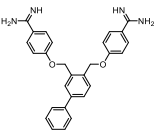
Checkerboard assays and FICI data against *E. coli* BW25113 *mcr-1* with rifampicin



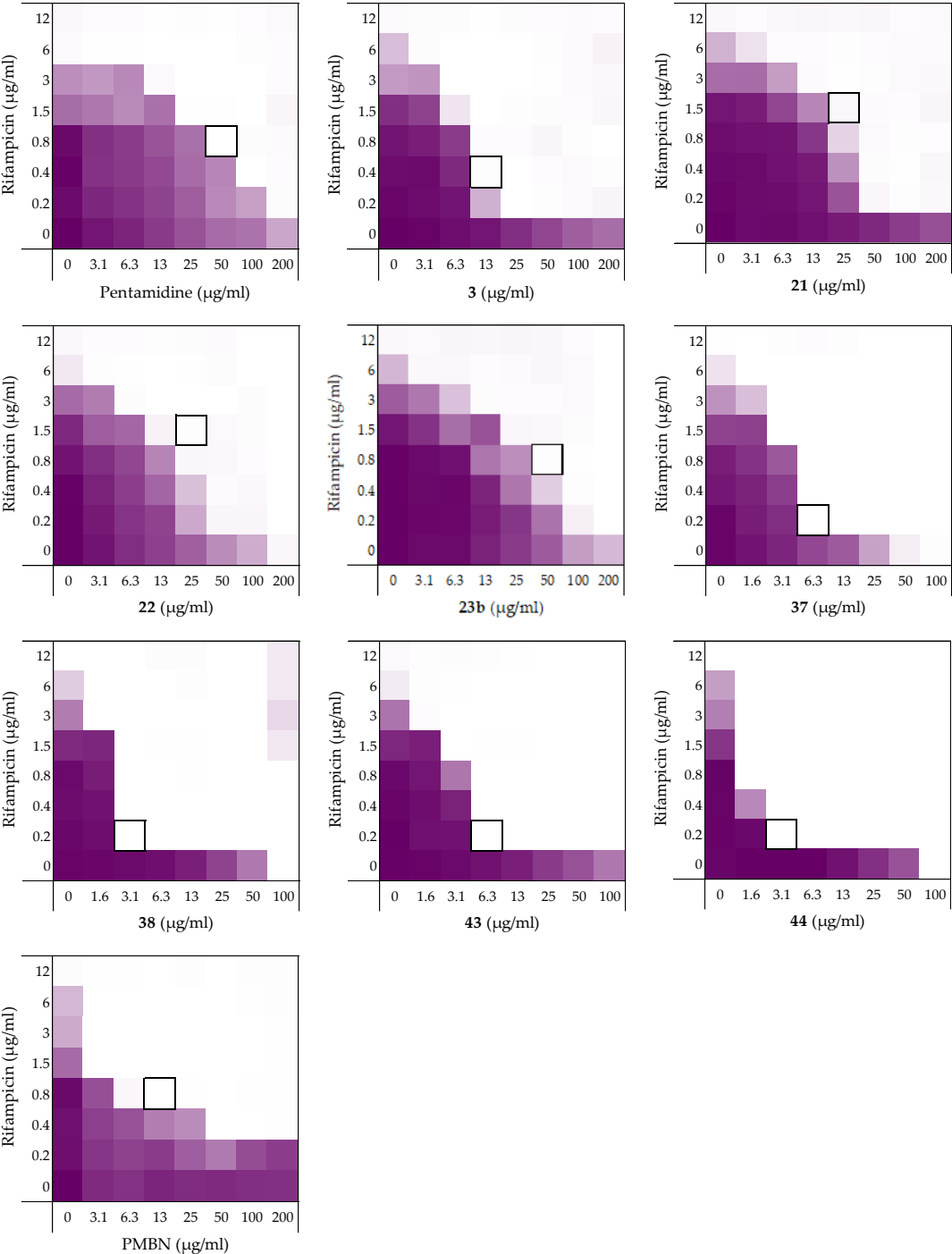


**Figure S8.** Checkerboard assays of compounds **1**, **3**, **21**, **22**, **23b**, **37**, **38**, **43**, **44**, and PMBN in combination with rifampicin versus *E. coli* BW25113 mcr-1. OD<sub>600</sub> values were measured using a plate reader and transformed to a gradient: purple represents growth, white represents no growth. In each case, the bounded box in the checkerboard assays indicates the minimal synergistic concentration (MSC) of compound and antibiotic resulting in the lowest FICI.

**Table S8.** Synergistic data of compounds **1**, **3**, **21**, **22**, **23b**, **37**, **38**, **43**, **44**, and PMBN of the checkerboard results for *E. coli* BW25113 mcr-1 with rifampicin as shown in Figure S8. All minimal inhibitory concentrations (MICs) and minimal synergistic concentrations (MSCs) are in µg/mL.

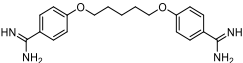
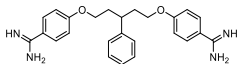
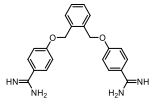
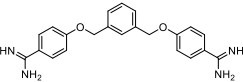
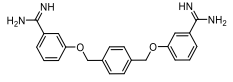
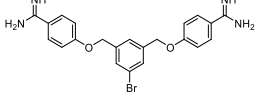
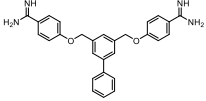
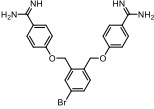
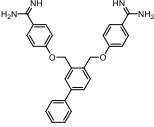
	Structures	MIC	MSC	MIC rif	MSC rif	FICI
<b>1</b>		>200	50	6	0.75	≤0.250
<b>3</b>		>200	12.5	6	0.19	≤0.063
<b>21</b>		>200	25	>6	0.38	≤0.094
<b>22</b>		>100	25	>6	0.38	≤0.156
<b>23b</b>		>200	50	>6	0.75	≤0.188
<b>37</b>		>50	6.25	>6	0.19	≤0.078
<b>38</b>		100	3.13	>6	0.09	≤0.039
<b>43</b>		200	6.25	>6	0.09	≤0.039
<b>44</b>		>100	3.13	>6	0.19	≤0.031
<b>PMBN</b>		>200	12.5	6	0.75	≤0.156

Checkerboard assays and FICI data against *E. coli* mcr-1 with rifampicin

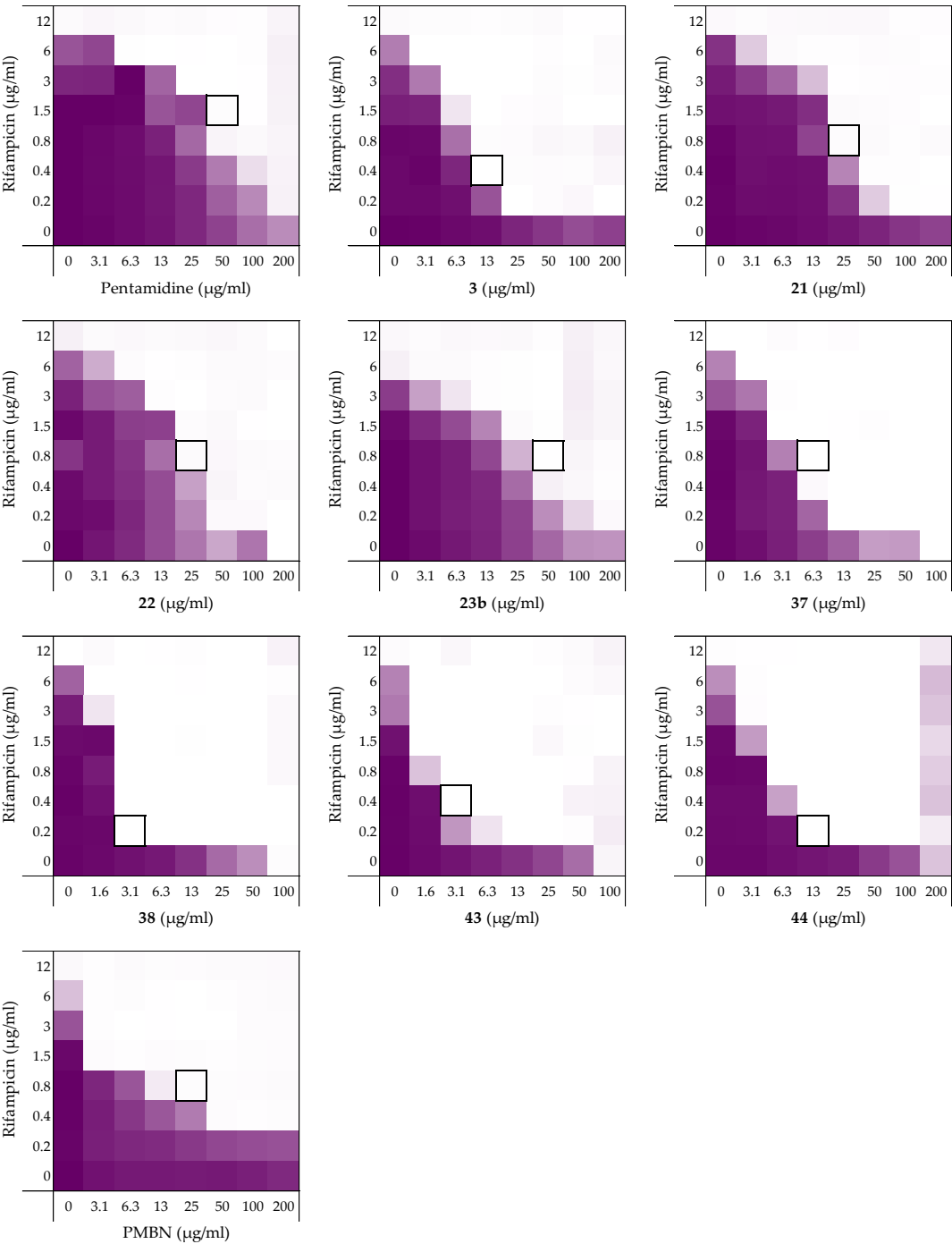


**Figure S9.** Checkerboard assays of compounds **1**, **3**, **21**, **22**, **23b**, **37**, **38**, **43**, **44**, and PMBN in combination with rifampicin versus *E. coli* mcr-1. OD<sub>600</sub> values were measured using a plate reader and transformed to a gradient: purple represents growth, white represents no growth. In each case, the bounded box in the checkerboard assays indicates the minimal synergistic concentration (MSC) of compound and antibiotic resulting in the lowest FICI.

**Table S9.** Synergistic data of compounds **1**, **3**, **21**, **22**, **23b**, **37**, **38**, **43**, **44**, and PMBN of the checkerboard results for *E. coli* mcr-1 with rifampicin as shown in Figure S9. All minimal inhibitory concentrations (MICs) and minimal synergistic concentrations (MSCs) are in µg/mL.

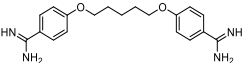
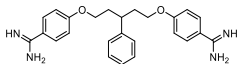
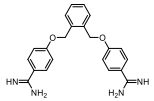
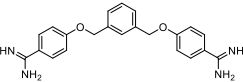
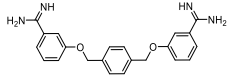
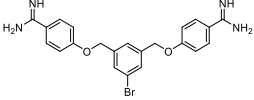
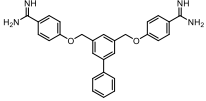
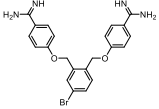
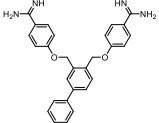
	Structures	MIC	MSC	MIC rif	MSC rif	FICI
<b>1</b>		>200	50	12	0.75	≤0.188
<b>3</b>		>200	12.5	12	0.38	≤0.063
<b>21</b>		>200	25	12	1.5	≤0.188
<b>22</b>		>200	25	12	1.5	≤0.188
<b>23b</b>		>200	50	12	0.75	≤0.188
<b>37</b>		100	6.25	12	0.19	0.078
<b>38</b>		100	3.13	12	0.19	0.047
<b>43</b>		>100	6.25	12	0.19	≤0.047
<b>44</b>		100	3.13	12	0.19	0.047
<b>PMBN</b>		>200	12.5	12	0.75	≤0.094

Checkerboard assays and FICI data against *E. coli* EQASmc<sup>r</sup>-1 with rifampicin

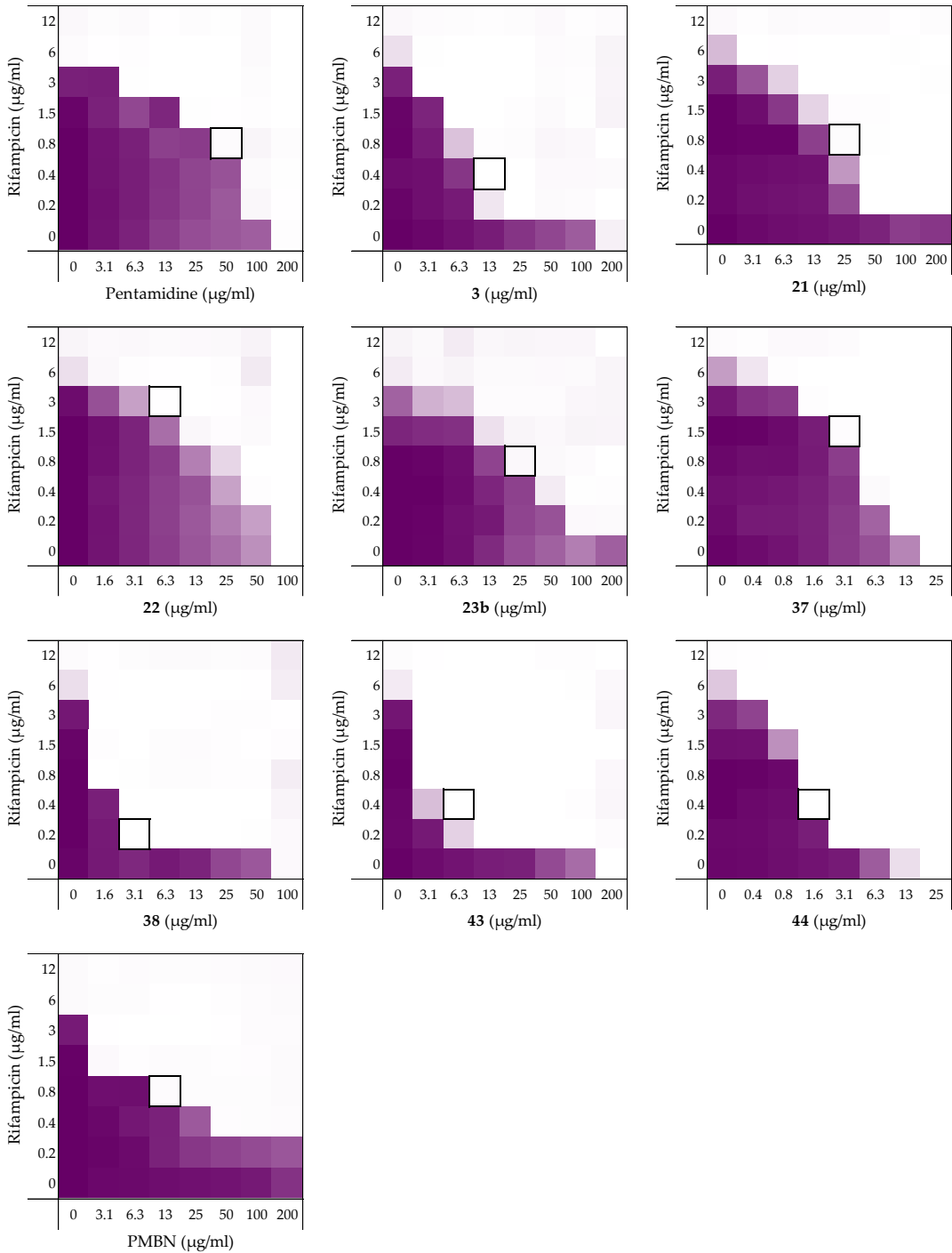


**Figure S10.** Checkerboard assays of compounds **1**, **3**, **21**, **22**, **23b**, **37**, **38**, **43**, **44**, and PMBN in combination with rifampicin versus *E. coli* EQASmc<sup>r</sup>-1. OD<sub>600</sub> values were measured using a plate reader and transformed to a gradient: purple represents growth, white represents no growth. In each case, the bounded box in the checkerboard assays indicates the minimal synergistic concentration (MSC) of compound and antibiotic resulting in the lowest FICI.

**Table S10.** Synergistic data of compounds **1**, **3**, **21**, **22**, **23b**, **37**, **38**, **43**, **44**, and PMBN of the checkerboard results for *E. coli* EQASmc<sup>r</sup>-1 with rifampicin as shown in Figure S10. All minimal inhibitory concentrations (MICs) and minimal synergistic concentrations (MSCs) are in µg/mL.

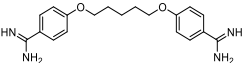
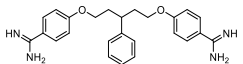
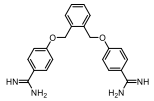
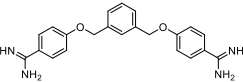
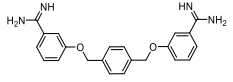
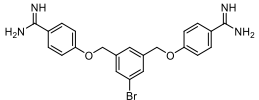
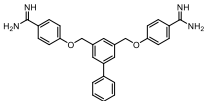
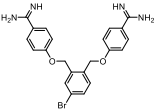
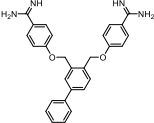
	Structures	MIC	MSC	MIC rif	MSC rif	FICI
<b>1</b>		>200	50	12	1.5	≤0.250
<b>3</b>		>200	12.5	12	0.38	≤0.063
<b>21</b>		>200	25	12	0.75	≤0.125
<b>22</b>		200	25	12	0.75	0.188
<b>23b</b>		>200	50	12	0.75	≤0.188
<b>37</b>		100	6.25	12	0.75	0.125
<b>38</b>		100	3.13	12	0.19	0.047
<b>43</b>		100	3.13	12	0.38	0.063
<b>44</b>		200	12.5	12	0.19	0.078
<b>PMBN</b>		>200	25	12	0.75	≤0.125

**Checkerboard assays and FICI data against *E. coli* EQASmc-2 with rifampicin**

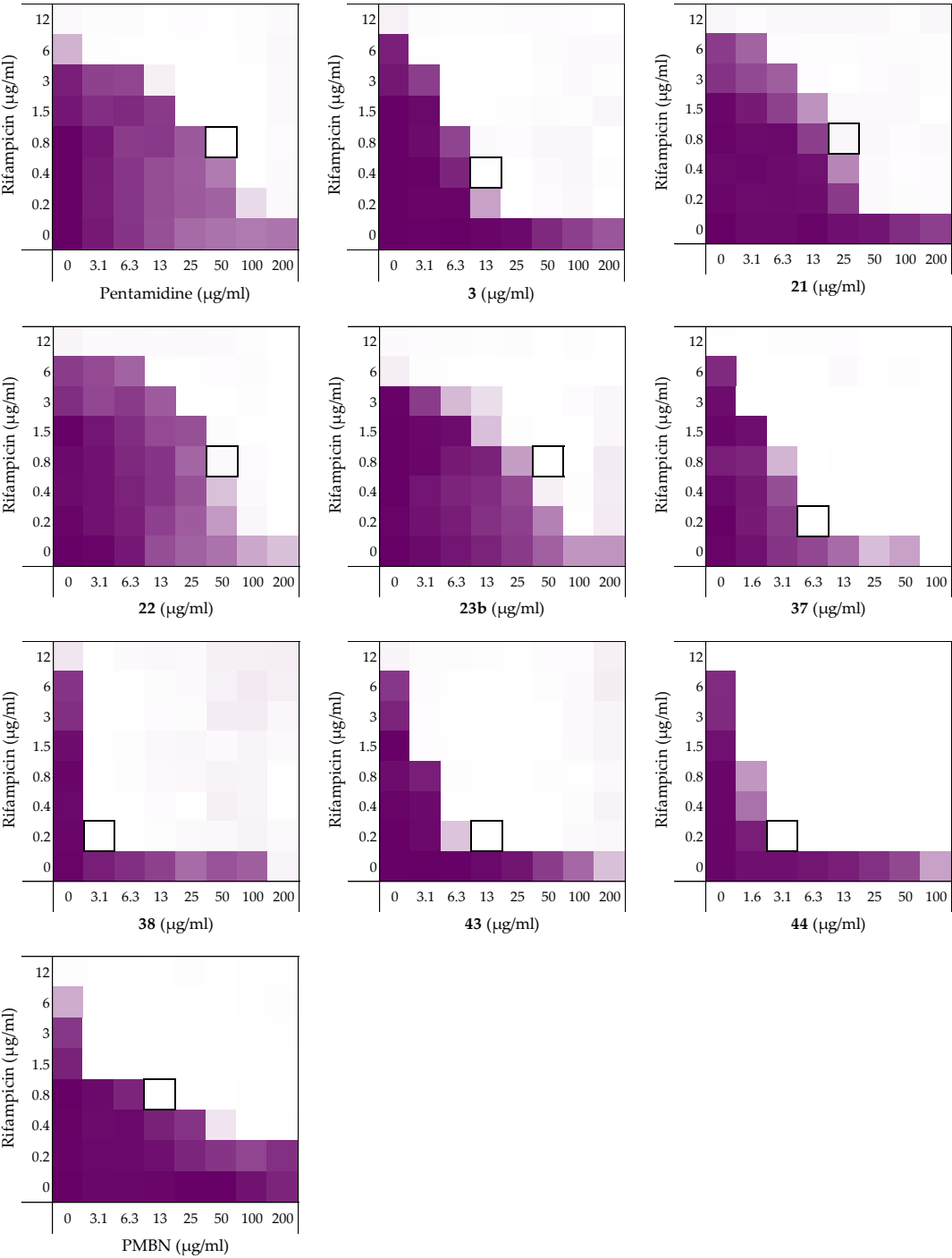


**Figure S11.** Checkerboard assays of compounds **1**, **3**, **21**, **22**, **23b**, **37**, **38**, **43**, **44**, and PMBN in combination with rifampicin versus *E. coli* EQASmc<sup>r</sup>-2. OD<sub>600</sub> values were measured using a plate reader and transformed to a gradient: purple represents growth, white represents no growth. In each case, the bounded box in the checkerboard assays indicates the minimal synergistic concentration (MSC) of compound and antibiotic resulting in the lowest FICI.

**Table S11.** Synergistic data compounds **1**, **3**, **21**, **22**, **23b**, **37**, **38**, **43**, **44**, and PMBN of the checkerboard results for *E. coli* EQASmc<sup>r</sup>-2 with rifampicin as shown in Figure S11. All minimal inhibitory concentrations (MICs) and minimal synergistic concentrations (MSCs) are in µg/mL.

	Structures	MIC	MSC	MIC rif	MSC rif	FICI
<b>1</b>		200	50	6	0.75	0.375
<b>3</b>		>200	12.5	12	0.38	≤0.063
<b>21</b>		>200	25	12	0.75	≤0.125
<b>22</b>		100	6.25	12	3	0.313
<b>23b</b>		>200	25	12	0.75	≤0.125
<b>37</b>		25	3.13	12	1.5	0.250
<b>38</b>		100	3.13	12	0.19	0.047
<b>43</b>		200	6.25	12	0.38	0.063
<b>44</b>		25	1.56	12	0.38	0.094
<b>PMBN</b>		>200	12.5	6	0.75	≤0.156

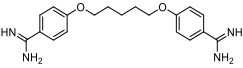
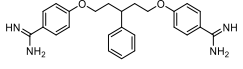
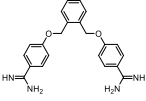
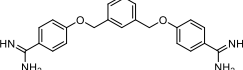
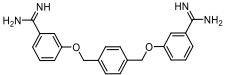
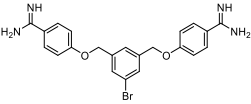
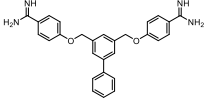
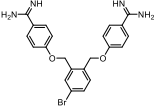
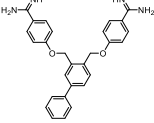
Checkerboard assays and FICI data against *E. coli* EQASmc-3 with rifampicin



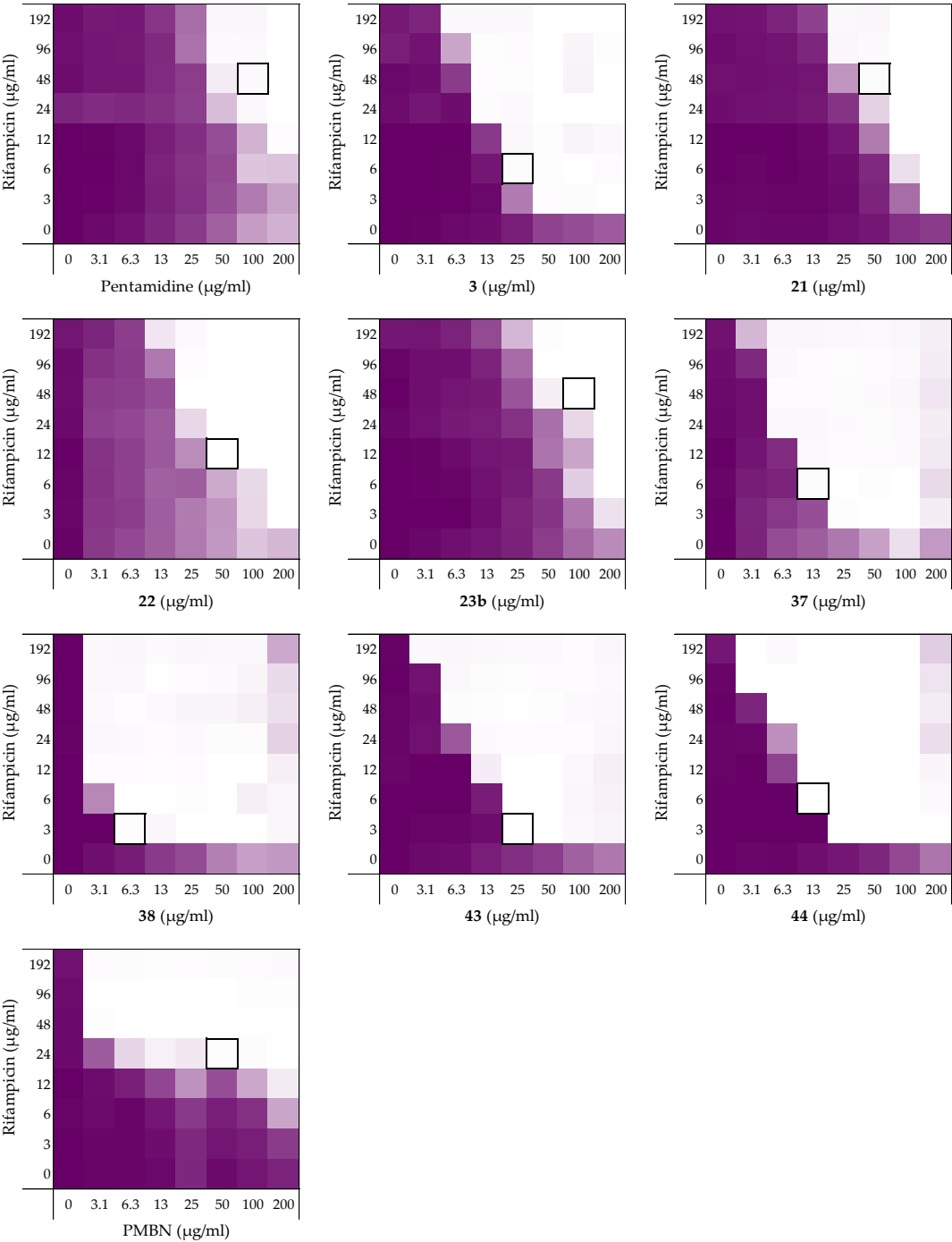


**Figure S12.** Checkerboard assays of compounds **1**, **3**, **21**, **22**, **23b**, **37**, **38**, **43**, **44**, and PMBN in combination with rifampicin versus *E. coli* EQASmc<sup>r</sup>-3. OD<sub>600</sub> values were measured using a plate reader and transformed to a gradient: purple represents growth, white represents no growth. In each case, the bounded box in the checkerboard assays indicates the minimal synergistic concentration (MSC) of compound and antibiotic resulting in the lowest FICI.

**Table S12.** Synergistic data of compounds **1**, **3**, **21**, **22**, **23b**, **37**, **38**, **43**, **44**, and PMBN of the checkerboard results for *E. coli* EQASmc<sup>r</sup>-3 with rifampicin as shown in Figure S12. All minimal inhibitory concentrations (MICs) and minimal synergistic concentrations (MSCs) are in µg/mL.

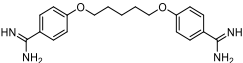
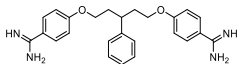
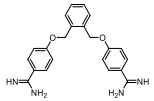
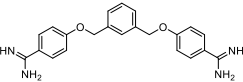
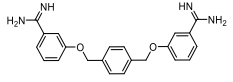
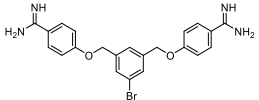
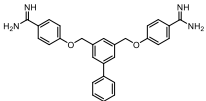
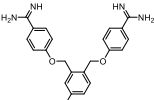
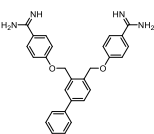
	Structures	MIC	MSC	MIC rif	MSC rif	FICI
<b>1</b>		>200	50	12	0.75	≤0.188
<b>3</b>		>200	12.5	12	0.38	≤0.063
<b>21</b>		>200	25	12	0.75	≤0.125
<b>22</b>		>200	50	12	0.75	≤0.188
<b>23b</b>		>200	50	12	0.75	≤0.188
<b>37</b>		100	6.25	12	0.19	0.078
<b>38</b>		200	3.13	12	0.19	0.031
<b>43</b>		>200	12.5	12	0.19	≤0.047
<b>44</b>		>100	3.13	12	0.19	≤0.031
<b>PMBN</b>		>200	12.5	12	0.75	≤0.094

Checkerboard assays and FICI data against *E. coli* RC00089 with rifampicin

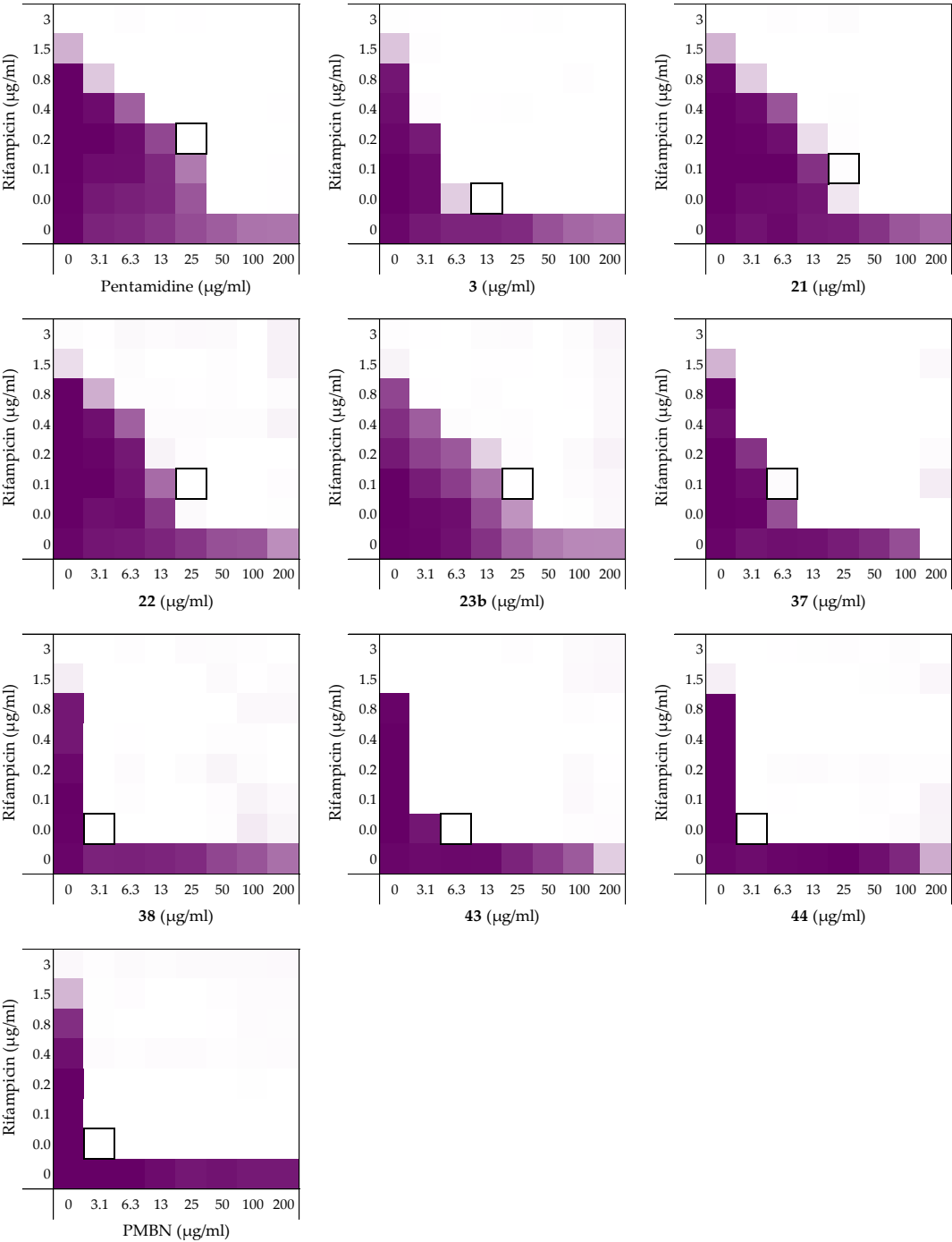


**Figure S13.** Checkerboard assays of compounds **1**, **3**, **21**, **22**, **23b**, **37**, **38**, **43**, **44**, and PMBN in combination with rifampicin versus *E. coli* RC00089. OD<sub>600</sub> values were measured using a plate reader and transformed to a gradient: purple represents growth, white represents no growth. In each case, the bounded box in the checkerboard assays indicates the minimal synergistic concentration (MSC) of compound and antibiotic resulting in the lowest FICI.

**Table S13.** Synergistic data of compounds **1**, **3**, **21**, **22**, **23b**, **37**, **38**, **43**, **44**, and PMBN of the checkerboard results for *E. coli* RC00089 with rifampicin as shown in Figure S13. All minimal inhibitory concentrations (MICs) and minimal synergistic concentrations (MSCs) are in µg/mL.

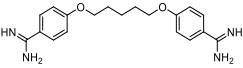
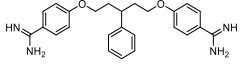
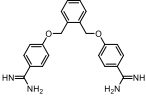
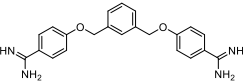
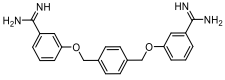
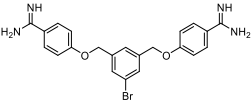
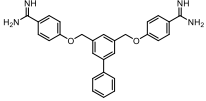
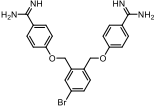
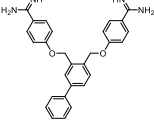
	Structures	MIC	MSC	MIC rif	MSC rif	FICI
<b>1</b>		>200	100	>192	48	≤0.375
<b>3</b>		>200	25	>192	6	≤0.078
<b>21</b>		>200	50	>192	48	≤0.250
<b>22</b>		>200	50	>192	12	≤0.156
<b>23b</b>		>200	100	>192	48	≤0.375
<b>37</b>		>200	12.5	>192	6	≤0.047
<b>38</b>		>200	6.25	>192	3	≤0.023
<b>43</b>		>200	25	>192	3	≤0.070
<b>44</b>		>200	12.5	>192	6	≤0.047
<b>PMBN</b>		>200	50	>192	24	≤0.188

Checkerboard assays and FICI data against *A. baumannii* ATCC17978 with rifampicin

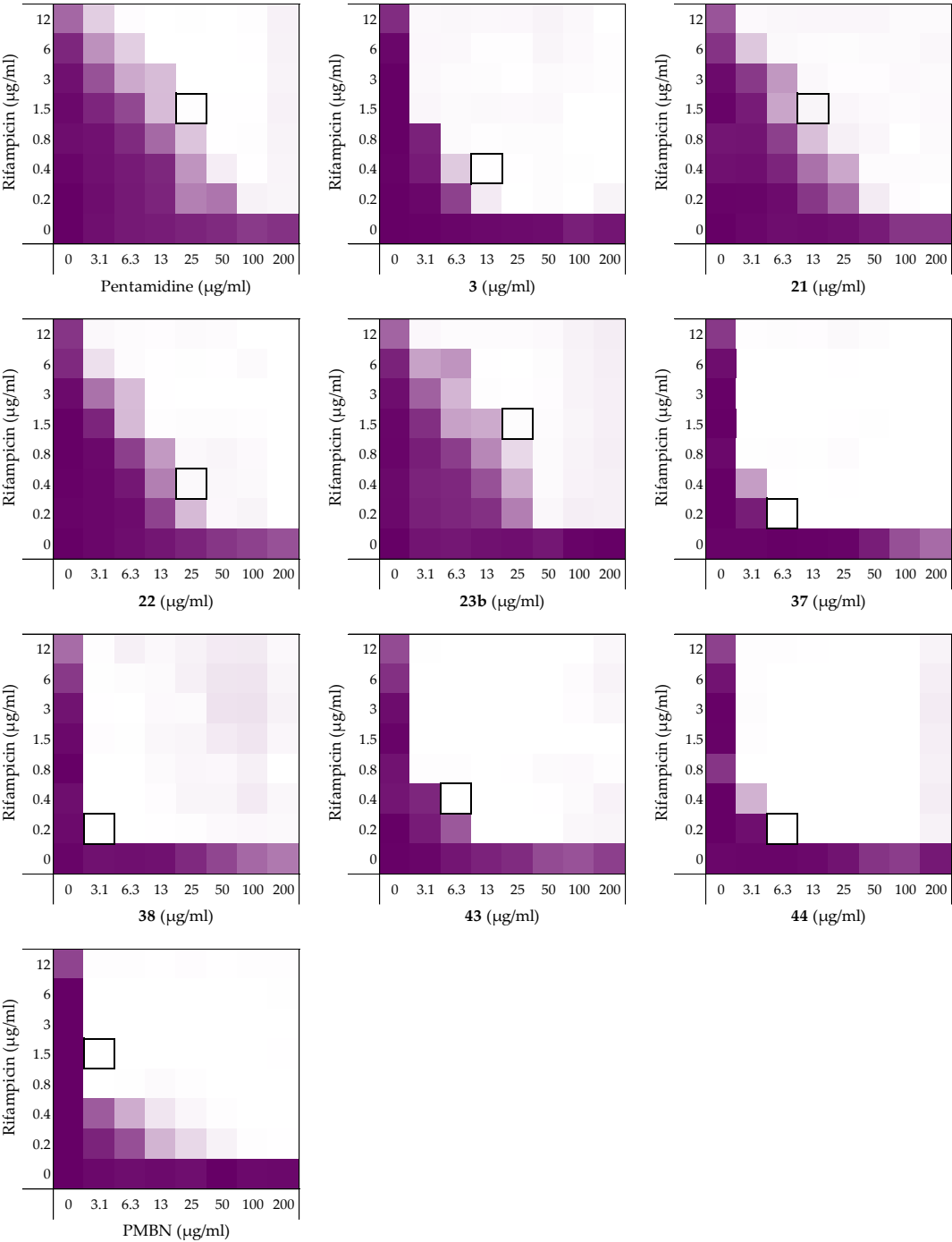


**Figure S14.** Checkerboard assays of compounds **1**, **3**, **21**, **22**, **23b**, **37**, **38**, **43**, **44**, and PMBN in combination with rifampicin versus *A. baumannii* ATCC17978. OD<sub>600</sub> values were measured using a plate reader and transformed to a gradient: purple represents growth, white represents no growth. In each case, the bounded box in the checkerboard assays indicates the minimal synergistic concentration (MSC) of compound and antibiotic resulting in the lowest FICI.

**Table S14.** Synergistic data of compounds **1**, **3**, **21**, **22**, **23b**, **37**, **38**, **43**, **44**, and PMBN of the checkerboard results for *A. baumannii* ATCC17978 with rifampicin as shown in Figure S14. All minimal inhibitory concentrations (MICs) and minimal synergistic concentrations (MSCs) are in µg/mL.

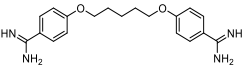
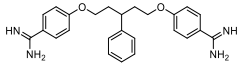
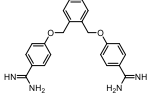
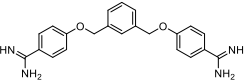
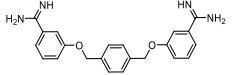
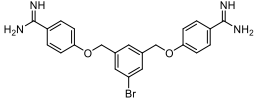
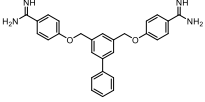
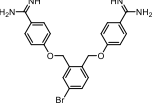
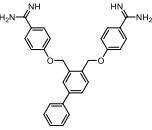
	Structures	MIC	MSC	MIC rif	MSC rif	FICI
<b>1</b>		>200	25	3	0.19	≤0.125
<b>3</b>		>200	12.5	3	0.05	≤0.047
<b>21</b>		>200	25	3	0.09	≤0.094
<b>22</b>		>200	25	3	0.09	≤0.094
<b>23b</b>		>200	25	3	0.09	≤0.094
<b>37</b>		>200	6.25	3	0.09	≤0.047
<b>38</b>		>200	3.13	3	0.05	≤0.023
<b>43</b>		>200	6.25	1.5	0.05	≤0.047
<b>44</b>		>200	3.13	3	0.05	≤0.023
<b>PMBN</b>		>200	3.13	3	0.05	≤0.023

Checkerboard assays and FICI data against *K. pneumoniae* ATCC13883 with rifampicin

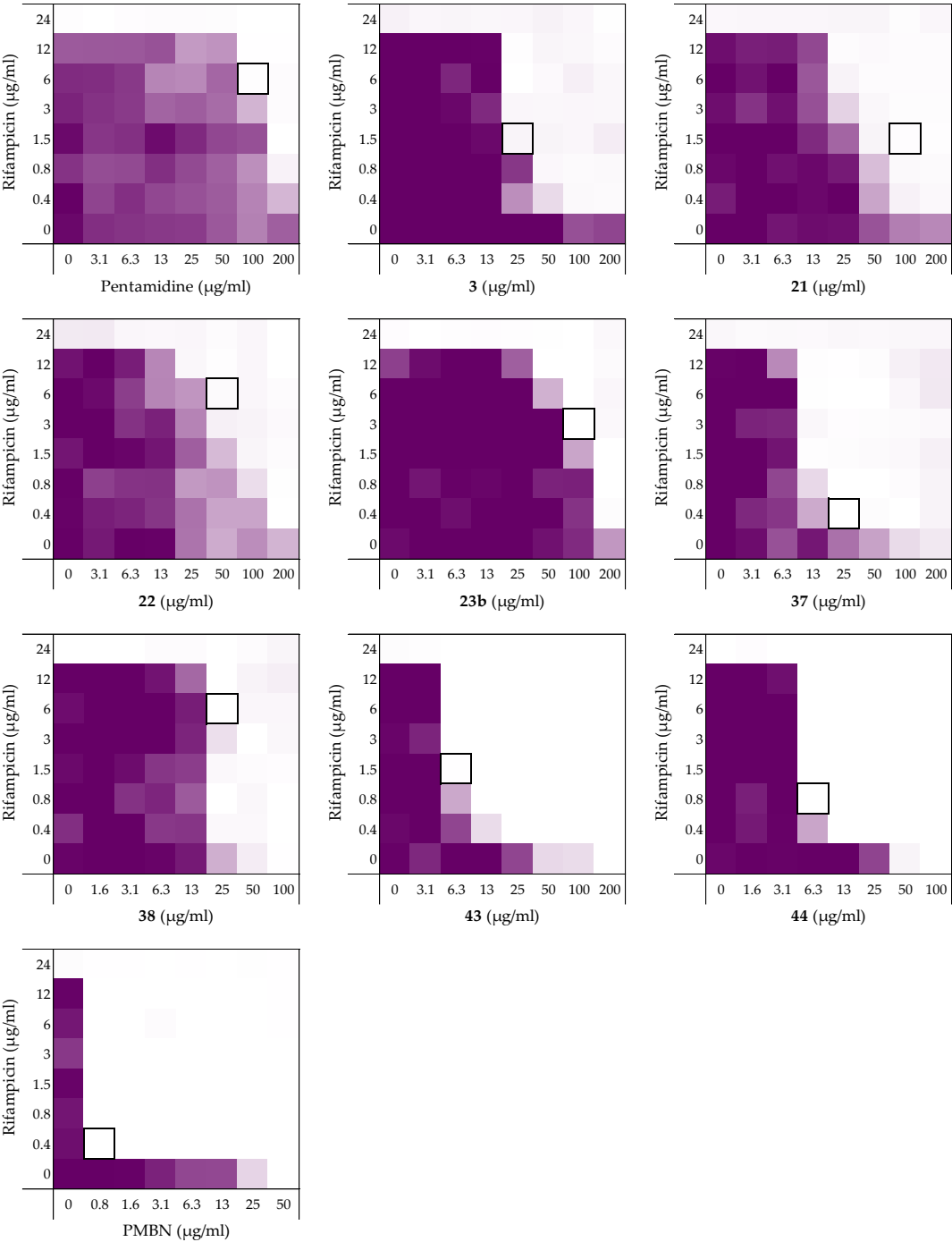


**Figure S15.** Checkerboard assays of compounds **1**, **3**, **21**, **22**, **23b**, **37**, **38**, **43**, **44**, and PMBN in combination with rifampicin versus *K. pneumoniae* ATCC13883. OD<sub>600</sub> values were measured using a plate reader and transformed to a gradient: purple represents growth, white represents no growth. In each case, the bounded box in the checkerboard assays indicates the minimal synergistic concentration (MSC) of compound and antibiotic resulting in the lowest FICI.

**Table S15.** Synergistic data of compounds **1**, **3**, **21**, **22**, **23b**, **37**, **38**, **43**, **44**, and PMBN of the checkerboard results for *K. pneumoniae* ATCC13883 with rifampicin as shown in Figure S15. All minimal inhibitory concentrations (MICs) and minimal synergistic concentrations (MSCs) are in µg/mL.

	Structures	MIC	MSC	MIC rif	MSC rif	FICI
<b>1</b>		>200	25	>12	1.5	≤0.125
<b>3</b>		>200	12.5	>12	0.38	≤0.047
<b>21</b>		>200	12.5	>12	1.5	≤0.094
<b>22</b>		>200	25	>12	0.38	≤0.078
<b>23b</b>		>200	25	>12	1.5	≤0.125
<b>37</b>		>200	6.25	>12	0.19	≤0.023
<b>38</b>		>200	3.13	>12	0.19	≤0.016
<b>43</b>		>200	6.25	>12	0.38	≤0.031
<b>44</b>		>200	6.25	>12	0.19	≤0.023
<b>PMBN</b>		>200	3.13	>12	1.5	≤0.070

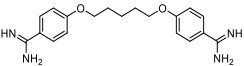
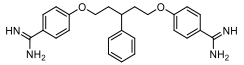
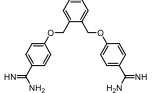
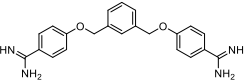
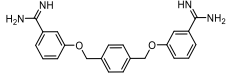
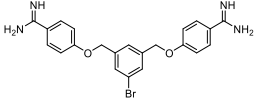
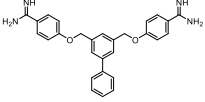
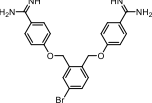
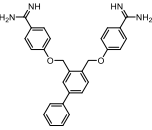
Checkerboard assays and FICI data against *P. aeruginosa* ATCC27853 with rifampicin



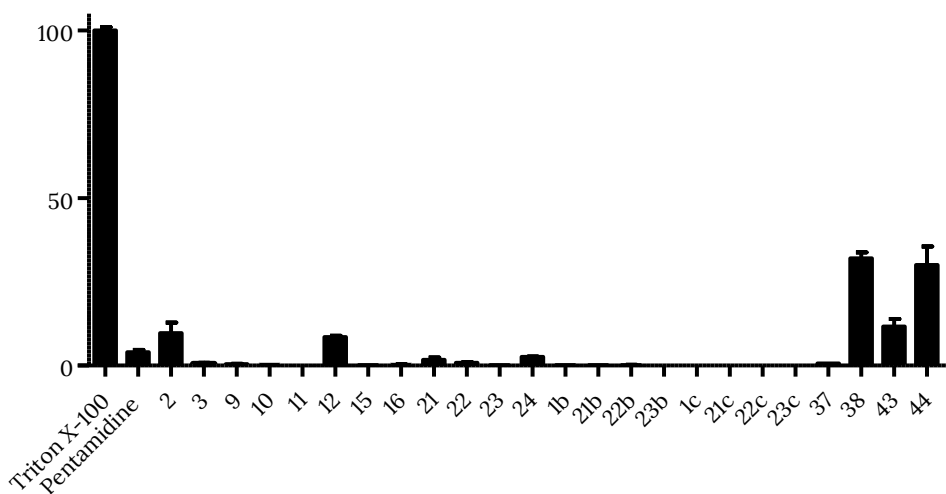


**Figure S16.** Checkerboard assays of compounds **1**, **3**, **21**, **22**, **23b**, **37**, **38**, **43**, **44**, and PMBN in combination with rifampicin versus *P. aeruginosa* ATCC27853. OD<sub>600</sub> values were measured using a plate reader and transformed to a gradient: purple represents growth, white represents no growth. In each case, the bounded box in the checkerboard assays indicates the minimal synergistic concentration (MSC) of compound and antibiotic resulting in the lowest FICI.

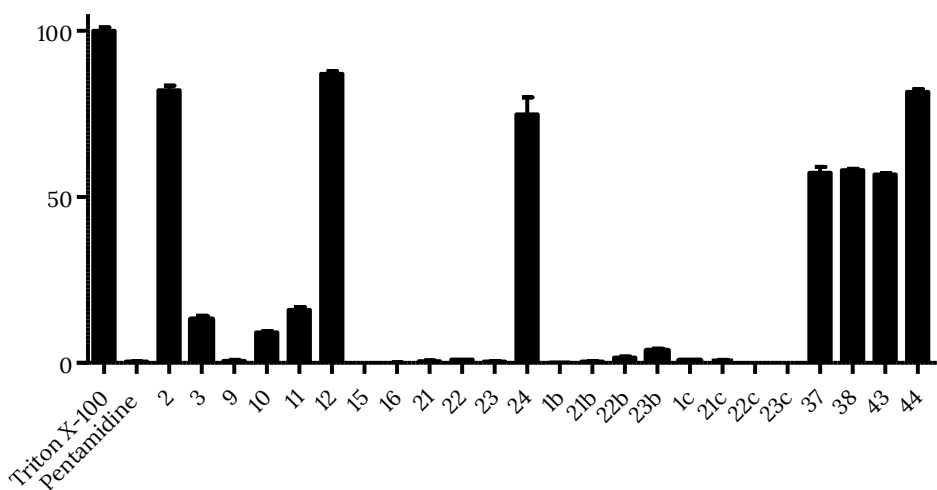
**Table S16.** Synergistic data of compounds **1**, **3**, **21**, **22**, **23b**, **37**, **38**, **43**, **44**, and PMBN of the checkerboard results for *P. aeruginosa* ATCC27853 with rifampicin as shown in Figure S16. All minimal inhibitory concentrations (MICs) and minimal synergistic concentrations (MSCs) are in µg/mL.

	Structures	MIC	MSC	MIC rif	MSC rif	FICI
<b>1</b>		>200	100	24	6	≤0.500
<b>3</b>		>200	25	24	1.5	≤0.125
<b>21</b>		>200	100	24	1.5	≤0.313
<b>22</b>		>200	50	>24	6	≤0.250
<b>23b</b>		>200	100	24	3	≤0.375
<b>37</b>		>200	25	24	0.38	≤0.078
<b>38</b>		100	25	24	6	0.500
<b>43</b>		200	6.25	24	1.5	0.094
<b>44</b>		100	6.25	24	0.75	0.094
<b>PMBN</b>		50	0.78	24	0.38	0.031

## Hemolysis assay

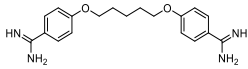
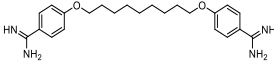
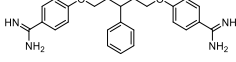
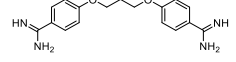
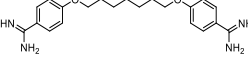
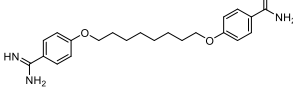
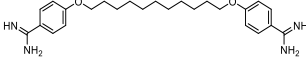
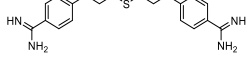
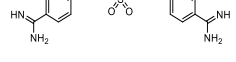
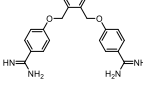
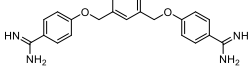
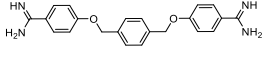
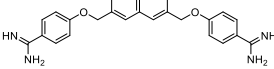
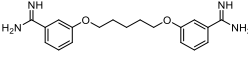
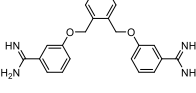


**Figure S17.** Hemolytic activity of all compounds (200  $\mu\text{g/mL}$ ) after 1 hour of incubation. The hemolysis assay was performed as described in materials and methods. Values below 10% were defined as non-hemolytic.<sup>76</sup> Error bars represent the standard deviation based on n=3 technical replicates.



**Figure S18.** Hemolytic activity of all compounds (200  $\mu\text{g/mL}$ ) after 20 hours of incubation. The hemolysis assay was performed as described in materials and methods. Values below 10% were defined as non-hemolytic.<sup>76</sup> Error bars represent the standard deviation based on n=3 technical replicates.

**Table S17.** Hemolytic activity of all compounds (200 µg/mL). The hemolysis assay was performed as described in materials and methods. Values <10% were defined as non-hemolytic.<sup>76</sup>

	Structures	Hemolysis 1 hour (%)	Hemolysis 20 hours (%)
1		4.0	0.4
2		9.7	82
3		0.5	13
9		0.4	0.6
10		0.3	9.2
11		0.0	16
12		8.5	87
15		0.2	0.0
16		0.2	0.1
21		1.7	0.5
22		0.9	11
23		0.2	0.4
24		2.6	75
1b		0.1	0.1
21b		0.1	0.4

<b>22b</b>		0.2	1.6
<b>23b</b>		0.0	3.7
<b>1c</b>		0.0	0.7
<b>21c</b>		0.0	0.4
<b>22c</b>		0.0	0.0
<b>23c</b>		0.0	0.0
<b>37</b>		0.6	57
<b>38</b>		32	58
<b>43</b>		12	57
<b>44</b>		30	82

### Outer membrane permeability assay

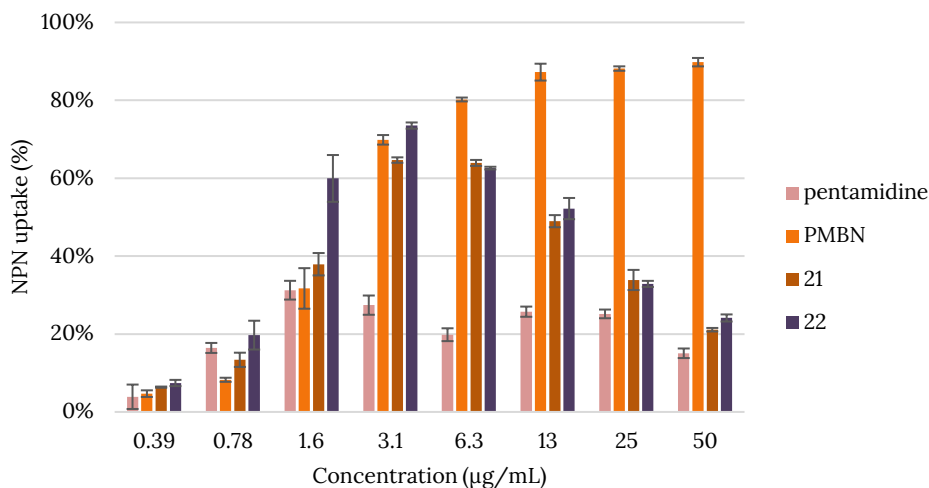


**Figure S19.** Outer membrane permeabilization assay of compounds **1**, **21**, **22**, and PMBN with *E. coli* BW25113 using N-phenyl-napthalen-1-amine (NPN) (at 0.01 mM) as fluorescent probe. The read-out was performed using a plate reader with  $\lambda_{\text{ex}}$  355 nm and  $\lambda_{\text{em}}$  420 nm. The NPN uptake values shown are relative to the uptake signal obtained upon treating the cells with 100 µg/mL colistin as previously reported.<sup>68</sup> Error bars represent the standard deviation based on n=3 technical replicates. Of note is the maximum NPN fluorescence measured for pentamidine and bis-amidines **21** and **22** at 3.1 µg/mL (0.01 mM). At higher bis-amidines concentrations, NPN fluorescence decreases, an effect not observed for PMBN.

## References

- (1) Amann, S.; Neef, K.; Kohl, S. Antimicrobial Resistance (AMR). *European Journal of Hospital Pharmacy* **2019**, 26 (3), 175–177. <https://doi.org/10.1136/ejpharm-2018-001820>.
- (2) UN Interagency Coordination Group on Antimicrobial Resistance. No Time to Wait: Securing the Future from Drug-Resistant Infections; Report to the Secretary-General of the United Nations. Geneva, WHO. **2019**. <https://www.who.int/antimicrobial-resistance/interagency-coordination-group/final-report/en/>.
- (3) WHO. Prioritization of pathogens to guide discovery, research and development of new antibiotics for drug-resistant bacterial infections including tuberculosis (WHO/EKP/IAU/2017.12), Geneva, WHO. **2017**
- (4) Macnair, C. R.; Brown, E. D. Outer Membrane Disruption Overcomes Intrinsic, Acquired, and Spontaneous Antibiotic Resistance. *mBio* **2020**, 11 (5), 1–15. <https://doi.org/10.1128/mBio.01615-20>.
- (5) Nikaido, H. The Role of Outer Membrane and Efflux Pumps in the Resistance of Gram-Negative Bacteria. Can We Improve Drug Access? *Drug Resistance Updates*. Churchill Livingstone January 1, 1998, pp 93–98. [https://doi.org/10.1016/S1368-7646\(98\)80023-X](https://doi.org/10.1016/S1368-7646(98)80023-X).
- (6) Vaara, M.; Vaara, T. Sensitization of Gram-Negative Bacteria to Antibiotics and Complement by a Nontoxic Oligopeptide. *Nature* **1983**, 303 (5917), 526–528. <https://doi.org/10.1038/303526a0>.
- (7) Stokes, J. M.; Macnair, C. R.; Ilyas, B.; French, S.; Côté, J. P.; Bouwman, C.; Farha, M. A.; Sieron, A. O.; Whitfield, C.; Coombes, B. K.; Brown, E. D. Pentamidine Sensitizes Gram-Negative Pathogens to Antibiotics and Overcomes Acquired Colistin Resistance. *Nature Microbiology* **2017**, 2. <https://doi.org/10.1038/nmicrobiol.2017.28>.
- (8) Stokes, J. M.; Davis, J. H.; Mangat, C. S.; Williamson, J. R.; Brown, E. D. Discovery of a Small Molecule That Inhibits Bacterial Ribosome Biogenesis. *eLife* **2014**, 3, e03574. <https://doi.org/10.7554/eLife.03574>.
- (9) Stokes, J. M.; French, S.; Ovchinnikova, O. G.; Bouwman, C.; Whitfield, C.; Brown, E. D. Cold Stress Makes Escherichia Coli Susceptible to Glycopeptide Antibiotics by Altering Outer Membrane Integrity. *Cell Chemical Biology* **2016**, 23 (2), 267–277. <https://doi.org/10.1016/j.chembiol.2015.12.011>.
- (10) Bean, D. C.; Wareham, D. W. Pentamidine: A Drug to Consider Re-Purposing in the Targeted Treatment of Multi-Drug Resistant Bacterial Infections? *Journal of Laboratory and Precision Medicine* **2017**, 2, 49–49. <https://doi.org/10.21037/jlpm.2017.06.18>.
- (11) Waller, D. G.; Sampson, A. P. Chemotherapy of Infections. In *Medical pharmacology and therapeutics*; Elsevier, 2018; pp 581–629. <https://doi.org/10.1016/B978-0-7020-7167-6.00051-8>.
- (12) Sands, M.; Kron, M. A.; Brown, R. B. Pentamidine: A Review. *Reviews of infectious diseases* **1985**, 7 (5), 625–634. <https://doi.org/10.1093/clinids/7.5.625>.
- (13) Goa, K. L.; Campoli-Richards, D. M. Pentamidine Isethionate: A Review of Its Antiprotozoal Activity, Pharmacokinetic Properties and Therapeutic Use in Pneumocystis Carinii Pneumonia. *Drugs* **1987**, 33 (3), 242–258. <https://doi.org/10.2165/00003495-198733030-00002>.
- (14) Libman, M. D.; Miller, M. A.; Richards, G. K. Antistaphylococcal Activity of Pentamidine. *Antimicrobial Agents and Chemotherapy* **1990**, 34 (9), 1795–1796. <https://doi.org/10.1128/AAC.34.9.1795>.
- (15) Maciejewska, D.; Zabiński, J.; Kaźmierczak, P.; Wójciuk, K.; Kruszewski, M.; Kruszewska, H. In Vitro Screening of Pentamidine Analogs against Bacterial and Fungal Strains. *Bioorganic and Medicinal Chemistry Letters* **2014**, 24 (13), 2918–2923. <https://doi.org/10.1016/j.bmcl.2014.04.075>.

- (16) Edwards, K. J.; Jenkins, T. C.; Neidle, S. Crystal Structure of a Pentamidine–Oligonucleotide Complex: Implications for DNA–Binding Properties. *Biochemistry* **1992**, 31 (31), 7104–7109. <https://doi.org/10.1021/bi00146a011>.
- (17) Sun, T.; Zhang, Y. Pentamidine Binds to tRNA through Non-Specific Hydrophobic Interactions and Inhibits Aminoacylation and Translation. *Nucleic Acids Research* **2008**, 36 (5), 1654–1664. <https://doi.org/10.1093/nar/gkm1180>.
- (18) Malkawi, R.; Iyer, A.; Parmar, A.; Lloyd, D. G.; Tze, E.; Goh, L.; Taylor, E. J.; Sarmad, S.; Maddar, A.; Lakshminarayanan, R.; Singh, I.; Yang, H.; Wierzbicki, M.; Bois, D. R. Du; Nowick, J. S.; Lee, H.; Song, W. Y.; Kim, M.; Lee, M. W.; Kim, S.; Park, Y. S.; Kwak, K.; Oh, M. H.; Kim, H. J.; Acedo, J. Z.; Chiorean, S.; Vederas, J. C.; Belkum, M. J. Van; Enterobacteriaceae, C.; Brennan-krohn, T.; Pironti, A.; Kirby, E.; Paracini, N.; Clifton, L. A.; Skoda, M. W. A.; Lakey, J. H.; Scherer, K. M.; Spille, J.; Sahl, H.; Grein, F.; Kubitscheck, U.; Brenna, E.; Cannavale, F.; Crotti, M.; Vitis, V. De; Gatti, F. G.; Migliazza, G.; Molinari, F.; Parmeggiani, F.; Romano, D.; Santangelo, S.; Cebrero-cangueiro, T.; Álvarez-marín, R.; Labrador-herrera, G.; Tomas, M.; Wiese, J.; Imhoff, J. F. Liquid Crystalline Bacterial Outer Membranes Are Critical for Antibiotic Susceptibility. *Biophysj* **2018**, 108 (August), 8–12. <https://doi.org/10.1002/ddr.21482>.
- (19) Cavalier, M. C.; Ansari, M. I.; Pierce, A. D.; Wilder, P. T.; McKnight, L. E.; Raman, E. P.; Neau, D. B.; Bezawada, P.; Alasady, M. J.; Charpentier, T. H.; Varney, K. M.; Toth, E. A.; MacKerell, A. D.; Coop, A.; Weber, D. J. Small Molecule Inhibitors of Ca<sup>2+</sup>-S100B Reveal Two Protein Conformations. *Journal of Medicinal Chemistry* **2016**, 59 (2), 592–608. <https://doi.org/10.1021/acs.jmedchem.5b01369>.
- (20) Lam, C.; Hildebrandt, J.; Schütze, E.; Wenzel, A. F. Membrane-Disorganizing Property of Polymyxin B Nonapeptide. *Journal of Antimicrobial Chemotherapy* **1986**, 18 (1), 9–15. <https://doi.org/10.1093/jac/18.1.9>.
- (21) Odds, F. C. Synergy, Antagonism, and What the Checkerboard Puts between Them. *Journal of Antimicrobial Chemotherapy* **2003**, 52 (1), 1–1. <https://doi.org/10.1093/jac/dkg301>.
- (22) Gromyko, A. V.; Popov, K. V.; Mosoleva, A. P.; Streltsov, S. A.; Grokhovsky, S. L.; Oleinikov, V. A.; Zhuze, A. L. DNA Sequence-Specific Ligands: XII. Synthesis and Cytological Studies of Dimeric Hoechst 33258 Molecules. *Russian Journal of Bioorganic Chemistry* **2005**, 31 (4), 344–351. <https://doi.org/10.1007/s11171-005-0047-z>.
- (23) Turner, A. D.; Pizzo, S. V.; Porter, N. A.; Rozakis, G. Photoreactivation of Irreversibly Inhibited Serine Proteinases. *Journal of the American Chemical Society* **1988**, 110 (1), 244–250. <https://doi.org/10.1021/ja00209a040>.
- (24) Tidwell, R. R.; Jones, S. K.; Geratz, J. D.; Ohemeng, K. A.; Cory, M.; Hall, J. E. Analogues of 1,5-Bis(4-Amidinophenoxy)Pentane (Pentamidine) in the Treatment of Experimental Pneumocystis Carinii Pneumonia. *Journal of Medicinal Chemistry* **1990**, 33 (4), 1252–1257. <https://doi.org/10.1021/jm00166a026>.
- (25) Stolić, I.; Avdičević, M.; Bregović, N.; Piantanida, I.; Glavaš-Obrovac, L.; Bajić, M. Synthesis, DNA Interactions and Anticancer Evaluation of Novel Diamidine Derivatives of 3,4-Ethylenedioxythiophene. *Croatica Chemica Acta* **2012**, 85 (4), 457–467. <https://doi.org/10.5562/cca2141>.
- (26) Ewins, A. J.; Barber, H. J.; Newbery, G.; Ashley, J. N.; Self, A. D. H. Verfahren Zur Herstellung von Diamidinderivaten. German patent DE 844897 C, 1952.
- (27) Roger, R.; Neilson, D. G. The Chemistry of Imidates. *Chemical Reviews* **2002**, 61 (2), 179–211. <https://doi.org/10.1021/CR60210A003>.
- (28) Bruncko, M.; McClellan, W. J.; Wendt, M. D.; Sauer, D. R.; Geyer, A.; Dalton, C. R.; Kaminski, M. A.; Weitzberg, M.; Gong, J.; Dellaria, J. F.; Mantel, R.; Zhao, X.; Nienaber, V. L.; Stewart, K.; Klinghofer, V.; Bouska, J.; Rockway, T. W.; Giranda, V. L. Naphthamidine Urokinase Plasminogen Activator Inhibitors with Improved Pharmacokinetic Properties. *Bioorganic*

- and *Medicinal Chemistry Letters* **2005**, 15 (1), 93–98. <https://doi.org/10.1016/j.bmcl.2004.10.026>.
- (29) Zhang, J.; Qian, K.; Yan, C.; He, M.; Jassim, B. A.; Ivanov, I.; Zheng, Y. G. Discovery of Decamidine as a New and Potent PRMT1 Inhibitor. *MedChemComm* **2017**, 8 (2), 440–444. <https://doi.org/10.1039/c6md00573j>.
- (30) Wendt, M. D.; Rockway, T. W.; Geyer, A.; McClellan, W.; Weitzberg, M.; Zhao, X.; Mantei, R.; Nienaber, V. L.; Stewart, K.; Klinghofer, V.; Giranda, V. L. Identification of Novel Binding Interactions in the Development of Potent, Selective 2-Naphthamidine Inhibitors of Urokinase. Synthesis, Structural Analysis, and SAR of N-Phenyl Amide 6-Substitution. *Journal of Medicinal Chemistry* **2004**, 47 (2), 303–324. <https://doi.org/10.1021/jm0300072>.
- (31) Abou-Elkhair, R. A. I.; Hassan, A. E. A.; Boykin, D. W.; Wilson, W. D. Lithium Hexamethyldisilazane Transformation of Transiently Protected 4-Aza/Benzimidazole Nitriles to Amidines and Their Dimethyl Sulfoxide Mediated Imidazole Ring Formation. *Organic Letters* **2016**, 18 (18), 4714–4717. <https://doi.org/10.1021/acs.orglett.6b02359>.
- (32) Maciejewska, D.; Zabinski, J.; Kaźmierczak, P.; Rezler, M.; Krassowska-Świebocka, B.; Collins, M. S.; Cushion, M. T. Analogs of Pentamidine as Potential Anti-Pneumocystis Chemotherapeutics. *European Journal of Medicinal Chemistry* **2012**, 48, 164–173. <https://doi.org/10.1016/j.ejmech.2011.12.010>.
- (33) Amin, K.; Dannenfelser, R.-M. In Vitro Hemolysis: Guidance for the Pharmaceutical Scientist. *Journal of Pharmaceutical Sciences* **2006**, 95 (6), 1173–1176. <https://doi.org/10.1002/JPS.20627>.
- (34) Wang, B.; Boykin, D.; Choudhary, M.; Kumar, A.; Yu, B.; Zhu, M. Amidines and Amidine Analogs for the Treatment of Bacterial Infections and Potentiation Antibiotics. World patent WO 2019/241566 A1, 2019.
- (35) Geratz, J. D.; Cheng, M. C. F.; Tidwell, R. R. Novel Bis(Benzamidino) Compounds with an Aromatic Central Link. Inhibitors of Thrombin, Pancreatic Kallikrein, Trypsin, and Complement. *Journal of Medicinal Chemistry* **1976**, 19 (5), 634–639. <https://doi.org/10.1021/jm00227a011>.
- (36) Vanden Eynde, J. J.; Mayence, A.; Huang, T. L.; Collins, M. S.; Rebholz, S.; Walzer, P. D.; Cushion, M. T. Novel Bisbenzamidines as Potential Drug Candidates for the Treatment of Pneumocystis Carinii Pneumonia. *Bioorganic and Medicinal Chemistry Letters* **2004**, 14 (17), 4545–4548. <https://doi.org/10.1016/j.bmcl.2004.06.034>.
- (37) Chauhan, P. M. S.; Niyer, R.; Bhakuni, D. S.; Shankhdhar, V.; Guru, P. Y.; Sen, A. B. Antiparasitic Agents: Part VI - Synthesis of 1,2-, 1,3- and 1,4-Bis(4-Substituted Aryloxy)Benzenes and Their Biological Activities. *Indian Journal of Chemistry - Section B Organic and Medicinal Chemistry* **1988**, 27 (1–12), 38–42.
- (38) Patrick, D. A.; Bakunov, S. A.; Bakunova, S. M.; Suresh Kumar, E. V. K.; Chen, H.; Jones, S. K.; Wenzler, T.; Barzecz, T.; Werbovetz, K. A.; Brun, R.; Tidwell, R. R. Synthesis and Antiprotozoal Activities of Dicationic Bis(Phenoxymethyl)Benzenes, Bis(Phenoxymethyl)Naphthalenes, and Bis(Benzyloxy)Naphthalenes. *European Journal of Medicinal Chemistry* **2009**, 44 (9), 3543–3551. <https://doi.org/10.1016/j.ejmech.2009.03.014>.
- (39) Bakunova, S. M.; Bakunov, S. A.; Patrick, D. A.; Kumar, E. V. K. S.; Ohemeng, K. A.; Bridges, A. S.; Wenzler, T.; Barszcz, T.; Jones, S. K.; Werbovetz, K. A.; Brun, R.; Tidwell, R. R. Structure-Activity Study of Pentamidine Analogues as Antiprotozoal Agents. *Journal of medicinal chemistry* **2009**, 52 (7), 2016–2035. <https://doi.org/10.1021/jm801547t>.
- (40) Ashley, J. N.; Barber, H. J.; Ewins, A. J.; Newbery, G.; Self, A. D. H. A Chemotherapeutic Comparison of the Trypanocidal Action of Some Aromatic Diamidines. *Journal of the Chemical Society (Resumed)* **1942**, No. 0, 103–116. <https://doi.org/10.1039/jr9420000103>.
- (41) Hamano, S.; Kanazawa, T.; Kitamura, S.-I. Bis-(Meta-Amidinophenoxy)-Compounds and Pharmacologically Acceptable Acid Addition Salts Thereof. U.S. patent US 4034010 A, 1977.



- (42) Goswami, R.; Mukherjee, S.; Wohlfahrt, G.; Ghadiyaram, C.; Nagaraj, J.; Chandra, B. R.; Sistla, R. K.; Satyam, L. K.; Samiulla, D. S.; Moilanen, A.; Subramanya, H. S.; Ramachandra, M. Discovery of Pyridyl Bis(Oxy)Dibenzimidamide Derivatives as Selective Matriptase Inhibitors. *ACS Medicinal Chemistry Letters* **2013**, 4 (12), 1152–1157. <https://doi.org/10.1021/ml400213v>.
- (43) Cavallo, G.; Metrangolo, P.; Milani, R.; Pilati, T.; Priimagi, A.; Resnati, G.; Terraneo, G. The Halogen Bond. *Chemical Reviews* **2016**, 116 (4), 2478–2601. <https://doi.org/10.1021/acs.chemrev.5b00484>.
- (44) Kong, N.; Liu, E. A.; Vu, B. T. Cis-Imidazolines. U.S. patent US 6617346 B1, 2003.
- (45) Huang, H.; Li, H.; Martásek, P.; Roman, L. J.; Poulos, T. L.; Silverman, R. B. Structure-Guided Design of Selective Inhibitors of Neuronal Nitric Oxide Synthase. *Journal of Medicinal Chemistry* **2013**, 56 (7), 3024–3032. <https://doi.org/10.1021/jm4000984>.
- (46) Suzuki, A. Organoborane Coupling Reactions (Suzuki Coupling). *Proceedings of the Japan Academy. Series B, Physical and Biological Sciences* **2004**, 80 (8), 359.
- (47) Martino, G.; Muzio, L.; Riva, N.; Gornati, D.; Seneci, P.; Eleuteri, S. Aminoguanidine Hydrazones as Retromer Stabilizers Useful for Treating Neurological Diseases. World patent WO 2020/201326 A1, 2020.
- (48) Innocenti, P.; Woodward, H.; O'Fee, L.; Hoelder, S. Expanding the Scope of Fused Pyrimidines as Kinase Inhibitor Scaffolds: Synthesis and Modification of Pyrido[3,4-d]Pyrimidines. *Organic & Biomolecular Chemistry* **2014**, 13 (3), 893–904. <https://doi.org/10.1039/C4OB02238F>.
- (49) García, D.; Foubelo, F.; Yus, M. Selective Lithiation of 4- and 5-Halophthalans. *Heterocycles* **2009**, 77 (2), 991–1005. [https://doi.org/10.3987/COM-08-S\(F\)85](https://doi.org/10.3987/COM-08-S(F)85).
- (50) Washington, J. A.; Wilson, W. R. Erythromycin: A Microbial and Clinical Perspective after 30 Years of Clinical Use (First of Two Parts). *Mayo Clinic Proceedings* **1985**, 60 (3), 189–203. [https://doi.org/10.1016/S0025-6196\(12\)60219-5](https://doi.org/10.1016/S0025-6196(12)60219-5).
- (51) Washington, J. A.; Wilson, W. R. Erythromycin: A Microbial and Clinical Perspective after 30 Years of Clinical Use (Second of Two Parts). *Mayo Clinic Proceedings* **1985**, 60 (4), 271–278. [https://doi.org/10.1016/S0025-6196\(12\)60322-X](https://doi.org/10.1016/S0025-6196(12)60322-X).
- (52) Farr, B.; Mandell, G. L. Rifampin. *Medical Clinics of North America* **1982**, 66 (1), 157–168. [https://doi.org/10.1016/S0025-7125\(16\)31449-3](https://doi.org/10.1016/S0025-7125(16)31449-3).
- (53) Levine, J. F. Vancomycin: A Review. *Medical Clinics of North America* **1987**, 71 (6), 1135–1145. [https://doi.org/10.1016/S0025-7125\(16\)30801-X](https://doi.org/10.1016/S0025-7125(16)30801-X).
- (54) Kirby, W. M. M.; Hudson, D. G.; Noyes, W. D. Clinical and Laboratory Studies of Novobiocin, a New Antibiotic. *A.M.A. Archives of Internal Medicine* **1956**, 98 (1), 1–7. <https://doi.org/10.1001/ARCHINTE.1956.00250250007001>.
- (55) Drugs@FDA: FDA-Approved Drugs. <https://www.accessdata.fda.gov/scripts/cder/daf/index.cfm?event=overview.process&ApplNo=050339> (accessed 2021-07-08).
- (56) Wesseling, C. M. J.; Wood, T. M.; Slingerland, C. J.; Bertheussen, K.; Lok, S.; Martin, N. I. Thrombin-Derived Peptides Potentiate the Activity of Gram-Positive-Specific Antibiotics against Gram-Negative Bacteria. *Molecules* **2021**, 26 (7), 1954. <https://doi.org/10.3390/molecules26071954>.
- (57) Thornsberry, C.; Hill, B. C.; Swenson, J. M.; McDougal, L. K. Rifampin: Spectrum of Antibacterial Activity. *Reviews of Infectious Diseases* **1983**, 5 (Supplement\_3), S412–S417. [https://doi.org/10.1093/CLINIDS/5.SUPPLEMENT\\_3.S412](https://doi.org/10.1093/CLINIDS/5.SUPPLEMENT_3.S412).
- (58) Ebbensgaard, A.; Mordhorst, H.; Aarestrup, F. M.; Hansen, E. B. The Role of Outer Membrane Proteins and Lipopolysaccharides for the Sensitivity of Escherichia Coli to Antimicrobial Peptides. *Frontiers in Microbiology* **2018**, 9 (SEP), 2153. <https://doi.org/10.3389/fmicb.2018.02153>.

- (59) Uchida, K.; Mizushima, S. A Simple Method for Isolation of Lipopolysaccharides from *Pseudomonas Aeruginosa* and Some Other Bacterial Strains. *Agricultural and Biological Chemistry* **1987**, 51 (11), 3107–3114. <https://doi.org/10.1080/00021369.1987.10868532>.
- (60) Furevi, A.; Stähle, J.; Muheim, C.; Gkatzis, S.; Udekwu, K. I.; Daley, D. O.; Widmalm, G. Structural Analysis of the O-Antigen Polysaccharide from *Escherichia Coli* O188. *Carbohydrate Research* **2020**, 498 (2020), 108051. <https://doi.org/10.1016/j.carres.2020.108051>.
- (61) Wang, Z.; Wang, J.; Ren, G.; Li, Y.; Wang, X. Influence of Core Oligosaccharide of Lipopolysaccharide to Outer Membrane Behavior of *Escherichia Coli*. *Marine Drugs* **2015**, 13 (6), 3325–3339. <https://doi.org/10.3390/md13063325>.
- (62) Doorduyn, D. J.; Heesterbeek, D. A. C.; Ruyken, M.; Haas, C. J. C. de; Stapels, D. A. C.; Aerts, P. C.; Rooijackers, S. H. M.; Bardoel, B. W. Polymerization of C9 Enhances Bacterial Cell Envelope Damage and Killing by Membrane Attack Complex Pores. *bioRxiv* **2021**, Epub, May 12, 2021. <https://doi.org/10.1101/2021.05.12.443779>.
- (63) Cox, G.; Sieron, A.; King, A. M.; De Pascale, G.; Pawlowski, A. C.; Koteva, K.; Wright, G. D. A Common Platform for Antibiotic Dereplication and Adjuvant Discovery. *Cell chemical biology* **2017**, 24 (1), 98–109. <https://doi.org/10.1016/J.CHEMBIOL.2016.11.011>.
- (64) Liu, Y. Y.; Wang, Y.; Walsh, T. R.; Yi, L. X.; Zhang, R.; Spencer, J.; Doi, Y.; Tian, G.; Dong, B.; Huang, X.; Yu, L. F.; Gu, D.; Ren, H.; Chen, X.; Lv, L.; He, D.; Zhou, H.; Liang, Z.; Liu, J. H.; Shen, J. Emergence of Plasmid-Mediated Colistin Resistance Mechanism MCR-1 in Animals and Human Beings in China: A Microbiological and Molecular Biological Study. *The Lancet Infectious Diseases* **2016**, 16 (2), 161–168. [https://doi.org/10.1016/S1473-3099\(15\)00424-7](https://doi.org/10.1016/S1473-3099(15)00424-7).
- (65) Nang, S. C.; Li, J.; Velkov, T. The Rise and Spread of Mcr Plasmid-Mediated Polymyxin Resistance. *Critical Reviews in Microbiology* **2019**, 45 (2), 131–161. <https://doi.org/10.1080/1040841X.2018.1492902>.
- (66) Vuorio, R.; Vaara, M. The Lipid A Biosynthesis Mutation LpxA2 of *Escherichia Coli* Results in Drastic Antibiotic Supersusceptibility. *Antimicrobial Agents and Chemotherapy* **1992**, 36 (4), 826–829. <https://doi.org/10.1128/AAC.36.4.826>.
- (67) Helander, I. M.; Mattila-Sandholm, T. Fluorometric Assessment of Gram-Negative Bacterial Permeabilization. *Journal of Applied Microbiology* **2000**, 88 (2), 213–219. <https://doi.org/10.1046/j.1365-2672.2000.00971.x>.
- (68) MacNair, C. R.; Stokes, J. M.; Carfrae, L. A.; Fiebig-Comyn, A. A.; Coombes, B. K.; Mulvey, M. R.; Brown, E. D. Overcoming Mcr-1 Mediated Colistin Resistance with Colistin in Combination with Other Antibiotics. *Nature Communications* **2018**, 9 (2018), 458. <https://doi.org/10.1038/s41467-018-02875-z>.
- (69) Li, X.; Sun, C. L. Piperidine and Piperazine Derivatives. World patent WO 2007/089462 A2, 2007.
- (70) Suzuki, N.; Kishimoto, K.; Yamazaki, K.; Kumamoto, T.; Ishikawa, T.; Margetić, D. Immobilized 1,2-Bis(Guanidinoalkyl)Benzenes: Potentially Useful for the Purification of Arsenic-Polluted Water. *Synlett* **2013**, 24 (19), 2510–2514. <https://doi.org/10.1055/S-0033-1338980>.
- (71) Berglund, A. J.; Bodner, M. J. Aryl Diamidines and Prodrugs Thereof for Treating Myotonic Dystrophy. U.S. patent US 2013/0281462 A1, 2013.
- (72) Lewis, J. E. M. Self-Templated Synthesis of Amide Catenanes and Formation of a Catenane Coordination Polymer. *Organic & Biomolecular Chemistry* **2019**, 17 (9), 2442–2447. <https://doi.org/10.1039/C9OB00107G>.
- (73) Akhtar, W. M.; Armstrong, R. J.; Frost, J. R.; Stevenson, N. G.; Donohoe, T. J. Stereoselective Synthesis of Cyclohexanes via an Iridium Catalyzed (5 + 1) Annulation Strategy. *Journal of the American Chemical Society* **2018**, 140 (38), 11916–11920. <https://doi.org/10.1021/jacs.8b07776>.

- (74) López-Cortina, S.; Medina-Arreguin, A.; Hernández-Fernández, E.; Berns, S.; Guerrero-Alvarez, J.; Ordoñez, M.; Fernández-Zertuche, M. Stereochemistry of Base-Induced Cleavage of Methoxide Ion on Cis- and Trans-1,4-Diphenylphosphorinanium Salts. A Different Behavior with a Phenyl Substituent. *Tetrahedron* **2010**, 66 (32), 6188–6194. <https://doi.org/10.1016/J.TET.2010.05.095>.
- (75) Wang, J.; Chou, S.; Xu, L.; Zhu, X.; Dong, N.; Shan, A.; Chen, Z. High Specific Selectivity and Membrane-Active Mechanism of the Synthetic Centrosymmetric  $\alpha$ -Helical Peptides with Gly-Gly Pairs. *Scientific Reports* **2015**, 5 (April), 1–19. <https://doi.org/10.1038/srep15963>.
- (76) Amin, K., Dannenfelser, R.-M. In vitro hemolysis: Guidance for the pharmaceutical scientist. *J. Pharm. Sci.* **2006**, 5 (6), 1173–1176. DOI: 10.1002/JPS.20627.





## Chapter 3

# Thrombin-derived peptides potentiate the activity of Gram-positive specific antibiotics against Gram-negative bacteria

Charlotte M. J. Wesseling,<sup>‡</sup> Thomas M. Wood,<sup>‡</sup> Cornelis J. Slingerland, Kristine Bertheussen, Samantha Lok, and Nathaniel I. Martin

<sup>‡</sup>These authors contributed equally to this work

Parts of this chapter have been published: *Molecules*. **2021**, 26 (7), 1954.

### Abstract

The continued rise of antibiotic resistance threatens to undermine the utility of the world's current antibiotic arsenal. This problem is particularly troubling when it comes to Gram-negative pathogens for which there are inherently fewer antibiotics available. To address this challenge, recent attention has been focused on finding compounds capable of disrupting the Gram-negative outer membrane as a means of potentiating otherwise Gram-positive-specific antibiotics. In this regard, agents capable of binding to the lipopolysaccharide (LPS) present in the Gram-negative outer membrane are of particular interest as synergists. Recently, thrombin-derived C-terminal peptides (TCPs) were reported to exhibit unique LPS-binding properties. We here describe investigations establishing the capacity of TCPs to act as synergists with the antibiotics erythromycin, rifampicin, novobiocin, and vancomycin against multiple Gram-negative strains including polymyxin-resistant clinical isolates. We further assessed the structural features most important for the observed synergy and characterized the outer membrane permeabilizing activity of the most potent synergists. Our investigations highlight the potential for such peptides in expanding the therapeutic range of antibiotics typically only used to treat Gram-positive infections.

# 1. Introduction

The rising tide of antibiotic resistance presents a clear threat to global health. This threat, coupled with the well-documented dearth of new antibiotics in the development pipeline, means that resistant pathogens are even more problematic.<sup>1</sup> Based on current trends, the World Health Organization (WHO) predicts that infections due to resistant bacteria will be the leading cause of death globally by 2050.<sup>2</sup> The WHO recently published its updated “pathogen threat list” of which three drug-resistant Gram-negative species were assigned top priority: carbapenem-resistant *Acinetobacter baumannii*, *Pseudomonas aeruginosa*, and *Enterobacteriaceae*.<sup>3</sup> The emergence and proliferation of such resistant Gram-negative pathogens is concerning given the limited number of viable treatment options available.<sup>3</sup>

It is well established that compared to Gram-positive pathogens, Gram-negative bacteria are more difficult to kill with antibiotics due to the presence of an additional barrier: the outer membrane (OM).<sup>4,5</sup> The OM protects Gram-negative bacteria from a large number of antibiotics that are used clinically to treat infections with Gram-positive bacteria.<sup>4</sup> Disruption of the OM has been widely investigated and in some cases proven to be an effective method to enable such antibiotics to function against Gram-negative bacteria.<sup>6–10</sup> In this regard, combinations of a membrane disruptor such as the well-studied polymyxin B nonapeptide (PMBN, Figure 1) along with macrolides or rifamycin-type antibiotics represent classic examples of such synergistic activity: the use of a combination leads to better results than a sum of each of the separate components.<sup>6,7,11–14</sup> Notably, the polymyxin derivative SPR741 (Figure 1), a selective OM disruptor developed by Spero Therapeutics, recently passed Phase I clinical trials.<sup>13,15,16</sup>

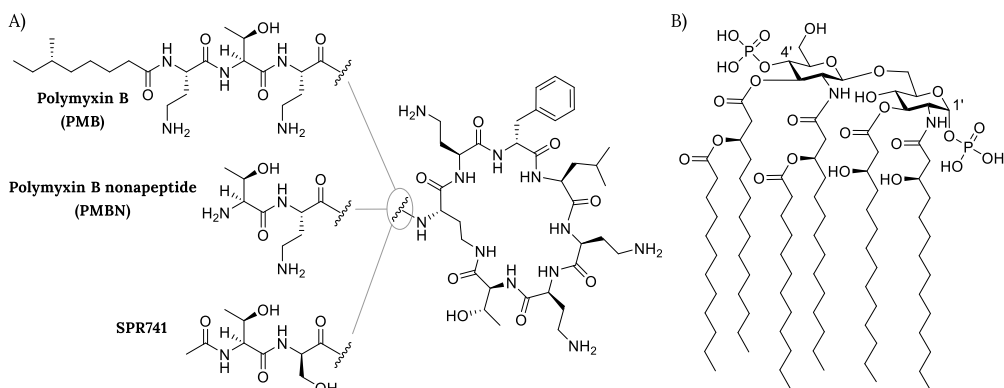


**Figure 1.** Structures of: A) polymyxin B (PMB), polymyxin B nonapeptide (PMBN), and SPR741; B) Lipid A component of the Gram-negative lipopolysaccharide (LPS).

Like its parent polymyxin B (Figure 1), SPR741 targets the bacterial lipopolysaccharide (LPS), a major component on the OM outer leaflet.<sup>4,14,17</sup> The core of LPS consists of Lipid A, a heavily lipidated disaccharide bearing phosphate groups at the 1' and

4' positions (Figure 1).<sup>4</sup> Small cations such as  $Mg^{2+}$  and  $Ca^{2+}$  bridge the negative charges of the phosphate groups and in doing so contribute to the tight packing of LPS.<sup>4,6</sup> It is generally held that highly positively charged compounds such as PMBN bind the negatively charged LPS with high affinity and in doing so interfere with LPS packing, leading to OM permeabilization.<sup>7,18–21</sup>

Compounds that bind to LPS with high affinity are also often referred to as endotoxin neutralizing compounds. Such compounds can demonstrate beneficial effects in reducing the inflammatory responses associated with systemic LPS exposure as in the case of sepsis.<sup>22–25</sup> In recent years, an increasing number of reports have appeared describing the synergistic effects of various positively charged small molecules and peptide-based compounds that interact with LPS.<sup>24–33</sup>

Given the apparent link between LPS binding, OM permeabilization, and antibiotic potentiation, we set out to identify literature compounds described as having affinity for LPS that had not yet been evaluated for synergy with Gram-positive specific antibiotics. This led us to the family of thrombin-derived C-terminal peptides (TCPs) reported by Schmidtchen and coworkers. In 2010, the Schmidtchen group first reported that peptide fragments from the C-terminus of thrombin, a key enzyme in the coagulation cascade, exhibit activity as host-defense peptides.<sup>34</sup> Subsequent structure activity studies by the same group identified peptide sequences with optimal antibacterial activity and recent NMR studies have elucidated the structural basis for their interaction with LPS.<sup>26,35,36</sup>

In the present study we set out to assess the potential for TCPs to potentiate the anti-Gram-negative activity of otherwise inactive Gram-positive specific antibiotics. To do so, synergy assays were first conducted using the TCPs described in the literature in combination with various antibiotics. Our initial studies revealed that, as we had hypothesized, the TCPs do indeed exhibit synergy. Building from these results we then prepared a number of new peptide analogues to assess the structural elements most important for synergy. Notably, we found that synergistic activity does not necessarily directly correlate with the inherent antibacterial activity of these peptides. We here report several new peptides inspired by thrombin-derived C-terminal peptides that display enhanced synergistic effects and reduced hemolytic activity.

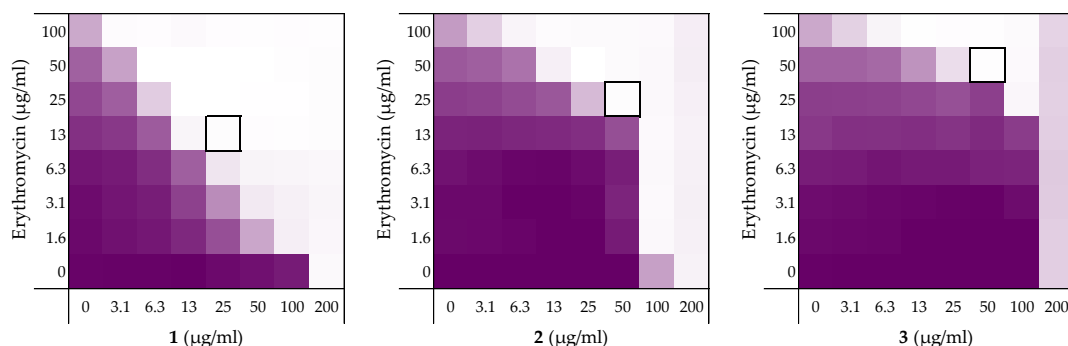


## 2. Results

### 2.1. Synergy with thrombin-derived C-terminal peptides

To begin, we selected four peptides previously described by the Schmidtchen group as LPS-binding.<sup>26</sup> The sequences of these peptides (**1–4**) are provided in Table 1 and range in length from 12 to 25 amino acids. Common to all four is the core sequence previously reported to be responsible for LPS binding.<sup>26</sup> The peptides were readily synthesized using solid-phase peptide synthesis (SPPS) and screened for synergistic activity using checkerboard assays. Synergy was initially assessed in combination with erythromycin (Figure 2, also see Supplementary data, Figure S1) and rifampicin (See Supplementary data, Figure S2) in Lysogeny Broth (LB) using *Escherichia coli* BW25113 as the indicator strain. Synergy is quantified by means of the fractional inhibitory concentration index (FICI) where an FICI of  $\leq 0.5$  is defined as synergistic and the lower the value, the more synergistic the combination.<sup>37</sup>

Prior to assessing synergy, the minimum inhibitory concentrations (MICs) of the peptides themselves were measured revealing that they exhibit little-to-no inherent activity with MICs equal to, or above, the maximum 200  $\mu\text{g/mL}$  concentration tested. The MICs of the companion antibiotics erythromycin and rifampicin were measured to be 100–200  $\mu\text{g/mL}$  and 8  $\mu\text{g/mL}$ , respectively (see Supplementary data, Tables S1 and S2). Using these parameters checkerboard assays were performed as illustrated in Figure 2. The results of the checkerboard assays performed with peptides **1–4** reveal clear differences in their synergistic potential. While the shortest peptide **1** exhibits potent synergy with erythromycin, the longer peptides **2–4** demonstrate comparatively little or no synergy (Table 1). In combination with rifampicin, peptides **1–4** all showed some synergistic activity with FICIs ranging from 0.094 to 0.313, but with peptide **1** again displaying the most potent synergy (see Supplementary data, Table S2). These preliminary findings served to validate our hypothesis that LPS-binding peptides derived from thrombin have the capacity to synergize with Gram-positive specific antibiotics. All peptides were also screened for hemolytic activity which revealed a clear trend: while the shorter peptides **1** and **2** showed no appreciable hemolytic activity, the longer peptide **3** and **4** were highly hemolytic (Table 1). This hemolysis data, combined with the synergistic activity observed, led us to select peptide **1** for further investigation.



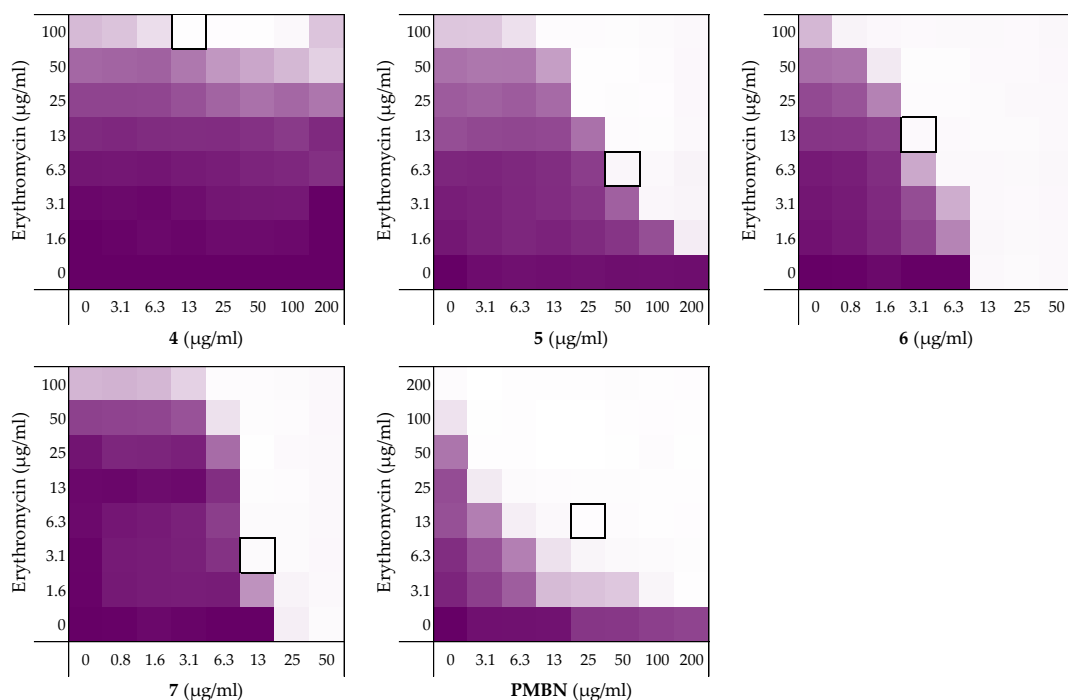


**Figure 2.** Checkerboard assays of the peptides **1-7** and PMBN in combination with erythromycin versus *E. coli* BW25113. In each case the bounded box in the checkerboard assays indicates the combination of peptide and antibiotic resulting in the lowest FICI (see Table 1). OD<sub>600</sub> values were measured using a plate reader and transformed to a gradient: purple represents growth, white represents no growth. An overview of all checkerboard assays with erythromycin can be found in the Supplementary data, Figure S1.

**Table 1.** Overview of the TCPs peptide sequence, synergistic and hemolytic activity.

	Peptide sequence	MIC	MSC <sub>peptide</sub>	FICI	Hemolysis <sup>b</sup>
<b>1</b>	H <sub>2</sub> N-VFRLKKWIQKVI-OH	200	25	0.188	0%
<b>2</b>	H <sub>2</sub> N-HVFRLKKWIQKVIDQFGE-OH	200	50	0.375	9%
<b>3</b>	H <sub>2</sub> N-FYTHVFRLKKWIQKVIDQFGE-OH	200	50	0.500	43%
<b>4</b>	H <sub>2</sub> N-GKYGFYTHVFRLKKWIQKVIDQFGE-OH	>200	12.5	>0.5 <sup>a</sup>	70%
<b>5</b>	Ac-VFRLKKWIQKVI-OH	>200	50	0.156	0%
<b>6</b>	H <sub>2</sub> N-VFRLKKWIQKVI-NH <sub>2</sub>	12.5	3.13	0.313	4%
<b>7</b>	Ac-VFRLKKWIQKVI-NH <sub>2</sub>	50	12.5	0.266	5%
<b>PMBN</b>		>200	25	0.125	-

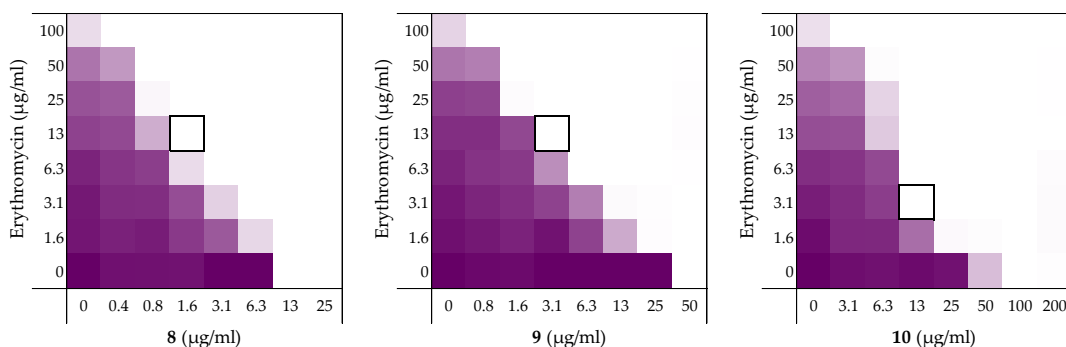
<sup>a</sup>Synergy defined as an FICI ≤ 0.5<sup>37</sup>; <sup>b</sup>Hemolysis was determined after a 20 hour incubation of the compounds (200 µg/ml) with defibrinated sheep blood (see Supplementary data, Figure S4 and Table S4).

Building on these findings and with peptide **1** as our lead synergist, we next explored the impact of changes to the N- and C-termini of the peptide. To this end,

peptides **5–7** were prepared to examine the impact of N-terminal acetylation and/or C-terminal amidation. N-terminal acetylation alone as in peptide **5** was found to have minimal effect on the inherent activity or synergistic potential of the peptide. By comparison, C-terminal amidation as in peptides **6** and **7** led to a significant increase in the inherent antibacterial activity with little impact on hemolytic activity. The reduced MIC values thus achieved, particularly notable for peptide **6**, provides a key advantage in that a lower concentration of peptide is required to achieve synergy: peptide **6** has a minimum synergistic concentration (MSC) of 3.125  $\mu\text{g}/\text{mL}$  versus 25  $\mu\text{g}/\text{mL}$  of its parent peptide **1** (Table 1). To assess whether peptide **6** employs an LPS mediated mechanism of action similar to peptide **1**, an LPS competition assay was also performed. Notably, the MIC of peptide **6** was found to increase from 12.5  $\mu\text{g}/\text{mL}$  to 200  $\mu\text{g}/\text{mL}$  in the presence of 1 mg/mL of LPS (See Supplementary data, Figure S4 and Table S4). This finding indicates that the antimicrobial activity of peptide **6** relies on LPS binding. Based on its enhanced activity and confirmed LPS-dependent mechanism, we next took peptide **6** forward for additional structure-activity studies by means of an alanine scan.

## 2.2. Alanine scan of peptide 6

To assess the role of the individual amino acids in peptide **6** and their specific contribution to both the inherent activity and synergistic activity of the peptide, an alanine scan was performed. Like the parent peptide, peptides **8–19** (Table 2) were synthesized as the C-terminus amides using microwave-assisted automated SPPS. As summarized in Table 2, the MICs of the alanine scan peptides ranged from 12.5  $\mu\text{g}/\text{mL}$ , as for peptide **6**, to above the maximum concentration tested of 200  $\mu\text{g}/\text{mL}$ . After establishing the individual MICs for peptides **8–19**, checkerboard assays were performed as shown in Figure 3. The FICI values thus obtained clearly show that the alanine exchange introduced in peptides **12**, **13**, and **17** leads to a complete loss of synergistic activity. Notably, the common feature in these three peptides is the replacement of a lysine residue with alanine. Moreover, while no longer synergistic with erythromycin, these peptides still have a relatively low MIC of 25  $\mu\text{g}/\text{mL}$ . Hemolysis data offers insight into this trend: the K $\Delta$ A peptides **12**, **13**, and **17** are all hemolytic, which suggests a nonselective membrane disruption mode of action. By comparison, none of the other alanine scan peptides show appreciable hemolytic activity (Table 2).



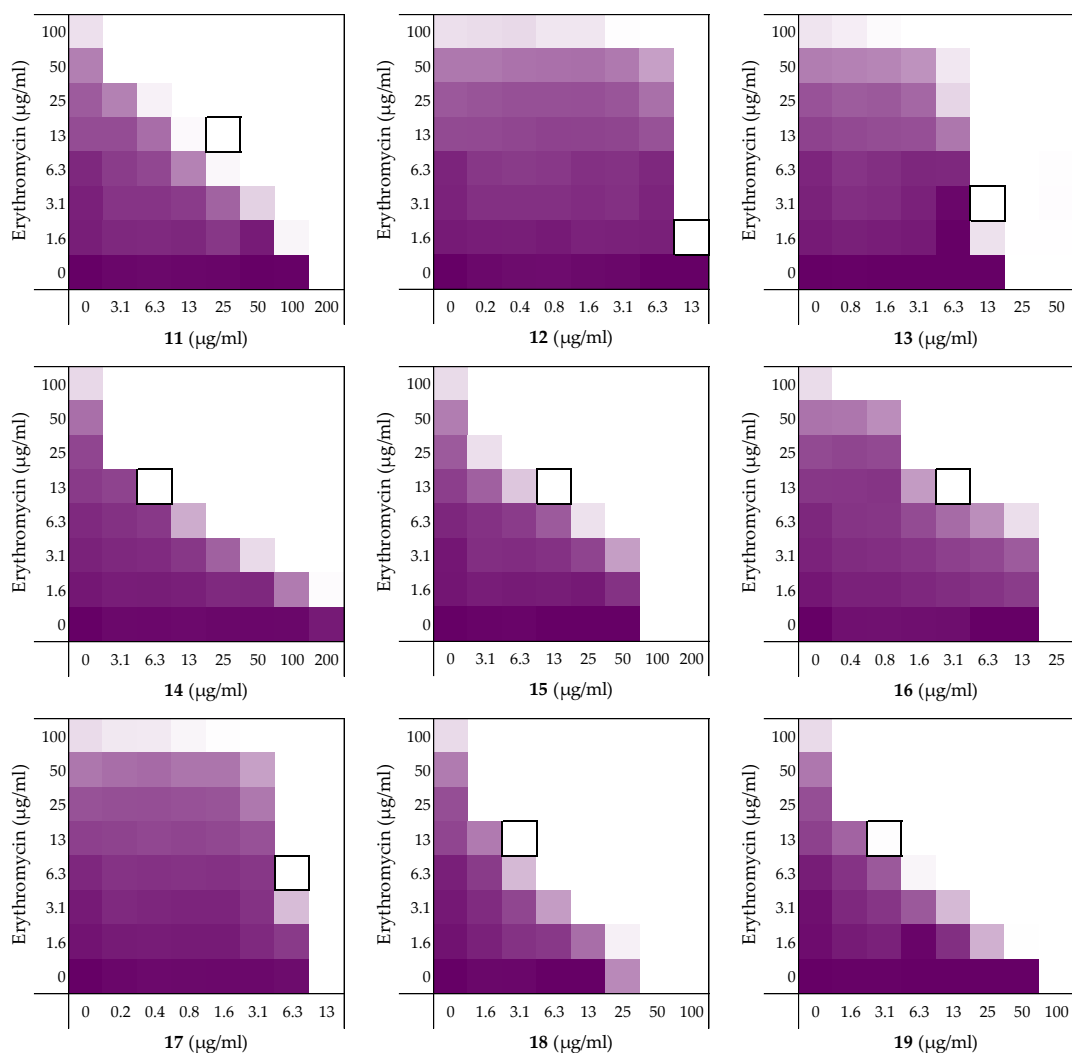


**Figure 3.** Checkerboard assays of the Ala-scan peptides **8-19** in combination with erythromycin versus *E. coli* BW25113. In each case the bounded box in the checkerboard assays indicates the combination of peptide and antibiotic resulting in the lowest FICI (see Table 2). OD<sub>600</sub> values were measured using a plate reader and transformed to a gradient: purple represents growth, white represents no growth. An overview of all checkerboard assays with erythromycin can be found in the Supplementary data, Figure S1.

Somewhat surprisingly, all of the other peptides prepared in the alanine scan study were found to exhibit more potent synergistic activity than peptide **6**. Notably, these peptides all exhibit synergy at concentrations lower than required for PMBN (see Table 1 and Table 2). In addition, an apparent trend emerges from the alanine scan data where decreased antimicrobial activity is inversely proportional to the synergistic activity of the peptides.

**Table 2.** Overview of the Ala-scan peptide sequences, antimicrobial, synergistic and hemolytic activity. MIC and FICI values were obtained from the checkerboard assay shown in Figure 3.

	Peptide sequence	MIC <sup>a</sup>	FICI	Hemolysis <sup>c</sup>
<b>6</b>	H <sub>2</sub> N-VFRLKKWIQKVI-NH <sub>2</sub>	12.5	0.313	4%
<b>8</b>	H <sub>2</sub> N- <b>A</b> FRLKKWIQKVI-NH <sub>2</sub>	12.5	0.188	2%
<b>9</b>	H <sub>2</sub> N-V <b>A</b> RLKKWIQKVI-NH <sub>2</sub>	50	0.125	0%
<b>10</b>	H <sub>2</sub> N-VF <b>A</b> LKKWIQKVI-NH <sub>2</sub>	100	0.141	4%
<b>11</b>	H <sub>2</sub> N-VFF <b>A</b> KKWIQKVI-NH <sub>2</sub>	200	0.188	1%
<b>12</b>	H <sub>2</sub> N-VFRL <b>A</b> KWIQKVI-NH <sub>2</sub>	25	>0.5 <sup>b</sup>	30%
<b>13</b>	H <sub>2</sub> N-VFRLK <b>A</b> WIQKVI-NH <sub>2</sub>	25	>0.5 <sup>b</sup>	19%
<b>14</b>	H <sub>2</sub> N-VFRLKK <b>A</b> IQKVI-NH <sub>2</sub>	>200	0.078	1%
<b>15</b>	H <sub>2</sub> N-VFRLKKW <b>A</b> QKVI-NH <sub>2</sub>	100	0.188	1%
<b>16</b>	H <sub>2</sub> N-VFRLKKW <b>I</b> AKVI-NH <sub>2</sub>	25	0.188	4%
<b>17</b>	H <sub>2</sub> N-VFRLKKWIQ <b>A</b> VI-NH <sub>2</sub>	12.5	>0.5 <sup>b</sup>	21%
<b>18</b>	H <sub>2</sub> N-VFRLKKWIQK <b>A</b> I-NH <sub>2</sub>	50	0.125	2%
<b>19</b>	H <sub>2</sub> N-VFRLKKWIQKV <b>A</b> -NH <sub>2</sub>	100	0.094	1%

<sup>a</sup>MSC data can be found in Supplementary data, Table S1; <sup>b</sup>Synergy defined as an FICI ≤0.5<sup>37</sup>;

<sup>c</sup>Hemolysis determined after a 20 hour incubation of the compounds (200 µg/ml) with defibrinated sheep blood. (see Supplementary data, Figure S4 and Table S4).

Among the non-hemolytic peptides generated in the alanine scan, only peptide **8** (V1ΔA) retains the same inherent antimicrobial activity as peptide **6** with an MIC of 12.5 µg/mL. It is, however, interesting to note that while replacement of other hydrophobic amino acids in peptide **6** with alanine as for **9**, **11**, **14**, **15**, **18**, and **19** did result in a decrease of antimicrobial activity, it also led to significant enhancement of synergistic activity (Table 2). Apparently, replacing the bulkier aromatic side-chains as in F2ΔA (**9**) and W7ΔA (**14**) is an especially favorable exchange when it comes to potentiating the activity of erythromycin. Notably, replacement of the C-terminal Ile residue as for I12ΔA (**19**) results in a strongly synergistic peptide, while replacing Ile in the center of the peptide as in I8ΔA (**15**) has a less profound effect. Moreover, while peptide **9** has the same FICI as PMBN (Table 1), peptides **14** and **19** are even more potent synergists.

As mentioned above, the cationic side-chains of the Lys residues present in peptide **6** are required for synergy and also serve to limit hemolysis. By comparison, alanine replacement of the polar but neutral glutamine, as in Q9ΔA (**16**), appears to have little effect. Moreover, the R3ΔA substitution in peptide **10**: the only other case wherein a positively charged side-chain was replaced by alanine, did not trigger hemolytic activity and retained synergistic activity. We therefore decided to also take peptide **10** along as part of a broader screening of the most potent synergistic peptides **14** and **19**.

### 2.3. Exploring the synergistic range

A well-studied example of synergy is the potentiation of erythromycin and rifampicin against Gram-negative bacteria by PMBN. Clinically, erythromycin and rifampicin are generally only used to treat infections due to Gram-positive pathogens as both exhibit rather limited activity against Gram-negative strains.<sup>38–40</sup> Other Gram-positive specific antibiotics, such as novobiocin and vancomycin, have also been shown to be capable of killing Gram-negative pathogens if combined with outer membrane disruptors.<sup>10</sup> To ascertain the potentiation range of peptides **6**, **10**, **14**, and **19** checkerboard assays with rifampicin, novobiocin, and vancomycin were performed. PMBN was also included to serve as a benchmark and to allow for comparison to other synergists described in literature.

In addition to investigating a broader panel of Gram-positive antibiotics, we were also curious to see how general the synergistic activity of peptides **6**, **10**, **14**, and **19** is against different Gram-negative pathogens. In the initial synergy assays performed the peptides were screened against the indicator strain *E. coli* BW25113. In the next phase of our study we selected a broader panel of Gram-negative bacteria selected from the WHO priority pathogen list. Specifically, we studied the capacity of peptides **6**, **10**, **14**, and **19** to enhance the activity of rifampicin against a range of *E. coli* strains including *mcr*-positive polymyxin-resistant isolates and strains of *A. baumannii*, *P. aeruginosa*, and *Klebsiella pneumoniae*.

#### 2.3.1. Synergy with rifampicin, novobiocin, and vancomycin

As noted above (Section 2.1), the MIC of rifampicin against *E. coli* BW25113 was established to be 8 µg/mL. By comparison, novobiocin and vancomycin showed no antimicrobial activity against the same strain at concentrations as high as 200 µg/mL. However, when these antibiotics were combined with peptides **6**, **10**, **14**, and **19** a clear synergistic effect was observed in all cases. As noted above, peptides **14** and **19** demonstrated the most potent synergy when combined with erythromycin (Table 2). This effect was largely maintained when **14** and **19** were tested with rifampicin, novobiocin, and vancomycin (Figure 4 and Supplementary data Figures S5 and S6). Table 3 provides an overview of the FICI values obtained for peptides **6**, **10**, **14**, and **19** in combination with these antibiotics. In general, peptide **19** was found to be the most potent synergist and notably was found to be even more effective than PMBN in potentiating the activity of both novobiocin and vancomycin against the indicator strain.

**Table 3.** FICI values of peptides **6**, **10**, **14**, and **19** against *E. coli* BW25113 in combination with “Gram-positive-specific” antibiotics rifampicin, novobiocin, and vancomycin.<sup>a</sup>

Peptides	Rifampicin	Novobiocin	Vancomycin
<b>6</b>	0.156	0.188	0.188
<b>10</b>	0.141	0.078	0.156
<b>14</b>	0.141	0.031	0.250
<b>19</b>	0.078	0.039	0.078
<b>PMBN</b>	0.063	0.047	0.156

<sup>a</sup>MIC and MSC data can be found in the Supplementary data, Table S2, S5 and S6.

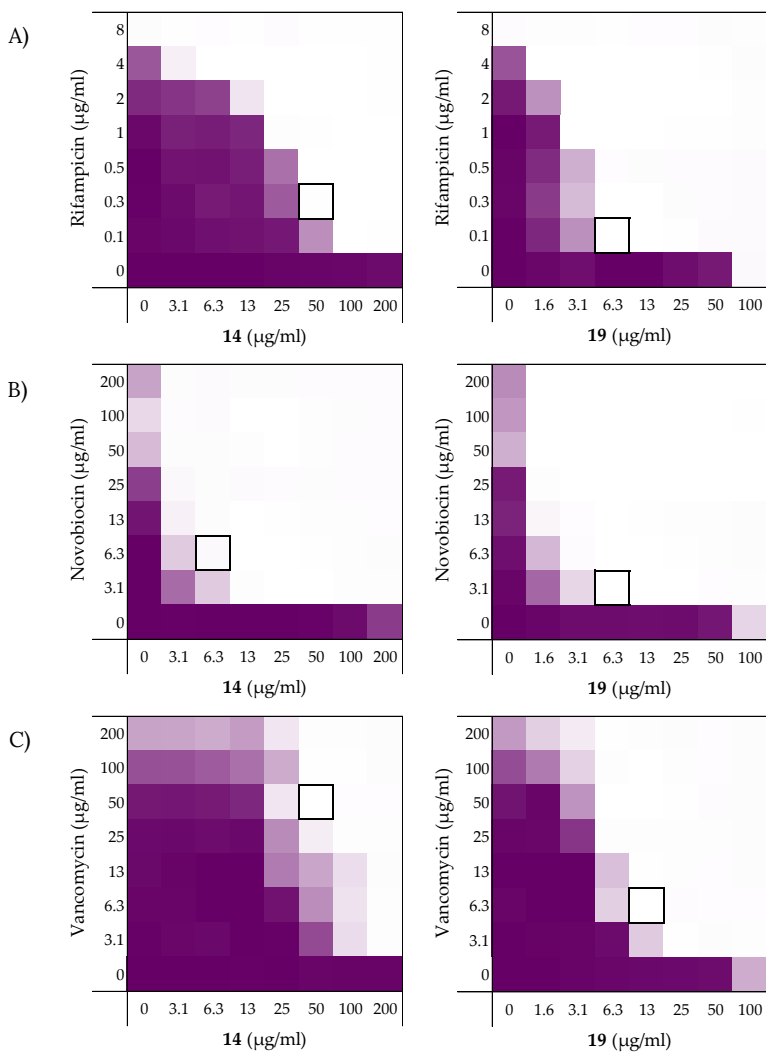


**Figure 4.** Checkerboard assays of the peptides **14** and **19** in combination with A) Rifampicin; B) Novobiocin; C) Vancomycin versus *E. coli* BW25113. In each case the bounded box in the checkerboard assays indicates the combination of peptide and antibiotic resulting in the lowest FICI (see Table 3). OD<sub>600</sub> values were measured using a plate reader and transformed to a gradient: purple represents growth, white represents no growth. Checkerboard assays of peptide **6**, **10** and PMBN in combination with rifampicin, novobiocin and vancomycin are available in the Supplementary data, Figure S2, S5 and S6.

### 2.3.2. Synergy towards other *E. coli* strains including *mcr*-positive clinical isolates

Next, the synergistic activity of peptides **6**, **10**, **14**, and **19** in combination with rifampicin was tested against *E. coli* strains ATCC25922 and W3110. These strains were selected given that *E. coli* ATCC25922 has a smooth LPS layer, while *E. coli* W3110 lacks the O-antigen, giving it a rough LPS layer similar to *E. coli* BW25113.<sup>41–43</sup> The susceptibility of Gram-negative bacteria to antibiotics is known to be related to their LPS structure and we therefore set out to assess whether this might affect the efficacy of the synergists as well.<sup>44</sup> While the four peptides exhibited MICs of 200 µg/mL or above against the ATCC25922 strain (see Supplementary data, Table S7), all were found to be potent synergists (Table 4 and Figure 5A). Interestingly, the ATCC25922 strain was found to be more susceptible to these synergistic effects than the BW25113 indicator strain used in our initial screens (Table 4). The results obtained with the W3110 strain provided an interesting contrast: while peptides **6** and **10** exhibited some inherent antimicrobial activity, neither showed any ability to synergize with rifampicin (see Table 4 and Supplementary data, Table S8). Peptides **14** and **19**, however, exhibited potent synergistic activity in combination with rifampicin with peptide **19** resulting in FICI values equal-to or lower than those obtained with the *E. coli* BW25113 indicator strain.

To examine the impact of structurally modified LPS on the synergistic activity of peptides **6**, **10**, **14**, and **19**, the screening was continued with *E. coli* strains bearing *mcr*-1, *mcr*-2 and *mcr*-3 genotypes known to confer polymyxin resistance. Specifically, *mcr*-positive bacteria encode for a phosphoethanolamine transferase that modifies the structure of lipid A leading to a loss of activity for polymyxin antibiotics.<sup>45,46</sup> Synergy was confirmed for all *mcr*-positive strains with EQAS*mcr*-1 and EQAS*mcr*-3 shown to be most susceptible to synergy (Figure 5B,C, Table 4 and see Supplementary data, Tables S9–S12). Interestingly, potent synergy was observed for all four peptides with rifampicin indicating that the structurally modified LPS present in these strains does not interfere with the synergistic activity of peptides **6**, **10**, **14**, and **19**.

**Table 4.** FICI values of peptides **6**, **10**, **14** and **19** in combination with rifampicin against different *E. coli* strains including *mcr*-resistant strains.<sup>a</sup>

Pathogen	6	10	14	19
<i>E. coli</i> BW25113	0.156	0.141	0.141	0.078
<i>E. coli</i> ATCC25922	0.047	0.031	0.031	0.031
<i>E. coli</i> W3110	>0.5 <sup>b</sup>	>0.5 <sup>b</sup>	0.188	0.078
<i>E. coli mcr</i> -1	0.141	0.078	0.125	0.125
<i>E. coli</i> EQAS <i>mcr</i> -1	0.078	0.078	0.094	0.094
<i>E. coli</i> EQAS <i>mcr</i> -2	0.094	0.141	0.094	0.125
<i>E. coli</i> EQAS <i>mcr</i> -3	0.078	0.078	0.047	0.031

<sup>a</sup>MIC and MSC data can be found in the Supplementary data, Tables S7–12; <sup>b</sup>Synergy is defined in literature as a FICI ≤0.5.<sup>37</sup>



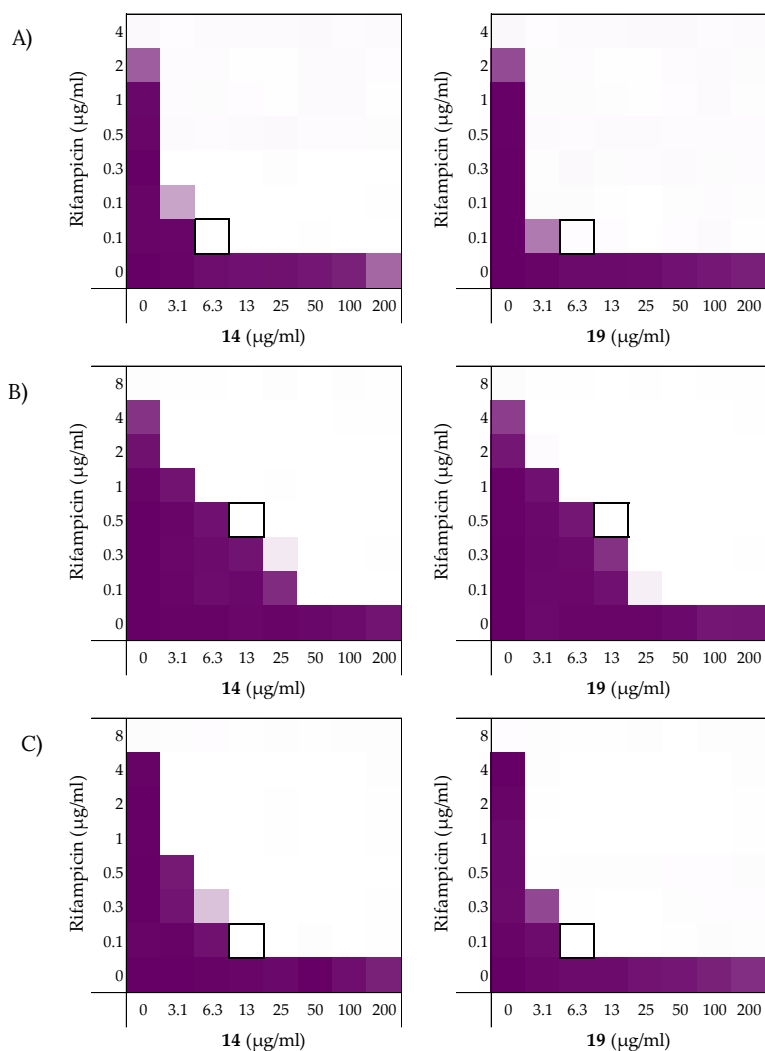
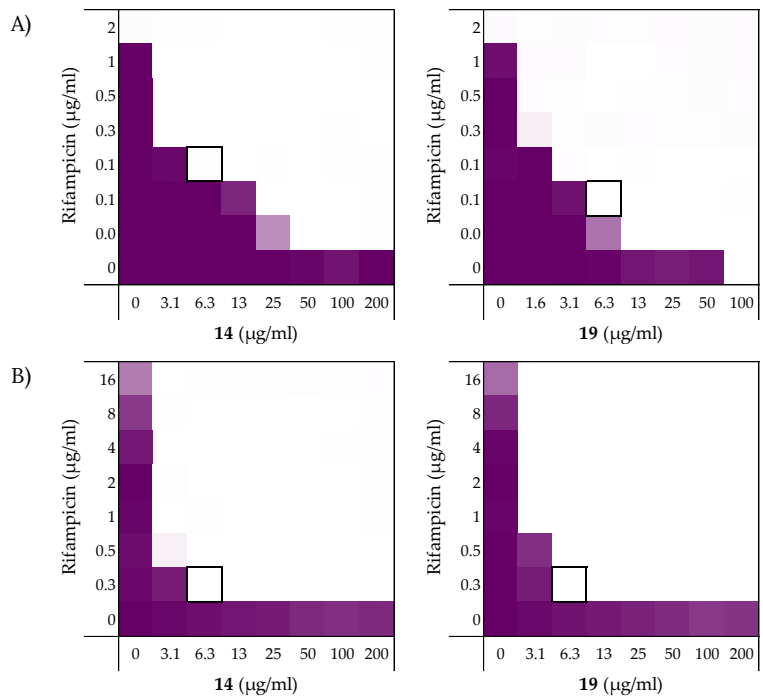


**Figure 5.** Checkerboard assays of the peptides **14** and **19** in combination with rifampicin versus: A) *E. coli* ATCC25922; and mcr-positive isolates B) EQASmcr-1 and C) EQASmcr-3. In each case the bounded box in the checkerboard assays indicates the combination of peptide and antibiotic resulting in the lowest FICI (see Table 4). OD<sub>600</sub> values were measured using a plate reader and transformed to a gradient: purple represents growth, white represents no growth. Checkerboard assays of peptide **6** and **10** of the strains shown above and all checkerboard assays of *E. coli* W3110, mcr-1 and EQASmcr-2 are available in the Supplementary data, Figure S7-12.

**2.3.3. Synergy towards *A. baumannii*, *K. pneumoniae*, and *P. aeruginosa***

After establishing the synergistic potential of peptides **6**, **10**, **14**, and **19** in combination with rifampicin against several *E. coli* strains, we turned our attention to other Gram-negative pathogens. For this part of the study we elected to use laboratory strains *A. baumannii* ATCC17978, *K. pneumoniae* ATCC13883, and *P. aeruginosa* ATCC27853. Rifampicin was again used as the companion antibiotic and we began by establishing its activity against these strains. While a relatively low MIC of 2 µg/mL was measured for rifampicin against the *A. baumannii* ATCC17978 strain, a much lower activity was found against *K. pneumoniae* ATCC13883 and *P. aeruginosa* ATCC27853 where the MICs measured were 32 µg/mL and 16 µg/mL respectively (see Supplementary data, Tables S13–S15).

As illustrated by checkerboard assays of **14** and **19** in Figure 6, all four peptides exhibited potent synergy against the *A. baumannii* and *K. pneumoniae* strains (Table 5). By comparison, significantly less synergy was observed with the *P. aeruginosa* strain with peptide **14** displaying the most potent synergistic activity. The results obtained with *A. baumannii* and *K. pneumoniae* were more in line with our previous findings where again, peptides **14** and **19** resulted in the most potent synergistic combinations with rifampicin. Impressively, a FICI of only 0.023 was detected for both peptides with the *K. pneumoniae* strain tested.



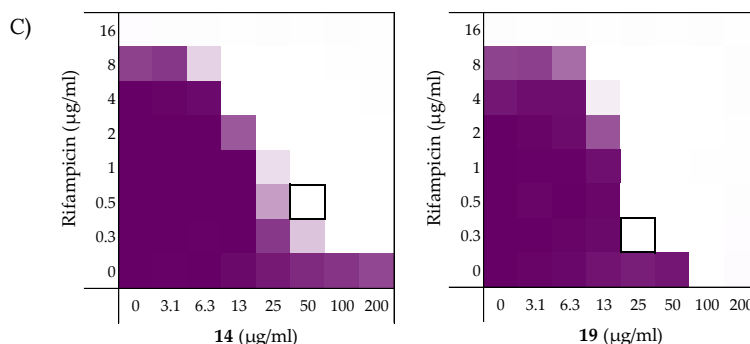


**Figure 6.** Checkerboard assays for peptides **14** and **19** in combination with rifampicin versus different Gram-negative pathogens: A) *A. baumannii* ATCC17978; B) *K. pneumoniae* ATCC13883; C) *P. aeruginosa* ATCC27853. In each case the bounded box in the checkerboard assays indicates the combination of peptide and antibiotic resulting in the lowest FICI (see Table 5). OD<sub>600</sub> values were measured using a plate reader and transformed to a gradient: purple represents growth, white represents no growth. Checkerboard assays of peptides **6** and **10** of the strains shown above are available in the Supplementary data, Figures S13-15.

**Table 5.** FICI values of peptides **6**, **10**, **14**, and **19** in combination with rifampicin against different Gram-negative pathogens.<sup>a</sup>

Pathogen	6	10	14	19
<i>A. baumannii</i> ATCC17978	0.125	0.125	0.078	0.094
<i>K. pneumoniae</i> ATCC13883	0.063	0.063	0.023	0.023
<i>P. aeruginosa</i> ATCC27853	>0.5 <sup>b</sup>	0.250	0.156	0.266

<sup>a</sup>MIC and MSC data can be found in the Supplementary data, Tables S13-15; <sup>b</sup>Synergy is defined in literature as a FICI ≤0.5.<sup>37</sup>

## 2.4. Mechanistic studies

The potentiation of antibiotics like erythromycin, rifampicin, novobiocin and vancomycin against Gram-negative bacteria is generally attained by disruption of the OM as previously described for PMBN.<sup>10</sup> The potent synergy observed for peptides **6**, **10**, **14**, and **19** with these antibiotics, coupled with the finding that the peptides are largely non-hemolytic, points to a mode of action involving selective permeabilization of the Gram-negative OM. To further investigate this hypothesis, a permeabilization assay using N-phenyl-napthalen-1-amine (NPN) on *E. coli* BW25113 was performed. This assay enables monitoring of OM disruption based upon the ability of NPN to enter the phospholipid layer which in turn results in a detectable increase in fluorescence.<sup>47</sup> As illustrated in Figure 7, a clear dose-dependent effect was observed for peptides **6**, **10**, **14**, and **19**. Taken along as a benchmark, PMBN was found to induce ca. 80% OM permeabilization at a concentration of 3.13 μg/mL. By comparison, the peptides matched or surpassed this effect at the higher concentrations tested.

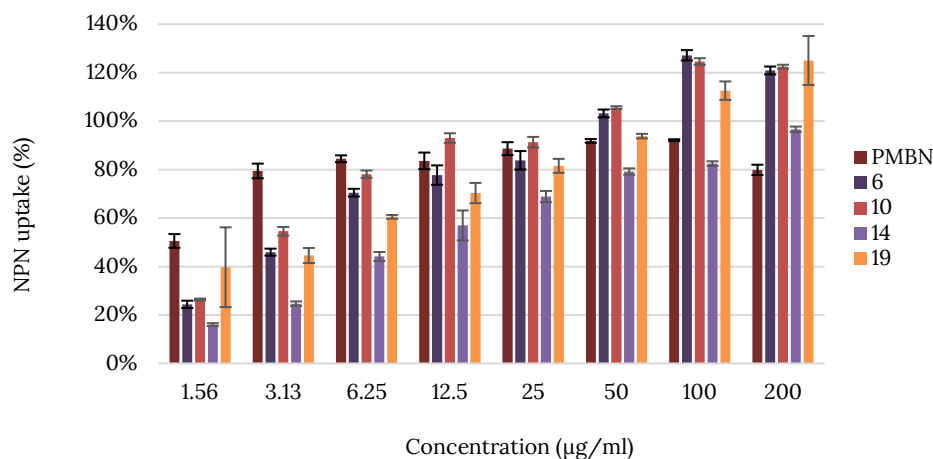


**Figure 7.** Permeabilization assay of *E. coli* BW25113 using N-Phenyl-1-naphthylamine (NPN) as fluorescent probe. The read-out was performed after 60 minutes of incubation using a plate reader with  $\lambda_{\text{ex}}$  355 nm and  $\lambda_{\text{em}}$  420 nm. The NPN uptake values shown are relative to the uptake signal obtained upon treating the cells with 100 µg/ml colistin as previously reported.<sup>48</sup> Error bars represent the standard deviation based on n=3 technical replicates. A read-out was also performed after 10 minutes of incubation (See Supplementary data, Figure 16).

## 2.5. Stereochemical studies

We next set out to probe the stereochemical parameters governing the OM disrupting activity of peptides **6**, **10**, **14**, and **19**. The result of the LPS competition assay with peptide **6** (described above in Section 2.1) as well as the published NMR studies on related thrombin-derived C-terminal peptides,<sup>26</sup> suggest that these peptides interact with LPS. At the core of the LPS structure is the bacterial phospholipid lipid A. Given that lipid A is a chiral biomolecule, we next prepared a series of stereochemical analogues of peptide **6** and characterized the impact on synergistic activity. These analogues included the all D-amino acid enantiomeric species **20**, the L-amino acid inverso peptide **21** and the all D-amino acid retro-inverso variant **22**.

Peptide **6** and enantiomer **20** were both found to exhibit appreciable inherent antimicrobial activity against *E. coli* BW25113, with MICs of 12.5 µg/mL and 6.25 µg/mL respectively (Table 6). Inversion of these peptides to give **21** and **22** led to a significant loss of antibacterial activity in both cases with MICs of >200 µg/mL and 100 µg/mL respectively. Checkerboard assays were next performed with erythromycin as the companion antibiotic using *E. coli* BW25113 as the indicator strain (Figure 8). Interestingly, the enantiomeric peptide **20** was found to exhibit no synergistic activity suggesting that the synergy observed for **6** is indeed stereospecific. Interestingly, the L-inverso peptide **21** did exhibit moderate synergistic activity, however, the D-retro-inverso peptide **22** was a much more potent synergist. Give that retro-inverso peptides can assume a side chain topology similar to that of the parent L-peptide,<sup>49</sup> these finding further support the stereospecific mechanism of peptide **6**. Similar results were obtained upon repeating the synergy assays for peptides **6**, **20–22** with rifampicin as the companion antibiotic (see Supplementary data, Figure S2 and Table S2).

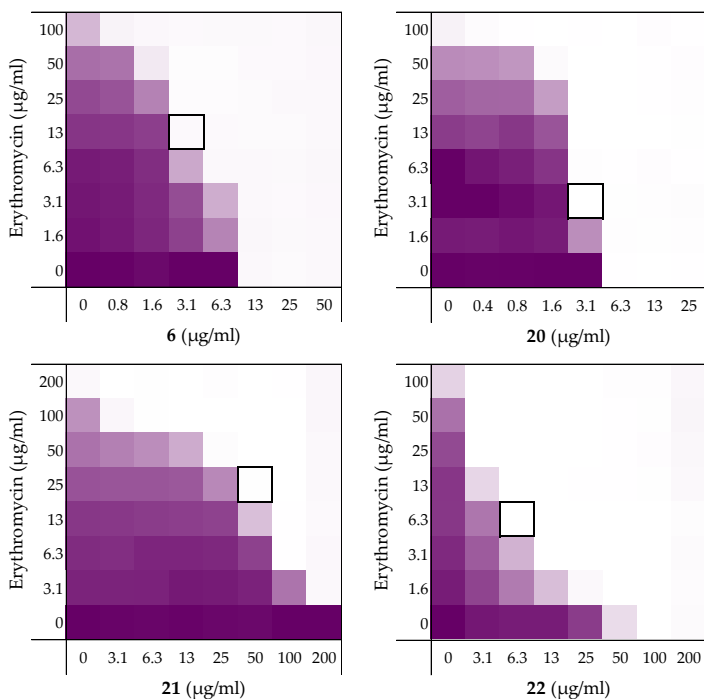


**Figure 8.** Checkerboard assays of the peptides **6**, and stereochemical analogues **20–22** in combination with erythromycin versus *E. coli* BW25113. In each case the bounded box in the checkerboard assays indicates the combination of peptide and antibiotic resulting in the lowest FICI (see Table 1). OD<sub>600</sub> values were measured using a plate reader and transformed to a gradient: purple represents growth, white represents no growth. An overview of all checkerboard assays with erythromycin can be found in the Supplementary data, Figure S1.

**Table 6.** Overview of the TCPs peptide sequence, synergistic and hemolytic activity.

	Peptide sequence <sup>a</sup>	MIC	MSC <sub>peptide</sub>	FICI	Hemolysis <sup>c</sup>
<b>6</b>	H <sub>2</sub> N-VFRLKKWIQKVI-NH <sub>2</sub>	12.5	3.13	0.313	4%
<b>20</b>	H <sub>2</sub> N-vfrlkkwiqkvi-NH <sub>2</sub>	6.25	3.13	>0.5 <sup>b</sup>	3%
<b>21</b>	H <sub>2</sub> N-IVKQIWKKLRFV-NH <sub>2</sub>	>200	50	0.250	2%
<b>22</b>	H <sub>2</sub> N-ivkqiwkklrfv-NH <sub>2</sub>	100	6.25	0.094	3%

<sup>a</sup>Lower case letters indicate D-amino acids; <sup>b</sup>Synergy defined as an FICI ≤0.5<sup>37</sup>; <sup>c</sup>Hemolysis determined after a 20 hour incubation of the compounds (200 µg/ml) with defibrinated sheep blood (see Supplementary data, Figure S4 and Table S4).

### 3. Discussion

The LPS-binding potential of the TCPs sparked our interest in these peptides as potential synergists. Indeed, the synergistic activity of peptides **1**, **2**, and **3** validated this hypothesis (See Table 2). Notably, this represents the first demonstration of the synergistic activity for these peptides even though their antimicrobial activity has been well-studied.<sup>26,35,36,50–52</sup> Peptide **1** exhibits synergy comparable to PMBN (Table 1). Amidation of the C-terminus of peptide **1** gave peptide **6** and led to a significant enhancement of inherent antibiotic activity, an effect also known for other antimicrobial peptides.<sup>53</sup> Most importantly, peptide **6** maintained synergistic activity leading to the lowest MSC and was therefore selected as a lead for further investigation.

While C-terminal amidation impacts the overall charge in peptide **6**, LPS-binding is still maintained as evidenced by the results of an LPS competition assay (Supplementary data, Figure S4 and Table S4). Moreover, stereochemical studies with peptide **6** suggests that synergistic activity is indeed stereospecific: loss of synergistic activity was observed for the mirror image of peptide **6**, D-peptide **20** (see Table 6). Similarly, in literature the mirror image of PMBN was described to have no synergistic activity.<sup>54</sup> Notable, however, is the finding that retro-inverso peptide **22** displays potent synergistic activity, in line with expectations given that the retro-inverso analogue features a topology similar to parent peptide **6**.<sup>49</sup>

Another indication of a mechanism involving LPS-binding comes from the antimicrobial activity observed for peptide **6** against wild-type and *mcr-1* strains of *E. coli*: while MIC values of 12.5 µg/mL and 6.25 µg/mL were measured against the reference BW25113 and W3110 strains, respectively, in the case of the *mcr-1,2,3* clinical isolates tested the MICs were much higher (50–100 µg/mL, see Supplementary data, Tables S2, S8–S12). A similar trend is also observed for the established LPS-binding polymyxin class of antibiotics.<sup>45,46</sup> Interestingly, the synergistic activity of peptide **6**, and the alanine-scan derived analogues **10**, **14**, and **19** is well retained against *mcr*-type stains which is not the case for PMBN (Table 4).<sup>31</sup>

The alanine scan provided insight into the roles of each amino acid in peptide **6** and resulted in the identification of three potent synergists: peptide **10**, **14**, and **19** (Table 2). All three peptides potentiated erythromycin, rifampicin, novobiocin, and vancomycin (Table 2 and Table 3). Peptide **19** was on par with PMBN and results in lower or equal FICIs of synergists recently described in literature.<sup>31,33</sup> Impressively, the potentiation of rifampicin by peptide **14** and **19** was also seen against multiple *E. coli* strains including the *mcr*-clinical isolates, *K. pneumoniae*, *P. aeruginosa*, and *A. baumannii* also with very low FICI values (Table 4 and Table 5). By comparison, peptide **10** displayed a slightly lower synergistic activity than peptide **14** and **19**, but was still equal to or better than peptide **6**. Interestingly, peptide **14** features the substitution of Ala for Trp, a residue often associated with membrane binding and antimicrobial activity.<sup>55–58</sup> Indeed, a significant loss of inherent antimicrobial activity is observed for peptide **14** relative to **6**. However, the finding that peptide **14** retains potent synergy suggests the Trp is not key for synergistic activity or OM permeabilization (Figure 7).

What is also clear from the alanine scan is the essentiality of the lysine side-chains, not only for maintaining synergy, but also for limiting hemolytic activity (Table 2). Comparable findings have been reported for PMB and PMBN which contain several positively charged Dab residues and replacing them with uncharged amino acids leads to a loss of antimicrobial activity for PMB and synergistic activity for PMBN.<sup>59</sup>

In summary, the peptides investigated in this study were found to exhibit potent and targeted synergy with multiple Food and Drug Administration (FDA)-approved Gram-positive-specific antibiotics. Importantly, this synergy was demonstrated against a range of Gram-negative species including *mcr*-resistant strains. The selective OM disrupting properties of these peptides and their potent synergy highlights the potential for such compounds to expand the number of antibiotic classes that can be effectively employed to kill Gram-negative bacteria.

## 4. Experimental section

### 4.1. Manual Peptide Synthesis for Carboxylic Acid C-terminus

Chlorotrityl resin (5.0 g, 1.60 mmol·g<sup>-1</sup>) was loaded with Fmoc-Ile-OH (1, 5) or Fmoc-Glu(OtBu)-OH (2-4). Resin loading was determined to be 0.44–0.57 mmol·g<sup>-1</sup>. Linear peptide encompassing the first amino acid until the last amino acid were assembled manually via standard Fmoc solid-phase peptide synthesis (SPPS) (resin bound AA:Fmoc-AA:BOP:DiPEA, 1:4:4:8 molar eq.) on a 0.1 mmol scale. DMF was used as solvent and Fmoc deprotections were carried out with piperidine:DMF (1:4 v:v). Amino acid side chains were protected as follows: tBu for Asp/Glu, Trt for Asn/Gln, Boc for Lys/Trp, Pbf for Arg. Following coupling and Fmoc deprotection of the final amino acid, N-terminal acylation was achieved for peptide 5 by coupling Ac2O using the same coupling conditions used for SPPS. The resin-bound peptides were next washed with CH<sub>2</sub>Cl<sub>2</sub> and subsequently treated with TFA:TIS:H<sub>2</sub>O (95:2.5:2.5, 10 mL) for 90 min. Resin beads were filtered off and the reaction mixture was added to cold MTBE:hexanes (1:1) and the resulting precipitate washed once more with MTBE:hexanes (1:1). The crude peptide was lyophilized from tBuOH:H<sub>2</sub>O (1:1) and purified with reverse phase HPLC. Pure fractions were pooled and lyophilized to yield the desired linear peptides as white powders, typically in 10–20 mg quantities. For peptide characterization and analysis see Supplementary data, Table S16 and pages S26–S28.

### 4.2. Automated Peptide Synthesis for C-terminal Amides

Rink Amide resin (150 mg, 0.684 mmol·g<sup>-1</sup>) was loaded into the reaction vessel of the CEM liberty blue peptide synthesizer for a 0.1 mmol scale. Linear peptides 6–22 were assembled using microwave irradiation at 90 °C (resin bound AA:Fmoc-AA:DIC:Oxyma, 1:5:5:5 molar eq.). DMF was used as solvent and Fmoc deprotections were carried out with piperidine:DMF (1:4, v:v). Amino acid side chains were protected as follows: tBu for Asp/Glu, Trt for Asn/Gln, Boc for Lys/Trp, Pbf, for Arg. Following coupling and Fmoc deprotection of the final amino acid, N-terminal acylation was achieved for peptide 7 by coupling Ac<sub>2</sub>O using microwave irradiation at 90 °C. The linear peptides were removed from the reaction vessel, washed with DCM and directly treated with TFA:TIS:H<sub>2</sub>O (95:2.5:2.5, 10 mL) for 90 min. Resin beads were filtered off and the reaction mixture was added to cold MTBE:hexanes (1:1) and the resulting precipitate washed once more with MTBE:hexanes (1:1). The crude peptides was lyophilized from tBuOH:H<sub>2</sub>O (1:1) and purified with reverse phase HPLC. Pure fractions were pooled and lyophilized to yield the desired linear peptides as white powders, typically in 20–60 mg quantities. For peptide characterization and analysis see Supplementary data.

### 4.3. Antimicrobial Assays

All peptides were screened for antimicrobial activity against *E. coli* BW25113, *E. coli* ATCC25922, and *E. coli* W3110. A select group of the peptides was further tested against *E. coli* mcr-1, *E. coli* EQASmcr-1, *E. coli* EQASmcr-2, *E. coli* EQASmcr-3, *K. pneumoniae* ATCC13883, *P. aeruginosa* ATCC27853, and *A. baumannii* ATCC17978. The antimicrobial assay was performed according to CLSI guidelines. Bacteria were plated out directly from their glycerol stocks on blood agar plates, incubated overnight at 37 °C, and then kept in the fridge. The blood agar plates were only used for 2 weeks and then replaced.

### 4.4. Minimum Inhibitory Concentration (MIC) Assay

A single colony from a blood agar plate was inoculated in Lysogeny Broth (LB) at 37 °C until a 0.5 optical density at 600nm (OD<sub>600</sub>) was reached (compared to the sterility control of LB). The bacterial suspension was diluted in fresh LB to 2.0 × 10<sup>6</sup> CFU/mL. The serial dilutions were prepared in polypropylene microtiter plates: a stock of the test compounds was prepared with a 2x final concentration in LB. 100 µl of the stock was added to the wells of the top row of which 50 µl was



used for the serial dilution. The bottom row of each plate was used as the positive (50 µl of LB) and negative controls (100 µl of LB) (6 wells each). 50 µl of the 2.0 x 10<sup>6</sup> CFU/mL bacterial stock was added to each well except for the negative controls, adding up to a total volume of 100 µl per well. The plates were sealed with a breathable seal and incubated for 20 hours at 37 °C and 600 rpm. The MIC was visually determined after centrifuging the plates for 2 minutes at 3000 rpm.

#### 4.5. Checkerboard Assays

Dilution series of both the test compound and antibiotic to be evaluated was prepared in LB media. To evaluate synergy, 25 µL of the test compound solutions were added to wells containing 25 µL of the antibiotic solution. This was replicated in three columns for each combination so as to obtain triplicates. To the resulting 50 µL volume of antibiotic + test compound was next added 50 µL of bacterial stock and the plates sealed. After incubation for 20 hours at 37 °C while shaking at 600 rpm, the breathable seals were removed and the plates shaken using a bench top shaker to ensure even suspension of the bacterial cells as established by visual inspection. The plates were then transferred to a Tecan Spark plate reader and following another brief shaking (20 seconds) the density of the bacterial suspensions measured at 600 nm (OD<sub>600</sub>). The resulting OD<sub>600</sub> values were transformed to a 2D gradient to visualize the growth/no-growth results. The FICI was calculated using Equation 1 where a FICI ≤ 0.5 indicating synergy.<sup>37</sup>

$$FICI = \frac{MSC_{ant}}{MIC_{ant}} + \frac{MSC_{syn}}{MIC_{syn}} \quad (1)$$

**Equation 1.** Calculation of the FICI: Calculation of FICI.  $MSC_{ant}$  = MIC of antibiotic in combination with synergist;  $MIC_{ant}$  = MIC of antibiotic alone;  $MSC_{syn}$  = MIC of synergist in combination with antibiotic;  $MIC_{syn}$  = MIC of synergist alone. In cases where the MIC of the antibiotic or synergist was found to exceed the highest concentration tested, the next highest concentration in the dilution series was used in determining the FICI and the result reported as ≤ the calculated value.

#### 4.6. Hemolysis Assay

The hemolytic activity of each analogue was assessed in triplicate. Red blood cells from defibrillated sheep blood obtained from Thermo Fisher were centrifuged (400 g for 15 minutes at 4°C) and washed with Phosphate-Buffered Saline (PBS) containing 0.002% Tween20 (buffer) for five times. Then, the red blood cells were normalized to obtain a positive control read-out between 2.5 and 3.0 at 415 nm to stay within the linear range with the maximum sensitivity. A serial dilution of the compounds (200 – 6.25 µg/mL, 75 µL) was prepared in a 96-well plate. The outer border of the plate was filled with 75 µL buffer. Each plate contained a positive control (0.1% Triton-X final concentration, 75 µL) and a negative control (buffer, 75 µL) in triplicate. The normalized blood cells (75 µL) were added and the plates were incubated at 37 °C for 1 hour or 20 hours while shaking at 500 rpm. A flat-bottom plate of polystyrene with 100 µL buffer in each well was prepared. After incubation, the plates were centrifuged (800 g for 5 minutes at room temperature) and 25 µL of the supernatant was transferred to their respective wells in the flat-bottom plate. The values obtained from a read-out at 415 nm were corrected for background (negative control) and transformed to a percentage relative to the positive control.

#### 4.7. LPS Competition Assay

The same protocol as the MIC assay was used to prepare the serial dilution of the compounds in 96-wells plates in duplicate resulting in two identical plates. A serial dilution of colistin was taken along as a control. The inoculation and preparation of the bacteria stock was performed as described for the MIC assay. The stock of bacteria was then split into two stocks. LPS (1 mg/mL final

concentration) was added to one of the stocks and added to one of the duplicate plates as described in the MIC assay. The normal bacteria stock was added to the remaining plate as described in the MIC assay. The plates were sealed with a breathable seal and incubated for 20 h at 37 °C and 600 rpm after which the MIC was visually determined.

#### 4.8. Membrane Permeability Assay Using N-phenylnaphthalen-1-amine (NPN)

The assay was performed based on protocols adapted from those described in literature.<sup>47,48</sup> Bacteria were inoculated overnight at 37 °C in LB, diluted the next day 50x in LB and grown to OD<sub>600</sub> of 0.5. The bacterial suspension was then centrifuged for 10 minutes at 1000 g at 25 °C. The pellet of bacteria was suspended in 5 mM HEPES buffer containing 20 mM glucose to a final concentration of OD<sub>600</sub> of 1.0. The compounds were serially diluted (25 µL) in triplicate in a black ½ area clear-bottom 96-well plate. 100 µg/mL final concentration of colistin in triplicate served as the positive control. Three wells were filled with 25 µL buffer to serve as the negative control. Additional controls of the compounds were made in triplicate using 25 µL of the highest concentration to detect interactions of the compounds with NPN in the absence of bacteria. A stock of 0.5 mM of NPN in acetone was prepared and diluted 12.5x in the buffer. 25 µL of the NPN solution was added to each well. 50 µL of the 1.0 OD<sub>600</sub> bacterial stock was then added to each well except for the controls of the compounds with NPN. To these wells 50 µL of buffer was added. After 60 minutes the plate was measured using Tecan plate reader with  $\lambda_{\text{ex}}$  355 nm  $\pm$  20 nm and  $\lambda_{\text{em}}$  420 nm  $\pm$  20 nm. The fluorescence values obtained were then transformed into a NPN uptake percentage using the following equation 2:

$$\text{NPN uptake (\%)} = (F_{\text{obs}} - F_0) / (F_{100} - F_0) \times 100\%, \quad (2)$$

**Equation 2.** consists of an observed value of fluorescence ( $F_{\text{obs}}$ ), which is corrected for background using the negative control ( $F_0$ ). This value is divided by the positive control corrected for background ( $F_{100}-F_0$ ) and multiplied by 100% to obtain the percentage.<sup>48,60</sup>

## Supplementary data

### General notes

All reagents employed were of American Chemical Society (ACS) grade or finer and were used without further purification unless otherwise stated. For compound characterization HRMS analysis was performed on a Shimadzu Nexera X2 UHPLC system with a Waters Acquity HSS C18 column (2.1 × 100 mm, 1.8 μm) at 30 °C and equipped with a diode array detector. The following solvent system, at a flow rate of 0.5 mL/min, was used: solvent A, 0.1 % formic acid in water; solvent B, 0.1 % formic acid in acetonitrile. Gradient elution was as follows: 95:5 (A/B) for 1 min, 95:5 to 15:85 (A/B) over 6 min, 15:85 to 0:100 (A/B) over 1 min, 0:100 (A/B) for 3 min, then reversion back to 95:5 (A/B) for 3 min. This system was connected to a Shimadzu 9030 QTOF mass spectrometer (ESI ionisation) calibrated internally with Agilent's API-TOF reference mass solution kit (5.0 mM purine, 100.0 mM ammonium trifluoroacetate and 2.5 mM hexakis(1H,1H,3H-tetrafluoropropoxy)phosphazine) diluted to achieve a mass count of 10000. Purity of the peptides was confirmed to be ≥ 95% by analytical RP-HPLC using a Shimadzu Prominence-i LC-2030 system with a Dr. Maisch Reprosil Gold 120 C18 column (4.6 × 250 mm, 5 μm) at 30 °C and equipped with a UV detector monitoring at 214 nm. The following solvent system, at a flow rate of 1 mL/min, was used: solvent A, 0.1 % TFA in water/acetonitrile, 95/5; solvent B, 0.1 % TFA in water/acetonitrile, 5/95. Gradient elution was as follows: 95:5 (A/B) for 2 min, 95:5 to 0:100 (A/B) over 13 min, 0:100 (A/B) for 2 min, then reversion back to 95:5 (A/B) over 1 min, 95:5 (A/B) for 2 min. The compounds were purified via preparative HPLC using a BESTA-Technik system with a Dr. Maisch Reprosil Gold 120 C18 column (25 × 250 mm, 10 μm) and equipped with a ECOM Flash UV detector monitoring at 214 nm. The following solvent system, at a flow rate of 12 mL/min, was used: solvent A, 0.1 % TFA in water/acetonitrile 95/5; solvent B, 0.1 % TFA in water/acetonitrile 5/95. Gradient elution was as follows: 95:5 (A/B) for 2 min, 95:5 to 0:100 (A/B) over 30 min, 0:100 (A/B) for 2 min, then reversion back to 95:5 (A/B) over 1 min, 95:5 (A/B) for 2 min.

### Peptide synthesis

Automated peptide synthesis. Peptides were synthesized by a microwave-assisted peptide synthesizer (Liberty Blue HT-12, CEM) using the following cycles of deprotection and coupling.

- 1) Fmoc deprotection: 90 °C, 80 W, 65 s with 20% piperidine in DMF, 3 mL/deprotection
- 2) AA coupling: Fmoc-AA-OH (0.2M in 2.5 mL DMF, 5 eq), DIC (1M in 1 mL DM, 10 eq) and Oxyma (1M in 0.5 mL DMF, 5 eq) at 76 °C, 80 W, 15 s before the temperature was increased to 90 °C, 80 W for 110s.

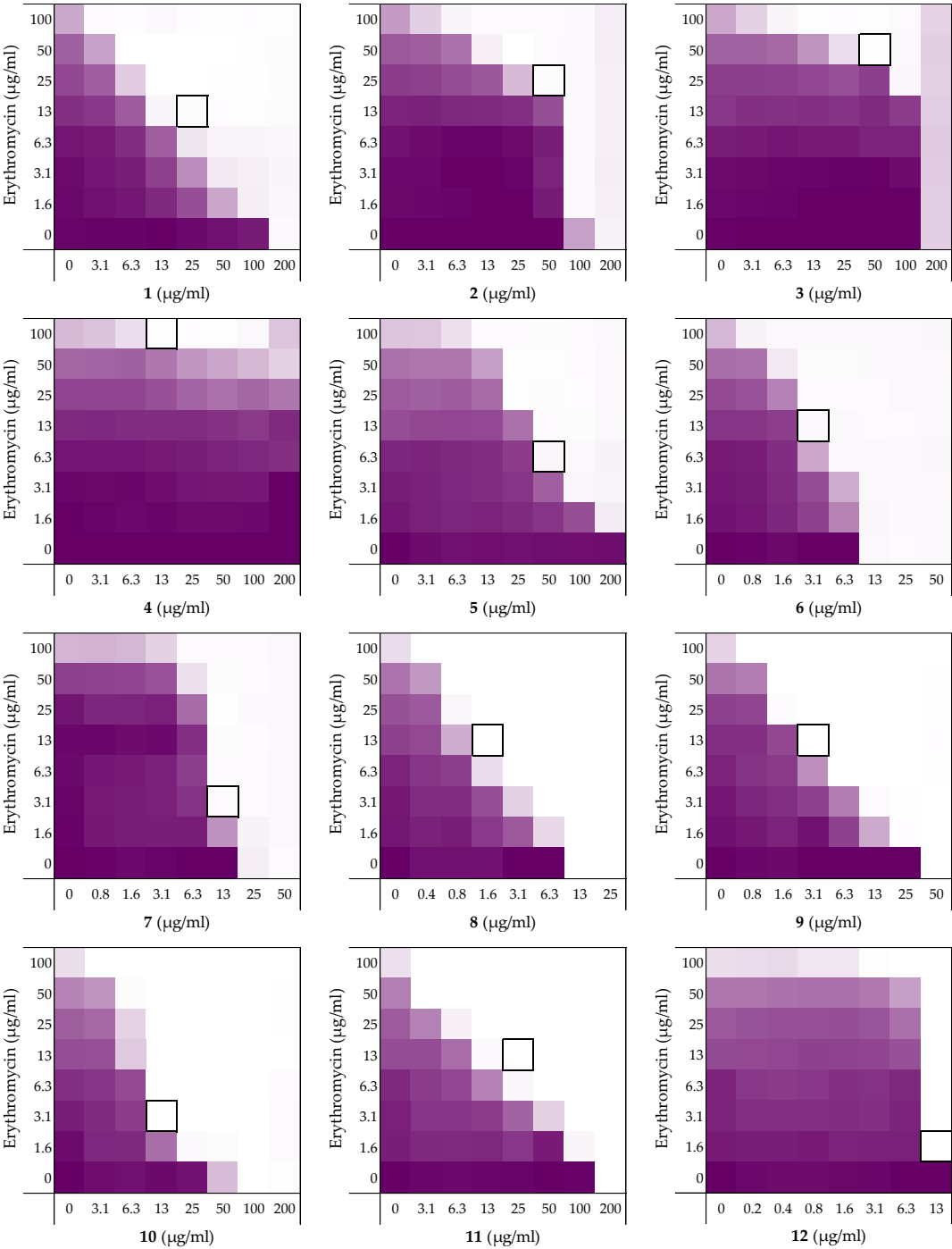
### Synthesis of C-terminal acid peptides.

Chlorotrityl resin was loaded with the first Fmoc-AA-OH (depending on the sequence). Linear peptide encompassing the first AA to the last AA was assembled manually via standard Fmoc solid-phase peptide synthesis (SPPS) (resin bound AA:Fmoc-AA:BOP:DiPEA, 1:4:4:8 molar eq.) on a 0.25 mmol scale. DMF was used as solvent and Fmoc deprotections were carried out with piperidine:DMF (1:4 v:v). Amino acid side chains were protected as follows: tBu for Ser/Asp/Glu/Tyr, Trt for Asn/Gln/His, Boc for Lys/Trp, and Pbf for Arg. Following coupling and Fmoc deprotection of the final AA, the resin was directly treated with TFA:TIS:H<sub>2</sub>O (95:2.5:2.5, 10 mL) for 90 min. The reaction mixture was added to cold MTBE:hexanes (1:1) and the resulting precipitate was centrifuged at 4500 rpm for 5 min, washed once more with MTBE:hexanes (1:1) and centrifuged at 4500 rpm for 5 min. The crude peptides were lyophilized from tBuOH:H<sub>2</sub>O (1:1) and purified with reverse phase HPLC. Pure fractions were pooled and lyophilized to yield the desired linear peptide products in >95% purity as white powders.

**Synthesis of C-terminal amide peptides.**

Rink Amide resin (150 mg, 0.684 mmol.g<sup>-1</sup>) was loaded into the CEM Liberty Blue peptide synthesizer for a 0.1mmol scale. Linear peptide encompassing the first amino acid to the last amino acid were assembled using microwave irradiation (resin bound AA:Fmoc-AA:DIC:Oxyma, 1:5:10:5 molar eq.). DMF was used as solvent and Fmoc deprotections were carried out with piperidine:DMF (1:4, v:v). Amino acid side chains were protected as follows: tBu for Ser/Asp/Glu/Tyr, Trt for Asn/Gln/His, Boc for Lys/Trp, and Pbf for Arg. Following coupling and Fmoc deprotection of the final AA, the resin was directly treated with TFA:TIS:H<sub>2</sub>O (95:2.5:2.5, 10 mL) for 90 min. The reaction mixture was added to cold MTBE:hexanes (1:1) and the resulting precipitate was centrifuged at 4500 rpm for 5 min, washed once more with MTBE:hexanes (1:1) and centrifuged at 4500 rpm for 5 min. The crude peptides were lyophilized from tBuOH:H<sub>2</sub>O (1:1) and purified with reverse phase HPLC. Pure fractions were pooled and lyophilized to yield the desired linear peptide products in >95% purity as white powders.

Checkerboard assays and FICI data against *E. coli* BW25113 with rifampicin



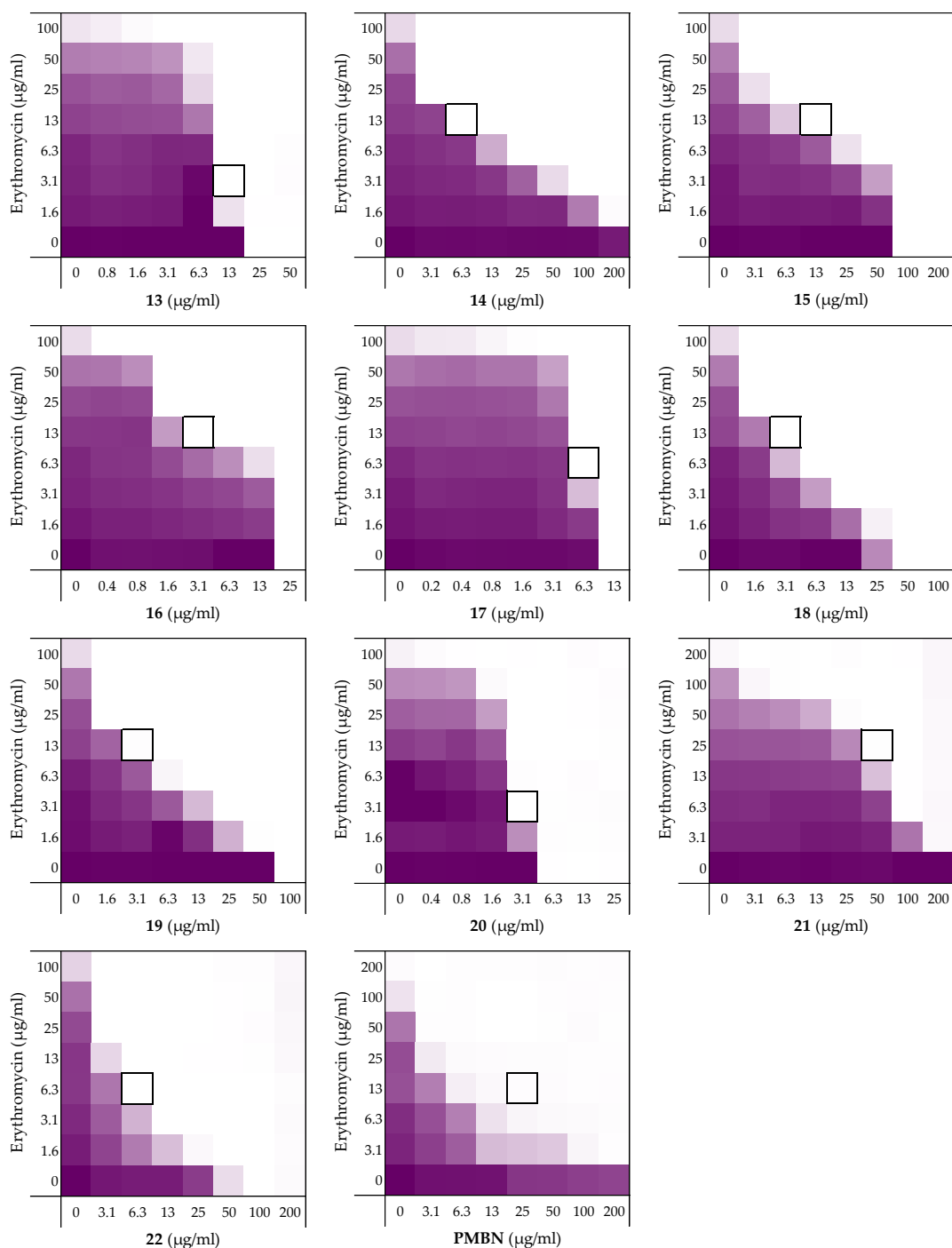


**Figure S1.** Checkerboard assays of peptides **1-22** and PMBN in combination with erythromycin versus *E. coli* BW25113. OD600 values were measured using a plate reader and transformed to a gradient: purple represents growth, white represents no growth. In each case, the bounded box in

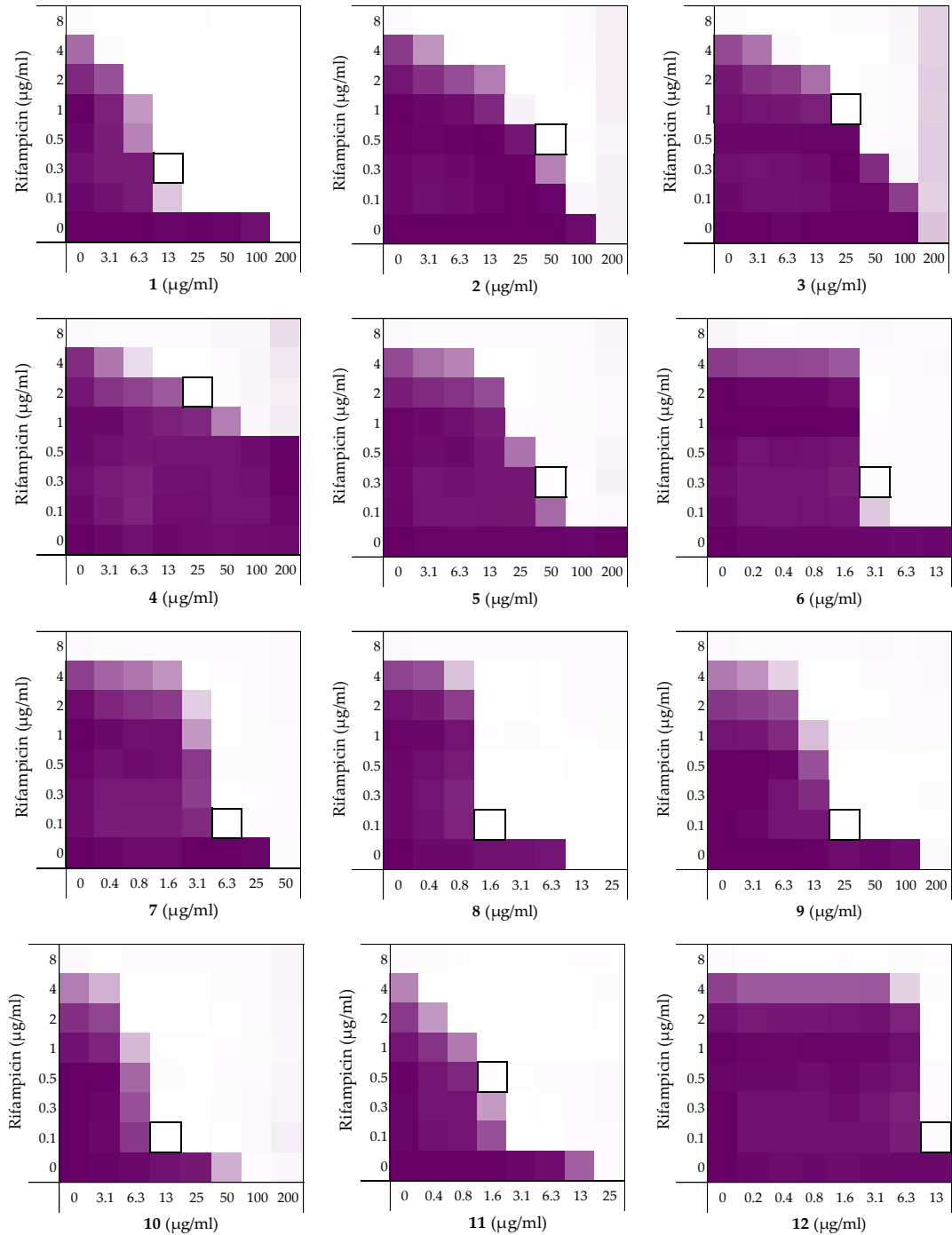
the checkerboard assays indicates the minimal synergistic concentration (MSC) of compound and antibiotic resulting in the lowest FICI.

**Table S1.** Synergistic data of peptides **1-22** and PMBN of the checkerboard assays with erythromycin as shown in Figure S1. All minimal inhibitory concentrations (MICs) and minimal synergistic concentrations (MSCs) are in µg/mL.

	MIC <sub>pep</sub>	MSC <sub>pep</sub>	MIC <sub>ery</sub>	MSC <sub>ery</sub>	FICI
<b>1</b>	200	25	>100	12.5	0.1875
<b>2</b>	200	50	>100	25	0.3750
<b>3</b>	200	50	>100	50	0.5000
<b>4</b>	>200	12.5	>100	100	>0.5 <sup>a</sup>
<b>5</b>	>200	50	>100	6.25	0.1563
<b>6</b>	12.5	3.125	>100	12.5	0.3125
<b>7</b>	50	12.5	>100	3.125	0.2656
<b>8</b>	12.5	1.563	>100	12.5	0.1875
<b>9</b>	50	3.125	>100	12.5	0.1250
<b>10</b>	100	12.5	>100	3.125	0.1406
<b>11</b>	200	25	>100	12.5	0.1875
<b>12</b>	25	12.5	>100	1.563	>0.5 <sup>a</sup>
<b>13</b>	25	12.5	>100	3.125	>0.5 <sup>a</sup>
<b>14</b>	>200	6.25	>100	12.5	0.0781
<b>15</b>	100	12.5	>100	12.5	0.1875
<b>16</b>	25	3.125	>100	12.5	0.1875
<b>17</b>	12.5	6.25	>100	6.25	>0.5 <sup>a</sup>
<b>18</b>	50	3.125	>100	12.5	0.1250
<b>19</b>	100	3.125	>100	12.5	0.0938
<b>20</b>	6.25	3.13	>100	3.125	>0.5 <sup>a</sup>
<b>21</b>	>200	50	200	25	0.2500
<b>22</b>	100	6.25	>100	6.25	0.0938
<b>PMBN</b>	>200	25	200	12.5	0.1250

<sup>a</sup> Synergy is defined as FICI ≤0.5.<sup>37</sup>

Checkerboard assays and FICI data against *E. coli* BW25113 with rifampicin





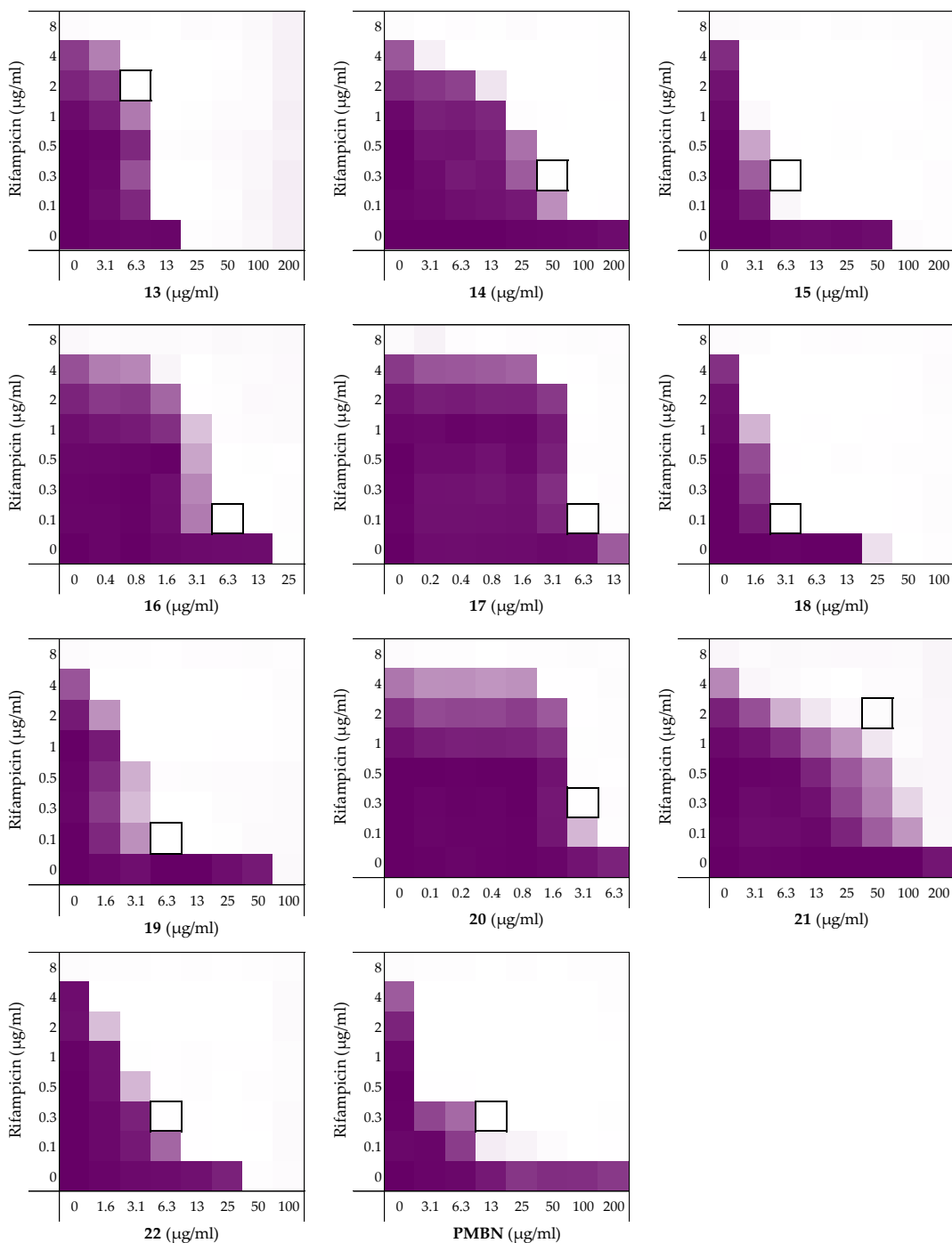


**Figure S2.** Checkerboard assays of peptides 1-22 and PMBN in combination with rifampicin versus *E. coli* BW25113. OD600 values were measured using a plate reader and transformed to a gradient: purple represents growth, white represents no growth. In each case, the bounded box in the

checkerboard assays indicates the minimal synergistic concentration (MSC) of compound and antibiotic resulting in the lowest FICI.

**Table S2.** Synergistic data of peptides **1-22** and PMBN of the checkerboard assays with erythromycin as shown in Figure S2. All minimal inhibitory concentrations (MICs) and minimal synergistic concentrations (MSCs) are in  $\mu\text{g/mL}$ .

	MIC <sub>pep</sub>	MSC <sub>pep</sub>	MIC <sub>rif</sub>	MSC <sub>rif</sub>	FICI
<b>1</b>	200	12.5	8	0.25	0.0938
<b>2</b>	200	50	8	0.5	0.3125
<b>3</b>	>200	25	8	1	0.1875
<b>4</b>	>200	25	8	2	0.3125
<b>5</b>	>200	50	8	0.25	0.1563
<b>6</b>	25	3.125	8	0.25	0.1563
<b>7</b>	50	12.5	8	0.125	0.2656
<b>8</b>	12.5	1.563	8	0.125	0.1406
<b>9</b>	200	25	8	0.125	0.1406
<b>10</b>	100	12.5	8	0.125	0.1406
<b>11</b>	25	1.563	8	0.5	0.1250
<b>12</b>	25	12.5	8	0.125	>0.5 <sup>a</sup>
<b>13</b>	25	6.25	8	2	0.5000
<b>14</b>	>200	50	8	0.125	0.1406
<b>15</b>	100	6.25	8	0.25	0.0938
<b>16</b>	25	6.25	8	0.125	0.2656
<b>17</b>	25	6.25	8	0.125	0.2656
<b>18</b>	50	3.125	8	0.125	0.0781
<b>19</b>	100	6.25	8	0.125	0.0781
<b>20</b>	12.5	3.125	8	0.25	0.2813
<b>21</b>	>200	50	8	2	0.3750
<b>22</b>	50	6.25	8	0.25	0.1406
<b>PMBN</b>	>200	12.5	8	0.25	0.0625

<sup>a</sup> Synergy is defined as FICI  $\leq 0.5$ .<sup>37</sup>

**LPS competition assay of peptide 6**

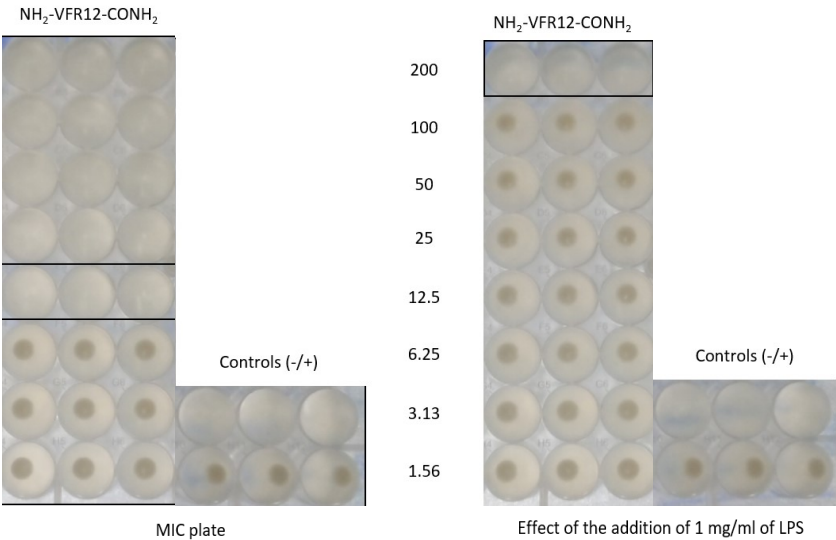


**Figure S3.** LPS competition assay of **6** with *E. coli* BW25113 in LB as described in materials and methods. A visual read-out was performed after centrifuging the plates for 2 minutes at 3000 rpm.

**Table S3.** Overview of LPS competition results using LB as medium. All results are obtained against *E. coli* BW25113 as shown in Figure S4.

	Peptide sequence	MIC	+ 1.0 mg/ml LPS
<b>6</b>	H <sub>2</sub> N-VFRLKKWIQKVI-NH <sub>2</sub>	12.5	200

## Hemolysis assay

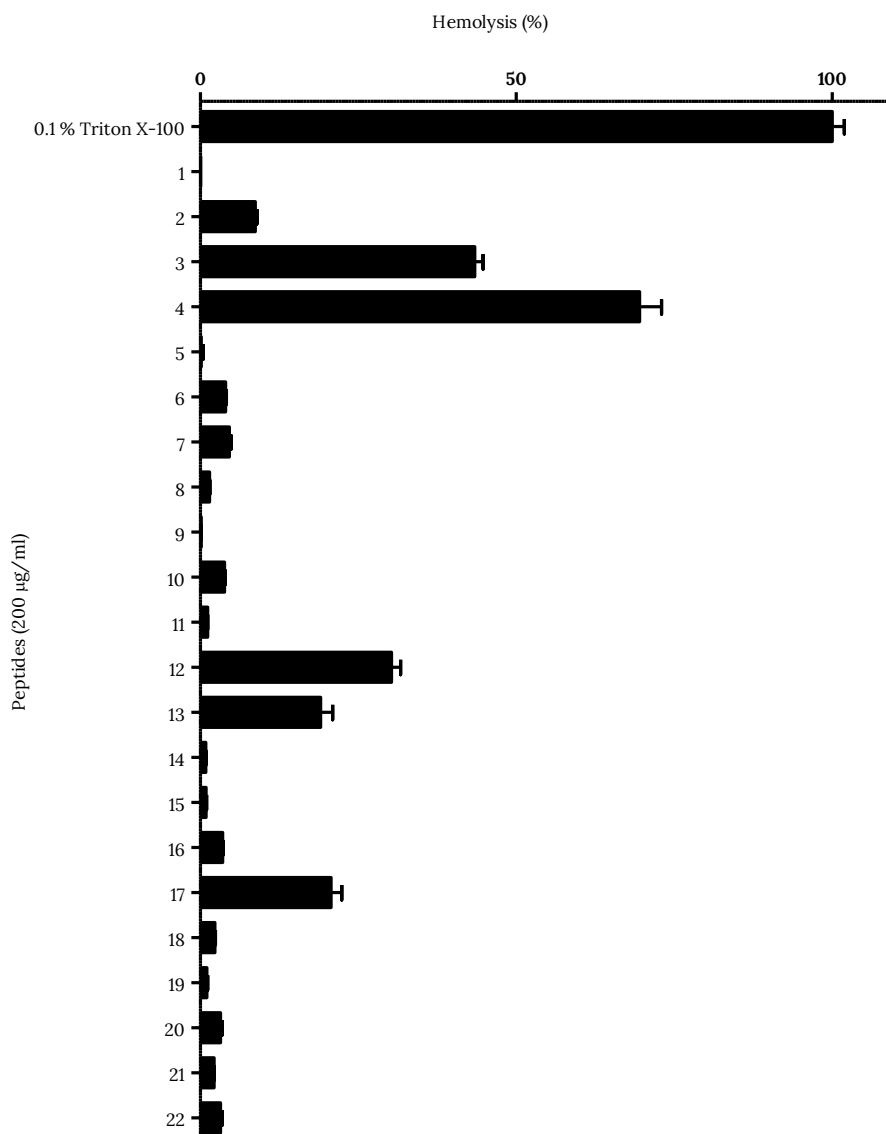


**Figure S4.** Hemolytic activity of peptides **1-22** (200 µg/ml). The hemolysis assay was performed as described in materials and methods. Values above 10% were defined as hemolytic for the peptides **1-4** in a previous study.<sup>35</sup> Error bars represent the standard deviation based on n=3 technical replicates.

**Table S4.** Hemolytic activity of peptides **1-22** (200 µg/ml). The hemolysis assay was performed as described in materials and methods. Values >10% were defined as hemolytic for the peptides **1-4** in a previous study.<sup>35</sup>

Compound	Peptide sequence	Hemolysis (%)
<b>1</b>	H <sub>2</sub> N-VFRLKKWIQKVI-OH	0.1
<b>2</b>	H <sub>2</sub> N-HVFRLKKWIQKVIDQFGE-OH	8.7
<b>3</b>	H <sub>2</sub> N-FYTHVFRLKKWIQKVIDQFGE-OH	43.4
<b>4</b>	H <sub>2</sub> N-GKYGFYTHVFRLKKWIQKVIDQFGE-OH	69.5
<b>5</b>	Ac-VFRLKKWIQKVI-OH	0.2
<b>6</b>	H <sub>2</sub> N-VFRLKKWIQKVI-NH <sub>2</sub>	4.0
<b>7</b>	Ac-VFRLKKWIQKVI-NH <sub>2</sub>	4.6
<b>8</b>	H <sub>2</sub> N- <b>A</b> FRLLKKWIQKVI-NH <sub>2</sub>	1.5
<b>9</b>	H <sub>2</sub> N-V <b>A</b> RLKKWIQKVI-NH <sub>2</sub>	0.1
<b>10</b>	H <sub>2</sub> N-VF <b>A</b> LKKWIQKVI-NH <sub>2</sub>	3.8
<b>11</b>	H <sub>2</sub> N-VF <b>R</b> AKKWIQKVI-NH <sub>2</sub>	1.1
<b>12</b>	H <sub>2</sub> N-VFRL <b>A</b> KWIKVI-NH <sub>2</sub>	30.2
<b>13</b>	H <sub>2</sub> N-VFRLK <b>A</b> WIKVI-NH <sub>2</sub>	19.0
<b>14</b>	H <sub>2</sub> N-VFRLKK <b>A</b> IQKVI-NH <sub>2</sub>	0.9
<b>15</b>	H <sub>2</sub> N-VFRLKKW <b>A</b> QKVI-NH <sub>2</sub>	0.9
<b>16</b>	H <sub>2</sub> N-VFRLKKWI <b>A</b> KVI-NH <sub>2</sub>	3.5
<b>17</b>	H <sub>2</sub> N-VFRLKKWIQ <b>A</b> VI-NH <sub>2</sub>	20.7
<b>18</b>	H <sub>2</sub> N-VFRLKKWIK <b>A</b> I-NH <sub>2</sub>	2.3
<b>19</b>	H <sub>2</sub> N-VFRLKKWIKV <b>A</b> -NH <sub>2</sub>	1.0
<b>20</b>	H <sub>2</sub> N-vfrlkkwiqkvi-NH <sub>2</sub>	3.2
<b>21</b>	H <sub>2</sub> N-IVKQIWKKLRfV-NH <sub>2</sub>	2.2
<b>22</b>	H <sub>2</sub> N-ivkqiwkklrfv-NH <sub>2</sub>	3.2

Checkerboard assays and FICI data against *E. coli* BW25113 with novobiocin

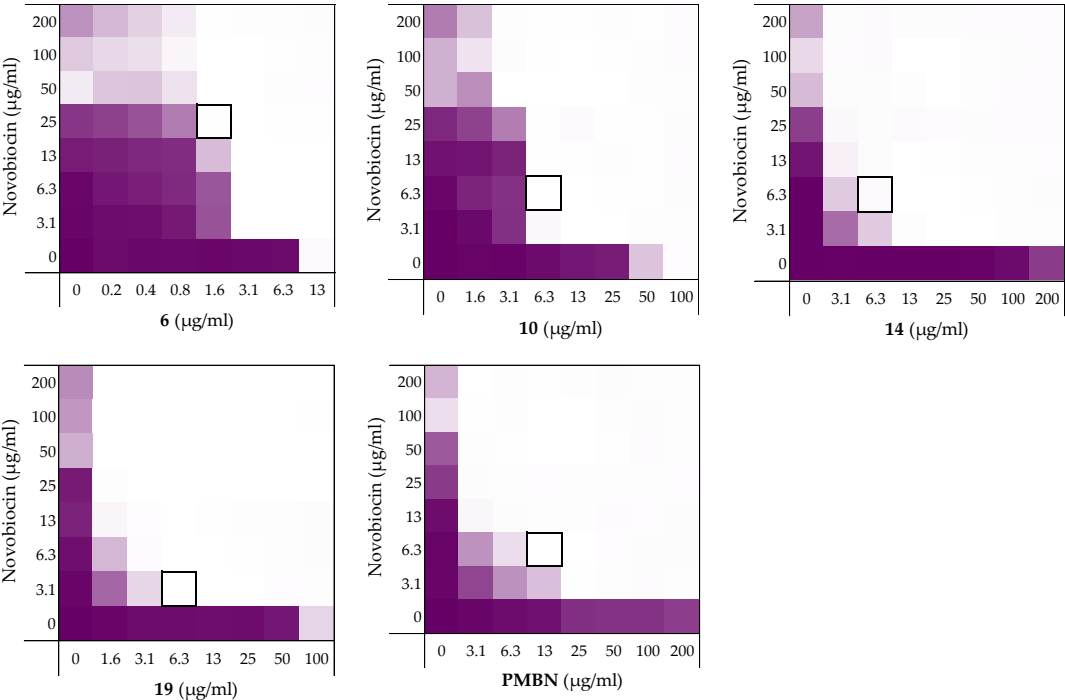


**Figure S5.** Checkerboard assays of the peptides **6**, **10**, **14**, **19** and PMBN in combination with novobiocin versus *E. coli* BW25113. OD600 values were measured using a plate reader and transformed to a gradient: purple represents growth, white represents no growth. In each case, the bounded box in the checkerboard assays indicates the minimal synergistic concentration (MSC) of compound and antibiotic resulting in the lowest FICI.

**Table S5.** Synergistic data of peptides **6**, **10**, **14**, **19** and PMBN of the checkerboard results for *E. coli* BW25113 with novobiocin displayed in Figure S5. All minimal inhibitory concentrations (MICs) and minimal synergistic concentrations (MSCs) are in  $\mu\text{g/mL}$ .

	MIC <sub>peptide</sub>	MSC <sub>peptide</sub>	MIC <sub>novo</sub>	MSC <sub>novo</sub>	FICI
<b>6</b>	12.5	1.563	>200	25	0.1875
<b>10</b>	100	6.25	>200	6.25	0.0781
<b>14</b>	>200	6.25	>200	6.25	0.0313
<b>19</b>	200	6.25	>200	3.125	0.0390
<b>PMBN</b>	>200	12.5	>200	6.25	0.0469

### Checkerboard assays and FICI data against *E. coli* BW25113 with vancomycin

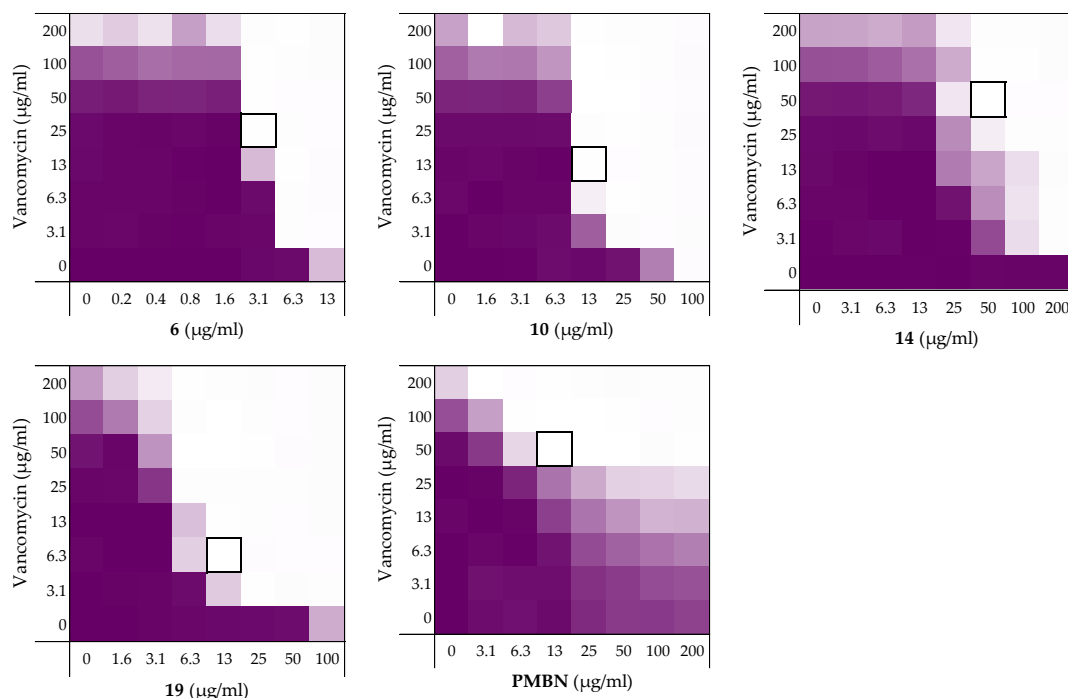


**Figure S6.** Checkerboard assays of the peptides **6**, **10**, **14**, **19** and PMBN in combination with vancomycin versus *E. coli* BW25113. OD600 values were measured using a plate reader and transformed to a gradient: purple represents growth, white represents no growth. In each case, the bounded box in the checkerboard assays indicates the minimal synergistic concentration (MSC) of compound and antibiotic resulting in the lowest FICI.

**Table S6.** Synergistic data of peptides **6**, **10**, **14**, **19** and PMBN of the checkerboard results for *E. coli* BW25113 with vancomycin displayed in Figure S6. All minimal inhibitory concentrations (MICs) and minimal synergistic concentrations (MSCs) are in μg/mL.

	MIC <sub>peptide</sub>	MSC <sub>peptide</sub>	MIC <sub>vanco</sub>	MSC <sub>vanco</sub>	FICI
<b>6</b>	25	3.125	>200	25	0.1875
<b>10</b>	100	12.5	>200	12.5	0.1563
<b>14</b>	>200	50	>200	50	0.2500
<b>19</b>	200	12.5	>200	6.25	0.0781
<b>PMBN</b>	>200	12.5	>200	50	0.1563

# Checkerboard assays and FICI data against *E. coli* ATCC25922 with rifampicin

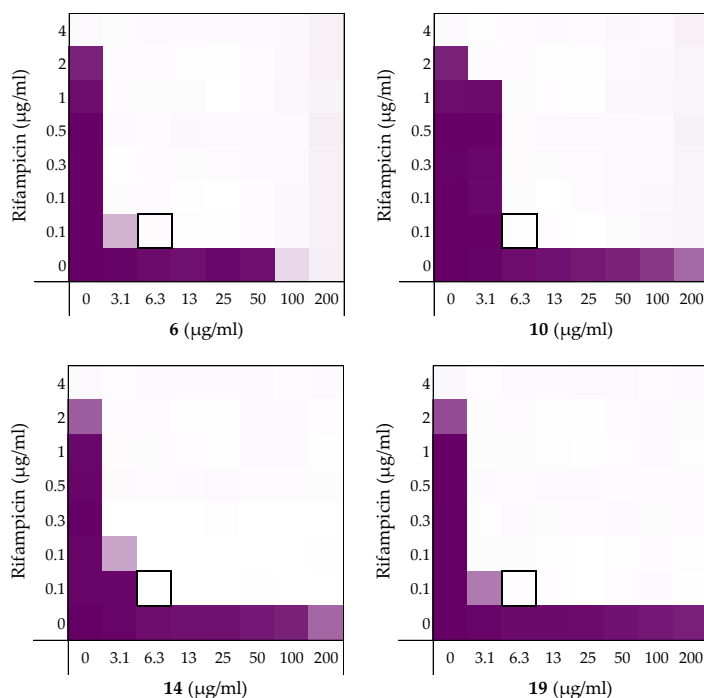


**Figure S7.** Checkerboard assays of the peptides **6**, **10**, **14**, and **19** in combination with rifampicin versus *E. coli* ATCC25922. OD600 values were measured using a plate reader and transformed to a gradient: purple represents growth, white represents no growth. In each case, the bounded box in the checkerboard assays indicates the minimal synergistic concentration (MSC) of compound and antibiotic resulting in the lowest FICI.

**Table S7.** Synergistic data of peptides **6**, **10**, **14**, and **19** of the checkerboard results for *E. coli* ATCC25922 with rifampicin displayed in Figure S7. All minimal inhibitory concentrations (MICs) and minimal synergistic concentrations (MSCs) are in µg/mL.

	MIC <sub>peptide</sub>	MSC <sub>peptide</sub>	MIC <sub>rif</sub>	MSC <sub>rif</sub>	FICI
<b>6</b>	200	6.25	4	0.063	0.0469
<b>10</b>	>200	6.25	4	0.063	0.0313
<b>14</b>	>200	6.25	4	0.063	0.0313
<b>19</b>	>200	6.25	4	0.063	0.0313



### Checkerboard assays and FICI data against *E. coli* W3110 with rifampicin

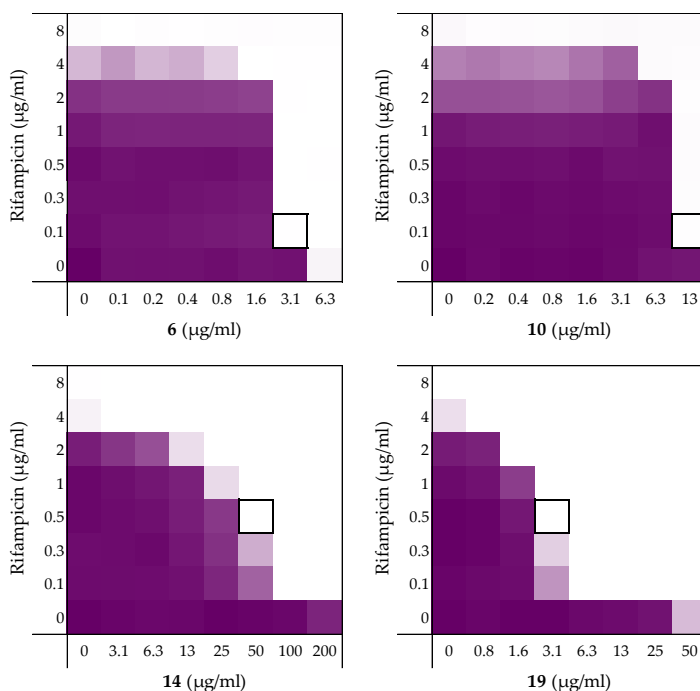


**Figure S8.** Checkerboard assays of the peptides **6**, **10**, **14**, and **19** in combination with rifampicin versus *E. coli* W3110. OD600 values were measured using a plate reader and transformed to a gradient: purple represents growth, white represents no growth. In each case, the bounded box in the checkerboard assays indicates the minimal synergistic concentration (MSC) of compound and antibiotic resulting in the lowest FICI.

**Table S8.** Synergistic data of peptides **6**, **10**, **14**, and **19** of the checkerboard results for *E. coli* W3110 with rifampicin displayed in Figure S8. All minimal inhibitory concentrations (MICs) and minimal synergistic concentrations (MSCs) are in µg/mL.

	MIC <sub>peptide</sub>	MSC <sub>peptide</sub>	MIC <sub>rif</sub>	MSC <sub>rif</sub>	FICI
<b>6</b>	6.25	3.125	8	0.125	>0.5 <sup>a</sup>
<b>10</b>	25	12.5	8	0.125	>0.5 <sup>a</sup>
<b>14</b>	>200	50	8	0.5	0.1875
<b>19</b>	100	3.125	8	0.5	0.0782

<sup>a</sup> Synergy is defined as FICI ≤ 0.5.<sup>37</sup>

### Checkerboard assays and FICI data against *E. coli* mcr-1 with rifampicin

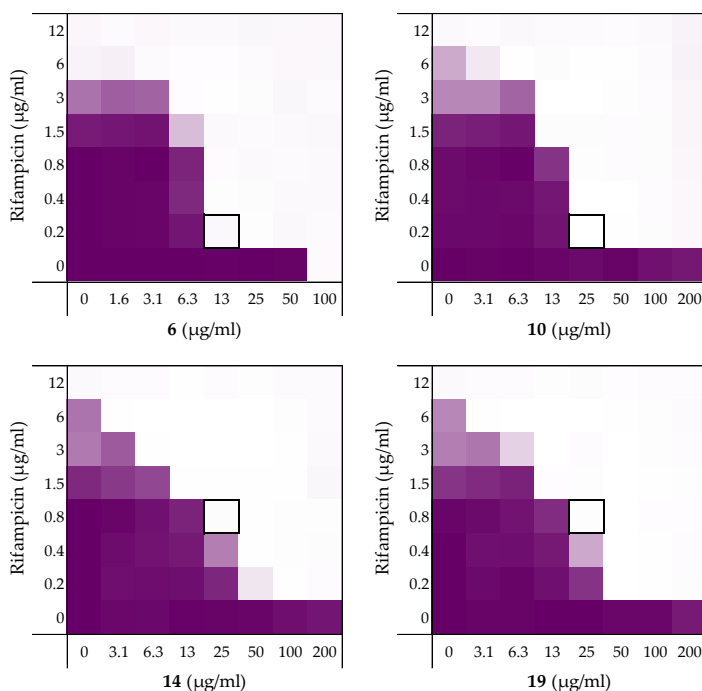


**Figure S9.** Checkerboard assays of the peptides **6**, **10**, **14**, and **19** in combination with rifampicin versus *E. coli* mcr-1. OD600 values were measured using a plate reader and transformed to a gradient: purple represents growth, white represents no growth. In each case, the bounded box in the checkerboard assays indicates the minimal synergistic concentration (MSC) of compound and antibiotic resulting in the lowest FICI.

**Table S9.** Synergistic data of peptides **6**, **10**, **14**, and **19** of the checkerboard results for *E. coli* mcr-1 with rifampicin displayed in Figure S9. All minimal inhibitory concentrations (MICs) and minimal synergistic concentrations (MSCs) are in µg/mL.

	MIC <sub>peptide</sub>	MSC <sub>peptide</sub>	MIC <sub>rif</sub>	MSC <sub>rif</sub>	FICI
<b>6</b>	100	12.5	12	0.188	0.1406
<b>10</b>	>200	25	12	0.188	0.0781
<b>14</b>	>200	25	12	0.75	0.1250
<b>19</b>	>200	25	12	0.75	0.1250

### Checkerboard assays and FICI data against *E. coli* EQASmc<sup>r</sup>-1 with rifampicin

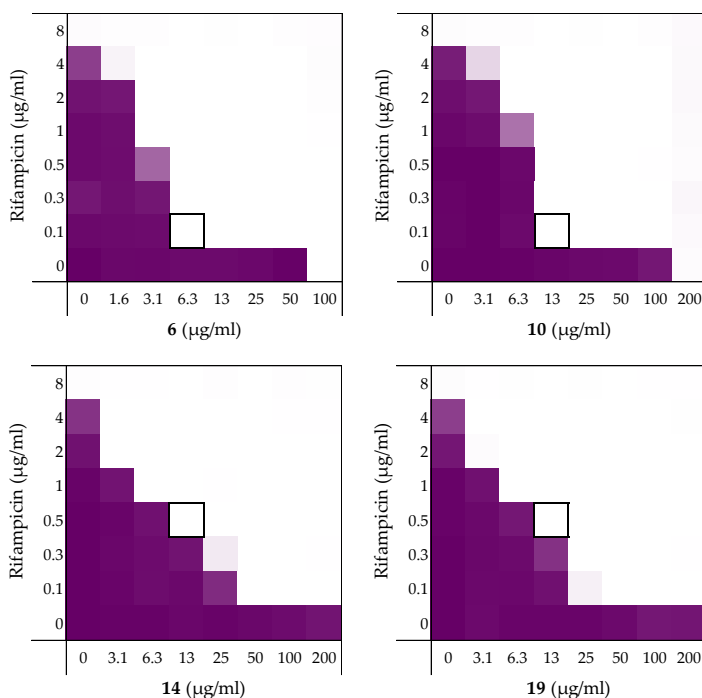


**Figure S10.** Checkerboard assays of the peptides **6**, **10**, **14**, and **19** in combination with rifampicin versus *E. coli* EQASmc<sup>r</sup>-1. OD600 values were measured using a plate reader and transformed to a gradient: purple represents growth, white represents no growth. In each case, the bounded box in the checkerboard assays indicates the minimal synergistic concentration (MSC) of compound and antibiotic resulting in the lowest FICI.

**Table S10.** Synergistic data of peptides **6**, **10**, **14**, and **19** of the checkerboard results for *E. coli* EQASmc<sup>r</sup>-1 with rifampicin displayed in Figure S10. All minimal inhibitory concentrations (MICs) and minimal synergistic concentrations (MSCs) are in µg/mL.

	MIC <sub>peptide</sub>	MSC <sub>peptide</sub>	MIC <sub>rif</sub>	MSC <sub>rif</sub>	FICI
<b>6</b>	100	6.25	8	0.125	0.0781
<b>10</b>	200	12.5	8	0.125	0.0781
<b>14</b>	>200	12.5	8	0.5	0.0938
<b>19</b>	>200	12.5	8	0.5	0.0938

### Checkerboard assays and FICI data against *E. coli* EQASmcr-2 with rifampicin

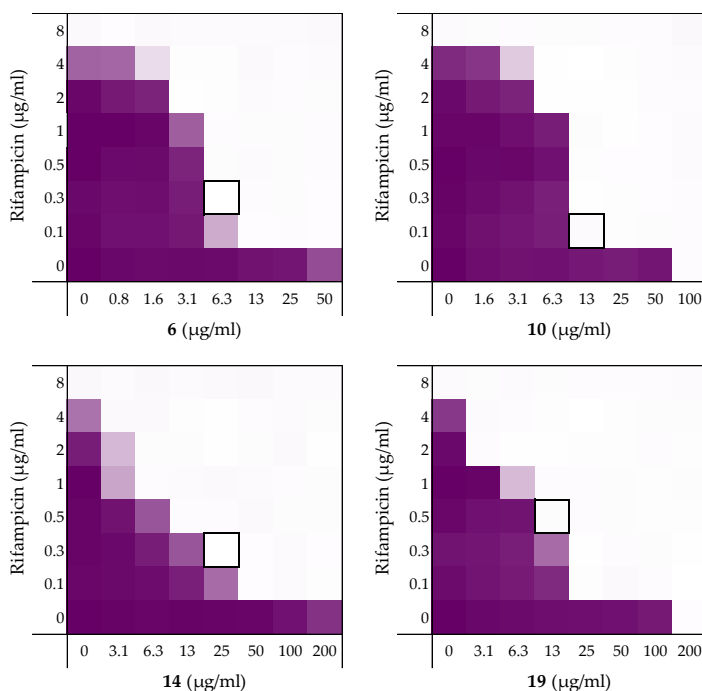


**Figure S11.** Checkerboard assays of the peptides **6**, **10**, **14**, and **19** in combination with rifampicin versus *E. coli* EQASmcr-2. OD600 values were measured using a plate reader and transformed to a gradient: purple represents growth, white represents no growth. In each case, the bounded box in the checkerboard assays indicates the minimal synergistic concentration (MSC) of compound and antibiotic resulting in the lowest FICI.

**Table S11.** Synergistic data of peptides **6**, **10**, **14**, and **19** of the checkerboard results for *E. coli* EQASmcr-2 with rifampicin displayed in Figure S11. All minimal inhibitory concentrations (MICs) and minimal synergistic concentrations (MSCs) are in µg/mL.

	MIC <sub>peptide</sub>	MSC <sub>peptide</sub>	MIC <sub>rif</sub>	MSC <sub>rif</sub>	FICI
<b>6</b>	100	6.25	8	0.25	0.0938
<b>10</b>	100	12.5	8	0.125	0.1406
<b>14</b>	>200	25	8	0.25	0.0938
<b>19</b>	200	12.5	8	0.5	0.1250

### Checkerboard assays and FICI data against *E. coli* EQASmc-3 with rifampicin

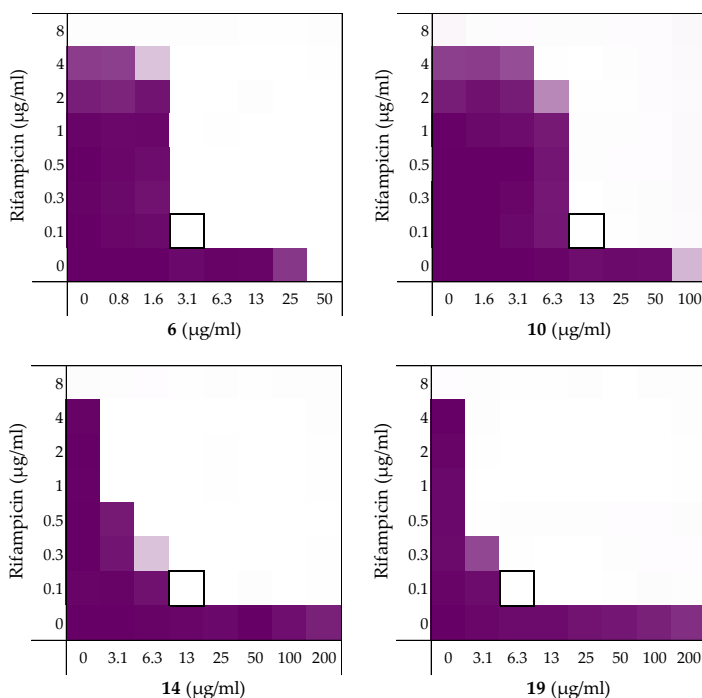


**Figure S12.** Checkerboard assays of the peptides **6**, **10**, **14**, and **19** in combination with rifampicin versus *E. coli* EQASmc-3. OD600 values were measured using a plate reader and transformed to a gradient: purple represents growth, white represents no growth. In each case, the bounded box in the checkerboard assays indicates the minimal synergistic concentration (MSC) of compound and antibiotic resulting in the lowest FICI.

**Table S12.** Synergistic data of peptides **6**, **10**, **14**, and **19** of the checkerboard results for *E. coli* EQASmc-3 with rifampicin displayed in Figure S12. All minimal inhibitory concentrations (MICs) and minimal synergistic concentrations (MSCs) are in µg/mL.

	MIC <sub>peptide</sub>	MSC <sub>peptide</sub>	MIC <sub>rif</sub>	MSC <sub>rif</sub>	FICI
<b>6</b>	50	3.125	8	0.125	0.0781
<b>10</b>	200	12.5	8	0.125	0.0781
<b>14</b>	>200	12.5	8	0.125	0.0469
<b>19</b>	>200	6.25	8	0.125	0.3125

### Checkerboard assays and FICI data against *A. baumannii* ATCC17978 with rifampicin

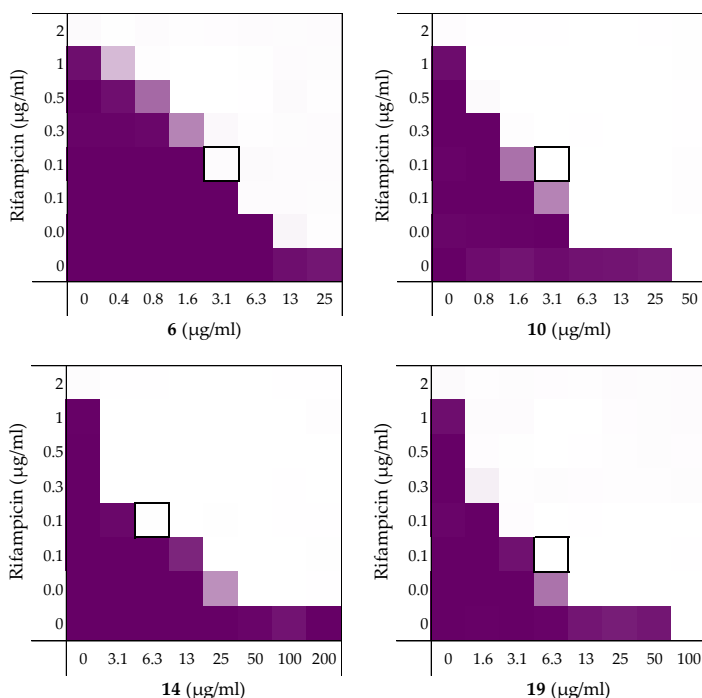


**Figure S13.** Checkerboard assays of the peptides **6**, **10**, **14**, and **19** in combination with rifampicin versus *A. baumannii* ATCC17978. OD600 values were measured using a plate reader and transformed to a gradient: purple represents growth, white represents no growth. In each case, the bounded box in the checkerboard assays indicates the minimal synergistic concentration (MSC) of compound and antibiotic resulting in the lowest FICI.

**Table S13.** Synergistic data of peptides **6**, **10**, **14**, and **19** of the checkerboard results for *A. baumannii* ATCC17978 with rifampicin displayed in Figure S13. All minimal inhibitory concentrations (MICs) and minimal synergistic concentrations (MSCs) are in µg/mL.

	MIC <sub>peptide</sub>	MSC <sub>peptide</sub>	MIC <sub>rif</sub>	MSC <sub>rif</sub>	FICI
<b>6</b>	50	3.125	2	0.125	0.1250
<b>10</b>	50	3.125	2	0.125	0.1250
<b>14</b>	>200	6.25	2	0.125	0.0781
<b>19</b>	100	6.25	2	0.063	0.0938

# Checkerboard assays and FICI data against *K. pneumoniae* ATCC13883 with rifampicin

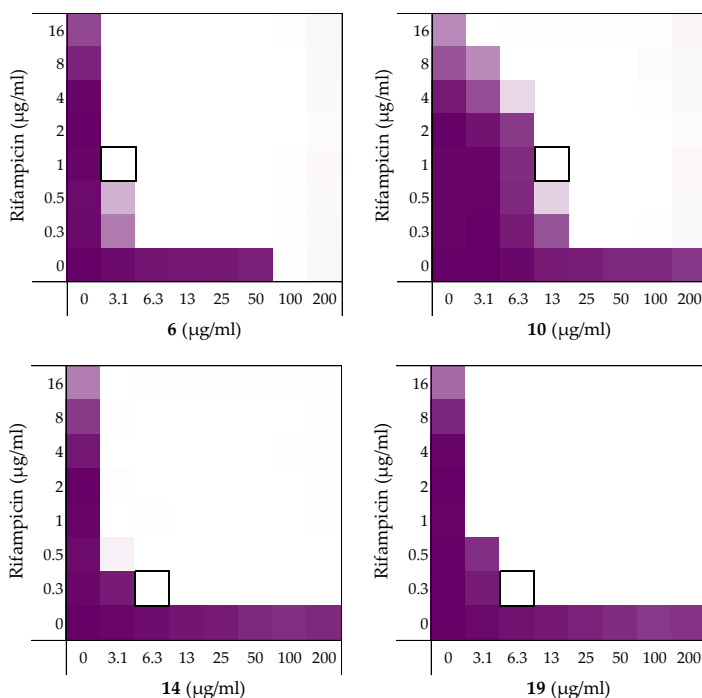


**Figure S14.** Checkerboard assays of the peptides **6**, **10**, **14**, and **19** in combination with rifampicin versus *K. pneumoniae* ATCC13883. OD600 values were measured using a plate reader and transformed to a gradient: purple represents growth, white represents no growth. In each case, the bounded box in the checkerboard assays indicates the minimal synergistic concentration (MSC) of compound and antibiotic resulting in the lowest FICI.

**Table S14.** Synergistic data of peptides **6**, **10**, **14**, and **19** of the checkerboard results for *K. pneumoniae* ATCC13883 with rifampicin displayed in Figure S14. All minimal inhibitory concentrations (MICs) and minimal synergistic concentrations (MSCs) are in µg/mL.

	MIC <sub>peptide</sub>	MSC <sub>peptide</sub>	MIC <sub>rif</sub>	MSC <sub>rif</sub>	FICI
<b>6</b>	100	3.125	32	1	0.0625
<b>10</b>	>200	12.5	32	1	0.0625
<b>14</b>	>200	6.25	32	0.25	0.0234
<b>19</b>	>200	6.25	32	0.25	0.0234

# Checkerboard assays and FICI data against *P. aeruginosa* ATCC27853 with rifampicin

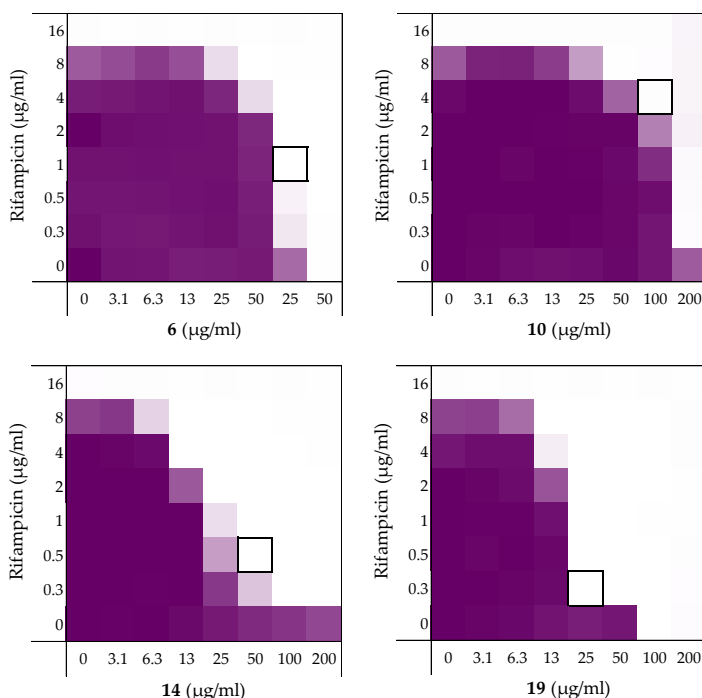


**Figure S15.** Checkerboard assays of the peptides **6**, **10**, **14**, and **19** in combination with rifampicin versus *P. aeruginosa* ATCC27853. OD600 values were measured using a plate reader and transformed to a gradient: purple represents growth, white represents no growth. In each case, the bounded box in the checkerboard assays indicates the minimal synergistic concentration (MSC) of compound and antibiotic resulting in the lowest FICI.

**Table S15.** Synergistic data of peptides **6**, **10**, **14**, and **19** of the checkerboard results for *P. aeruginosa* ATCC27853 with rifampicin displayed in Figure S15. All minimal inhibitory concentrations (MICs) and minimal synergistic concentrations (MSCs) are in µg/mL.

	MIC <sub>peptide</sub>	MSC <sub>peptide</sub>	MIC <sub>rif</sub>	MSC <sub>rif</sub>	FICI
<b>6</b>	50	25	16	1	>0.5 <sup>a</sup>
<b>10</b>	>200	100	16	4	0.2500
<b>14</b>	>200	50	16	0.5	0.1563
<b>19</b>	100	25	16	0.25	0.2656

<sup>a</sup> Synergy is defined as FICI ≤ 0.5.<sup>37</sup>



### Membrane permeability assay using NPN

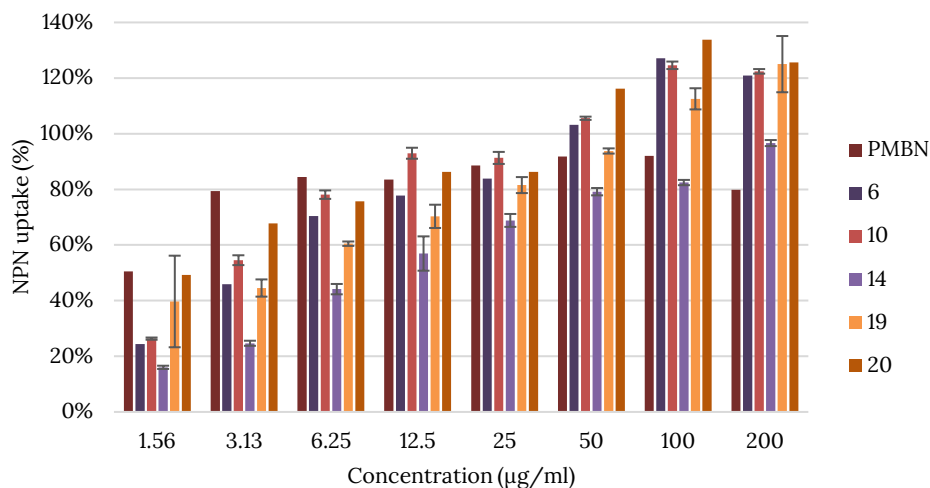


**Figure S16.** Outer membrane permeabilization assay of peptides **6**, **10**, **14**, **19**, **20**, and PMBN with *E. coli* BW25113 using N-phenyl-naphthalen-1-amine (NPN) (at 0.01 mM) as fluorescent probe. The read-out was performed using a plate reader with  $\lambda_{\text{ex}}$  355 nm and  $\lambda_{\text{em}}$  420 nm. The NPN uptake values shown are relative to the uptake signal obtained upon treating the cells with 100 µg/mL colistin as previously reported.<sup>48</sup> Error bars represent the standard deviation based on n=3 technical replicates.

## Peptide characterization and analysis

### HRMS characterization

**Table S16.** Overview of the HRMS results obtained using a Shimadzu Nexera X2 UHPLC system with a Waters Acquity HSS C18 column (2.1 × 100 mm, 1.8 μm) at 30 °C and equipped with a diode array detector. This system was connected to a Shimadzu 9030 QTOF mass spectrometer (ESI ionisation) calibrated internally with Agilent's API-TOF reference mass solution kit (5.0 mM purine, 100.0 mM ammonium trifluoroacetate and 2.5 mM hexakis(1H,1H,3H-tetrafluoropropoxy)phosphazine) diluted to achieve a mass count of 10000.

	Peptide sequence	[M+H] <sup>+</sup> calculated	[M+H] <sup>+</sup> found
1	H <sub>2</sub> N-VFRLKKWIQKVI-COOH	1557.9998	1557.9993
2	H <sub>2</sub> N-HVFRLKKWIQKVIDQFGE-COOH	2271.2767	2271.2791
3	H <sub>2</sub> N-FYTHVFRLKKWIQKVIDQFGE-COOH	2682.4561	2682.4579
4	H <sub>2</sub> N-GKYGFYTHVFRLKKWIQKVIDQFGE-COOH	3087.6573	1544.3326 <sup>a</sup>
5	Ac-VFRLKKWIQKVI-COOH	1600.0104	1600.0110
6	H <sub>2</sub> N-VFRLKKWIQKVI-CONH <sub>2</sub>	1557.0158	1557.0153
7	Ac-VFRLKKWIQKVI-CONH <sub>2</sub>	1599.0263	1599.0259
8	H <sub>2</sub> N- <b>A</b> FRLKKWIQKVI-CONH <sub>2</sub>	1528.9845	1528.9753
9	H <sub>2</sub> N-V <b>A</b> RLLKKWIQKVI-CONH <sub>2</sub>	1480.9845	1480.9846
10	H <sub>2</sub> N-VF <b>A</b> LKKWIQKVI-CONH <sub>2</sub>	1471.9518	1471.9523
11	H <sub>2</sub> N-VFR <b>A</b> KKWIQKVI-CONH <sub>2</sub>	1514.9688	1514.9685
12	H <sub>2</sub> N-VFRL <b>A</b> KWIQKVI-CONH <sub>2</sub>	1499.9579	1499.9580
13	H <sub>2</sub> N-VFRLK <b>A</b> WIQKVI-CONH <sub>2</sub>	1499.9579	1499.9578
14	H <sub>2</sub> N-VFRLKK <b>A</b> IQKVI-CONH <sub>2</sub>	1441.9736	1441.9736
15	H <sub>2</sub> N-VFRLKKW <b>A</b> QKVI-CONH <sub>2</sub>	1514.9688	1514.9696
16	H <sub>2</sub> N-VFRLKKW <b>I</b> AQVI-CONH <sub>2</sub>	1499.9943	1500.0008
17	H <sub>2</sub> N-VFRLKKW <b>I</b> Q <b>A</b> VI-CONH <sub>2</sub>	1499.9579	1499.9646
18	H <sub>2</sub> N-VFRLKKWIQ <b>K</b> <b>A</b> I-CONH <sub>2</sub>	1528.9845	1528.9912
19	H <sub>2</sub> N-VFRLKKWIQKV <b>A</b> -CONH <sub>2</sub>	1514.9688	1514.9753
20	H <sub>2</sub> N-vfrlkkwiqkvi-CONH <sub>2</sub>	1557.0158	1557.0156
21	H <sub>2</sub> N-IVKQIWKKLRFV-CONH <sub>2</sub>	1557.0158	1557.0151
22	H <sub>2</sub> N-ivkqiwwklrfv-CONH <sub>2</sub>	1557.0158	1557.0222

<sup>a</sup> In this case only the [M+2H]<sup>2+</sup> was observed

## References

- (1) Freire-Moran, L.; Aronsson, B.; Manz, C.; Gyssens, I. C.; So, A. D.; Monnet, D. L.; Cars, O. Critical Shortage of New Antibiotics in Development against Multidrug-Resistant Bacteria—Time to React Is Now. *Drug Resistance Updates* **2011**, 14 (2), 118–124. <https://doi.org/10.1016/j.drug.2011.02.003>.
- (2) Amann, S.; Neef, K.; Kohl, S. Antimicrobial Resistance (AMR). *Eur J Hosp Pharm* **2019**, 26 (3), 175–177. <https://doi.org/10.1136/ejpharm-2018-001820>.
- (3) Willyard, C. The Drug-Resistant Bacteria That Pose the Greatest Health Threats. *Nature* **2017**, 543 7643, 15–15. <https://doi.org/10.1038/nature.2017.21550>.
- (4) Nikaido, H. Molecular Basis of Bacterial Outer Membrane Permeability Revisited. *Microbiology and Molecular Biology Reviews* **2003**, 67 (4), 593–656. <https://doi.org/10.1128/MMBR.67.4.593-656.2003>.
- (5) Silhavy, T. J.; Kahne, D.; Walker, S. The Bacterial Cell Envelope. *Cold Spring Harbor Perspectives in Biology* **2010**, 1–16. <https://doi.org/10.1101/cshperspect.a000414>.
- (6) Vaara, M.; Vaara, T. Sensitization of Gram-Negative Bacteria to Antibiotics and Complement by a Nontoxic Oligopeptide. *Nature* **1983**, 303 (5917), 526–528. <https://doi.org/10.1038/303526a0>.
- (7) Vaara, M. Agents That Increase the Permeability of the Outer Membrane. *Microbiol Rev* **1992**, 56 (3), 395–411.
- (8) Rojas, E. R.; Billings, G.; Odermatt, P. D.; Auer, G. K.; Zhu, L.; Miguel, A.; Chang, F.; Weibel, D. B.; Theriot, J. A.; Huang, K. C. The Outer Membrane Is an Essential Load-Bearing Element in Gram-Negative Bacteria. *Nature* **2018**, 559 (7715), 617–621. <https://doi.org/10.1038/s41586-018-0344-3>.
- (9) Kimura, Y.; Matsunaga, H.; Vaara, M. Polymyxin B Octapeptide and Polymyxin B Heptapeptide Are Potent Outer Membrane Permeability-Increasing Agents. *J Antibiot (Tokyo)* **1992**, 45 (5), 742–749. <https://doi.org/10.7164/antibiotics.45.742>.
- (10) Lam, C.; Hildebrandt, J.; Schütze, E.; Wenzel, A. F. Membrane-Disorganizing Property of Polymyxin B Nonapeptide. *Journal of Antimicrobial Chemotherapy* **1986**, 18 (1), 9–15. <https://doi.org/10.1093/jac/18.1.9>.
- (11) Viljanen, P.; Vaara, M. Susceptibility of Gram-Negative Bacteria to Polymyxin B Nonapeptide. *Antimicrobial Agents and Chemotherapy* **1984**, 25 (6), 701–705. <https://doi.org/10.1128/AAC.25.6.701>.
- (12) Viljanen, P.; Koski, P.; Vaara, M. Effect of Small Cationic Leukocyte Peptides (Defensins) on the Permeability Barrier of the Outer Membrane. *Infect Immun* **1988**, 56 (9), 2324–2329.
- (13) Tyrrell, J. M.; Aboklaish, A. F.; Walsh, T. R.; Vaara, T.; Vaara, M. The Polymyxin Derivative NAB739 Is Synergistic with Several Antibiotics against Polymyxin-Resistant Strains of Escherichia Coli, Klebsiella Pneumoniae and Acinetobacter Baumannii. *Peptides* **2019**, 112, 149–153. <https://doi.org/10.1016/j.peptides.2018.12.006>.
- (14) Vaara, M. Polymyxin Derivatives That Sensitize Gram-Negative Bacteria to Other Antibiotics. *Molecules* **2019**, 24 (2), 249. <https://doi.org/10.3390/molecules24020249>.
- (15) FDA Approves New Antibacterial Drug to Treat Complicated Urinary Tract Infections as Part of Ongoing Efforts to Address Antimicrobial Resistance | FDA.
- (16) Spero Therapeutics Highlights SPR741 Phase 1 and Preclinical Data at the 28th European Congress of Clinical Microbiology and Infectious Diseases | Spero Therapeutics, Inc.
- (17) Vaara, M.; Siikanen, O.; Apajalahti, J.; Fox, J.; Frimodt-Møller, N.; He, H.; Poudyal, A.; Li, J.; Nation, R. L.; Vaara, T. A Novel Polymyxin Derivative That Lacks the Fatty Acid Tail and Carries Only Three Positive Charges Has Strong Synergism with Agents Excluded by the Intact Outer Membrane. *Antimicrobial Agents and Chemotherapy* **2010**, 54 (8), 3341–3346. <https://doi.org/10.1128/AAC.01439-09>.

- (18) Kubesch, P.; Maass, G.; Tummler, B.; Boggs, J.; Luciano, L. Interaction of Polymyxin B Nonapeptide with Anionic Phospholipids. *Biochemistry* **1987**, 26 (8), 2139–2149. <https://doi.org/10.1021/bi00382a012>.
- (19) Vaara, M.; Viljanen, P. Binding of Polymyxin B Nonapeptide to Gram-Negative Bacteria. *Antimicrobial Agents and Chemotherapy* **1985**, 27 (4), 548–554. <https://doi.org/10.1128/AAC.27.4.548>.
- (20) Vaara, M. Polymyxin B Nonapeptide Complexes with Lipopolysaccharide. *FEMS Microbiology Letters* **1983**, 18 (1–2), 117–121. <https://doi.org/10.1111/j.1574-6968.1983.tb00461.x>.
- (21) Peterson, A. A.; Hancock, R. E. W.; McGroarty, E. J. Binding of Polycationic Antibiotics and Polyamines to Lipopolysaccharides of *Pseudomonas Aeruginosa*. *Journal of Bacteriology* **1985**, 164 (3), 1256–1261. <https://doi.org/10.1128/jb.164.3.1256-1261.1985>.
- (22) Cavaillon, J. M.; Adib-Conquy, M. Bench-to-Bedside Review: Endotoxin Tolerance as a Model of Leukocyte Reprogramming in Sepsis. *Critical Care* **2006**, 10 (5), 1–8. <https://doi.org/10.1186/cc5055>.
- (23) Fenton, M. J.; Golenbock, D. T. LPS-Binding Proteins and Receptors. *Journal of Leukocyte Biology* **1998**, 64 (1), 25–32. <https://doi.org/10.1002/jlb.64.1.25>.
- (24) Rosenfeld, Y.; Shai, Y. Lipopolysaccharide (Endotoxin)-Host Defense Antibacterial Peptides Interactions: Role in Bacterial Resistance and Prevention of Sepsis. *Biochimica et Biophysica Acta - Biomembranes* **2006**, 1758 (9), 1513–1522. <https://doi.org/10.1016/j.bbamem.2006.05.017>.
- (25) Brandenburg, K.; Heinbockel, L.; Correa, W.; Lohner, K. Peptides with Dual Mode of Action: Killing Bacteria and Preventing Endotoxin-Induced Sepsis. *Biochimica et Biophysica Acta - Biomembranes* **2016**, 1858 (5), 971–979. <https://doi.org/10.1016/j.bbamem.2016.01.011>.
- (26) Saravanan, R.; Holdbrook, D. A.; Petrlova, J.; Singh, S.; Berglund, N. A.; Choong, Y. K.; Kjellström, S.; Bond, P. J.; Malmsten, M.; Schmidtchen, A. Structural Basis for Endotoxin Neutralisation and Anti-Inflammatory Activity of Thrombin-Derived C-Terminal Peptides. *Nat Commun* **2018**, 9 (1), 2762. <https://doi.org/10.1038/s41467-018-05242-0>.
- (27) Dong, N.; Li, X. R.; Xu, X. Y.; Lv, Y. F.; Li, Z. Y.; Shan, A. S.; Wang, J. L. Correction to: Characterization of Bactericidal Efficiency, Cell Selectivity, and Mechanism of Short Interspecific Hybrid Peptides (Amino Acids, (2018), 50, 3–4, (453–468), 10.1007/S00726-017-2531-1). *Amino Acids* **2018**, 50 (7), 967–967. <https://doi.org/10.1007/s00726-018-2584-9>.
- (28) Jerala, R.; Porro, M. Endotoxin Neutralizing Peptides. *Current Topics in Medicinal Chemistry* **2005**, 4 (11), 1173–1184. <https://doi.org/10.2174/1568026043388079>.
- (29) Kaconis, Y.; Kowalski, I.; Howe, J.; Brauser, A.; Richter, W.; Razquin-Olazarán, I.; Inígo-Pestaña, M.; Garidel, P.; Rössle, M.; De Tejada, G. M.; Gutschmann, T.; Brandenburg, K. Biophysical Mechanisms of Endotoxin Neutralization by Cationic Amphiphilic Peptides. *Biophysical Journal* **2011**, 100 (11), 2652–2661. <https://doi.org/10.1016/j.bpj.2011.04.041>.
- (30) De Tejada, G. M.; Heinbockel, L.; Ferrer-Espada, R.; Heine, H.; Alexander, C.; Bárcena-Varela, S.; Goldmann, T.; Correa, W.; Wiesmüller, K. H.; Gisch, N.; Sánchez-Gómez, S.; Fukuoka, S.; Schürholz, T.; Gutschmann, T.; Brandenburg, K. Lipoproteins/Peptides Are Sepsis-Inducing Toxins from Bacteria That Can Be Neutralized by Synthetic Anti-Endotoxin Peptides. *Scientific Reports* **2015**, 5 (August), 1–15. <https://doi.org/10.1038/srep14292>.
- (31) Stokes, J. M.; MacNair, C. R.; Ilyas, B.; French, S.; Côté, J.-P.; Bouwman, C.; Farha, M. A.; Sieron, A. O.; Whitfield, C.; Coombes, B. K.; Brown, E. D. Pentamidine Sensitizes Gram-Negative Pathogens to Antibiotics and Overcomes Acquired Colistin Resistance. *Nat Microbiol* **2017**, 2 (5), 1–8. <https://doi.org/10.1038/nmicrobiol.2017.28>.
- (32) Hancock, R. E. Alterations in Outer Membrane Permeability. *Annu Rev Microbiol* **1984**, 38, 237–264. <https://doi.org/10.1146/annurev.mi.38.100184.001321>.

- (33) Li, Q.; Cebrián, R.; Montalbán-López, M.; Ren, H.; Wu, W.; Kuipers, O. P. Outer-Membrane-Acting Peptides and Lipid II-Targeting Antibiotics Cooperatively Kill Gram-Negative Pathogens. *Commun Biol* **2021**, 4 (1), 1–11. <https://doi.org/10.1038/s42003-020-01511-1>.
- (34) Papareddy, P.; Rydengård, V.; Pasupuleti, M.; Walse, B.; Mörgelin, M.; Chalupka, A.; Malmsten, M.; Schmidtchen, A. Proteolysis of Human Thrombin Generates Novel Host Defense Peptides. *PLoS pathogens* **2010**, 6 (4). <https://doi.org/10.1371/journal.ppat.1000857>.
- (35) Kasetty, G.; Papareddy, P.; Kalle, M.; Rydengård, V.; Mörgelin, M.; Albiger, B.; Malmsten, M.; Schmidtchen, A. Structure-Activity Studies and Therapeutic Potential of Host Defense Peptides of Human Thrombin. *Antimicrobial Agents and Chemotherapy* **2011**, 55 (6), 2880–2890. <https://doi.org/10.1128/AAC.01515-10>.
- (36) Holdbrook, D. A.; Singh, S.; Choong, Y. K.; Petrlova, J.; Malmsten, M.; Bond, P. J.; Verma, N. K.; Schmidtchen, A.; Saravanan, R. Influence of PH on the Activity of Thrombin-Derived Antimicrobial Peptides. *Biochimica et Biophysica Acta - Biomembranes* **2018**, 1860 (11), 2374–2384. <https://doi.org/10.1016/j.bbamem.2018.06.002>.
- (37) Odds, F. C. Synergy, Antagonism, and What the Chequerboard Puts between Them. *Journal of Antimicrobial Chemotherapy* **2003**, 52 (1), 1–1. <https://doi.org/10.1093/jac/dkg301>.
- (38) Washington, J. A.; Wilson, W. R. Erythromycin: A Microbial and Clinical Perspective after 30 Years of Clinical Use (First of Two Parts). *Mayo Clinic Proceedings* **1985**, 60 (3), 189–203. [https://doi.org/10.1016/S0025-6196\(12\)60219-5](https://doi.org/10.1016/S0025-6196(12)60219-5).
- (39) Washington, J. A.; Wilson, W. R. Erythromycin: A Microbial and Clinical Perspective after 30 Years of Clinical Use (Second of Two Parts). *Mayo Clinic Proceedings* **1985**, 60 (4), 271–278. [https://doi.org/10.1016/S0025-6196\(12\)60322-X](https://doi.org/10.1016/S0025-6196(12)60322-X).
- (40) Farr, B.; Mandell, G. L. Rifampin. *Medical Clinics of North America* **1982**, 66 (1), 157–168. [https://doi.org/10.1016/S0025-7125\(16\)31449-3](https://doi.org/10.1016/S0025-7125(16)31449-3).
- (41) Furevi, A.; Stähle, J.; Muheim, C.; Gkotzis, S.; Udekwu, K. I.; Daley, D. O.; Widmalm, G. Structural Analysis of the O-Antigen Polysaccharide from *Escherichia Coli* O188. *Carbohydrate Research* **2020**, 498 (2020), 108051–108051. <https://doi.org/10.1016/j.carres.2020.108051>.
- (42) Uchida, K.; Mizushima, S. A Simple Method for Isolation of Lipopolysaccharides from *Pseudomonas Aeruginosa* and Some Other Bacterial Strains. *Agricultural and Biological Chemistry* **1987**, 51 (11), 3107–3114. <https://doi.org/10.1080/00021369.1987.10868532>.
- (43) Ebbensgaard, A.; Mordhorst, H.; Aarestrup, F. M.; Hansen, E. B. The Role of Outer Membrane Proteins and Lipopolysaccharides for the Sensitivity of *Escherichia Coli* to Antimicrobial Peptides. *Frontiers in Microbiology* **2018**, 9 (SEP), 2153–2153. <https://doi.org/10.3389/fmicb.2018.02153>.
- (44) Wang, Z.; Wang, J.; Ren, G.; Li, Y.; Wang, X. Influence of Core Oligosaccharide of Lipopolysaccharide to Outer Membrane Behavior of *Escherichia Coli*. *Marine Drugs* **2015**, 13 (6), 3325–3339. <https://doi.org/10.3390/md13063325>.
- (45) Liu, Y. Y.; Wang, Y.; Walsh, T. R.; Yi, L. X.; Zhang, R.; Spencer, J.; Doi, Y.; Tian, G.; Dong, B.; Huang, X.; Yu, L. F.; Gu, D.; Ren, H.; Chen, X.; Lv, L.; He, D.; Zhou, H.; Liang, Z.; Liu, J. H.; Shen, J. Emergence of Plasmid-Mediated Colistin Resistance Mechanism MCR-1 in Animals and Human Beings in China: A Microbiological and Molecular Biological Study. *The Lancet Infectious Diseases* **2016**, 16 (2), 161–168. [https://doi.org/10.1016/S1473-3099\(15\)00424-7](https://doi.org/10.1016/S1473-3099(15)00424-7).
- (46) Nang, S. C.; Li, J.; Velkov, T. The Rise and Spread of Mcr Plasmid-Mediated Polymyxin Resistance. *Critical Reviews in Microbiology* **2019**, 45 (2), 131–161. <https://doi.org/10.1080/1040841X.2018.1492902>.
- (47) Helander, I. M.; Mattila-Sandholm, T. Fluorometric Assessment of Gram-Negative Bacterial Permeabilization. *Journal of Applied Microbiology* **2000**, 88 (2), 213–219. <https://doi.org/10.1046/j.1365-2672.2000.00971.x>.

- (48) MacNair, C. R.; Stokes, J. M.; Carfrae, L. A.; Fiebig-Comyn, A. A.; Coombes, B. K.; Mulvey, M. R.; Brown, E. D. Overcoming Mcr-1 Mediated Colistin Resistance with Colistin in Combination with Other Antibiotics. *Nat Commun* **2018**, 9 (1), 458. <https://doi.org/10.1038/s41467-018-02875-z>.
- (49) Van Regenmortel, M. H. V.; Muller, S. D-Peptides as Immunogens and Diagnostic Reagents. *Current Opinion in Biotechnology* **1998**, 9 (4), 377–382. [https://doi.org/10.1016/S0958-1669\(98\)80011-6](https://doi.org/10.1016/S0958-1669(98)80011-6).
- (50) Singh, S.; Kalle, M.; Papareddy, P.; Schmidtchen, A.; Malmsten, M. Lipopolysaccharide Interactions of C-Terminal Peptides from Human Thrombin. *Biomacromolecules* **2013**, 14 (5), 1482–1492. <https://doi.org/10.1021/bm400150c>.
- (51) Oliva, R.; Battista, F.; Cozzolino, S.; Notomista, E.; Winter, R.; Del Vecchio, P.; Petraccone, L. Encapsulating Properties of Sulfobutylether- $\beta$ -Cyclodextrin toward a Thrombin-Derived Antimicrobial Peptide. *Journal of Thermal Analysis and Calorimetry* **2019**, 138 (5), 3249–3256. <https://doi.org/10.1007/s10973-019-08609-7>.
- (52) Burdukiewicz, M.; Sidorczuk, K.; Rafacz, D.; Pietluch, F.; Chilimoniuk, J.; Rödiger, S.; Gagat, P. Proteomic Screening for Prediction and Design of Antimicrobial Peptides with AmpGram. *International Journal of Molecular Sciences* **2020**, 21 (12), 4310–4310. <https://doi.org/10.3390/ijms21124310>.
- (53) Mura, M.; Wang, J.; Zhou, Y.; Pinna, M. The Effect of Amidation on the Behaviour of Antimicrobial Peptides. **2016**, 195–207. <https://doi.org/10.1007/s00249-015-1094-x>.
- (54) Tsubery, H.; Ofek, I.; Cohen, S.; Fridkin, M. The Functional Association of Polymyxin B with Bacterial Lipopolysaccharide Is Stereospecific: Studies on Polymyxin B Nonapeptide. *Biochemistry* **2000**, 39 (39), 11837–11844. <https://doi.org/10.1021/bi000386q>.
- (55) Jin, Y.; Mozsolits, H.; Hammer, J.; Zmuda, E.; Zhu, F.; Zhang, Y.; Aguilar, M. I.; Blazyk, J. Influence of Tryptophan on Lipid Binding of Linear Amphipathic Cationic Antimicrobial Peptides. *Biochemistry* **2003**, 42 (31), 9395–9405. <https://doi.org/10.1021/bi034338s>.
- (56) Yau, W. M.; Wimley, W. C.; Gawrisch, K.; White, S. H. The Preference of Tryptophan for Membrane Interfaces. *Biochemistry* **1998**, 37 (42), 14713–14718. <https://doi.org/10.1021/bi980809c>.
- (57) Wimley, W. C.; White, S. H. Experimentally Determined Hydrophobicity Scale for Proteins at Membrane Interfaces. *Nature Structural Biology* **1996**, 3 (10), 842–848. <https://doi.org/10.1038/nsb1096-842>.
- (58) Strøm, M. B.; Haug, B. E.; Skar, M. L.; Stensen, W.; Stiberg, T.; Svendsen, J. S. The Pharmacophore of Short Cationic Antibacterial Peptides. *Journal of Medicinal Chemistry* **2003**, 46 (9), 1567–1570. <https://doi.org/10.1021/jm0340039>.
- (59) Velkov, T.; Thompson, P. E.; Nation, R. L.; Li, J. Structure–Activity Relationships of Polymyxin Antibiotics. *J. Med. Chem.* **2010**, 53 (5), 1898–1916. <https://doi.org/10.1021/jm900999h>.
- (60) Wang, J.; Chou, S.; Xu, L.; Zhu, X.; Dong, N.; Shan, A.; Chen, Z. High Specific Selectivity and Membrane-Active Mechanism of the Synthetic Centrosymmetric  $\alpha$ -Helical Peptides with Gly-Gly Pairs. *Scientific Reports* **2015**, 5 (April), 1–19. <https://doi.org/10.1038/srep15963>.





## Chapter 4

# Exploring Gram-positive specific antibiotics potentiation by human serum against Gram-negative bacteria

Charlotte M.J. Wesseling, Nathaniel I. Martin, Suzan H.M. Rooijackers, and Bart W. Bardoel

### Abstract

The rise of antibiotic resistance will lead to millions of deaths worldwide if left unchecked. Especially Gram-negative bacteria are inherently harder to target due to the outer membrane that functions as an additional barrier. Recent work has shown the ability of human serum to potentiate Gram-positive specific antimicrobials nisin and vancomycin against Gram-negative bacteria and thus expanding their range. Serum contains proteins of the complement system that upon activation trigger the formation of the membrane attack complex that damages the outer membrane of Gram-negative bacteria. Damage to the outer membrane allows some Gram-positive specific antimicrobial agents to reach their targets. In this study, the potential of human serum for synergy with multiple classes of Gram-positive specific antibiotics was systematically investigated via inner membrane permeability and bacterial viability assays. Three Gram-negative bacteria were selected for screening: *E. coli*, *K. pneumoniae* and *P. aeruginosa*. Inner membrane permeability was observed for most Gram-negative bacteria when treated with a mixture of serum + nisin or serum + vancomycin. For *E. coli* the combination of serum with daptomycin, telavancin, oritavancin, or dalbavancin also resulted in a moderate increase of inner membrane permeability. The viability of *E. coli* was significantly reduced when incubated with serum in combination with nisin, erythromycin, quinupristin & dalfopristin, rifampicin, vancomycin, or dalbavancin compared to serum or the antibiotics alone. By comparison, for *K. pneumoniae* only nisin, rifampicin, and vancomycin displayed a significant synergistic effect when combined with serum. Serum was also found to potentiate nisin, rifampicin, vancomycin, as well as quinupristin & dalfopristin against *P. aeruginosa*. This study reveals that the immune system can sensitize different Gram-negative bacteria toward several Gram-positive specific antibiotics.



## 1. Introduction

The rise of antimicrobial resistance, combined with the lowered discovery rate of new antibiotic classes, has already led to the inability to treat infections in some patients.<sup>1–4</sup> Most notable is the growing resistance among *Klebsiella pneumoniae*, *Escherichia coli*, *Pseudomonas aeruginosa*, and *Acinetobacter baumannii* against the few remaining antibiotic treatments leading these multidrug resistant pathogens to be assessed at the highest threat level by the World Health Organization.<sup>1</sup> Gram-negative bacteria are inherently harder to target by antibiotics, due to the presence of an additional barrier: the outer membrane (OM).<sup>2,5–7</sup> Apart from the impermeable OM itself, the entry of compounds for Gram-negative bacteria is highly restricted by porins and selective uptake, for example, through siderophores.<sup>8–10</sup> In addition, efflux pumps effectively transport the few compounds that do gain entry out of the cell and upregulation of these pumps is often directly related to resistance.<sup>9,10</sup>

Disruption of the OM with adjuvants has the potential to counter this inherent resistance and results in the potentiation of antibiotics normally excluded by the OM.<sup>5,11</sup> Several synergistic molecules have been well-described over the past decades even leading to the first successful Phase I clinical trial with such a synergist (Chapter 1).<sup>5,11</sup> Human serum has also been reported to potentiate antibiotics against Gram-negative bacteria.<sup>12–14</sup> In addition, human serum has been described to form pores in cell membranes through the membrane attack complex (MAC).<sup>15–17</sup> Only recently these two findings were combined and systematically investigated in a report describing the potentiation of antimicrobial compounds nisin and vancomycin by the MAC pores.<sup>18</sup>

The MAC consists of five different proteins (C5b6789<sub>18</sub>) and results from a step-wise activation process called the complement cascade (Figure 1).<sup>19</sup> The recognition of the bacterial surface leads to activation of the classical pathway of the complement system. This results in the deposition of surface-bound convertases.<sup>20–22</sup> Then, cleavage of component C3 into C3a and C3b occurs by the surface-bound convertases.<sup>20</sup> This leads to the covalent linkage by a thioester of C3b to the membrane and the high density of C3b deposition leads to the formation of a C5 convertase.<sup>23,24</sup> The conversion of C5 to C5b requires rapid binding of C6 or it tends to aggregate.<sup>25,26</sup> The C5b6 complex recruits the C7 component and subsequently C8 to result in the C5b-8 complex.<sup>27,28</sup> The recruitment of 18 copies of C9 finalizes the transmembrane MAC pore with an inner diameter of 11 nm. In addition to the permeabilization of the outer membrane, human serum at higher concentrations is also able to disrupt the inner membrane leading to bacterial killing.<sup>18,29</sup>

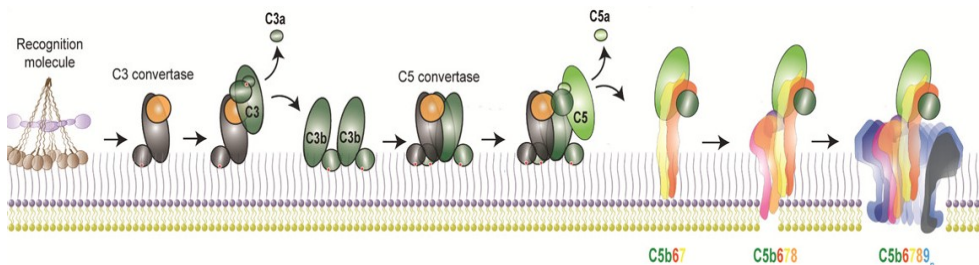


**Figure 1.** Overview of the step-wise formation of the membrane attack complex (MAC). Image by Doorduijn (2019)<sup>30</sup>

The difference in efficiency between outer and inner membrane permeabilization creates a window in which antimicrobial compounds normally inactive against Gram-negative bacteria such as nisin and vancomycin, can synergize with serum (Figure 2).<sup>18</sup> This leads to faster killing of bacteria and the killing occurs at lower serum or antibiotic concentrations.<sup>18</sup> The potentiation of other Gram-positive specific antibiotics against Gram-negative bacteria has not yet been explored systematically. The potentiation by serum could shine a new light on the range of antibiotic activity in the human body and would contribute to understanding the interactions of human serum with bacteria and antibiotics.

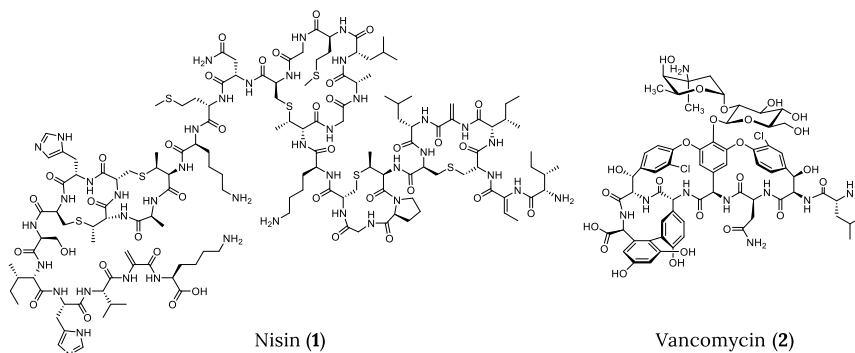
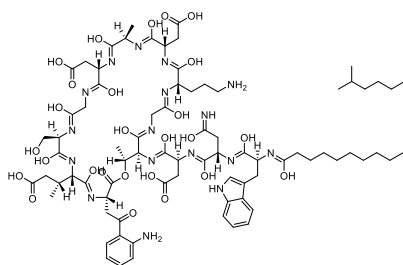


**Figure 2.** Molecular structures of antimicrobial nisin (1) and antibiotic vancomycin (2)

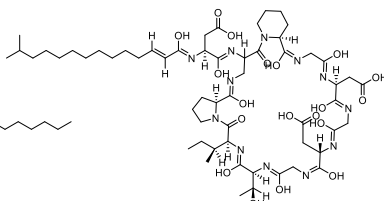
Therefore, in this chapter, the inner membrane permeability and bacterial viability of Gram-negative bacteria was analyzed in order to screen for synergy between serum and selected Gram-positive specific antibiotics (Table 1 and Figure 3). The selection of the specific antibiotics of the classes requires in some cases an additional explanation. Of note is oxacillin, which is part of the first generation of semisynthetic penicillins that do not have broad-spectrum activity (unlike the later generation penicillins).<sup>31</sup> The antimicrobial agent nisin and antibiotic vancomycin serve as controls since their synergy with serum has already been established against *E. coli*, *K. pneumoniae*, and *P. aeruginosa*.<sup>18</sup> Laspartomycin, apart from nisin, is the only antibacterial in our study that is not clinically used, but like vancomycin, nisin, bacitracin and oxacillin it targets the cell wall synthesis and was therefore included (Table 1).<sup>32,33</sup> Lastly, since vancomycin and serum were already reported as a potent synergistic combination, telavancin, oritavancin and dalbavancin were included for a more in-depth structure activity relationship study of glycopeptides with serum (Figure 3).<sup>18</sup>

**Table 1.** Overview of the antibiotics of each class screened for potentiation by human serum

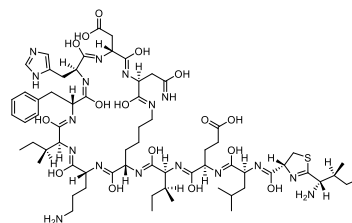
Antibiotic	Class	Target	Route of administration
1	Nisin	Lantibiotic	Cell wall synthesis; pyrophosphate of Lipid II and pore formation in the membrane
2	Vancomycin	Glycopeptide	Cell wall synthesis; D-Ala-D-Ala motif of Lipid II peptide
3	Daptomycin	Lipopeptide	Calcium-dependent binding to phosphatidylglycerol, depolarization and permeabilization of the membrane <sup>4</sup>
4	Laspartomycin	Lipopeptide	Cell wall synthesis; undecaprenyl phosphate
5	Bacitracin	Polypeptide	Cell wall synthesis; undecaprenyl pyrophosphate
6	Oxacillin	Penicillins	Cell wall synthesis; DD-transpeptidase
7	Fusidic acid	Steroid antibiotics	Inhibition of protein synthesis; EF-G
8	Lincomycin	Lincosamides	50S
9	Linezolid	Oxazolidinone	50S
10	Erythromycin	Macrolide	50S
11	Quinupristin & dalbapristin	Streptogramins	50S
12	Rifampicin	Rifamycins	RNA polymerase



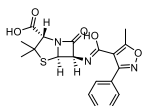
Daptomycin (3)



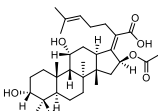
Laspartomycin (4)



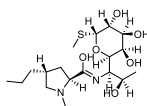
Bacitracin (5)



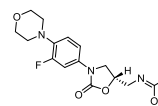
Oxacillin (6)



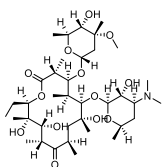
Fusidic acid (7)



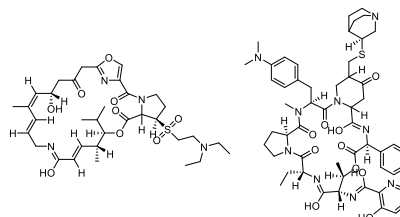
Lincomycin (8)



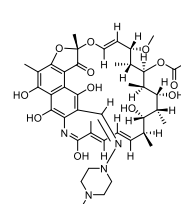
Linezolid (9)



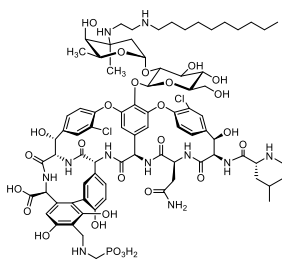
Erythromycin (10)



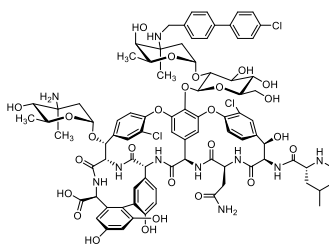
Quinupristin & dalfopristin (11)



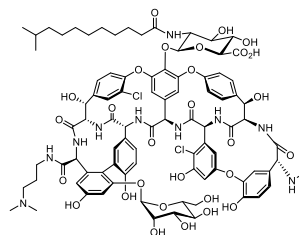
Rifampicin (12)



Telavancin (13)



Oritavancin (14)



Dalbavancin (15)

**Figure 3.** Molecular structures of the Gram-positive specific antibiotics screened in combination with human serum

## 2. Results

### 2.1. Inner membrane permeability assay reveals glycopeptides, nisin, and daptomycin as synergists

The inner membrane permeability assay used was based on the previous work that reported the potentiation of nisin and vancomycin by MAC.<sup>18</sup> SYTOX Green functions as the probe for inner membrane permeability, since this nucleic acid stain cannot penetrate intact bacterial cells. Gram-positive specific antibiotics were screened against *E. coli*, *K. pneumoniae*, and *P. aeruginosa* to establish their effectiveness in the presence of serum. The intensity of the SYTOX Green signal was monitored over 2 hours (Supporting information, Figure S1-S15). For the read-out, we selected the 2-hour time point where the expected synergy of nisin and human serum is clearly visible and absent when serum was heat-inactivated (Figure 4).

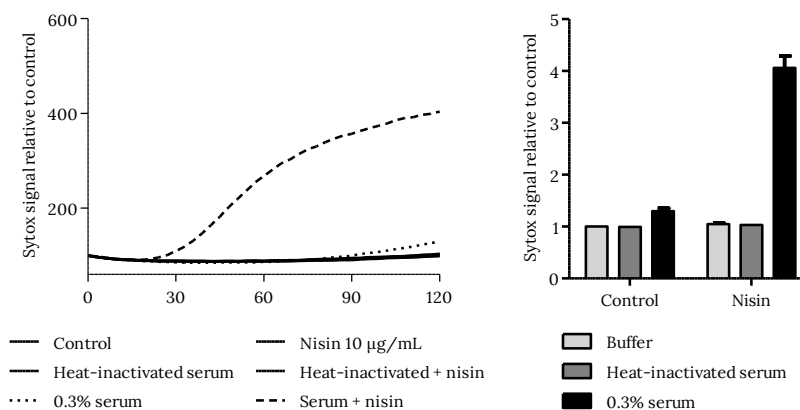


**Figure 4.** Inner membrane permeability assay using SYTOX Green of *E. coli* following incubation with buffer (control), 0.3% heat-inactivated serum, and 0.3% serum with or without 10 µg/mL nisin at 37 °C. SYTOX Green intensity was measured every 3 minutes for 120 minutes in a microplate fluorometer. Values were depicted as relative values to the control condition and represent mean  $\pm$  SD of three independent experiments.

Next, *E. coli* was screened with a 0.3% serum concentration in combination with the different antibiotics (Figure 5A). After 2 hours of incubation inner membrane permeability increased when bacteria were treated with serum in combination with nisin or vancomycin compared to serum only (Figure 5A). A moderate increase in inner membrane permeability was observed for daptomycin, oritavancin, and dalbavancin (Figure 5A).

For *K. pneumoniae* and *P. aeruginosa*, the concentration of serum was based on a previous study (10% and 1% serum respectively).<sup>18</sup> The bacteria were screened with medium, serum, and heat-inactivated serum in the absence and presence of antibiotics. At the 2-hour time point, serum alone already caused inner membrane damage for *K. pneumoniae* and *P. aeruginosa* (Supporting information Figure S16). Therefore, a different time point was taken for which the SYTOX Green signal for nisin in combination with serum was higher as the serum control (Supporting information Figure S1). For *K. pneumoniae* this was at 15 minutes and for *P. aeruginosa* at 90 minutes (Figure 5B-C).

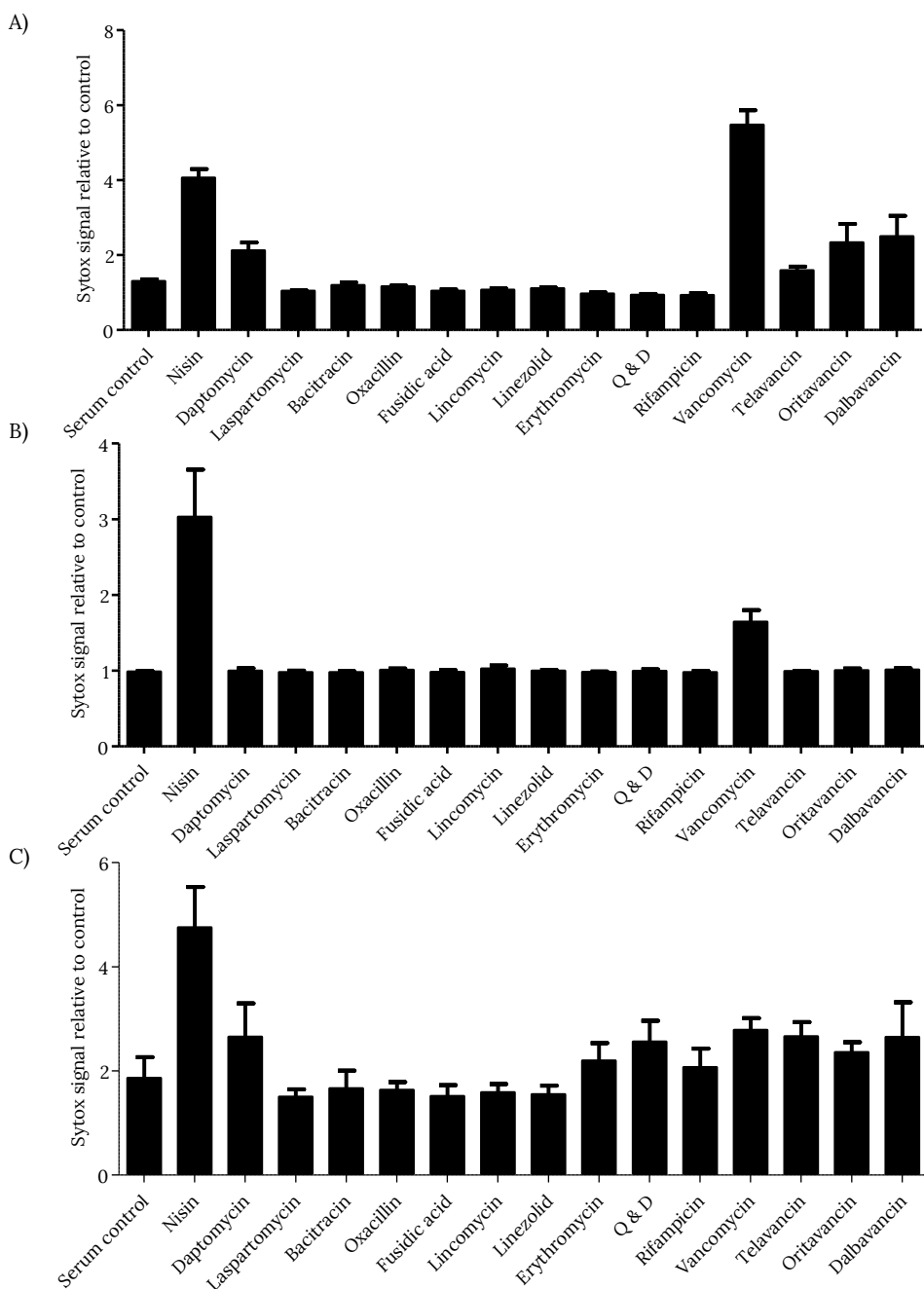


**Figure 5.** Inner permeability assay data with serum for A) *E. coli* at 2 hours; B) *K. pneumoniae* at 15 minutes; C) *P. aeruginosa* at 90 minutes. The antibiotics (10  $\mu\text{g}/\text{mL}$ , except for erythromycin (5, 2.5, 5  $\mu\text{g}/\text{mL}$  respectively) and rifampicin (5, 2.5, 2.5  $\mu\text{g}/\text{mL}$  respectively) were screened in combination with serum (0.3% for *E. coli*, 10% for *K. pneumoniae*, and 1% for *P. aeruginosa*). Values were depicted as relative values to the buffer control conditions and represent mean  $\pm$  SD of three independent experiments.

In addition to the nisin and serum combination, only vancomycin in combination with serum resulted in an increase in SYTOX Green signal for *K. pneumoniae* compared to the serum control. Erythromycin, quinupristin & dalbapristin (Q&D), and rifampicin combined with serum display a slight increase in inner membrane permeability compared to the serum control, but this effect falls within the standard deviation (Figure 5C). These screenings thus revealed the combinations of serum with nisin, daptomycin, or the glycopeptides resulted in increased levels of inner membrane damage compared to serum controls in at least one of the three Gram-negative strains.

## 2.2. Validation of the inner membrane permeability by a bacterial viability assay

The antibiotics that resulted in increased inner membrane permeability when combined with serum were selected for further screening in a bacterial viability assay. This included nisin, daptomycin, vancomycin, telavancin, oritavancin, and dalbavancin. Also, given the unresolved effects on *P. aeruginosa* inner membrane permeability observed for erythromycin, Q & D, and rifampicin when combined with serum, these antibiotics were added to the screen. Bacitracin was also selected as a negative control. While the inner membrane permeability assay used in the previous section provides a very sensitive read-out, the bacterial viability assay here employed allows for the determination of whether the combination of serum with antibiotic has a significant effect on bacterial viability.

Notably, bacterial viability was found to be affected by antibiotic concentration of 10 µg/mL for rifampicin and erythromycin in the absence of serum (Supporting information, Figure S17-18). To validate the effect of serum potentiation, inherent activity of the antibiotics should preferably not be detected. For this reason, serial dilutions of erythromycin and rifampicin were screened against the bacteria (Supporting information, Figures S17-18) and the concentrations of both adjusted accordingly for *E. coli*, *K. pneumoniae*, and *P. aeruginosa*.

Bacterial viability was measured under similar conditions as for the inner membrane permeability assay. The combination of serum with antibiotics showed a significant reduction in bacterial viability for nisin, rifampicin, Q & D, vancomycin, and dalbavancin for *E. coli* (Figure 6A). The combinations of serum with daptomycin, telavancin, and oritavancin, also led to reduced bacterial viability, but not significantly. Bacitracin, which was taken along as an additional negative control, showed similar levels of viability as the control. Additionally, heat-inactivated serum in combination with antibiotics was also screened and these combinations had no effect on viability (Supporting Information, Figure S19, S22, and S23).

For *K. pneumoniae*, a concentration of 10% serum was selected, which was found to reduce bacterial viability by 90% (Figure 6B). However, addition of rifampicin, nisin, and vancomycin further decreased viability significantly, while erythromycin and Q & D resulted in a moderate decrease in viability compared to serum alone (Figure 6B). Heat-inactivated serum in combination with these antibiotics did not display this effect (Supporting information, Figure S20, S22, and S23). The effect of serum with bacitracin, daptomycin, telavancin, oritavancin, and dalbavancin on bacterial viability was found to be negligible.

Similar to *K. pneumoniae*, serum also resulted in more than one log reduction of bacterial viability for *P. aeruginosa* when added at a concentration of 1% (Figure 6C). The

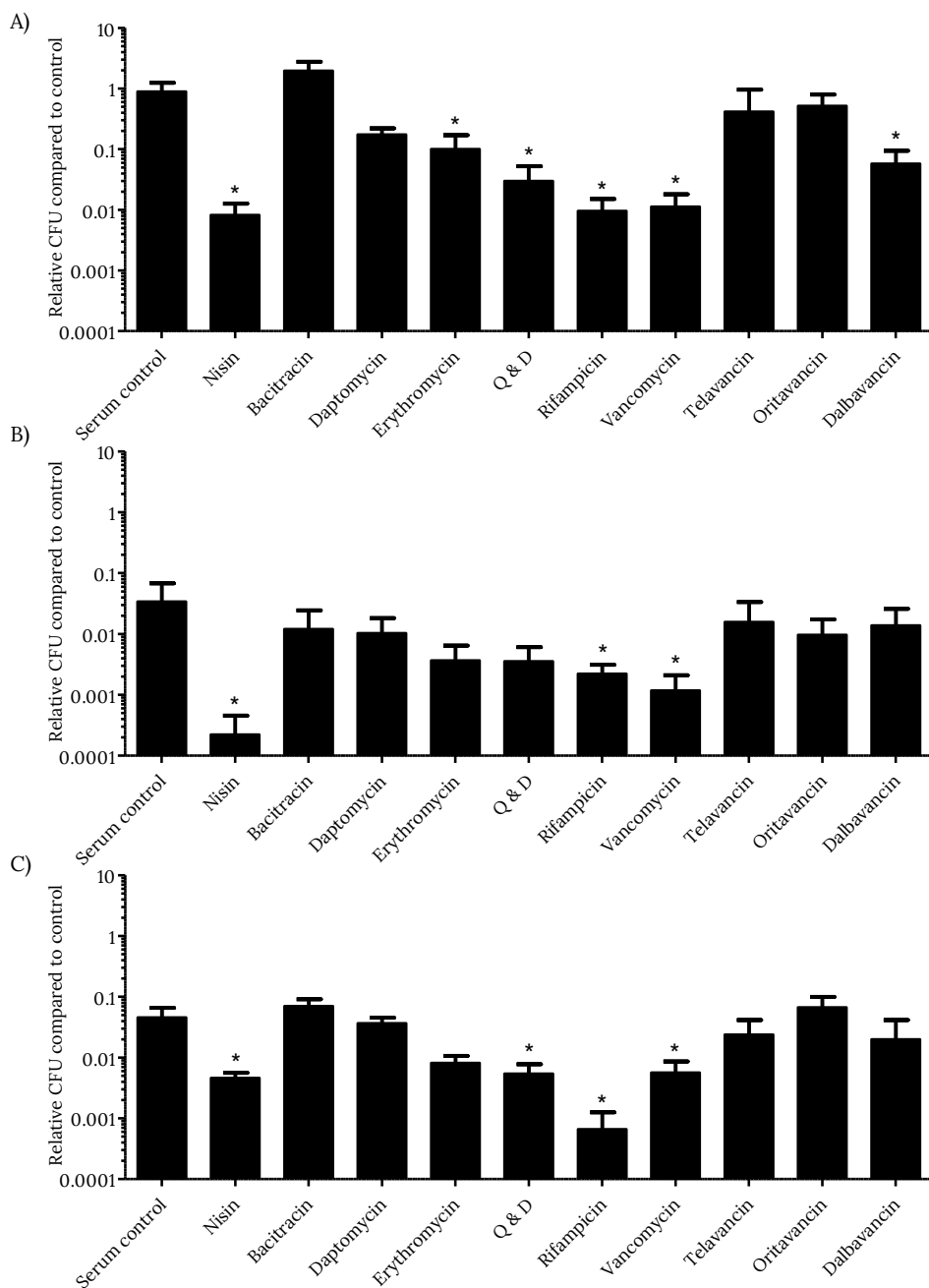


**Figure 6.** Synergy between serum and antibiotics: viability of A) *E. coli*; B) *K. pneumoniae*; C) *P. aeruginosa*. 2 hours of incubation with serum (0.3% for *E. coli*, 10% for *K. pneumoniae*, and 1% for *P. aeruginosa*) with 10 µg/mL antibiotics (for erythromycin 5, 2.5, 5 µg/mL and rifampicin 5, 2.5, 2.5 µg/mL respectively) at 37 °C with shaking. CFU counts were normalized to buffer controls. Data represent mean ± SD of three independent experiments and were analyzed by an one-way ANOVA and Dunnett test (\* $p < 0.05$ ) using the serum as control group.



combinations of serum with nisin, vancomycin, rifampicin, or Q & D significantly reduced the bacterial viability compared to the serum control (Figure 6C). Again, this effect was absent in the heat-inactivated serum with antibiotics combinations (Supporting information, Figure S21, S22, and S23). Erythromycin with serum did lower the bacterial viability visibly, but not significantly.

### 2.3. Potentiation by human serum differs among the glycopeptide antibiotics

In addition to vancomycin, the glycopeptides telavancin, oritavancin, and dalbavancin were selected to investigate the potentiation with serum within a class of antibiotics. For *E. coli*, a large increase in inner membrane permeability was observed for vancomycin, while for oritavancin, dalbavancin, and telavancin only a moderate increase was detected in the presence of serum (Figure 5A). In agreement with these findings, vancomycin combined with serum resulted in a significant decrease in bacterial viability (Figure 7A) while telavancin and oritavancin did not affect the viability. Notable, however, was the finding that dalbavancin also resulted in a significant reduction of bacterial viability (Figure 7A).

The combinations of telavancin, oritavancin, and dalbavancin with serum did not affect the inner membrane permeability of *K. pneumoniae*, nor its bacterial viability (Figure 5B and 7B). Vancomycin + serum resulted in both inner membrane permeability and a significant reduction in bacterial viability (Figure 5B and 7B). For *P. aeruginosa*, the inner membrane permeability was only slightly increased with the different glycopeptides (Figure 5C) with only vancomycin + serum causing a reduction of bacterial viability (Figure 7C).

These results were compared to different parameters of the glycopeptides (Table 2). The inherent activity of vancomycin is the least potent against Gram-positive bacteria, which seems contrary to our data on glycopeptide potentiation against Gram-negative bacteria. The greater lipophilicity and/or serum protein binding of the next generation glycopeptides relative to vancomycin could provide an explanation as to these findings. However, the significant reduction of *E. coli* viability by dalbavancin would seem to argue against this possibility.

**Table 2.** Inherent activity, (calculated) lipophilicity and protein binding of the glycopeptides

Glycopeptide	MIC <sub>90</sub> (μg/mL) <sup>55,56</sup>	XLogP3-AA	Protein binding <sup>65,66</sup>
<b>Vancomycin</b>	1	-2.6 <sup>57</sup>	30-55%
<b>Telavancin</b>	0.06	-2.1 <sup>58</sup>	90%
<b>Oritavancin</b>	0.12	1.5 <sup>59</sup>	85%
<b>Dalbavancin</b>	0.03	3.8 <sup>60</sup>	93%

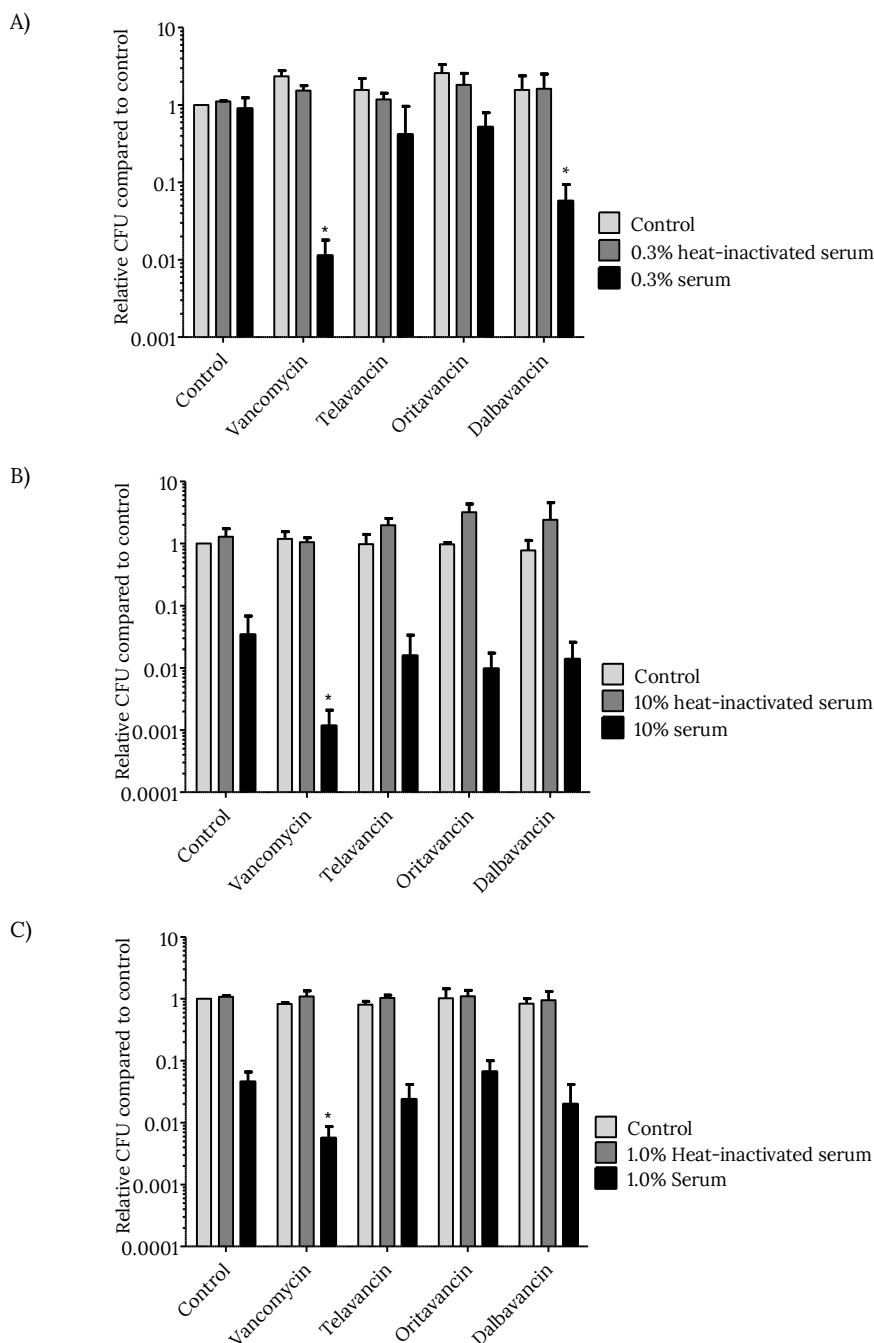


**Figure 7.** Synergy between serum and glycopeptide antibiotics. The viability of A) *E. coli*; B) *K. pneumoniae*; and C) *P. aeruginosa* was screened after 2 hours of incubation with buffer, heat-inactivated serum or serum with 10  $\mu\text{g}/\text{mL}$  antibiotics at 37  $^{\circ}\text{C}$  with shaking. CFU counts were normalized to buffer controls. Data represent mean  $\pm$  SD of three independent experiments and were analyzed by an one-way ANOVA and Dunnett test (\* $p < 0.05$ ) using the serum as control group.

### 3. Discussion and conclusion

The potentiation of antibiotics towards Gram-negative bacteria can be achieved by the addition of a chemical synergist capable of disrupting the outer membrane (Chapter 1). Although this field has been widely explored, mainly the discovery of new synergists is reported in addition to the work focused on the (clinical) development of the polymyxin derived synergists (Chapter 1).<sup>5</sup> The previous work by Heesterbeek *et al.* already illustrated that exogenous OM disruptors might not even be required in the presence of serum.<sup>18</sup> Based on the OM disruption mechanism of serum, an expanded screening of antibiotics, such as rifampicin, clindamycin, and erythromycin, often described as the antibiotic partners of the outer membrane disrupting chemical synergists, was suggested in the previous study.<sup>18</sup> In our investigation we therefore systematically explored the potentiation of many more Gram-positive specific antibiotic classes against *E. coli*, *K. pneumoniae*, and *P. aeruginosa*.

The inner membrane permeability assay was employed as a screening tool and clearly revealed the potentiation of nisin against three different Gram-negative bacterial species. For *E. coli* and *K. pneumoniae*, inner membrane damage was enhanced when serum was combined with vancomycin. Of note was the inherent activity of serum as a result of the prolonged incubation time compared to the previous study.<sup>18</sup> This effect was particularly visible for both *K. pneumoniae* and *P. aeruginosa*: at the 2-hour time point the effect of serum overshadowed the results with antibiotics. The inner membrane permeability assay, however, does allow for a dynamic read-out and selection of different time points. Still, ideally a serum concentration should be selected that results in no or a minimal increase in inner membrane permeability.

Other aspects to consider in the selection of the optimal serum concentration is the balanced nature of the choice: since on the one hand you pursue the minimal amount of inner membrane permeability by serum itself, but on the other hand the potentiation of antibiotics should be as potent as possible. Another aspect to consider is the length of incubation, since length of exposure to serum plays a role in the permeabilization of the inner membrane. While longer incubation might positively or negatively influence the gap between the serum and serum in combination with antibiotic signals, the dynamic read-out ensures that this effect can be monitored (Supporting information, Figure S1-S15). Lastly, the mode-of-action of different antibiotics, and therefore the speed of inhibition, should be considered in the selection of an incubation time and consequently the serum concentration. In the case, a different type of assay, such as the bacterial viability assay with an overnight incubation might prove more appropriate.

The effect of the 2-hour incubation with the selected serum concentration also results in a reduction in bacterial viability for *K. pneumoniae* and *P. aeruginosa* in the serum control. A lower serum concentration will reduce this effect. However, it is questionable whether the synergistic effect will be more pronounced: a lower concentration of serum will result in less pores and therefore lower influx of antibiotics.

Apart from screening different classes of antibiotics, several antibiotics of the glycopeptide class (vancomycin, telavancin, oritavancin, and dalbavancin) were selected to investigate their potentiation with serum. The reported synergy of vancomycin with serum against all three strains was clearly visible in the bacterial viability data and in the inner membrane permeability data of *E. coli* and *K. pneumoniae*. Also, the inner membrane permeability data for *E. coli* showed a moderate increase in permeability for

oritavancin, dalbavancin, and telavancin combined with serum (Figure 5A). Interestingly, only the combinations of serum with vancomycin and dalbavancin resulted in a significant reduction in bacterial viability for *E. coli*. When comparing the potentiation of the glycopeptides by serum against Gram-negative bacteria to the inherent activity of the glycopeptides against Gram-positive bacteria, the inherent activity of vancomycin is the least potent, but vancomycin does show the most potent synergy with serum. Characteristics such as lipophilicity and serum protein binding may explain the activity of vancomycin. However, the synergy of dalbavancin with serum against *E. coli* counters this hypothesis. In all assays a very low concentration of serum was employed and equates to low number of pores. The rate of influx could therefore be an important factor in potentiation by serum, since the accumulation of the glycopeptides in the periplasm is key for their activity against Gram-negative bacteria.

In line with the previous study, the combination of nisin and vancomycin showed a significantly reduced bacterial viability compared to the serum control (Figure 7 and Supporting information, Figure S22A).<sup>18</sup> These antimicrobial compounds both target bacterial cell wall synthesis, which resulted in the selection of bacitracin, another inhibitor of this process, as a suitable negative control (Supporting information, Figure S22B).<sup>34–37,61</sup> In addition to nisin and vancomycin, rifampicin also resulted in a significant reduction in viability against all three Gram-negative bacteria screened at concentrations of 5 µg/mL (Supporting information, Figure S23C). Of note, is the small effect of rifampicin itself on the Gram-negative bacteria, which is slightly visible in the *P. aeruginosa* data. Rifampicin, is known as an antibiotic partner to many outer membrane disrupting synergists (Chapter 1) and synergy of rifampicin with serum has been reported against an *E. coli* K-12.<sup>14</sup>

Two more antibiotics were significantly potentiated by serum against at least one strain: erythromycin and Q & D (Supporting information, Figure S23A-B). The macrolide antibiotic erythromycin targets the 50S subunit of the bacterial ribosome and inhibits the protein synthesis.<sup>62</sup> Its activity has been described as bacteriostatic against Gram-positive bacteria.<sup>63</sup> Q & D are two peptides marketed as Synercid, a synergistic combination, that also targets the bacterial protein synthesis.<sup>64,65</sup> Contrarily to erythromycin, Q & D is bactericidal against Gram-positive bacteria.<sup>65</sup> Like rifampicin, erythromycin has been widely described in synergy literature, specifically with outer membrane disruptors (Chapter 1). Interestingly, the study reporting potentiation of rifampicin by serum, also mentions that no synergy was found for erythromycin, contrary to our results.<sup>14</sup> For Q & D, we did not manage to find literature describing potentiation by serum against Gram-negative bacteria. A outer membrane disruptor derived of polymyxin was reported to potentiate Q & D against *E. coli*.<sup>5,66</sup>

Of interest is the lack of inner membrane permeability signal for erythromycin and rifampicin, since in literature for rifampicin an increase in SYTOX Green was reported for *E. coli*<sup>67</sup> and the effect of erythromycin was also screened using SYTOX Green against both Gram-positive and Gram-negative bacteria.<sup>68</sup> Contrarily to erythromycin and rifampicin, serum + daptomycin did display an increase in inner membrane permeability, however, it did not impact bacterial viability significantly (Supporting information, Figure S22C). The mechanisms of action of daptomycin is still being ironed out in literature, the current consensus is the insertion into the membrane after oligomerization results in depolarization leading to the inhibition of growth and division of cells.<sup>44–46</sup> The sensitivity of the SYTOX Green in combination with such a

membrane-targeting mechanism could provide an additional explanation for this difference between the two assays. The sensitivity of the inner membrane permeability assay could be another explanation as there is a one-log reduction in viability for *E. coli*. Daptomycin only seems to have an effect with serum on *E. coli* and it could be speculated that the protein binding of daptomycin, could interfere with its inherent activity since the serum concentration employed is higher for *K. pneumoniae* and *P. aeruginosa* bacterial viability assays.<sup>69</sup> Recently, a study also reported daptomycin tolerance in the Gram-positive bacteria *Staphylococcus aureus* triggered by human serum.<sup>70</sup>

In conclusion, a systematic screening of Gram-positive specific antibiotics in combination with serum against three different Gram-negative bacteria was performed. A clear increase in inner membrane damage and bacterial viability is seen for nisin and vancomycin in the presence of serum. However, for the other tested antibiotics increases in inner membrane damage could not be validated with a significant change in bacterial viability. An exception was the potentiation of human serum with dalbavancin against *E. coli* as the moderate increase in SYTOX Green fluorescence correlated to a significant reduction in bacterial viability. In addition, this study has revealed the need for optimization of the serum concentration and identified the optimal concentrations of rifampicin and erythromycin. Also, in the case of rifampicin, erythromycin, and Q & D, only the bacterial viability assay revealed that these antibiotics were significantly potentiated by serum. An alternative screening method might be more suitable for these antibiotics than the inner membrane permeability assay using SYTOX Green. Most importantly, this study reports new synergistic combinations of serum and Gram-positive specific antibiotics, further revealing how the complement system can work together with Gram-positive specific antibiotics to kill Gram-negative bacteria.

## 4. Materials and methods

### 4.1. Antibiotics

All antibiotics employed were of American Chemical Society (ACS) grade or finer and were used without further purification unless otherwise stated. Nisin was HPLC purified as this antibiotic was not obtained in an ACS grade.

### 4.2. Serum preparation

For normal human serum preparation, blood was drawn from healthy volunteers and allowed to clot for 15 minutes at RT. After centrifugation (10 min, 4000 rpm), serum was collected, pooled and stored at -80 °C. Heat-inactivated serum was obtained by incubating serum for 30 min at 56 °C.

### 4.3. Bacterial inner membrane permeabilization assay using SYTOX Green

The assay was performed based on a protocol described in literature.<sup>18</sup> Bacteria were grown an OD<sub>600nm</sub> of 0.5 in Lysogeny Broth (LB) medium, pelleted by centrifugation and resuspended to OD<sub>600nm</sub> of 1.0 in RPMI 1640 (ThermoFisher) supplemented with 0.05% HSA. The bacteria were diluted by a ten-fold, final concentration of OD<sub>600nm</sub> ~ 0.05. For *E. coli* the bacteria were incubated with 0 or 0.3% serum or 0.3% heat-inactivated serum. For *P. aeruginosa* the selected concentration was 1% and for *K. pneumoniae* 10%. Incubations were done in the presence of 1 µM SYTOX Green Nucleic Acid stain (Thermofisher). Fluorescence was measured in a microplate reader (CLARIOstar, Labtech) at 37 °C under shaking conditions for 2 hours. Synergy experiments were performed by incubating bacteria with the antibiotics in a 10 µg/mL final concentration except for rifampicin and erythromycin: erythromycin 5, 2.5, 5 µg/mL and rifampicin 5, 2.5, 2.5 µg/mL for *E. coli*, *K. pneumoniae* and *P. aeruginosa* respectively

### 4.4. Bacterial viability assay

The assay was performed based on a protocol described in literature.<sup>18</sup> Bacteria were prepared as described above and incubated with buffer, serum or blood (drawn from healthy volunteers) in the presence or absence of antibiotics (10 µg/ml, except for rifampicin and erythromycin, as described above). For CFU/ml determination, serial dilutions were made in PBS and bacteria were plated onto agar plates followed by colony enumeration after overnight incubation. Relative viability was calculated as the number of CFU/ml relative to the buffer control.

### 4.5. Statistical testing

Statistical analysis was performed using a one-way ANOVA and Dunnett test (\*p < 0.05) using the serum as control group in Graphpad. The tests and n-values used to calculate p-values are also mentioned in the figure captions.

### 4.6. Ethics statement

Human blood was isolated after informed consent was obtained from all subjects in accordance with the Declaration of Helsinki. Approval was obtained from the medical ethics committee of the UMC Utrecht, The Netherlands.

## Supporting information

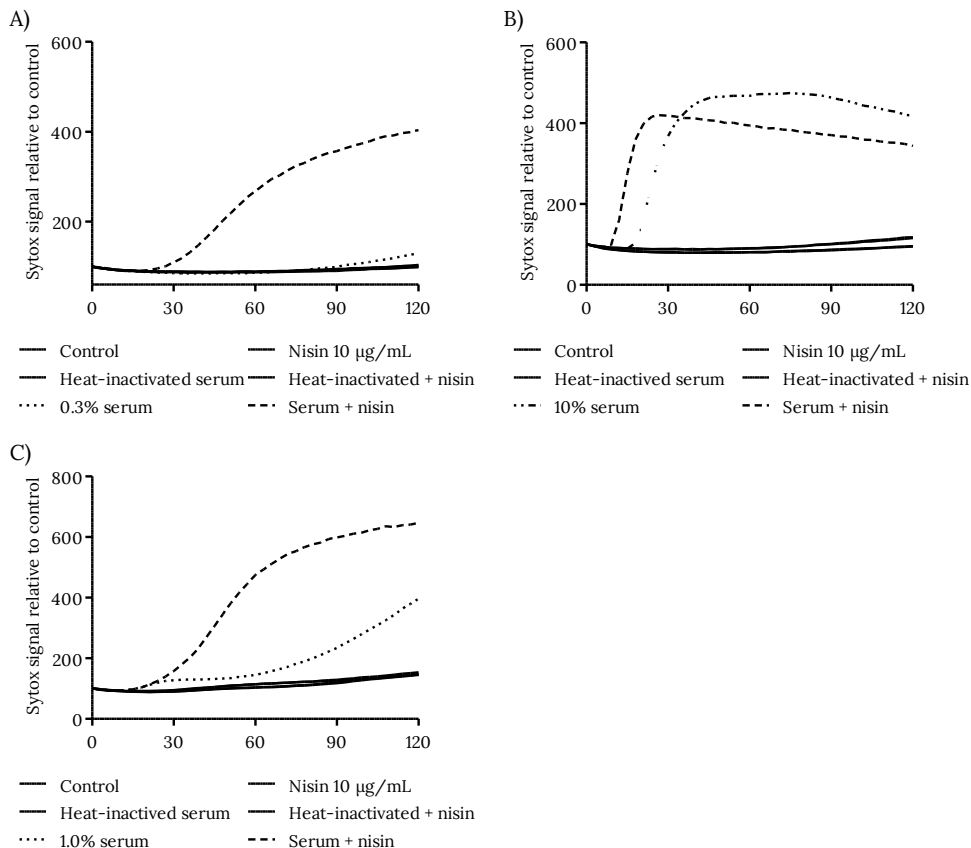


**Figure S1.** Dynamic read-out of the inner permeability assays for nisin with A) *E. coli*; B) *K. pneumoniae*; C) *P. aeruginosa*. The bacteria were incubated with buffer (control), heat-inactive serum, and serum with or without 10  $\mu\text{g/mL}$  nisin at 37 °C. The concentrations of serum used were 0.3%, 10%, and 1.0% respectively. SYTOX Green intensity was measured every 3 minutes for 120 minutes in a microplate fluorometer. Values were corrected and represent mean  $\pm$  SD of three independent experiments.

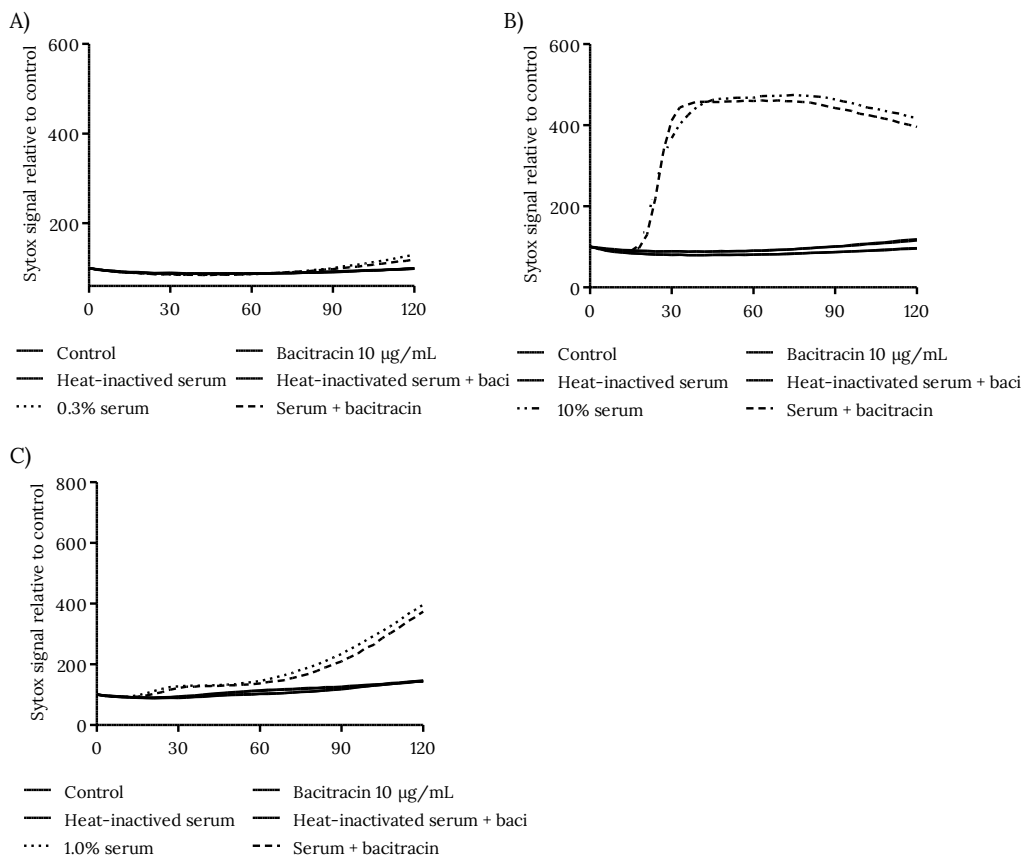


**Figure S2.** Dynamic read-out of the inner permeability assays for bacitracin with A) *E. coli*; B) *K. pneumoniae*; C) *P. aeruginosa*. The bacteria were incubated with buffer (control), heat-inactive serum, and serum with or without 10 µg/mL bacitracin at 37 °C. The concentrations of serum used were 0.3%, 10%, and 1.0% respectively. SYTOX Green intensity was measured every 3 minutes for 120 minutes in a microplate fluorometer. Values were corrected and represent mean  $\pm$  SD of three independent experiments.



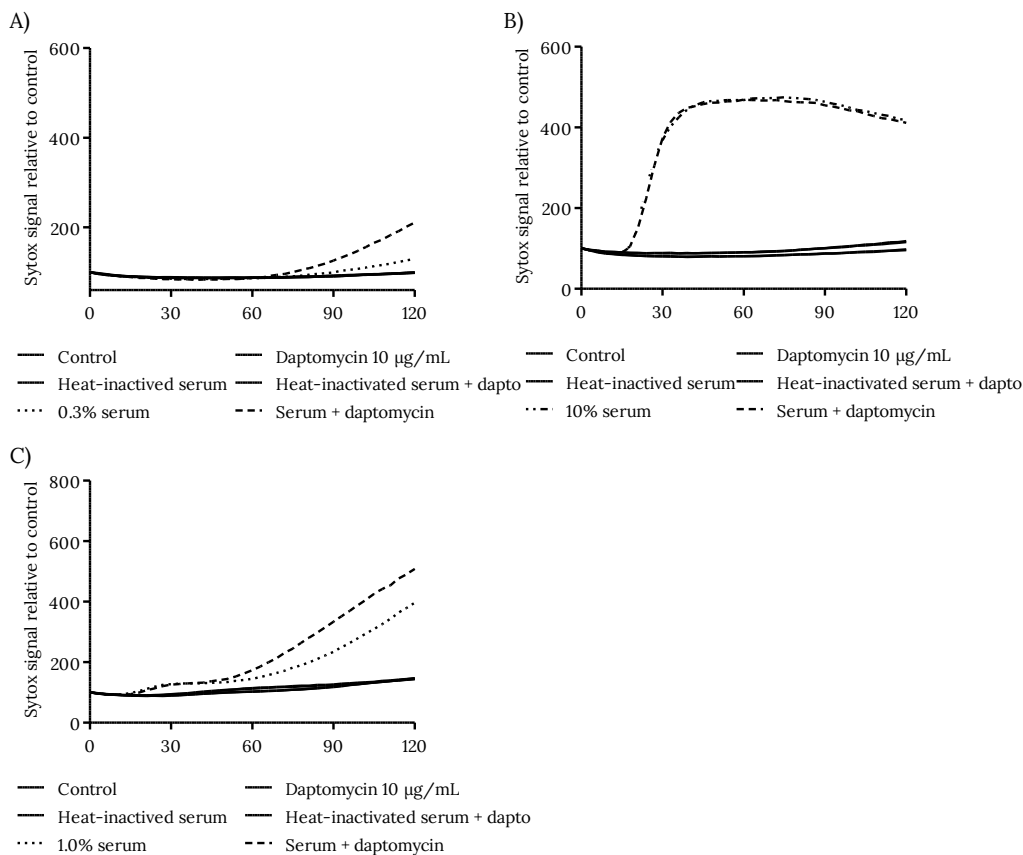


**Figure S3.** Dynamic read-out of the inner permeability assays for daptomycin with A) *E. coli*; B) *K. pneumoniae*; C) *P. aeruginosa*. The bacteria were incubated with buffer (control), heat-inactive serum, and serum with or without 10 µg/mL daptomycin at 37 °C. The concentrations of serum used were 0.3%, 10%, and 1.0% respectively. SYTOX Green intensity was measured every 3 minutes for 120 minutes in a microplate fluorometer. Values were corrected and represent mean ± SD of three independent experiments.

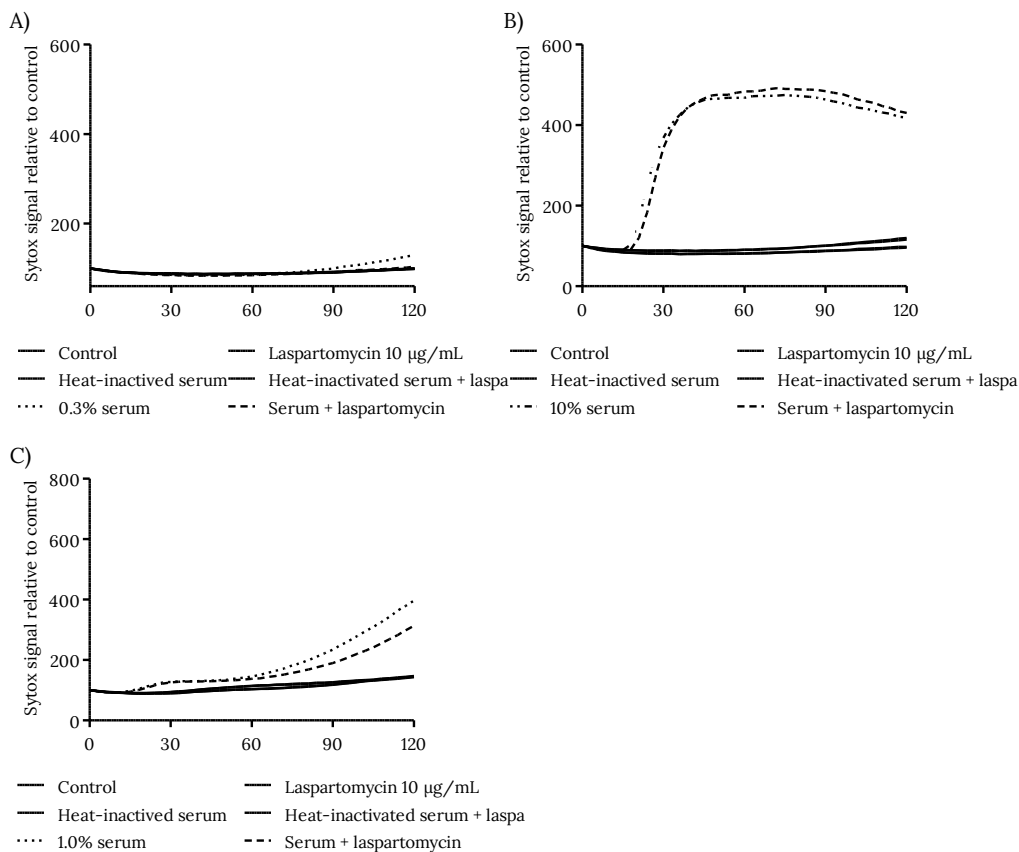


**Figure S4.** Dynamic read-out of the inner permeability assays for laspartomycin with A) *E. coli*; B) *K. pneumoniae*; C) *P. aeruginosa*. The bacteria were incubated with buffer (control), heat-inactive serum, and serum with or without 10 µg/mL laspartomycin at 37 °C. The concentrations of serum used were 0.3%, 10%, and 1.0% respectively. SYTOX Green intensity was measured every 3 minutes for 120 minutes in a microplate fluorometer. Values were corrected and represent mean ± SD of three independent experiments.

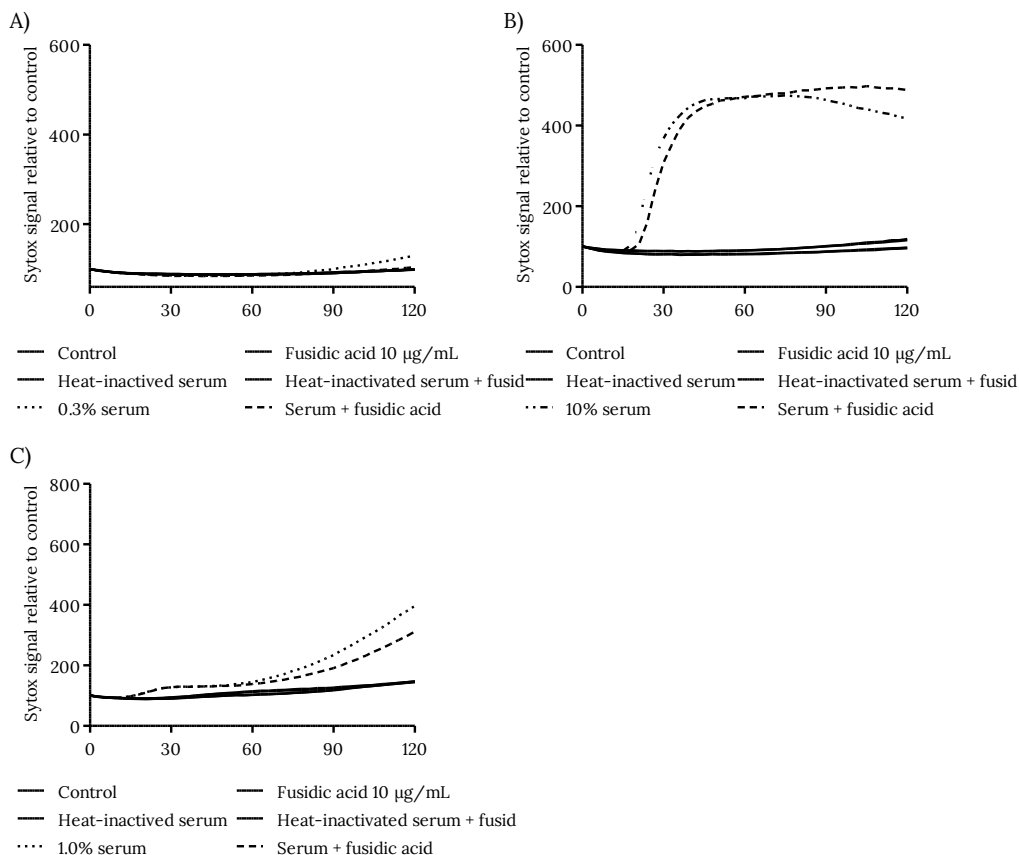


**Figure S5.** Dynamic read-out of the inner permeability assays for fusidic acid with A) *E. coli*; B) *K. pneumoniae*; C) *P. aeruginosa*. The bacteria were incubated with buffer (control), heat-inactive serum, and serum with or without 10 µg/mL fusidic acid at 37 °C. The concentrations of serum used were 0.3%, 10%, and 1.0% respectively. SYTOX Green intensity was measured every 3 minutes for 120 minutes in a microplate fluorometer. Values were corrected and represent mean ± SD of three independent experiments.

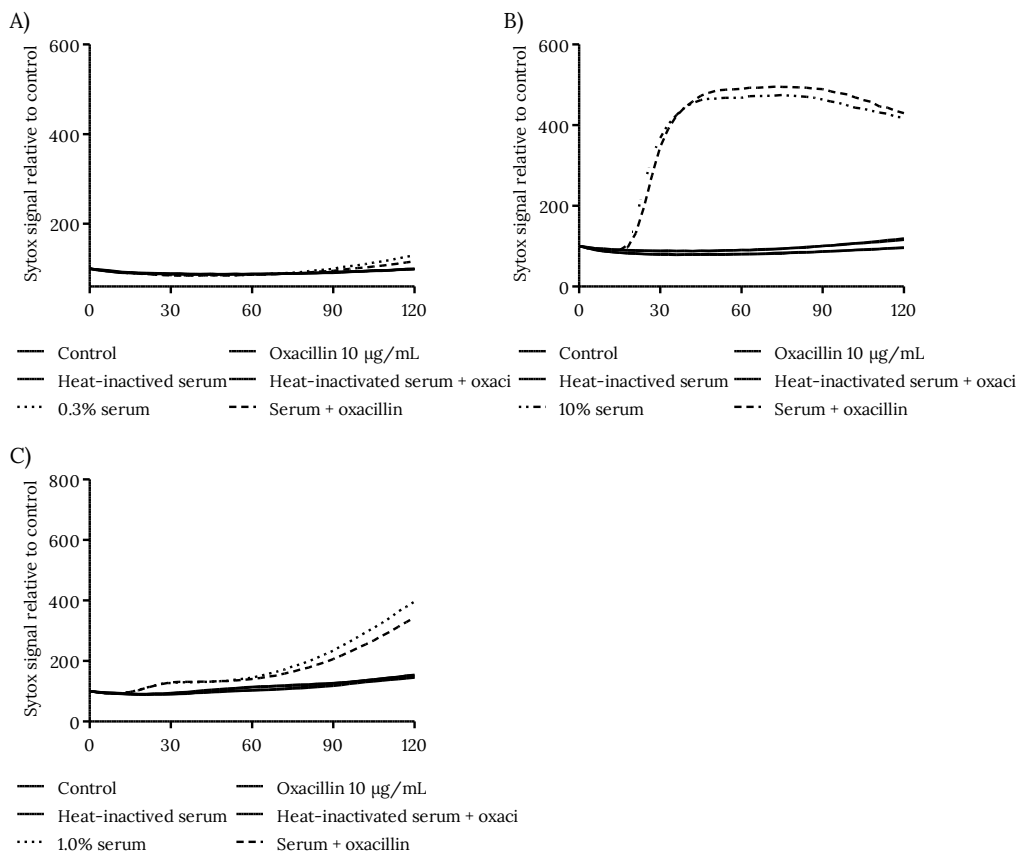


**Figure S6.** Dynamic read-out of the inner permeability assays for oxacillin with A) *E. coli*; B) *K. pneumoniae*; C) *P. aeruginosa*. The bacteria were incubated with buffer (control), heat-inactive serum, and serum with or without 10 µg/mL oxacillin at 37 °C. The concentrations of serum used were 0.3%, 10%, and 1.0% respectively. SYTOX Green intensity was measured every 3 minutes for 120 minutes in a microplate fluorometer. Values were corrected and represent mean ± SD of three independent experiments.

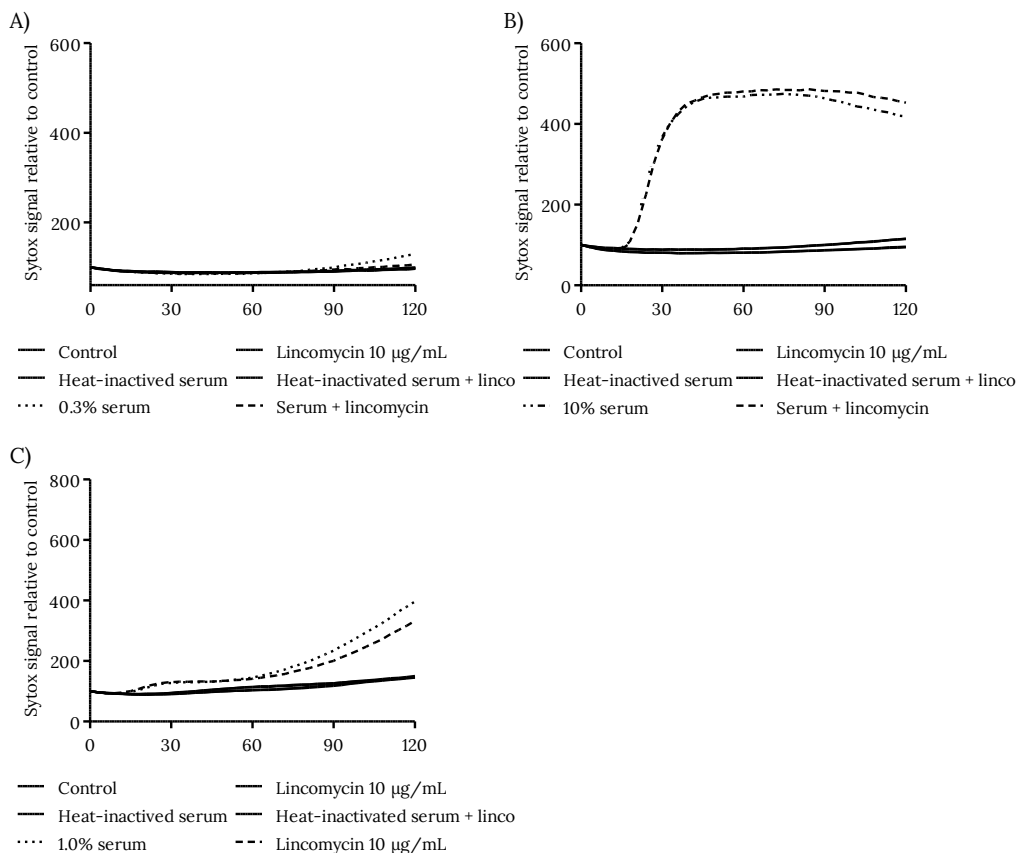


**Figure S7.** Dynamic read-out of the inner permeability assays for lincomycin with A) *E. coli*; B) *K. pneumoniae*; C) *P. aeruginosa*. The bacteria were incubated with buffer (control), heat-inactive serum, and serum with or without 10 µg/mL lincomycin at 37 °C. The concentrations of serum used were 0.3%, 10%, and 1.0% respectively. SYTOX Green intensity was measured every 3 minutes for 120 minutes in a microplate fluorometer. Values were corrected and represent mean ± SD of three independent experiments.

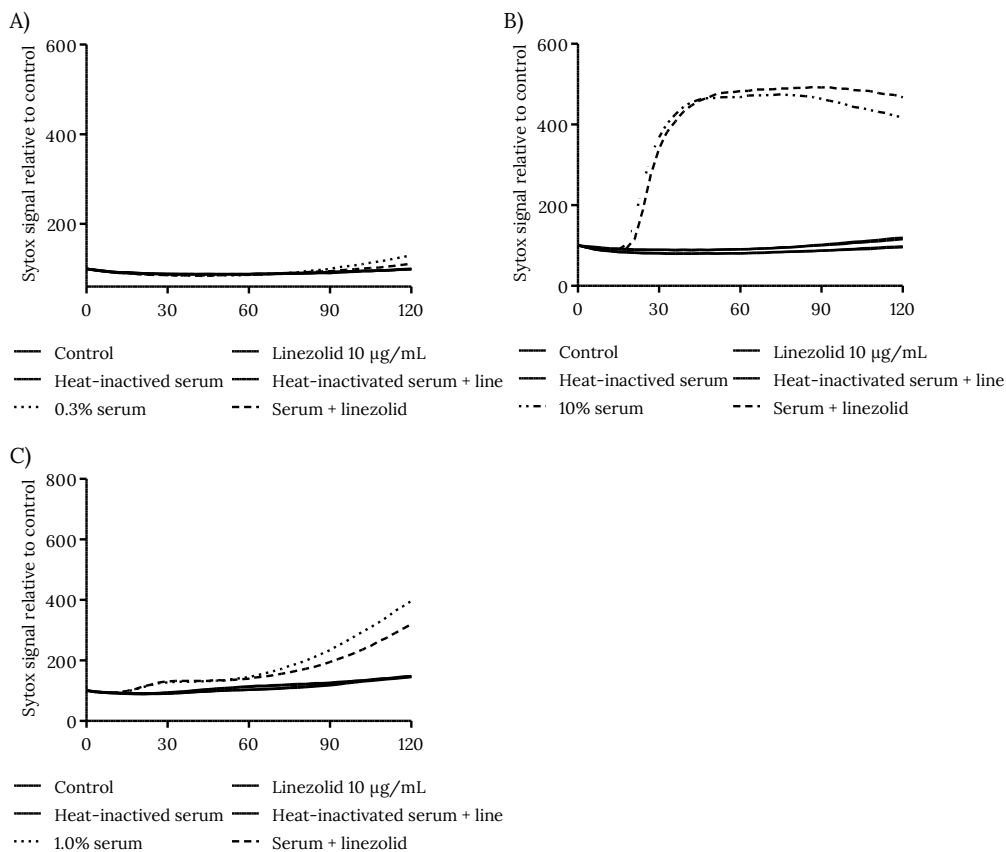


**Figure S8.** Dynamic read-out of the inner permeability assays for linezolid with A) *E. coli*; B) *K. pneumoniae*; C) *P. aeruginosa*. The bacteria were incubated with buffer (control), heat-inactivate serum, and serum with or without 10 µg/mL linezolid at 37 °C. The concentrations of serum used were 0.3%, 10%, and 1.0% respectively. SYTOX Green intensity was measured every 3 minutes for 120 minutes in a microplate fluorometer. Values were corrected and represent mean ± SD of three independent experiments.

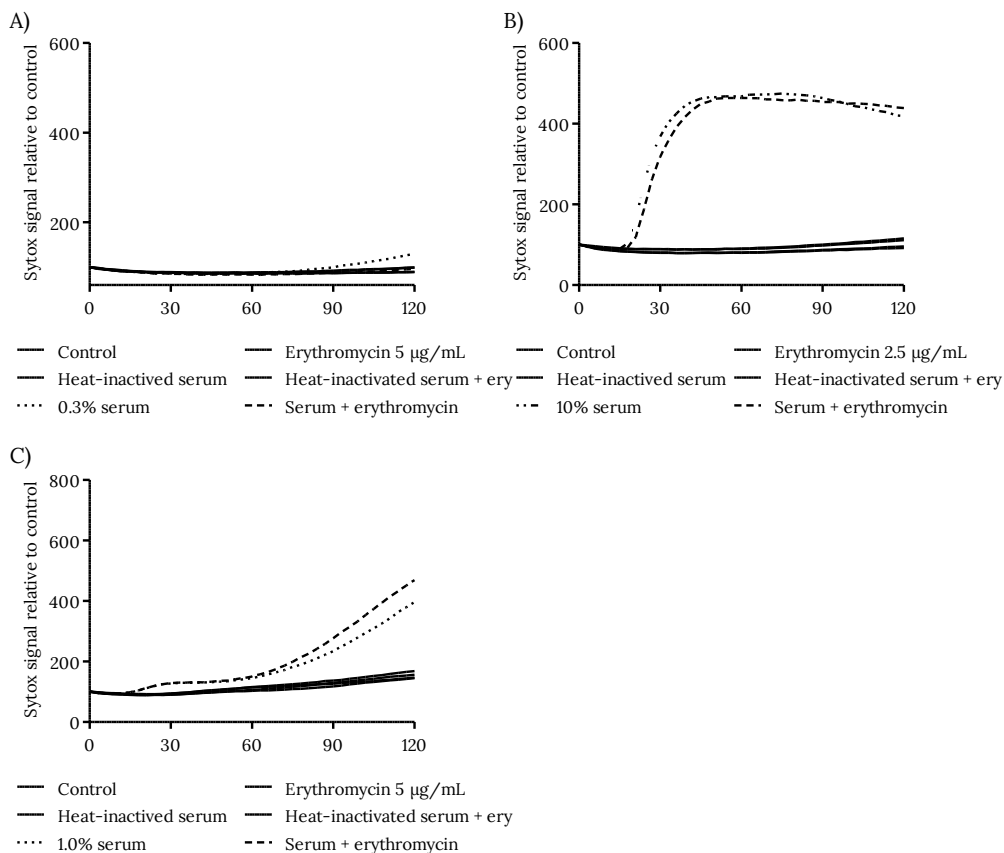


**Figure S9.** Dynamic read-out of the inner permeability assays for erythromycin with A) *E. coli*; B) *K. pneumoniae*; C) *P. aeruginosa*. The bacteria were incubated with buffer (control), heat-inactive serum, and serum with or without 5, 2.5, and 5  $\mu\text{g/mL}$  erythromycin respectively at 37 °C. The concentrations of serum were 0.3%, 10%, and 1.0% respectively. SYTOX Green intensity was measured every 3 minutes for 120 minutes in a microplate fluorometer. Values were corrected and represent mean  $\pm$  SD of three independent experiments.

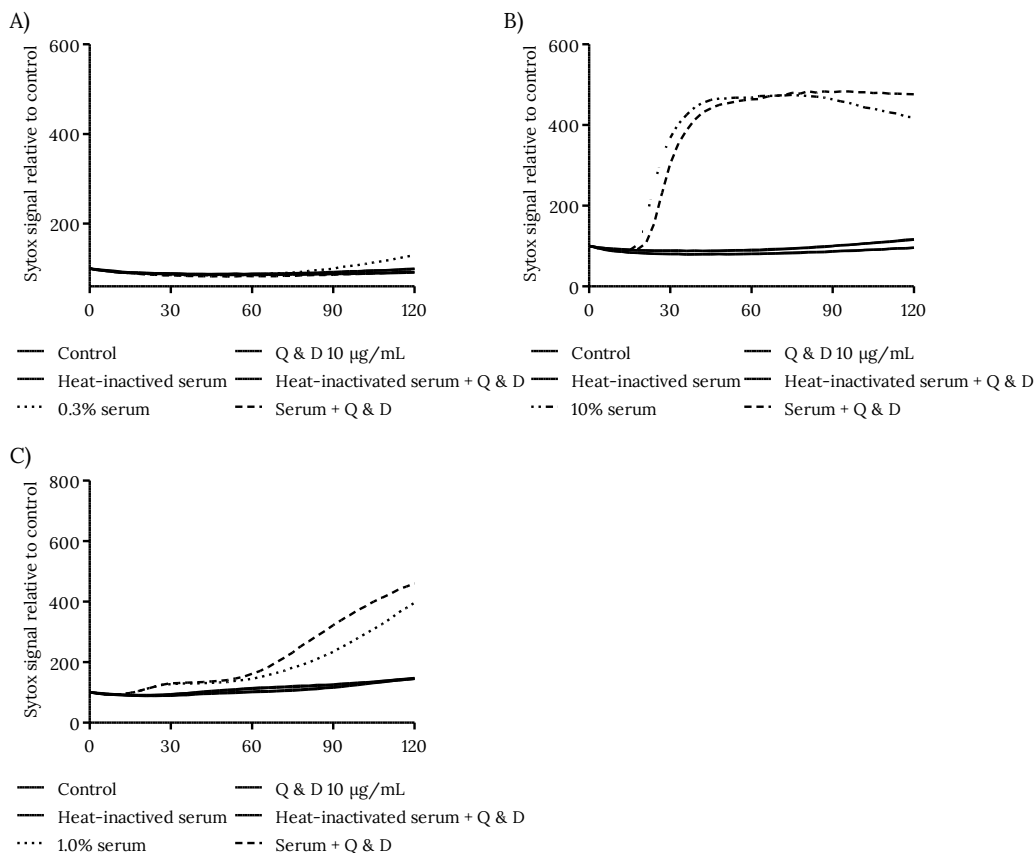


**Figure S10.** Dynamic read-out of the inner permeability assays for quinupristin & dalbapristin (Q & D) with A) *E. coli*; B) *K. pneumoniae*; C) *P. aeruginosa*. The bacteria were incubated with buffer (control), heat-inactive serum, and serum with or without 10 µg/mL Q & D at 37 °C. The concentrations of serum used were 0.3%, 10%, and 1.0% respectively. SYTOX Green intensity was measured every 3 minutes for 120 minutes in a microplate fluorometer. Values were corrected and represent mean  $\pm$  SD of three independent experiments.



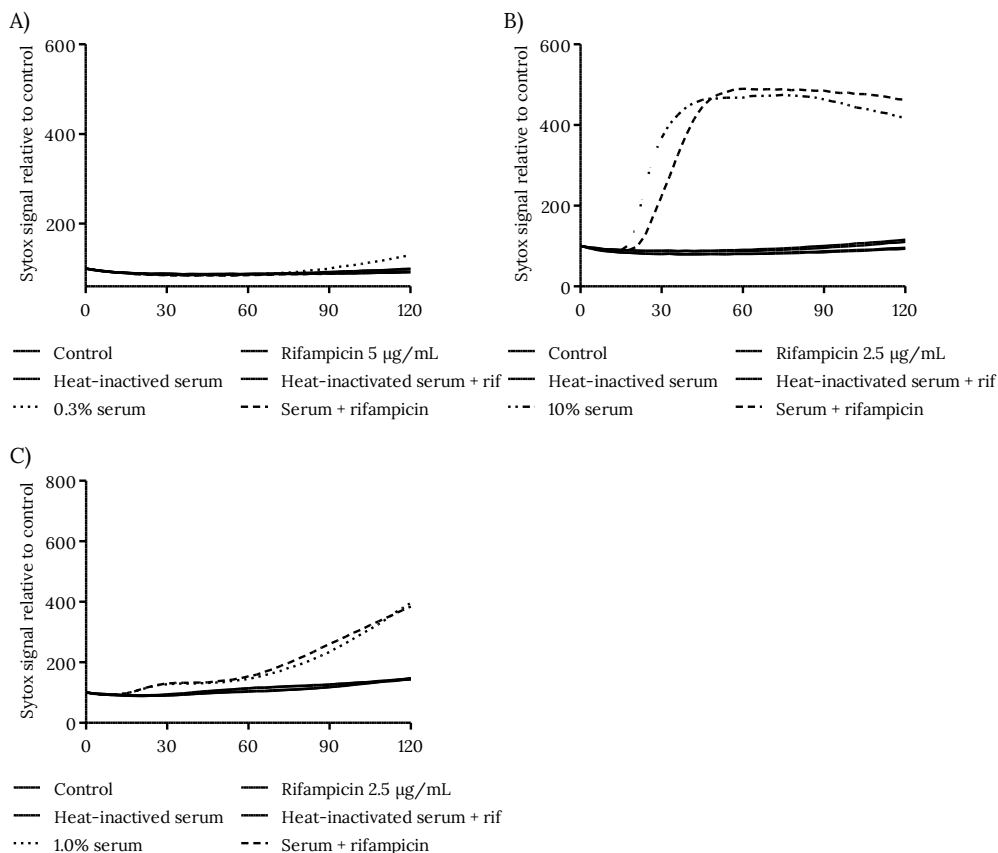


**Figure S11.** Dynamic read-out of the inner permeability assays for rifampicin with A) *E. coli*; B) *K. pneumoniae*; C) *P. aeruginosa*. The bacteria were incubated with buffer (control), heat-inactive serum, and serum with or without 5, 2.5, and 2.5 µg/mL rifampicin respectively at 37 °C. The concentrations of serum used were 0.3%, 10%, and 1.0% respectively. SYTOX Green intensity was measured every 3 minutes for 120 minutes in a microplate fluorometer. Values were corrected and represent mean  $\pm$  SD of three independent experiments.

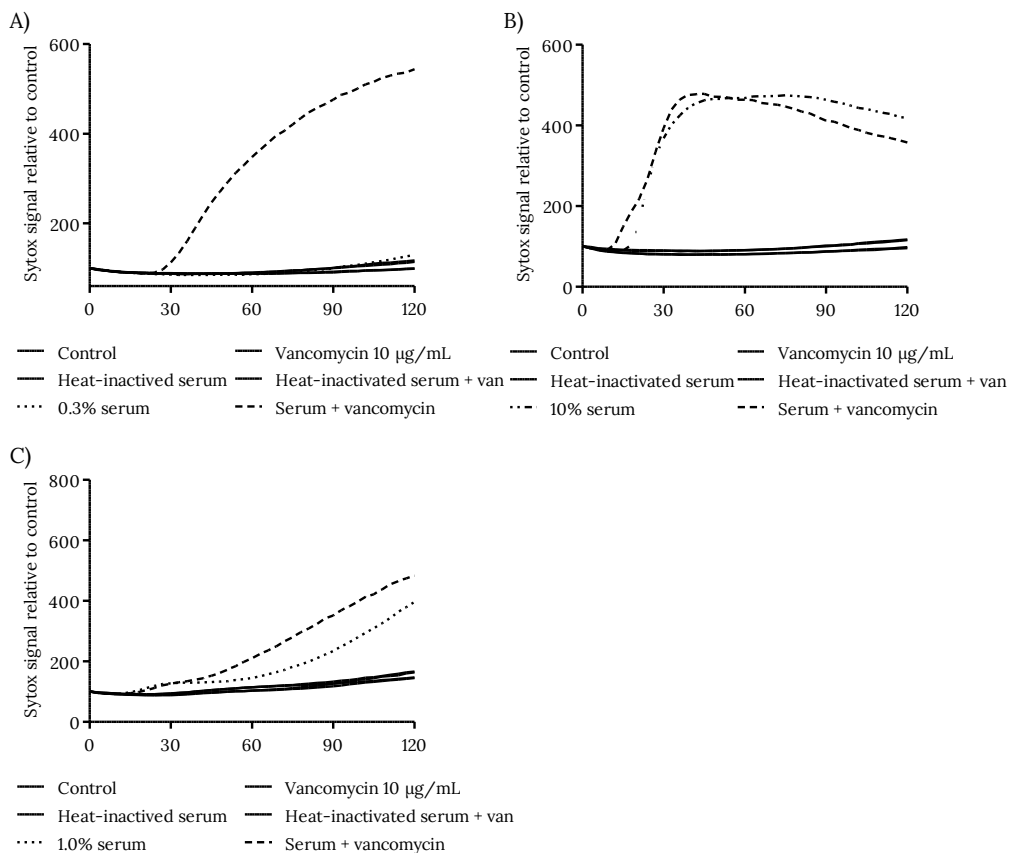


**Figure S12.** Dynamic read-out of the inner permeability assays for vancomycin with A) *E. coli*; B) *K. pneumoniae*; C) *P. aeruginosa*. The bacteria were incubated with buffer (control), heat-inactive serum, and serum with or without 10 µg/mL vancomycin at 37 °C. The concentrations of serum used were 0.3%, 10%, and 1.0% respectively. SYTOX Green intensity was measured every 3 minutes for 120 minutes in a microplate fluorometer. Values were corrected and represent mean ± SD of three independent experiments

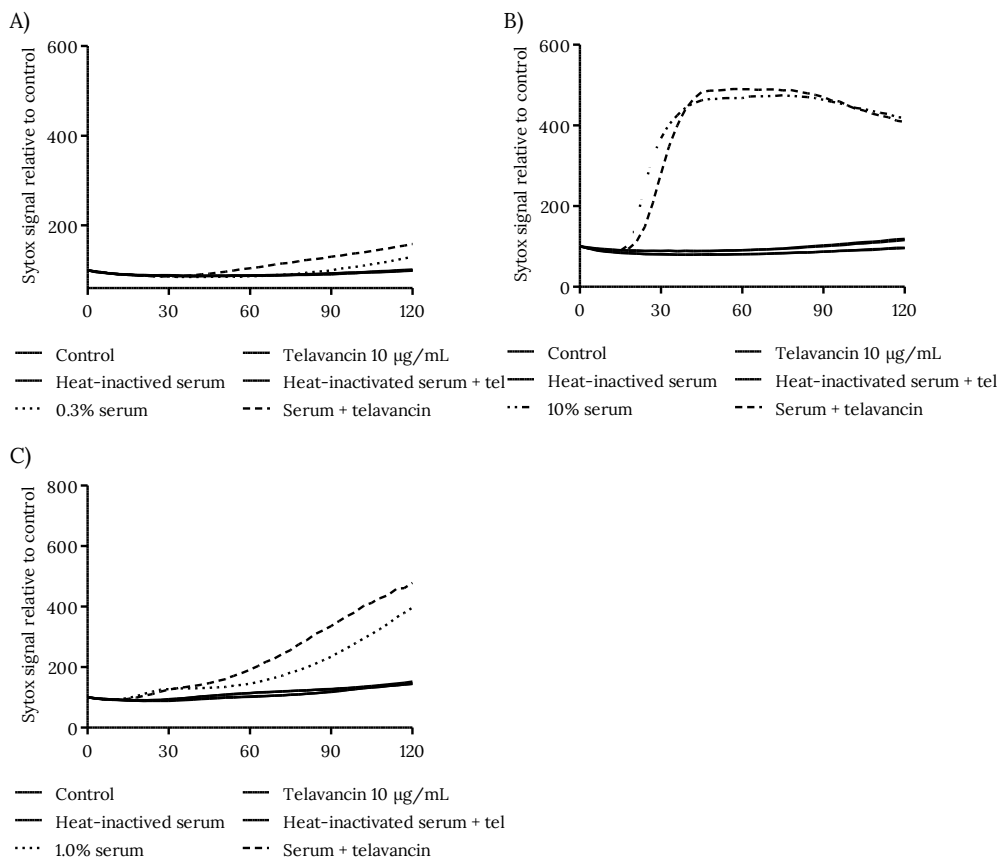


**Figure S13.** Dynamic read-out of the inner permeability assays for telavancin with A) *E. coli*; B) *K. pneumoniae*; C) *P. aeruginosa*. The bacteria were incubated with buffer (control), heat-inactive serum, and serum with or without 10 µg/mL telavancin at 37 °C. The concentrations of serum used were 0.3%, 10%, and 1.0% respectively. SYTOX Green intensity was measured every 3 minutes for 120 minutes in a microplate fluorometer. Values were corrected and represent mean ± SD of three independent experiments.

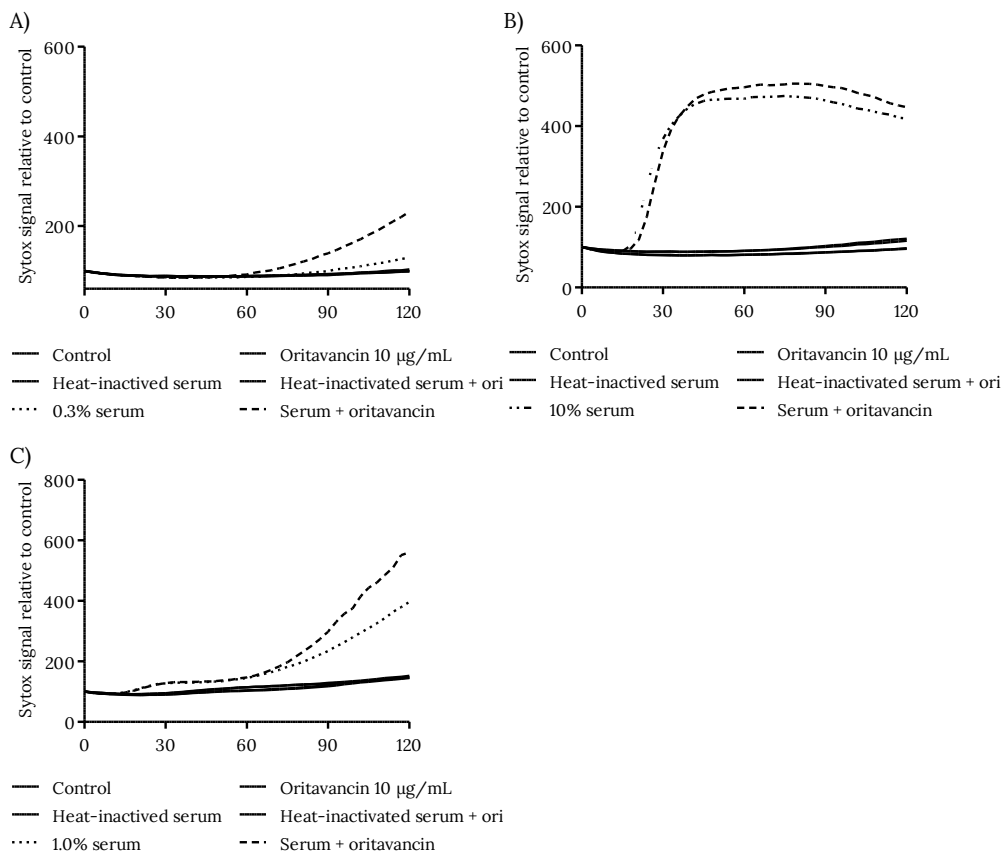


**Figure S14.** Dynamic read-out of the inner permeability assays for oritavancin with A) *E. coli*; B) *K. pneumoniae*; C) *P. aeruginosa*. The bacteria were incubated with buffer (control), heat-inactive serum, and serum with or without 10  $\mu\text{g/mL}$  oritavancin at 37 °C. The concentrations of serum used were 0.3%, 10%, and 1.0% respectively. SYTOX Green intensity was measured every 3 minutes for 120 minutes in a microplate fluorometer. Values were corrected and represent mean  $\pm$  SD of three independent experiments

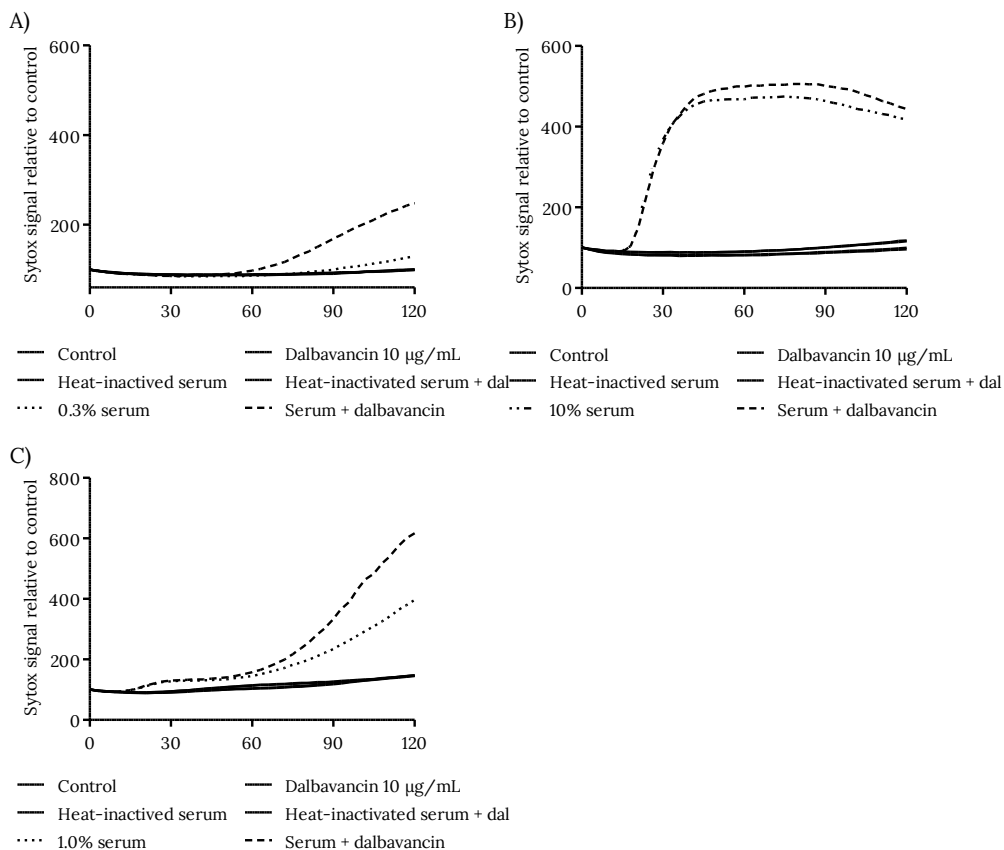


**Figure S15.** Dynamic read-out of the inner permeability assays for dalbavancin with A) *E. coli*; B) *K. pneumoniae*; C) *P. aeruginosa*. The bacteria were incubated with buffer (control), heat-inactive serum, and serum with or without 10 µg/mL dalbavancin at 37 °C. The concentrations of serum used were 0.3%, 10%, and 1.0% respectively. SYTOX Green intensity was measured every 3 minutes for 120 minutes in a microplate fluorometer. Values were corrected and represent mean ± SD of three independent experiments

**SYTOX read-out of *K. pneumoniae* and *P. aeruginosa* at 2 hours**

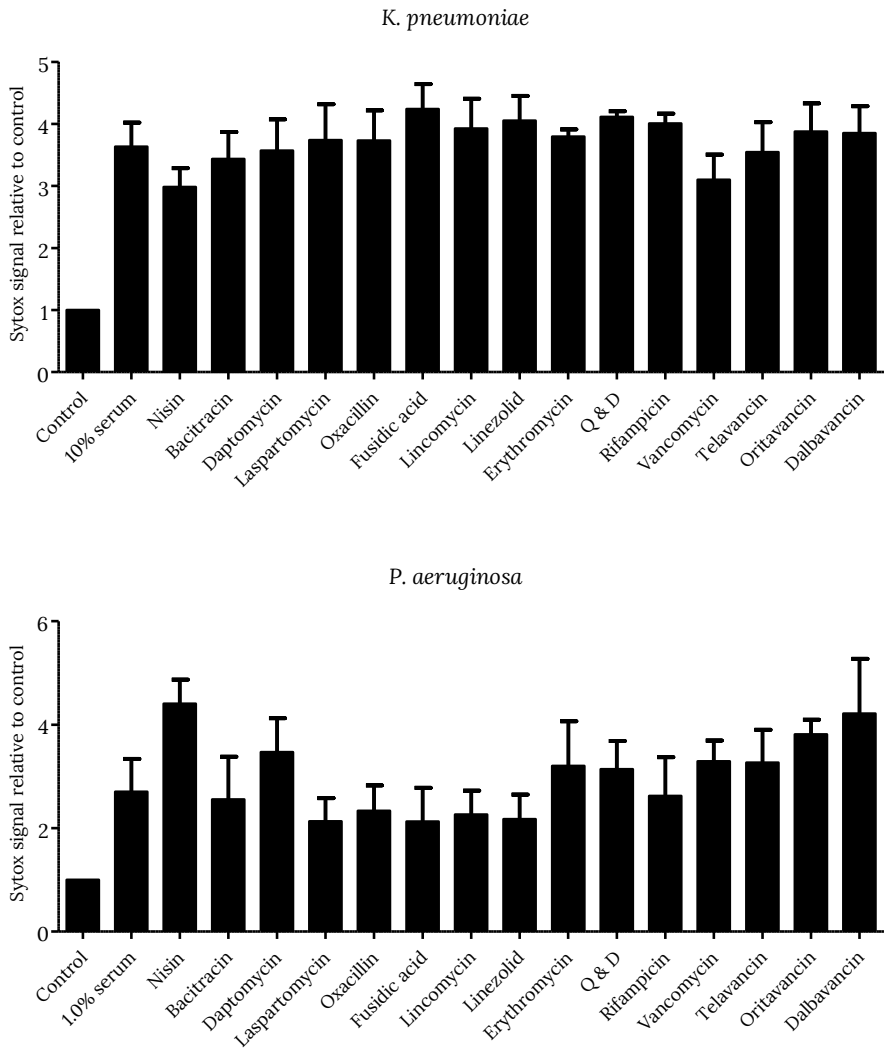


**Figure S16.** Inner permeability assay data of *K. pneumoniae* and *P. aeruginosa* at 2 hours. The antibiotics (10  $\mu\text{g}/\text{mL}$ , except for erythromycin (2.5, 5  $\mu\text{g}/\text{mL}$  respectively) and rifampicin (2.5, 2.5  $\mu\text{g}/\text{mL}$  respectively) were screened in combination with serum (10% for *K. pneumoniae*, and 1% for *P. aeruginosa*). Values were depicted as relative values to the control condition and represent mean  $\pm$  SD of three independent experiments.

### Erythromycin concentrations vs. CFU/mL

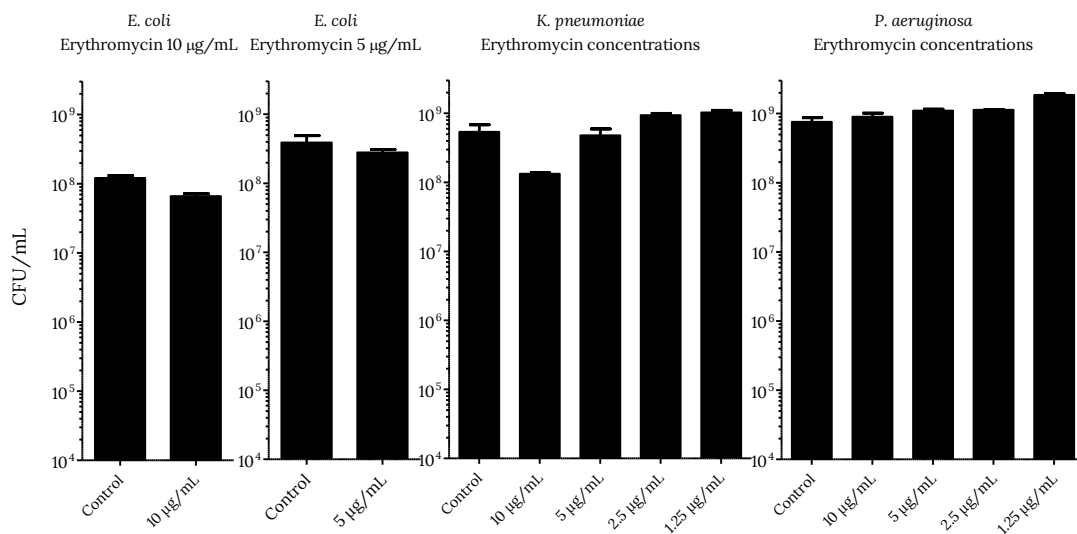


**Figure S17.** Bacterial viability assay for establishing inherent activity of erythromycin. The viability of the bacteria was screened after 2 hours of incubation with buffer with concentrations of 10, 5 or 10 to 1.25 µg/mL at 37 °C with shaking. Data represent mean ± SD of 2 technical replicates from a single experiment.

### Rifampicin concentrations vs. CFU/mL

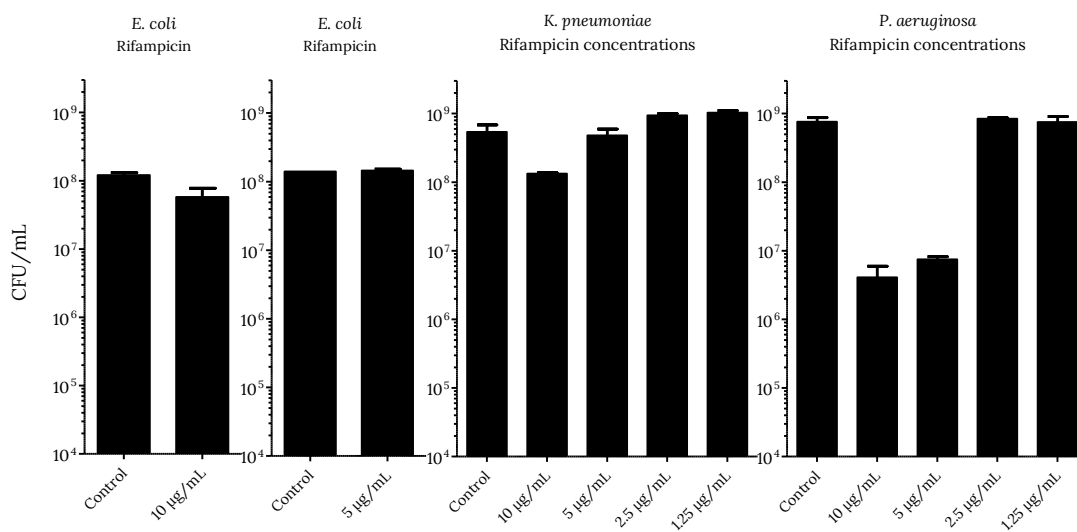


**Figure S18.** Bacterial viability assay for establishing inherent activity of rifampicin. The viability of the bacteria was screened after 2 hours of incubation with buffer with concentrations of 10, 5, or 10 to 1.25 µg/mL at 37 °C with shaking. Data represent mean ± SD of 2 technical replicates from a single experiment.

Overview results of bacterial viability assay

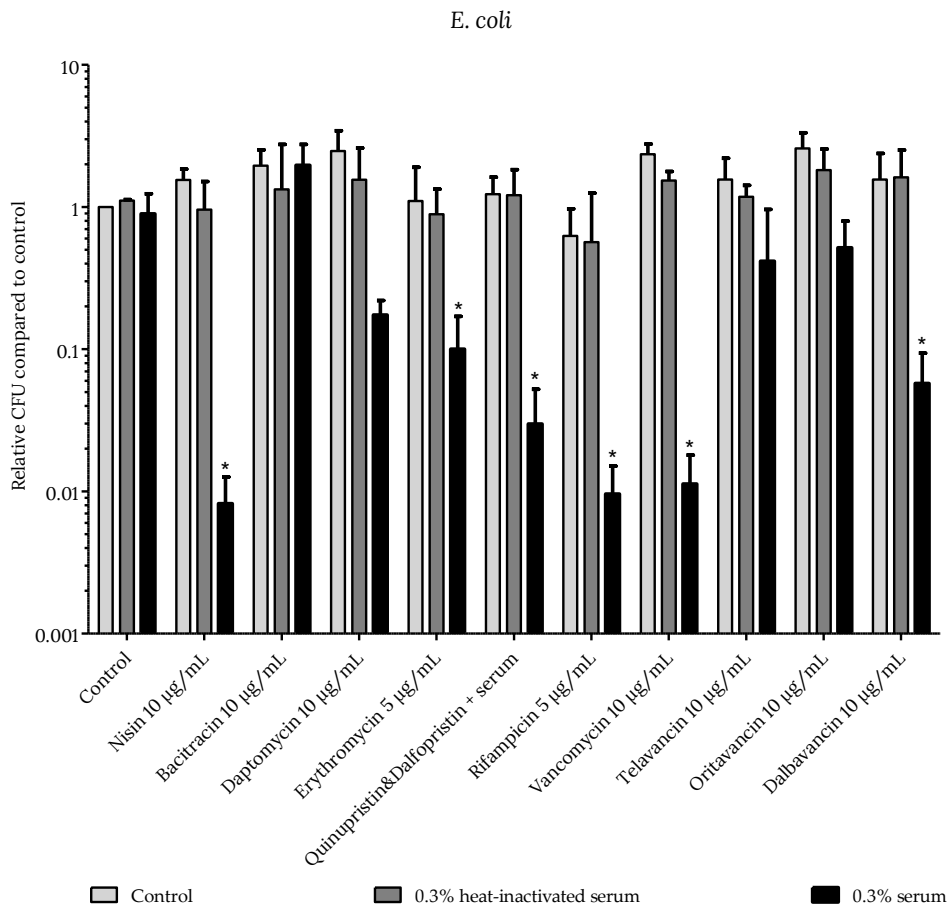


**Figure S19.** Synergy between serum and antibiotics in the bacterial viability assay. The viability of *E. coli* was screened after 2 hours of incubation with buffer, 0.3% heat-inactivated serum or 0.3% serum with 10 µg/mL antibiotics at 37 °C with shaking. CFU counts were normalized to buffer controls. Dashed line represent detection limit. Data represent mean ± SD of three independent.



*K. pneumoniae*

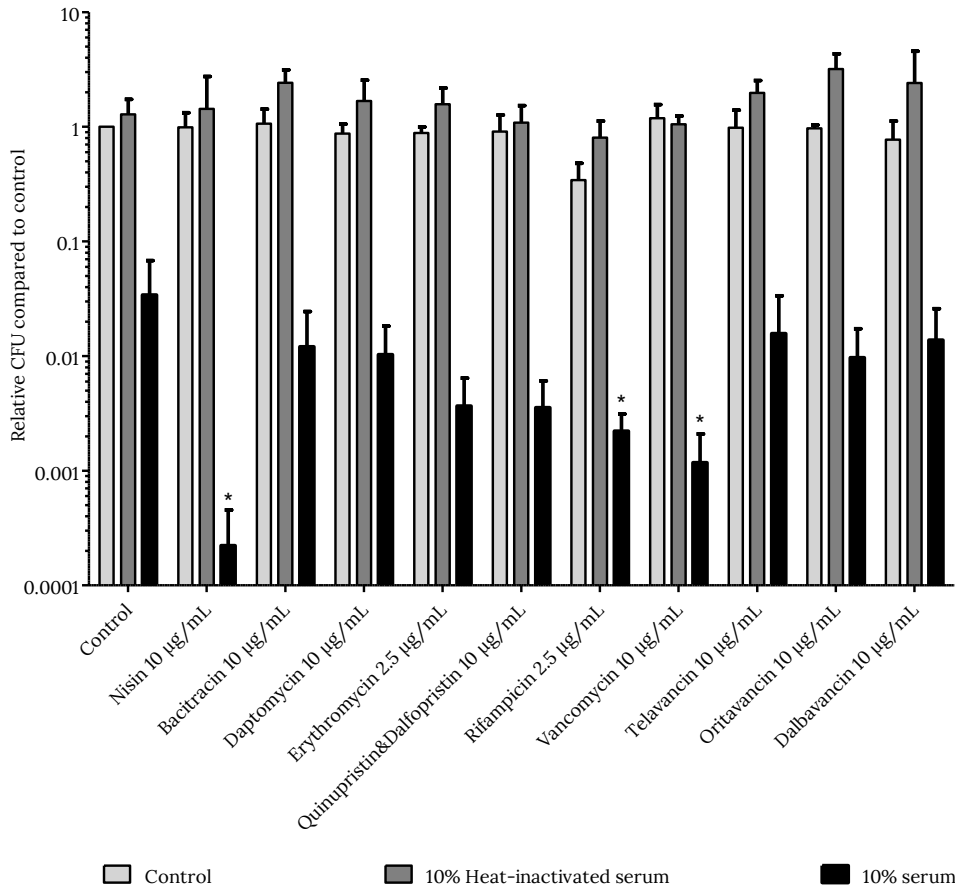


**Figure S20.** Synergy between serum and antibiotics in the bacterial viability assay. The viability of *K. pneumoniae* was screened after 2 hours of incubation with buffer, 10% heat-inactivated serum or 10% serum with 10 µg/mL antibiotics at 37 °C with shaking. CFU counts were normalized to buffer controls. Dashed line represent detection limit. Data represent mean ± SD of three independent.

*P. aeruginosa*

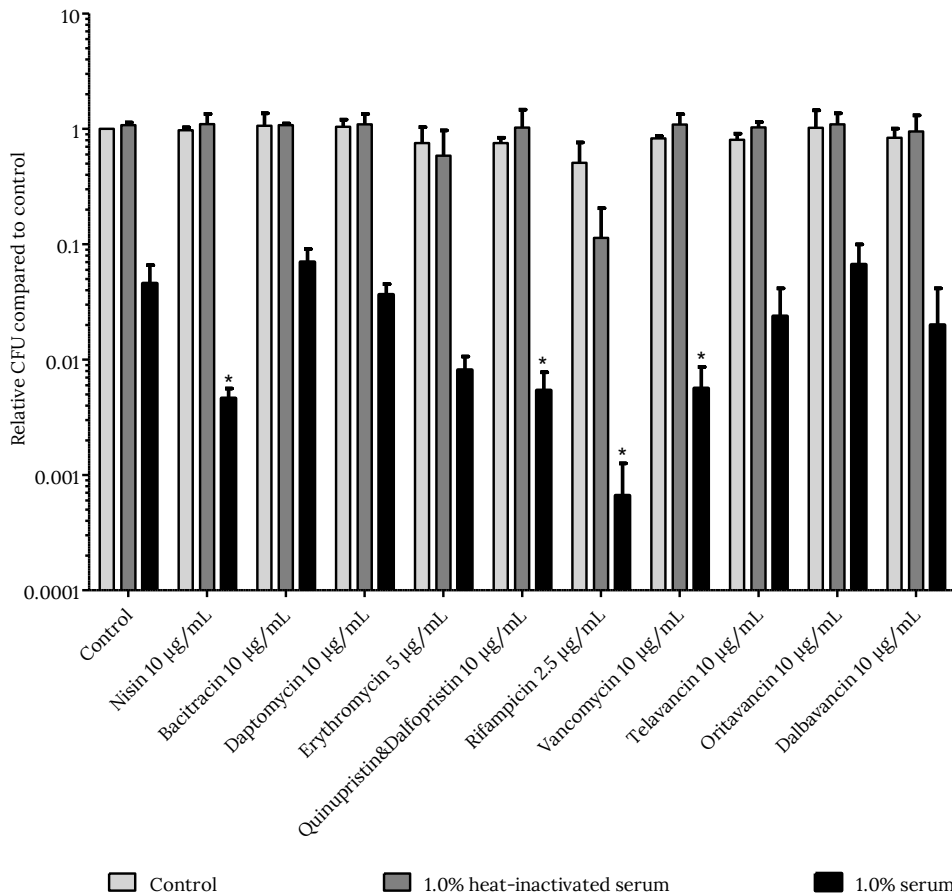


**Figure S21.** Synergy between serum and antibiotics in the bacterial viability assay. The viability of *P. aeruginosa* was screened after 2 hours of incubation with buffer, 1.0% heat-inactivated serum or 1.0% serum with 10 µg/mL antibiotics at 37 °C with shaking. CFU counts were normalized to buffer controls. Dashed line represent detection limit. Data represent mean ± SD of three independent.

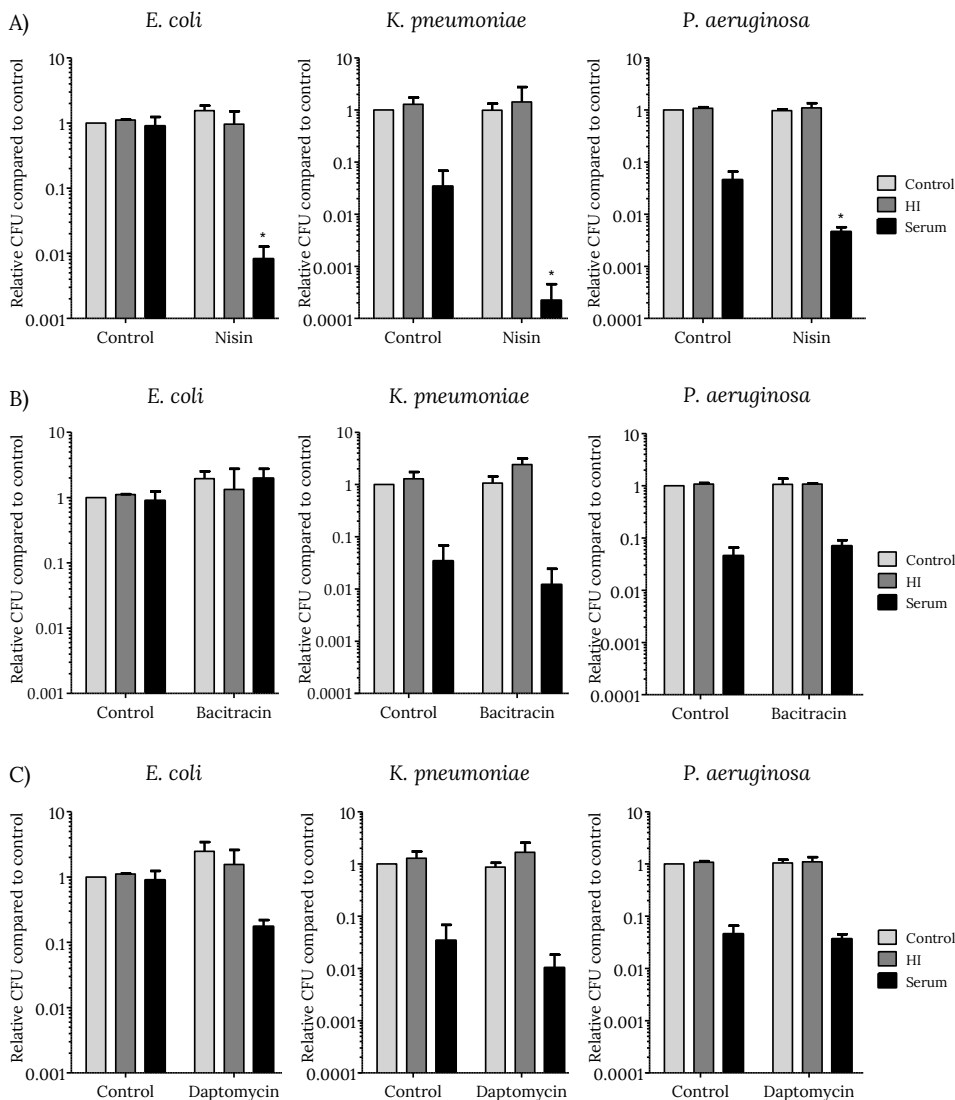


**Figure S22.** Synergy between serum and antibiotics A) nisin; B) daptomycin; C) bacitracin. The viability of *E. coli*, *K. pneumoniae*, and *P. aeruginosa* was screened after 2 hours of incubation with buffer, heat-inactivated serum (HI) or serum with 10  $\mu\text{g}/\text{mL}$  antibiotics at 37  $^{\circ}\text{C}$  with shaking. Concentrations of serum differed per pathogen and were 0.3%, 10% and 1.0% respectively. CFU counts were normalized to buffer controls. Data represent mean  $\pm$  SD of three independent experiments and were analyzed by an one-way ANOVA and Dunnett test (\* $p < 0.05$ ) using the serum as control group.

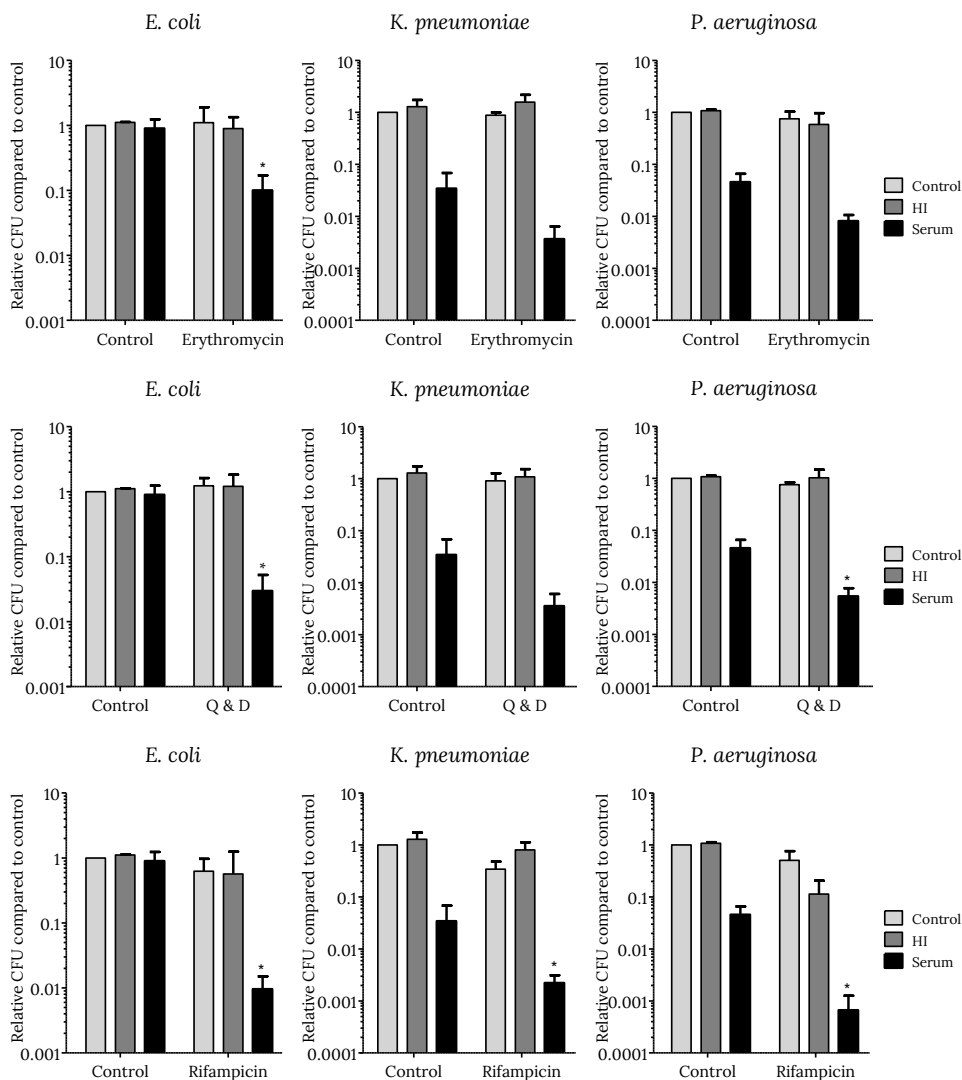


**Figure S23.** Synergy between serum and antibiotics A) erythromycin; B) quinupristin & dalfopristin; C) rifampicin. The viability of *E. coli*, *K. pneumoniae*, and *P. aeruginosa* was screened after 2 hours of incubation with buffer, heat-inactivated serum or serum with antibiotics at 37 °C with shaking. Concentrations of serum differed per pathogen and were 0.3%, 10% and 1.0% respectively. Erythromycin and rifampicin concentrations had to be lowered due to their inherent activity at the 10 µg/mL. Erythromycin was dosed at 5, 2.5, and 5 µg/mL for the pathogens respectively and rifampicin concentrations were 5, 2.5, and 2.5 µg/mL respectively. CFU counts were normalized to buffer controls. Data represent mean ± SD of three independent experiments and were analyzed by an one-way ANOVA and Dunnett test (\*p < 0.05) using the serum as control group.

## References

- (1) World Health Organization. Prioritization of Pathogens to Guide Discovery, Research and Development of New Antibiotics for Drug-Resistant Bacterial Infections, Including Tuberculosis; WHO/EMP/IAU/2017.12; World Health Organization, 2017.
- (2) Freire-Moran, L.; Aronsson, B.; Manz, C.; Gyssens, I. C.; So, A. D.; Monnet, D. L.; Cars, O. Critical Shortage of New Antibiotics in Development against Multidrug-Resistant Bacteria—Time to React Is Now. *Drug Resist. Updat.* **2011**, *14* (2), 118–124. <https://doi.org/10.1016/j.drug.2011.02.003>.
- (3) Amann, S.; Neef, K.; Kohl, S. Antimicrobial Resistance (AMR). *Eur. J. Hosp. Pharm.* **2019**, *26* (3), 175–177. <https://doi.org/10.1136/ejhpharm-2018-001820>.
- (4) Brown, E. D.; Wright, G. D. Antibacterial Drug Discovery in the Resistance Era. *Nature* **2016**, *529* (7586), 336–343. <https://doi.org/10.1038/nature17042>.
- (5) Vaara, M. Polymyxin Derivatives That Sensitize Gram-Negative Bacteria to Other Antibiotics. *Molecules* **2019**, *24* (2), 249. <https://doi.org/10.3390/molecules24020249>.
- (6) Nicolau, D. P. Carbapenems: A Potent Class of Antibiotics. *Expert Opin. Pharmacother.* **2008**, *9* (1), 23–37. <https://doi.org/10.1517/14656566.9.1.23>.
- (7) Nikaido, H.; Nakae, T. The Outer Membrane of Gram-Negative Bacteria. In *Advances in Microbial Physiology*; Rose, A. H., Morris, J. G., Eds.; Academic Press, **1980**; Vol. 20, pp 163–250. [https://doi.org/10.1016/S0065-2911\(08\)60208-8](https://doi.org/10.1016/S0065-2911(08)60208-8).
- (8) Ghai, I.; Ghai, S. Understanding Antibiotic Resistance via Outer Membrane Permeability. *Infect. Drug Resist.* **2018**, *11*, 523–530. <https://doi.org/10.2147/IDR.S156995>.
- (9) Nikaido, H. Molecular Basis of Bacterial Outer Membrane Permeability Revisited. *Microbiol. Mol. Biol. Rev.* **2003**, *67* (4), 593–656. <https://doi.org/10.1128/MMBR.67.4.593-656.2003>.
- (10) Delcour, A. H. Outer Membrane Permeability and Antibiotic Resistance. *Biochim. Biophys. Acta BBA - Proteins Proteomics* **2009**, *1794* (5), 808–816. <https://doi.org/10.1016/j.bbapap.2008.11.005>.
- (11) Vaara, M. Agents That Increase the Permeability of the Outer Membrane. *Microbiol. Rev.* **1992**, *56* (3), 395–411.
- (12) Citterio, L.; Franzky, H.; Palarasah, Y.; Andersen, T. E.; Mateiu, R. V.; Gram, L. Improved In Vitro Evaluation of Novel Antimicrobials: Potential Synergy between Human Plasma and Antibacterial Peptidomimetics, AMPs and Antibiotics against Human Pathogenic Bacteria. *Res. Microbiol.* **2016**, *167* (2), 72–82. <https://doi.org/10.1016/j.resmic.2015.10.002>.
- (13) Dutcher, B. S.; Reynard, A. M.; Beck, M. E.; Cunningham, R. K. Potentiation of Antibiotic Bactericidal Activity by Normal Human Serum. *Antimicrob. Agents Chemother.* **1978**, *13* (5), 820–826. <https://doi.org/10.1128/AAC.13.5.820>.
- (14) Fietta, A.; Mangiarotti, P.; Grassi, G. G. Effects of Antibiotics on the Bactericidal Activity of Human Serum. *J. Antimicrob. Chemother.* **1982**, *9* (2), 141–148. <https://doi.org/10.1093/jac/9.2.141>.
- (15) Borsos, T.; Dourmashkin, R. R.; Humphrey, J. H. Lesions in Erythrocyte Membranes Caused by Immune Haemolysis. *Nature* **1964**, *202*, 251–252. <https://doi.org/10.1038/202251a0>.
- (16) Dourmashkin, R. R.; Rosse, W. F. Morphologic Changes in the Membranes of Red Blood Cells Undergoing Hemolysis. *Am. J. Med.* **1966**, *41* (5), 699–710. [https://doi.org/10.1016/0002-9343\(66\)90031-3](https://doi.org/10.1016/0002-9343(66)90031-3).
- (17) Mayer, M. M. Mechanism of Cytolysis by Complement. *Proc. Natl. Acad. Sci. U. S. A.* **1972**, *69* (10), 2954–2958. <https://doi.org/10.1073/pnas.69.10.2954>.
- (18) Heesterbeek, D. A. C.; Martin, N. I.; Velthuisen, A.; Duijst, M.; Ruyken, M.; Wubbolts, R.; Rooijackers, S. H. M.; Bardoel, B. W. Complement-Dependent Outer Membrane Perturbation Sensitizes Gram-Negative Bacteria to Gram-Positive Specific Antibiotics. *Sci. Rep.* **2019**, *9* (1), 3074. <https://doi.org/10.1038/s41598-019-38577-9>.
- (19) Müller-Eberhard, H. J. The Membrane Attack Complex of Complement. *Annu. Rev. Immunol.* **1986**, *4*, 503–528. <https://doi.org/10.1146/annurev.iy.04.040186.002443>.
- (20) Merle, N. S.; Church, S. E.; Fremaux-Bacchi, V.; Roumenina, L. T. Complement System Part I - Molecular Mechanisms of Activation and Regulation. *Front. Immunol.* **2015**, *6*, 262. <https://doi.org/10.3389/fimmu.2015.00262>.

- (21) Gros, P.; Milder, F. J.; Janssen, B. J. C. Complement Driven by Conformational Changes. *Nat. Rev. Immunol.* **2008**, 8 (1), 48–58. <https://doi.org/10.1038/nri2231>.
- (22) Heesterbeek, D. A. C.; Angelier, M. L.; Harrison, R. A.; Rooijakkers, S. H. M. Complement and Bacterial Infections: From Molecular Mechanisms to Therapeutic Applications. *J. Innate Immun.* **2018**, 10 (5–6), 455–464. <https://doi.org/10.1159/000491439>.
- (23) Rawal, N.; Pangburn, M. K. Structure/Function of C5 Convertases of Complement. *Int. Immunopharmacol.* **2001**, 1 (3), 415–422. [https://doi.org/10.1016/s1567-5769\(00\)00039-4](https://doi.org/10.1016/s1567-5769(00)00039-4).
- (24) Berends, E. T. M.; Gorham, R. D.; Ruyken, M.; Soppe, J. A.; Orhan, H.; Aerts, P. C.; de Haas, C. J. C.; Gros, P.; Rooijakkers, S. H. M. Molecular Insights into the Surface-Specific Arrangement of Complement C5 Convertase Enzymes. *BMC Biol.* **2015**, 13, 93. <https://doi.org/10.1186/s12915-015-0203-8>.
- (25) DiScipio, R. G.; Linton, S. M.; Rushmere, N. K. Function of the Factor I Modules (FIMs) of Human Complement Component C6. *J. Biol. Chem.* **1999**, 274 (45), 31811–31818. <https://doi.org/10.1074/jbc.274.45.31811>.
- (26) Doorduyn, D. J.; Bardeel, B. W.; Heesterbeek, D. A. C.; Ruyken, M.; Benn, G.; Parsons, E. S.; Hoogenboom, B. W.; Rooijakkers, S. H. M. Bacterial Killing by Complement Requires Direct Anchoring of Membrane Attack Complex Precursor C5b-7. *PLOS Pathog.* **2020**, 16 (6), e1008606. <https://doi.org/10.1371/journal.ppat.1008606>.
- (27) Preissner, K. T.; Podack, E. R.; Müller-Eberhard, H. J. The Membrane Attack Complex of Complement: Relation of C7 to the Metastable Membrane Binding Site of the Intermediate Complex C5b-7. *J. Immunol. Baltim. Md 1950* **1985**, 135 (1), 445–451.
- (28) Brannen, C. L.; Sodetz, J. M. Incorporation of Human Complement C8 into the Membrane Attack Complex Is Mediated by a Binding Site Located within the C8 $\beta$  MACPF Domain. *Mol. Immunol.* **2007**, 44 (5), 960–965. <https://doi.org/10.1016/j.molimm.2006.03.012>.
- (29) Heesterbeek, D. A. C.; Bardeel, B. W.; Parsons, E. S.; Bennett, I.; Ruyken, M.; Doorduyn, D. J.; Gorham, R. D.; Berends, E. T.; Pyne, A. L.; Hoogenboom, B. W.; Rooijakkers, S. H. Bacterial Killing by Complement Requires Membrane Attack Complex Formation via Surface-Bound C5 Convertases. *EMBO J.* **2019**, 38 (4), e99852. <https://doi.org/10.15252/embj.201899852>.
- (30) Doorduyn, D. J.; Rooijakkers, S. H. M.; Heesterbeek, D. A. C. How the Membrane Attack Complex Damages the Bacterial Cell Envelope and Kills Gram-Negative Bacteria. *BioEssays* **2019**, 41 (10), 1900074. <https://doi.org/10.1002/bies.201900074>.
- (31) Wright, A. J. The Penicillins. *Mayo Clin. Proc.* **1999**, 74 (3), 290–307. <https://doi.org/10.4065/74.3.290>.
- (32) Kleijn, L. H. J.; Oppedijk, S. F.; 't Hart, P.; van Harten, R. M.; Martin-Visscher, L. A.; Kemmink, J.; Breukink, E.; Martin, N. I. Total Synthesis of Laspartomycin C and Characterization of Its Antibacterial Mechanism of Action. *J. Med. Chem.* **2016**, 59 (7), 3569–3574. <https://doi.org/10.1021/acs.jmedchem.6b00219>.
- (33) Wood, T. M.; Martin, N. I. The Calcium-Dependent Lipopeptide Antibiotics: Structure, Mechanism, & Medicinal Chemistry. *MedChemComm* **2019**, 10 (5), 634–646. <https://doi.org/10.1039/C9MD00126C>.
- (34) Breukink, E.; de Kruijff, B. The Lantibiotic Nisin, a Special Case or Not? *Biochim. Biophys. Acta BBA - Biomembr.* **1999**, 1462 (1), 223–234. [https://doi.org/10.1016/S0005-2736\(99\)00208-4](https://doi.org/10.1016/S0005-2736(99)00208-4).
- (35) Wiedemann, I.; Breukink, E.; Kraaij, C. van; Kuipers, O. P.; Bierbaum, G.; Kruijff, B. de; Sahl, H.-G. Specific Binding of Nisin to the Peptidoglycan Precursor Lipid II Combines Pore Formation and Inhibition of Cell Wall Biosynthesis for Potent Antibiotic Activity. *J. Biol. Chem.* **2001**, 276 (3), 1772–1779. <https://doi.org/10.1074/jbc.M006770200>.
- (36) Rubinstein, E.; Keynan, Y. Vancomycin Revisited – 60 Years Later. *Front. Public Health* **2014**, 2, 217. <https://doi.org/10.3389/fpubh.2014.00217>.
- (37) Patel, S.; Preuss, C. V.; Bernice, F. Vancomycin. In *StatPearls*; StatPearls Publishing: Treasure Island (FL), 2021.
- (38) Taylor, S. D.; Palmer, M. The Action Mechanism of Daptomycin. *Bioorg. Med. Chem.* **2016**, 24 (24), 6253–6268. <https://doi.org/10.1016/j.bmc.2016.05.052>.
- (39) Kotsogianni, I.; Wood, T. M.; Alexander, F. M.; Cochrane, S. A.; Martin, N. I. Binding Studies Reveal Phospholipid Specificity and Its Role in the Calcium-Dependent Mechanism of

- Action of Daptomycin. *ACS Infect. Dis.* **2021**, 7 (9), 2612–2619. <https://doi.org/10.1021/acsinfecdis.1c00316>.
- (40) Gray, D. A.; Wenzel, M. More Than a Pore: A Current Perspective on the In Vivo Mode of Action of the Lipopeptide Antibiotic Daptomycin. *Antibiotics* **2020**, 9 (1), 17. <https://doi.org/10.3390/antibiotics9010017>.
  - (41) Humphries, R. M.; Pollett, S.; Sakoulas, G. A Current Perspective on Daptomycin for the Clinical Microbiologist. *Clin. Microbiol. Rev.* **2013**. <https://doi.org/10.1128/CMR.00030-13>.
  - (42) Huang, H. W. Daptomycin, Its Membrane-Active Mechanism vs. That of Other Antimicrobial Peptides. *Biochim. Biophys. Acta BBA - Biomembr.* **2020**, 1862 (10), 183395. <https://doi.org/10.1016/j.bbamem.2020.183395>.
  - (43) Patel, S.; Saw, S. Daptomycin. In StatPearls; StatPearls Publishing: Treasure Island (FL), 2021.
  - (44) Storm, D. R. Mechanism of Bacitracin Action: A Specific Lipid-Peptide Interaction\*. *Ann. N. Y. Acad. Sci.* **1974**, 235 (1), 387–398. <https://doi.org/10.1111/j.1749-6632.1974.tb43278.x>.
  - (45) Ming, L.-J.; Epperson, J. D. Metal Binding and Structure-Activity Relationship of the Metalloantibiotic Peptide Bacitracin. *J. Inorg. Biochem.* **2002**, 91 (1), 46–58. [https://doi.org/10.1016/S0162-0134\(02\)00464-6](https://doi.org/10.1016/S0162-0134(02)00464-6).
  - (46) Nguyen, R.; Khanna, N. R.; Safadi, A. O.; Sun, Y. Bacitracin Topical. In StatPearls; StatPearls Publishing: Treasure Island (FL), 2021.
  - (47) Biedenbach, D. J.; Rhomberg, P. R.; Mendes, R. E.; Jones, R. N. Spectrum of Activity, Mutation Rates, Synergistic Interactions, and the Effects of PH and Serum Proteins for Fusidic Acid (CEM-102). *Diagn. Microbiol. Infect. Dis.* **2010**, 66 (3), 301–307. <https://doi.org/10.1016/j.diagmicrobio.2009.10.014>.
  - (48) Spížek, J.; Řezanka, T. Lincomycin, Clindamycin and Their Applications. *Appl. Microbiol. Biotechnol.* **2004**, 64 (4), 455–464. <https://doi.org/10.1007/s00253-003-1545-7>.
  - (49) Bartlett, J. G.; Sutter, V. L.; Finegold, S. M. Treatment of Anaerobic Infections with Lincomycin and Clindamycin. *N. Engl. J. Med.* **1972**, 287 (20), 1006–1010. <https://doi.org/10.1056/NEJM197211162872002>.
  - (50) Azzouz, A.; Preuss, C. V. Linezolid. In StatPearls; StatPearls Publishing: Treasure Island (FL), 2021.
  - (51) Farzam, K.; Nessel, T. A.; Quick, J. Erythromycin. In StatPearls; StatPearls Publishing: Treasure Island (FL), 2021.
  - (52) Bryson, H. M.; Spencer, C. M. Quinupristin-Dalfopristin. *Drugs* **1996**, 52 (3), 406–415. <https://doi.org/10.2165/00003495-199652030-00006>.
  - (53) Miyazaki, S.; Tateda, K.; Ono, A.; Ishii, Y.; Matsumoto, T.; Furuya, N.; Yamaguchi, K. In Vitro and In Vivo Antibacterial Activities of Quinupristin-Dalfopristin, a Novel Injectable Streptogramin, against Gram-Positive Cocci and Gram-Negative Respiratory Tract Pathogens. *J. Infect. Chemother.* **1998**, 4 (2), 64–70. <https://doi.org/10.1007/BF02489963>.
  - (54) Beloor Suresh, A.; Rosani, A.; Wadhwa, R. Rifampin. In StatPearls; StatPearls Publishing: Treasure Island (FL), 2021.
  - (55) Jalali, V. al; Zeitlinger, M. Clinical Pharmacokinetics and Pharmacodynamics of Telavancin Compared with the Other Glycopeptides. *Clin. Pharmacokinet.* **2018**, 57 (7), 797. <https://doi.org/10.1007/s40262-017-0623-4>.
  - (56) Sweeney, D.; Shinabarger, D. L.; Arhin, F. F.; Belley, A.; Moeck, G.; Pillar, C. M. Comparative in Vitro Activity of Oritavancin and Other Agents against Methicillin-Susceptible and Methicillin-Resistant Staphylococcus Aureus. *Diagn. Microbiol. Infect. Dis.* **2017**, 87 (2), 121–128. <https://doi.org/10.1016/j.diagmicrobio.2016.11.002>.
  - (57) PubChem. Vancomycin <https://pubchem.ncbi.nlm.nih.gov/compound/14969> (accessed 2022-04-03).
  - (58) PubChem. Telavancin <https://pubchem.ncbi.nlm.nih.gov/compound/3081362> (accessed 2022-04-03).
  - (59) PubChem. Oritavancin <https://pubchem.ncbi.nlm.nih.gov/compound/16136912> (accessed 2022-04-03).
  - (60) PubChem. Dalbavancin <https://pubchem.ncbi.nlm.nih.gov/compound/16134627> (accessed 2022-04-03).

- (61) Johnson, B. A.; Anker, H.; Meleney, F. L. Bacitracin: A New Antibiotic Produced by a Member of the *B. Subtilis* Group. *Science* **1945**, 102 (2650), 376–377. <https://doi.org/10.1126/science.102.2650.376>.
- (62) Washington, J. A.; Wilson, W. R. Erythromycin: A Microbial and Clinical Perspective after 30 Years of Clinical Use (First of Two Parts). *Mayo Clin. Proc.* **1985**, 60 (3), 189–203. [https://doi.org/10.1016/S0025-6196\(12\)60219-5](https://doi.org/10.1016/S0025-6196(12)60219-5).
- (63) Washington, J. A.; Wilson, W. R. Erythromycin: A Microbial and Clinical Perspective after 30 Years of Clinical Use (Second of Two Parts). *Mayo Clin. Proc.* **1985**, 60 (4), 271–278. [https://doi.org/10.1016/S0025-6196\(12\)60322-X](https://doi.org/10.1016/S0025-6196(12)60322-X).
- (64) Verbist, L.; Verhaegen, J. Comparative In-Vitro Activity of RP 59500. *J. Antimicrob. Chemother.* **1992**, 30 Suppl A, 39–44. [https://doi.org/10.1093/jac/30.suppl\\_a.39](https://doi.org/10.1093/jac/30.suppl_a.39).
- (65) Finch, R. G. Antibacterial Activity of Quinupristin/Dalfopristin. *Drugs* **1996**, 51 (1), 31–37. <https://doi.org/10.2165/00003495-199600511-00007>.
- (66) Corbett, D.; Wise, A.; Langley, T.; Skinner, K.; Trimby, E.; Birchall, S.; Doral, A.; Sandiford, S.; Williams, J.; Warn, P.; Vaara, M.; Lister, T. Potentiation of Antibiotic Activity by a Novel Cationic Peptide: Potency and Spectrum of Activity of SPR741. *Antimicrob. Agents Chemother.* **2017**, 61 (8), e00200–17. <https://doi.org/10.1128/AAC.00200-17>.
- (67) Mortimer, F. C.; Mason, D. J.; Gant, V. A. Flow Cytometric Monitoring of Antibiotic-Induced Injury in *Escherichia Coli* Using Cell-Impermeant Fluorescent Probes. *Antimicrob. Agents Chemother.* **2000**, 44 (3), 676–681. <https://doi.org/10.1128/AAC.44.3.676-681.2000>.
- (68) Louvet, J.-N.; Attik, G.; Dumas, D.; Potier, O.; Pons, M.-N. Simultaneous Gram and Viability Staining on Activated Sludge Exposed to Erythromycin: 3D CLSM Time-Lapse Imaging of Bacterial Disintegration. *Int. J. Hyg. Environ. Health* **2011**, 214 (6), 470–477. <https://doi.org/10.1016/j.ijheh.2011.02.001>.
- (69) Lee, B. L.; Sachdeva, M.; Chambers, H. F. Effect of Protein Binding of Daptomycin on MIC and Antibacterial Activity. *Antimicrob. Agents Chemother.* **1991**, 35 (12), 2505–2508. <https://doi.org/10.1128/AAC.35.12.2505>.
- (70) Ledger, E. V. K.; Mesnage, S.; Edwards, A. M. Human Serum Triggers Antibiotic Tolerance in *Staphylococcus Aureus*. *Nat. Commun.* **2022**, 13 (1), 2041. <https://doi.org/10.1038/s41467-022-29717-3>.





## **Chapter 5**

### **Intrinsic antimicrobial activity of bis-amidines against Gram-positive bacteria**

*Charlotte M.J. Wesseling, Samantha Lok, Shanice Veraar, and Nathaniel I. Martin*

## 1. Introduction

Antimicrobial resistance (AMR) is on the rise. In the 5 year period between 2014 and 2019, annual deaths worldwide due to AMR rose from 700k to 1.27 million.<sup>1-4</sup> The rightly coined “overlooked pandemic” requires attention, not only by controlling and reducing the use of antibiotics, but also by developing new antibiotics to revive the dried-up pipeline.<sup>2,3,5</sup> In addition to developing new antibiotics, another strategy for addressing the threat of AMR is by examining the potential for repurposing approved drugs as antimicrobial agents.<sup>5-8</sup>

Pentamidine (**1**, Figure 1) is a simple bis-amidine, was first synthesized in the 1930s, and is an effective antiparasitic drug. Pentamidine is on the WHO’s list of essential medicines and it freely distributed in developing countries where parasitic diseases are endemic.<sup>9,10</sup> Beyond its antiparasitic activity, pentamidine has also been investigated as an anti-cancer agent and shows inhibition of *Escherichia coli* and *Staphylococcus aureus* growth, exhibiting moderate antimicrobial activity against Gram-positive bacteria.<sup>11-18,10,19-24</sup> Its adverse side-effects are also well-documented and include nephrotoxicity, tachycardia, hypotension, hypoglycaemia, and local reactions to the injection.<sup>9,10,25,26</sup> Efforts are being made to reduce the nephrotoxicity of pentamidine, such as employing nanotechnology.<sup>27</sup> Pentamidine is seen as a promising repurposing candidate as exemplified by the wide range of therapeutical applications proposed and/or approved.<sup>27</sup>

Recently, the possibility to repurpose pentamidine as a potentiator of Gram-positive antibiotics against Gram-negative bacteria was reported by Brown and coworkers.<sup>11</sup> Compelling *in vivo* data from systemic murine models with colistin-sensitive and -resistant *Acinetobacter baumannii* strains showed pentamidine to be highly effective in enhancing the antibacterial activity of novobiocin.<sup>11</sup> The results of this study highlight the potential of repurposing pentamidine as a combination treatment against Gram-negative bacteria.<sup>5-8,11</sup> In addition, this study explored the structure-activity relationship (SAR) of pentamidine and commercially available analogues.<sup>11</sup> Building on this work, our group recently conducted a follow-up SAR study wherein a number of novel bis-amidines inspired by pentamidine (Figure 1) were synthesized and assessed for antibiotic synergy (see Chapter 2 of this thesis).<sup>12</sup>

A number of the bis-amidines prepared in our earlier study showed strong potentiation of several Gram-positive analogues.<sup>12</sup> Disruption of the Gram-negative outer membrane (OM) was established as the mode of potentiation for these compounds and for this reason the selectivity of membrane disruption was also explored by means of a hemolysis assay.<sup>11,12</sup> Several analogues proved to be hemolytic when tested under stringent conditions including high concentrations and long incubation times (20 hours).<sup>12</sup> From these studies however, compounds **3** and **4** emerged as having potent OM disrupting ability and low hemolytic activity (Figure 1).<sup>12</sup> Still, a question remained, while compounds **3** and **4** showed the highest OM disruption, compounds **6-9** displayed lower OM disruption (data not shown), but potentiated the activity of antibiotics even stronger.<sup>12</sup> This finding prompted us to also perform a preliminary screen of these analogues for inherent antibacterial activity against a selected *S. aureus* strain.

In literature several SAR studies of pentamidine analogues against *S. aureus* have been reported.<sup>21,28-30</sup> As mentioned before, the development of new antibiotics is key in combating AMR.<sup>3,31</sup> A systematic analysis of the AMR numbers of 2019 revealed that of the Gram-positive bacteria *S. aureus* and *Streptococcus pneumoniae* were each responsible for more than 250.000 deaths in 2019, while deaths associated with AMR *Enterococcus faecium* lay between 100.000 and 250.000 deaths.<sup>1</sup> According to the WHO's priority list, vancomycin-resistant *E. faecium* and methicillin- and vancomycin-resistant *S. aureus* are classified as priority 2 “high”, while *S. pneumoniae* is classified as priority 3 “medium”.<sup>31</sup> The work described in this chapter work aimed to assess and improve the inherent activity of our new pentamidine analogues towards Gram-positive bacteria, specifically *S. aureus* and *E. faecium*.

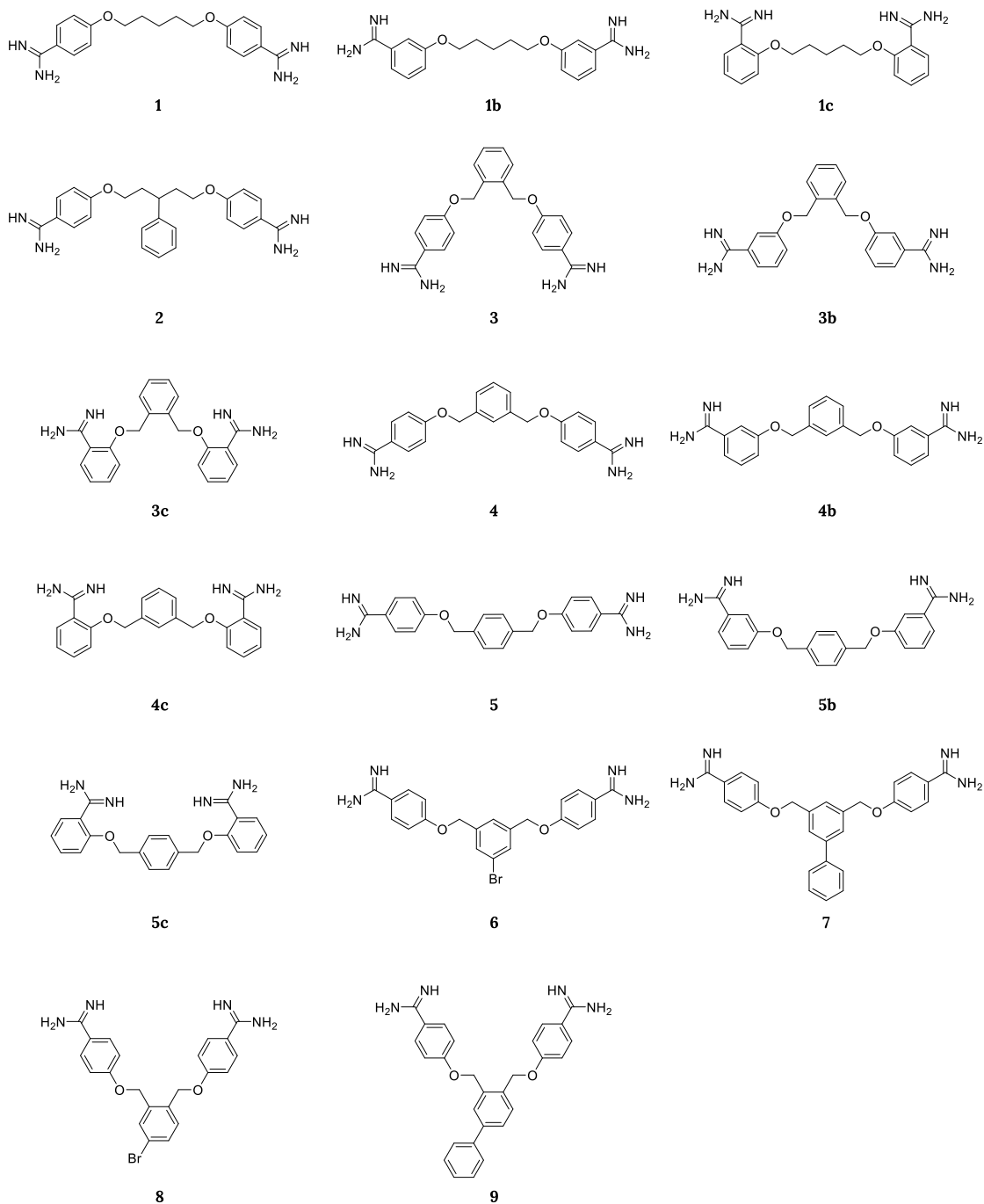


**Figure 1.** Overview of pentamidine (**1**) and the bis-amidines described as potentiators by the group of Brown (**2**)<sup>11</sup> and from our previous publication (**1b**, **1c**, and **3-9**) (see Chapter 2).<sup>12</sup>

## 2. Results and Discussion

The inherent antibacterial activity of the pentamidine-inspired bis-amidines from our previous study (Figure 1),<sup>12</sup> were established by determining the minimum inhibitory concentration (MIC) of each compound against *S. aureus* (ATCC 29213) grown in lysogeny broth (LB). Table 1 provides a summary of the MIC values thus obtained, along with the FICI values for each compound (based on the synergy observed when combined with erythromycin and tested against *E. coli*) as well as the hemolytic activity determined for each compound.

**Table 1.** Overview of the antimicrobial and hemolytic activity of the previously described bis-amidines. The minimal inhibitory concentration (MIC) is determined against *S. aureus* ATCC 29213 ( $\mu\text{g/mL}$ ). The hemolytic activity is determined at 128  $\mu\text{g/mL}$  after 20 hours of incubation. The hemolytic activity is normalized to the positive control (0.1% Triton X-100) and a value of <10% is considered non-hemolytic.<sup>32</sup>

	MIC ( $\mu\text{g/mL}$ )	FICI	% Hemolysis
<b>Pentamidine (1)</b>	8-16	0.500	0.0
<b>1b</b>	16	$\leq 0.375$	0.0
<b>1c</b>	>128	>0.5 <sup>a</sup>	0.0
<b>2</b>	2	$\leq 0.063$	6.6
<b>3</b>	16	$\leq 0.125$	0.0
<b>3b</b>	32	$\leq 0.313$	0.5
<b>3c</b>	>128	>0.5 <sup>a</sup>	0.0
<b>4</b>	16	$\leq 0.094$	0.0
<b>4b</b>	4	$\leq 0.250$	0.9
<b>4c</b>	128	>0.5 <sup>a</sup>	0.2
<b>5</b>	8	$\leq 0.313$	0.5
<b>5b</b>	8	$\leq 0.250$	0.3
<b>5c</b>	128	>0.5 <sup>a</sup>	0.1
<b>6</b>	4	$\leq 0.063$	13
<b>7</b>	1	$\leq 0.047$	10
<b>8</b>	1	$\leq 0.094$	14
<b>9</b>	1	$\leq 0.078$	78
<b>Vancomycin</b>	1	-	<5% <sup>33</sup>

<sup>a</sup>The fractional inhibitory concentration index (FICI) values were taken from Table 1 of the previous SAR study with bis-amidines (See Chapter 2).<sup>12</sup> These values were calculated from checkerboard assays with erythromycin against *E. coli* BW25113 in LB.<sup>12</sup>

The effect of the bis-amidine geometries on inherent activity roughly reflected the trends observed for their synergistic activity.<sup>12</sup> For example, when the amidine moieties are located at the *ortho* position as **1c**, **3c**, **4c**, and **5c**, a significant reduction of inherent activity results is noted relative to the corresponding *para*-amidine analogues

**1, 3, 4,** and **5**. Similarly, these *ortho* analogues were found to also been largely devoid of synergistic potential with a fractional inhibitory concentration index (FICI) above 0.5.<sup>12</sup> Conversely, in the case of the *meta*-amidine analogues prepared (**1b**, **3b**, **4b** and **5b**), the antibacterial activities measured were found to be similar to *para*-substituted compounds. Notably, the compound with the most potent *in vitro* antibacterial activity among the *ortho*-, *meta*-, *para*- series of analogues prepared was *meta* analogue **4b** which was found to exhibit a 2- to 4-fold enhancement compared to pentamidine (Table 1).

Overall, the lowest MICs were observed for the bis-amidines **7-9** (Table 1), which showed a significant 16-fold improvement compared to pentamidine. Notable in this regard are a previously reported SAR studies that yielded pentamidine analogues which in some cases showed enhanced activity against MRSA strains.<sup>21</sup> A closer look at these reports revealed the use of Mueller-Hinton broth (MHB) as medium.<sup>28</sup> MHB is a medium that is normally adjusted with cations, Mg<sup>2+</sup> and Ca<sup>2+</sup>, and the absence of cations could hypothetically improve MIC values of positively charged bis-amidines. Re-evaluation of a selection of our analogues in MHB and cation-adjusted MHB (CAMHB) resulted in lower MIC for a majority of the analogues (Table 2). For instance, the MIC of pentamidine, originally 8-16 µg/mL in LB, dropped to 2 µg/mL in MHB and 4 µg/mL in CAMHB. By comparison, the MICs of the most potent compounds **7** and **9** dropped to 0.5 µg/mL in MHB, while for **8** the MIC did not change when screening in different media.

**Table 2.** The effect of different media on the antimicrobial activity of bis-amidines **1-4** and **6-9**. The minimal inhibitory concentration (MIC) is determined against *S. aureus* ATCC29213 (µg/mL).

	LB	MHB	CAMHB
<b>Pentamidine (1)</b>	8-16	2	4
<b>2</b>	2	1	1
<b>3</b>	16	4	8
<b>4</b>	16	4	8
<b>6</b>	4	1	1
<b>7</b>	1	0.5	0.5
<b>8</b>	1	1	1
<b>9</b>	1	0.5	1
<b>Vancomycin</b>	1	0.5	1

Analogues **7-9** exhibited the most potent antibacterial activity and were not impacted by the use of different growth media conditions. However, assessment of hemolytic activity clearly reveals bis-amidines **6-9** to be hemolytic (Table 1). As mentioned in our previous SAR study (Chapter 2), an increase in lipophilicity is often associated with an increase in hemolysis.<sup>12</sup> However, lipophilicity alone does not explain the high difference in hemolytic activity between **7** and **9** (10% and 78%, respectively, Table 1) with our data clearly showing that the geometry of the aromatic linker plays a role. To further explore this effect, the *meta*-oriented bis-amidine analogues **6b**, **7b**, **8b**,

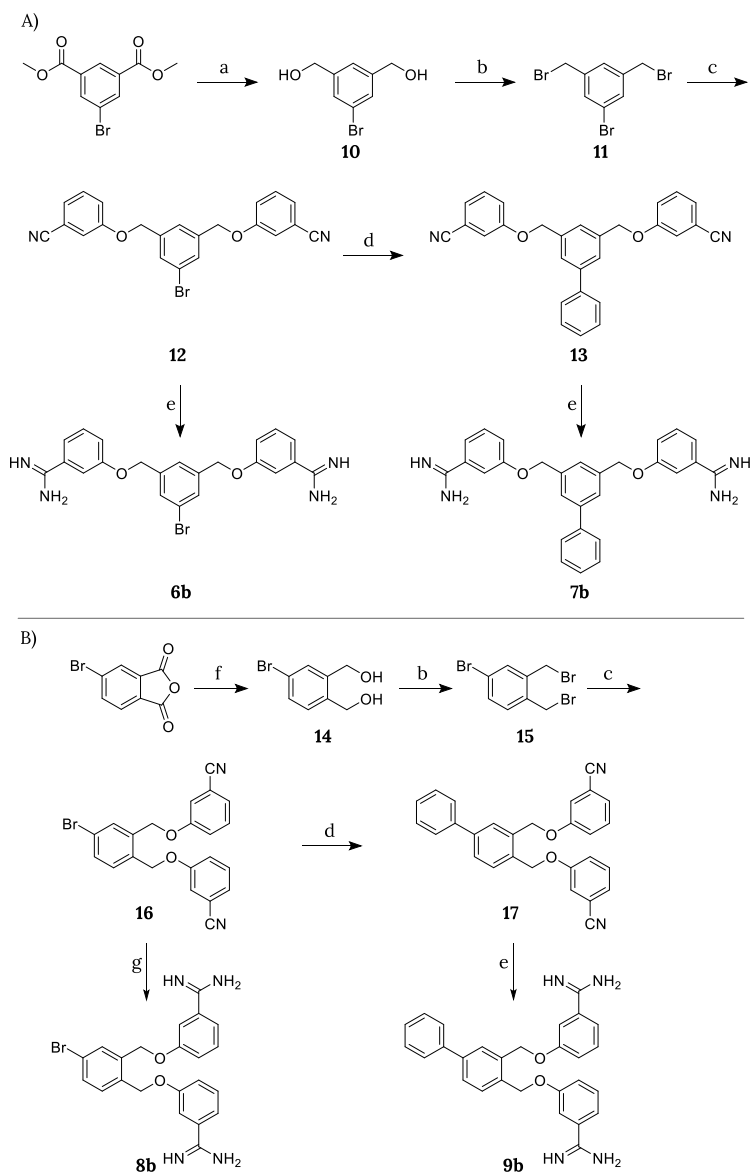
and **9b** were synthesized (Scheme 1). The synthetic routes used in their preparation were largely based on the reported syntheses of analogues **6**, **7**, **8**, and **9** as described in Chapter 3.<sup>12</sup> In the case of **6b** and **7b** compound **11** served as a common intermediate.<sup>12,34,35</sup> In the subsequent Williamson ether synthesis, however, 3-cyanophenol instead of 4-cyanophenol was used to yield **12**.<sup>12,36</sup> Transformation to the bis-amidine products was then performed as for **6** and **7** as described in Chapter 2.<sup>12</sup> Likewise, the first three steps in the synthesis of **8b** and **9b** were identical to their parent compounds **8** and **9** with the only difference being the use the 4-cyanophenol for 3-cyanophenol.<sup>12,37</sup> As for bis-amidine **8**, the use of LHMDs resulted in the loss of the bromo-group in bis-amidine **8b**.<sup>12</sup> Therefore, the same three-step reaction used to obtain **8** was employed and yielded **8b**.<sup>12,38</sup> The aforementioned Suzuki coupling was performed on bis-nitrile **16** as for bis-nitrile **12**.<sup>39–41</sup> Bis-amidine **9b** was obtained from **16** using LHMDs as described before.<sup>12</sup>

The newly obtained analogues **6b**, **7b**, **8b**, and **9b** were then screened for antimicrobial activity against *S. aureus* (ATCC 29213) and their hemolytic activity also assessed. The compounds were compared to their parent compounds **6**, **7**, **8**, **9** (Table 3). Bis-amidine **2** was also included, due to its relatively low MIC values in all media (see Table 2) and its low hemolytic activity. Based on the values thus obtained for antibacterial and hemolytic activity, an estimate for the therapeutic window of the compounds was calculated (Table 3). The calculate therapeutic wind was based on the difference between MIC and the concentration at which the hemolytic activity was below 10% (see caption Table 3). It should be noted that these estimated therapeutic window values should only be see as indicative given that they are based on *in vitro* assays. Nonetheless, such an analysis can provide an indication of selectivity of the compounds for bacterial cells vs erythrocytes.

**Table 3.** MIC values of pentamidine analogues **2** and **6–9b** in LB broth for *S. aureus* ATCC 29213. The therapeutic window is calculated from the highest non-hemolytic concentration divided by the MIC (µg/ml). If the compound is still hemolytic at 32 µg/ml, the value ≤16 µg/ml was used in the calculation. The MIC values, the percentage of hemolysis at different concentrations, and the therapeutic window for the other bis-amidines can be found in the Supplementary data, Table S1.

	MIC (µg/ml)	% Hemolysis (128 µg/ml)	% Hemolysis (64 µg/ml)	% Hemolysis (32 µg/ml)	Therapeutic window
<b>2</b>	2	6.6	0.6	0.0	64
<b>6</b>	4	13	1.8	0.0	16
<b>6b</b>	1	4.2	0.6	0.0	128
<b>7</b>	1	10	3.6	2.3	64
<b>7b</b>	0.5	84	49	11	≤32
<b>8</b>	1	14	3.4	0.7	64
<b>8b</b>	1	4.8	0.8	0.0	128
<b>9</b>	1	78	54	22	≤16
<b>9b</b>	4	61	44	21	≤4





**Scheme 1.** Reagents and conditions: (a) (i) DIBALH, DCM, 0 °C, 1 h; (ii) Rochelle salt (quench), rt, overnight (96%); (b) PPh<sub>3</sub>, CBr<sub>4</sub>, DCM, rt, 2 h (55-74%); (c) 4-cyanophenol, NaH, DMF, 80 °C, 1 h (quant.); (d) phenylboronic acid, Pd(dppf)Cl<sub>2</sub>·DCM, THF/Na<sub>2</sub>CO<sub>3</sub>(aq) (1:1), 65 °C, 18 h (81-83%); (e) (i) LHMDs, THF, rt, 48 h; (ii) HCl (dioxane), 0 °C-rt, overnight (21-93%); (f) (i) LAH, ZnCl<sub>2</sub>, THF, rt, 6 h; (ii) Rochelle salt (quench), rt, overnight (95%); (g) (i) NH<sub>2</sub>OH·HCl, DIPEA, EtOH, 85 °C, 6 h; (ii) Ac<sub>2</sub>O, AcOH, rt, 4 h; (iii) Zn powder, AcOH, 35 °C, 6 h (10%).

Interestingly, the newly synthesized compounds **6b**, **7b**, **8b**, and **9b** exhibit both a greater range of hemolytic activity (4.2-84%) and antibacterial activity (0.5 – 4 µg/mL) compared to the *para*-amidine analogues **6**, **7**, **8**, and **9** (Table 3). Again, the relation between hemolytic activity and antibacterial activity doesn't seem to be directly correlated: **6b** and **8b** are non-hemolytic and have MIC values of 1 µg/mL, whereas **9b** is hemolytic and has a MIC of 4 µg/mL. In contrast, the more potent analogue, **7b**, with an MIC of 0.5 µg/mL also exhibits the highest hemolytic activity. The therapeutic window calculations here provide a convenient means of comparing all analogues revealing **6b** and **8b** as the most selective.

In addition to *S. aureus* ATCC 29213, several other strains of *S. aureus* and *E. faecium* were selected for MIC assays to establish the range of activity of the bis-amidines (Table 4). The selected strains include vancomycin-resistant strains (*S. aureus* LIM2 (intermediate-resistant) and VRS3b and *E. faecium* E155 and 7314) and methicillin-resistant *S. aureus* (MRSA) strains (COL and USA300) to further establish the activity of bis-amidines against drug resistant organisms. The MIC values shown in Table 4 were obtained using LB broth as growth media. The same assays were also run in MHB and CAMHB (Supplementary data, Table S3-4). In the case of *E. faecium* strains, TSB was also employed as medium for the MIC assays (Supplementary data Table S5). Based on the therapeutic window of the bis-amidines (Table 3), a selection of the bis-amidines is displayed in Table 4 (therapeutic window ≥ 64).

**Table 4.** MIC values (µg/ml) of pentamidine (**1**) and bis-amidines with a therapeutic window ≥ 64 (**2**, **6b**, **7**, **8**, and **8b**) in LB broth for *S. aureus* and *E. faecium* strains. The maximum concentration tested for pentamidine (**1**) was 64 µg/ml and for vancomycin 128 µg/ml. Results of the other bis-amidines is located in Supplementary data, Table S2.

	<i>S. aureus</i>					<i>E. faecium</i>	
	ATCC 29213	LIM2	VRS3b	COL	USA300	E155	7314
<b>1</b>	8-16	>64	8	8	16	>64	64
<b>2</b>	2	32	2	2	4	16	16
<b>6b</b>	1	16	0.5	0.5	2	32	16
<b>7</b>	1	4	0.25	0.5	1	4	16
<b>8</b>	1	16	1	1	2	16	16
<b>8b</b>	1	32	2	4	8	32	32
<b>Vancomycin</b>	1	4	128	2	<2	>128	128

Of this selection, bis-amidine **7** clearly displays the most potent overall antibacterial activity (Table 4). Only against the *E. faecium* strains and *S. aureus* LIM2, were MIC values for **7** above 4 µg/ml. This compound was assessed as beingh borderline hemolytic at 128 µg/ml (10%, Table 3). The most selective bis-amidines **6b** and **8b**, based on the therapeutic window as determined for *S. aureus* ATCC 29213, display even less activity against *E. faecium* and *S. aureus* LIM2 (≤16 µg/ml, Table 4). However, against the other strains, **6b** displays similar MIC values (maximum a 2-fold difference) to those

measured for **7**. Given that these values were obtained in LB, the effects of other growth media on the MIC values of bis-amidines **6b** and **7** were assessed. To this end, the activities of **6b** and **7** were established against *S. aureus* strains in LB, MHB, and CAMHB and for *E. faecium* also in TSB (Table 5). Interestingly, in the other growth media, the *S. aureus* LIM2 and *E. faecium* 7314 strains appeared to more susceptible to bis-amidine **7**. While for **6b** no such enhancement of activity was observed. There was, however, an improvement seen for **6b** in CAMHB against the *E. faecium* strain E155. In some cases **6b** even shows 2-fold lower MIC values in MHB and CAMHB compared to **7**. Still, overall, bis-amidine **7** is clearly the more potent compound.

A final detail that does require some attention is the overall trend seen for *S. aureus* LIM2 and *E. faecium* E155 and 7314: in general these strains seem less susceptible to pentamidine and bis-amidine analogues compared to the other strains tested (Table 4 and 5, See supplementary data, Table S2-S5). In the case of *S. aureus* LIM2 this could be the results of a thickened cell wall, often seen for vancomycin intermediate-resistant *S. aureus* strains.<sup>42-44</sup> *E. faecium* E155 and 7314 carry the VanA and VanB resistance gene responsible for their vancomycin-resistance, similar to *S. aureus* VRS3b, which is susceptible to the bis-amidines.

Possibly, the *E. faecium* strains are harder to target because of other factors contributing to their inherent insensitivity to the bis-amidines. In terms of resistance, in the literature there is mention of MDR efflux pumps that result in increased resistance to pentamidine<sup>45-48</sup>. The chromosomally-encoded NorA or the plasmid-encoded QacA and QacB are most commonly reported for *S. aureus*, but a QacA/B plasmid has also been found in an isolated *E. faecium* strain.<sup>45-55</sup> Given that there is no literature reporting the presence of this gene or plasmids in the aforementioned strains, we cannot draw a firm conclusion as of yet. Still, future studies to address this point could include strains with either the QacA, QacB, and QacC plasmid or with the NorA gene.<sup>47,50,51,55</sup>

**Table 5.** MIC values (µg/ml) of bis-amidines **6b** and **7** for *S. aureus* and *E. faecium* strains in different broths. The maximum concentration tested for vancomycin was 128 µg/ml. Results of the other bis-amidines is located in Supplementary data, Table S2-S5.

		<i>S. aureus</i>				<i>E. faecium</i>	
	ATCC 29213	LIM2	VRS3b	COL	USA300	E155	7314
<b>LB</b>							
<b>6b</b>	1	16	0.5	0.5	2	32	16
<b>7</b>	1	4	0.25	0.5	1	4	16
<b>Vancomycin</b>	1	4	128	2	<2	>128	128
<b>MHB</b>							
<b>6b</b>	0.5	8	0.5	0.125	0.5	8	8
<b>7</b>	0.5	2	0.25	0.25	1	2	2
<b>Vancomycin</b>	0.5	4	128	2	1	>128	>128
<b>CAMHB</b>							
<b>6b</b>	0.5	16	0.5	0.25	0.5	2	16
<b>7</b>	0.5	4	0.5	0.5	1	2	2
<b>Vancomycin</b>	1	4	128	2	1	>128	>128
<b>TSB</b>							
<b>6b</b>	-	-	-	-	-	32	16
<b>7</b>	-	-	-	-	-	4	4
<b>Vancomycin</b>	-	-	-	-	-	64	128

### 3. Conclusion

In this study we examined the inherent antibacterial activity of the bis-amidines previously investigated as antibiotic synergists (see Chapter 2). This revealed bis-amidine **7** to have potent antibacterial activity against *S. aureus* and *E. faecium* strains (majority of the MIC values  $\leq 2$   $\mu\text{g}/\text{ml}$ ). An estimation of the selectivity of **7** and the other bis-amidine studied was achieved by comparing the concentrations at which they exhibit hemolytic activity versus their MIC values. This revealed compound **7** to have relatively large therapeutic window (64-fold difference between hemolytic activity concentration and MIC against *S. aureus* ATCC 29213 screened in LB).

A focused SAR study also revealed the optimal positioning of the amidine group to be *para* and *meta*-in terms of antibacterial activity, while the *ortho*-amidine analogues displayed little-to-no activity. In addition, increasing the linker hydrophobicity, increased both the inherent activity and hemolytic activity. However, the positioning of the linker relative to the amidines clearly also plays a role given that a direct correlation of lipophilicity to hemolytic activity couldn't be made when comparing bis-amidines **6-9b**. These trends are similar to the trends observed for the synergistic potential of the same bis-amidines in the previous SAR study focused on potentiation of Gram-positive antibiotics against Gram-negative bacteria.<sup>11,12</sup>

Based on the results from the SAR study reported in Chapter 2, it appeared that the bis-amidines studied might have a secondary mode of action that contributed to their synergistic activity; the disruption of the OM alone, could not explain the trends seen in the FICI.<sup>12</sup> The trends observed for the inherent *in vitro* activity of the bis-amidines towards Gram-positive bacteria suggest that this is indeed the case, especially since Gram-positive bacteria don't have an OM.

## 4. Materials and methods

**General procedures.** All reagents employed were of American Chemical Society (ACS) grade or finer and were used without further purification unless otherwise stated. For compound characterization,  $^1\text{H}$  NMR spectra were recorded at 400 MHz with chemical shifts reported in parts per million (ppm) downfield relative to  $\text{CHCl}_3$  (7.26) or DMSO ( $\delta$  2.50).  $^1\text{H}$  NMR data are reported in the following order: multiplicity (s, singlet; d, doublet; t, triplet; q, quartet and m, multiplet), coupling constant (J) in hertz (Hz) and the number of protons. Where appropriate, the multiplicity is preceded by br, indicating that the signal was broad.  $^{13}\text{C}$  NMR spectra were recorded at 101 MHz with chemical shifts reported relative to  $\text{CDCl}_3$  ( $\delta$  77.16) or DMSO ( $\delta$  39.52). HRMS analysis was performed on a Shimadzu Nexera X2 UHPLC system with a Waters Acquity HSS C18 column ( $2.1 \times 100$  mm,  $1.8 \mu\text{m}$ ) at  $30^\circ\text{C}$  and equipped with a diode array detector. The following solvent system, at a flow rate of  $0.5 \text{ mL/min}$ , was used: solvent A,  $0.1\%$  formic acid in water; solvent B,  $0.1\%$  formic acid in acetonitrile. Gradient elution was as follows: 95:5 (A/B) for 1 min, 95:5 to 15:85 (A/B) over 6 min, 15:85 to 0:100 (A/B) over 1 min, 0:100 (A/B) for 3 min, then reversion back to 95:5 (A/B) for 3 min. This system was connected to a Shimadzu 9030 QTOF mass spectrometer (ESI ionisation) calibrated internally with Agilent's API-TOF reference mass solution kit ( $5.0 \text{ mM}$  purine,  $100.0 \text{ mM}$  ammonium trifluoroacetate and  $2.5 \text{ mM}$  hexakis(1H,1H,3Htetrafluoropropoxy) phosphazine) diluted to achieve a mass count of 10000. Purity of the final compounds **6b**, **7b**, **8b**, and **9b** was confirmed to be  $\geq 95\%$  by analytical RPHPLC using a Shimadzu Prominence-i LC-2030 system with a Dr. Maisch Reprosil Gold 120 C18 column ( $4.6 \times 250$  mm,  $5 \mu\text{m}$ ) at  $30^\circ\text{C}$  and equipped with a UV detector monitoring at  $214 \text{ nm}$ . The following solvent system, at a flow rate of  $1 \text{ mL/min}$ , was used: solvent A,  $0.1\%$  TFA in water/acetonitrile, 95/5; solvent B,  $0.1\%$  TFA in water/acetonitrile, 5/95. Gradient elution was as follows: 95:5 (A/B) for 2 min, 95:5 to 0:100 (A/B) over 30 min, 0:100 (A/B) for 1 min, then reversion back to 95:5 (A/B) over 1 min, 95:5 (A/B) for 3 min. The compounds were purified via preparative HPLC using a BESTA-Technik system with a Dr. Maisch Reprosil Gold 120 C18 column ( $25 \times 250$  mm,  $10 \mu\text{m}$ ) and equipped with a ECOM Flash UV detector monitoring at  $214 \text{ nm}$ . The following solvent system, at a flow rate of  $12 \text{ mL/min}$ , was used: solvent A,  $0.1\%$  TFA in water/acetonitrile 95/5; solvent B,  $0.1\%$  TFA in water/acetonitrile 5/95. Unless stated otherwise in the protocol, the gradient elution was as follows: 70:30 (A/B) to 0:100 (A/B) over 25 min, 0:100 (A/B) for 3 min, then reversion back to 70:30 (A/B) over 1 min, 70:30 (A/B) for 1 min.

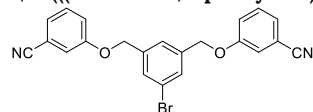
### 4.1. Synthesis

**(5-bromo-1,3-phenylene)dimethanol (10)** Protocol as described in literature.<sup>34</sup> Dimethyl 5-bromoisophthalate (2.3 g, 8.3 mmol) was dissolved in dry DCM (25 mL) under argon atmosphere. The solution was then cooled to  $0^\circ\text{C}$  using an ice bath and DIBALH (40 mL,  $1 \text{ M}$  hexane solution, 4.8 eq.) was added dropwise. The mixture was stirred from  $0^\circ\text{C}$  to room temperature for 1 hour. The reaction was quenched with Rochelle salt (60 mL, sat. aq.) and the biphasic mixture was stirred at room temperature overnight. The layers were separated and the aqueous layer was two times extracted with diethyl ether. The organic layers were combined, washed with water and brine, dried over  $\text{Na}_2\text{SO}_4$  and concentrated in vacuo. The crude product was purified using column chromatography (DCM/EtOAc = 1:1) and afforded compound **18** (1.8 g, 96%).  $^1\text{H}$  NMR (400 MHz, MeOD)  $\delta$  7.42 (s, 2H), 7.28 (s, 1H), 4.58 (s, 4H), 3.35 (s, 2H).  $^{13}\text{C}$  NMR (101 MHz, MeOD)  $\delta$  145.51, 129.42, 124.82, 123.31, 64.29.

**1-bromo-3,5-bis(bromomethyl)benzene (11)** Protocol as described in literature.<sup>56</sup> To a solution of compound **10** (1.0 g, 4.6 mmol) in dry DCM (50 mL) was added  $\text{PPh}_3$  (2.5 g, 9.7 mmol, 2.1 eq.) and  $\text{CBr}_4$  (3.2 g, 9.7 mmol, 2.1 eq.) and the mixture was stirred at room temperature for two hours under argon atmosphere. The reaction was quenched

with water (30 mL) and the product was extracted from the aqueous layer with DCM three times. The combined organic layers were washed with water and brine, dried over Na<sub>2</sub>SO<sub>4</sub> and concentrated in vacuo. The crude product was purified by column chromatography (petroleum ether 100%) to give compound **19** (0.87 g, 55%). <sup>1</sup>H NMR (400 MHz, CDCl<sub>3</sub>) δ 7.51 – 7.45 (m, 2H), 7.34 (s, 1H), 4.53 (d, J = 4.0 Hz, 1H), 4.41 (d, J = 4.2 Hz, 3H). <sup>13</sup>C NMR (101 MHz, CDCl<sub>3</sub>) δ 140.42, 140.11, 132.11, 132.09, 131.64, 128.40, 127.90, 122.83, 44.89, 31.64, 31.59.

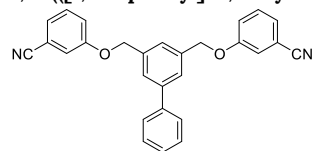
**3,3'-(((5-bromo-1,3-phenylene)bis(methylene))bis(oxy))dibenzonitrile (12)** These conditions were



based on literature protocols.<sup>36</sup> 3-cyanophenol (0.49 g, 4.1 mmol, 2.4 eq.) was suspended in dry DMF (6 mL) under argon atmosphere. The suspension was cooled to 0 °C using an ice bath and NaH (160 mg, 60% dispersion in mineral oil, 2.4 eq.) was slowly

added. The reaction was stirred for 30 minutes, the ice bath was removed and compound **11** (0.59 g, 1.7 mmol) was added. The reaction mixture was heated to 80 °C, stirred for 1 hour, and then cooled to room temperature. Water (18 mL) was added to the mixture to obtain precipitation and give compound **12** (0.72 g, quant.). <sup>1</sup>H NMR (400 MHz, CDCl<sub>3</sub>) δ 7.58 – 7.54 (m, 2H), 7.43 – 7.37 (m, 3H), 7.29 (dt, J = 7.6, 1.2 Hz, 2H), 7.21 – 7.17 (m, 4H), 5.07 (s, 4H). <sup>13</sup>C NMR (101 MHz, CDCl<sub>3</sub>) δ 158.45, 138.79, 130.69, 130.23, 125.33, 124.61, 123.34, 120.16, 118.68, 117.88, 113.54, 69.27.

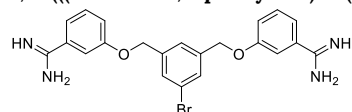
**3,3'-([1,1'-biphenyl]-3,5-diylbis(methylene))bis(oxy))dibenzonitrile (13)** Conditions were based on



protocols described in literature.<sup>40,41</sup> Dibenzonitrile intermediate **12** (0.15 g, 0.36 mmol) was dissolved in a 3:1 mixture of THF and 2 M Na<sub>2</sub>CO<sub>3</sub> (aq.) of 4 mL, respectively. Phenylboronic acid (65 mg, 0.54 mmol, 1.5 eq.) and Pd(dppf)Cl<sub>2</sub>·DCM (26 mg, 0.03 mmol, 0.1 eq.) were added. The reaction mixture was heated to 65 °C for 18 hours and then partitioned between DCM and NaHCO<sub>3</sub> (sat. aq.). The

aqueous layer was three times extracted with DCM, the organic layers were combined and dried over Na<sub>2</sub>SO<sub>4</sub>. The solvent was evaporated under reduced pressure and the crude product was purified using column chromatography (petroleum ether/EtOAc = 4:1) to obtain compound **13** (0.12 g, 83%). <sup>1</sup>H NMR (400 MHz, CDCl<sub>3</sub>) δ 7.70 – 7.61 (m, 4H), 7.54 – 7.48 (m, 3H), 7.47 – 7.40 (m, 3H), 7.34 – 7.24 (m, 6H), 5.21 (s, 4H). <sup>13</sup>C NMR (101 MHz, CDCl<sub>3</sub>) δ 158.77, 142.63, 140.34, 137.22, 130.63, 129.07, 128.01, 127.38, 126.33, 125.23, 125.14, 120.25, 118.79, 117.96, 113.47, 70.22.

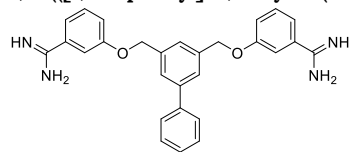
**3,3'-(((5-bromo-1,3-phenylene)bis(methylene))bis(oxy))dibenzimidamide (6b)** This protocol was



based on the synthesis of structurally similar amidine containing compounds previously described in literature.<sup>12,57-</sup>

<sup>60</sup> Compound **12** (100 mg, 0.24 mmol) was dissolved in a solution of LHMDs (2.0 mL, 1 M THF solution, 8.0 eq.) under argon atmosphere. The reaction was stirred at room temperature for 48 hours or longer until complete conversion to the bis-amidine (monitored by LCMS). The solution was cooled to 0 °C and quenched with HCl (3.6 mL, 4 M dioxane solution, 60 eq.). The mixture was stirred at room temperature for 30 minutes, then diluted with diethyl ether and filtered. The precipitate was purified by preparative HPLC with the gradient 30-100% in 30 minutes to give compound **6b** (23 mg, 21%). <sup>1</sup>H NMR (400 MHz, DMSO) δ 9.28 (s, 4H), 9.16 (s, 4H), 7.62 (d, J = 1.4 Hz, 2H), 7.56 – 7.48 (m, 3H), 7.43 (t, J = 2.1 Hz, 2H), 7.39 – 7.29 (m, 4H), 5.18 (s, 4H). <sup>13</sup>C NMR (101 MHz, DMSO) δ 165.26, 158.15, 139.57, 130.51, 129.92, 129.52, 125.78, 121.87, 120.64, 119.92, 114.66, 68.65. HRMS (ESI): calculated for C<sub>22</sub>H<sub>21</sub>BrN<sub>4</sub>O<sub>2</sub> [M+H]<sup>+</sup> 453.0926, found 453.0921.

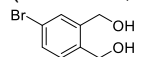
**3,3'-((([1,1'-biphenyl]-3,5-diylbis(methylene))bis(oxy))dibenzimidamide (7b)**



Following the procedure as described above for compound **6b**, using compound **13** (110 mg, 0.26 mmol), LHMS (2.5 mL, 1 M THF solution, 9.4 eq.) and HCl (4.5 mL, 4 M dioxane solution, 68 eq.), afforded the crude product. The crude product was purified using HPLC with a 30–100% gradient for 30 minutes to obtain the pure compound **7b** (112 mg, 93%).

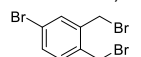
<sup>1</sup>H NMR (400 MHz, DMSO)  $\delta$  9.36 (s, 4H), 9.28 (s, 4H), 7.68 (d,  $J$  = 1.6 Hz, 2H), 7.64 – 7.58 (m, 2H), 7.52 – 7.39 (m, 7H), 7.38 – 7.31 (m, 5H), 5.22 (s, 4H). <sup>13</sup>C NMR (101 MHz, DMSO)  $\delta$  165.46, 158.42, 140.80, 139.61, 137.69, 130.49, 129.56, 129.15, 127.93, 126.84, 126.12, 125.93, 120.49, 120.06, 114.57, 69.59. HRMS (ESI): calculated for C<sub>28</sub>H<sub>26</sub>N<sub>4</sub>O<sub>2</sub> [M+H]<sup>+</sup> 451.2135, found 451.2129.

**(4-bromo-1,2-phenylene)dimethanol (14)**



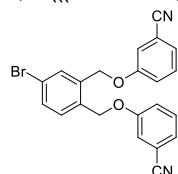
Conditions were based on protocol reported in literature.<sup>61</sup> LAH (15 mL, 1 M THF solution, 2 eq.) and ZnCl<sub>2</sub> (0.61 g, 4.5 mmol, 0.6 eq.) were suspended in dry THF (30 mL) and cooled to 0 °C, then 4-bromophthalic anhydride (1.7 g, 7.5 mmol) was slowly added. The mixture was stirred at room temperature for 6 hours under argon atmosphere. The mixture was cooled to 0 °C and quenched with Rochelle salt (30 mL, sat. aq.) and the biphasic mixture was stirred at room temperature overnight. The layers were separated and the aqueous layer was extracted with diethyl ether two times and the combined organic layers were washed with water and brine, dried over Na<sub>2</sub>SO<sub>4</sub> and concentrated in vacuo. The crude product was purified by column chromatography (DCM/EtOAc = 1:1) to give compound **24** (1.5 g, 95%). <sup>1</sup>H NMR (400 MHz, CDCl<sub>3</sub>)  $\delta$  7.48 (d,  $J$  = 2.1 Hz, 1H), 7.42 (dd,  $J$  = 8.0, 2.1 Hz, 1H), 7.18 (d,  $J$  = 8.0 Hz, 1H), 4.62 (d,  $J$  = 2.6 Hz, 4H), 3.20 (s, 2H). <sup>13</sup>C NMR (101 MHz, CDCl<sub>3</sub>)  $\delta$  141.49, 138.18, 129.88, 128.77, 127.92, 122.30, 64.53, 64.40, 64.31, 63.49, 63.47, 31.08, 23.80.

**4-bromo-1,2-bis(bromomethyl)benzene (15)**



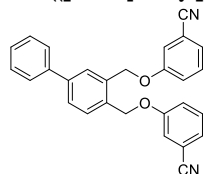
Following the procedure described for compound **11**, using compound **14** (1.5 g, 7.0 mmol) as starting material, afforded compound **40** (1.8 g, 74%). <sup>1</sup>H NMR (400 MHz, CDCl<sub>3</sub>)  $\delta$  7.52 (d,  $J$  = 2.1 Hz, 1H), 7.43 (dd,  $J$  = 8.2, 2.1 Hz, 1H), 7.24 (d,  $J$  = 8.2 Hz, 1H), 4.59 (s, 2H), 4.58 (s, 2H). <sup>13</sup>C NMR (101 MHz, CDCl<sub>3</sub>)  $\delta$  138.65, 135.67, 134.02, 132.69, 132.58, 131.24, 129.60, 123.17, 66.00, 42.46, 42.32, 30.14, 29.32, 29.12, 29.00, 28.83, 15.43.

**3,3'-(((4-bromo-1,2-phenylene)bis(methylene))bis(oxy))dibenzonitrile (16)**



Following the procedure as described above for compound **13**, using compound **15** (0.84 g, 2.4 mmol), afforded compound **16** as a crude product. After the precipitation, the weight of the precipitate was too high. The precipitate was then dissolved in DMF, water was added, and the precipitated compound **16** was collected (1.2 g, quant.). <sup>1</sup>H NMR (400 MHz, CDCl<sub>3</sub>)  $\delta$  7.68 (d,  $J$  = 2.1 Hz, 1H), 7.55 (dd,  $J$  = 8.1, 2.1 Hz, 1H), 7.44 – 7.34 (m, 4H), 7.31 – 7.25 (m, 3H), 7.20 – 7.14 (m, 2H), 5.12 (d,  $J$  = 6.6 Hz, 4H). <sup>13</sup>C NMR (101 MHz, CDCl<sub>3</sub>)  $\delta$  158.38, 136.48, 132.95, 132.13, 132.07, 131.07, 130.77, 130.75, 129.53, 129.21, 125.50, 125.44, 123.21, 120.12, 120.11, 118.60, 117.71, 117.70, 113.60, 113.58, 67.95, 67.62.

**3,3'-(((1,1'-biphenyl)-3,4-diylbis(methylene))bis(oxy))dibenzonitrile (17)**

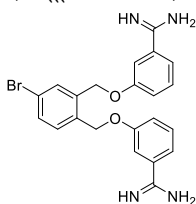


Following the procedure as described above for compound **13**, using compound **16** (150 mg, 0.36 mmol) afforded compound **17** (0.12 g, 81%). <sup>1</sup>H NMR (400 MHz, CDCl<sub>3</sub>)  $\delta$  7.80 (s, 1H), 7.73 – 7.63 (m, 3H), 7.59 – 7.42 (m, 5H), 7.37 – 7.32 (m, 3H), 7.30 – 7.22 (m, 4H), 5.37 – 5.22 (m, 4H). <sup>13</sup>C NMR (101 MHz, CDCl<sub>3</sub>)  $\delta$  158.65, 142.30, 140.16, 134.77, 134.27, 133.08, 130.70, 130.66, 130.17, 129.54, 129.21, 129.07, 128.36, 127.99, 127.78, 127.30, 125.28, 125.25, 125.21, 120.20, 120.16, 118.71, 117.78, 117.75, 113.52, 77.48,

77.16, 76.84, 68.63, 68.55, 68.37.

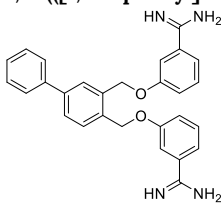


**3,3'-(((4-bromo-1,2-phenylene)bis(methylene))bis(oxy))dibenzimidamide (8b)** Conditions were



based on literature.<sup>38</sup> To a suspension of compound **16** (130 mg, 0.31 mmol) and DIPEA (0.28 mL, 1.6 mmol, 5 eq.) in EtOH (5.0 mL) was added  $\text{NH}_2\text{OH}\cdot\text{HCl}$  (104 mg, 1.5 mmol, 4.8 eq.). The reaction mixture was stirred at 85 °C overnight. The mixture was concentrated in vacuo and the residue was dissolved in AcOH (3.0 mL) and  $\text{Ac}_2\text{O}$  (0.14 mL, 1.5 mmol, 4.8 eq.) was added. The reaction was stirred overnight and then concentrated in vacuo. The residue was co-evaporated with toluene three times and then suspended in AcOH (4.0 mL) under argon atmosphere. Zinc powder (30 mg, 0.92 mmol, 1.5 eq.) was added and the mixture was stirred at 35 °C for 6 hours. Upon completion, the reaction mixture was filtered through Celite®, the Celite® was rinsed with acetone and all collected fractions were concentrated in vacuo. The crude product purified by preparative HPLC (gradient 30-100%, 30 minutes) to afford the final compound **8b** (14.7 mg, 10%).  $^1\text{H}$  NMR (400 MHz, DMSO)  $\delta$  9.25 (s, 4H), 8.99 (s, 4H), 7.72 (d,  $J$  = 2.1 Hz, 1H), 7.62 – 7.40 (m, 6H), 7.40 – 7.32 (m, 4H), 5.28 (d,  $J$  = 10.6 Hz, 4H). HRMS (ESI): calculated for  $\text{C}_{22}\text{H}_{21}\text{BrN}_4\text{O}_2$   $[\text{M}+\text{H}]^+$  453.0926, found 453.0919.

**3,3'-(((1,1'-biphenyl)-3,4-diylbis(methylene))bis(oxy))dibenzimidamide (9b)** Following the



procedure as described above for compound **6b**, using compound **17** (110 mg, 0.26 mmol), LHMDS (2.5 mL, 1 M THF solution, 9.4 eq.) and HCl (4.6 mL, 4 M dioxane solution, 68 eq.), afforded the crude product. The crude product was purified using HPLC with a 30-100% gradient for 30 minutes to obtain the pure compound **9b** (64 mg, 53%).  $^1\text{H}$  NMR (400 MHz, DMSO)  $\delta$  9.27 (dd,  $J$  = 15.0, 2.7 Hz, 8H), 7.80 (d,  $J$  = 1.9 Hz, 1H), 7.68 – 7.54 (m, 4H), 7.49 – 7.38 (m, 6H), 7.37 – 7.28 (m, 5H), 5.32 (d,  $J$  = 9.1 Hz, 4H).  $^{13}\text{C}$  NMR (101 MHz, DMSO)  $\delta$  165.42, 165.39, 158.28, 140.24, 139.43, 135.39, 134.01, 130.45, 129.51, 129.11, 127.87, 127.28, 126.77, 126.64, 120.52, 119.99, 114.78, 114.68, 67.67, 67.31. HRMS (ESI): calculated for  $\text{C}_{28}\text{H}_{26}\text{N}_4\text{O}_2$   $[\text{M}+\text{H}]^+$  451.2135, found 451.2128.

## 4.2. Antimicrobial assays

All compounds were screened for antimicrobial activity against *S. aureus* ATCC29213. A select group of the pentamidine analogues was further tested against *S. aureus* LIM2, *S. aureus* VRS3b, *S. aureus* MRSA Col, *S. aureus* USA300, *E. faecium* E155, and *E. faecium* 7314. The antimicrobial assay was performed according to CLSI guidelines. Bacteria were plated out directly from their glycerol stocks on blood agar plates, incubated overnight at 37 °C, and then kept in the fridge. The blood agar plates were only used for 2 weeks and then replaced.

## 4.3. Minimal inhibitory concentration (MIC) assay using Lysogeny Broth (LB)

A single colony from a blood agar plate was inoculated in LB at 37 °C until a 0.5 optical density at 600nm ( $\text{OD}_{600}$ ) was reached (compared to the sterility control of LB). The bacterial suspension was diluted in fresh LB to  $2.0 \times 10^6$  CFU/mL. The serial dilutions were prepared in polypropylene microtiter plates: a stock of the test compounds was prepared with a 2x final concentration in LB. 100  $\mu\text{L}$  of the stock was added to the wells of the top row of which 50  $\mu\text{L}$  was used for the serial dilution. The bottom row of each plate was used as the positive (50  $\mu\text{L}$  of LB) and negative controls (100  $\mu\text{L}$  of LB) (6 wells each). 50  $\mu\text{L}$  of the  $2.0 \times 10^6$  CFU/mL bacterial stock was added to each well except for the negative controls, adding up to a total volume of 100  $\mu\text{L}$  per well. The plates were sealed with a breathable seal and incubated for 20 hours at 37 °C and 600 rpm. The MIC was visually determined after centrifuging the plates for 2 minutes at 3000 rpm.

#### **4.4. MIC using Mueller Hinton Broth (MHB), cation-adjusted MHB (CAMHB), and tryptic soy broth (TSB).**

Protocol identical to the MIC assays with LB except for the use of TSB as broth for the inoculation and the use of MHB, CAMHB, or TSB for the bacterial suspensions and serial dilutions.

#### **4.5. Hemolysis assays.**

The hemolytic activity of each analogue was assessed in triplicate. Red blood cells from defibrinated sheep blood obtained from Thermo Fisher were centrifuged (400 g for 15 minutes at 4°C) and washed with Phosphate-Buffered Saline (PBS) containing 0.002% Tween20 (buffer) for five times. Then, the red blood cells were normalized to obtain a positive control read-out between 2.5 and 3.0 at 415 nm to stay within the linear range with the maximum sensitivity. A serial dilution of the compounds (128 – 4 µg/mL, 75 µL) was prepared in a 96-well plate. The outer border of the plate was filled with 75 µL buffer. Each plate contained a positive control (0.1% Triton-X final concentration, 75 µL) and a negative control (buffer, 75 µL) in triplicate. The normalized blood cells (75 µL) were added and the plates were incubated at 37 °C for 1 hour or 20 hours while shaking at 500 rpm. After incubation, the plates were centrifuged (800 g for 5 minutes at room temperature). A flat-bottom plate of polystyrene with 100 µL buffer in each well was prepared. To this plate 25 µL of the supernatant was transferred to their respective wells in the flat-bottom plate. The values obtained from a read-out at 415 nm were corrected for background (negative control) and transformed to a percentage relative to the positive control.

# Supplementary data

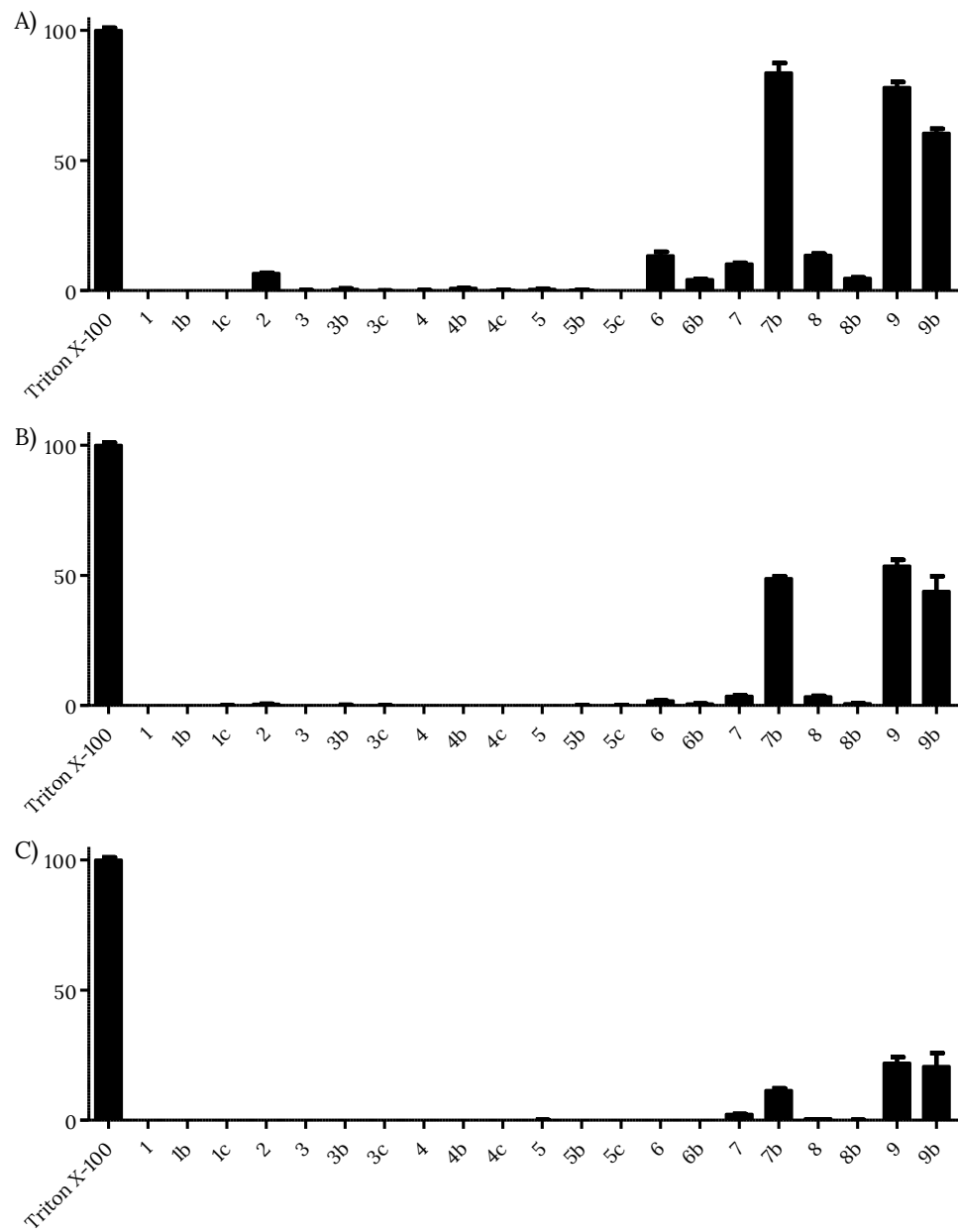


**Figure S1.** Hemolytic activity of all compounds after 20 hours of incubation. Concentration tested: A) 128 µg/mL; B) 64 µg/mL; C) 32 µg/mL. The hemolysis assay was performed as described in materials and methods. Values below 10% were defined as non-hemolytic.<sup>32</sup> Error bars represent the standard deviation based on n=3 technical replicates.

**Table S1.** MIC values (µg/ml) of pentamidine analogues in LB broth for *S. aureus* ATCC29213. Hemolytic activity of all compounds (128-32 µg/mL). The hemolysis assay was performed as described in materials and methods. Values below 10% were defined as non-hemolytic (see gray background for ≥ 10%).<sup>32</sup> Values are the average of on n=3 technical replicates. The therapeutic window is calculated by dividing the highest non-hemolytic concentration by the MIC.

	MIC (µg/ml)	% Hemolysis (128 µg/ml)	% Hemolysis (64 µg/ml)	% Hemolysis (32 µg/ml)	Therapeutic window
<b>1</b>	8-16	0.0	0.0	0.0	16-8
<b>1b</b>	16	0.0	0.0	0.0	8
<b>1c</b>	>128	0.0	0.0	0.0	-
<b>2</b>	2	6.6	0.6	0.0	64
<b>3</b>	16	0.0	0.0	0.0	8
<b>3b</b>	32	0.5	0.1	0.0	4
<b>3c</b>	>128	0.0	0.0	0.0	-
<b>4</b>	16	0.0	0.0	0.0	8
<b>4b</b>	4	0.9	0.0	0.0	32
<b>4c</b>	128	0.2	0.0	0.0	1
<b>5</b>	8	0.5	0.0	0.1	16
<b>5b</b>	8	0.3	0.1	0.0	16
<b>5c</b>	128	0.1	0.1	0.0	1
<b>6</b>	4	13	1.8	0.0	16
<b>6b</b>	1	4.2	0.6	0.0	128
<b>7</b>	1	10	3.6	2.3	64
<b>7b</b>	0.5	84	49	11	≤32
<b>8</b>	1	14	3.4	0.7	64
<b>8b</b>	1	4.8	0.8	0.0	128
<b>9</b>	1	78	54	22	≤16
<b>9b</b>	4	61	44	21	≤4

**Table S2.** MIC values (µg/ml) of pentamidine analogues **1-4** and **6-9b** in LB broth for *S. aureus* and *E. faecium* strains. The maximum concentration tested for the bis-amidines was 32 µg/ml and vancomycin 128 µg/ml.

	<i>S. aureus</i>					<i>E. faecium</i>	
	ATCC 29213	LIM2	VRS3b	COL	USA300	E155	7314
<b>1</b>	8-16	>64	8	8	16	>64	64
<b>2</b>	2	32	2	2	4	16	16
<b>3</b>	16	>32	8	8	16	>32	>32
<b>4</b>	16	>32	16	16	16	16	32
<b>6</b>	4	16	2	2	2	16	32
<b>6b</b>	1	16	0.5	0.5	2	32	16
<b>7</b>	1	4	0.25	0.5	1	4	16
<b>7b</b>	0.5	4	0.125	0.25	1	8	8
<b>8</b>	1	16	1	1	2	16	16
<b>8b</b>	1	32	2	4	8	32	32
<b>9</b>	1	4	0.25	<0.5	1	2	4
<b>9b</b>	4	8	1	0.5	<2	4	8
<b>Vancomycin</b>	1	4	128	2	<2	>128	128

**Table S3.** MIC values (µg/ml) of pentamidine analogues **1-4** and **6-9b** in MHB broth for *S. aureus* and *E. faecium* strains. The maximum concentration tested for the pentamidine analogues was 32 µg/ml and vancomycin 128 µg/ml.

	<i>S. aureus</i>					<i>E. faecium</i>	
	ATCC 29213	LIM2	VRS3b	COL	USA300	E155	7314
<b>1</b>	2	>32	8	4	8	32	32
<b>2</b>	1	16	2	0.5	1	8	16
<b>3</b>	4	>32	4	4	8	>32	>32
<b>4</b>	4	32	4	4	8	8	>32
<b>6</b>	1	4	0.5	0.5	1	2	8
<b>6b</b>	0.5	8	0.5	0.125	0.5	8	8
<b>7</b>	0.5	2	0.25	0.25	1	2	2
<b>7b</b>	0.5	2	0.25	0.125	0.5	2	2
<b>8</b>	1	4	0.25	0.5	1	4	8
<b>8b</b>	0.5	2	0.5	0.25	1	2	4
<b>9</b>	0.5	2	0.5	0.5	1	1	1
<b>9b</b>	1	8	1	1	2	16	16
<b>Vancomycin</b>	0.5	4	128	2	1	>128	>128

**Table S4.** MIC values (µg/ml) of pentamidine analogues **1-4** and **6-9b** in CAMHB broth for *S. aureus* and *E. faecium* strains. The maximum concentration tested for the bis-amidines was 32 µg/ml (except for pentamidine with the *E. faecium* strains) and vancomycin 128 µg/ml.

	<i>S. aureus</i>					<i>E. faecium</i>	
	ATCC 29213	LIM2	VRS3b	MRSA Col	USA300	E155	7314
<b>1</b>	4	>32	8	4	8	>64	64
<b>2</b>	1	32	1	1	2	16	32
<b>3</b>	8	>32	8	4	8	32	32
<b>4</b>	8	>32	4	4	8	32	32
<b>6</b>	1	8	1	1	1	>32	16
<b>6b</b>	0.5	16	0.5	0.25	0.5	2	16
<b>7</b>	0.5	4	0.5	0.5	1	2	2
<b>7b</b>	0.5	4	0.25	0.5	1	2	4
<b>8</b>	1	16	0.5	0.25	1	8	8
<b>8b</b>	1	32	1	1	2	2	16
<b>9</b>	1	4	0.5	0.5	1	2	2
<b>9b</b>	0.5	4	0.5	0.5	2	1	4
<b>Vancomycin</b>	1	4	128	2	1	>128	>128

**Table S5.** MIC values (µg/ml) of pentamidine analogues **1-4** and **6-9b** in TSB broth for *E. faecium* E155 and 7314. The maximum concentration tested for the bis-amidines was 128 µg/ml and vancomycin 128 µg/ml.

	<i>E. faecium</i>	
	E155	7314
<b>1</b>	128	128
<b>2</b>	>2	>2
<b>3</b>	>128	>128
<b>4</b>	64	128
<b>6</b>	16	32
<b>6b</b>	32	16
<b>7</b>	4	4
<b>7b</b>	4	8
<b>8</b>	16	16
<b>8b</b>	8	8
<b>9</b>	<2	<2
<b>9b</b>	64	32
<b>Vancomycin</b>	64	128

## References

- (1) Murray, C. J.; Ikuta, K. S.; Sharara, F.; Swetschinski, L.; Aguilar, G. R.; Gray, A.; Han, C.; Bisignano, C.; Rao, P.; Wool, E.; et al. Global Burden of Bacterial Antimicrobial Resistance in 2019: A Systematic Analysis. *The Lancet* **2022**, 399 (10325), 629–655. [https://doi.org/10.1016/S0140-6736\(21\)02724-0](https://doi.org/10.1016/S0140-6736(21)02724-0).
- (2) Laxminarayan, R. The Overlooked Pandemic of Antimicrobial Resistance. *The Lancet* **2022**, 399 (10325), 606–607. [https://doi.org/10.1016/S0140-6736\(22\)00087-3](https://doi.org/10.1016/S0140-6736(22)00087-3).
- (3) O'Neill, J. *Tackling Drug-Resistant Infections Globally: Final Report and Recommendations*; Report; Government of the United Kingdom, 2016.
- (4) O'Neill, J. *Antimicrobial Resistance: Tackling a Crisis for the Health and Wealth of Nations*; Report; Government of the United Kingdom, 2014.
- (5) Thakare, R.; Kaul, G.; Shukla, M.; Kesharwani, P.; Srinivas, N.; Dasgupta, A.; Chopra, S. Chapter 5 - Repurposing Nonantibiotic Drugs as Antibacterials. In *Drug Discovery Targeting Drug-Resistant Bacteria*; Kesharwani, P., Chopra, S., Dasgupta, A., Eds.; Academic Press, 2020; pp 105–138. <https://doi.org/10.1016/B978-0-12-818480-6.00005-9>.
- (6) Farha, M. A.; Brown, E. D. Drug Repurposing for Antimicrobial Discovery. *Nature Microbiology* **2019**, 4 (April), 565–577. <https://doi.org/10.1038/s41564-019-0357-1>.
- (7) Schweizer, F. *Repurposing Antibiotics to Treat Resistant Gram-Negative Pathogens*. In *Antibiotic Drug Resistance*; John Wiley & Sons, Ltd, 2019; pp 453–476. <https://doi.org/10.1002/9781119282549.ch18>.
- (8) Bean, D. C.; Wareham, D. W. Pentamidine: A Drug to Consider Re-Purposing in the Targeted Treatment of Multi-Drug Resistant Bacterial Infections? *Journal of Laboratory and Precision Medicine* **2017**, 2, 49–49. <https://doi.org/10.21037/jlpm.2017.06.18>.
- (9) Trypanosomiasis, human African (sleeping sickness) [https://www.who.int/news-room/fact-sheets/detail/trypanosomiasis-human-african-\(sleeping-sickness\)](https://www.who.int/news-room/fact-sheets/detail/trypanosomiasis-human-african-(sleeping-sickness)) (accessed 2022 -02 -15).
- (10) Sands, M.; Kron, M. A.; Brown, R. B. Pentamidine: A Review. *Reviews of infectious diseases* **1985**, 7 (5), 625–634. <https://doi.org/10.1093/clinids/7.5.625>.
- (11) Stokes, J. M.; MacNair, C. R.; Ilyas, B.; French, S.; Côté, J.-P.; Bouwman, C.; Farha, M. A.; Sieron, A. O.; Whitfield, C.; Coombes, B. K.; Brown, E. D. Pentamidine Sensitizes Gram-Negative Pathogens to Antibiotics and Overcomes Acquired Colistin Resistance. *Nat Microbiol* **2017**, 2 (5), 1–8. <https://doi.org/10.1038/nmicrobiol.2017.28>.
- (12) Wesseling, C. M. J.; Slingerland, C. J.; Veraar, S.; Lok, S.; Martin, N. I. Structure-Activity Studies with Bis-Amidines That Potentiate Gram-Positive Specific Antibiotics against Gram-Negative Pathogens. *ACS Infect. Dis.* **2021**. <https://doi.org/10.1021/acsinfecdis.1c00466>.
- (13) Herrera-Espejo, S.; Cebreiro-Cangueiro, T.; Labrador-Herrera, G.; Pachón, J.; Pachón-Ibáñez, M. E.; Álvarez-Marín, R. In Vitro Activity of Pentamidine Alone and in Combination with Antibiotics against Multidrug-Resistant Clinical *Pseudomonas Aeruginosa* Strains. *Antibiotics* **2020**, 9 (12), 885. <https://doi.org/10.3390/antibiotics9120885>.
- (14) Wu, C.; Xia, L.; Huang, W.; Xu, Y.; Gu, Y.; Liu, C.; Ji, L.; Li, W.; Wu, Y.; Zhou, K.; Feng, X. Pentamidine Sensitizes FDA-Approved Non-Antibiotics for the Inhibition of Multidrug-Resistant Gram-Negative Pathogens. *Eur J Clin Microbiol Infect Dis* **2020**, 39 (9), 1771–1779. <https://doi.org/10.1007/s10096-020-03881-0>.
- (15) Edwards, K. J.; Jenkins, T. C.; Neidle, S. Crystal Structure of a Pentamidine-Oligonucleotide Complex: Implications for DNA-Binding Properties. *Biochemistry* **1992**, 31 (31), 7104–7109. <https://doi.org/10.1021/bi00146a011>.
- (16) Sun, T.; Zhang, Y. Pentamidine Binds to tRNA through Non-Specific Hydrophobic Interactions and Inhibits Aminoacylation and Translation. *Nucleic Acids Research* **2008**, 36 (5), 1654–1664. <https://doi.org/10.1093/nar/gkm1180>.
- (17) Paracini, N.; Clifton, L. A.; Skoda, M. W. A.; Lakey, J. H. Liquid Crystalline Bacterial Outer Membranes Are Critical for Antibiotic Susceptibility. **2018**. <https://doi.org/10.1073/pnas.1803975115>.

- (18) Cavalier, M. C.; Ansari, M. I.; Pierce, A. D.; Wilder, P. T.; McKnight, L. E.; Raman, E. P.; Neau, D. B.; Bezawada, P.; Alasady, M. J.; Charpentier, T. H.; Varney, K. M.; Toth, E. A.; MacKerell, A. D.; Coop, A.; Weber, D. J. Small Molecule Inhibitors of Ca<sup>2+</sup>-S100B Reveal Two Protein Conformations. *Journal of Medicinal Chemistry* **2016**, 59 (2), 592–608. <https://doi.org/10.1021/acs.jmedchem.5b01369>.
- (19) Amos, H.; Vollmayer, E. Effect of pentamidine on the growth of *Escherichia coli*. *J Bacteriol* **1957**, 73 (2), 172–177.
- (20) Libman, M. D.; Miller, M. A.; Richards, G. K. Antistaphylococcal Activity of Pentamidine. *Antimicrobial Agents and Chemotherapy* **1990**, 34 (9), 1795–1796. <https://doi.org/10.1128/AAC.34.9.1795>.
- (21) Maciejewska, D.; Zabiński, J.; Kaźmierczak, P.; Wójciuk, K.; Kruszewski, M.; Kruszewska, H. In Vitro Screening of Pentamidine Analogs against Bacterial and Fungal Strains. *Bioorganic and Medicinal Chemistry Letters* **2014**, 24 (13), 2918–2923. <https://doi.org/10.1016/j.bmcl.2014.04.075>.
- (22) Bichowsky-Slomnitzki, L. The Effect of Aromatic Diamidines on Bacterial Growth. *J Bacteriol* **1948**, 55 (1), 27–31.
- (23) Rolain, J.-M.; Fenollar, F.; Raoult, D. In Vitro Activity of Pentamidine against *Tropheryma Whipplei*. *International Journal of Antimicrobial Agents* **2011**, 38 (6), 545–547. <https://doi.org/10.1016/j.ijantimicag.2011.07.015>.
- (24) Minnick, M. F.; Hicks, L. D.; Battisti, J. M.; Raghavan, R. Pentamidine Inhibits *Coxiella Burnetii* Growth and 23S rRNA Intron Splicing in Vitro. *International Journal of Antimicrobial Agents* **2010**, 36 (4), 380–382. <https://doi.org/10.1016/j.ijantimicag.2010.05.017>.
- (25) Waller, D. G.; Sampson, A. P. Chemotherapy of Infections. In *Medical pharmacology and therapeutics*; Elsevier, 2018; pp 581–629. <https://doi.org/10.1016/B978-0-7020-7167-6.00051-8>.
- (26) Goa, K. L.; Campoli-Richards, D. M. Pentamidine Isethionate: A Review of Its Antiprotozoal Activity, Pharmacokinetic Properties and Therapeutic Use in *Pneumocystis Carinii* Pneumonia. *Drugs* **1987**, 33 (3), 242–258. <https://doi.org/10.2165/00003495-198733030-00002>.
- (27) Andreana, I.; Bincoletto, V.; Milla, P.; Dosio, F.; Stella, B.; Arpicco, S. Nanotechnological Approaches for Pentamidine Delivery. *Drug Deliv. and Transl. Res.* **2022**. <https://doi.org/10.1007/s13346-022-01127-4>.
- (28) Liu, Y.; Hu, X.; Wu, Y.; Zhang, W.; Chen, X.; You, X.; Hu, L. Synthesis and Structure-Activity Relationship of Novel Bisindole Amidines Active against MDR Gram-Positive and Gram-Negative Bacteria. *European Journal of Medicinal Chemistry* **2018**, 150, 771–782. <https://doi.org/10.1016/j.ejmech.2018.03.031>.
- (29) Donkor, I. O.; Clark, A. M. In Vitro Antimicrobial Activity of Aromatic Diamidines and Diimidazolines Related to Pentamidine. *European Journal of Medicinal Chemistry* **1999**, 34 (7), 639–643. [https://doi.org/10.1016/S0223-5234\(00\)80032-X](https://doi.org/10.1016/S0223-5234(00)80032-X).
- (30) Bistrović, A.; Krstulović, L.; Stolić, I.; Drenjančević, D.; Talapko, J.; Taylor, M. C.; Kelly, J. M.; Bajić, M.; Raić-Malić, S. Synthesis, Anti-Bacterial and Anti-Protozoal Activities of Amidinobenzimidazole Derivatives and Their Interactions with DNA and RNA. *Journal of Enzyme Inhibition and Medicinal Chemistry* **2018**, 33 (1), 1323–1334. <https://doi.org/10.1080/14756366.2018.1484733>.
- (31) WHO. Global Priority List of Antibiotic-Resistant Bacteria to Guide Research, Discovery, and Development of New Antibiotics. **2017**, 7.
- (32) Amin, K.; Dannenfelser, R.-M. In Vitro Hemolysis: Guidance for the Pharmaceutical Scientist. *Journal of Pharmaceutical Sciences* **2006**, 95 (6), 1173–1176. <https://doi.org/10.1002/JPS.20627>.
- (33) van Groesen, E.; Slingerland, C. J.; Innocenti, P.; Mihajlovic, M.; Masereeuw, R.; Martin, N. I. Vancomyxins: Vancomycin-Polymyxin Nonapeptide Conjugates That Retain Anti-Gram-Positive Activity with Enhanced Potency against Gram-Negative Strains. *ACS Infect. Dis.* **2021**, 7 (9), 2746–2754. <https://doi.org/10.1021/acsinfecdis.1c00318>.
- (34) Kong, N.; Liu, E. A.; Vu, B. T. Cis-Imidazolines. U.S. patent US 6617346 B1, 2003.



- (35) Huang, H.; Li, H.; Martásek, P.; Roman, L. J.; Poulos, T. L.; Silverman, R. B. Structure-Guided Design of Selective Inhibitors of Neuronal Nitric Oxide Synthase. *Journal of Medicinal Chemistry* **2013**, 56 (7), 3024–3032. <https://doi.org/10.1021/jm4000984>.
- (36) Gromyko, A. V.; Popov, K. V.; Mosoleva, A. P.; Streltsov, S. A.; Grokhovsky, S. L.; Oleinikov, V. A.; Zhuze, A. L. DNA Sequence-Specific Ligands: XII. Synthesis and Cytological Studies of Dimeric Hoechst 33258 Molecules. *Russian Journal of Bioorganic Chemistry* **2005**, 31 (4), 344–351. <https://doi.org/10.1007/s11171-005-0047-z>.
- (37) García, D.; Foubelo, F.; Yus, M. Selective Lithiation of 4- and 5-Halophthalans. *Heterocycles* **2009**, 77 (2), 991–1005. [https://doi.org/10.3987/COM-08-S\(F\)85](https://doi.org/10.3987/COM-08-S(F)85).
- (38) Goswami, R.; Mukherjee, S.; Wohlfahrt, G.; Ghadiyaram, C.; Nagaraj, J.; Chandra, B. R.; Sistla, R. K.; Satyam, L. K.; Samiulla, D. S.; Moilanen, A.; Subramanya, H. S.; Ramachandra, M. Discovery of Pyridyl Bis(Oxy)Dibenzimidamide Derivatives as Selective Matriptase Inhibitors. *ACS Medicinal Chemistry Letters* **2013**, 4 (12), 1152–1157. <https://doi.org/10.1021/ml400213v>.
- (39) Suzuki, A. Organoborane Coupling Reactions (Suzuki Coupling). *Proceedings of the Japan Academy. Series B, Physical and Biological Sciences* **2004**, 80 (8), 359–359.
- (40) Martino, G.; Muzio, L.; Riva, N.; Gornati, D.; Seneci, P.; Eleuteri, S. Aminoguanidine Hydrazones as Retromer Stabilizers Useful for Treating Neurological Diseases. WO 2020/201326 A1, 2020.
- (41) Innocenti, P.; Woodward, H.; O'Fee, L.; Hoelder, S. Expanding the Scope of Fused Pyrimidines as Kinase Inhibitor Scaffolds: Synthesis and Modification of Pyrido[3,4-d]Pyrimidines. *Organic & Biomolecular Chemistry* **2014**, 13 (3), 893–904. <https://doi.org/10.1039/C4OB02238F>.
- (42) G C, B.; Sahukhal, G. S.; Elasri, M. O. Role of the MsaABCR Operon in Cell Wall Biosynthesis, Autolysis, Integrity, and Antibiotic Resistance in *Staphylococcus Aureus*. *Antimicrobial Agents and Chemotherapy* 63 (10), e00680–19. <https://doi.org/10.1128/AAC.00680-19>.
- (43) Samanta, D.; Elasri, M. O. The MsaABCR Operon Regulates Resistance in Vancomycin-Intermediate *Staphylococcus Aureus* Strains. *Antimicrobial Agents and Chemotherapy* **2014**, 58 (11), 6685–6695. <https://doi.org/10.1128/AAC.03280-14>.
- (44) Sieradzki, K.; Tomasz, A. Alterations of Cell Wall Structure and Metabolism Accompany Reduced Susceptibility to Vancomycin in an Isogenic Series of Clinical Isolates of *Staphylococcus aureus*. *Journal of Bacteriology* **2003**, 185 (24), 7103–7110. <https://doi.org/10.1128/JB.185.24.7103-7110.2003>.
- (45) Schindler, B. D.; Kaatz, G. W. Multidrug Efflux Pumps of Gram-Positive Bacteria. *Drug Resistance Updates* **2016**, 27, 1–13. <https://doi.org/10.1016/j.drup.2016.04.003>.
- (46) Costa, S. S.; Viveiros, M.; Amaral, L.; Couto, I. Multidrug Efflux Pumps in *Staphylococcus Aureus*: An Update. *Open Microbiol J* **2013**, 7, 59–71. <https://doi.org/10.2174/1874285801307010059>.
- (47) Paulsen, I. T.; Brown, M. H.; Skurray, R. A. Characterization of the Earliest Known *Staphylococcus Aureus* Plasmid Encoding a Multidrug Efflux System. *Journal of Bacteriology* **1998**, 180 (13), 3477–3479. <https://doi.org/10.1128/JB.180.13.3477-3479.1998>.
- (48) Mitchell, B. A.; Brown, M. H.; Skurray, R. A. QacA Multidrug Efflux Pump From *Staphylococcus Aureus*: Comparative Analysis of Resistance to Diamidines, Biguanidines, and Guanylhidrazones. *Antimicrobial Agents and Chemotherapy* **1998**, 42 (2), 475–477. <https://doi.org/10.1128/AAC.42.2.475>.
- (49) Hassan, K. A.; Skurray, R. A.; Brown, M. H. Transmembrane Helix 12 of the *Staphylococcus Aureus* Multidrug Transporter QacA Lines the Bivalent Cationic Drug Binding Pocket. *Journal of Bacteriology* **2007**, 189 (24), 9131–9134. <https://doi.org/10.1128/JB.01492-07>.
- (50) Hsieh, P.-C.; Siegel, S. A.; Rogers, B.; Davis, D.; Lewis, K. Bacteria Lacking a Multidrug Pump: A Sensitive Tool for Drug Discovery. *PNAS* **1998**, 95 (12), 6602–6606. <https://doi.org/10.1073/pnas.95.12.6602>.
- (51) Chan, K.-F.; Zhao, Y.; Chow, L. M. C.; Chan, T. H. Synthesis of (±)-5'-Methoxyhydnocarpin-D, an Inhibitor of the *Staphylococcus Aureus* Multidrug Resistance Pump. *Tetrahedron* **2005**, 61 (16), 4149–4156. <https://doi.org/10.1016/j.tet.2005.02.024>.

- (52) Dashtbani-Roozbehani, A.; Brown, M. H. Efflux Pump Mediated Antimicrobial Resistance by Staphylococci in Health-Related Environments: Challenges and the Quest for Inhibition. *Antibiotics* **2021**, 10 (12), 1502. <https://doi.org/10.3390/antibiotics10121502>.
- (53) Rizzotti, L.; Rossi, F.; Torriani, S. Biocide and Antibiotic Resistance of Enterococcus Faecalis and Enterococcus Faecium Isolated from the Swine Meat Chain. *Food Microbiology* **2016**, 60, 160–164. <https://doi.org/10.1016/j.fm.2016.07.009>.
- (54) Alotaibi, S. M. I.; Ayibieke, A.; Pedersen, A. F.; Jakobsen, L.; Pinholt, M.; Gumpert, H.; Hammerum, A. M.; Westh, H.; Ingmer, H. 2017. Susceptibility of Vancomycin-Resistant and -Sensitive Enterococcus Faecium Obtained from Danish Hospitals to Benzalkonium Chloride, Chlorhexidine and Hydrogen Peroxide Biocides. *Journal of Medical Microbiology* 66 (12), 1744–1751. <https://doi.org/10.1099/jmm.0.000642>.
- (55) Mayer, S.; Boos, M.; Beyer, A.; Fluit, A. C.; Schmitz, F.-J. Distribution of the Antiseptic Resistance Genes QacA, QacB and QacC in 497 Methicillin-Resistant and -Susceptible European Isolates of Staphylococcus Aureus. *Journal of Antimicrobial Chemotherapy* **2001**, 47 (6), 896–897. <https://doi.org/10.1093/jac/47.6.896>.
- (56) Huang, H.; Li, H.; Martásek, P.; Roman, L. J.; Poulos, T. L.; Silverman, R. B. Structure-Guided Design of Selective Inhibitors of Neuronal Nitric Oxide Synthase. *Journal of Medicinal Chemistry* **2013**, 56 (7), 3024–3032. <https://doi.org/10.1021/jm4000984>.
- (57) Bruncko, M.; McClellan, W. J.; Wendt, M. D.; Sauer, D. R.; Geyer, A.; Dalton, C. R.; Kaminski, M. A.; Weitzberg, M.; Gong, J.; Dellaria, J. F.; Mantei, R.; Zhao, X.; Nienaber, V. L.; Stewart, K.; Klinghofer, V.; Bouska, J.; Rockway, T. W.; Giranda, V. L. Naphthamidine Urokinase Plasminogen Activator Inhibitors with Improved Pharmacokinetic Properties. *Bioorganic and Medicinal Chemistry Letters* **2005**, 15 (1), 93–98. <https://doi.org/10.1016/j.bmcl.2004.10.026>.
- (58) Zhang, J.; Qian, K.; Yan, C.; He, M.; Jassim, B. A.; Ivanov, I.; Zheng, Y. G. Discovery of Decamidine as a New and Potent PRMT1 Inhibitor. *MedChemComm* **2017**, 8 (2), 440–444. <https://doi.org/10.1039/c6md00573j>.
- (59) Wendt, M. D.; Rockway, T. W.; Geyer, A.; McClellan, W.; Weitzberg, M.; Zhao, X.; Mantei, R.; Nienaber, V. L.; Stewart, K.; Klinghofer, V.; Giranda, V. L. Identification of Novel Binding Interactions in the Development of Potent, Selective 2-Naphthamidine Inhibitors of Urokinase. Synthesis, Structural Analysis, and SAR of N-Phenyl Amide 6-Substitution. *Journal of Medicinal Chemistry* **2004**, 47 (2), 303–324. <https://doi.org/10.1021/jm0300072>.
- (60) Abou-Elkhair, R. A. I.; Hassan, A. E. A.; Boykin, D. W.; Wilson, W. D. Lithium Hexamethyldisilazane Transformation of Transiently Protected 4-Aza/Benzimidazole Nitriles to Amidines and Their Dimethyl Sulfoxide Mediated Imidazole Ring Formation. *Organic Letters* **2016**, 18 (18), 4714–4717. <https://doi.org/10.1021/acs.orglett.6b02359>.
- (61) García, D.; Foubelo, F.; Yus, M. Regioselective Reductive Opening of Substituted Phthalans: Synthetic Applications. *Tetrahedron* **2008**, 64 (19), 4275–4286. <https://doi.org/10.1016/j.tet.2008.02.072>.



## **Chapter 6**

### Summary and Future Outlook

## 1. Summary

Extending our current arsenal of antibiotics is key in winning the arms-race between humans and resistant bacteria. Classes of antibiotics otherwise limited to the treatment of Gram-positive pathogens may be potentiated to Gram-negative bacteria by disruption of their additional outer membrane. The work described in this thesis focusses on the development of novel synergists designed to selectively disrupt the outer membrane of Gram-negative bacteria.

In **Chapter 1** an overview is presented of the current literature on outer membrane disrupting synergistic compounds. This overview includes linear and cyclic cationic peptides, positively charged peptide-mimics, small molecules, either chelating, lipophilic, or positively charged, cationic steroids, and derivatives of aminoglycoside antibiotics. Synergy is defined by a fractional inhibitory concentration index (FICI) of  $\leq 0.5$  (Equation 1). The FICI functions as a numerical representation of potentiation: the lower the number, the stronger the synergistic combination. However, the drawback of focusing on FICI is that one loses sight of the concentration at which the synergy occurs. Selectivity for the outer membrane over membranes of human cells is vital and often overlooked in literature reports. A red blood cell based hemolysis assay can provide insight into this selectivity. This review aims to provide an assessment of the body of literature which facilitates the comparison of published synergistic agents and therefore aid the optimization and development of synergists.

$$\text{FICI} = \frac{\text{MSC}_{\text{ant}}}{\text{MIC}_{\text{ant}}} + \frac{\text{MSC}_{\text{syn}}}{\text{MIC}_{\text{syn}}} \quad (1)$$

**Equation 1.** Calculation of FICI.  $\text{MSC}_{\text{ant}}$  = MIC of antibiotic in combination with synergist;  $\text{MIC}_{\text{ant}}$  = MIC of antibiotic alone;  $\text{MSC}_{\text{syn}}$  = MIC of synergist in combination with antibiotic;  $\text{MIC}_{\text{syn}}$  = MIC of synergist alone.

In **Chapter 2** the synergistic potential of bis-amidines was explored. Pentamidine, an anti-parasitic drug, has been reported to potentiate Gram-positive specific antibiotics against Gram-negative bacteria and a limited structure-activity relationship (SAR) study was described using a commercially available set of pentamidine analogues. In **Chapter 2**, this SAR was expanded with synthesized bis-amidines allowing for specific modifications to be compared. A screening using checkerboard assays revealed hits with improved FICI values. However, a hemolysis assay revealed that the most potent hits resulted in high percentages of hemolysis. Our focus shifted towards bis-amidines **21** and **22** containing a xylene linker which showed no hemolytic activity (Figure 1). A wide range of potentiation was confirmed by screening of compounds **21** and **22** in combination with several antibiotics: erythromycin, rifampicin, vancomycin, and novobiocin. Synergy was first assessed in *E. coli* and subsequently established for *K. pneumoniae*, *A. baumannii*, *P. aeruginosa*, and resistant *E. coli* strains.

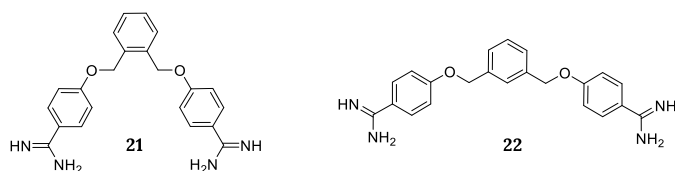


**Figure 1.** Molecular structures of the most potent, non-hemolytic bis-amidines **21** and **22**

Thrombin-derived peptides have been reported to bind to lipopolysaccharide (LPS), a major component of the outer membrane of Gram-negative bacteria. We hypothesized that LPS-binding results in outer membrane disruption by these peptides as seen for other synergists. In **Chapter 3** screening of four thrombin-derived peptides confirmed this hypothesis through potentiation of erythromycin and rifampicin against *E. coli*. Optimization of the lead peptide was achieved through amidation of the C-terminus followed by an alanine scan. Of the 12 alanine scan peptides, the peptides with the highest synergy and lowest hemolytic activity are presented in Table 1. The range of potentiation was investigated as reported for the bis-amidines in **Chapter 2**. Again, the synergistic activity for the optimized peptides extended to multiple antibiotics, resistant *E. coli* strains and other Gram-negative bacteria.

**Table 1.** Overview of the thrombin-derived peptides sequence, synergistic and hemolytic activity.

Peptide	Peptide sequence	MIC <sup>a</sup>	MSC <sub>peptide</sub> <sup>b</sup>	FICI <sup>c</sup>	Hemolysis <sup>d</sup>
<b>6</b>	H <sub>2</sub> N-VFRLKKWIQKVI-NH <sub>2</sub>	12.5	3.13	0.313	4%
<b>14</b>	H <sub>2</sub> N-VFRLKKAIQKVI-NH <sub>2</sub>	>200	6.25	0.078	1%
<b>19</b>	H <sub>2</sub> N-VFRLKKWIQKVA-NH <sub>2</sub>	100	3.13	0.094	1%

<sup>a</sup>Minimum inhibitory concentration (MIC); <sup>b</sup>Minimum synergistic concentration (MSC); <sup>c</sup>Fractional inhibitory concentration index (FICI); <sup>d</sup>Hemolysis after 20 hours of incubation of the compounds (200 µg/ml) with defibrinated sheep blood.

Recently, human serum was reported to potentiate both vancomycin and nisin against Gram-negative bacteria. The membrane-attack complex (MAC) present in human serum was found to be responsible for this potentiation through pore formation in bacterial membranes. This finding was further supported by the loss of synergy upon inhibition of MAC. The potentiation of other Gram-positive specific antibiotics by human serum was explored in **Chapter 4**. The inner membrane permeability assay produced nisin and vancomycin as hits against *E. coli*, while only modest activity was observed for daptomycin and the other glycopeptide antibiotics tested; telavancin, oritavancin, and dalbavancin. The bacterial viability assay functioned as a validation of these hits: the viability of *E. coli* was significantly reduced by nisin, vancomycin, and dalbavancin in the presence of serum. The bacterial viability assay also revealed other antibiotics with a significant effect on bacterial viability on *E. coli* in combination with serum: erythromycin, quinupristin & dalfopristin, and rifampicin. Unfortunately, the serum concentrations employed resulted in a reduction of viability for *K. pneumoniae* and *P. aeruginosa*, which overshadowed the results of the antibiotics. Prolonged exposure or

high concentration of human serum leads to inner membrane permeabilization and subsequent bactericidal activity by serum alone. Therefore, further optimization of the serum concentration would be recommended. Still, the current data clearly indicates that nisin, rifampicin, and vancomycin are potentiated against *K. pneumoniae* and nisin, quinupristin & dalfopristin, rifampicin, and vancomycin synergize with serum against *P. aeruginosa*.

Pentamidine has been reported as moderately active against Gram-positive bacteria. Therefore, the bis-amidines described in **Chapter 2** were screened for their antibacterial activity against Gram-positive bacteria in **Chapter 5**. The lowest minimum inhibitory concentration (MIC) observed was 0.25 µg/mL. However, like in **Chapter 2**, the most potent bis-amidines were found to be hemolytic. The range of hemolytic activity was quite broad even though several bis-amidines had similar lipophilic structures. To investigate whether the orientation of the linker compared to the amidine-position could be responsible for the difference in hemolysis, a set of bis-amidines was synthesized with altered amidine positions. Of the four novel bis-amidines synthesized, bis-amidine **6b** was found to be non-hemolytic whilst retaining activity (Figure 2). Together with the slightly hemolytic bis-amidine **7**, the antibacterial activity was evaluated against multiple Gram-positive strains in different growth media. Overall, bis-amidine **7** was found to be more potent than compound **6b**. A therapeutic window has been proposed based on the large difference between the concentration resulting in hemolysis (128 µg/mL) and the MIC values (0.25-4 µg/mL) for bis-amidine **7**.

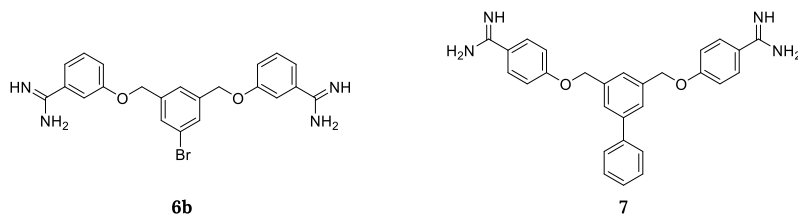


**Figure 2.** Chemical structures of the most potent bis-amidines **6b** and **7**



## 2. Future outlook

### 1.1. Bis-amidines

Both SARs performed on the bis-amidines have revealed clear and important trends; their hemolytic activity is driven by the compounds' lipophilicity as well as the orientation of the linker and positioning of the amidine moiety. Using CLogP as a measure of lipophilicity, the CLogP values of the bis-amidines were plotted against both the FICI values and the percentage of hemolysis (Figure 3).

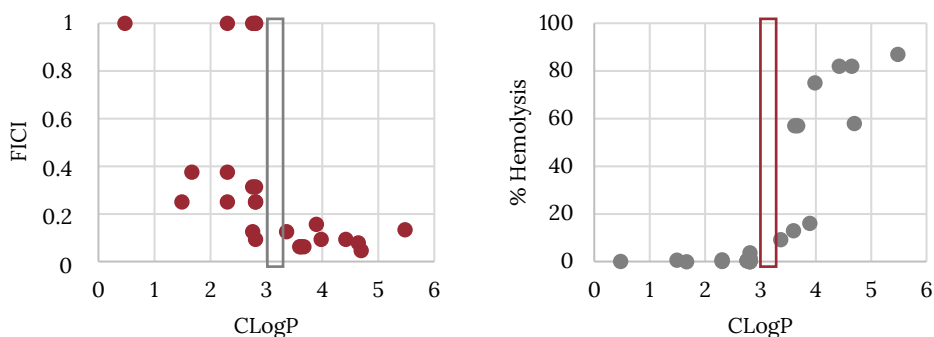


**Figure 3.** CLogP values of screened bis-amidines plotted vs. the FICI values or hemolysis percentages

The graphs indicate that a CLogP of 3.0 to 3.3 could be the ideal lipophilicity for minimal hemolysis and potent synergy. The lipophilicity of lead compound **22** (CLogP 2.809, Figure 1) could be slightly increased by the introduction of a methyl group (Figure 4A). The ideal position of the methyl group can be investigated through the synthesis of three analogues and, if successful, the same approach could be applied to the other two lead compounds: bis-*para*-amidine **21** (Figure 1) and bis-*meta*-amidine **23b** (Chapter 2).

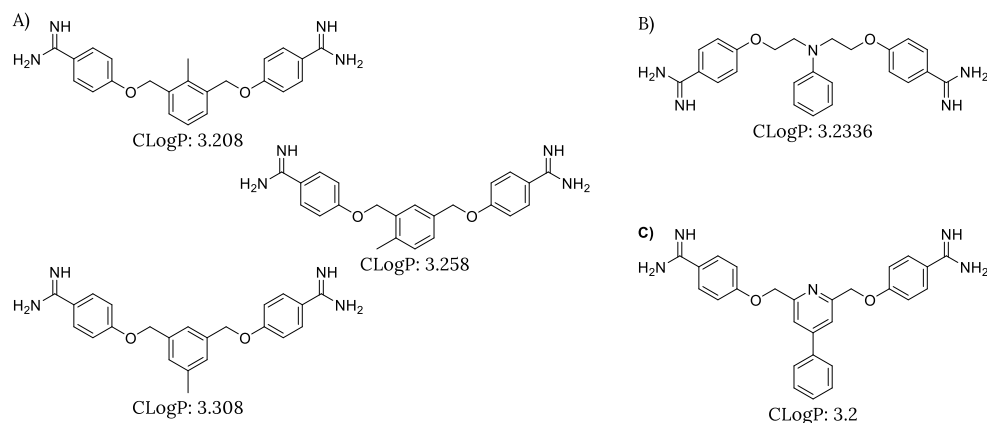


**Figure 4.** Structures of proposed bis-amidines and their ClogP values calculated by Chemdraw. A) Proposed methylation of compound **22** (Figure 1) to increase its lipophilicity; B) Optimized lead by the Brown group; C) Introduction of the nitrogen group in compound **7** (Figure 3) to reduce its lipophilicity.



A recent paper by the Brown group, which initially reported the synergistic potential of pentamidine, revealed a new lead compound based off of their original SAR study (Figure 4B).<sup>1,2</sup> The introduction of a nitrogen in the lead compound reduces its lipophilicity. In our own SAR study we had reported the parent compound of this analogue to be hemolytic (**Chapter 2**), while the new analogue was reported to be non-hemolytic (after 45 minutes of incubation).<sup>1</sup> The CLogP value calculated for this compound is 3.2, well within the proposed optimal range proposed and the nitrogen could also be implemented in our most potent, but hemolytic, bis-amidine **7** (Figure 2 and 4C).

While bis-amidines represent interesting leads as antibiotic synergists, the clinical history of pentamidine offers important insights into the side-effects, nephrotoxicity, hypotension, and hypoglycaemia associated with such compounds.<sup>3-5</sup> In addition to standard cytotoxicity screens (i.e. with HEK293 cells), the ADME and PK profile of the new analogues will certainly also need to be determined. Recent work from the Brown group provides not only a convenient ADME screening roadmap, but also assays tailored for the specific side-effects of pentamidine (QT prolongation and cell cycle arrest with HepG2 cells).<sup>1</sup> The PK profile of the new bis-amidines is also highly relevant since the clinical efficacy is dependent on how well this profile matches that of the antibiotics it potentiates. In literature *in vivo* potentiation of novobiocin with both pentamidine and the new lead compound has been established in mouse models.<sup>1,2</sup> It could be predicted that other structurally similar bis-amidines are likely to exhibit similar PK profiles.

## 1.2. Synergistic peptides

The original paper describing thrombin-derived peptides as LPS-binding is part of the research field focusing on sepsis and endotoxin-neutralization.<sup>6</sup> LPS is an endotoxin, binding LPS can lead to endotoxin-neutralization, and sepsis research could therefore provide a wealth of new leads for outer membrane disrupting synergists. Vice-versa, this field could also benefit from the LPS-binding outer membrane synergists reported.

The thrombin-derived peptides reported in **Chapter 3** can be further optimized by investigating truncations of the C- and N-termini and preparation of the mirror-image enantiomers using D-amino acids as D-peptides are more resistant to proteolysis.

Another experimental approach could be a systematic modification of the peptide sequence: to evaluate which set of amino acids needs to be kept intact as a group (for example, from VFRLKKWIQKVI to IVFRLKKWIQKV). A strongly synergistic peptide with a similar sequence was reported by the Kuipers group<sup>7</sup> in which the RLKKW sequence shifted towards the C-terminal end of the peptide (Table 2).

**Table 2.** Overview of the thrombin- and cathelicidin-derived peptides sequences.

	Peptide sequence
<b>6</b>	H <sub>2</sub> N-VF <b>RLKKW</b> IQKVI-NH <sub>2</sub>
<b>L-11</b>	H <sub>2</sub> N-RIVQ <b>RIKKW</b> LR-NH <sub>2</sub>

While peptide based synergists have in some cases shown potent *in vitro* activity, their *in vivo* efficacy is hampered by degradation and rapid clearance. In this regard, serum/plasma stability assays can provide insight into the stability and the sites of proteolytic degradation. Given the clinical potential of peptide-based therapeutics, a variety of modification have been investigated as a means of improving their stability. These strategies include replacing specific L-amino acids with D-amino acids, capping the termini, as well as completely transforming the peptide to its mirror image as was reported for **L-11**.<sup>7-14</sup> The plasma stability of this peptide was greatly improved upon transforming this peptide to its mirror image **D-11**.<sup>7</sup> Notably, while the mirror image form of our most potent peptide synergist **6** was not synergistic (see **Chapter 3**), the enantiomeric peptide did display antimicrobial activity suggesting the possibility to further optimize its inherent and/or synergistic activity.

### 1.3. Synergy with human serum

As described in both the summary and in **Chapter 4**, the optimal serum concentration for *K. pneumoniae* and *P. aeruginosa* needs further investigation. Subsequently, the screening of antibiotics and synergists can be repeated with these two strains. In addition, preliminary data was obtained for *A. baumannii* indicating that 25% of serum could potentiate nisin, although the data was hard to reproduce and the serum concentration needs further optimization.

With an optimal serum concentration established, the screening could be expanded to include more Gram-positive specific antibiotics. For example, from the macrolides only erythromycin was screened, while reports of potentiation of clarithromycin by chemical outer membrane disruptors has been reported.<sup>15</sup> This could result in new hits, as the potentiation of antibiotics by human serum is not equal for every member of an antibiotic class. This is evident from the data obtained for several glycopeptides: while dalbavancin and vancomycin resulted in a significant reduction in viability for *E. coli* in the presence of serum, no effect was observed for telavancin and oritavancin.

After screening with a fixed concentration of antibiotic, the antibiotic concentration required for potentiation can be investigated and optimized. The screenings could also be followed-up with time-kill assays. This would provide insight into the bacteriostatic or bactericidal activity of the serum and antibiotic combination. Resistance assay are also recommended as the resistance against the Gram-positive antibiotics is only known for Gram-positive species.

Traditional antibiotic susceptibility assays have generally neglected to consider the potential for serum proteins, including those of the innate immune system, to enhance the activity of antibiotics. While the *in vitro* research in **Chapter 4** points toward this intriguing possibility, it remains to be seen if *in vivo* assays would corroborate this synergistic effect, since the synergy is dependent on a window of time and serum concentration. Furthermore, it should be noted that the synergistic effect is limited to bacterial cells that are in contact with serum. With this in mind, the formation of biofilms, known to reduce the efficacy of antibiotics, could also limit the synergistic activity of serum. Further studies are needed to more fully elucidate the extent to which serum proteins can effectively potentiate antibiotics.

## References

- (1) MacNair, C. R.; Farha, M. A.; Serrano-Wu, M. H.; Lee, K. K.; Hubbard, B.; Côté, J.-P.; Carfrae, L. A.; Tu, M. M.; Gaulin, J. L.; Hunt, D. K.; Hung, D. T.; Brown, E. D. Preclinical Development of Pentamidine Analogs Identifies a Potent and Nontoxic Antibiotic Adjuvant. *ACS Infect. Dis.* **2022**. <https://doi.org/10.1021/acsinfecdis.1c00482>.
- (2) Stokes, J. M.; MacNair, C. R.; Ilyas, B.; French, S.; Côté, J.-P.; Bouwman, C.; Farha, M. A.; Sieron, A. O.; Whitfield, C.; Coombes, B. K.; Brown, E. D. Pentamidine Sensitizes Gram-Negative Pathogens to Antibiotics and Overcomes Acquired Colistin Resistance. *Nat Microbiol* **2017**, 2 (5), 1–8. <https://doi.org/10.1038/nmicrobiol.2017.28>.
- (3) Waller, D. G.; Sampson, A. P. (2018) Chemotherapy of infections. In *Medical pharmacology and therapeutics*, 5th ed., pp 581–629, Elsevier.
- (4) Sands, M.; Kron, M. A.; Brown, R. B. Pentamidine: a review. *Rev. Infect. Dis.*, **1985**, 7 (5), 625–634. DOI: 10.1093/clinids/7.5.625.
- (5) Goa, K. L.; Campoli-Richards, D. M. Pentamidine isethionate: A review of its antiprotozoal activity, pharmacokinetic properties and therapeutic use in *Pneumocystis carinii* pneumonia. *Drugs*, **1987**, 33 (3), 242–258. DOI: 10.2165/00003495-198733030-00002.
- (6) Saravanan, R.; Holdbrook, D. A.; Petrlova, J.; Singh, S.; Berglund, N. A.; Choong, Y. K.; Kjellström, S.; Bond, P. J.; Malmsten, M.; Schmidtchen, A. Structural Basis for Endotoxin Neutralisation and Anti-Inflammatory Activity of Thrombin-Derived C-Terminal Peptides. *Nat Commun* **2018**, 9 (1), 2762. <https://doi.org/10.1038/s41467-018-05242-0>.
- (7) Li, Q.; Cebrián, R.; Montalbán-López, M.; Ren, H.; Wu, W.; Kuipers, O. P. Outer-Membrane-Acting Peptides and Lipid II-Targeting Antibiotics Cooperatively Kill Gram-Negative Pathogens. *Commun Biol* **2021**, 4 (1), 1–11. <https://doi.org/10.1038/s42003-020-01511-1>.
- (8) Seo, M.-D.; Won, H.-S.; Kim, J.-H.; Mishig-Ochir, T.; Lee, B.-J. Antimicrobial Peptides for Therapeutic Applications: A Review. *Molecules* **2012**, 17 (10), 12276–12286. <https://doi.org/10.3390/molecules171012276>.
- (9) Adessi, C.; Soto, C. Converting a Peptide into a Drug: Strategies to Improve Stability and Bioavailability. *Curr. Med. Chem.* **2002**, 9 (9), 963–978. <https://doi.org/10.2174/0929867024606731>.
- (10) Ovadia, O.; Greenberg, S.; Laufer, B.; Gilon, C.; Hoffman, A.; Kessler, H. Improvement of Drug-like Properties of Peptides: The Somatostatin Paradigm. *Expert Opin. Drug Discov.* **2010**, 5 (7), 655–671. <https://doi.org/10.1517/17460441.2010.493935>.
- (11) Godballe, T.; Nilsson, L. L.; Petersen, P. D.; Jenssen, H. Antimicrobial  $\beta$ -Peptides and  $\alpha$ -Peptoids. *Chem. Biol. Drug Des.* **2011**, 77 (2), 107–116. <https://doi.org/10.1111/j.1747-0285.2010.01067.x>.
- (12) Zhang, L.; Bulaj, G. Converting Peptides into Drug Leads by Lipidation. *Curr. Med. Chem.* **2012**, 19 (11), 1602–1618. <https://doi.org/10.2174/092986712799945003>.
- (13) Gentilucci, L.; De Marco, R.; Cerisoli, L. Chemical Modifications Designed to Improve Peptide Stability: Incorporation of Non-Natural Amino Acids, Pseudo-Peptide Bonds, and Cyclization. *Curr. Pharm. Des.* **2010**, 16 (28), 3185–3203. <https://doi.org/10.2174/138161210793292555>.
- (14) deGruyter, J. N.; Malins, L. R.; Baran, P. S. Residue-Specific Peptide Modification: A Chemist's Guide. *Biochemistry* **2017**, 56 (30), 3863–3873. <https://doi.org/10.1021/acs.biochem.7b00536>.
- (15) Blankson, G.; Parhi, A. K.; Kaul, M.; Pilch, D. S.; LaVoie, E. J. Structure-Activity Relationships of Potentiators of the Antibiotic Activity of Clarithromycin against *Escherichia Coli*. *European Journal of Medicinal Chemistry* **2019**, 178, 30–38. <https://doi.org/10.1016/j.ejmech.2019.05.075>.



## Appendices







## Samenvatting

Het uitbreiden van het huidige repertoire aan antibiotica is essentieel om de wapenwedloop tussen mens en resistente bacteriën te winnen. Klassen van antibiotica die qua behandeling gelimiteerd zijn tot Grampositieve pathogenen kunnen ook worden ingezet tegen Gramnegatieve bacteriën mits de integriteit van het buitenmembraan verstoord is. Het onderzoek beschreven in deze dissertatie omvat de ontwikkeling van nieuwe synergetische additieven aan antibiotica die ontworpen zijn om selectief de structurele integriteit van het buitenmembraan van Gramnegatieve bacteriën te verstoren.

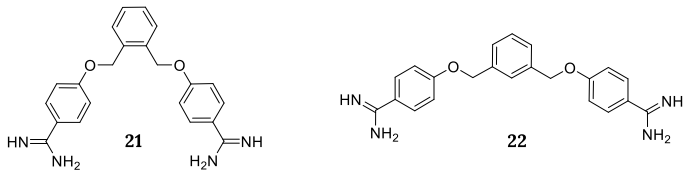
In **Hoofdstuk 1** wordt een overzicht van de huidige literatuur op het gebied van buitenmembraan verstorende synergetische moleculen gepresenteerd. Dit overzicht omvat lineaire en cyclische, positief geladen peptiden, positief geladen peptidenmimics, kleine moleculen met chelerende of lipofiele eigenschappen of positief ladingen, positief geladen steroïden en derivaten van aminoglycosiden antibiotica. Synergie wordt gedefinieerd door een fractioneel remmende concentratie-index (FICI) kleiner dan 0.5 (Vergelijking 1). De FICI fungeert als een numerieke representatie van de potentiëring: hoe kleiner het getal, hoe sterker de synergetische combinatie. Een bezwaar tegen een eenzijdige focus op FICI is dat men de concentratie waarmee de synergie plaatsvindt uit het oog verliest. Een ander belangrijk aspect in de evaluatie van buitenmembraan verstorende moleculen is de selectiviteit voor dit specifieke membraan. In de literatuur kan dit aspect over het hoofd worden gezien terwijl slechts een simpel hemolyse experiment met rode bloedcellen al enig inzicht in deze selectiviteit verschaft. Dit overzicht van de huidige literatuur heeft als doel om een vergelijking tussen gepubliceerde synergetische chemische verbindingen te faciliteren en kan derhalve bijdragen aan de optimalisatie en ontwikkeling van synergetische moleculen.

$$FICI = \frac{MSC_{ant}}{MIC_{ant}} + \frac{MSC_{syn}}{MIC_{syn}} \quad (1)$$

**Vergelijking (1).** FICI berekening.  $MSC_{ant}$  = minimale remmende concentratie (MIC) van een antibioticum in combinatie met de synergist;  $MIC_{ant}$  = MIC van het antibioticum zelf;  $MSC_{syn}$  = MIC van de synergist in combinatie met het antibioticum;  $MIC_{syn}$  = MIC van de synergist zelf.

In **Hoofdstuk 2** wordt het synergetische potentieel van bis-amidines onderzocht. Recentelijk onderzoek toonde aan dat pentamidine, een anti-parasitair medicijn, ook het gebruik van Grampositieve antibiotica tegen Gramnegatieve bacteriën faciliteerde. Daarnaast werd ook een structuur-activiteit relatie (SAR) studie beschreven gelimiteerd tot commercieel verkrijgbare pentamidine analogen. In **Hoofdstuk 2** werd deze SAR studie verder uitgebreid met de synthese van bis-amidines waardoor een directe vergelijking van specifieke modificaties mogelijk werd. Screening middels checkerboard testen resulteerde in hits met verbeterde FICI waardes. Echter, de hemolyse screening toonde aan dat de meest potente hits ook hoge percentages van hemolyse veroorzaakten. Door deze bevinding verschoof onze aandacht naar bis-amidines **21** en **22** die een xyleen linker bevatten en niet in hemolyse resulteerden. (Afbeelding 1). Het brede spectrum van synergie van de chemische verbindingen **21** en **22** werd bevestigd in combinatie met verschillende antibiotica: erythromycine, rifampicine,

vancomycine en novobiocine. Synergie werd eerst vastgesteld met *Escherichia coli* en vervolgens ook aangetoond tegen *Klebsiella pneumoniae*, *Acinetobacter baumannii*, *Pseudomonas aeruginosa* en resistente *E. coli* stammen.



**Abbeelding 1.** Moleculaire structuren van de potente, niet-hemolytische bis-amidines **21** en **22**

In de literatuur werd de binding van peptiden, afgeleid van trombine, met lipopolysacharide (LPS), een essentiële component van het Gramnegatieve buitenmembraan, gerapporteerd. Wij veronderstelden dat het binden van deze peptiden met het LPS zou kunnen leiden tot een verstoring van het buitenmembraan aangezien dit principe ook geldt voor andere synergetische moleculen. In **Hoofdstuk 3** bevestigde een screening van vier peptiden afgeleid van trombine deze hypothese aangezien er synergie met erythromycine en rifampicine voor *E. coli* werd geobserveerd. De optimalisatie van de lead peptide werd bereikt met een C-terminus amidatie gevolgd door een alanine scan. Van de 12 alanine scan peptiden zijn de peptiden resulterend in de hoogste synergie en laagste hemolyse weergegeven in Tabel 1. Het spectrum van synergie werd op een vergelijkbare wijze onderzocht zoals beschreven voor de bis-amidines in **Hoofdstuk 2**. Opnieuw was er sprake van een brede synergistische activiteit: ditmaal bij de geoptimaliseerde peptiden in combinatie met meerdere antibiotica en voor resistente *E. coli* stammen en andere Gramnegatieve bacteriën.

**Tabel 1.** Overzicht van de peptiden afgeleid van het eiwit trombine: sequentie, synergetische en hemolytische activiteit.

Peptide	Peptide sequentie	MIC <sup>a</sup>	MSC <sub>peptide</sub> <sup>b</sup>	FICI <sup>c</sup>	Hemolyse % <sup>d</sup>
<b>6</b>	H <sub>2</sub> N-VFRLKKWIQKVI-NH <sub>2</sub>	12.5	3.13	0.313	4%
<b>14</b>	H <sub>2</sub> N-VFRLKKAIQKVI-NH <sub>2</sub>	>200	6.25	0.078	1%
<b>19</b>	H <sub>2</sub> N-VFRLKKWIQKVA-NH <sub>2</sub>	100	3.13	0.094	1%

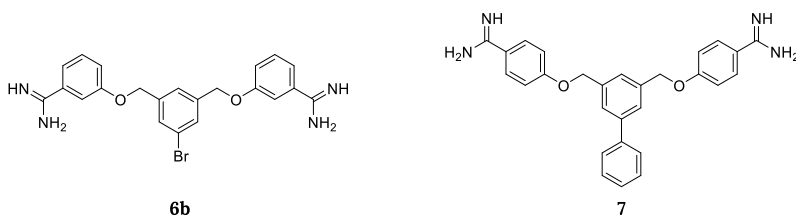
<sup>a</sup>Minimale remmende concentratie (MIC); <sup>b</sup>Minimale synergistische concentratie (MSC); <sup>c</sup>Fractionele remmende concentratie-index (FICI); <sup>d</sup>Hemolyse percentage na 20 uur incubatie van de chemische verbindingen (200 µg/ml) met gedefibrineerd schapenbloed.

Recentelijk werd de synergie tussen human serum met zowel vancomycine en nisine voor Gramnegatieve bacteriën gerapporteerd. Het membraan-aanval complex (MAC) aanwezig in humaan bloed bleek verantwoordelijk voor deze synergie door het vormen van poriën in bacteriële membranen. Deze bevinding werd verder ondersteund doordat inhibitie van het MAC leidde tot een verlies van synergie. De synergie van andere Grampositieve antibiotica met humaan serum werd verder onderzocht in **Hoofdstuk 4**. Een cytoplasmamembraan permeabiliteitstest resulteerde in nisine en vancomycine als hits voor *E. coli*, terwijl alleen een bescheiden effect werd geobserveerd voor daptomycine en de overige geteste glycopeptide-antibiotica; telavancine, oritavancine en dalbavancine. Een bacteriële levensvatbaarheid test had als rol om deze hits te



valideren: de levensvatbaarheid van de *E. coli* cellen werd significant gereduceerd met nisine, vancomycine en dalbavancine in de aanwezigheid van serum. Daarnaast onthulde de bacteriële levensvatbaarheid test ook dat andere antibiotica in combinatie met serum een significant effect hadden op de levensvatbaarheid van *E. coli* cellen: erythromycine, quinupristine & dalbopristine en rifampicine. Helaas resulteerden de serum concentraties voor *K. pneumoniae* en *P. aeruginosa* zelf al in een reductie van levensvatbaarheid. Dit effect overschaduwde de resultaten met antibiotica. Langdurige blootstelling of blootstelling aan hoge concentraties humaan serum leidt tot de permeabilisatie van het bacteriële cytoplasmamembraan met een bacteriedodende activiteit tot gevolg. De optimalisatie van de serum concentratie is daarom raadzaam. Desalniettemin is de huidige data al een sterke indicatie dat nisine, rifampicine en vancomycine synergie vertonen met serum voor *K. pneumoniae*. Nisine, quinupristine & dalbopristine, rifampicine en vancomycine demonstreren synergie met serum tegen *P. aeruginosa*.

Een bescheiden activiteit van pentamidine tegen Grampositieve bacteriën was reeds bekend in de literatuur. Om deze reden volgde een screening van de bis-amidines uit **Hoofdstuk 2** voor antibacteriële activiteit tegen Grampositieve bacteriën in **Hoofdstuk 5**. De laagste minimale remmende concentratie (MIC) die werd geobserveerd was 0.25 µg/mL. Zoals tevens het geval in **Hoofdstuk 2**, bleken de meest potente bis-amidines hemolytisch te zijn. Het was echter opmerkelijk dat de hemolytische waarden aanzienlijk uit elkaar lagen, terwijl meerdere bis-amidines een overeenkomstig lipofiele structuur hadden. Om te onderzoeken of de oriëntatie van de linker ten opzichte van de amidine positie een rol speelde, werd er een nieuwe set van bis-amidines gesynthetiseerd met een aangepaste amidine positie. Van de vier nieuwe gesynthetiseerde bis-amidines was bis-amidine **6b** niet hemolytisch met het behoud van de inherente activiteit (Afbeelding 2). Tezamen met de minimaal hemolytische bis-amidine **7** werd de antibacteriële activiteit geëvalueerd voor meerdere Grampositieve stammen in verschillende groeimedia. Over het geheel bleek bis-amidine **7** potenter te zijn dan bis-amidine **6b**. Dit leidde tot het voorstel voor een therapeutisch venster aangezien de verschillen tussen de concentratie die hemolyse veroorzaakten (128 µg/mL) en de MIC waarden (0.25-4 µg/mL) voor bis-amidine **7** zeer groot waren.



**Afbeelding 2.** Chemische structuren van de meest potente bis-amidines **6b** en **7**

## Sources of bacterial strains

Utrecht University Medical Center (UMC), Microbiology department, Heidelberglaan 100, 3584 CX Utrecht, The Netherlands

*E. coli* BW25113  
*E. coli* 552060.1  
*E. coli* mcr-1  
*S. aureus* USA300  
*E. faecium* E7314  
*E. faecium* E155

Utrecht University, Molecular Pharmacy, Universiteitsweg 99, 3584 CG Utrecht, the Netherlands

*S. aureus* ATCC29213

Leiden University Medical Center (LUMC), Department of Medical Microbiology, Albinusdreef 2, 2333 ZA Leiden, The Netherlands

*A. baumannii* ATCC17978  
*E. coli* ATCC25922  
*K. pneumoniae* ATCC13883  
*P. aeruginosa* ATCC27853

Wageningen Bioveterinary Research, Bacteriology and Epidemiology, Houtribweg 39, 8221 RA Lelystad, The Netherlands

*E. coli* EQASmcr-1/EQAS 2016 412016126  
*E. coli* EQASmcr-2/EQAS 2016 KP37  
*E. coli* EQASmcr-3/EQAS 2017 2013-SQ352

BEI resources

*S. aureus* COL  
*S. aureus* LIM2  
*S. aureus* VRS3b

## List of publications

### From this thesis:

Al Ayed, K.;<sup>‡</sup> Ballantine, R.D.;<sup>‡</sup> Hoekstra, M.; Bann, S.J.; Wesseling, C.M.J.; Bakker, A.T.; Zhong, Z.; Li, Y.; Bröchle, N.C.; Stelt, M. van der; Cochrane, S.A.; Martin, N.I. (2022) Synthetic studies with the brevicidine and laterocidine lipopeptide antibiotics including analogues with enhanced properties and in vivo efficacy, *Chem. Sci.*, **2022**,13, 3563–3570.

<sup>‡</sup>denotes shared first authorship

Wesseling, C.M.J.; Slingerland, C.J.; Veraar, S.; Lok, S.; Martin, N.I. (2021) Structure-activity studies with bis-amidines that potentiate Gram-positive specific antibiotics against Gram-negative pathogens, *ACS Infect. Dis.* **2021**, 7, 12, 3314–3335.

Wesseling, C.M.J.;<sup>‡</sup> Wood, T.M.;<sup>‡</sup> Slingerland, C.J.; Bertheussen, K.; Lok, S.; Martin, N.I. (2021) Thrombin-Derived Peptides Potentiate the Activity of Gram-Positive-Specific Antibiotics against Gram-Negative Bacteria, *Molecules* **2021**, 26, 1954.

<sup>‡</sup>denotes shared first authorship

### Other

Bruin, G. de; Rooden, E.J. van; Ward, D.; Wesseling, C.M.J.; Nieuwendijk, A.M.C.H. van den; Boeckel, C.A.A. van; Driessen, C.; Kisselev, A.F.; Florea, B.I.; Stelt, M. van der; Overkleeft, H.S. (2017) Asymmetric synthesis of lysine analogues with reduced basicity, and their incorporation into proteasome inhibitors, *Eur. J. Org. Chem.* **2017**(39): 5921–5934.

### Manuscripts in preparation

Wesseling, C.M.J.; Martin, N.I. Synergy by perturbing the outer membrane: access for Gram-positive specific antibiotics. (submitted)

## Curriculum Vitae

Charlotte Marie José Wesseling was born in Woerden, the Netherlands on the 3<sup>rd</sup> of April, 1990. She attended secondary school at the Coornhert Gymnasium in Gouda, during which she followed the extracurricular pre-university program of Leiden University, LAPP-TOP. After graduating from secondary school in 2008 she spend a year in Spain where she learned to speak Spanish, passed the DELE Inicial and Intermedio exams, and worked at the winery Elias Mora.

Back in the Netherlands, she started her Bachelor degree in Molecular Science & Technology at both Leiden University and TU Delft in 2009. During her bachelor, she elected a minor in Latin American Studies and she performed a research internship on the “Synthesis of a new diacylglycerol lipase- $\beta$  inhibitor building block based on the structure of tetrahydrolipstatin” under the supervision of prof. dr. Mario van der Stelt.

After obtaining her BSc in 2013, she continued her studies with a Research Master in Chemistry at Leiden University, specializing in Design & Synthesis and Biochemistry which she successfully completed in 2016. She performed a research internship for both specializations. In the first internship she worked on the “Synthesis of selective inhibitors of the catalytically active subunits of the proteasome” under the supervision of prof. dr. Hermen Overkleeft. She also performed a research internship in Berlin on the “Total synthesis of dehydroalanine containing lanthipeptides” under the supervision of prof. dr. Roderich Süßmuth.

In 2017, Charlotte joined the research group of prof. dr. Nathaniel Martin at Utrecht University as a PhD candidate, where she worked on several projects including the synergistic activity of pentamidine and thrombin-derived peptides. In July 2018 the research group transferred to the Institute of Biology Leiden at Leiden University, where she continued her PhD. Her chapter on the synergistic combinations of serum with conventional Gram-positive specific antibiotics was performed in the department of Microbiology in the group of prof. dr. Suzan H.M. Rooijackers at the UMC. Charlotte has published two research papers and a review article has been submitted for publication. Parts of her work have been presented as a poster during Chains 2017, 2018, 2019, 2020, HIPS symposium 2021 and an oral presentation at the IBL cluster meeting.

“Als je goed  
om je heen kijkt  
zie je dat alles  
gekleurd is”

- K. Schippers